

CARDIFF UNIVERSITY

Mechanics, Materials and Advanced Manufacturing

OPTIMISATION OF TOOL LIFE THROUGH NOVEL DATA  
ACQUISITION AND DECISION MAKING TECHNIQUES

Jacob L Hill

A thesis submitted in partial fulfilment for  
the degree of Doctor of Philosophy

2020

# Abstract

Variations in the operation and management of machine tool cutting processes will cause deviations in the quality of the manufactured parts. Current process management approaches combat these variations using combinations of pre- and/or post- process operator centred actions. The experience of the Author, and indications from involved industry partners, indicates that the associated "conservative" approaches to tool life management is costing between five and ten percent of the money spent on cutting tools, here amounting to two million pounds per annum. The additional cost of quality arising from process related variations cannot be accurately assessed.

This research enables the real time assessment of CNC milling cutting processes and the management of process variations. Innovative systems, programs and algorithms are developed through the course of this research project for the on-line monitoring of cutting tool health. These innovations include: the development of a cross-section area model to indicate variable metal removal in milling processes, the conversion of limited load data into process energy consumption, the engineering of an embedded tool wear data acquisition program, the application of an offline cubic change-point detection algorithm to quantitatively identify changes in cutting tool wear behaviour, the implementation of the density evaluation and separation algorithm to enable the separation of cutting and non-cutting process control signals, the development of novel Dispersion Plots, and the development of novel 3D process plots for illustrating instantaneous cutting tool condition.

In support of these innovations specially defined methods of signal analysis are deployed to acquire information for the assessment of enabled and complex health features. The approach is autonomous and based upon learning from the acquisition and analysis of information directly from the machine controller. This approach limits the impact on the operation and availability of the machine tool and mitigates any further impact on the capacity of the machine tools in question.

Decision making is enabled within the deployed diagnostic techniques. This provides the opportunity for plant-wide tool condition status monitoring and data visualisation. The deployed approach enables researchers to engineer machine systems that can provide more accurate, reliable and repeatable machine operations, with less waste and better managed processes.

It is shown that there is significant value in the process control data that was acquired throughout this study. The data is used to show the deployed cutting tool condition based on current and imminent machining requirements. It is also deployed to estimate the expected end of useful life for specific cutting tools and to generate innovative models of the cutting process. These models will enable Engineers to improve the cutting processes and to optimise the assessment of cutting tool condition and life.

# Acknowledgements

The author would like to acknowledge those who provided support and valuable company throughout this difficult undertaking. Without the friendship and support from supervisors, fellow PhD students, Cardiff University staff, and from friends and family, this endeavour would have been impossible.

Particular thanks go to Paul Prickett for their invaluable help and encouragement, and to Roger Grosvenor for their support and enthusiasm. Their patience made this work possible. Appreciation also goes to Craig Ryan for supporting the necessary empirical work and for their friendship throughout the four years, to Paul O'Regan and Jian Qin for their friendship (and coffee), and to Bethany Keenan for welcome distractions and research opportunities.

Acknowledgement also goes to Renishaw for enabling this research opportunity through their funding, their continued involvement and their provision of resources and information. Especially to David Miles and Robert Horsley for their support and advice. Most importantly, thanks go to Gareth Hankins, who helped keep this research grounded, focused and realistic.

Last but by no means least, appreciation goes to Naomi Eaton and Becca Morgan, and to wider friends and family for their constant encouragement and understanding.

# Contents

<b>1</b>	<b>Introduction</b>	<b>1</b>
1.1	Thesis aim and objectives . . . . .	3
1.2	Thesis scope and content . . . . .	4
<b>2</b>	<b>Literature Review</b>	<b>5</b>
2.1	Industry and manufacturing . . . . .	5
2.1.1	Industry 4.0, connected factories and the IIOT . . . . .	6
2.1.2	Machine tools . . . . .	8
2.2	Cutting tools . . . . .	12
2.2.1	Tool wear . . . . .	14
2.2.2	Machining strategies . . . . .	18
2.2.3	Tool management approaches . . . . .	20
2.2.3.1	Challenges and innovations . . . . .	20
2.2.3.2	Tool life equations . . . . .	21
2.3	Tool condition monitoring . . . . .	23
2.3.1	Complementary industrial solutions . . . . .	24
2.3.2	Data acquisition . . . . .	25
2.3.3	The ambiguity of acquired data . . . . .	29
2.3.4	Data and signal processing . . . . .	30
2.3.4.1	Prognostics and remaining useful life . . . . .	33
2.4	The research gap . . . . .	35
<b>3</b>	<b>Enabling Technologies and Methods</b>	<b>37</b>
3.1	Research framework . . . . .	37
3.2	Enabling technologies . . . . .	39
3.2.1	Machine tool and numerical controller . . . . .	39
3.2.1.1	Communication setup . . . . .	42
3.2.1.2	PC specification . . . . .	44

3.2.2	Coordinate measurement machine . . . . .	44
3.2.2.1	Fixturing . . . . .	46
3.2.2.2	Tactile probes . . . . .	47
3.2.2.3	Skidded probes . . . . .	47
3.3	Applications . . . . .	48
3.3.1	Application 1: Cylinders . . . . .	48
3.3.2	Application 2: Slots . . . . .	50
3.3.3	Application 3: Connecting-Rods . . . . .	51
3.3.4	Application 4: OMI-bodies . . . . .	52
3.3.5	Cutting tools . . . . .	53
3.4	Process assurance . . . . .	53
3.4.1	CMM suitability . . . . .	54
3.4.2	Machine tool capability . . . . .	57
3.5	Summary . . . . .	57
<b>4</b>	<b>Tool Monitoring System Development</b>	<b>59</b>
4.1	Data acquisition and initial processing . . . . .	59
4.1.1	Activity detection . . . . .	61
4.1.2	Data acquisition . . . . .	64
4.1.3	Integrated processing . . . . .	66
4.1.4	Error handling . . . . .	68
4.1.5	Files and storage . . . . .	68
4.1.6	Limitations . . . . .	69
4.1.6.1	Memory . . . . .	69
4.1.6.2	Sampling frequency . . . . .	70
4.1.6.3	Implementation . . . . .	70
4.2	Eliciting process features . . . . .	70
4.2.1	Innovation . . . . .	71
4.2.2	Implementation . . . . .	72
4.2.2.1	Import data . . . . .	73
4.2.2.2	Locate feature data . . . . .	75
4.2.2.3	Eliminate outliers . . . . .	78

4.2.2.4	Trim repeating values . . . . .	80
4.2.2.5	Apportion data and plot . . . . .	81
4.2.2.6	Additional memory improvements . . . . .	81
4.3	Converting unsuitable data . . . . .	82
4.3.1	Convert spindle motor output . . . . .	82
4.3.2	Convert axes motor output . . . . .	84
4.3.3	Calculate resultant force and direction . . . . .	84
4.3.4	Implementing data conversions . . . . .	85
4.4	Summary . . . . .	86
<b>5</b>	<b>Cylinder Wear Investigation</b>	<b>87</b>
5.1	Qualitative condition assessment . . . . .	88
5.2	Quantitative condition assessment . . . . .	92
5.2.1	Form measurement . . . . .	92
5.2.1.1	Depth, diameter and cylindricity variation . . . . .	92
5.2.1.2	Developed equation for cross-section wear . . . . .	96
5.2.1.3	Form observations from scanned measurement . . . . .	99
5.2.2	Finish measurement . . . . .	101
5.2.2.1	Ra versus Rz . . . . .	102
5.2.2.2	Best-fit polynomial and cumulative sum . . . . .	103
5.3	Application of MTData: Spindle motor load . . . . .	109
5.3.1	Signal and condition observations . . . . .	111
5.3.1.1	Micro value . . . . .	111
5.3.1.2	Macro value . . . . .	114
5.3.2	Development of RUL algorithm . . . . .	118
5.3.3	RUL correlation with form and finish . . . . .	127
5.4	Application of MTData: Spindle rotation . . . . .	131
5.4.1	Applications, advantages, limitations and disadvantages . . . . .	133
5.5	Application of MTData: Axis motor load . . . . .	134
5.6	Application of MTData: Ancillary signals . . . . .	137
5.6.1	Potential applications, advantages and complementary uses . . . . .	138
5.7	Challenges - limitations of the Cylinder application . . . . .	140

<b>6</b>	<b>Slotting Investigation</b>	<b>141</b>
6.1	Qualitative condition assessment . . . . .	142
6.2	Quantitative condition assessment . . . . .	144
6.3	Application of MTData: Spindle motor load . . . . .	149
6.4	Application of MTData: Axis motor load . . . . .	153
6.4.1	Axis separation . . . . .	155
6.4.2	Dispersion heat maps . . . . .	157
6.5	Application of MTData: Spindle rotation . . . . .	160
6.6	Challenges and next steps . . . . .	162
<b>7</b>	<b>Con-Rod Investigation</b>	<b>163</b>
7.1	Qualitative condition assessment . . . . .	164
7.2	Quantitative condition assessment . . . . .	166
7.3	Application of MTData: Axis position data . . . . .	169
7.4	Application of MTData: Spindle motor load . . . . .	177
7.5	Application of MTData: Axis motor load . . . . .	180
7.6	Application of MTData: Spindle rotation . . . . .	185
7.7	Challenges and next steps . . . . .	187
<b>8</b>	<b>OMI-body Investigation</b>	<b>188</b>
8.1	RAMTICs . . . . .	188
8.1.1	Refurbished cutting tools . . . . .	189
8.2	Laboratory implementation . . . . .	190
8.3	Industrial implementation . . . . .	193
8.3.1	Initial observations . . . . .	195
8.3.2	MTData investigation . . . . .	196
8.3.2.1	Cutting tool breakage . . . . .	196
8.3.2.2	Instantaneous condition . . . . .	198
8.3.2.3	Spindle signals . . . . .	202
8.3.2.4	Axis loads . . . . .	207
8.4	Challenges and next steps . . . . .	209
<b>9</b>	<b>Discussion</b>	<b>210</b>

<b>10 Conclusions and future opportunities</b>	<b>214</b>
10.1 Research contributions . . . . .	216
10.2 Future development . . . . .	217
<b>11 References</b>	<b>219</b>
<b>Appendix:</b>	
<b>A Programs</b>	<b>231</b>
A.1 PAc . . . . .	231
A.2 PAc flowchart . . . . .	231
A.3 DENSE program . . . . .	231
A.4 CMM scan data processing . . . . .	231
A.5 Excel VBA functions . . . . .	231
<b>B Effects of variable cutter engagement</b>	<b>243</b>
B.1 Pre-mill theory and derivation . . . . .	245
B.1.1 Edge lengths . . . . .	245
B.1.2 Arc lengths . . . . .	246
B.1.3 Adjustment factor . . . . .	247
B.1.4 Effective pre-mill length . . . . .	247
B.2 Pre-mill examples . . . . .	248
B.2.1 Pre-mill 1 . . . . .	249
B.2.2 Pre-mill 2 . . . . .	251
B.2.3 Pre-mill 3 . . . . .	253
B.2.4 Final material removal (Pre-mill 4) . . . . .	255
B.3 Pre-mill effect on process data . . . . .	257
B.3.1 Spindle rotational speed . . . . .	257
B.3.2 Spindle motor load and relative energy . . . . .	260
B.3.3 Axis motor loads . . . . .	262
B.4 Practical challenges facing implementation . . . . .	267
B.5 Summary . . . . .	268

<b>C</b>	<b>DMIS</b>	<b>270</b>
C.1	Programs . . . . .	270
C.2	Process assurance . . . . .	270
C.3	Calibration certificate (CMM) . . . . .	270
C.4	Calibration certificate (surface finish) . . . . .	270
C.5	I-MR charts . . . . .	270
<b>D</b>	<b>Additional documents</b>	<b>271</b>
D.1	Naming conventions . . . . .	271
D.2	DENSE additional figures . . . . .	271
D.3	Sycon help file . . . . .	271
D.4	Sycon project files . . . . .	271
D.5	Mazak API specification . . . . .	271
D.6	PC specification . . . . .	271
<b>E</b>	<b>Data files</b>	<b>272</b>
E.1	Experiment log . . . . .	272
E.2	Register audit . . . . .	272
E.3	Dispersion plots . . . . .	272
E.4	Application data files . . . . .	272

# List of Figures

1.1	Example probability curve sample for the estimated life of an unspecified cutting tool	2
2.1	Image of the iSMART factory concept, reproduced from yamazakimazak2020c . . . . .	7
2.2	Material hardness versus temperature, reproduced from Astakhov and Davim (2008) .	13
2.3	Material hardness versus toughness, reproduced from Astakhov and Davim (2008) . .	13
2.4	Images of different wear mechanisms, reproduced from Sandvik Coromant (2020b) . .	14
2.5	Indications of flank wear, reproduced from ISO 8688-2:1989 . . . . .	16
2.6	Cutting tool flank wear curves, reproduced from Black and Kohser (2012 p594) . . . .	17
2.7	Misappropriating Taylor’s tool wear curves, adapted from Prakash and Kanthababu 2013	17
2.8	Chip thickness versus shear stress - reproduced from Taniguchi (1994), from Shaw (2003)	19
2.9	Hypothesised origins of process variation, reproduced from Hill et al. (2019) . . . . .	29
2.10	Concept of RUL based on component health, reproduced from Okoh et al. (2014) . . .	35
3.1	Process and application timeline . . . . .	38
3.2	Mazak Vertical Centre Smart 430A VMC . . . . .	40
3.3	FCU7 installation and Ethernet cable routing . . . . .	42
3.4	Basic wiring schematic for COMX-CIFX physical connection . . . . .	43
3.5	MT and PC backend connections . . . . .	43
3.6	CMM and REVO-2 head . . . . .	45
3.7	Fixture example . . . . .	46
3.8	Surface finish probe and modules . . . . .	47
3.9	Cylinder CAD drawing . . . . .	48
3.10	Two-dimensional path schematics for Cylinder application . . . . .	49
3.11	Slot CAD model . . . . .	50
3.12	Conrod CAD model . . . . .	51
3.13	Variation in K direction cosine during scanning . . . . .	55
3.14	Collected probe debris after scanning measurement . . . . .	56
3.15	SFM-A2 acting on the 3.0 $\mu$ m roughness specimen . . . . .	56

3.16	Proportional gauge error versus AAE (pie-chart) . . . . .	57
4.1	High-level outline of the communication process . . . . .	60
4.2	Process logic illustrating activity detection (grey), DAQ (blue) and processing (green)	61
4.3	Pseudo code illustrating implementation of activity detection . . . . .	62
4.4	Pseudo code illustrating inter-process management . . . . .	63
4.5	MTData string-output composition . . . . .	64
4.6	IF-ELSE DAQ logic . . . . .	64
4.7	Pseudo code illustrating time-specific data filtering . . . . .	65
4.8	Priority scales . . . . .	66
4.9	Pseudo code illustrating initial processing . . . . .	67
4.10	Comparison of XYZ before and after correction of byte processing (axes omitted) . . .	68
4.11	Normally distributed DENSE theory for cutting process . . . . .	71
4.12	Simple linear structure diagram for DENSE . . . . .	72
4.13	Screen capture of omidef.dat . . . . .	73
4.14	MATLAB script for importing process data . . . . .	74
4.15	MATLAB script for generating plot objects . . . . .	75
4.16	MATLAB script for location of features . . . . .	76
4.17	MATLAB script to edit process data using DENSE conditions . . . . .	76
4.18	Example metadata plots for the Cylinder application . . . . .	77
4.19	Cylinder-Wear application DENSE result . . . . .	77
4.20	Outlier examples from arbitrary sample of MTData (shielded outliers noted) . . . . .	78
4.21	MATLAB script for first implementation of CC filter . . . . .	79
4.22	MATLAB script for second implementation of CC filter . . . . .	79
4.23	MATLAB script for repetition filter . . . . .	80
4.24	MATLAB script for visualising process data by creating plot of cutting tool paths . . .	81
4.25	Spindle speed-power-torque characteristic, recreated from Yamazaki Mazak (2015b) . .	83
4.26	MATLAB script for implementing conversion of percentage load data . . . . .	85
5.1	Observed cutting tool states following Cylinder application . . . . .	88
5.2	Flank and notch wear observed following Cylinder application . . . . .	89
5.3	Disintegrated tool (catastrophic failure) . . . . .	89

5.4	Irreparably damaged Cylinders due to catastrophic cutting tool failures . . . . .	90
5.5	Cutting tool failure with minimal workpiece damage . . . . .	91
5.6	Qualitative analysis of Cylinder condition at stages in the cutting process . . . . .	91
5.7	Trends in form measurements for CD . . . . .	93
5.8	Comparison of depth measurements from four tests . . . . .	94
5.9	Form measurements for CG and CH . . . . .	95
5.10	Diameter deviation for four tests considering an appropriate upper threshold . . . . .	96
5.11	CSAM deviation for four tests . . . . .	97
5.12	Cumulative CSAM deviation for four tests . . . . .	98
5.13	Cumulative CSAM deviation for tests CD, CI, CJ, CK, CL, and CM . . . . .	99
5.14	Example 3D plots of geometry variation in the Cylinder applications . . . . .	100
5.15	Roughness measurements for CD, comparing Ra, RzDIN, and RzISO . . . . .	102
5.16	Comparing RzISO for each side of the slot wall (set CD) . . . . .	102
5.17	Surface finish envelope plot for CD, CE, CF and CG, showing the combined average trend . . . . .	103
5.18	Geometry envelope plot for CD, CE, CF, and CG, showing the combined average trend	104
5.19	QSUM investigation for CD surface finish trends . . . . .	105
5.20	Upper QSUM plots for CD, CE, CF, and CG geometry data sets . . . . .	106
5.21	CG surface imperfection . . . . .	107
5.22	Qualitative breakpoint correlation using radar plot for CD, CE, CF, and CG . . . . .	107
5.23	Box-plot comparison of the geometry and surface finish measures estimates for EOL .	108
5.24	Quantised SML MTDData for CD . . . . .	109
5.25	PEC for CD prior to Hampel filter . . . . .	110
5.26	Process energy consumption plots for CD, CE, CF, and CG, after a single Hampel filter	110
5.27	Single Cylinder spindle motor load for a 10mm cutting tool (with failure) . . . . .	111
5.28	Single Cylinder spindle motor load for an arbitrary 10mm cutting tool (no failure) . .	113
5.29	Unprocessed spindle motor load line plot for CD . . . . .	114
5.30	Variations in SML upper peak envelope for CD based on peak distribution . . . . .	116
5.31	SML upper peak envelope with 900pt separation for CD and CE . . . . .	116
5.32	PEC plots for CD and CE illustrating general trend . . . . .	118
5.33	Best-fit cubic for CE PEC trend . . . . .	120

5.34	Standard cubic illustrating four condition stages based on inflection points . . . . .	120
5.35	Normalised best-fit for CE PEC, showing SP and mean part numbers . . . . .	122
5.36	p-fit curves for CE PEC indicating FRL effect for values of 1, 10, and 20 . . . . .	123
5.37	e-fit plot for CE PEC (FRL=0) . . . . .	123
5.38	CE PEC predicted e-fit curves from 48-190 parts . . . . .	125
5.39	CE response plot for PEC e-fit predictions of cutting tool condition . . . . .	125
5.40	RUL predictions for CD, CE, and CF . . . . .	126
5.41	Standardised comparison of CE PEC (with uncertainty) and CSAM trends . . . . .	127
5.42	Standardised comparison of CE PEC (with uncertainty) and surface finish trends . . . . .	128
5.43	CSAM and PEC inflection comparison using radar plot for CD, CE, CF, and CG . . . . .	129
5.44	Surface finish and PEC EOL comparison using radar plot for CD, CE, CF, and CG . . . . .	130
5.45	Spindle rotational speed for CE015 . . . . .	131
5.46	Probability density functions for two CE peak envelopes (upper and lower) . . . . .	132
5.47	Probability density functions for three CE peak envelopes (upper) . . . . .	132
5.48	Frequency-amplitude image for CE SRS . . . . .	133
5.49	Comparison between SRS and X-axis motor load, with and without cutting . . . . .	134
5.50	Axis motor loads (raw signals) for CD . . . . .	135
5.51	Frequency-amplitude image for CD XML . . . . .	136
5.52	Change in axis load over a single (arbitrary) Cylinder (Jet colourmap) . . . . .	137
5.53	3D process visualisation compiled using in-process axis position data . . . . .	138
5.54	3D process visualisation illustrating feature quality using SML overlay . . . . .	139
6.1	Photographs of the 10mm Slots (SA), illustrating the workpiece dimensions . . . . .	143
6.2	Slot width variation (top and bottom) for arbitrary points (SB003) . . . . .	144
6.3	Surface waviness along Slot wall . . . . .	145
6.4	Min, avg, and max scanned width measurements for SB (inc. SB003) . . . . .	146
6.5	Estimated (average) peripheral edge wear based on a 12mm Slot width . . . . .	147
6.6	Estimated (average) peripheral edge wear based on the upper width of a 12mm Slot . . . . .	148
6.7	Upper QSUM trends for SB peripheral wear, with 1, 2, and $3\sigma$ thresholds . . . . .	149
6.8	Upper QSUM moving average for SB peripheral wear, with 1, 2, and $3\sigma$ thresholds . . . . .	149
6.9	Raw SML signal for all 12mm Slots (SB003 and SB004026) . . . . .	150
6.10	PEC trend for all completed 12mm Slots . . . . .	150

6.11	PEC trend with cubic best-fit for 12mm Slots (SB) . . . . .	151
6.12	e-fit plot for SB PEC (FRL = 10) . . . . .	151
6.13	SB response plot for PEC e-fit predictions of cutting tool condition . . . . .	152
6.14	SB PEC predicted e-fit curves from 48-141 parts . . . . .	152
6.15	Percentage axis motor load signals for SB (including SB003) . . . . .	154
6.16	Percentage axis motor load signals for single test (seven Slots) . . . . .	155
6.17	Single Slot signal components (SB004-1) . . . . .	156
6.18	Single Slot primary signal component for SB004 (first Slot) . . . . .	156
6.19	XML dispersion heat map for all 12mm Slots . . . . .	158
6.20	XML dispersion heat maps for first and last Slots . . . . .	158
6.21	YML dispersion heat map for all 12mm Slots . . . . .	159
6.22	ZML dispersion heat map for all 12mm Slots . . . . .	160
6.23	SRS dispersion heat map for all 12mm Slots . . . . .	161
6.24	SRS dispersion heat maps for first and last Slots . . . . .	161
7.1	Photograph of the Con-Rod application . . . . .	163
7.2	Inner-surface condition of the Con-Rod for arbitrary part (unknown cutting tool state) . . . . .	165
7.3	Outer-surface condition of the Con-Rod for arbitrary part (unknown cutting tool state) . . . . .	165
7.4	Cumulative CSAM deviation for 40 of the manufactured Con-Rods . . . . .	166
7.5	RzNOV surface finish measurements for the inner, top, and side of all 42 Con-Rods . . . . .	167
7.6	Scanned measurements for arbitrary Con-Rod indicating point-to-point variation . . . . .	168
7.7	Point-to-point form variation measured from best-fit radius . . . . .	169
7.8	Exaggerated geometry of the Con-Rod large bore . . . . .	169
7.9	3D process plot using axis position data (Con-Rod #2) . . . . .	170
7.10	3D process plot using axis position data – defined cutting tools (Con-Rod #2) . . . . .	171
7.11	3D process plot separating by process - roughing and finishing (Con-Rod #2) . . . . .	172
7.12	3D process plot for optimised cutting process (Con-Rod #26) . . . . .	172
7.13	3D process plots for rotational speed and feed rate for Con-Rod #15 (all cutting tools) . . . . .	173
7.14	3D process plots showing instantaneous SML for Con-Rod #15 (all cutting tools) . . . . .	174
7.15	3D process plots showing instantaneous SRS for R021EM12 (Con-Rod #15) . . . . .	175
7.16	3D process plots showing instantaneous SML for R021EM12 (Con-Rod #15) . . . . .	176
7.17	SML for arbitrary Con-Rod, separating different cutting tools . . . . .	178

7.18	R021EM12 PEC per part for all 42 Con-Rods (one Con-Rod is one part) . . . . .	178
7.19	Combined PEC per part for all 42 Con-Rods (one Con-Rod is one part) . . . . .	179
7.20	Raw load signals for axis motors for Con-Rod application (R021EM12 only) . . . . .	180
7.21	xPEC and yPEC for R021EM12 during the Con-Rod application (R021EM12 only) . . . . .	181
7.22	XML dispersion heat map for all 42 Con-Rods (R021EM12 only) . . . . .	182
7.23	YML dispersion heat map for all 42 Con-Rods (R021EM12 only) . . . . .	183
7.24	Trends in core statistics for the given XML dispersion heat maps . . . . .	184
7.25	SRS results for worn and new cutting tools . . . . .	185
7.26	SRS dispersion heat map for R021EM12 (parts 16-42) . . . . .	186
8.1	RAMTICs at Renishaw, reproduced from Renishaw2020b . . . . .	189
8.2	Photographs of laboratory made OMI-bodies (new cutting tools) . . . . .	190
8.3	Photos of laboratory made OMI-bodies (worn cutting tools) . . . . .	191
8.4	Measured (M) cutting tool (H008) diameter using TS27R . . . . .	192
8.5	Spindle motor PEC results for the laboratory-made OMI-bodies . . . . .	193
8.6	Evidence of stop signatures in the SML signal for abnormal MTData set . . . . .	195
8.7	SML plot to compare worn and new cutting tools with a potential breakage . . . . .	197
8.8	Final 60 seconds of the cutting process for T8 (possible cutting tool failure) . . . . .	198
8.9	OMI-body process position data - all cutting tools (MMC) . . . . .	199
8.10	OMI-body process position data for only H008 cutting tools (MMC) . . . . .	199
8.11	OMI-body process model for H008 indicating instantaneous SML (MMC) . . . . .	200
8.12	OMI-body process model for T3 comparing relative health using MTData overlays . . . . .	201
8.13	OMI-body process model for T8 showing potential process anomalies . . . . .	202
8.14	Spindle PEC trends for the MMC OMI-bodies (first batch, H008 cutting tools) . . . . .	203
8.15	Spindle PEC trends for the MMC OMI-bodies (second batch, H008 cutting tools) . . . . .	204
8.16	SRS dispersion heat maps for the three H008 cutting tools (second batch of OMI-bodies) . . . . .	205
8.17	Trends in core statistics for the H008 SRS dispersion heat maps (MMC) . . . . .	206
8.18	sPEC compared with zPEC for T3 (second batch) illustrative purposes. . . . .	207
8.19	XML dispersion heat maps for the H008 cutting tools (second batch of OMI-bodies) . . . . .	208
B.1	Cutting tool failures for both minimum and maximum material removal . . . . .	243
B.2	X and Y position plots indicating relative cutting tool load . . . . .	244

B.3	Pre-mill occurrences for 10mm Cylinder wear tests (inner pocket) . . . . .	248
B.4	Pre-mill overlap during first slotting cut . . . . .	249
B.5	Relative impact of pre-mill 1 on AMR . . . . .	251
B.6	Pre-mill overlap at start of circular partial cut . . . . .	251
B.7	Relative impact of pre-mill 2 on AMR . . . . .	253
B.8	Final pre-mill overlap for circular partial cut . . . . .	253
B.9	Relative impact of pre-mill 3 on AMR . . . . .	254
B.10	Final region of metal to be removed during circular partial cut . . . . .	255
B.11	Relative impact of FMR on AMR . . . . .	256
B.12	Pre-mill impact on the material removal process . . . . .	257
B.13	Inner-pocket examples for eAMR and aAMR . . . . .	258
B.14	Material removed per cut compared with the equivalent SRS . . . . .	258
B.15	Correlation of pre-mill regions with significant SRS deviations (QSUM) . . . . .	259
B.16	Comparison of the eAMR and the aAMR with the SML . . . . .	261
B.17	Energy required to remove 1mm <sup>2</sup> of bright mild steel during pocket milling . . . . .	262
B.18	Axis loads versus AMR . . . . .	263
B.19	Cumulative sum for X-axis percentage load compared with material removal during wear test . . . . .	265
B.20	Cumulative sum for Y-axis percentage load compared with material removal during wear test . . . . .	266

# List of Tables

3.1	Key MT components . . . . .	39
3.2	Key MT attributes . . . . .	41
3.3	Laboratory PC specification . . . . .	44
3.4	Stage information for equivalent part manufacture . . . . .	49
3.5	Cutting tool details and nominal dimensions . . . . .	53
3.6	CMM measurement techniques . . . . .	54
3.7	Scan results for different velocities . . . . .	55
4.1	Key process parameters . . . . .	66
4.2	Spindle speed-power-torque characteristic ranges and power law coefficients . . . . .	83
4.3	Axis motor characteristics . . . . .	84
5.1	Breakpoints for CD-CG, for both geometry and surface finish measurements . . . . .	106
5.2	Data for single Cylinder machined using an arbitrary 10mm cutting tool (with failure) . . . . .	112
5.3	Initial coefficients for p-fit adjustment factor . . . . .	122
5.4	CD, CE, CF, and CG e-fit characteristics, calculated for both CSAM and PEC . . . . .	128
6.1	Slotting test information and cutting parameters . . . . .	142
7.1	Qualitative information for Con-Rod cutting tools . . . . .	164
7.2	Spindle PEC signal statistics for worn cutting tools and new cutting tools . . . . .	179
7.3	Axis PEC signal statistics for worn cutting tools and new cutting tools . . . . .	181
8.1	OMI-body cutting tool details (laboratory version) . . . . .	191
8.2	OMI-body cutting tool details (MMC version) . . . . .	194
B.1	Pre-mill 1 material engagement . . . . .	250
B.2	Pre-mill 2 material engagement . . . . .	252
B.3	Pre-mill 3 material engagement . . . . .	254
B.4	FMR material engagement . . . . .	256

# Nomenclature

$\alpha$	Chauvenet's Criterion Outlier Band
$\gamma$	Probable Fit Curve Adjustment Factor
$\sigma$	Standard Deviation
$\varnothing$	Diameter
$\omega$	Rotational Speed
$C_X$	Angle respective to X-Axis
$C_Z$	Angle respective to Z-Axis
$d$	Diameter
$E$	Energy
$F_S$	Sampling Frequency
$N$	Number of Samples
$P_{max}$	Rated Power
$R$	Resultant Load
$T_{max}$	Rated Torque
$T$	Cutting time
$Tn$	Cutting tool number
$Tt$	Cutting tool usage time
$V$	Cutting speed
AAE	Acceptable Artefact Error
AAMR	Actual Area of Material Removed
ACL	Application Control Limit
AFC	Active Feed Control
AKA	Also Known As
AM	Additive Manufacturing
AMR	Area of Material Removed
AMV	Actual Machine Volume
API	Application Programming Interface
ASCII	American Standard Code for Information Interchange
AVC	Active Vibration Control
BUE	Built-up-edge
CAD	Computer Aided Design
CAXIS	Colour Axis
CC	Chauvenet's Criterion
CCL	Chauvenet's Criterion Limit
CCPD	Cubic Change Point Detection

CMM	Coordinate Measurement Machine
CNC	Computer Numerical Control
CPU	Central Processing Unit
CS	Cutting Speed
CSAM	Cross-Section Area Method
CSV	Comma Separated Variable
DAQ	Data Acquisition
DAT	Data
DENSE	Density Evaluation and Separation Algorithm
DIAG	Diagnostics
DMIS	Dimensional Measuring Interface Standard
DOC	Depth of Cut
DOE	Design of Experiments
DSP	Digital Signal Processing
DTW	Differential Tool Wear
EAMR	Estimated Area of Material Removed
EC	Ethernet Cable
ECC	Electrical Control Cabinet
EFIT	Estimated Difference Plot
EIP	Ethernet Industrial Protocol
EMV	Effective Machine Volume
ENG	Extreme Negative Gradient
EOL	End of Life
EOUL	End of Useful Life
EPG	Extreme Positive Gradient
EPL	Effective Pre-mill Length
EWMA	Exponentially Weighted Moving Averages
FFT	Fast Fourier Transform
FMEA	Failure Modes and Effects Analysis
FMR	Final Material Removal
FMS	Flexible Manufacturing System
FRL	Forced Remaining Life
FWT	Fast Wavelet Transform
GEO	Geometry
GUI	Graphical User Interface
HSS	High Speed Steel
HVM	High Value Manufacturing
ICG	In Cycle Gauging
ICT	Information and Communication Technologies

IOT	Industrial Internet of Things
IO	Input Output
IPM	Intelligent Process Monitoring
IPMM	Intelligent Process Monitoring and Management
LB	Large Bore
MCS	Machine Coordinate System
MMC	Miskin Manufacturing Center
MRR	Material Removal Rate
MT	Machine Tool
MTData	Machine Tool Data
NC	Numerical Controller
NG	Negative Gradient
OEE	Overall Equipment Effectiveness
OEM	Original Equipment Manufacturer
OMI	Optical Machine Interface
OT	Outside Temperature
OTS	Online Tool Setter
PAc	Parameter Acquisition and Monitoring Application
PC	Personal Computer
PCD	Polycrystalline diamond
PCS	Part Coordinate System
PDE	Probability Density Estimate
PDF	Probability Density Function
PDIFF	Proportional Difference
PEC	Process Energy Consumption
PFIT	Probable Fit Curve
PFTU	Probe Feature Tactile Unique
PG	Positive Gradient
PLC	Programmable Logic Controller
PSTU	Probe Size Tactile Unique
QC	Quality Control
QSUM	Cumulative Sum
RA	Roughness Average
RAM	Random Access Memory
RAMTIC	Renishaw's Automated Milling, Turning and Inspection Centre
RAUC	Relative Area Under the Curve
REN	Relative Energy
RFR	Resultant Feed Rate
RMS	Root Mean Square

RPI	Requested Packet Interval
RT	Room Temperature
RTE	Real Time Ethernet
RUL	Remaining Useful Life
RZ	Roughness Total
SB	Small Bore
SF	Surface Finish
SFM	Surface Finish Module
SFP	Surface Finish Probe
SML	Spindle Motor Load
SP	Stationary Point
SPT	Speed Power Torque
SRS	Spindle Rotational Speed
STFT	Short Time Fourier Transform
TC	Tool Changer
TCM	Tool Condition Monitoring
VB	Flank Wear
VBA	Visual Basic for Applications
VCS	Vertical Centre Smart
VMC	Vertical Machining Centre
VMR	Volume of Material Removed
XML	X-axis Motor Load
YML	Y-Axis Motor Load
ZML	Z-Axis Motor Load

# 1 | Introduction

The research detailed in this thesis considers the acquisition and utilisation of data generated during the enactment of cutting processes on a vertical machining centre (VMC). It does so to promote the concepts associated with the utilisation of the advanced information and communication technologies (ICT) that are evident within the controllers of such machines and processes. These ICT systems are being continuously developed as part of the global initiative that can be associated with the concepts of the Industrial Internet of Things (IIoT). In this context Industry 4.0 is becoming increasingly cited within research. This is evidenced in Chapter 2, Section 2.1.1. However commercial implementation is still lacking, as is general understanding of the concept. Surveys on behalf of the Institution of Mechanical Engineers (Professional Engineering 2019) indicated that just 13% of companies have openly implemented Industry 4.0 concepts (of which a proportion will be those developing and selling such technologies) whilst 61% admit to not fully understanding the concept. Nevertheless, >42% noted an increase in predictive maintenance investment, whilst >41% noted plans to invest in big data. Both of which are often promoted when investigating Industry 4.0.

That said, driven by process sustainability and healthy competition Industry has progressed towards smarter manufacturing. Included in this progress is a degree of condition-based monitoring. Modern machine tools are often capable of actively monitoring their processes. They are also able to adjust control to maintain cutting speeds and the feed rate, or to enact inbuilt functions to protect the machine from damage. However, further improvements are possible and therefore more research is justified. It is the case that cutting tools continue to hinder both the automation and sustainability of the machining process. This often forms the basis of conservative management approaches as variations in cutting tool condition will cause deviations in the quality of the manufactured part.

Current process management approaches combat these variations using pre-process or post-process operator centred actions. This has enabled greater control over product quality and reduced the incidence of cutting tool failures. Sometimes in-process routines are also enacted, aimed at ensuring the quality of the machined product. It is not uncommon for modern machine tools to have the capacity to account for cutting tool wear and thus attempt to eliminate the effect on product geometry, or to identify broken cutting tools and thus prevent extensive damage to the workpiece. These systems are beneficial in a commercial sense; however, they have little consideration for the health of the cutting tool. Indeed, it is possible that degradation to cutting tool health may be obscured by such methods. The research presented herein indicates that methods for monitoring the health of cutting tools can be integrated into the machining process and will complement the current process management routines. This will help if the chosen approaches are able to work alongside the available pre-process, in-process and post-process routines employed by manufacturing organisations. It is noted that the availability of effective implementations is limited, despite the vast scale of research proposals available. This

indicates that efforts towards industry specific solutions for active tool condition monitoring and prediction of remaining cutting tool life, is desirable and warranted.

This research was approached with three motivations. The first motivation comes from the industrial sponsor, Renishaw plc. It is estimated that Renishaw spend in the region of £2 million per year on cutting tools and aim to avoid 25% of that by embracing the tacit intelligence arising from cutting processes. As part of that, the author envisages that between 5% and 10% of this cost may be avoided by transitioning from the current conservative approaches for managing cutting tools, towards more intelligent methods that appreciate the actual health of each cutting tool. Where the use of each cutting tool is based on the measured life remaining rather than the assumed life remaining. To illustrate the basis of this claim, Figure 1.1 considers a brief exploration by the author into current conservative approaches. The figure considers a sample batch of cutting tools that were deliberately run to failure. It is provided to show the cost of conservatively managing cutting tools.

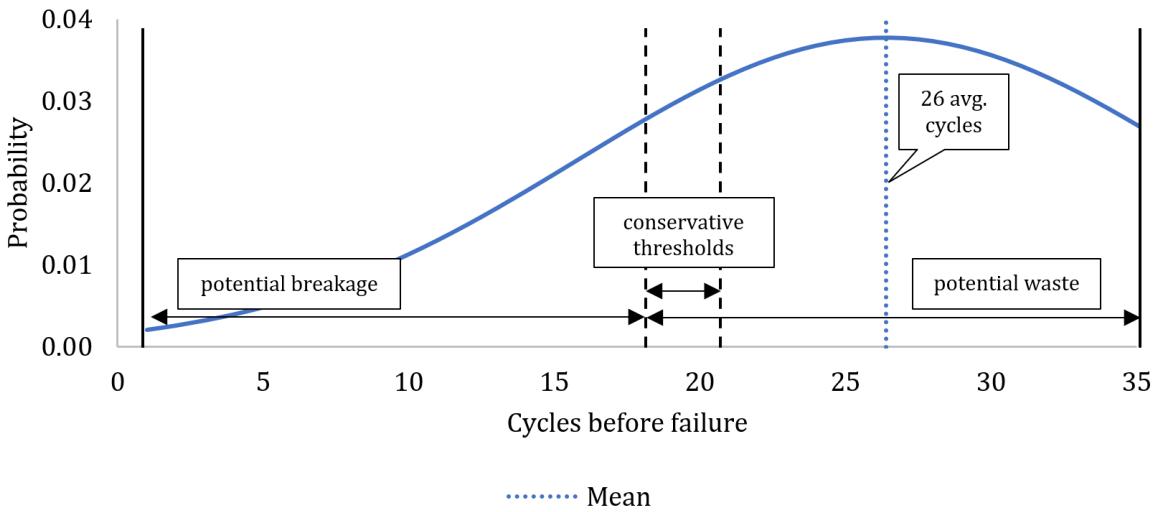


Figure 1.1. Example probability curve sample for the estimated life of an unspecified cutting tool

Figure 1.1 shows that an example cutting tool would last (on average) 26 cycles before failure. In this context “cycles” is used loosely to refer to the deployment of the cutting tool to machine a fixed number of parts. Being conservative in the management of such cutting tools will therefore mean limiting use to either 18 (70%) or 21 (80%) cycles depending on the acceptable risk to the process of cutting tool failure. This wastes five or more potential cycles per cutting tool. In the more extreme cases 14 or more cycles may be wasted. It is thus necessary that the management of cutting tools is revised to consider the actual condition of each cutting tool to save money on cutting tools and reduce the avoidable waste. This may be enabled through efficient use of smart process data acquired from machine tool architecture.

The second motivation was to optimise the management and contribute to the understanding of the degradation of cutting tools. Research shows that cutting tools remain the least optimised component within machine tools and contribute significantly to avoidable process waste. Reducing this waste will considerably improve the sustainability of the material removal process. In response, this thesis will

consider options for active monitoring of cutting tools and approaches for determining the remaining life of cutting tools. The research is targeted specifically towards practical or commercial applications and for eventual installation within a manufacturing environment. Specially chosen methods of signal analysis will be deployed to autonomously acquire information for the assessment of enabled health features. This will benefit from the acquisition and analysis of information directly from the machine tool controller. This work considers the diagnosis of cutting tool condition using the information acquired from a smart machine tool. This tacit knowledge, relating to the management and control of specific cutting processes, enables smart operations but also enables access to process information without demanding significant alteration to the system or process.

The operation and further enhancement of the deployed approach will meet the aims of the third motivation for this research, which is to demonstrate to machine tool manufacturers the potential for better utilising the information they currently generate to control and enact machining processes. This will enable researchers to engineer machine systems that can provide more accurate, reliable and repeatable machine operations, with less waste and better managed processes. In this research the co-operation of the machine tool manufacturer, Mazak, was secured and this provided the important access to otherwise hidden sources of information.

## **1.1 Thesis aim and objectives**

The aim of this thesis is to present concepts that will enable the accurate assessment of cutting tool condition and life in the context of current and imminent machining requirements. This is considered through five distinct objectives:

- To consider the current understanding and state-of-art of both academic and commercial innovations with respect to Industry 4.0 enabled manufacturing and cutting tool condition monitoring
- To design and test a prototype monitoring system capable of acquiring control data from a modern machine tool. Any derived system must prove the concept is feasible and should establish the value in such an approach and the value in acquiring such information
- To develop concept software capable of evaluating process data to identify the cutting process and the instantaneous cutting tool condition or general health. The concept software should respect the potential uncertain nature of the data and must establish the specific signal regions with value through appropriate implementation of signal filtering/processing
- To investigate any acquired process information to identify the likely sources, causes and ramifications of the data in terms of the cutting tool health, cutting tool or process diagnostics and cutting tool or process prognostics
- To establish the efficacy of the previous objectives and to identify methods appropriate for tool condition monitoring. Approaches must respect the boundaries between laboratory-based testing and commercial implementations and should appreciate the necessary stages for taking a laboratory-based concept through to commercial use.

## 1.2 Thesis scope and content

The scope of this thesis is to consider a new way of using information acquired directly from a machine tool controller to better manage cutting tool life. It does not set out to investigate tool life itself, but rather to demonstrate the potential for such an approach. In this context the thesis will show how it is possible to acquire machine control and process signals directly from a machine tool controller. Such signals are then used to analyse the nature of the cutting process being enacted and to indicate tool health. The potential of such an approach is demonstrated in the context of the presence of such signals within industry, stressing the explicit and implicit value of the information made available. The work presented utilises a 3-axis machine tool, deployed for end-mill cutting operations with uncoated cutting tools and using fully-flooded cutting conditions unless explicitly noted. The cutting parameters, materials, material properties and cutting operations will not be a focus of this work other than to confirm the integrity of, and future value in, the acquired data. This will not be a study into the implicit nature of cutting tools, nor the specific determination of cutting tool condition, but will explore routes for enabling such studies through proactive management of valuable process data. This thesis will explore potential uses for process signals to offer alternative approaches to existing methods, such as MTConnect and Taylor's tool wear curves and equations. Herein this thesis is divided into six major parts:

**Literature review** - discussing the current state-of-art of Industry 4.0, machine tools, cutting tools, the machining process and cutting tool condition monitoring. The main themes considered are diagnostics, prognostics and remaining useful life. In addition, the review more specifically considers the management cycle of cutting tools, including discussion on the application, deterioration and subsequent replacement.

**Enabling technologies and applications** – considers the equipment necessary to support this research and the empirical approaches necessary to properly ascertain cutting tool wear and to properly derive effective monitoring strategies. The capabilities of the technologies and applications presented are outlined explicitly.

**Tool monitoring system development** - presents the initial investigations into the management of cutting tools using the tacit intelligence afforded by their environment and the controlling functions.

**Wear investigations** – the initial developments are expanded in response to four specific applications. Each considers the value inherent to the process data and the value in identifying the instantaneous process state (diagnostics) and the progressive process state (prognostics). The wear investigations promote increased process complexity and will be presented as single factor experiments.

**Discussions and conclusions** – summary of the research completed, considering the contributions made and the future opportunities arising from the investigations presented herein.

## 2 | Literature Review

This review seeks to demonstrate why this thesis is necessary. It questions where research has failed to adequately understand the needs of industry and where industry has failed to appreciate the provisions of research. This chapter reviews the contributions from academics and from industrial organisations towards modern manufacturing systems and the development of intelligent processes, systems and factories. The review considers the two predominant methods for the assessment of cutting tool condition. First a direct assessment of the cutting tool, through measurement, or through either qualitative or quantitative comparisons between healthy and unhealthy cutting tools. Second an indirect assessment, with the condition of the cutting tool inferred from manufactured parts, or from process data. The process data may be derived through observation, or from the process directly considering implicit process feedback, control data, or from secondary sources, including vibration analysis, acoustic emission, force measurement and power consumption. More detail will be afforded to methods considered in subsequent chapters, specifically the assessment of cutting tool condition from the form of the manufactured part and from ‘smart’ machine data.

### 2.1 Industry and manufacturing

It is widely accepted that industry has gone through several “revolutions” to reach the current state-of-art. Most familiar is the first of these revolutions, Industry 1 is better-known as the industrial revolution. It covered the transition from isolated pockets of manufacturing, better described as ‘home-made’ goods, towards centralised manufacturing. This involved the development of machine tools and the beginnings of mass-production. Industry 1 is synonymous with the origin of factories, big-business and consumerism. The second revolution, Industry 2, continued these trends. Innovation in energy saw progress from steam to oil, gas and processed electricity. Progress also came in the form of the combustion engine and air travel. For manufacturing, Industry 2 acknowledges the contributions from innovators such as Henry Ford and Edison. Innovation in manufacturing came by the development of the assembly line and true mass-production. The third revolution, Industry 3, is also known as the digital revolution. Industry 3 marked a shift away from analogue technology and relates to the exponential increase in computing capability. This increase in capability had a marked effect on manufacturing and the available manufacturing techniques. Within machine tools with greater processing capability comes the ability to prolong the cutting process, to speed up the cutting process and to introduce optimised cutting strategies.

Each industrial revolution can be linked to an increasing need for manufacturing capability and the associated capability to create the machines and systems required to achieve this. This was propelled by the invention of computer numerical control (CNC). It can be inferred that process variation - arising from human error and inconsistency between operators - needed to be reduced, hence the decision to

“hard-wire” repeatability into operations. All three industrial revolutions are also intrinsically linked with the ethical/moral dilemmas centred around the health of the public and of the planet. These dilemmas form the basis of sustainability in manufacture, the reduction of waste and the introduction of lean manufacturing techniques. This drive towards sustainability in manufacture is one motivation behind the desire of manufacturing organisations to reduce waste; however, the main motivation will be improving the economy of a process. Reducing the incidence of cutting tool failures and improving the quality and integrity of manufactured components is always desirable. This can be approached by appropriately monitoring the process, whether that is indirectly, or through more invasive quality control. As the environmental impact becomes a primary focus, the reduction in all aspects of process waste becomes more valuable. A review commissioned by the UK Government in 2013 indicated that 2020 would see emphasis on process and material efficiency (Tennant 2013). Research by Cosgrove et al. (2019), Rance et al. (2019) and Zhou et al. (2019) indicates that this has happened. It is further implied by Tennant (2013) that policy changes will be necessary to optimise sustainable manufacturing; however, changes in public opinion and healthy competition between organisations may push through sustainable changes regardless. These priorities imply that systematic changes to promote process sustainability should be at the forefront for manufacturing organisations.

### **2.1.1 Industry 4.0, connected factories and the IIOT**

It has become impossible to escape the ideology that industry is manifesting a fourth revolution, Industry 4.0. This is not because Industry 4.0 is necessarily being implemented now but because Industry 4.0 is anticipated. A survey published by the IMechE (Professional Engineering 2019) found that only 13% of companies claimed to have implemented Industry 4.0 and 10% of companies were planning to. Manufacturing equipment has the increasing potential to be “self-aware”. This may evoke the illusion of self-managed and/or self-contained factories as is often theorised by proponents of Industry 4.0; however, as yet it simply means that the equipment is fitted with sensors that can provide feedback for most aspects of the process. This could be mistaken for an extension of the digital revolution; however, it is argued by Schwab (2016), Kagermann et al. (2013), MacDougall (2014) and Xu (2017) that the distinction lies in the pace of innovation, the specifics of the emerging technologies and the scale of the change.

Regardless of the label given, some of the innovations arising from the Industry 4.0 technology advancements are still notable. These include the capacity to further optimise sustainable manufacturing by providing greater traceability to processes. Where efficient energy consumption of manufacturing processes is sought after, the innovations presented by Industry 4.0 perhaps provide new avenues for monitoring such consumption (Cosgrove et al. 2019, Qin et al. 2017, Qin 2019, Qin et al. 2020). Additionally, Industry 4.0 is seemingly a catalyst for connected factories. A notable innovation in the UK for instance is Mazak’s (soon to be) iSMART factory in Worcester (Yamazaki Mazak 2019). Mazak note that their iSMART factories apply Industry 4.0 concepts (Figure 2.1) enabling them to improve their products and to boost their sales. Other examples outside of the UK include the three Mazak iSMART factories in the USA and Japan (Yamazaki Mazak 2020c) and Siemens’ Amberg Fac-

tory in Germany (Greenfield 2016, Staufer 2019). All commercial offerings for Industry 4.0, the IIOT and connected factories are competing products. Potential “solutions” exist from Mazak, Rexroth, Siemens and Marposs.

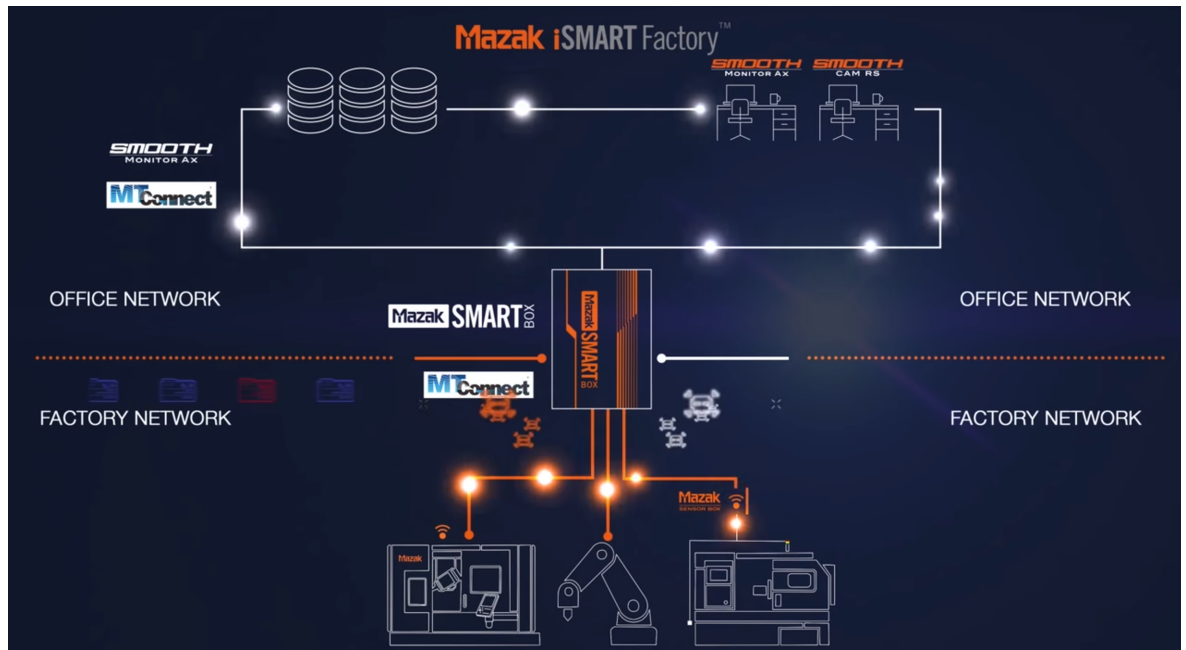


Figure 2.1. Image of the iSMART factory concept, reproduced from yamazakimazak2020c

Mazak offer the “Mazak SmartBox” which they claim works with all machines (Yamazaki Mazak 2015a, Yamazaki Mazak 2020d). At the time of writing, the caveat to this impressive claim is that the buyer is responsible for the integration, set-up, connection, software configuration and all-round installation, unless the machine is a Mazak. For other machines, this perhaps becomes the “Mazak Box” considering all the Smart is outsourced. The box can be retrofitted to legacy equipment, has enough computing capability for the incorporation of significant data processing and allows data to be networked to enable remote viewing (Allcock 2018).

Rexroth offer ODIN (Rexroth 2019). A system based on machine learning principles and one that offers manufacturing organisations the chance to send process information away for maintenance recommendations in “good time”. This may suit some organisations; however, many will be unwilling to share sensitive process information with another company. In addition, “good time” may not be enough. Where an anomaly is a significant fault, this must be detected in time or else significant costs may be incurred.

Siemens present a similar cloud-based solution in their MindSphere offering (Siemens 2020a). In contrast to Rexroth, Siemens offer just the platform to enable connectivity, rather than the entire solution. True connection and data analysis are left to individuals to customise, as necessary. This will perhaps be more tempting to organisations that wish to prioritise the privacy of their data; however, as with all data made available to the cloud privacy concerns may be ultimately unavoidable.

From Marposs is the ARTIS system (Marposs 2020a, Marposs 2020b). Unlike both Rexroth and Siemens, ARTIS is a machine tool specific system offering data acquisition and analysis for metal

cutting machine tools. The system provides solutions for machine, process and cutting tool monitoring by way of plug-in modules. The system is primarily aimed at protecting the integrated systems from damage through evaluation of process data to determine system and process health. The limitation of the ARTIS system is the same as the Mazak SmartBox in that integration with machines may be limited. Equally, the black box nature of the system does not encourage trust in the data output, nor trust in allowing the modules free reign to tamper with the workings of the integrated machine tool.

It is noted that many solutions encourage the acquisition of all information that is available. These approaches attempt to work with the mass of information by offering ‘intelligent’ interpretations of the data, sometimes implying the use of computation-heavy techniques (Rexroth 2020, Marposs 2020b). There are few repeatable or sensible interpretations of this data from a commercial sense. Where attempts are made to interpret the vast quantities of process data (typically referred to as “big data”), the results are often overly simplified, generic, or they fail to consider the ambiguity of the information generated by such complex systems. This will be revisited in Section 2.3.3. Additionally, all the data is often retained. In many cases, approaches require that the data be transferred off-site for processing, with results returned either periodically, or when necessary (if an anomaly is detected). In a data sensitive world, this is both challenging and potentially risky for organisations to adopt. Additionally, as the data footprint of these ‘smart’ machines increase, the rate at which the data can be sent, processed and returned is affected negatively. This infers that optimising the data use requires on-site processing. It is likely that monitoring manufacturing operations will create significant storage and downstream processing issues for such vast quantities of potentially sensitive information (Singh et al. 2020, Liu et al. 2020). Although this challenge is not fully appreciated by many organisations, despite the clear advantages to processing data at the source and only archiving any high-value data, it is noted that some organisations have recognised the need for value rather than volume (Tyrrell 2017, Red Lion 2020).

Understandably the goal is for future factories to be self-sustaining through automation by being connected. Such improvements benefit manufacturing in that they enable prolonged machining time, lower ongoing cost due to the reduced labour required and remote investigation into ongoing processes. Future factories themselves benefit from the exponential increase in cloud computing technology that has enabled applications of the IIOT to proliferate. Such technologies have enabled greater integration between factory and office networks (MacDougall 2014). In theory this enables engineers to monitor process availability and health remotely; however, when issues arise it does still question how robust the systems will be. Nevertheless, motivation is the driver of innovation. Without the enthusiasm for Industry 4.0, for the IIOT and for sustainable, sustaining manufacturing, the current drive in research funding and pace of industry involvement would not be as persistent as it has been.

### **2.1.2 Machine tools**

Manufacturing traditionally refers to subtractive methods, or the removal of material; however, innovations in additive manufacturing (AM) has recently prompted some researchers, including Rance

et al. (2019), to question the future of traditional techniques. The claim is that AM is less wasteful and has a greater capability to introduce complexity into manufactured components (Davim 2020). Yet, despite these arguments, subtractive manufacturing will always have a place in the production chain. AM has limitations in all-in-one manufacture and traditional techniques are often still required to improve the final quality of components and to achieve desired tolerances (Flynn et al. 2016, Stavropoulos et al. 2018). Nevertheless, change must still be implemented within conventional reductive processes in favour of sustainable manufacturing. Such change must start at the core of the material removal process.

At the heart of the material removal process is the machine tool. A machine tool is defined as a system capable of independent manufacturing. Their development came from the need to repeatedly machine components with a high degree of accuracy and precision. Machine tools are most often configured as a milling machine or a turning machine, or combinations of both. They are capable of automatically switching cutting tools in-process, with some able to switch workpieces. Machine tools are sometimes referred to as machining centres as they are effectively capable of all in one manufacture. It is even the case that newer machines come with AM capabilities built in (Flynn et al. 2016).

Machine tools have advanced from mechanically driven and manually operated machines developed in the first industrial revolution, through to CNC, electrical drives and automated production. These stages have been compared to the Industrial revolutions by Xu (2017) and Liu et al. (2019). The increasing independence of modern machine tools and the advent of CNC has shifted the responsibilities of an operator from a control-based role to a supervisory-based role. Instead of an active role in the actual machining of parts, operators now prepare machines between cycles and react to process changes and anomalies that the machine tools are not capable of controlling. Operators will often manage multiple machine tools. This reduces the cost of labour and promotes the idea of connected factories. Research by Xu (2017), Sobie et al. (2018), Liu et al. (2018), and Liu and Xu (2017) indicates that momentum is gathering towards connected factories, which (if implemented properly) will increase the capability of one operator to manage more machines, as well as enabling remote monitoring and management of connected machine tools.

Nevertheless, the capacity for independent operation of the machine tool is still limited. This can be attributed to three primary determinants: error, inconsistency and interference. Error includes both human error and sensor error. Inconsistency refers to variations in the process, cutting tools and materials used. Such variations will affect the accuracy of automated processes unless there is enough flexibility in the system. Inconsistencies limit the independence of a system as it encourages intervention by engineers to both determine the cause of any variation and to verify process anomalies that may arise due to such variation. Lastly, the independence of a machine tool is invariably affected by the constant intrusion by human elements and programmed elements of the systems. Interference is largely attributable to the above determinants in that both errors and inconsistencies will promote increased interference. However, in some cases further interference is also encountered. Factors for all three determinants can be expanded:

**Human error** can be mitigated by automating procedures and by limiting any manual operation of the machine tool. Human error may remain in process code, or during procedures that are not automated. If this error is significant, it can be debilitating to automated processes in that it introduces a potential mode of failure (Jones 2020).

**Sensor error** includes systematic errors and false readings. Such errors may invariably increase the rate of false alarms and subsequently decrease confidence in the system. Decreased confidence in an automated system renders it useless as it may no longer be adopted or will be subject to increased interruption from operators (Wheeler et al. 2010). This reduces the benefit of automation and the independence of the machine tools.

**Process variations** arise from programming inconsistencies and can perhaps be attributed to human error, or indeed different practice employed by different operators (Jones 2020). Variations may also arise when there is too much flexibility in an automated system. If the algorithms for deriving the cutting tool paths vary per iteration, it introduces an inconsistency to the process that may affect how the process is enacted. During evaluation of the process this may be mistakenly identified as stochastic variation, when it may arise due to a rounding error when deriving the most appropriate path for the cutting tool.

**Cutting tool variation** arises because no two cutting tools can be identical. There will always be discrepancies between cutting tools in terms of the coating finish, material composition, general finish and significant geometries (for example diameter) (Meier 2019). Inconsistencies will be further introduced by the setting of the tool in the tool holder, including runout, balance and effective tool length. It is thought that cutting tools are a significantly limiting factor in machine tool capability and a barrier against effective implementation of automated processes. This is due to their relative weakness compared to other components in the machine tool.

**Material variation** can result in features that are comparable to cutting tool variation. Material discrepancies arise between and within batches that will cause variation during manufacturing. This will include variation in material hardness, localised hardness, chemical composition and differences in billet geometries (Meier 2019). If such variation has negligible instantaneous impact on the cutting process anomalies (and thus false alarms) may be avoided. However, the long term or cumulative effects on the process or the cutting tool may become significant. A further variable is that the machining of a billet releases residual stresses in the material and can induce additional stresses when creating certain geometries (Fuh and Wu 1995, Ma and Feng 2016). This can cause the finished component to warp. Such distortion can occur during machining and when released from the MT fixturing. Such distortion will affect the instantaneous conditions experienced by the cutting tool during machining and will also introduce errors that require correction and therefore prolonged cutting cycles.

**Human interference** in automated systems can be limited by controlling how easy the system is to access. Some systems may not allow constant or easy access; therefore, interference may be limited. However, for systems where access is enabled, interference cannot be eliminated. This

may result from operators responding to perceived or actual anomalies in the process, taking action to slow or stop the process to investigate. Where there is an issue such intervention can only be beneficial, especially if not identified by the system. However, where there is no issue, interventions will be costly. It may also be the case that operators are opposed to the implementation of process monitoring. Such systems will inevitably be able to, and used to, monitor the effectiveness of the operators themselves. No research has been identified that seriously considers how operators view the implementation of remote monitoring and management of machine tools. The few articles located are primarily positive, including one by Bither (2016) noting the enthusiasm for such software. Additionally, Albert (2017) noted the opportunities made available by machine monitoring to improve operations, yet also noted the effect on productivity attributable to operators. It is noted that comments by Albert (2017) were almost entirely positive, including the encouragement of healthy competition, rewards, or training. However, there is little to stop organisations taking a more confrontational approach that perhaps benefits the business at the expense of the operator. Perhaps in contrast to the articles, it has been observed by the author in the context of this research that operators are remarkably suspicious when monitoring applications are installed.

**Programmed interference** is likely to be the result of human error. This may be through error thresholds being set too low and therefore programmed control attempting to limit damage that may never occur. However, interference will also arise through the simple act of maintaining the process. When cutting speeds dip due to increased resistances to cutting, the controller will increase the speed to compensate. Similarly, when cutting speeds rise due to reduced resistances to cutting the controller will reduce speeds to compensate. This compensation will inevitably add a “stochastic element” to the process. Not because the interference is truly random, but because the interventions may be hard to predict.

The capability of CNC machine tools has increased over time and will be further increased as researchers and OEMs pursue enhancements associated with Industry 4.0 (Renishaw 2020c, Rexroth 2020, Yamazaki Mazak 2020a, MTConnect Institute 2020, Siemens 2020b). This includes the MTConnect standard. MTConnect offers a method for standardising the information output from a machine tool controller by translating the native outputs into a standard or “universal” format. The benefits of this are notable, as data that is otherwise challenging to define and/or utilise becomes standard across machine tools. However, MTConnect is limited in value as it is ultimately another middle management program at the front-end of the machine tool controller. For that reason, MTConnect will inevitably restrict the effective and potential rate for utilising process data in real-time. This is because the method introduces data processing and management too late in the process.

Machine tools are somewhat convolutedly linked to Industry 4.0 by the similarly named Machine Tool 4.0. Xu (2017) and Liu et al. (2019) have collaboratively released several papers proposing such an initiative. Machine Tool 4.0 promotes the idea of “cyber-physical” machine tools whereby processes are enacted physically by the machine tool controlled by CNC and modelled digitally by way of “digital

twins” or similar technologies (Cai et al. 2017, Liu et al. 2019). Such approaches are a catalyst for generating huge volumes of data. Machine tool manufacturers do attempt to process the data at source, offering ‘smart’ functions intended to protect the machine and part from damage (Yamazaki Mazak 2014b). However, currently these approaches are often automatically applied to the real-time control of the machining operation to mitigate any detected changes and thus extend the effectiveness of the machining process. They do not aim to provide evidence or supply data of any change affected, but rather support the continued operation in a practical context and wholly rely on the machine operator to implement them effectively. Such methods are in effect relying on tacit knowledge related to the management of the cutting process that is built into modern advanced “smart” CNC systems.

## 2.2 Cutting tools

If the machine tool is the heart of the material removal process, cutting tools are the heart of the machine tool and are instrumental in the material removal process. A cutting tool must be chosen specifically for the application for which it is intended. It has been indicated by Dolinsek et al. (2001) and Black and Kohser (2012 p569) that for any machining to be effective the cutting tool must:

- be harder than the workpiece
- have high thermal stability
- resist wear
- be resistant to impacts (unintended or otherwise)
- not react chemically with the workpiece or the lubrication
- be an appropriate geometry and style for the required application

Besides the coolant, cutting tools are one of the consumables within machine tools that have the greatest impact on process conditions. It is noted by Cao et al. (2017) that cutting tools have the greatest impact on the outcome of the cutting process due to their direct interaction with the workpiece. This interaction affects the resultant geometries, surface finish and part quality. Cutting tools have developed on the basis that they must last for as long as possible and remove material as effectively as possible. This means that one of the underlying objectives of much research has been towards developing cutting tool materials that enable the cutting of progressively harder material, at faster speeds, without breaking. Cutting tool materials have progressed from high speed steel (HSS), to various carbides, ceramics and polycrystalline diamonds (PCDs) amongst others. An effective comparison of the different cutting tool materials is provided in Figure 2.2 and Figure 2.3 reproduced below. Figure 2.2 indicates the relative material hardness as temperature increases. Figure 2.3 indicates the relationship between material hardness and toughness.

Figure 2.2 and Figure 2.3 underline the variability within and between cutting tools, even between those produced from similar materials. The information provided can be used to establish the best cutting tool for a given application, or to estimate the life expectancy of a cutting tool for a specific

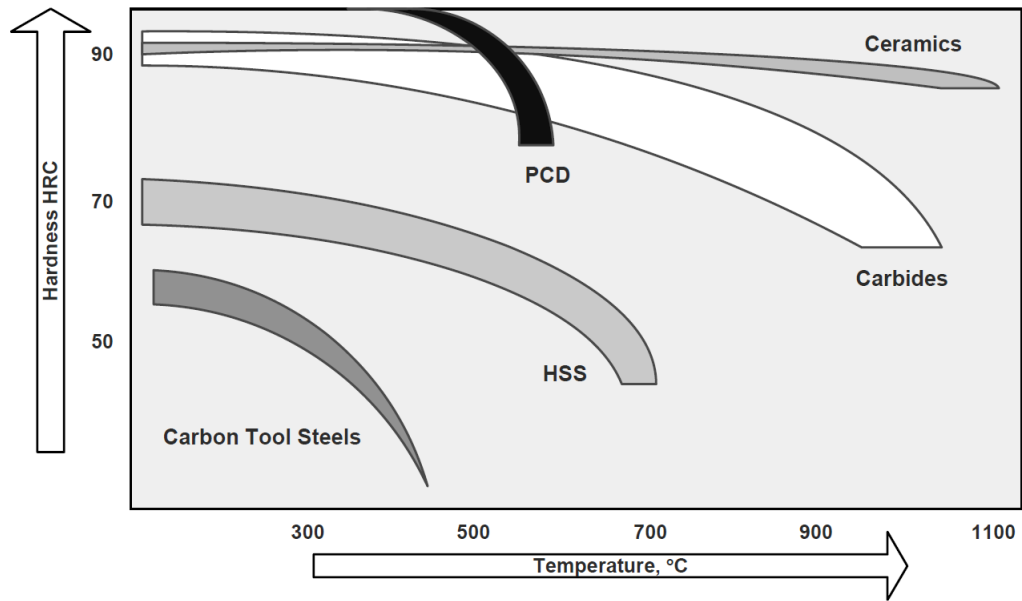


Figure 2.2. Material hardness versus temperature, reproduced from Astakhov and Davim (2008)

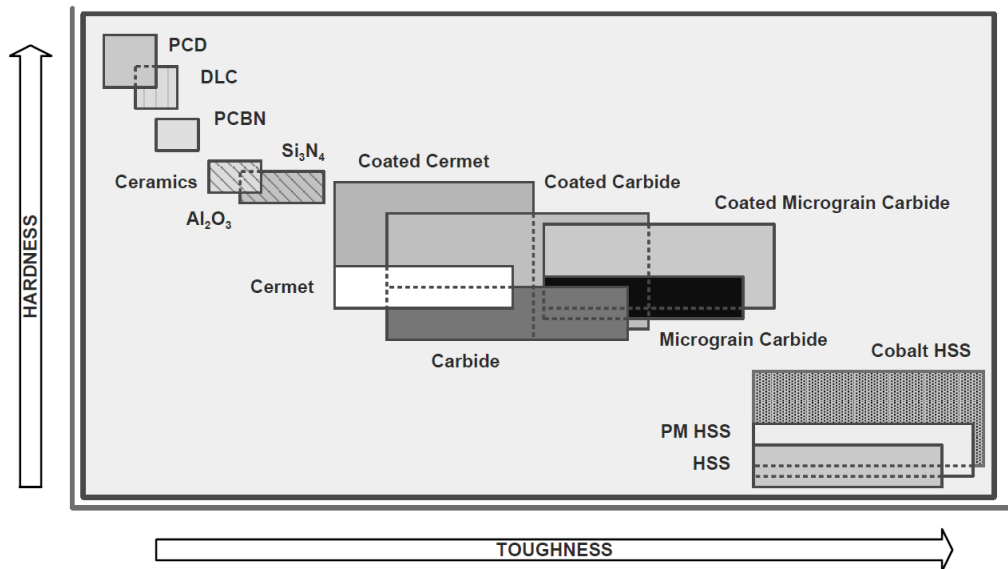


Figure 2.3. Material hardness versus toughness, reproduced from Astakhov and Davim (2008)

use. For example, HSS is effective at absorbing energy before breakage; however, it cannot cope with very high-speed cutting, nor hard workpiece materials. That said, HSS will cope better with anomalies in the manufacturing process without failing than harder materials. For example, carbide cutting tools are more likely to brittle fracture due to their relatively low toughness. However, compared to HSS the carbide cutting tools are likely to last longer before significantly deteriorating or breaking. In response to the two-sided nature of the above, a popular approach is to coat cutting tools to improve their cutting characteristics. Coatings can improve properties to offer decent toughness, whilst improving hardness. Astakhov and Davim (2008) notes that this enables cutting tools to better resist the effects of the cutting process, including friction, heat and damage. Attention is directed to information by Bhushan and Gupta (1991), Astakhov and Davim (2008) and Sandvik Coromant (2020a).

Despite the innovations in cutting tool materials, it is still the case that one of the weakest parts

in a machine tool are the cutting tools employed. Manufacturing operations are limited, in part, by the need to periodically check the condition of the cutting tools and to replace those that are damaged or failed. A large part of the process planning for metal cutting is therefore invested into the management of cutting tools (Conradie et al. 2017). Research has suggested that cutting tools account for a quarter of machining costs (Sakharov et al. 1990, Ghosh et al. 2018, Wong et al. 2020). This value is likely to be an over estimation as the 25% figure was originally stated in 1990. It seems unlikely that relative costs remain unchanged in 30 years; although it is not unreasonable to assume that the cost of cutting tools remains a significant proportion of the total machining costs. Especially when the industrial partner for this research has indicated costs for cutting tools in excess of £2million per annum. This will, in part, be due to the tendency for cutting tools to fail, and to wear, in ways that are detrimental to the manufacturing process and the quality of the produced parts.

### 2.2.1 Tool wear

The act of cutting material is fundamentally damaging to the tool that is removing the metal. This damage, or wear, to the cutting tool can eventually lead to total failure. It is also the case that some forms of wear can be instantly detrimental to the cutting process and therefore constitute immediate failure. Cutting tools can fail in several different ways. Herein these will be referred to as “failure modes”. Common modes of cutting tool failure include (but are not limited to) abrasive wear of the cutting tool flank or nose, adhesive wear (also known as built-up-edge (BUE)), chipping and tooth shear (or total failure). The failure modes that have most importance to the research in this thesis are expanded below. Further details and additional failure modes, that are not necessary herein, can be found in research by Dolinsek et al. (2001), Liu et al. (2002) and Okoh et al. (2014). Visual examples of each of the considered cutting tool failures are provided in Figure 2.4.

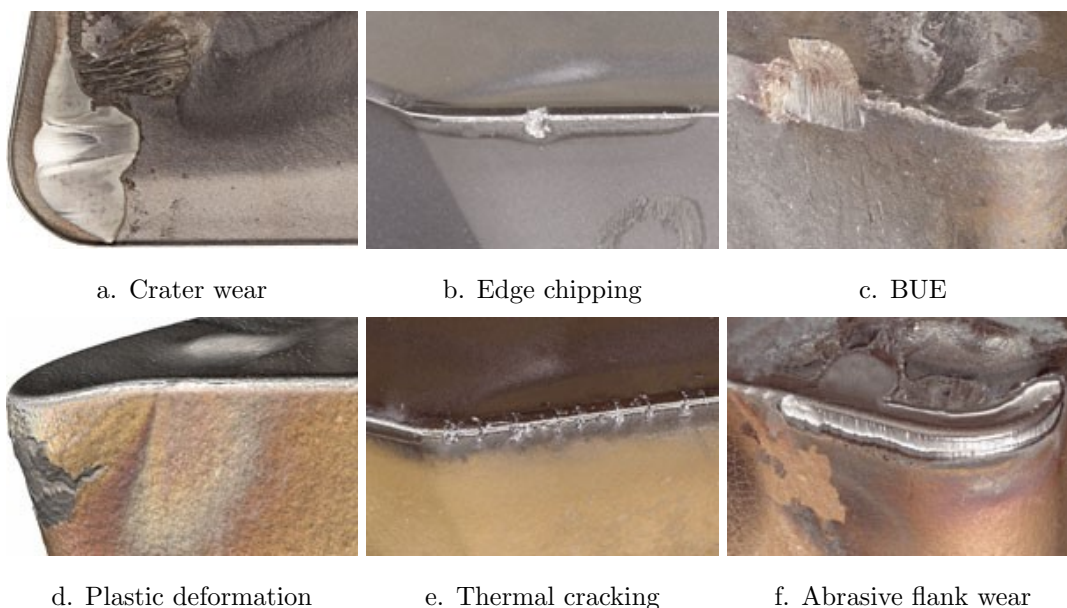


Figure 2.4. Images of different wear mechanisms, reproduced from Sandvik Coromant (2020b)

**Cratering** - Affects the surface of a cutting tool behind the cutting edge, where the impact from chips or swarf from the workpiece wear away the surface of the cutting tool. Cratering is relatively common but can be reduced by using cutting tool materials, or coatings, with a higher hardness.

**Chipping** - Unpredictable failure where an edge of the tool breaks away. Chipping is considered random; however, the risk of chipping may be reduced by using a stronger grade of cutting tool or changing the lead angle.

**BUE** - Caused when material from the workpiece builds up on the rake face, effectively adding material to the mass of the cutting tool. The extra material can break away taking material from the cutting tool with it. BUE is common, especially when machining ductile materials such as soft steel, aluminium and copper. Using faster cutting speeds, higher rake angles and use of high-pressure cutting fluid can help to reduce the likelihood of a BUE occurring.

**Deformation** - Where the tool has deformed and deviated from the original shape (warped) due to excessive heat or heat build-up. Deformation wear is dependent on material properties and cutting parameters and can be prevented by utilising a cutting tool material capable of the required cutting speeds.

**Thermal cracking** - Cracking of the tool due to inconsistent or sudden changes in temperature. Occurs often when a tool endures a rapid heating or cooling cycle. The likelihood of thermal cracking can be minimised by reducing how often the cutting process is interrupted or by using the correct cutting fluid.

**Edge and/or flank wear** - Represents the gradual, abrasive wear that will inevitably accompany all cutting operations. With a hard or abrasive material this wear will accelerate. Edge and flank wear can also be contributed to by other wear types, including cratering and separation of a BUE. General wear of the cutting tool is often assimilated to flank wear as noted in ISO 8688-2:1989 (Figure 2.5). When this wear is uniform the greatest impact on process quality will be to the geometry of the components. If the wear is not uniform the greatest impact on process quantity will be to the surface finish.

ISO 8688-2:1989 recommends that an appropriate threshold for flank wear is 0.3mm of average wear, or 0.5mm of localised (maximum per tooth) wear for cutting tools. This is illustrated in Figure 2.5 where VB1 illustrates uniform flank wear, VB2 non-uniform flank wear, VB3 localised flank wear and KT indicates face wear. Notwithstanding, Astakhov (2007) argues that such criteria are “subjective and insufficient”. It is true that the given thresholds hold no account for the work undertaken by, or the conditions subjected to, the cutting tool, nor the specific style or geometry of the cutting tool employed. However, despite this argument, the suggested thresholds are still relevant if used as a guide or starting point rather than at face value. Ultimately, the acceptable limits for flank wear will be entirely process and cutting tool specific. This concept is explored in the main body of the research reported in this thesis.

Cutting tool flank wear is often mapped against the general wear curves considered by Taylor (1906). It is noted that cutting tools go through an initial phase of rapid wear, a secondary

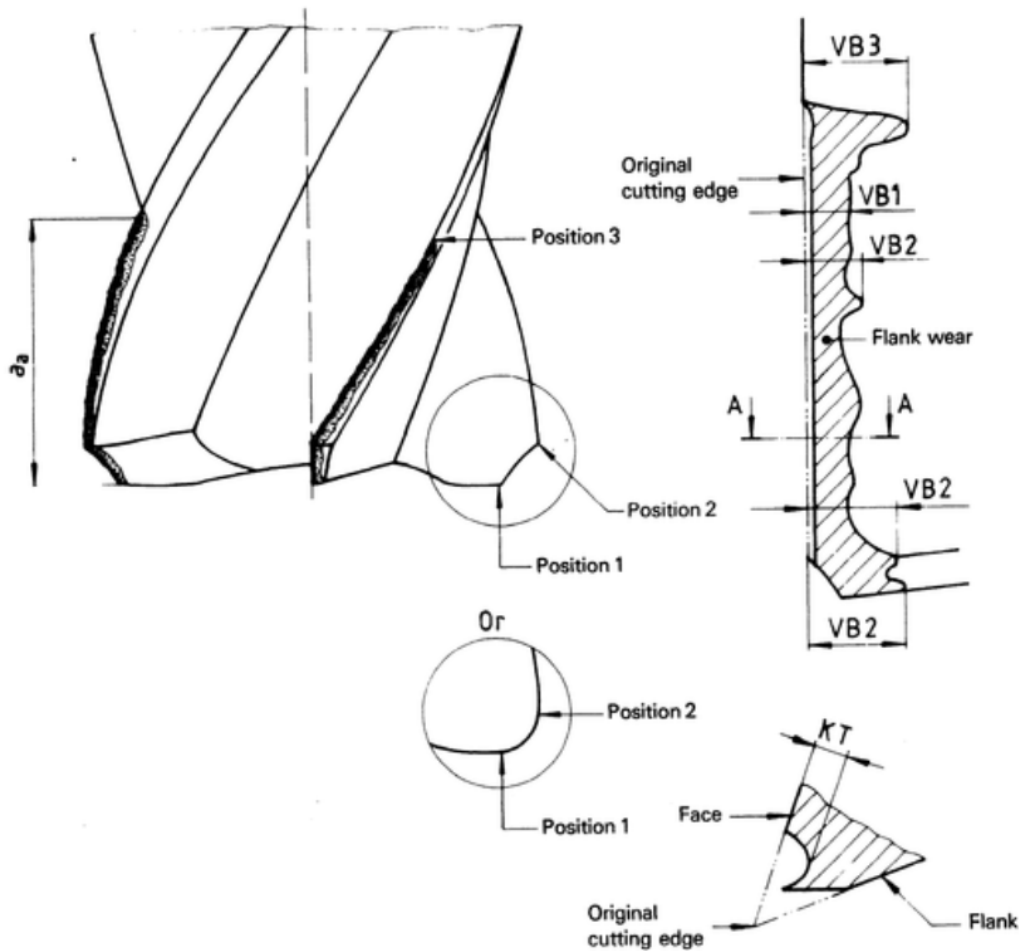


Figure 2.5. Indications of flank wear, reproduced from ISO 8688-2:1989

phase of gradual wear and a final stage of rapid wear to failure. An example of these curves is presented in Figure 2.6. The curves identify the relationship between the flank wear (shown here in imperial units) of a cutting tool and cutting speed ( $V$ ) and the enabled cutting time ( $T$ ). It is noted that a large body of research has previously applied the tool wear curves to describe the progressive trend in the wear of their cutting tools. For example, Prakash and Kanthababu (2013) implies that their flank wear versus time follows the same pattern of initial, gradual and rapid wear proposed by Taylor. However, arguably their progressive wear region as indicated in Figure 2.7 is more rapid than their accelerated wear region. It is therefore noted that not all cutting tools will wear in such an explicit fashion. Care must be taken to ensure that any diagnosis appreciates the actual wear, not the expected or indeed desired wear.

**Breakage** - Can occur because of the above failure modes and represents the ultimate failure of the cutting tool. Breakage can occur when a worn or damaged cutting tool is used but also if a cutting tool has inherent flaws (even when new) or when a cutting tool is used inappropriately or subjected to excessive loads. All cutting tools have a finite life and will not last indefinitely; however, it is unlikely that a process will be allowed to reach the breakage of a cutting tool as the negative effects on the process will be significant. This will prompt the replacement of the cutting tool before breakage occurs.

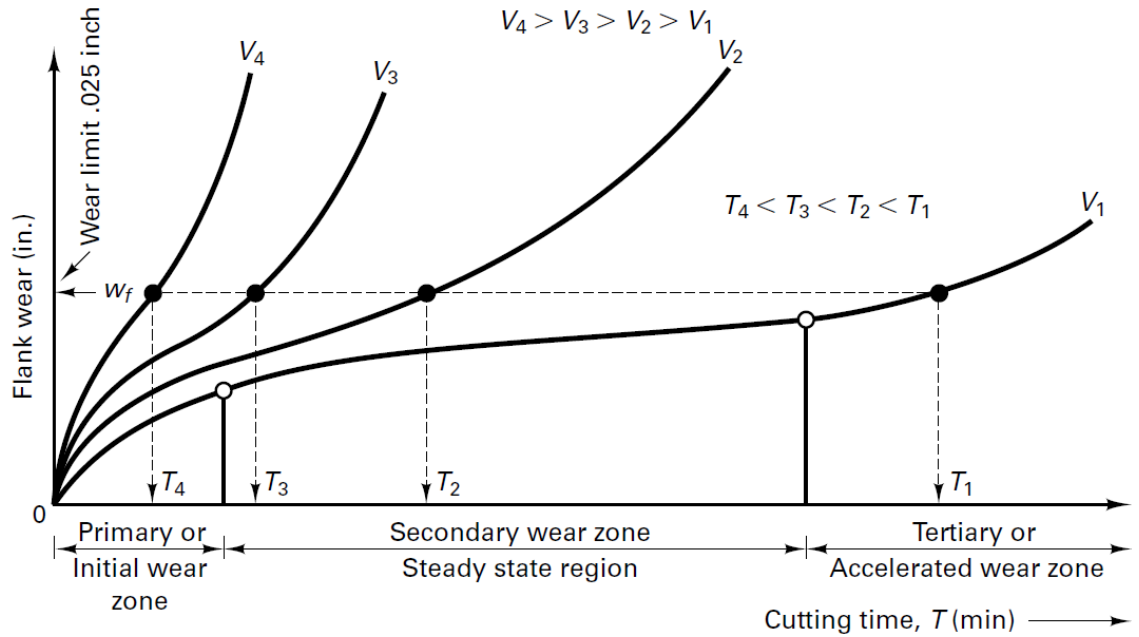


Figure 2.6. Cutting tool flank wear curves, reproduced from Black and Kohser (2012 p594)

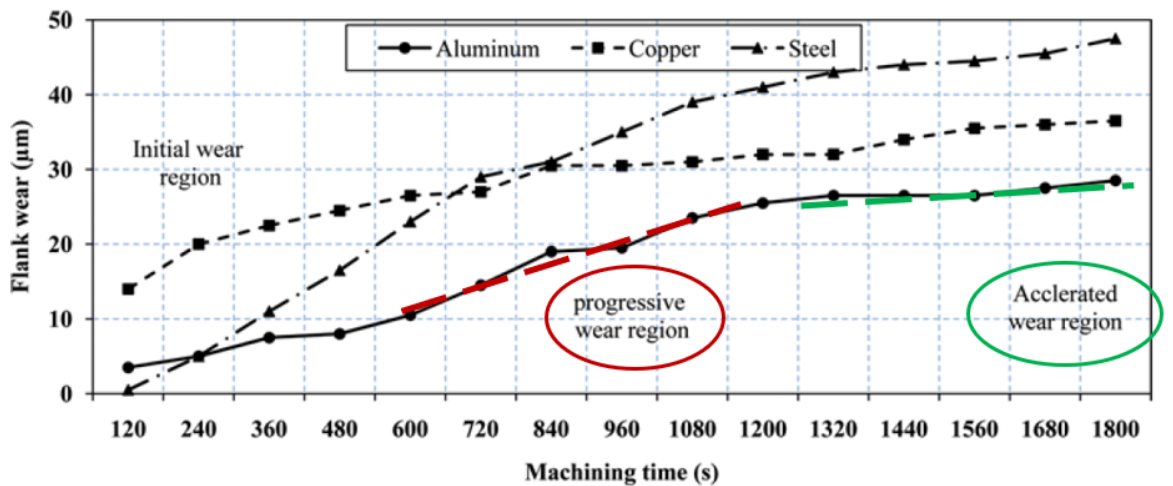


Figure 2.7. Misappropriating Taylor's tool wear curves, adapted from Prakash and Kanthababu 2013

Published research on cutting tool wear suggests it can be represented as a stochastic process (Amer et al. 2007, Karandikar et al. 2013, Zhou and Xue 2018). This posits that nothing can be done to predict or to prevent some failures from occurring. Similarly, when these failures do occur nothing can be done to predict when or how the cutting tool itself will fail totally. This negative approach does little to promote investigation into each failure mode, or to genuinely appreciate all facets of the cutting process and the interaction between the machine tool, the cutting tool and the workpiece material. It is noted by Astakhov (2004), that few studies seek to understand the relationship between the cutting tool surface and the cutting material. This is despite the significant volume of research into the wear mechanisms and failure modes of cutting tools (Dolinsek et al. 2001, Liu et al. 2002, Okoh et al. 2014).

Notwithstanding, the damage effected on a cutting tool is essentially irrelevant as the actual point

at which cutting tools have worn appreciably, or failed, depends entirely on the needs of the specific process and the allowable condition of the machined component. This is appreciated by Astakhov (2004), noting that quantitative characteristics are necessary, including dimensional criteria such as cutting tool length and diameter. This is relevant because an intact cutter with a severely deteriorated flank still has the capacity to machine components, but they will have a poor finish and quality. If this is of little consequence, then the cutting tool can be considered to still have remaining useful life. However, if the quality or finish of the component matters, then a cutting tool employed for only a short time and with negligible deterioration may have *no* remaining useful life. It therefore seems that the actual condition of the cutting tool is effectively irrelevant. The important metric is perhaps the instance at which the cutting tools should be replaced. This can be identified by comparing the specific process characteristics at the chosen instance versus the process threshold.

### 2.2.2 Machining strategies

Most process optimisations aim to save time and resources; reduce errors, energy and system loads; and improve the process economy, quality and output. It is also the case that optimising the machining strategies can help to promote longer cutting tool life and better quality of machined components. However, all approaches remain limited in that they either impact negatively on other aspects of the process, or the process assumptions required for such approaches to be functional limit their wider application. The optimisation of the milling process is therefore an ever-evolving field with the focus of process optimisation often aimed at the control of the process or the cutting algorithms employed:

**Control** - There are increasing levels of implementation of functions embedded within the CNC controller. These applications are often introduced by the original equipment manufacturers (OEM). Such approaches include spindle load management, volumetric error compensation, or closed-loop spindle velocity controls (Yamazaki Mazak 2014b). However, these functions may be limited in that they remain relatively hidden to the machine operators and to separate condition monitoring systems. If not accounted for these functions can potentially interfere with separately optimised, or retrofit, processes, algorithms and systems. Process parameters are also targeted to find optimum combinations of cutting speed, feed rates, or cutter-material engagement. Both Othmani et al. (2011) and Yusup et al. (2012) provide relevant summaries of the many approaches.

**Cutting tool paths** - Effort is continually aimed at developing and implementing alternative cutting algorithms to reduce the material contact time. This targets reductions in machining time, which in turn leads to a higher process output. According to Abdullah et al. (2017) and Santhakumar et al. (2018), it is usual for approximately 50% of the machining time to be attributed to the roughing cycles. Optimisations are therefore targeted specifically at these cycles, rather than interfering with the finishing cycles. Approaches also target the path of the cutting tool, specifically aiming to reduce cutting forces or to achieve constant cutting forces (Sui et al. 2016, Sui and Li et al. 2016).

An additional focus of process optimisation is the behaviour and the gradual wear of any cutting tool used within a machine tool. The importance of accurately characterising the behaviour and the condition cannot be understated. The improper use of a cutting tool can result in a damaged product (scrap), a damaged tool and a damaged machine, leading to lengthy downtime and economic losses (Amer et al. 2007, Lee et al. 1992). Additionally, suboptimal use can have similar consequences. In this context it has been observed that removing small cuts during the milling process results in failed cuts, rubbing and/or burnishing (Dornfeld et al. 2006, Astakhov 2007, Warfield 2020, Dasarathi 2016). It is also noted that Shaw (2003) comments on the impact of the size effect in metal cutting, where a decrease in chip size results in an increase in resistance to the cutting motion (Figure 2.8). This increase in resistance is noted to be down to a reduction in the probability of encountering material defects such as grain boundaries and slip planes. Shaw (2003) further notes that metals are

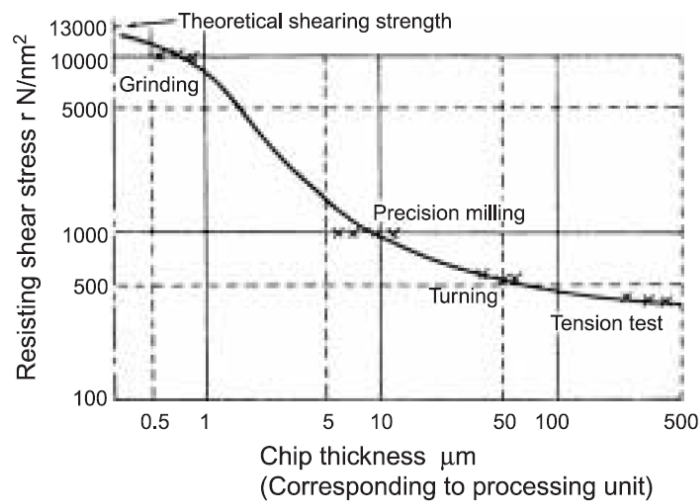


Figure 2.8. Chip thickness versus shear stress - reproduced from Taniguchi (1994), from Shaw (2003)

not homogeneous and thus will not act equally when cut. The size effect may increase the possibility of failed cuts. It may also prove to be important when considering the forces acting on the cutting tool as the resistance to motion may cause anomalies in the observed force magnitudes for small cuts.

One phenomenon linked to both the behaviour and condition of the machining process is the overlap between each pass of the cutting tool. Research that comments specifically on this overlap seeks to reduce or to eliminate it (Kim 2007, Kariuki et al. 2014). This is often linked to efforts in pursuit of minimising process cycle times, attempting to maintain process settings (for example the material removal rate (MRR)), or seeking improvements in part quality, cutting tool life, process time and process cost. However, as commented by Adesta et al. (2017), irrespective of the efficiency of the process, the overlap can be reduced but cannot be eliminated entirely. As this overlap introduces slight variation in the rate of material removal, knowing the effect it has on the milling process will always be beneficial. This could, and should, be included within intelligent process monitoring (IPM) methods and systems.

### 2.2.3 Tool management approaches

The most commonly adopted approaches for reducing the incidence of cutting tool failures is to replace them before they can be expected to fail. This often anticipates prolonged machining time during which the machine should be safe to leave unattended (Koepfer 2012). To reduce the risks associated with poor use or unexpected failure, manufacturers tend towards combinations of both proactive and reactive approaches to the management of cutting tools. According to research by Wiklund (1998), Liu et al. (2015), and Zhou and Xue (2018) replacements are often based on a set schedule, with a healthy safety margin of 20% of the cutting tool total life. This is sometimes referred to as a form of preventative maintenance, or a proactive approach to cutting tool management. However, when unexpected failures are met, or immediately negative deficiencies in the process are found, process adjustments or system replacements may be implemented in response to the problem. This approach is reactive maintenance and/or management of the cutting tools and is costly. Unfortunately, reactive management is a by-product of the proactive (conservative) approaches taken. Unless processes are monitored and failures are predicted, reactive management cannot be avoided.

Additionally, whilst there is merit in proactively managing cutting tools, such approaches will inevitably increase process waste. Tool life estimates will be based on experience with, or the history of, each cutting tool. These life estimates may be adjusted based on recent performance, or based on process changes, but (as noted) there will always be that margin for error, or safety factor. This means that cutting tool use is far from optimised. Research estimates from Zhou and Xue (2018), and estimates from the industrial partner, indicate that for some processes 20-30% of the potential cutting tool life is wasted. For these processes, a sizeable proportion of unnecessary process waste may originate from the cutting tools. This stems from the methods employed to manage the cutting tools. Most are conservative methods and none tackle the root problem, meaning that process waste and costs are often higher than necessary.

#### 2.2.3.1 Challenges and innovations

The effective management of cutting tools is sometimes limited by factors that discourage the implementation of better, or optimised, approaches. Such challenges may encourage the implementation of conservative management approaches. These challenges include access to the cutting tool, unexpected cutting tool wear and material distortion.

Access to the cutting tool applies to either operator access or equipment access. Access to operators is often limited by the need for prolonged machining time. Accessing the cutting tools in-process contributes to machine downtime and thus reduces the overall equipment effectiveness (OEE). OEE, when used correctly, is a useful metric for improving the efficiency of a system based on availability, performance and quality elements (Williamson 2006, Gupta and Vardhan 2016). Equally, access may be limited by design. In automated factories machines may control the flow of material, as well as cutting tools. Access to each machine tool may be limited for safety reasons. Equipment access on the other hand refers to the capacity to introduce extra content to the machine tool volume to enable

process or condition monitoring. The ability to retrofit sensors to legacy equipment enables them to connect to modern machines and enables an upgrade that requires less capital than purchasing a new system entirely (Siddiqui 2008). However, the main limitation will be that every extra sensor requires space in the machine tool to install, operator training to utilise and engineer expertise to understand. It is therefore understood that extra sensors can significantly reduce the effective machine volume (EMV), may increase operating costs and may be underutilised in many installations.

Unexpected tool wear may occur because of changes to the workpiece, environment, or process. Regarding the workpiece, there may be localised hard regions (Meier 2019) such as occlusions; or the material may have a different composition entirely. This may be due to subtle differences between batches, or because a different material has been introduced to cut cost or to improve material properties. Changes in the environment that may promote a different mode of tool wear include thermal or chemical variations (due to the cutting process, or the coolant). Unexpected tool wear is difficult to account for (Zhou and Xue 2018), therefore by implementing conservative management approaches the risk of such failures will be mitigated to an extent. Progressing from such “safe” strategies increases risk but with an increase in rewards such as optimised cutting tool life and reduced process waste.

Material distortion (Section 2.1.2) may also contribute towards unexpected wear of the cutting tool. If components experience warp in-process, such distortion will change the conditions experienced by the cutting tool, thus changing the rate of wear and hence the life expectancy of the cutting tool. Depending on the severity of the distortion and the capability of (or redundancy within) the management of the cutting tools this may outstrip the ability of the process to safely manage the tool or ensure a replacement is available at the best time. It should be noted that some systems have the capability to identify such distortion through appropriate use of the artifacts. This has significant potential to complement monitoring strategies by providing information regarding geometric inconsistencies during the machining process.

### 2.2.3.2 Tool life equations

The application of tool life equations is another example of a conservative approach to the management of cutting tools. Example tool life equations include derivatives from Taylor (1906), Astakhov (2004) and Kandrak and Palmai (2014), but numerous alternatives also exist (Karandikar et al. 2013). All iterations purport to offer an improvement over others, and perhaps do, but only for the specific process from which they were derived. Three example tool life equations are expanded below.

**Taylor (1906):**

$$VT^n = C \tag{2.1}$$

The tool life equation from Taylor (1906) noted a power-law relationship between cutting time and total life.  $V$  is the cutting speed (m/min),  $T$  is the tool life (min),  $n$  is a constant related to the cutting tool and  $C$  is a constant related to almost all other input parameters (but is found to

be equal to V for a tool life of a single minute). Both n and C are acquired empirically, or from tabulated values (empirically derived by someone else). Whilst easier to gain the values from tables it is worth noting that they can vary between authors giving markedly different results in practice. Amendments to the extended tool life equation typically consider the effect of the feed rate (mm/rev) and the depth of cut (mm), each also being empirically derived (Black and Kohser 2012 p596).

**Astakhov (2004):**

$$v_h = \frac{dv_r}{dT} = \frac{h_r - h_{r-i}}{T - T_i} = \frac{vh_{i-r}}{1000} = \frac{vf h_s}{100} \quad (2.2)$$

$$h_s = \frac{dh_r}{dS} = \frac{(h_r - h_{r-i})100}{(l - l_i)f} \quad (2.3)$$

Astakhov (2004) presents two equations for the “proper assessment of tool wear”. The first equation considers the rate of perpendicular wear (wear of the cutting tool nose,  $v_h$  ( $\mu\text{m}/\text{min}$ )), the second considers the rate of radial wear (peripheral/flank wear,  $h_s$  ( $\mu\text{m}/10^3\text{sm}^2$ )). Both consider the change in the dimensions of the cutting tool for a specific distance machined. These could be considered an improvement over Taylor’s equations as they give context to the changes and thus may be more suitable for commercial processes where geometric tolerances are specified. Nevertheless, processes that incorporate in-cycle gauging (ICG) will be capable of adjusting for any dimensional changes in the cutting tool, especially changes to the length and the diameter. This could render these equations obsolete in practice, as the geometry of the cutting tool should have little consequence on the remaining useful life. Notwithstanding, Astakhov (2004) notes that these enable the direct comparison of different tool and process combinations.

**Kundrak and Palmai (2014):**

$$T = \frac{A}{v_c^3 + B \cdot v_c^2 + C \cdot v_c} \quad (2.4)$$

$$T = \frac{\sum_1^n \Delta t_i (v_{ci}^3 + B \cdot v_{ci}^2 + C \cdot v_{ci})}{v_c^3 + B \cdot v_c^2 + C \cdot v_c} \quad (2.5)$$

$$T = \frac{\int_{t_1}^{t_2} [v_c^3(t) + B \cdot v_c^2(t) + C \cdot v_c(t)] dt}{v_c^3 + B \cdot v_c^2 + C \cdot v_c} \quad (2.6)$$

Where A, B and C are process specific constants.  $v_c$  and  $v_{ci}$  are the considered cutting speeds. Equation (2.4) is only suitable when the cutting speed remains constant. Where the cutting speed is not constant Kundrak and Palmai (2014) presents the second two equations for step changes in cutting speed and continuously changing cutting speed, respectively. These do perhaps improve upon Taylor’s equations, as they allow for changes in the cutting speed; however, it could be argued that one of the primary benefits of Taylor’s equations is the simplicity. Kundrak and Palmai (2014) further fails to appreciate the concerns raised by Astakhov (2004) in that context (beyond that of the cutting speed) is required to appreciate cutting tool life.

All tool life equations seek to incorporate various cutting parameters to establish the remaining useful life of a cutting tool. Unfortunately, such approaches often require extensive empirical investigation to appropriately populate the equations. This is compounded for those equations that have numerous constants to establish. It is also the case that establishing how each cutting parameter affects the total cutting tool life does not necessarily mean that the same will hold true for another similar, or even an identical process. Ahmed (2018) has identified several authors, each providing different results for equivalent processes. Such variation is not sensible when determining the remaining life of a cutting tool. Four further limitations to note are:

- All the tool life equations can only offer a single snapshot of the process in a specific condition, at a specific time
- Unexpected failure or sudden damage to the cutting tool cannot be accounted for
- The tool life equations are computationally heavy and are often derived for specific processes, materials and cutting tools
- The tool life equations represent attempts to model the changes in the condition of a cutting tool, based on the current conditions and based on an assumed extrapolation. It is noted that even small changes in the conditions, settings, or behaviour of the cutting tool may render the results of the tool life equations to be void.

These limitations affect the wider application of the equations. This is especially true for commercial processes as model-based approaches may be considered too academic. Additionally, commercial processes are often complex and will not be adapted to enable the use of such tool wear equations. The focus will be on the economy of the process, not necessarily on optimising the process simply for an easier assessment of the potential remaining life of a cutting tool.

## 2.3 Tool condition monitoring

Tool condition monitoring (TCM) refers to the strategies employed for the acquisition and subsequent analysis of information relating to the condition of the cutting tool. Whilst process monitoring is popular and there is a high uptake of monitoring systems in commercial organisations, active or in-process TCM is less popular. This is not because such systems would not benefit organisations, but because the provided solutions are often complex, unworkable for different applications, costly, or invasive (Hill et al. 2019). Nevertheless, research into TCM has remained popular since the turn of the millennium with multiple review papers presented, including: Frankowiak et al. (2005), Li (2012), Lauro et al. (2014), Elattar et al. (2016), Cao et al. (2017), and Zhou and Xue (2018).

It is suggested that there exist two overarching approaches for the assessment of cutting tool condition. The first is a direct assessment of the tool, through measurement, or through comparison between healthy and unhealthy tools. The second is an indirect assessment, with the cutting tool condition often inferred from the quality of the manufactured parts, from analysis of the process vibration,

acoustic emissions, forces on the cutting tool or the machine axes, power consumption, or debris in the coolant.

Direct assessment of cutting tools is popular because it identifies the exact condition of a cutting tool, rather than the implied condition. It is also the case that to directly assess the cutting tool is perhaps less complex than attempting to decipher the condition indirectly, as what you see is effectively what you get. Direct assessment is possible by eye. Especially when the condition of the cutting tool is substantially deteriorated and when the precise way the cutting tool has worn is not as important as the fact the cutting tool has worn at all. Indeed, some of the approaches employed by manufacturing organisations are often deliberately straightforward. Cutting tools and components are typically assessed by eye, or with a fingernail, only using measurement equipment when strictly necessary. This keeps the process moving and is sufficient when quality is based on appearance and not specific tolerances. More capable approaches would be necessary when the cutting tool has worn but the visual difference is negligible.

On the other hand, indirect assessment of cutting tools is popular because of the possibility to gain the benefits afforded by monitoring the cutting tool, without the necessary downtime, or invasive nature of direct approaches. However, that is not to say that indirect approaches are not invasive. Popular approaches do implement retrofit equipment into the working volume of machine tools, including cameras, probes, dynamometers, thermometers and vibration sensors. It is rarely appreciated that approaches that require extra materials, sensors and/or foreign objects within the machine tool may prove to be detrimental as the working volume reduces. This reduction in the working volume constrains both the number and the size of parts that can be manufactured. It is thus not surprising that Prickett and Johns (1999) noted that any decision to forego additional sensors is a preferred approach. Instead one should rely on monitoring machine tool architecture.

### **2.3.1 Complementary industrial solutions**

There exists a growing number of in-process solutions available to ensure that the geometry and finish of components is maintained, without the need for retrospective quality assessment and remanufacture. These primarily consider the re-dimensioning of, and in-cycle assessment of, cutting tools. These include ICG approaches and programmed control solutions (including active process controls).

**ICG** - Cutting tools can be measured using the appropriate equipment and their respective dimensions can be updated within the NC. During the process, the parts can be periodically measured using an in-machine probe to identify any deviation in machined dimensions. This difference is taken as an offset value and tool dimensions are again updated. This accounts for the gradual tool wear and effectively masks the effect of wear from the finished product. These systems can potentially complement TCM implementations through the provision of geometric information relating to both the cutting tool and the process. Geometric information may be acquired pre-process and in-process by using online measurement systems. Pre-process information is often in aid of locating the workpiece and setting the part datum. In-process information is often

used to determine cutting tool offsets and to ensure components are machined to the required tolerances.

**Programmed control** - Modern CNC machine tools include functions that may complement TCM approaches. These perhaps benefit separate TCM systems as they provide separate indications of the process condition. For example, Active Feed Control (AFC) enables the machine tool to adjust the applied feed rate according to the effective load on the spindle. When the load exceeds a threshold input by the operator, the machine tool overrides the specified feed to reduce the load below that threshold. This is beneficial for when a cutting tool cannot cope with extreme loads and is perhaps beneficial for any system developed to monitor the feed rate for anomalies. However, it is also appreciated that AFC is detrimental to the process efficiency as the reduced feed will add time to the process. AFC may also affect the rate at which the cutting tool depreciates due to the reduced overall cutting speed. Other included functions may be detrimental to the effectiveness of certain TCM systems, for example Active Vibration Control (AVC). When AVC is active it is inevitable that approaches attempting to monitor process vibrations will suffer due to the process adapting to account for and to minimise such vibrations.

ICG, programmed control and other solutions proposed by manufacturing organisations have value; however, consensus on the necessary output or reaction from such systems is limited. Many are content to provide the data with no liability for the process, others retain or delete their information when it may be useful to other systems. Nevertheless, complementing such systems, or accounting for the use of such solutions in industry, is critical to ensure developments are adopted commercially and that they derive the most value from the systems already implemented.

### 2.3.2 Data acquisition

Effective TCM relies (in part) on the successful acquisition of information from the cutting tool and process. Assessment of tool condition from the form of the manufactured part is practiced. Some studies, including work by Cerce et al. (2015) and Yang et al. (2017), take a direct approach by assessing the geometry of the cutting tool itself in-progress. Others evaluate the variation in geometric form (of the manufactured part) and attribute this variation to the deterioration of the cutting tool (Liu et al. 2010, Zhang and Zhou 2013, Li et al. 2014, Ahmed et al. 2017). The methods are predominantly post-process oriented and better suited for diagnostics than active process control. The methods are viable from an academic perspective and enable the better understanding of tool wear phenomena, but they have a limited bearing on the continuous management of machining operations. It may be considered that these studies evaluating geometric form fail to consider arguments made by fellow academics and industrial organisations. Both Astakhov (2004) and Shaw (1984) recognise that the association between geometry and cutting tool condition is tricky to quantify and the individual features difficult to apportion to responsible process variations. It must be noted that the terminology differs between the contrasting opinions, possibly indicating that the geometry is adequate for

the prediction of tool life, but inadequate for an indication of condition. This corroborates with the argument that complex systems may generate ambiguous information (Hill et al. 2019). In addition, industrial organisations add further complexity with innovations that hide or mitigate tool condition, including for instance re-dimensioning cutting tools in-process using ICG. From an economic and competitive stance, removing the geometric variation is both sensible and beneficial. According to Renishaw (2011) dimension related post-processing can be eliminated or at least significantly reduced. ICG could provide the information necessary for approaches considering geometric variation through appropriate use of the data arising from the re-dimensioning of cutting tools. However, it is acknowledged that, as it stands, the information is rarely retained for more than the correction of tool offsets.

In lieu of geometrical variation, some studies evaluate the variation in surface integrity (of the manufactured part) and attribute this variation to the deterioration of the cutting tool. This method is more popular within industrial organisations, being complimentary to the re-dimensioning of cutting tools. The approach has proven to be popular for turning operations (Kwon et al. 2004, Karim et al. 2013, Danesh and Khalili 2015). Equally, Shaw (1984) indicates that the surface finish ( $R_a$ ) when plotted against cutting time is comparative to conventional (Direct) measures of wear, following a similar trend to the Taylor tool life curves proposed by Taylor (1906). This would indicate potential for the surface finish to show the tool condition. However, it has been reported by Li et al. (2014), Wilkinson et al. (1997) and Waydande et al. (2016) that the surface integrity is highly susceptible to changes in machining parameters and tool geometry when considering the milling process. Li et al. (2014) further reports that individually surface roughness is unsuitable for assessing part quality and that some types of wear affecting part integrity can be missed due to “smearing”. Although, it is noted that no suggestion is made indicating an impediment in the ability to detect tool wear. The primary issue instead appears to be with quality control of the machined part. Nevertheless, effective implementation of such an analysis may be impractical when the additional measurement apparatus is considered. This indicates that analysis of the surface integrity is equivalent to geometry analysis for the assessment of cutting tool condition, with perhaps added potential with respect to systems implementing ICG. Being inherently post-process, the analysis of surface integrity falls in with others that either detect poor condition too late, resulting in scrapped parts, or detract from the process efficiency when measured in-process. This indicates an inadequacy in the current form classification approaches for monitoring time-dependent tool condition.

An alternative approach is to consider monitoring machine tool architecture. This approach is popular with proposals designed for most of the machine tool components. Objects of interest currently include the spindle motor, the spindle rotational speed and the axis motor loads in X, Y and Z.

**Machine tool spindle** - approaches are primarily focused on analysing the forces and/or vibrations occurring during the manufacturing process (Azmi 2015, Ma and Jia 2016, Yao et al. 2018). Other approaches also consider the power consumption of the spindle motor (Tseng and Chou 2002, Axinte and Gindy 2004, Lee et al. 2007, Fu et al. 2007, Abbass and Al-Habaibeh 2015).

Analysis of the spindle forces are typically enacted using a dynamometer. This enables the components of the forces on the cutting tool (usually  $F_x$ ,  $F_y$  and  $F_z$ ) to be measured and combined using the square root of the sum of each squared. For example, Ma and Jia (2016) considers the cutting forces on a coated carbide cutting tool for different spindle speeds using a Kistler dynamometer. Dynamometers are an effective means of measuring cutting forces. However, it is noted that they are often expensive and complex and they are not suitable for commercial applications (Xie et al. 2017).

An alternative approach is to use a smart spindle, one that effectively has the capability to monitor the cutting forces without any table-based equipment. Research from Cao et al. (2017) and from Xie et al. (2017) considers this concept, suggesting that the cutting forces may be calculated using integrated strain gauges, accelerometers, or displacement probes. Whilst this reduces the necessary equipment within the working volume of the machine tool, it will significantly add to the cost of the spindle when new. It will also add to the cost and complexity of ongoing maintenance. These considerations may outweigh the benefits afforded by such a system.

Analysis of the spindle vibration is another method that seeks to establish the forces on the cutting tool. Yao et al. (2018) considered a method using table-based accelerometers, approaches using smart spindles are also noted by Cao et al. (2017) and Xie et al. (2017). Alternatively, an approach using sensors embedded behind cutting inserts has been presented by Luo et al. (2018). Embedded sensors take up less room and do not add to the cost of the spindle. Luo et al. (2018) also notes that such an approach allows the consideration of each insert separately; however, they do not consider the potential risk in installing sensors in an aggressive environment.

Alternatively, some research does away with as many intrusive sensors as possible. A popular approach is to monitor the spindle current. Abbass and Al-Habaibeh (2015) notes that such an approach is easy to implement due to the low cost of the sensors and the simple installation. It is also perhaps easy to enable as modern machine tools tend to have current sensors built in. These tend to be provided to complement the process control systems and assist in protecting the machine from damage (see Section 2.3.1). Research into the use of the spindle current and/or power for TCM is extensive. For example, research from both Lee et al. (2007) and Abbass and Al-Habaibeh (2015) identifies that the spindle current and the spindle motor power are able to indicate the condition of a cutting tool and that using the spindle power specifically can be very successful. The sensitivity of spindle power for TCM has also been investigated by Axinte and Gindy (2004). They determined that spindle power lacked the capability to differentiate between separate teeth and therefore fails to identify instantaneous wear, unless it is significant. However, they did note that spindle power was suitable for identifying gradual wear.

Fu et al. (2007) on the other hand investigated the input resistance (impedance) of the spindle motor, identifying that the cutting tool wear was appropriately identified from the signals along with additional process information. They noted that use of the resistance may be better than

using the spindle current due to less influence from the voltage signal. Although, they note that in a practical context this becomes negligible and ultimately the only context that matters is a practical one.

Interest has also been directed at the rotation of the spindle. Research by Girardin et al. (2010) and Soshi et al. (2014) indicates that the rotational speed is a useful means for monitoring the condition of the cutting tool. Both assess the rotational speed and indicate that it is affected by the milling process. This is evidenced by irregular loads on the cutting tool. Girardin et al. (2010) goes as far as to identify cutting tool wear from these observations. Although, they fail to appreciate that they consider two extreme cases (a new cutting tool versus a broken cutting tool) and not gradual wear. Therefore, the only evidence provided is in favour of breakage detection and not wear monitoring. Moreover, it is noted that many modern machine tools are smart and often compensate for changes in the rotational speed to maintain programmed values. As observed for ICG, this may obscure cutting tool wear from the rotational speed signals. It is also noted in research by Gebler et al. (2018) that although rotational speed may be sensitive to changes in a process, differentiating the events that caused the changes in the process is much harder due to similarities in the resulting signal characteristics.

**Axis motors** - Approaches are often akin to those implemented for the spindle and the signals are noted to provide similar information for cutting tool wear and damage (Rivero et al. 2008). Access to the axis motor currents (or perhaps impedance) affords the same benefits as access to the spindle motor in that no additional sensors are required. This is because almost all modern machine tools will have the monitoring capability built in and the sensitivity of the approach is considered to be acceptable (Rivero et al. 2008, Comacho et al. 2011). However, similar caveats exist for the X, Y and Z loads as did when considering the spindle rotation. It is noted that both inbuilt functions AVC and AFC may introduce unpredictable noise to the system. Care must be taken to establish the possible impact of these functions to avoid the misappropriation of their actions as changes in the condition of the cutting tool or of the process. Equally, according to Vogl et al. (2015), degradation of the machine tool axes is unpredictable and that will introduce further noise to the system. However, Vogl et al. (2015) acknowledge that monitoring the axes is generally effective and may contribute positively to monitoring systems.

Deciding on the best approach requires consideration of two issues, data suitability and data quantity. A sensible approach will acquire all available data during an event as inevitably, post-process, the data is no longer available. However, all available data is not necessarily all sensible data. Therefore, a practical approach must assess all available data and acquire only that which is necessary. Given this consideration developed approaches tend to limit their consideration to selected variables, reducing the complexity of the data. However, most confirm that additional data would be necessary for effective implementation of the approaches (Zhou and Xue 2018). This indicates that a single variable is relatively ineffective at identifying deviations from nominal yet may be effective when considered in addition to others.

### 2.3.3 The ambiguity of acquired data

Fundamentally, an argument can be made that accessible data is not necessarily suitable data. To resolve some of these issues, one must consider if the information gleaned from a machine tool is implying:

- A deterioration of, or change in, the entire system
- The deterioration of a system subset - e.g. axis drives or spindle
- Causal changes in the process - i.e. new cutters, materials, changed feeds/speeds
- Different process plans and/or machining methods employed by different operators

Machine tools are complex systems that generate a lot of information, not all of which is useful or indeed the information sought in the first instance. Sources of information are identified in the Ikishawa fishbone diagram (Figure 2.9). Each source of information is a potential red herring for those attempting to identify the condition of a cutting tool without appropriate consideration of the machine tool “ecosystem”.

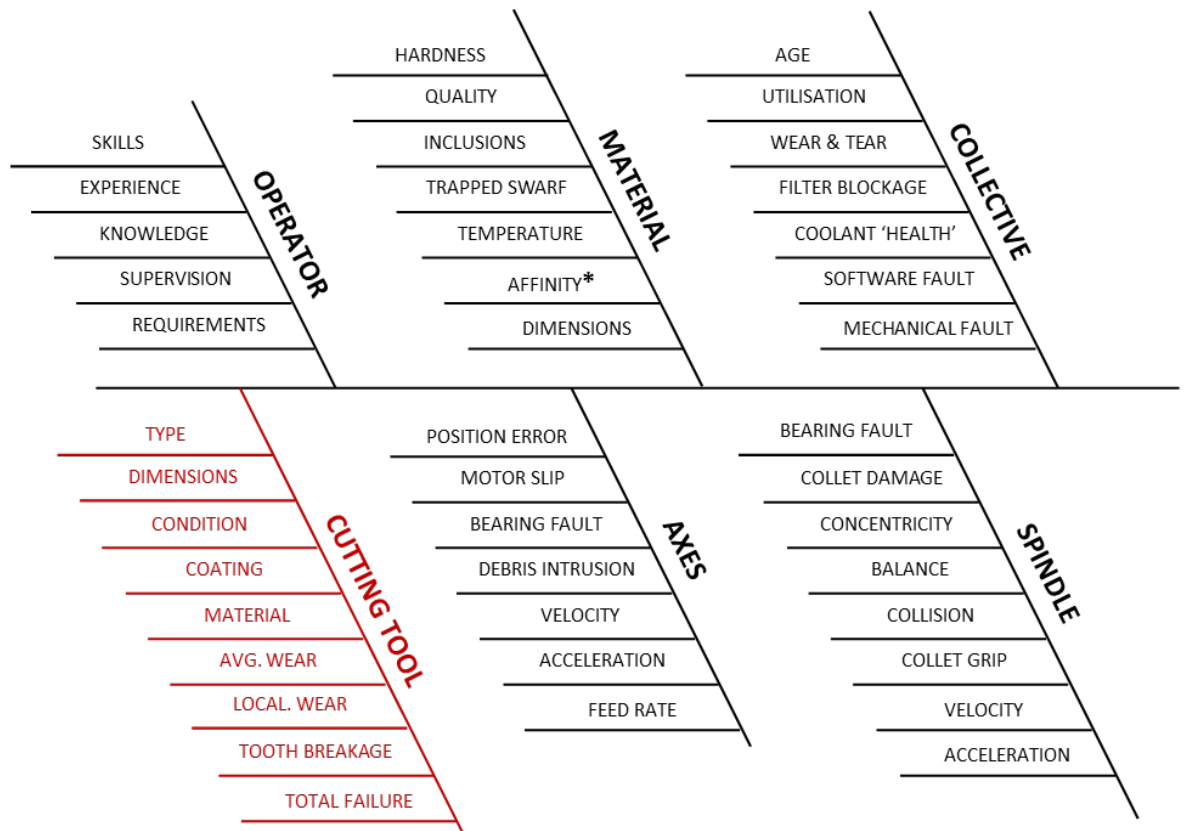


Figure 2.9. Hypothesised origins of process variation, reproduced from Hill et al. (2019)

Figure 2.9 illustrates some of the underlying reasons for a changing or variable process and visually emphasises the contributions from cutting tools. It is presented in argument that the exact cause of an observed process change is hard to determine, or confirm, with confidence. It also justifies why systems that monitor and/or diagnose complex systems, such as machine tools, require the (often)

strict assumptions and need significant process competence or experience. This implies that the perfect solution for TCM is process specific. It is noted from Figure 2.9 that affinity\* refers to metallurgical affinity; Lopez de Lacalle et al. (2011) and Hosseini and Kishawy (2014) both note that higher affinity between tool and material is likely to result in additional process complications.

It is noted that some researchers have attempted to characterise machine tools as a singular, all-inclusive entity (Laloix et al. 2018, Xu 2017). Other researchers are seeking to exploit machine tool intelligence to construct a digital representation of the entity creating so-called digital twins (Sobie et al. 2018, Liu et al. 2018, Liu and Xu 2017). These approaches are promising and seek to capitalise on the increasing intelligence and connectivity of machine tools. However, most of them fall short of realising the complexity of the system and hence generate ambiguous information. Further to the data ambiguity, difficulties arise when considering specific components, the interaction between components, or the normal (baseline) versus abnormal states for an unknown process.

On the other hand, Grosvenor and Prickett (2011) present a more sensible paper that reinforces the importance of digital signal processing (DSP) techniques alongside analysis techniques such as FMEA. Adhering to this approach (or similar) may reduce the challenge in designating process data to the correct source, whilst also encouraging an appreciation of the limitations of the available data. That ever-prominent peak in the data may not infer the condition of the cutting tool, but instead perhaps a bearing fault, or the effects from trapped swarf.

### **2.3.4 Data and signal processing**

With respect for the potential factors contributing to process information and when a suitable method of data acquisition has been implemented, the cutting tool condition must be considered from the acquired data. Many different approaches exist in the literature that claim to be better than the last for the determination of cutting tool condition. A few approaches will be considered in order to appreciate the possibilities and to identify both good and bad practice to take forward into the rest of this thesis.

In the context of this thesis data and signal processing techniques hope to extract features from raw signals to enable decision makers to identify the state of a cutting tool. Depending on the approach taken, such features may be abrupt changes in the signal, changes to the signal characteristics, or they may be different signals altogether. According to Siddiqui (2008), options are limited to either model-based methods, or feature-based methods.

Model-based approaches have become popular within the last decade due to advances in computational capability and in cloud-computing (Liu et al. 2019). Such approaches encompass the recent advancements in digital twin technologies. These approaches attempt to digitally replicate the machining process with input from the machine program and feedback from the process. Modelling the process in this way enables engineers to identify processes that deviate from normal by comparing the physical process with the digital twin. Notwithstanding, these approaches remain demanding on the network, are relatively costly, can show the variation but not explain the behaviour and mostly

represent a perfect version of the system and thus struggle to accurately represent what they are attempting to model (Ogewell 2018, Witte 2020). This will make it challenging to accurately identify subtle and/or gradual changes, or differences between the process and the model. Further reading on model-based approaches can be found in work by Siddiqui (2008), Si et al. (2011) or Liu et al. (2019).

Feature-based approaches on the other hand can be further differentiated between time-domain and frequency-domain approaches. Time-domain approaches attempt to identify cutting tool health features by determining the characteristics of the process signals in real time. This can mean the determination of signal characteristics at one point in time and comparing such with another point in time. Signal characteristics may include the frequency or amplitude of the signal, signal statistics such as Kurtosis, standard deviation or variance, or perhaps simpler measures including the moving average, or maximum/minimum values. Another approach would be to apply a signal threshold based on the general, or as-new behaviour of a cutting tool. Using the same signal characteristics, if the signal exceeded a set threshold it may indicate a change in the condition of the cutting tool, or a breakage. Time-domain approaches are simple to implement and are sometimes the basis of preinstalled functions for smart machine tools. However, the challenge with time-domain approaches is that they are often complex and difficult to compare appropriately. Whilst significant changes to the condition of a cutting tool may be easy to identify, subtle changes may be lost within the signal. A possible remedy would be to simplify the information through suitable implementation of filtering; however, such an approach risks eliminating key health identifiers from the signals.

Frequency-domain approaches are also popular and attempt to simplify the process signals by separating them into their constituent frequencies (Peng and Chu 2004, Siddiqui 2008, Zhu et al. 2009, Lee et al. 2017). This is achieved by “transforming” the signal from the time domain to the frequency domain. Ways to achieve this “transformation” include use of the Fast Fourier Transform (FFT), the Short Time Fourier Transform (STFT) and the Fast Wavelet Transform (FWT). Sufficient detail regarding the theory and implementation of both the FFT and the STFT can be found in work by Amer et al. (2007), or Siddiqui (2008 pp94-100). Further detail for the FWT can be found in Peng and Chu (2004). Frequency-domain approaches are popular as specific frequencies relating to the health or deterioration of the cutting tool can be isolated and identified. It is also the case that two signals may appear similar in the time-domain yet have quite different underlying frequencies.

It is clear that each of the FFT, SFT and FWT are computationally heavy as noted by Amer et al. (2007). Peng and Chu (2004) further comment that the FWT is superior to both the FFT and the STFT for the analysis of transient signals. The FFT is more suited to a single stationary signal and the STFT has trouble including both low and high frequency components of a signal. Reference was also made to the STFT only being suitable for quasi-stationary signal analysis (stationary at the scale of the window) Although, Peng and Chu (2004) noted that methods based on the FFT were still more popular than the WT with results from the latter being difficult to process and having problems with frequency aliasing.

Perhaps more appealing in a commercial sense will be “simple” statistical DSP approaches. Techniques

that have value include Shewhart control charts, the cumulative sum (QSUM) and exponentially weighted moving averages (EWMA). These approaches have value due to their straightforward nature and will be considered for deploying DSP in Chapter 5 and Chapter 6.

Further to using DSP techniques for the detection of cutting tool wear, some research has looked specifically at identifying what process is occurring and when. Efforts aim to associate key process changes with key data changes and prevent the misdiagnosis of a slightly different cutting cycle with an actual process anomaly. Work by Li et al. (2008) looked at the signal changes when a cutting tool enters or exits a workpiece and identifies that both the entry and the exit cuts are distinct changes. It was noted that their system should be capable of detecting these events. Whilst perhaps the entry is distinguishable, the exit cut is less distinct than implied. Another investigation by Siddiqui (2008) indicated that entry into and exit from a workpiece can prove confusing to most condition monitoring systems, especially threshold-based approaches that look for distinct changes in the signal. Knowing the process can go some way towards mitigating the risk of entry/exit cycles raising false alarms.

Research by Cai et al. (2017) considered the response of the X, Y and Z axis signals to different operations including face, shoulder, contour, or pocket milling, drilling and chamfering. The signal was categorised by using the machine tool process code (G-code) and thus relied on prior knowledge of the process occurring to enable accurate decision making as to which process is occurring. Whether the process identification could be approached blind (i.e. identifying future operations based on the known signal characteristics) was not considered. A further limitation was that the work failed to appreciate the risk that a process anomaly has a similar characteristic to a specific process. Depending on the degree of similarity an anomaly may be missed. Similarly, the work fails to identify the thresholds applied to each process. A slightly different application of a process may significantly change the signal characteristics.

It is noted that many TCM systems avoid attempting to detect specific processes on their own merit, instead opting to use existing knowledge to locate specific processes. This approach is sensible since the mischaracterisation of a process may change how a cutting tool is monitored and thus not effectively identify the cutting tool health. Nevertheless, the need to redefine any and every process, or to train models to appreciate the current or future processes is inefficient and prevents ad-hoc use of a TCM system. This may limit the commercial appeal of an approach and is thus an area that should be investigated.

Some attempts to determine the condition of the cutting tool from the process data seem flawed. Ma and Jia (2016) attempts to predict the trend in the cutting force based on the cutting tool area and the spindle speed. However, it is noted that they overly simplify the acquired force signals and ultimately fit an adjusted profile of the process to the force data. It is thus unsurprising that the trend in the force measurements approximates the trend in the process activity as they effectively go full circle and compare two related signals. Another study by Xiong et al. (2016) attempts to simulate process vibrations during the cutting process. They claim that two acquired signals are similar enough for a model to reflect the true vibration. However, it may be noted that there are regions in the signal that

do not correspond and that simply because two signals have a comparable amplitude and frequency, does not mean the two signals are the same. These are not isolated instances and each highlights the importance of rigor in any developed DSP approach. Care must be taken when comparing two related or similar signals as the similarities between them may be more than a coincidence. Equally, when two signals are similar, the difference must be quantified. Otherwise one could assume signals are carbon copies when really, they differ where it matters.

#### 2.3.4.1 Prognostics and remaining useful life

It has been said that to effectively reduce process waste requires the implementation of appropriate TCM approaches, especially those that employ tool and process prognostics (Grosvenor and Prickett 2011). Prognostics is the systematic evaluation of developing faults or changes in a process and the estimation of how these progress through to end-of-life, or failure. In this circumstance, end-of-life is deemed the natural end to a process, not necessarily catastrophic failure. Prognostics is not diagnostics. Diagnostics looks back on a process to determine what happened where and why. Prognostics is employed in-process (or alongside processes) to look at concurrent events and predict these forward such that the potential consequences of any detected event can be mitigated. In the event that the consequences are beneficial, knowing in advance ensures that such benefits can be fully exploited. Elattar et al. (2016), Jain and Lad (2016) and Rigamonti et al. (2016) note that effective implementation of prognostic systems provides numerous benefits, including improved machine availability and mitigation of process risk. In manufacturing, the theoretical potential, or ‘added value’ offered by the appropriate application of prognostics includes:

- Improvements in process efficiency through prediction of machine and/or cutting tool failures. This allows for appropriate remedial action to be determined early and hence applied quickly (improving the measure of machine availability).
- Reduction of risk through detection and management of damaged or failing cutting tools and equipment, hence reducing the occurrence of scrap products and eliminating the detrimental effects of damaged cutting tools on the process or systems.

However, the approach is not without risk. Engel et al. (2000), Line and Clements (2006) Wheeler et al. (2010), Saxena et al. (2010) and Gugulothu et al. (2017) all identify that there are limitations to current prognostics approaches, including system inaccuracy, false alarms and low user confidence. Many practical prognostic approaches remain limited in capability and according to Acuna and Orchard (2018) may be fundamentally lacking. Research by Wheeler et al. (2010) refers to the difficulty in obtaining accurate data, that not all faults can be identified and that not all faults will be diagnosed correctly. It can thus be inferred that prognostic methods suffer from issues that limit their adoption and the confidence in their use, including:

**False alarms** - Both Bain and Orwig (2000) and Wheeler et al. (2010) identify that false alarms contribute to a reduction in effective useful life and come at a high cost to the process and the

end-user, both economically and in terms of confidence. Efforts to reduce the impact of false alarms is necessary for approaches to be accepted and successful.

**Prediction inaccuracy** - Inaccurate predictions of cutting tool health, or useful life, have the potential to result in unanticipated failures or for reductions in product quality to go unobserved. Many methods for prognostics claim high accuracy in use, however these claims are based on the enactment of given process conditions and often fail to translate from study to industry. The uncertainty this presents lowers the appeal of the given methods (Elattar et al. 2016, Line and Clements 2006, Saxena et al. 2010).

**Process limitations** - Many approaches are proven for one process and assumed applicable to similar processes. The process-specific nature of a chosen method can be a determining factor in the acceptance of a system. If the system benefits cannot be accurately quantified the approach is unlikely to gain acceptance (Elattar et al. 2016, Saxena et al. 2010, Wheeler et al. 2010).

Prognostics, as it pertains to the monitoring of cutting tools, is again difficult to properly define and to ensure that false alarms or incorrect predictions are avoided. This relates back to the complexity of process variation and the limitations inherent in current prognostic approaches (Hill et al. 2018). This can be set in an industrial context where, whilst the general consensus prevails that industry is engaged in developing and applying process monitoring and prognostics, the packages available remain limited. Innovations have been found to primarily involve mass data capture, with limited process control (Section 2.1.1). Regarding intelligent machine tools, implemented systems predominantly aim to predict when the process exceeds pre-established limits. For controlled and thus repeatable processes, these systems may suffice. However, for situations where the thresholds are unknown, the approach must be adapted to identify the potential limits from the data available.

To make progress it is possible to propose that the prediction of the remaining useful life (RUL) for specific cutting tools could be considered more achievable. RUL is a measure of how long a cutting tool has left before theoretical failure. In this context failure is not necessarily breakage of the cutting tool, but rather the point at which it is no longer economical to continue being used. In some instances, this may represent cutting tool failure; however, in most cases setting the point at the incidence of actual failure will be too late. RUL can be generalised against the flank wear curves presented in Figure 2.6 (Section 2.2.1). Although, this may not appreciate the true nature of cutting tool deterioration (as explained in Section 2.2.1). Figure 2.10 illustrates the concept of RUL from the perspective of component health.

Okoh et al. (2014) noted that there are three types of approach for the prediction of RUL. Model-based, analytical-based and knowledge-based. It is implied that hybrid is a fourth type; however, it is simply a combination of the main three. Notwithstanding, the prediction of RUL can effectively be summarised into just two (overlapping) approaches, model-based and data-driven. Model-based approaches will be based on the same methods as has been identified for general DSP techniques; therefore, attention is directed to Section 2.3.4. Data-driven approaches are (as implied) based on the

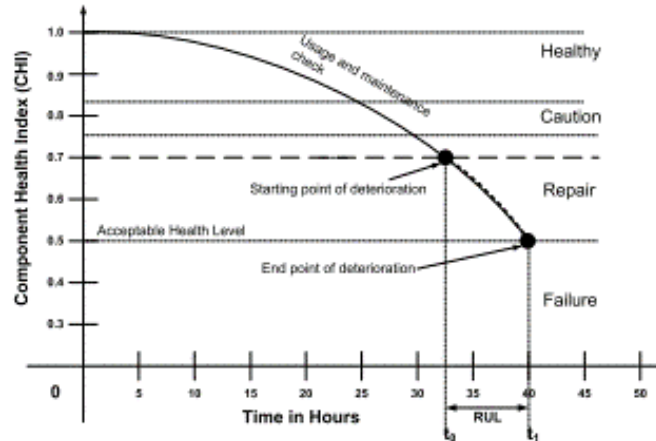


Figure 2.10. Concept of RUL based on component health, reproduced from Okoh et al. (2014)

use of current or historical data in order to determine the estimated RUL. Approaches may consider the similarities, or differences between a current cutting tool and a past cutting tool to determine whether the behaviour is comparable. Alternatively, approaches may consider the current behaviour of a cutting tool and forecast this behaviour forward to determine future behaviour. These approaches may be applied statistically, either employing some form of a health index, or based on auto regressive models (Si et al. 2011). It is also popular to utilise neural network approaches to automate these procedures (Heng et al. 2009); however, such approaches are not considered herein.

Another popular approach for estimating the RUL is with a probability density function (PDF) or using Bayesian inference models (Wiklund 1998, Engel et al. 2000, Karandikar et al. 2013, Wang and Gao 2016). Such approaches account for the likelihood that a prediction is correct; however, Engel et al. (2000) notes that an exact prediction of RUL is unrealistic as the probability that the prediction is 100% accurate is zero. It is suggested that an estimation of the RUL should not be considered without appropriate confidence bounds. Nevertheless, the implementation of methods to predict the RUL of a cutting tool or process is not the be all and end all for a process. From a commercial sense, one cannot simply rely on RUL to solve all the problems with cutting tool wear and failure as instantaneous condition is still important. If the health of a cutting tool changes suddenly and thus affects the cutting process, this needs to be identified before it becomes a significant problem.

## 2.4 The research gap

Industry has progressed towards smarter manufacturing and a degree of condition-based monitoring. Modern machine tools are often capable of actively monitoring their processes and adjusting to maintain speeds or feeds, or enacting inbuilt functions to protect the machine from damage. It is also not uncommon for modern machine tools to have the capacity to account for cutting tool wear and thus eliminate the effect on product geometry, or to identify broken cutting tools and thus prevent extensive damage to the workpiece. Further innovation comes from the many involved industries in favour of “smart factories”. This includes methods for acquiring and monitoring machine data such as MTConnect. Such methods are valuable in their own right; however, it was noted that such imple-

mentations cannot be suitable for high-speed or real-time data acquisition and process monitoring. It is therefore evidenced that effective implementations are limited. This indicates that efforts towards effective and industry specific solutions for active TCM and tool/process prognostics are still desirable and warranted.

It is also the case that two major problems face much of the research considered. The first problem is that often a new cutting tool is compared with a failed, or severely damaged cutting tool. This exaggerates the change and fails to provide evidence that the developed system can detect anything less than a significant change in the condition of a cutting tool. This is despite the authors often remarking that their approach can detect gradual or subtle wear. It is also the case that the failed cutting tools used are often far beyond any sensible state of deterioration, meaning that detection would come a little too late.

The second problem is that developed approaches are often far removed from a practical or commercial context. In other words, methods are often approached in a time-accelerated fashion or aiming to wear the cutting tool in a short space of time. This is a limitation of laboratory-based efforts, in that wearing out a cutting tool without trying to wear the cutting tool is not feasible in a reasonable time scale. For that reason, the cutting tool wear is often accelerated and thus does not represent practical or commercial cutting conditions. Yet the authors tend not to appreciate this difference and the enthusiasm from industry gains little in the way of workable solutions.

Nevertheless, cutting tools continue to either fail prematurely, or to get replaced early. Additionally, despite the popularity within academia, TCM has not been adopted as successfully within industry. Perhaps the nature of the cutting tools themselves and of the manufacturing processes introduce more influencing factors than is feasible to consider or account for. Or the cost versus benefits of such TCM systems confines them to academia as being promising in theory, but impractical and expensive in context. Ultimately however, (in the current state) TCM has not been able to translate from the controlled conditions of academic research to the relatively messy applications within industry.

In response, this thesis will consider options for active TCM and tool/process prognostics targeted specifically towards practical or commercial applications and for eventual installation within a manufacturing environment. This work considers the diagnosis of cutting tool condition using the information acquired from a smart machine tool. This tacit knowledge, relating to the management and control of specific cutting processes, enables smart operations but also enables access to process information without demanding significant alteration to the system or process.

## 3 | Enabling Technologies and Methods

This chapter expands on the equipment used and the specific applications adopted and/or developed to support this research. The efficacy of the processes employed will be determined together with comments on the suitability of the approaches and of the potential results.

Firstly a research framework is provided. This identifies the main research elements and highlights the development timeline that determined each application considered in subsequent chapters. The influences between industry and research are discussed.

Secondly, the equipment is outlined including the relevance of each identified item and the broader context for why each is necessary. This includes equipment with direct relevance to the development and deployment of monitoring strategies. These include the CNC machine tool, the physical connection for data transfer and the specification of the attached PC. The equipment necessary for verifying any process variation and for calibrating the cutting tool monitoring strategies are also included. These objects are indirectly relevant for the development of monitoring strategies. Their value is stated and the practicality of using such equipment within a manufacturing environment is discussed. A Coordinate Measurement Machine (CMM) is considered, using both tactile probes and skidded probes.

Thirdly, the applications employed to support this research will be defined. In this context “application” considers both the specific cutting tools employed and the material products designed to enact cutting tool wear. The design of, and reasoning for, each application will be included, as well as how each item fits within the broader scope of the project. The limitations of each application will also be considered to fully appreciate how each contributes to the project outcomes. The information on the necessary empirical studies will be outlined as appropriate in later sections and is available in Appendix E.1.

Lastly, brief gauge studies will be presented. The studies are included to underline the efficacy of the applications and of the studies undertaken herein. This foundation will ensure that results are valid and that each analysis is not influenced by the methods used to gather the data. The process assurance studies included will be brief and will not be a comprehensive or exhaustive evaluation of the equipment and methods used.

### 3.1 Research framework

First it is necessary to establish the methodology and the decisions leading to each application outlined in later sections. It is also necessary to establish the progression from laboratory-based investigations towards commercial-style manufacturing. Figure 3.1 provides the development timeline, indicating the stages at which each application was employed. The four applications were employed in a specific order to maximise value at each development stage. The Cylinders built upon previous research.

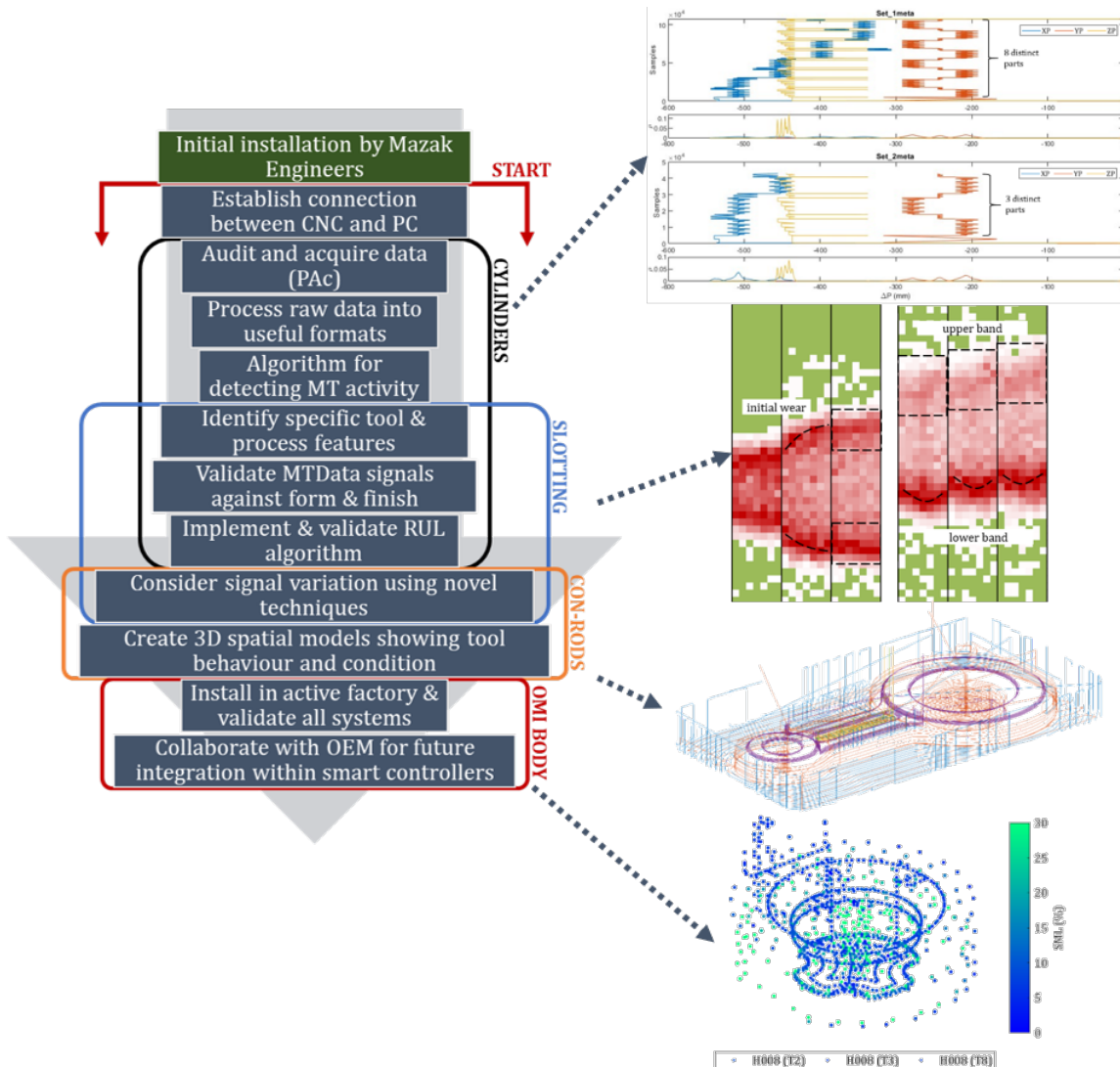


Figure 3.1. Process and application timeline

This meant that there was a proven basis from which to establish communications, audit data and process data into useful formats. Starting with the Cylinders better enabled the data acquisition programming and inspired the development of advanced algorithms (presented in Chapter 4). The Slotting application was introduced after the Cylinders to shift the focus to specific signals, notably the axis loads. They also provided a chance to validate the systems being developed. The Slotting application was more basic than the Cylinders but provided the means to confirm specific signals (identified by the Cylinders) before transitioning to more complex designs. After the Slots, Connecting Rods (Con-Rods) were investigated. The Con-Rods were a valuable resource for increasing complexity and for considering the behaviours of different cutting tools. The Con-Rods inspired the development of spatial models and shifted the investigation away from wear-focused testing towards product-focused testing. This shift provided the first half of a bridge between research and industry and can be considered as a laboratory-based case study. Following the Con-Rods, a Renishaw product, the OMI-body, was investigated. This was a complex process, truly representative of commercial manufacturing, that enabled the system efficacy to be validated in a factory environment. The OMI-body can also be considered as a commercial-style case study, providing the second half of a bridge between research and

industry. This offered the potential for access to real life manufacturing at high levels of production. This potential cannot be proven through laboratory-based testing alone, nor by showing the viability of a system using specially designed applications created to prove the success of the system.

It is important to clarify what is meant by optimisation in the context of this work. Optimisation will herein refer to the effective use of data and information, it will not focus on the best or the perfect processes. In other words, this work will not seek to optimise the life of cutting tools, nor the economy of the cutting process. Neither will specific optimisation methods be deployed (e.g. Taguchi, or six sigma). Instead this work will establish valuable methods for deploying the control data native to machine tools and will offer opportunities for making the most effective use of this resource. It is also important to clarify the importance of bridging the gap between research and industry. Without careful management approaches cannot be confidently deployed from the straightforward and controlled conditions often tied to laboratory work to the complex, messy and production focussed conditions of industrial manufacturing. It has been noted that commercial-style applications are warranted; however, firstly applications that are laboratory-based are necessary to simplify the analysis of any generated data. Then more applications may be appraised to bridge the gap between research and industry, introducing multiple cutting tools, a more complex process and a process optimised for purposes other than the specific deterioration of cutting tools.

## 3.2 Enabling technologies

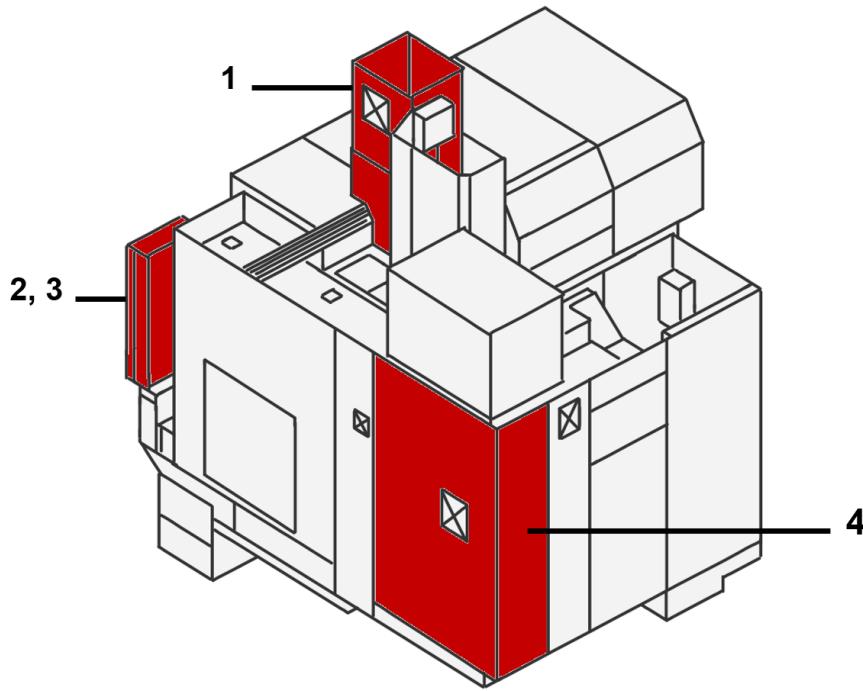
### 3.2.1 Machine tool and numerical controller

This work considers the application of existing MT architecture to investigate generated process data and to develop novel cutting tool monitoring strategies. To action this, a Mazak Vertical Centre Smart 430A VMC (VCS) was acquired and adopted for this research. It was equipped with a Mazatrol matrix nexus 2 CNC controller (NC). The VCS and NC are both shown in Figure 3.2. The key components of the VCS are emphasized in Figure 3.2a and listed in Table 3.1. These components are those that will be considered in greater detail in this and later sections.

Table 3.1. Key MT components

Component	Name	Primary use
1	Spindle	Cutting action
2, 3	NC and auxiliary operating panels	Control
4	Electrical control cabinet	Access & maintenance

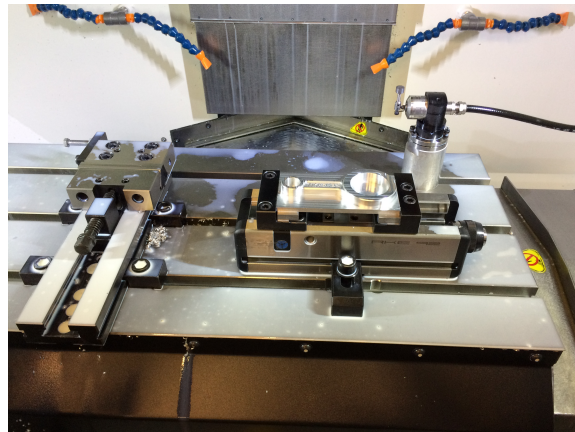
The VCS and NC combination is herein referred to as the MT, unless explicitly separated or stated otherwise. Table 3.2 provides key MT attributes. The “unique pocket” action of the magazine returned cutting tools to their original pocket after use. An alternative action would be “swap pocket”, returning cutting tools to the pocket of the next cutting tool used. Neither “unique pocket” or “swap pocket” are official terms used by the OEM.



a. Isometric Mazak wireframe - rear



b. Mazak front exterior



c. Mazak table area

Figure 3.2. Mazak Vertical Centre Smart 430A VMC

The MT was acquired to ensure parity with the systems used by the industrial sponsor of this project. Importantly, the combination is also representative of the typical shop-floor MT employed within generic manufacturing organisations. This can be inferred from the information present in the literature (Chapter 2). It should also be noted that the MT can employ the majority of the “smart functions” often packaged with such systems. Functions include active vibration control, volumetric error compensation and active feed rate control. These were discussed in Chapter 2.

The primary difference between the MT studied and the systems typically employed within manufacturing organisations is the relatively small table area and working volume of the MT (Table 3.2). Nevertheless, being relatively small does not reduce the relevance of the control functions accessed and utilised, nor the study undertaken herein. This point was proven with the successful deployment of the developed tools within a larger MT located in the partner organisation, as detailed in Chapter 8. The

Table 3.2. Key MT attributes

System	Attribute	Value	Unit
Spindle	Max power	18.5	kW
	Speed range	40 - 12000	rpm
	Type	7/24 taper, No. 40	–
X-Axis	Max power	1.5	kW
	Travel	0.560	m
	Precision	0.1	micron
Y-Axis	Max power	3.5	kW
	Travel	0.430	m
	Precision	0.1	micron
Z-Axis	Max power	3.5	kW
	Travel	0.510	m
	Precision	0.1	micron
Capacity	Table area (total)	0.387	m <sup>2</sup>
	Table area (usable)	0.241	m <sup>2</sup>
	Actual machine volume (AMV)	0.123	m <sup>3</sup>
	Effective machine volume (EMV)	0.099	m <sup>3</sup>
	Max (allowable) mass	500	kg
Feed	Rapid	42	m/min
	Cutting range	0.001 - 8	m/min
Magazine	Capacity	30	–
	Action	Unique pockets*	–

MT additionally accommodates two build fixtures, an in-process TS27R “online tool setter” (OTS) and an optical machine interface (OMI) to communicate with the inspection probe occupying pocket 30 of the MT tool magazine. The EMV is further reduced from the AMV by the operator-adjusted table offset of 100mm.

The OTS was utilised for an on-machine (online) estimate of the initial dimensions of the cutting tools. Measuring a cutting tool online is more reliable than measuring offline as the tool is seated within the machine, hence behaving as in-situ. It is also easier to assess the true working dimensions of the cutting tool, as the spindle is rotated during measurement. Notwithstanding, both the accuracy and the precision of the dimension measurements will be limited by the capability of the OTS employed. In this set-up the TS27R utilised is stated to have a  $1.00\mu\text{m}$  repeatability in each direction (when impacted with a controlled contact velocity of  $0.48\text{mm}/\text{min}$ ). Additionally, the OTS will only return a dimension averaged over the 8mm cross-section directly measured. This will differ from measurements taken using ICG approaches, or measurements taken offline. Offline measurements will theoretically be more accurate and precise. However, the true accuracy will suffer due to the variation introduced by simply accessing the cutting tool and removing the workpiece from the MT vice (see Section 3.4).

Both the VCS and NC were necessary to support this research. Without them the tacit intelligence could not be appropriately established without resorting to digital models or simulations. As discussed in the literature (Chapter 2), it is believed that any approach that neglects to base findings on empirical work, or that fails to support models or simulations with suitable empirical validation, cannot be trusted. It is noted that the empirical work conducted herein and the data produced by it may be used by other researchers to update, or to validate, their simulations or digital twins. It is noted that the MT was calibrated prior to commencing empirical studies. The machine was maintained at regular intervals. It is important to state that the MT supplier collaborated in forming the hardware interface necessary to conduct this research. This provided access to information and inbuilt functions not normally available to MT users. They did so in direct response to specifications and requests for information generated by the author. Unless otherwise stated however all of the systems and software described in this thesis were produced by the author.

### 3.2.1.1 Communication setup

The MT retains much of the processing power within the NC unit. Access to this required an Ethernet cable (EC) running from an FCU7 series extension unit (Figure Figure 3.3), retrofitted to the NC, through to the electrical control cabinet (ECC). The FCU7 series extension unit is a COMX 100XX-

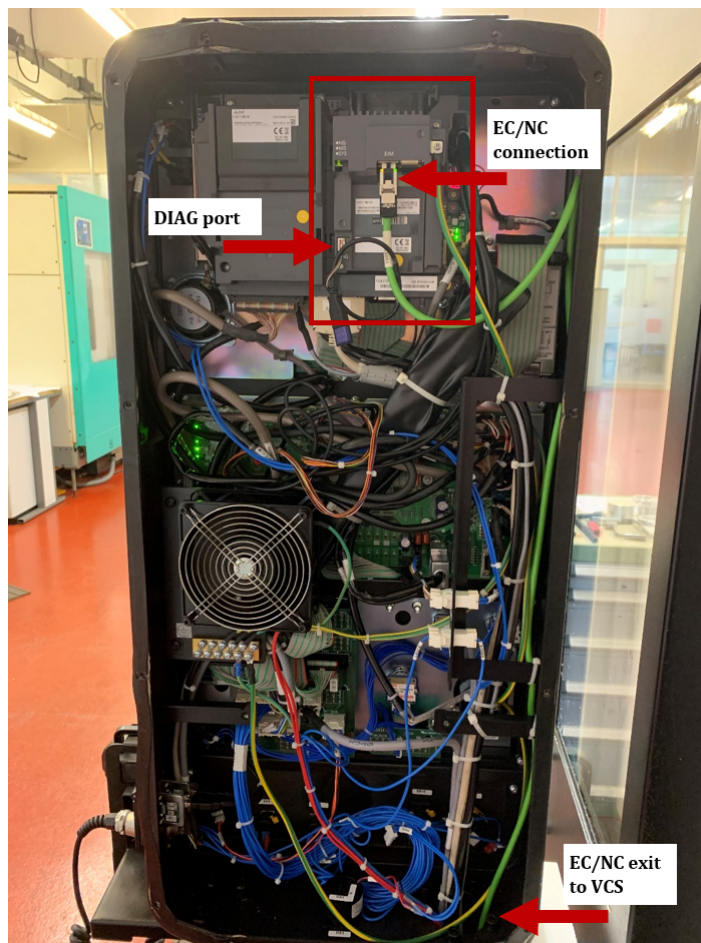


Figure 3.3. FCU7 installation and Ethernet cable routing

RE/EIM Ethernet IP Master device and enables external transfer of NC data when a suitable Ethernet IP (EIP) Slave device is available. The ECC houses all the servo drives, but more importantly allows external access to the EC via an RJ45 adaptor. The cable can be routed from the ECC to an external PC, enabling one-way transfer of information from the NC. The simplified wiring schematic is provided in Figure 3.4. The PC was provided with a Hilscher CifX50E-RE interface board (CifX-

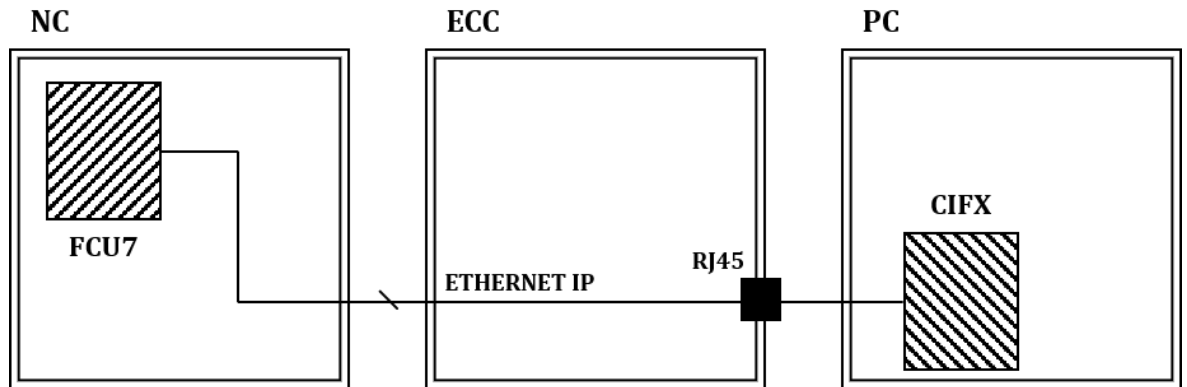


Figure 3.4. Basic wiring schematic for COMX-CIFX physical connection

B). The CifX-B requires a physical connection to the MT via an EC to the RJ45 adaptor, from one of the on-board channels (CH0) (Figure 3.5). The board also required a digital connection - made possible as the CifX-B is an EIP Slave device and therefore a suitable gateway device (CIFX RE EIS[CIFX RE/EIS]). The FCU7, herein referred to as COMX, can be configured by directly accessing

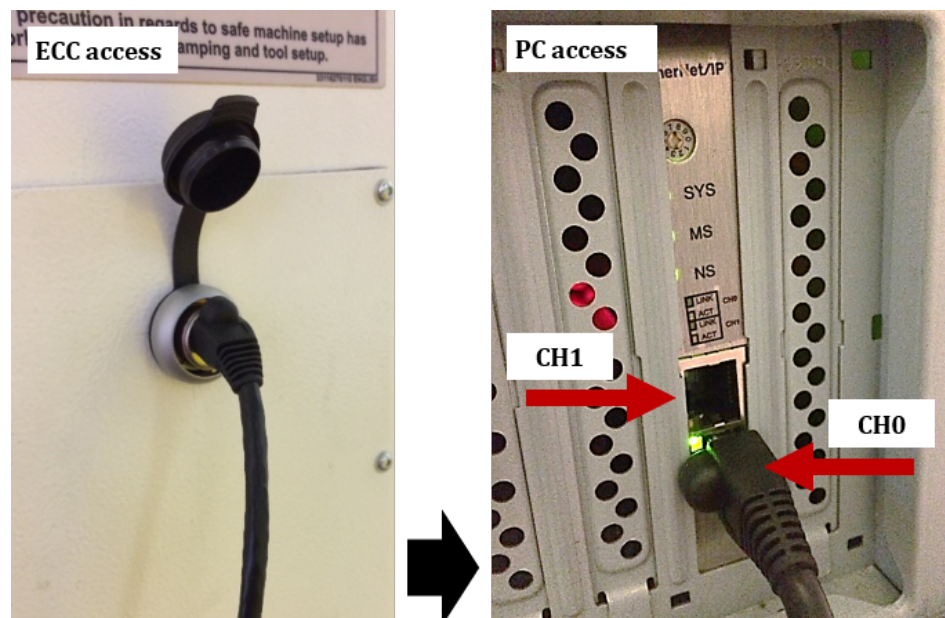


Figure 3.5. MT and PC backend connections

the unit (removing the back panel of the NC) and connecting to the DIAG port with an external (additional PC). Configuration of the CifX-B can be achieved simply using the PC housing the unit. Configuration of both the COMX and the CifX-B is enabled with SYCON.net software, the method of which is outlined in Appendix D.3 - A document created by the author in collaboration with a

Hilscher Engineer. The specific SYCON.net project files (created by the author) that will enable trouble-free communication between a COMX and a CifX-B are provided in Appendix D.4.

It is important to stress that accessing and exploiting the MT control signals minimises any impact on day-to-day machining operations while also avoiding the need to retrofit equipment or sensors. Such an approach may be equipped to operational MT units, without any downtime, reduction in capacity or reduction in capability. This approach was proven to be effective by the implementation into a MT operated by the partner organisation, as detailed in Chapter 8.

### 3.2.1.2 PC specification

The dedicated PC was purchased to support this project. The key details of the PC specification are detailed in Table 3.3. The full PC specification is included in Appendix D.6. It is noted that the specification of the PC could be improved to maximise performance. Primary attributes that would benefit from an upgrade include the system RAM, storage and the CPU. Other attributes would have negligible effect on the performance or capability for data acquisition.

Table 3.3. Laboratory PC specification

System	Attribute	Value
CPU	Spec	Intel Core 2 Duo E8400
	Cores / Threads	2 / 2
	Frequency	3.00GHz
	Technology	45nm
Memory	Format	DIMM
	Type	DDR2
	Width	64bits
	Size (individual)	4096MB (2048MB)
Storage	Capacity	149.0GB
	Bus type	SATA (11)
	Speed	7200rpm
PCI	Express (single slot) for CifX-B	
Operating System	Microsoft Windows 7 (6.1) Professional 64-bit SP1 (7601)	
Network state	No network connection	

### 3.2.2 Coordinate measurement machine

All tangible measures of process variation were acquired using a Mitutoyo Euro Apex CMM with a retrofit Renishaw REVO-2 five-axis head. The system was interfaced through Renishaw's Modus software. The programs written to control the system are expanded in the investigative Chapters 5-8. The CMM and the REVO-2 are pictured in Figure 3.6. CMMs represent significant capital outlay and can require substantial real estate when positioned on the shop floor. Further to space and cost restraints, appropriate use of a CMM requires time, a controlled environment and significant



a. CMM home location



b. REVO-2 (Renishaw 2019)

Figure 3.6. CMM and REVO-2 head

operator expertise. Such resources are therefore typically associated with high value products, such as in aerospace industries, which have a need for precisely manufactured and measured products. This makes outsourcing measurement of components more economical (and more popular) for many organisations, rather than investing in in-house solutions. This is particularly the case for high-volume products. Indeed, for many MT based manufacturers CMMs are not widely utilised beyond product conception, initial production checks or research studies such as this. Alternative approaches are often preferred, lower-cost equipment is used and simpler approaches taken. This includes the use of Equators (Renishaw 2020a), shadowgraphs (Davidhazy 2006), go/no-go gauges (Oddy 2015, Marposs 2020c), microscopes (Conroy and Armstrong 2005) and simple inspection routines as part of process quality control (QC) – mostly visual checks of every  $n$ th part. Nevertheless, CMMs can be effective at characterising a machined part due to their accuracy and reliability versus alternative approaches.

A CMM is traditionally a mechanical-based tactile metrology instrument; however, recent advances in non-contact measurement approaches means that retrofit equipment also offers non-contact methods of measurement. Although noted, such approaches are not employed for this study. The REVO-2 appended to the CMM allows additional measurement strategies to be considered beyond those possible for fixed heads. The benefits afforded by the additional degrees of freedom mean that parts may be almost entirely evaluated without any re-positioning of the component. This includes the capability to assess surface finish when combined with the right probes. Notwithstanding, additional complexity means additional measurement uncertainty. The suitability of the additional strategies employed is evaluated in Section 3.4. The CMM can specify feature coordinates relative to either the machine coordinate system (MCS) or the part coordinate system (PCS) and can determine the deviation of a point from the nominal position. The MCS is based on the CMM range in each axis, relative to the home position at the top-rear-left (noted in Figure 3.6). The PCS on the other

hand is user-generated and equates measurements relative to the datum position of the part under consideration. Both provide the same information but from different perspectives. The alignment necessary to generate the PCS is discussed relative to each application.

The CMM excels when features are defined beyond individual touch points, for example, circles, cylinders and lengths. This allows feature deviations to be expressed in terms relevant to the object of interest (e.g. circle diameter). This gives more meaning to each measurement as an under-size diameter is more understandable than perhaps a coordinate that is at (65,72,0) rather than at the nominal (67,71,-1). Notwithstanding, these improvements in user-friendliness come at the cost of reduced transparency in measurement. Algorithms applied by the CMM software would evaluate each feature differently if the arguments provided are not explicit enough. For example, one cycle may evaluate a diameter based on 32 scanned points, the subsequent sample may evaluate the diameter based on 33 scanned points. Such deviation could be avoided by explicitly identifying the points to include. However, which points, and the exact position of each point, may still not be guaranteed. Assessment of the gauge suitability is briefly considered in Section 3.4.

### 3.2.2.1 Fixturing

The applications are fixed to the bed of the CMM for the duration of the measurement process. In most cases, the fixturing is specific to each application and is designed to reduce unwarranted movement of the components when impacted by the CMM. In this research a modular “fixture kit” was utilised. An example fixture design is provided in Figure 3.7 for the Cylinder and Slot applications used in this study. The same design is implemented for both due to the same billet (and therefore

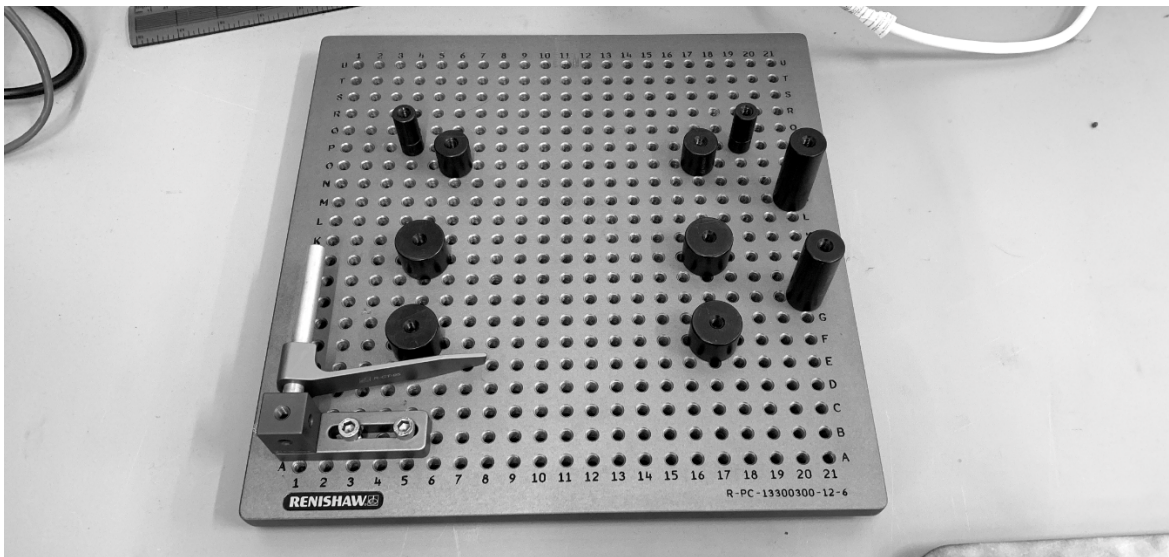


Figure 3.7. Fixture example

external dimensions) used for each. Figure 3.7 shows that the applications are raised on supports with a sliding clamp available to reduce lateral movement. It is noted that not all movement will be negated, however it is important to reduce the movement as much as is feasible to reduce the measurement variance (Dove 2014, O’Regan 2020).

### 3.2.2.2 Tactile probes

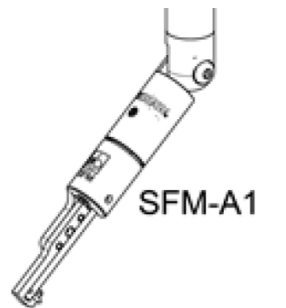
Two tactile probes were employed for the measurement of each component, the RSP2-RSH250 (RSP2) and the RSP3-3-SH25-3A (RSP3). The name of each probe identifies the combination of modules each is comprised of. The RSP2 is used for part alignment and for measurements taken by head scan. The larger tip diameter of the RSP2 relative to the RSP3 was deemed to be superior for alignment as imperfections in the finish of the measured components would be effectively filtered by the tip. The RSP3 is used for most diameter measurements and for waviness investigations due to the smaller tip being more suitable for accessing hard-to-reach regions. The RSP3 was not capable of head scans, however, was the only one of the two capable of Z+ CMM scanning. Some applications were evaluated using only one of either tactile probe combinations. This was enacted to balance the benefit afforded by either probe against the additional time expense required to change the probe mid-cycle.

### 3.2.2.3 Skidded probes

The addition of a Renishaw surface finish probe (SFP2) introduced measurement of surface finish during inspection routines using the CMM. Figure 3.8 shows the SFP2 and the surface finish modules (SFM) A1 and A2. The SFP2 was calibrated using a roughness specimen, itself calibrated in accor-



a. SFP2 module, reproduced from Renishaw (2020d)



b. SFM-A1 straight tip (Renishaw 2020d)



c. SFM-A2 cranked tip

Figure 3.8. Surface finish probe and modules

dance with ISO 4288:1988 and ISO 4287:1998+A1:2009. The calibration of the roughness specimen considered only the roughness average (Ra) and the roughness total (Rz). The full calibration cer-

tificate is available in Appendix C.4. The initial gauge assessment of the SFP2 in combination with SFM-A1 and SFM-A2 is provided in Section 3.4.

### 3.3 Applications

Four applications were developed to investigate the feasibility for using machine tool controller data for the evaluation of cutting tool health. Each application was engineered separately to identify the tacit value offered when observing key parameters and/or groups of parameters. Each subsequent application was considered to account for shortcomings in the previous and to assist with the evaluation of process signals and hence the development of cutting tool monitoring strategies. The applications consisted of Cylinders, Slots, Con-Rods and OMI-bodies. This section identifies the application designs and the benefits afforded to the study. The detailed investigations into each of the applications are in later individual Chapters. The cutting tools employed for each application, including the nominal dimensions, are listed at the end of the section.

#### 3.3.1 Application 1: Cylinders

The first of the four applications were adopted for parity with other researchers within the IPMM group at Cardiff University. The part drawing is given in Figure 3.9. Measurements are not indicated for the central slots as they are a secondary process and mostly ignored herein.

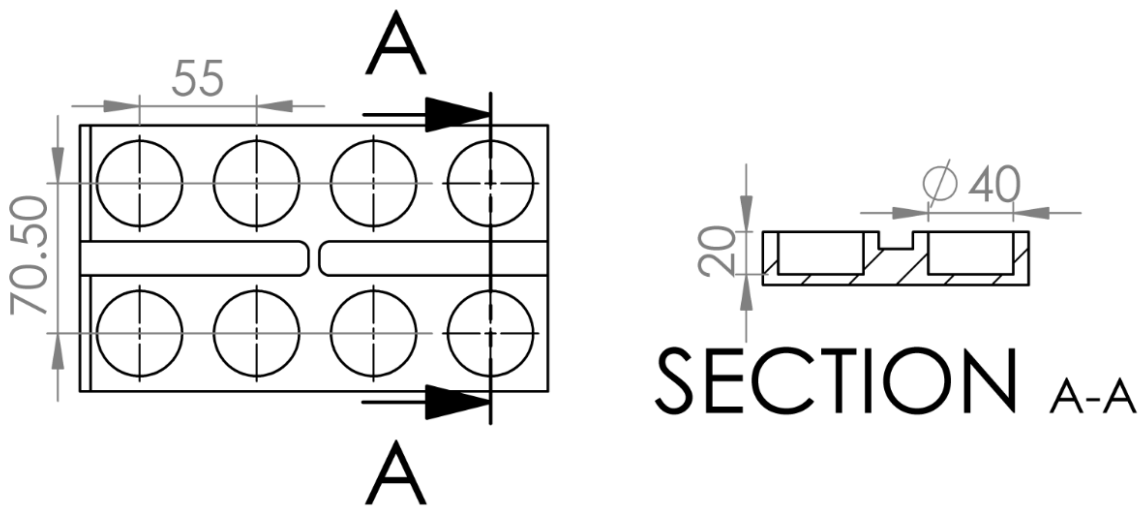


Figure 3.9. Cylinder CAD drawing

The application consisted of eight homogeneous pockets and eight unidirectional slots. These were machined into a billet of bright mild steel (125x25x220 mm) of initially unknown material properties. Each pocket was manufactured in four stages, each stage henceforth considered equivalent to a single machined part. This definition allowed the direct comparison of each element (i.e. part) of Cylinder manufacture across the whole investigation. The unidirectional slots were machined in two passes; each pass was equated to a single machined part. Segregating the process in this way resulted in 48

equivalent parts per section of steel. The process continued for each cutting tool until either four billets (consisting of 192 parts) were completed or the cutting tool broke. Two-dimensional path information is given in Figure 3.10, the cutting cycles are outlined in Table 3.4.

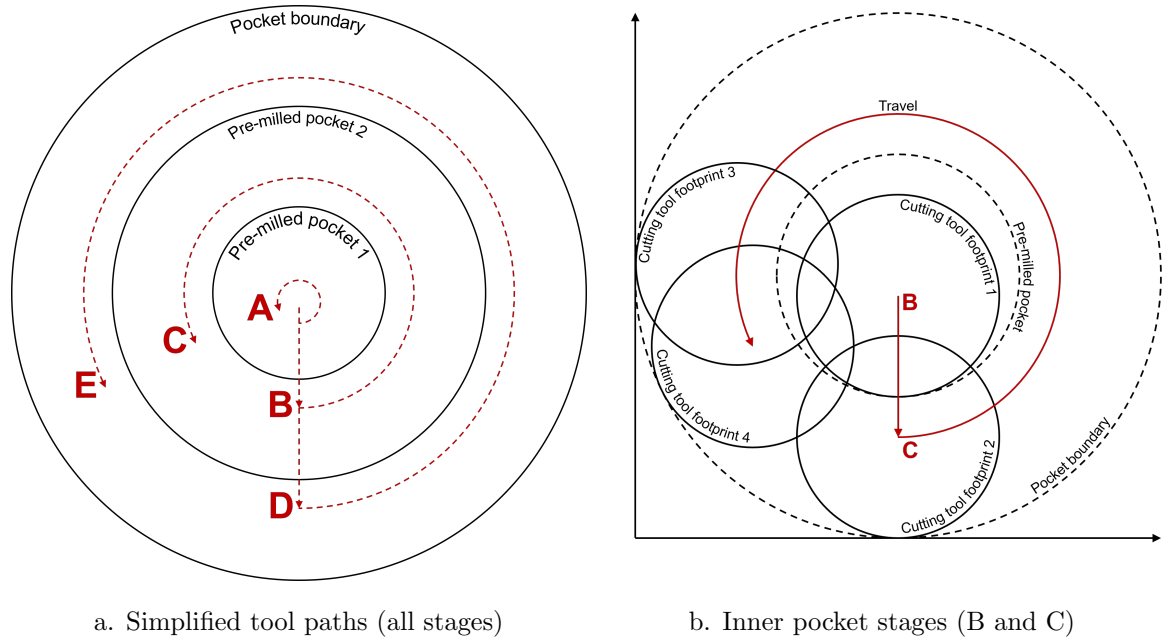


Figure 3.10. Two-dimensional path schematics for Cylinder application

Table 3.4. Stage information for equivalent part manufacture

Stage	Operation	Movement axes	Relative Feed
A	Helical	-Z	1.0
B	Slotting	-Y	1.0
C	Circular partial	X and Y	2.0
D	Slotting	-Y	1.0
E	Circular partial	X and Y	2.5

The Cylinder application was designed to identify cutting tool wear and usefully also indicated differential cutting tool wear (DTW) due to the four-part depths. DTW being caused by regions of the cutting tool not being utilised equally. The Cylinders were manufactured without modified tool offsets. In other words, the effects of cutting tool wear were not accounted for in-process. This allowed the effects of such degradation to propagate through to the final geometry and finish of the parts. The design of the application meant that the reduction in the cross-section of the cutting tool (due to peripheral wear) should be affected on the diameter of each part. The reduction in part diameter may hence be appropriated as peripheral wear, with appreciation for any dynamic effects from the cutting process. Dynamic effects may arise from chatter, deflection of the cutting tool, BUE and swarf. Benefits of the Cylinder applications include:

- Rapid cutting tool wear due to the high material engagement and aggressive cutting cycles

- Simple geometries, enabling relatively quick post-process inspection routines
- Pocket geometries are common in the literature, meaning high comparability to other studies
- Uniform cycles simplify the trends in cutting tool wear

The primary limitations of the Cylinder applications include:

- Hidden (post-process) cutting phases due to multiple part depths
- Challenging access for surface finish measurement
- Incomparable with real-world operations due to the uniform, excessively aggressive, cutting cycles.
- Relatively unrealistic rate of cutting tool wear

It is noted that most of the benefits and limitations are based on the same design features. This initial study was designed to produce high rates of tool wear. The experiment design (Design of Experiments (DOE)) was to employ a single factor strategy to investigate cutting tool wear. To achieve this all experiments were completed with fixed cutting parameters, with equivalent cutting tools and using equal cutting conditions. 50 Cylinder tests were completed. This number was arbitrary and limited by time and resource constraints; however, the number was still deemed appropriate as it provided enough data to evidence repeatable results. The design of the cutting strategies enabled the evaluation of cutting tool wear.

### 3.3.2 Application 2: Slots

The second application was designed to simplify the continued assessment of the machine tool controller data. An example part model is given in Figure 3.11. The Slots were introduced to simplify

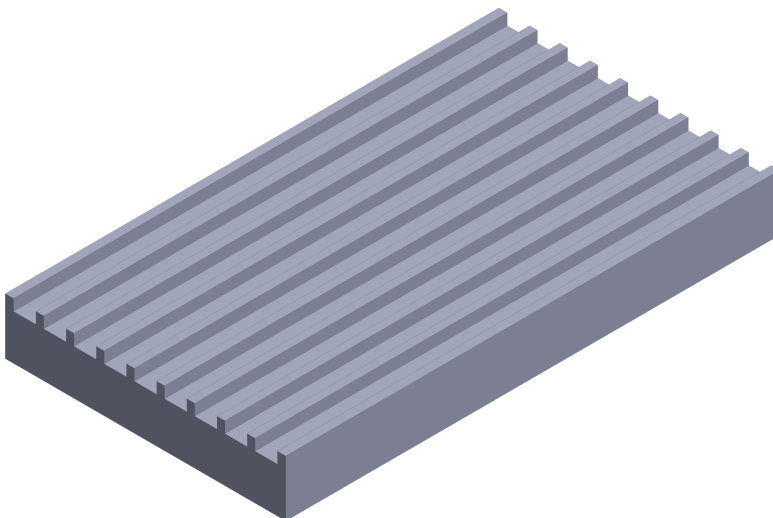


Figure 3.11. Slot CAD model

the necessary processing of directional data and to remove the hidden machining phases noted for the Cylinder application. It was noted that the multiple depths necessary to machine the pockets

prevented explicit recognition of cutting depth in any calculation of material removal post-process. All cuts were in the X-direction only. The cutting tool entered the material at the necessary depth and exited the material at the same depth. This ensured that the only spatial change in the process was the X-axis position. Additionally, the Slots were machined in a single pass and were started from the same end for each pass. Again, these process strategies fixed all variables such that the experiments were focused on tool wear monitoring. 24 experiments were completed in this way, employing a single cutting tool. This enabled the changing condition of the cutting tool to be established. It was not taken further as the cutting tool was not expected to fail and thus further cutting would be a waste of resources. The Slot application was designed as a stepping stone towards a better understanding of the process data. The design benefits from being simple and therefore straightforward to evaluate; however, the design is limited by being less akin to a realistic product. It was also noted that the per-unit material removal is significantly less than noted for the Cylinder applications, therefore (as noted) timely cutting tool deterioration was not possible.

### 3.3.3 Application 3: Connecting-Rods

The third application considered a more complicated process in the machining of an aluminium artefact designed to represent the essential features of a Con-Rod. It introduced into this research the use of multiple cutting tools within a machining cycle. A part model is in Figure 3.12.

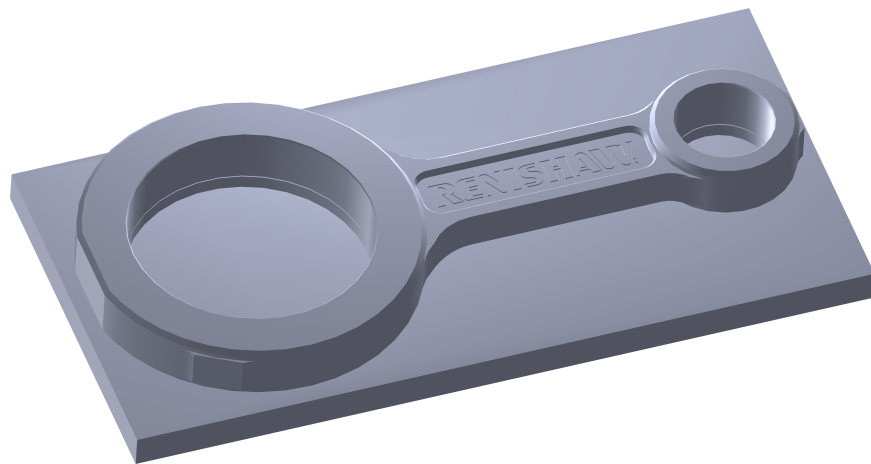


Figure 3.12. Conrod CAD model

Prior to this project the Con-Rod application was already being manufactured at Cardiff University to complement an undergraduate lab-based metrology module. As part of the 20-week laboratory, one to two Con-Rods are machined per week. This regular manufacture of the Con-Rod enables an investigation into the behaviour of the cutting tools used during a process that was not primarily designed to wear out said cutting tools. This directly contrasts with the Cylinder applications and progresses the investigation towards a more realistic process. The main limitation of this approach is that the cutting tools are not anticipated to deteriorate significantly within a reasonable time scale. Benefits of the Con-Rod application include:

- Realistic process – bridging gap between wear testing and production processes
- Multiple cutting tools – providing additional data and indications of variability between different cutting tool geometries
- Multiple machining processes – indicating cutting tool behaviour during intermittent machining

The limitations of the Con-Rod application again reflect the benefits. This is because the additional complexity of the process makes it harder to ascertain true cutting tool behaviour amongst the natural variation in the process. The Con-Rods were still a single factor experiment focussing on cutting tool wear. The manufacturing of each of the 42 Con-Rods sampled was homogeneous. However, this limited the number evaluated to 42 as no more were manufactured with fixed or similar cutting conditions. An additional limitation is as discussed previously - each cutting tool is not anticipated to wear to the point of failure within the period of this study.

### 3.3.4 Application 4: OMI-bodies

The fourth application was introduced to bridge the final gap between the previous academic studies and industrial products. The OMI-body is a product manufactured en-mass by the industrial sponsor and allows the efficacy of the process thus far to be tested. The process can then be deployed onto a second MT located in an actual setting, to monitor the manufacture of an actual product. As outlined in Chapter 8 it should be noted that, in a reflection of the production methods used, eight OMI bodies were manufactured in one process. This required the use of an eight-part fixture and greatly added to the challenges associated with monitoring this process. Due to the complicated nature of the OMI body, only one of the cutting tools used in the manufacture of the component will be investigated. The other cutting tools may be considered, but not in any considerable detail. Benefits of the OMI body include:

- Production component – therefore entirely representative of a realistic process
- Manufactured in high volume thus providing enough data
- Complicated process and hence more opportunity to rigorously test any developed strategies
- Known (from experience) cutting tool contact limits – allowing a comparison between known limits and the predicted limits

The primary limitations of the OMI body include:

- Complexity may be challenging to evaluate
- “Enough data” may be considerable and therefore time consuming to evaluate
- Production environments may obscure or limit traceability regarding breakages, damage, or process anomalies

It is noted that the term “enough data” is used as the true quantity is subjective. In this context, the author considers “enough data” to be an amount sufficient for a reliable sample size, yet not so much that manual manipulation and analysis of the data is impractical.

### 3.3.5 Cutting tools

Table 3.5 identifies the cutting tools employed during each of the four applications. A mix of HSS and carbide cutters are considered, none are coated. Table 3.5 provides cutting tool information (sorted by application), including the nominal cutting tool dimensions. Variation in the nominal diameter and length is expected for individual cutting tools. This is measured in-process through use of the TS27R unless explicitly stated to the contrary. All cutting tools employed per application are included for information; however, not all are referenced in later sections.

Table 3.5. Cutting tool details and nominal dimensions

Application	Cutting tool	Detail (where available)	Diameter (mm)	Length (mm)
Cylinders	HSS10	HSS 4-flute square-end-mill	10.00	130.00
	HSS16	HSS 4-flute square-end-mill	16.00	130.00
Slots	HSS10	HSS 4-flute square end mill	10.00	130.00
	HSS12	HSS 4-flute square-end-mill	12.00	130.00
Conrods	R020EM16	HSS 3-flute square-endmill	16.00	135.00
	R021EM12	HSS 3-flute square-endmill	12.00	130.00
	R023EM06	HSS 3-flute square-endmill	06.00	115.00
	R024EM03	HSS 3-flute ball-nose	03.00	112.00
	R025ENP6	HSS engraving tool	00.60	122.00
OMI body (lab.)	D806	Carbide 3-flute ripper cutter	16.00	155.00
	C900	Carbide 2-flute spot drill	06.00	115.00
	H058	Carbide 3-flute slot drill	08.00	110.00
	H008	Carbide 3-flute slot drill	12.00	136.00
OMI Body (prod.)	H008SD01	Carbide 3-flute slot drill	12.00	136.00
	C900SD01	Carbide 2-flute spot drill	06.00	115.00
	H058SD03	Carbide 3-flute slot drill	08.00	110.00
	C853CD01	Carbide drill	02.60	134.00
	E800CD02	Carbide drill	04.30	154.00
	F363GC01	Carbide grooving cutter	12.00	122.00
	E616CD03	Carbide drill	02.80	139.00
	E801CD04	Carbide drill	03.30	143.00
	D635TM01	1.0 pitch threadmill insert	01.00	120.00
	D806RC01	Carbide 3-flute ripper cutter	16.00	155.00
E950TM01	15-degree tapermill	12.00	130.00	

### 3.4 Process assurance

This section is concerned with verifying the quality and hence suitability of the process data, of the measurement methods and of the gauges employed during this study (where applicable). Whilst

process assurance normally means to control the quality of a system or process, in this context the term is used to mean the evaluation of process fitness, or suitability. Judging the origin of the process data and of the results provides both basis and value to the subsequent analysis. This gives the study rigour because data sources are evaluated comprehensively thus making results traceable and repeatable.

### 3.4.1 CMM suitability

First an assessment of the CMM suitability for measurement of form is required. The CMM employed for this study was calibrated in accordance with ISO 10360-2:2009 to ensure that measurements remain traceable. In addition, the temperature of the laboratory environment was maintained at a consistent 19 ( $\pm 1$ ) degrees Celsius throughout any measurement process. The CMM techniques are outlined in Table 3.6, listing the target features and the measurement techniques. Table 3.6 indicates three primary CMM techniques to assess: touch trigger, CMM-scanning and head-scanning. These thus informed the brief measurement systems analysis approaches considered.

Table 3.6. CMM measurement techniques

Feature	Technique(s)
Diameter	Head-scanning, CMM-scanning
Distance	Touch trigger, CMM-scanning
Roughness	CMM-scanning

#### Touch-trigger measurement -

Is the acquisition of discrete points to generate a feature, or to assess a single point. The observations from the reverification of the CMM indicate a probe uncertainty of  $0.11\mu\text{m}$ , a tip-size error of  $0.52\mu\text{m}$  (PSTU) and a feature error of  $3.79\mu\text{m}$  (PFTU). An investigation into the possible effect of these errors on the measurements taken in this research was therefore conducted. This is provided in Appendix C.2 and indicates that taking discrete points is not a suitable technique for the applications considered.

#### Scanning measurement -

An alternative technique for acquiring data to generate a feature is to scan the surface. This approach drags the probe across the surface, taking multiple discrete points sequentially. Using multiple points reduces the likelihood of extreme values skewing the results and reduces the variability (introduced by surface quality) from taking a measurement in a slightly different location. The CMM scan is applied in two configurations: unidirectional and circular. The DMIS programs written by the author to acquire data for both configurations are in Appendix C.1. The expanded investigation into unidirectional scanning is in Appendix C.2. The assessment of circular head-scanning and circular CMM-scanning was enacted using the Cylinder application. Different approaches for the measurement of the Cylinders were taken to assess the variation attributed to probe velocity and probe starting position. The two types of scanning were then compared. It is reiterated that the RSP2 was the

only probe capable of head scanning. For that reason, both CMM-scanning and head-scanning measurements presented in evidence were taken using the RSP2. Table 3.7 provides the measurement average, range and standard deviation results for both scanning techniques, over three measurement velocities (for 20 repeat measurements). The CMM-scan was not enacted at 25% velocity due to the

Table 3.7. Scan results for different velocities

Technique	Statistic	100% velocity	50% velocity	25% velocity
Head-scanning	Average (mm)	39.625	39.624	39.626
	Range (mm)	0.219	0.213	0.220
	Standard deviation (mm)	0.093	0.091	0.093
CMM-scanning	Average (mm)	39.624	39.624	
	Range (mm)	0.218	0.214	
	Standard deviation (mm)	0.093	0.091	

probe consistently crashing during the measurement. This was due to an imperfection in the Cylinder form. It was observed that the probe was only able to navigate the imperfection when scanning at higher speeds. This observation is noted to be an advantage of head scanning versus CMM scanning. It is acknowledged that the problem only arises due to the issue with the Cylinder form; however, this affects the broader ability of the CMM to be used in automated environments. The three velocities were chosen arbitrarily as the relationship between measurement velocity and variation was not the subject of the investigation. The results indicate that the effect (of the velocities chosen) on the measurement is negligible. It was also determined that the starting position of the probe had negligible effect on the measurement variation.

It is noted that dragging the probe challenges the reliable measurement of surfaces using scanning techniques. Figure 3.13 illustrates the effect on the K direction cosine for vertical (unidirectional) scanning. Another side-effect is the propensity of the probe to collect debris (Figure 3.14). Collection

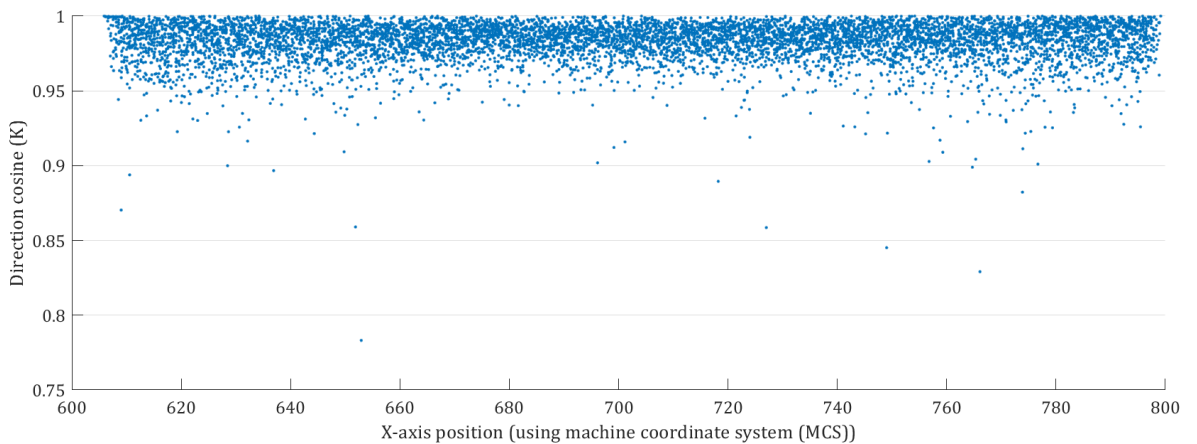


Figure 3.13. Variation in K direction cosine during scanning

of matter throughout the measurement will contribute to the deterioration in the reliability of each

subsequent measurement. The effects of surface debris may be mitigated by regular and thorough cleaning of the probe and surface to be measured.



Figure 3.14. Collected probe debris after scanning measurement

### Roughness -

As the CMM is further employed for the measurement of surface finish, further evaluation of the capability of the required modules is necessary. The assessment of finish was conducted using the roughness specimen shown in Figure 3.15. The roughness specimen had a calibrated Ra of  $3.0\mu\text{m}$



Figure 3.15. SFM-A2 acting on the  $3.0\mu\text{m}$  roughness specimen

and was used for the assessment of the SFP2 as the true roughness value is traceable. The capability of each surface finish module was reviewed against the specimen by repeating the approach taken in certification 317546 (Appendix C.4). Measurements were taken over an evaluation length of 6.4mm with a 0.4mm cut-off length either end (to remove data captured during probe acceleration and deceleration). The measurements were taken repeatedly ( $\gg 20$  repeats). Only the values of Ra and Rsm were evaluated as they were specified for the roughness specimen. The results for Rsm indicated no variation from the nominal 0.1mm. The results for Ra indicated negligible variation. Figure 3.16 illustrates the proportional gauge error versus acceptable artefact error (AAE). Further breakdown of the gauge variation is given in Appendix C.2, including the gauge capability.

It can be determined that the SFP2, in combination with either the SFM-A1 or the SFM-A2, is suitable for the measurements required herein. It can be safely assumed that variation in the measurement is

primarily attributable to the artefact and not the probe error. Herein the SFM-A2 will be employed for roughness measurements due to the slightly reduced bias ( $0.013\mu\text{m}$  vs  $0.019\mu\text{m}$ ).

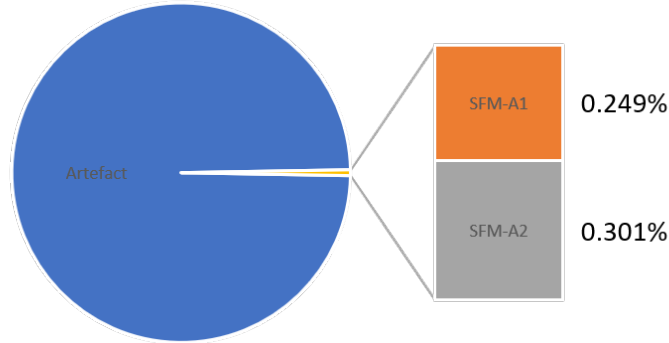


Figure 3.16. Proportional gauge error versus AAE (pie-chart)

### 3.4.2 Machine tool capability

The capability of the MT may be measured through the ability to create the correct components repeatedly. This can be assessed by comparing the machined parts on a separate system, for example the CMM. The capability of the MT to manufacture each part for each application can also be assessed by looking at the measurement of machined features. Although, it is noted that effects of tool wear should be separated. It could be argued that the MT and CMM could share similar systematic errors. If systematic errors are occurring in both systems, they would not be easy to identify as differences between the two and may not be observed in the measured components. Possible examples would be axis straightness, squareness, lateral play or scale mismatches. Notwithstanding, the CMM is calibrated to determine whether such errors exist. Passing the calibration implies that the errors are not occurring in the CMM and therefore could be observed in the MT.

A further argument is that the machining of a billet releases residual stresses in the material and can induce additional stresses when creating certain geometries. This is discussed in Chapters 2 and 5. This distortion must not be appropriated as a change in the health of the process, or a change in the health of the cutting tool. It should be identified as a limitation introduced by the billet and indicates that the material should be stress-relieved prior to machining and after machining (but before removal from the fixture). It is noted that such distortion will affect the geometry of the final product and therefore must be corrected during manufacture. The issue is raised as the effect has a notable effect on the results and must be acknowledged herein.

## 3.5 Summary

This Chapter investigated the manufacturing environments employed for the empirical work instigated during this project. It was shown that the specific equipment used is not particularly special or unique. Nor are the applications considered special, beyond the novel ways that they are utilised. A graduated approach has been taken to progress the development from predominantly laboratory-based

approaches, through to what are considered “real-world” applications. This forces the introduction of management approaches that are practical and can be implemented relatively easily by most manufacturing organisations hoping to improve their awareness of their manufacturing systems and their capabilities. Gauge studies were presented to discuss the limitations of the measurement systems employed. These studies help to better understand the capabilities and limitations of the systems. This provides a solid basis for any future evaluation of the data gleaned from such systems and prevents measurement error from being appropriated as changes to system health, or the health of the cutting tool. Acknowledging that measurement variability will exist allows results to be assessed objectively.

## 4 | Tool Monitoring System Development

In a competitive market effort must be made to optimise manufacturing processes and reduce their impact on the environment. This Chapter describes the steps taken to develop algorithms for on-line monitoring of cutting tool health and the engineering of a suitable monitoring system for cutting tool wear. The approach exploits NC architecture to acquire machine tool information that is not widely available, understood, or used for purposes other than creating superficial infographics. The intention was to ensure minimal interference from ancillary processes and hardware. Data acquisition (DAQ) from machine tools has high value, as highlighted by the rise in popularity of Industry 4.0 (see Chapter 2). Systems aiming to exploit said value have been increasing over the last decade; however, it should be noted that such systems and approaches are (and should always be) secondary to the machining process. Therefore, it is expected that data solutions should be minimal and integrated within the machine tool and NC where suitable. This Chapter outlines the necessary information required to enable optimised communication between NC units and an external PC. This builds on the applications introduced in Chapter 3 and is organised into three primary sections:

### **Data acquisition and initial processing**

Considers the development and implementation of enabling technologies, introducing the embedded tool wear DAQ system and the initial organisation of process data. The section details the communication standard between the NC and a PC. Specific attention is given to the details of the PAc DAQ program.

### **Eliciting process features**

Introduces the novel density evaluation and separation (DENSE) algorithm. This was developed to enable process identification without prior knowledge of the machining cycle. The DENSE application was developed as a proof of concept post-processor and indicates the necessary steps needed to make system data manageable.

### **Converting unsuitable data**

Of the process data generated herein, it was identified that the motor load signals as acquired were found wanting. In response, it was identified that many of these signals may be converted into a usable state using the appropriate motor characteristics. Novel stages are considered to enable the conversion of quantised spindle and axis load signals into energy curves.

## 4.1 Data acquisition and initial processing

Following configuration of both the COMX and the CifX-B and enabling of the communication network between the two, the control data (herein referred to as “MTData”) must be made available by the OEM. In this research project access to “internal” MT controller functions was enabled with

the collaboration of Mazak, the OEM. It should be noted that, unless otherwise stated, all of the procedures and functions outlined here in were designed by the author. Where necessary requests were submitted to the OEM for access to a required signal and/or data source. Making the MTDData available is essentially a process of forwarding the contents of specific registers (determined by the PLC software) to the on-board memory of the COMX as a 480 byte string variable. The number of accessible registers is limited over concerns with the potential impact on the ordinary operation of the NC. In this implementation the MTDData is made available by the NC every 0.0284 seconds (35.2Hz). Access to the MTDData is enabled by the COMX at a reduced rate of 10Hz (100ms between samples), again due to concerns with the performance of the NC under load. An overview of the process logic is given in Figure 4.1.

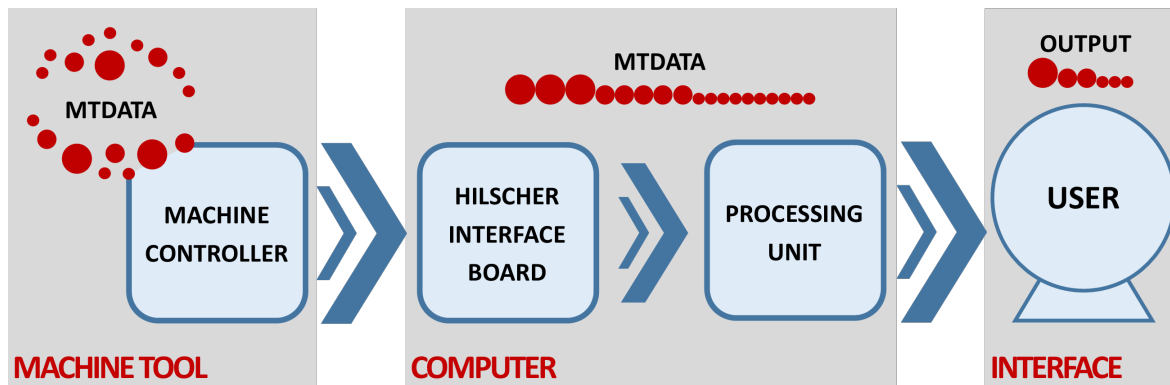


Figure 4.1. High-level outline of the communication process

The MTDData is effectively the closed-loop information, available to the NC, which enables process control and an “intelligent” response to changing process conditions. The accessible information includes typical machine parameters, including the machine feed rate, spindle rotational speed, machine temperatures, etc. All parameters are derived from internal pre-installed sensors, identified by the OEM as beneficial in the typical control, usage and/or maintenance of the machine. As no additional machine volume needs to be sacrificed for retrofit sensors, this is a highly valuable approach to monitoring machine tools.

The author-specified MTDData was transferred from the controller to the user over the EIP network for collection in the external PC. Data was acquired from the local memory of the CifX-B by implementing a modular program (written by the author in procedural programming language C), designed to communicate with the board. The developed program was named the Parameter Acquisition and Monitoring Application (herein shortened to PAc). The application was designed to alternate between two primary modes, data acquisition and data processing. Within these two modes, primary functions included:

- Establish communication with the NC - either continuously, or at the start of processes
- Establish data structs to contain parameter information
- Obtain each parameter from the NC and handle errors as necessary - should individual parameters fail, purge all for current time step and note error

- Append parameters to local memory – recommended in comma separated variable (CSV) format for live access
- Close communication connection with NC.

Secondary functions (implemented separately) included:

- Reduce local files by removing unnecessary data
- Compress data files to allow for efficient network transfer
- Create/update log files to promote system traceability.

Secondary functions would benefit the system if implemented within the PAc structure but are not necessary to ensure proper functionality. Primary functions are further defined in latter sections. The simplified program logic is presented in Figure 4.2. The figure outlines the overall structure of the PAc real-time Ethernet (RTE) application developed to facilitate communication between the MT and the attached PC. An expanded outline of the process is provided in Appendix A.2 and additional detail of the process logic is provided in Appendix D.5.

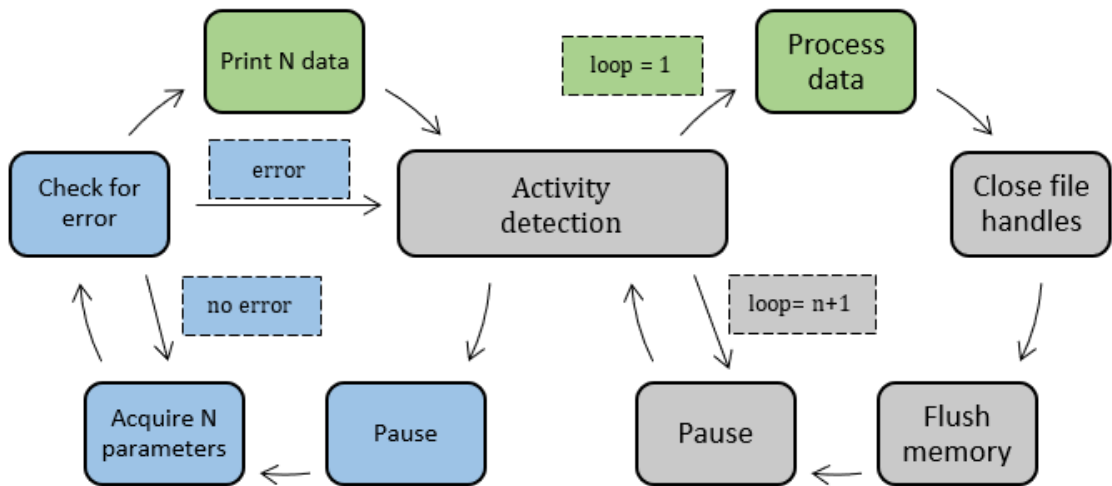


Figure 4.2. Process logic illustrating activity detection (grey), DAQ (blue) and processing (green)

#### 4.1.1 Activity detection

The first of the primary functions was activity detection. The program checked the VMC for activity and initiated DAQ when appropriate. Activity detection was centred on the initiation within the MT controller of a suitable part program. When a program enabling the manufacture of a part was detected the DAQ began. The running of a part program was proven as the basis for the process check as it was found to be suitable as a solitary input. Most other inputs require additional arguments to find the action of an entire process. Two examples are the rotational speed of, and the load on, the main spindle. The movement of the spindle may show an active process; however, the sensor will also detect rotation when the spindle is manually rotated by an operator (this can result in false positive actions). Equally, basing a process on the rotation of a spindle must assume that the spindle rotation

will drop to zero when the process is complete. For a complex process it should be expected that the spindle rotation will drop to zero several times. On the other hand, when a load is detected on the spindle a process must be occurring and it must be more than manual rotation of the spindle. However, it will also be the case that certain cutting operations, for example cutting with optimised parameters, may register negligible load. These processes will therefore become false negatives. It should also be noted that the two spindle inputs are not complementary - use of both will afford the same limitations.

Therefore, the decision would be that both the spindle rotation and the spindle load would *not* be suitable inputs for detecting an active process as more signals would be needed to properly frame the process. The part program on the other hand should begin at the start of the process and will continue until the process is complete. There are, however, still limitations to using the part program. These limitations include:

- Macro-programs or linked programs may cause start/stop behaviour. This can be mitigated by preventing a new process being registered if an earlier run was within a defined (short) period. However, this may be challenging when two separate processes are run without much downtime between as they may be mistakenly combined into a single process.
- Monitoring the part program will include all the non-contact processes, including tool changes, tool setting, part and tool probing, general machine movements and tool and material loading. This will bloat the MTDData file and will introduce signals that do not relate to the condition of the cutting tool. Whilst the additional data will be beneficial for diagnosing machine condition, the signals must be filtered out to prevent any impact on the evaluation of cutting tool condition.

The enactment of activity detection can be appraised through simplified extracts from the developed PAc program, herein referred to as pseudo code (Figure 4.3).

```

while (!_ACTION) {
    SUM_OF_PARTS = 0;
    RETURN = xChannelIORead(HANDLE, AREA, OFFSET, SIZE, PART1, TIMEOUT);
    if (CIFX_NO_ERROR != RETURN) {
        RETURN = ErrChk(RETURN, CLOCK);
    }
    ...
    SUM_OF_PARTS = PART1 + PART2 + PART3;
    if (SUM_OF_PARTS > 0) { /* START DAQ CYCLE */
        /*
        ACTION      = LOOP CONTROL - DETECT USER INPUT
        RETURN      = ERROR NO. IF UNSUCCESSFUL, OTHERWISE CIFX_NO_ERROR
        HANDLE      = CHANNEL HANDLE (DEFAULT ZERO)
        AREA        = READ AREA (DEFAULT ZERO)
        OFFSET      = OFFSET FROM START
        SIZE        = STRING LENGTH TO READ
        PART#       = TARGET DATA ARRAY
        TIMEOUT     = ALLOWABLE (MAXIMUM) DELAY
        CLOCK       = TIME STAMP FOR ERROR TRACEABILITY
        */
    }
}

```

Figure 4.3. Pseudo code illustrating implementation of activity detection

The pseudo code replaces variables with placeholders in an attempt to make it easier to understand. Repetitive lines of code are removed and denoted by ellipses. The activity detection was enacted before, and within, the DAQ stages of the program to find when the process began and when the process ended. The implementation consisted of three CIFS API calls to xChannelIORead. The process was split in three parts to accommodate the three offsets that make up the output for program execution. Each of the xChannelIORead calls is followed by a call to the ErrChk function IF the API call fails (discussed in Section 4.1.4). IF the API call does not fail the program starts the DAQ cycle (discussed in Section 4.1.2). The pseudo code provided in Figure 4.4 indicates the process management steps taken when process activity has been detected. Following the DAQ cycle (when the process has ended)

```

/* CREATE DATA FILE NAME BASED ON CURRENT DATE & TIME */
NOW = time(NULL);
localtime_s(TIME, &NOW);
strftime(String, SIZE, FORMAT_STRING, TIME);

strcpy(NAME, ABBREV);
strcat_s(NAME, SIZE, String);
...

/* OPEN THE DATA FILE (APPEND) */
FILE = fopen(NAME, TYPE);
if (FILE != NULL) {
    /* UPDATE & RE-FORMAT TIME */
    ...
    /* CREATE FILE HEADER */
    fprintf(FILE, FORMAT_STRING);
    ...
    /* CREATE CONSOLE HEADER */
    printf(FORMAT_STRING);
    ...
    /* RESET ERROR RETURN & OBTAIN TIME1 & TIME3 */
    TIME1 = GetTickCount64();
    TIME3 = TIME1;
    RETURN = CIFS_NO_ERROR;
    printf(FORMAT_STRING);

    /* COLLECT DATA UNTIL PROGRAM END */
    while (!ACTION && RETURN != PROCESS_STOP) {
/*
ACTION           = LOOP CONTROL - DETECT USER INPUT
RETURN           = ERROR NO. IF UNSUCCESSFUL, OTHERWISE CIFS_NO_ERROR
NOW              = CURRENT TIME (UNFORMATTED)
TIME             = TIME STRUCT
STRING           = CHARACTER ARRAY
SIZE             = LENGTH OF CHARACTER ARRAY
TYPE             = FILE ACCESS TYPE (READ/WRITE/APPEND/ETC)
FILE             = DATA FILE (CSV)
NAME            = FILE NAME STRING
FORMAT_STRING    = STRING CONTENT AND FORMAT -> "CONTENT %s"
TIME1           = INITIAL TIME (TICK) FOR TOTAL PROCESS
TIME3           = INITIAL TIME (TICK) FOR EACH TOOL
*/
}

```

Figure 4.4. Pseudo code illustrating inter-process management

further process management steps are taken to reset the process, flush the input stream and restart the activity detection. These steps distinguish between each process and allows for the monitoring of subsequent, or end-to-end processes, without needing human intervention. This prevents data-loss from missed processes without combining, or stringing together, similar or subsequent cycles. Separating each process, or program, within a cycle allows the previous cycles to be processed whilst the current cycle is being monitored. This optimises both the time and data management of the

acquisition process.

### 4.1.2 Data acquisition

It has been identified that the MTData was made available as a 480 byte string variable. This was accessed in 8-bit byte segments to match the organisation of information within the string and to separate the data into manageable chunks. This concept is illustrated in Figure 4.5.

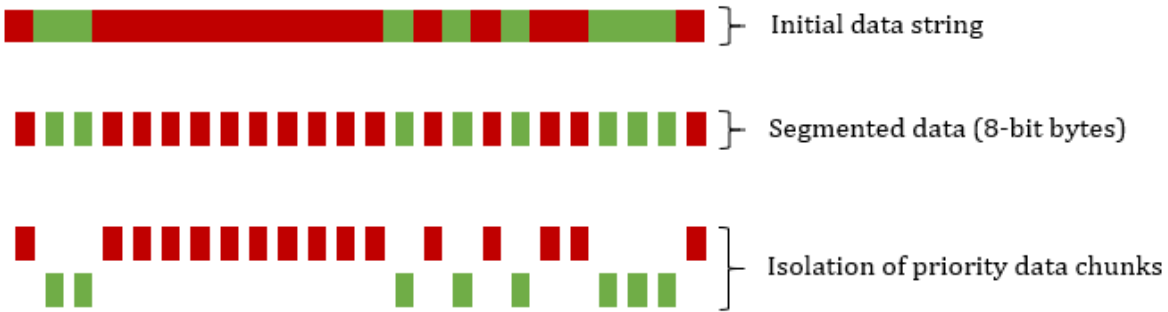


Figure 4.5. MTData string-output composition

Data is then nominally acquired using the previously identified xChannelIORead API. These calls are nested within an IF-ELSE structure to prevent collection of partial data sets (see Figure 4.6). When an error occurs the current stream is flushed and the process returns to the first IO variable (IO 1).

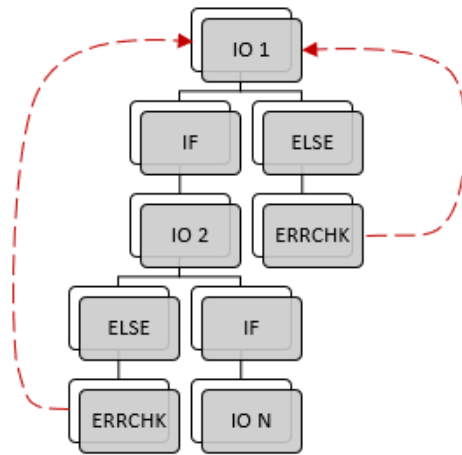


Figure 4.6. IF-ELSE DAQ logic

IF no error occurs, the program continues until all IO variables have been collected (IO N). This approach ensured complete data sets at each time interval. It is noted that partial data sets would cause confusion in latter processing stages due to discrepancies between each parameter when viewed or analysed separately. It is also noted that, by discarding the entire time interval, when variables are missing the missed data can be identified by the perceived variation in the sampling frequency. This may assist in subsequent “syncing” of data sets, when setting them up for comparison. Following successful acquisition of all variables, the program checks the tool in use, the usage times (according to

the PC) and filters the data according to the resolution of the system Tick using the GetTickCount64() function (specific to the windows platform). The implementation of this is demonstrated using the pseudo code provided in Figure 4.7. Data is then passed to the eject function for integrated processing and to be stored locally to the PC (see Section 4.1.3).

```

if (ACTION != 0) {
    /* CHECK CURRENT TOOL */
    if (CURR_TOOL != PREV_TOOL) {
        ...
        PREV_TOOL = CURR_TOOL;
    }
    /* CHECK USAGE TIMES */
    TIME2 = GetTickCount64() - TIME1;
    ...
    /* PASS NON-REPETITIVE DATA TO EJECT FUNCTION */
    if (TIME2 != TIME_CHECK) {
        eject(FILE, TIME2, CURR_TOOL, DATA);
        ...
    }
    /* UPDATE TIME_CHECK */
    TIME_CHECK = TIME2;
}
else { /* ELSE STOP ACQUISITION */ }
/*
ACTION      = ACCESS CONTROL - IF ZERO CODE IS NOT EXECUTED
CURR_TOOL   = READ AREA (DEFAULT ZERO)
PREV_TOOL   = OFFSET FROM START
TIME1       = STRING LENGTH TO READ
TIME2       = TARGET DATA ARRAY
TIME_CHECK  = TIME STAMP FOR ERROR TRACEABILITY
FILE        = DATA FILE (CSV)
DATA        = ALL ACQUIRED DATA - INC. TOOL AND USAGE TIMES
*/

```

Figure 4.7. Pseudo code illustrating time-specific data filtering

The OEM made the key parameters available through the COMX interface as requested, but of the available data not all has value in determining the health of the cutting tools. An example of this is the temperature of the primary spindle. Whilst important in the overall health monitoring of the MT, the temperature of the spindle has no significant use for the diagnosis of cutter health. As all parameters may be acquired for future cycles there is no pressing need to acquire all signals all the time. Therefore, to reduce the necessary storage capacity and to reduce the requested packet sizes only parameters deemed by the author to be immediately important are acquired from the MT. The list of parameters deemed to be important does change as the understanding of the process changes, therefore those acquired per test also changes. The full register audit (carried out by the author) is provided in Appendix E.2. This was provided to the OEM to inform and support subsequent developments. Table 4.1 indicates the parameters that were identified as having the most value for the evaluation of cutting tool and/or process health. Priority scales are indicated in Figure 4.8. The tests for which each were acquired are additionally indicated in the experiment log (located in Appendix E.1).

Parameter priority values indicate the relative importance of each variable (A-C) and the sampling frequency weighting (1-4). A frequency rating of 1 indicates that continuous sampling is of most benefit, whilst a sampling frequency of 4 indicates that infrequent sampling will be enough in most cases. This could (for future implementations) be exploited to maximise the performance of such

Table 4.1. Key process parameters

Parameter	Abbreviation	SF / Unit	Priority
Tool No.	Tn	1 / —	A4
Spindle rotational speed	SRS	0.001 / rpm	B1
Resultant feed rate	RFR	0.1 / mm.s <sup>-1</sup>	C2
Tool usage time	Tt	0.001 / s	B4
Spindle 1 motor load	SML	1 / %	A1
Axis 1 motor load	XML	1 / %	C1
Axis 2 motor load	YML	1 / %	C1
Axis 3 motor load	ZML	1 / %	C1
Axis 1 position	XP	0.0001 / mm	B1
Axis 2 position	YP	0.0001 / mm	B1
Axis 3 position	ZP	0.0001 / mm	B1

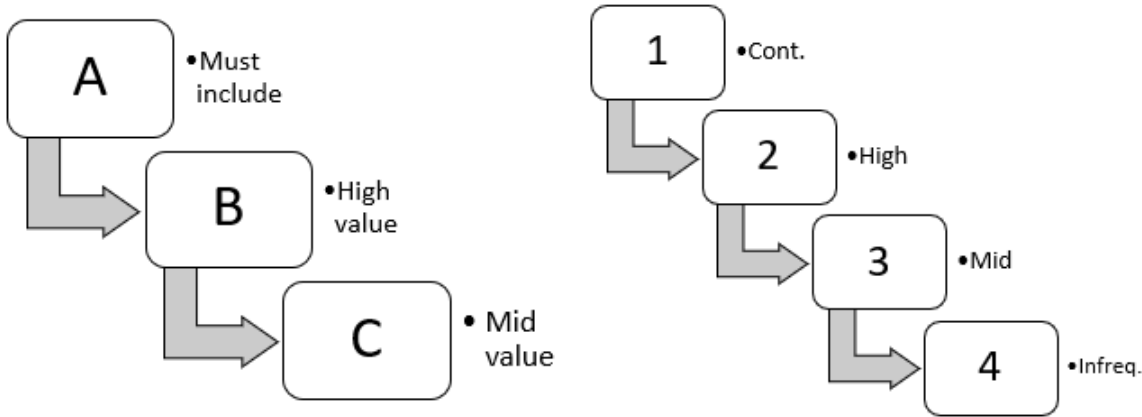


Figure 4.8. Priority scales

applications and to increase the overall average of the sampling frequency. However, it is still suggested that continuous sampling should be limited to the fastest appropriate RPI to avoid unnecessary pressure on the PC, or the NC (for integrated systems) CPU.

The system must acquire the key process parameters from suitable sources within the MT architecture. Where data is available in a semi-processed form, this should be prioritised over other locations. The method of acquisition will ultimately depend on the parameter in question. The rate of acquisition should depend on the process speed and on downstream functionality. Where sampling frequency must be compromised against sample precision it is recommended that an assessment into the merits of each is undertaken to find an appropriate balance. This was discussed in Chapter 2.

### 4.1.3 Integrated processing

Most of the MTData processing was developed to prove such concepts were suitable for the data acquired during this study. As such, much of the processing was written in separate programs, using separate development systems, and enacted at various times in the process cycle. However, it was

found early on that some of the processing steps would help the user and improve the overall process effectiveness if they were implemented at certain stages within the process cycle. This included the primary conversion of the MTData from segmented 8-bit bytes of information, into each of the targeted process parameters. This was enacted here to simplify the data files and to bring a necessary processing stage into the acquisition of the data, thus consolidating the processes. The pseudo code is given in Figure 4.9. The figure illustrates the initial processing for the time, X-position data and for the RFR, SRS and SML.

```

TIME = TIME / FLOAT1;
...
if (POS[3] != 0) {
  XPOS = ((255 - POS[0]) + ((255 - POS[1]) * 255) + ((255 - POS[2]) * 255 * 255) +
  ((255 - POS[3]) * 255 * 255 * 255)) / FLOAT2;
}
else {
  XPOS = (POS[0] + (POS[1] * 255) + (POS[2] * 255 * 255) + (POS[3] * 255 * 255 *
  255)) / FLOAT2;
}
...

RESULT2 = (IN2[0] + (255 * IN2[1]) + (255 * 255 * IN2[2])) / FLOAT3;
RESULT3 = (IN3[0] + (255 * IN3[1]) + (255 * 255 * IN3[2])) / FLOAT4;
RESULT4 = (IN4[0] + (255 * IN4[1]) + (255 * 255 * IN4[2]));

// PRINT FORMATTED DATA TO SCREEN & FILE
fprintf(FILE, FORMAT_STRING, TIME, TOOL, TIME, RESULT2-4, XYZ_LOAD, XPOS, YPOS, ZPOS);

printf(FORMAT_STRING, TOOL, TIME, RESULT2-4);
/*
  TIME           = TIMER TICK VALUE (PROCESS AND/OR TOOL)
  POS            = AXIS POSITION VALUE
  FLOAT#         = VARIABLE FLOAT VALUE (TO GENERATE DECIMALS)
  RESULT#       = PROCESSED DATA (SML/RFR/SRS)
  TOOL          = CUTTING TOOL ID NUMBER
  XYZ_LOAD      = XYZ LOAD DATA (INTEGER PERCENTAGES)
  IN#          = ACQUIRED (RAW) DATA (SML/RFR/SRS)
  FILE         = DATA FILE (CSV)
  FORMAT_STRING = STRING CONTENT AND FORMAT -> "CONTENT %s"
*/

```

Figure 4.9. Pseudo code illustrating initial processing

Each byte is 8-bits (ISO 2382-1:1993), with a value of 0-255 and a range of 256, or  $2^8$ . The string size of 480 bytes indicates that up to 480 registers could be made available; however, not all registers occupy a single byte of memory. For example, the “total switched on time” for the MT requires 4 bytes of memory. This allows a maximum integer value of  $255 \times 255 \times 255 \times 255$  or  $255^4$ . It is thus estimated that 150 MT parameters have been made available, although it is noted that not all will be active for any given MT. The VCS considered in this study has only one spindle, however, registers for eight spindles are made available as standard (see Appendix E.2). This indicates that the available registers should be tailored to each machine rather than being a standard list applicable to all MT units.

For registers that required multiple bytes for their output, the original value needed to be re-calculated from each byte. This process was indicated in the pseudo code (Figure 4.9). It is noted that the axes positions (X, Y and Z) were output as negative values. It is known that bytes cannot represent negative values; and it was identified through initial investigations that the X, Y and Z results were incorrect when processed in the same way as positive registers. Hence, they were handled by inverting

the approach and calculating *away* from 2554. There was still some conversion error (for X 0.78%, for Y 0.00%, for Z 0.39%) measured in-process by comparing the controller stated spindle position with the X, Y, and Z axis positions acquired using PAC; however, the result was improved. Figure 4.10 shows the difference between the two methods of processing for the X and Y axes, indicating that both accuracy and precision were improved by altering the approach.

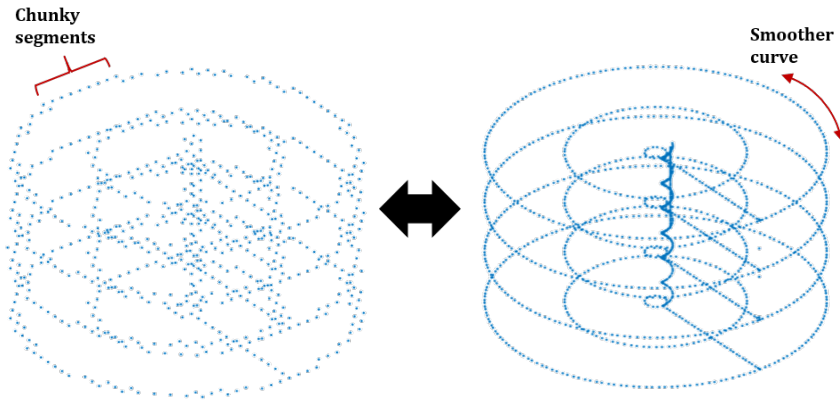


Figure 4.10. Comparison of XYZ before and after correction of byte processing (axes omitted)

To achieve decimal values, the precision was achieved by dividing the integer value by the necessary float amount. For example, a resultant feed rate of  $120.1\text{mm}\cdot\text{s}^{-1}$  was achieved by dividing the provided integer of 1201 by 10.0.

#### 4.1.4 Error handling

The primary error handling was enacted by the ErrChk function. The function was written to log each error and then return to the previous function. The ErrChk function can be found in Appendix A.1. It is noted that the error was saved with both the error code and the date and time of the occurrence. When an error occurred multiple times or occurred constantly for a period (e.g. if the Ethernet cable disconnected from the PC), the first instance of the error would be recorded along with the final instance of the error. This provided the duration of an error, without logging infinite errors and filling the PC memory. The errors are logged to enable engineers processing the data to separate anomalies that arise from the communication of data from any anomalies that arise from the process. This will prevent false positives.

#### 4.1.5 Files and storage

It has been mentioned that the PAC program has been developed as a proof of concept. Nevertheless, even prototypes must prove that such systems, or similar systems, will be robust enough to cope with the rigour of real-world use. One significant consideration for TCM is the created data sets and the space that these large data sets require. It is thus necessary to consider the impact that the created data sets will have, and to optimise the generated data to avoid unnecessary waste. This will prove

that the developed system is robust and, in keeping with the main aim of reducing process waste, will reduce the “digital waste” generated.

One approach would be to reduce the number of acquired parameters, avoiding any that have no immediate value. This will reduce file sizes to a degree; however, the most value lies in optimising the sizes such that multiple parameters may be acquired. It was consequently established that the file sizes varied considerably due to variation in:

- sampling frequencies
- number of acquired parameters
- parameter precision
- general complexity of the created file structure
- file formatting
- time taken by each process
- processed state of each parameter

Over time most of the above variations were controlled to reduce the overall file sizes. Initial files were approximately 250MB for a one-hour process, despite acquiring only three parameters. The large file sizes were primarily due to excessive sampling, inefficient file structures and the parameters being unprocessed. It was acknowledged that 250MB per hour was unsustainable and could not be transferred to continuous manufacturing processes as the increased number of processes would rapidly overwhelm even generous storage solutions. This would substantially affect the cost of implementation.

In response, the file output was changed to CSV with ASCII encoding and the sampling frequency of the program was controlled to match the MT output. Also, each of the parameters were pre-processed where possible (see Section 4.2), the file structure was simplified, and unnecessary rows were removed. This resulted in the same one-hour process, acquiring 12 parameters, achieving a file size of approximately 10MB. This indicated a 96% reduction in the file size. To put this in perspective, it would herein be possible to monitor a continuous manufacturing process for 24 hours, with the resulting files taking up less storage than the unoptimised version required for just one hour. It is noted that this may be improved further; however, the system would, in the current state, be capable of monitoring a continuous manufacturing process. This would no longer raise concerns with the resulting output other than for analysing the cutting tool and process health.

## **4.1.6 Limitations**

### **4.1.6.1 Memory**

The local memory of the Matrix 2 NC is assumed to be less than 500 MB. This severely limits the extent to which data can be stored locally. Obtaining 12 parameters at 10 Hz results in 0.6 kB.s<sup>-1</sup>. This would reach the estimated capacity within 176 hours (assuming 80% available capacity, 20% native applications and/or programs). It is assumed that data will be transferred across a network to local,

regional, or cloud storage for archiving and/or processing. It should be an option to save temporary data to the local memory, however, the default setting should be to delete local data following each process. It would be advised that the local capacity is monitored (if possible) to prevent storage of excess data (to the detriment of the MT). When capacity is reached data should be purged or transferred to an appropriate medium (if chosen by the user). If no user is available data should be purged by default.

#### 4.1.6.2 Sampling frequency

It is assumed that the application can realistically achieve a sampling frequency of 10 Hz minimum. Increasing the sampling frequency may be possible in future applications; however, was limited herein due to the potential to disrupt the ordinary control and operation of the machine tool. Justification should be sought for frequencies below this threshold. Achievable frequencies greater than the threshold should be identified for individual parameters to facilitate faster data acquisition when warranted.

#### 4.1.6.3 Implementation

It is noted that the current implementation of the PAc program has been designed to cope with the existing (limited) access to the MT architecture. The software has been designed to prove that the available data has tacit value for the evaluation of both cutting tool and process health and behaviour. It is accepted that the implementation is perhaps also limited; however, future proponents of this technology could, and should, expect integration within the controller. OEMs that deliberately avoid sensible approaches for accessing such data will inevitably set themselves behind their competition as their offering will have limited appeal.

## 4.2 Eliciting process features

Diagnosing variation within manufacturing cycles requires a detailed knowledge of the machined features. Such knowledge allows for the isolation of individual features which helps with any subsequent analysis of the process and control data. Having no knowledge of the machining process *will* increase the uncertainty attributed to the identification of significant system variability. Any ability to detect subtle changes will be eliminated entirely.

In addition to the above points, limited process knowledge restricts the ability to trim available data to remove machine movements, outliers, sub-processes and similar, all of which may negatively affect any decisions based on the process and control data. Machine tools employ rapid table movements between operations, thus reducing the overall process duration. These rapid movements put additional strain on the axes motors, resulting in artificially high observed loads. Similarly, adjustments to the rotational velocity of the machine tool spindle will result in spindle load outliers. Typically, these adjustments are enacted whilst offset from the machined component to ensure appropriate cutting conditions are employed for the actual machining process. These activities, herein referred to as “non-cutting activities”, are entirely necessary during the operation of a MT; however, the resultant process data from such activities is not relevant to the assessment of cutting tool health.

It can thus be seen that isolating each of the actual cutting processes from non-cutting activities within the overall machining process is important. Such an approach will enable engineers to better appreciate the conditions more likely to have been encountered by the cutting tool, rather than the conditions most likely being encountered by the entire VCS. In practice this is implemented by applying domain knowledge to the resulting process and control data. This requires a competent individual, holding the relevant knowledge, to separate each process manually. This consumes significant money, time and resources, hence proving unpopular to industrial organisations. However, the approach is necessary when introducing unknown or new components. Advances in virtual systems allow this process to be applied on a larger scale, costing less money, time and resource. This requires the virtual machine to consider each phase of the process and determine the feature by comparing the physical process to the virtual process. If the physical process differs from the virtual process, as a result of intrinsic differences, the approach is likely to fail. The approach is also not cost effective in the case of one-off or unique components.

#### 4.2.1 Innovation

This indicates that an improved approach is required to elicit process features, particularly for instances in which the process is unknown, new, or a one-off. It is also acknowledged that any approach must be computationally simple. The system will need to run in tandem with the DAQ process, as well as any other data processing stages. In response, herein is presented an innovative method for isolating the manufactured component within the working volume of a MT. The author hypothesises that the machining process may be determined by considering the relative densities of the controlled axes positions. The main assumption being that the process density shall be greatest during the cutting process due to the reduced movement and the prolonged contact time required for the effective removal of material. It is further assumed that the process density can be *approximated* as a normal distribution (Figure 4.11).

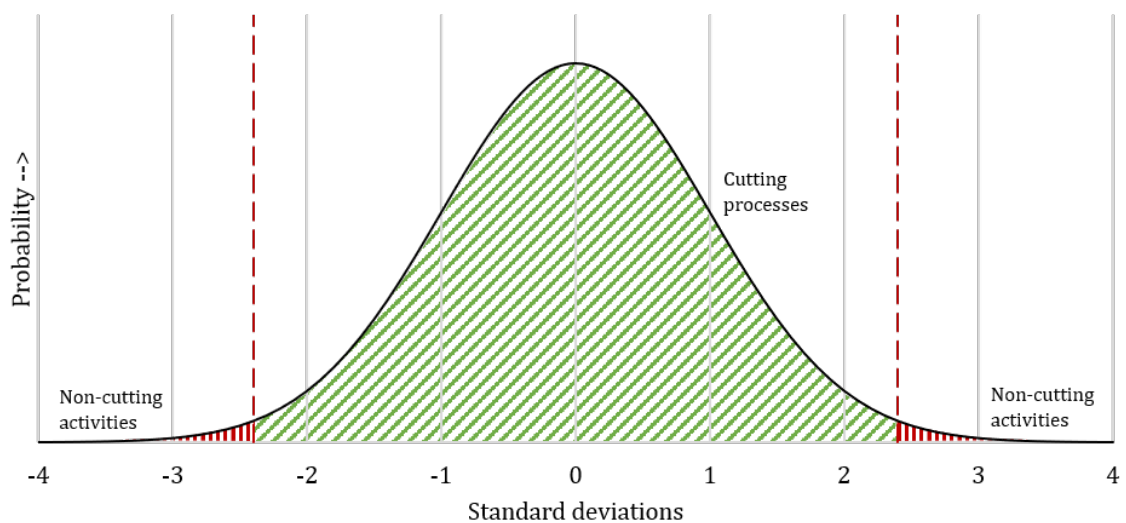


Figure 4.11. Normally distributed DENSE theory for cutting process

The body of the distribution should pertain to the cutting process whilst the tails of the distribution will represent the instances during which cutting does not occur. The proportion of the process contained within the tails of the distribution will be process dependent. It is acknowledged that this would require partial intervention by an Engineer to establish the likely limits. This could be following an initial production run, or during the low-volume feasibility studies, from which one set of results can be used to establish the best process distribution. It is also sensible for the process distribution to be updated as the process history is developed.

Every time a process is completed, the acquired data enables engineers to establish whether the currently applied distribution is effectively capturing the entire process. If sections of the process are missing, the distribution may be adjusted to capture a greater percentage of the output. Similarly, it may be established that too much of each process is being captured. The distribution would then be adjusted to capture a reduced percentage of the output. The distributions would then be applied to all appropriate axes (not all distributions will be equivalent) to locate the machined part within the working volume of the VCS.

#### 4.2.2 Implementation

The author developed the DENSE algorithm to take process-generated data, analyse the individual coordinate densities and return the features identified to be the machining process. This is a novel approach for locating the machined part from the X, Y and Z axis feedback. The full DENSE program, written using MATLAB script, can be found in Appendix A.3. Figure 4.12 shows the high-

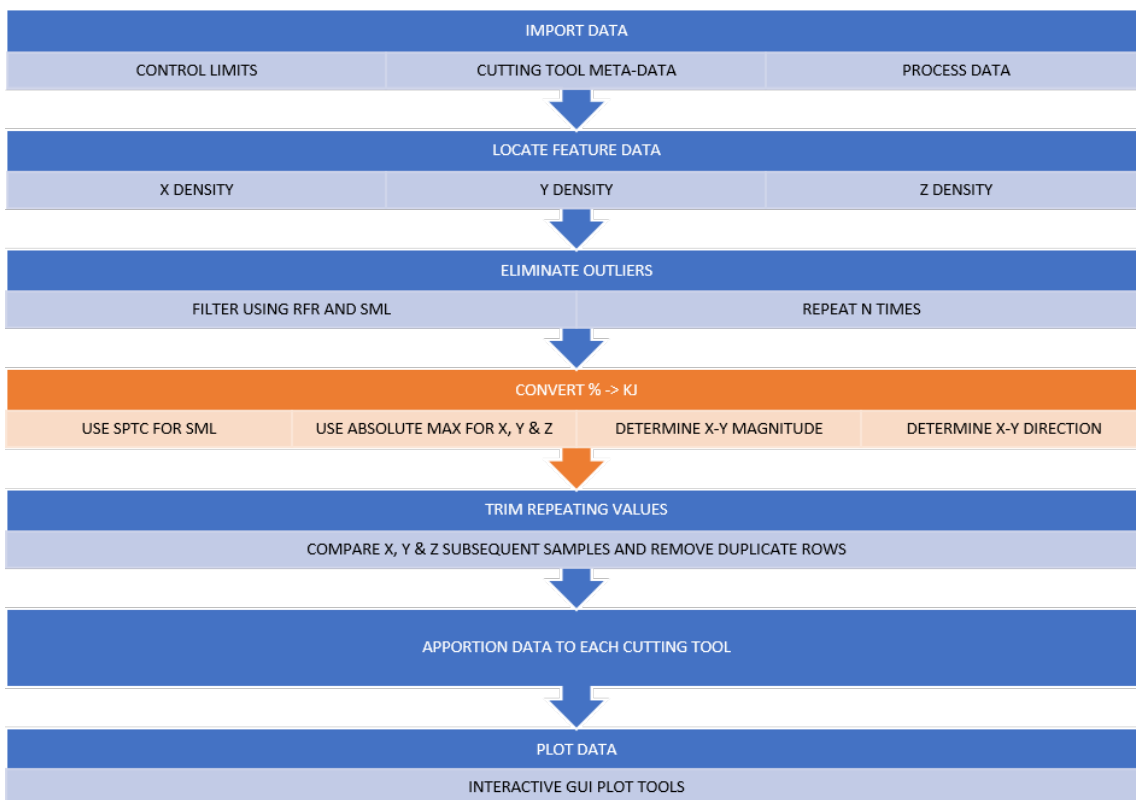


Figure 4.12. Simple linear structure diagram for DENSE

level program logic. It is noted that the fourth part of the program “Convert % – > kJ” is highlighted. Whilst the fourth part is built into the DENSE algorithm, it is not required to isolate the machined part within the machine volume. The conversion of MTDData parameters from percentages into energy is a novel development that will be discussed in Section 4.3.

#### 4.2.2.1 Import data

First the process definitions are identified. This includes the pre-established control limits for the best-fit process distribution and the cutting tool metadata. An indication of the definition file is provided in Figure 4.13.

CL#,,,,,	Specific control limit search term
0.008,,,,,	<b>X, Y, Z non-cutting percentages</b>
0.01,,,,,	
0.02,,,,,	
TI#,,,,,	Specific tool info. search term
1,X000XX00,0,*****,,0,0,UNK	<b>Tool information</b>
2,H008SD01,1,SLOTDRILL*,136,12,USE	
3,H008SD02,2,SLOTDRILL*,136,12,USE	
4,C900SD01,0,SPOTDRILL*,115,6,USE	
5,X000XX00,0,*****,,0,0,UNK	
6,X000XX00,0,*****,,0,0,UNK	
7,H058SD03,0,SLOTDRILL*,110,8,USE	
8,H008SD04,3,SLOTDRILL*,136,12,USE	
9,X000XX00,0,*****,,0,0,UNK	
10,X000XX00,0,*****,,0,0,UNK	
11,X000XX00,0,*****,,0,0,UNK	
12,C853CD01,0,CARBDRILL*,134,2.6,USE	
13,X000XX00,0,*****,,0,0,UNK	
14,X000XX00,0,*****,,0,0,UNK	
15,X000XX00,0,*****,,0,0,UNK	
16,X000XX00,0,*****,,0,0,UNK	
17,E800CD02,0,CARBDRILL*,154,4.3,USE	
18,X000XX00,0,*****,,0,0,UNK	
19,X000XX00,0,*****,,0,0,UNK	
20,X000XX00,0,*****,,0,0,UNK	
21,F363GC01,0,GROOVING*,122,12,USE	
22,E616CD03,0,CARBDRILL*,139,2.8,USE	
23,E801CD04,0,CARBDRILL*,143,3.3,USE	
24,D635TM01,0,THREADMILL,120,12,USE	
25,D806RC01,0,RIPPER****,155,16,USE	
26,E950TM01,0,TAPERMILL*,130,12,USE	
27,X000XX00,0,*****,,0,0,UNK	
28,X000XX00,0,*****,,0,0,UNK	
29,X000XX00,0,*****,,0,0,UNK	
30,X000XX00,0,*****,,0,0,UNK	

Figure 4.13. Screen capture of omidef.dat

Figure 4.13 indicates the estimated X, Y, then Z values for the non-cutting activities of the OMI body application. These are treated as control limits, or threshold values. It is noted that the value for  $X < Y < Z$ . This will be influenced by the relative part dimensions. Following the X, Y and Z control limits, the cutting tool metadata provides all the necessary information required for cataloguing each tool and for appropriating the correct process data to each tool. The cutting tool metadata should be available for all processes as the VCS could not successfully operate without knowing what tool is necessary for which operation. The VCS requires basic information to complete each operation, including the diameter and length of each cutting tool. This information may not be explicitly available prior to a process, as there may be pre-process stages during which the cutting tools are evaluated. This is

more likely to be the case for processes incorporating ICG. Nevertheless, this information could (and should) be made available from the ICG output. Alternatively, the information may be added later in the process if the end-user is happy to delay the post-processing. When the process definitions have been imported, the MTData can be imported. An extract from the MATLAB script is provided in Figure 4.14.

```

for szR = 1 : size(fName,2)
    fID = fopen(fName{szR}, 'r');
    datArr = textscan(fID, '%s%s%s%s%s%s%s%s%s', inf-9, ...
        'Delimiter', ',', 'EmptyValue', 0.0, 'HeaderLines', 9, 'ReturnOnError', 0);
    fclose(fID);
    OArr{szR,1} = cat(2,datArr{:,:});

    % -Check for bad data
    bad = find(contains(OArr{szR,1}(:,1), '*H80C4*'));
    tmp = zeros(size(OArr{szR,1},1),12);

    if isempty(bad)
        tmp = cellfun(@str2num,OArr{szR,1});
    else
        tmp(1:bad(1)-1,:) = cellfun(@str2num,OArr{szR,1}(1:bad(1)-1,:));
        for N = 1:size(bad,1)-1
            tmp(bad(N)+7:bad(N+1)-1,:) = cellfun(@str2num, ...
                OArr{szR,1}(bad(N)+7:bad(N+1)-1,:));
            pb.Message = 'Removing bad data...';
        end
        tmp(bad(end)+7:end,:) = cellfun(@str2num,OArr{szR,1}(bad(end)+7:end,:));
    end

    tmp(tmp(:,1)==0,:) = [];
    OArr{szR,1} = tmp;
    pb.Message = 'Loading data...';
end

```

Figure 4.14. MATLAB script for importing process data

An example graphical user interface (GUI) is demonstrated in Appendix D.2 to illustrate the use of the system for diagnostic process evaluation. It is anticipated that if such a system was implemented in real-time, a GUI may be unnecessary as the process would benefit if implemented as a background process, cleaning up the data as it was generated. The sample code snippet provided imports an entire CSV file. This assumes that the process has finished and is therefore diagnostic or semi real-time, rather than real-time. However, the theory could be implemented in real-time if desired, simply by accessing the data file intermittently. It is noted that to facilitate such a change may require the implementation of additional stages. This would ensure that variation in the relative weighting of the non-cutting process movements remains comparable to the weighting of the actual cutting processes. It should be noted that the for-loop facilitating the data import includes a check for “bad data”. This check is included to remove any instances in which the file header is repeated. When PAC misidentifies a finished process, it can exit to the monitoring phase. When the process is re-identified this will automatically create a new file header within the existing process data file. These additional headers do not process well during later stages of the DENSE program. It therefore makes sense to remove this “bad data” at the earliest opportunity to prevent downstream issues. The file header is easily located within each data file due to the inclusion of the specific search string \*H80C4\*. This approach reduces the overhead required to find each unnecessary file header at the cost of an additional row within the file. As the files are ASCII CSV files, this additional row adds approximately eight bytes to the required file size per recurrence.

#### 4.2.2.2 Locate feature data

When the data has been imported and the bad data has been removed the resulting data set is stored in active memory. Any on-machine probe data is then removed for separate evaluation. This is not currently utilised, however it retains value as it may enable a crossover between MTData and ICG systems. Figure 4.15 indicates the necessary script and includes the instructions for the “metadata plots”. The plots would not, at this stage in the program, have any content; however, to consolidate the process interruptions, and therefore optimise the process, the necessary objects are generated outside of the actual data processing loop.

```
% -Allocate each set to datArr
datArr = cat(2,OArr{sLp,1}(:,1:9),OArr{sLp,1}(:,10:12) .* Mult);

% -Ignore probe data
tmp = cell(30,1);
tmp{30,1} = datArr(datArr(:,2)==30,:);
datArr(datArr(:,2)==30,:) = [];

% -Request metadata plot
if strcmp(opt,'YES') == 1
    set(0,'CurrentFigure',axB);
    bulim = (mod(szR,2)~=0)*(szR+1) + (mod(szR,2)==0)*(szR);
    if (sLp <= bulim/2)
        % -Axes posi (2D line)
        subplot(6,bulim/2,[sLp,sLp+bulim/2]); plot(datArr(:,10:12));
        xlabel('Samples'); title(['Set\_',num2str(sLp),'meta']); view([90 -90]);
        % -Density (2D line)
        subplot(6,bulim/2,sLp+bulim);
        ksdensity(datArr(:,10),(0:Mult:value)');
        hold on; ksdensity(datArr(:,11),(0:Mult:value)');
        ksdensity(datArr(:,12),(0:Mult:value)'); hold off;
        ylabel('\rho'); xlabel(' ');
    else
        % -Axes posi (2D line)
        subplot(6,bulim/2,[sLp+bulim,sLp+(ceil(bulim*1.5))]);
        plot(datArr(:,10:12));
        xlabel('Samples'); title(['Set\_',num2str(sLp),'meta']); view([90 -90]);
        % -Density (2D line)
        subplot(6,bulim/2,sLp+(2*bulim));
        ksdensity(datArr(:,10),(0:Mult:value)');
        hold on; ksdensity(datArr(:,11),(0:Mult:value)');
        ksdensity(datArr(:,12),(0:Mult:value)'); hold off;
        xlabel('\DeltaP (mm)'); ylabel('\rho');
    end
end
```

Figure 4.15. MATLAB script for generating plot objects

Figure 4.15 shows that the metadata plots were generated in pairs. It is assumed that assessment of individual processes is of limited value, as this approach limits the ability to accurately compare each process with another. Therefore, it is expected that processes will be assessed either in pairs, or in greater numbers. This could mean comparing a standard process with each new process – to establish the differences from normal. Or alternatively, comparing each subsequent process to assess the variation over time. Figure 4.16 shows the implementation of the DENSE theory as a three part for loop with nested switch function. Each loop represents a coordinate axis. The switch case enables backwards compatibility with older data sets for which the X, Y, and Z position data is inverted.

The density variable was pre-allocated memory using  $density = zeros(ceil(value(1)),2,3)$ ; where  $value = (max(tmp)+1)$ ; and  $tmp(N) = max(max(OArrN,1(:,10:12)))$ . The algorithm then calculates the probability density estimate (PDE) for each axis across a standard set of samples (0:Mult:value).

```

% -Consider the density of the coordinate axes to locate the likely feature data
for N = 1 : 3
    switch Mult
        case -1
            [density(:,2,N), density(:,1,N)] = ...
                ksdensity(datArr(:, (9+N)), (0:Mult:value)');
            density(density(:,2,N) <= (CL(N) * max(density(:,2,N))), :, N) = 0;
            dense_lim(N,1,sLp) = min(density(:,1,N));
            dense_lim(N,2,sLp) = max(density(density(:,1,N)<-10,1,N));
        otherwise
            [density(:,2,N), density(:,1,N)] = ...
                ksdensity(datArr(:, (9+N)), (0:Mult:value-1)');
            density(density(:,2,N) <= (CL(N) * max(density(:,2,N))), :, N) = 0;
            dense_lim(N,1,sLp) = min(density(density(:,1,N)>10,1,N));
            dense_lim(N,2,sLp) = max(density(:,1,N));
    end
end

```

Figure 4.16. MATLAB script for location of features

Then, using logical indexing, every PDE value that is less than or equal to the sum of the maximum PDE (for the current axis) and the ACL, is reduced to zero. The corresponding samples are also reduced to zero. This allows the minimum and the maximum sample to be identified (not within 10 points of zero - (0,0,0)) as all samples that had a PDE less than the cut-off have been eliminated. Those eliminated samples refer to the non-cutting activities, whilst the remaining samples refer to the actual cutting process. The maximum cannot be within 10 points of (0,0,0), as (0,0,0) is the home location within the MT and the coordinate at which the MT changes the cutting tool. Whilst the MT may spend a significant portion of time at or in the vicinity of (0,0,0), it is unlikely that cutting is occurring. To prevent this affecting the DENSE algorithm, the home location (0,0,0) is negated.

Each density limit can then be applied to the data as a series of conditions (applied using logical indexing). This approach removed the need for a loop and thus optimised the speed of the process significantly. Six conditions are generated: two per axis, representing the upper and the lower thresholds. The conditions are then applied (again using logical indexing) to the entire data set simultaneously, by deleting all data rows that satisfy one or more of the conditions. A predicted feature plot is then created to show that the DENSE algorithm was successful. This is shown in Figure 4.17.

```

% -Define the density conditions
conditions = datArr(:,10) < dense_lim(1,1,sLp) | ...
    datArr(:,10) > dense_lim(1,2,sLp) | ...
    datArr(:,11) < dense_lim(2,1,sLp) | ...
    datArr(:,11) > dense_lim(2,2,sLp) | ...
    datArr(:,12) < dense_lim(3,1,sLp) | ...
    datArr(:,12) > dense_lim(3,2,sLp);

% -Edit/append datArr to OArr
datArr(conditions,:) = [];
OArr{sLp,2} = datArr;

% -Request predicted feature plot
if strcmp(opt,'YES') == 1
    set(0,'CurrentFigure',axA);
    % -Plot feature (3D scatter)
    subplot(2,ceil(szR/2),sLp);
    scatter3(datArr(:,10),datArr(:,11),datArr(:,12),'.');
    daspect([1 1 1]);
    title(['Set\ ',num2str(sLp)]);
    xlabel('\Delta x'); ylabel('\Delta y'); zlabel('\Delta z');
end

```

Figure 4.17. MATLAB script to edit process data using DENSE conditions

To illustrate the DENSE process two sets of Cylinders were made available, with the second set being

a partial set of three. This arose due to the cutting tool breaking but is used here to assess the abilities of this process. This difference enables the efficacy of the DENSE algorithm to be tested. If the algorithm is simply finding what is known to be there, when there is an unknown, the process should fail. The generated metaplots for the two example Cylinder applications are provided in Figure 4.18. The plots show differences in the geometries of the processes despite having the same underlying program. The located feature data that accompanies the metaplots is provided in Figure 4.19.

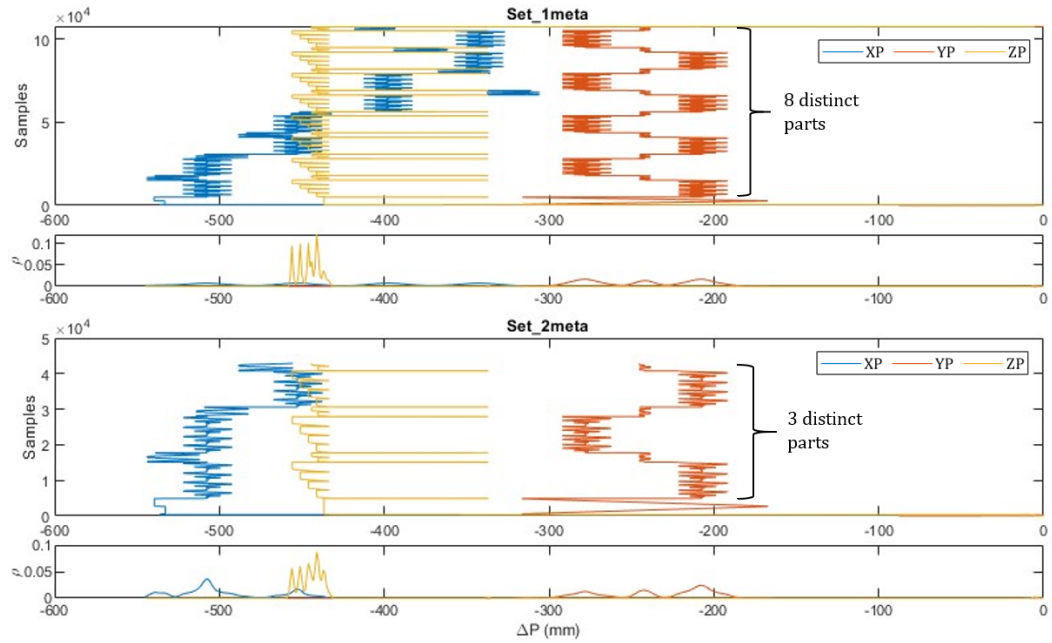


Figure 4.18. Example metadata plots for the Cylinder application

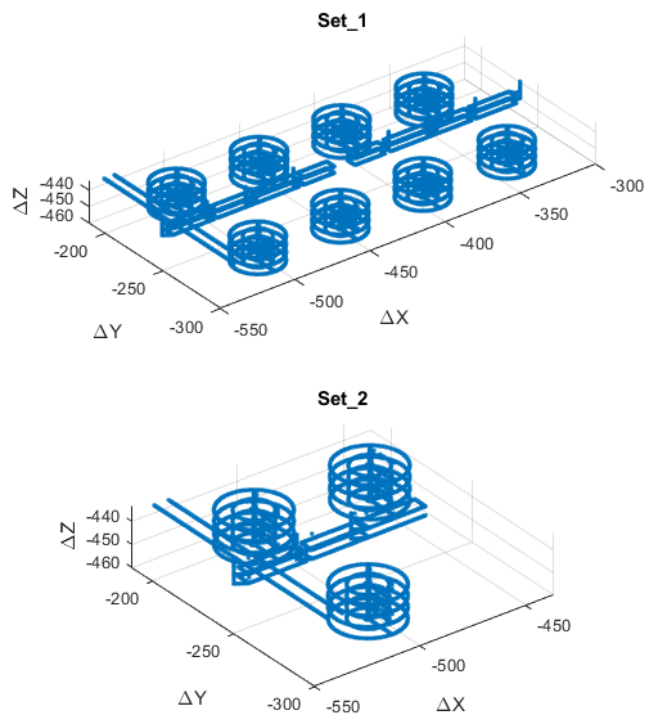


Figure 4.19. Cylinder-Wear application DENSE result

Figure 4.19 shows that the DENSE algorithm was successful at locating the entire part, without retaining any excessive movements. It also indicates that the algorithm successfully managed the partial process for set 2, with the same initial limits and no additional non-cutting activities observed in the results.

#### 4.2.2.3 Eliminate outliers

It is acknowledged that some non-cutting activities will be enacted within the part volume. An example would be milling pockets, or complex geometries, as the tool must eventually retract from the feature. Such a movement is not removing material and hence must be negated from any tool condition analysis. Equally, some rapid movements, or changes to the rotational velocity of the machine tool, may be enacted close to the part volume. In those instances, the DENSE approach may fail to remove such activities.

In response, an additional filter stage was considered. The novel approach chosen was to employ Chauvenet’s Criterion (CC) as a filter to eliminate the remaining RFR and SML extremes. CC is an approach for identifying outliers, based on probabilities derived from the number of samples. An explanation for the approach (as well as the limitations of) can be found in work by Limb et al. (2017). The approach was targeted specifically at the SRS, RFR and the SML as those parameters were found to be most susceptible to outliers from non-cutting activities. For example, the SML peaked significantly when there was a change in the rotational velocity, whilst the RFR peaked significantly when there was a rapid movement. This is illustrated for the RFR and the SML in Figure 4.20.

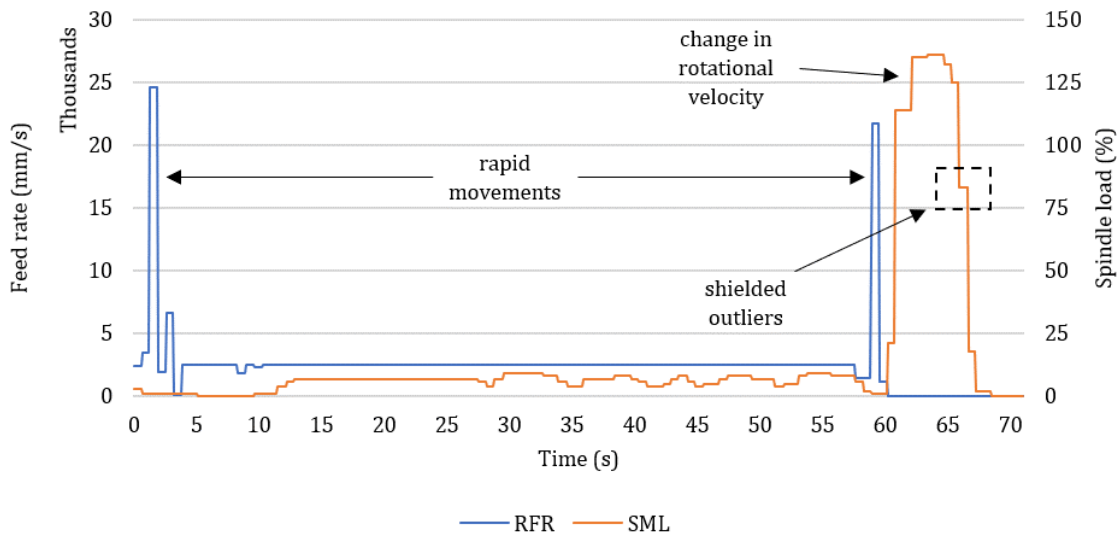


Figure 4.20. Outlier examples from arbitrary sample of MTData (shielded outliers noted)

Figure 4.21 shows the MATLAB script for implementing the CC in the DENSE program. The outlier threshold is calculated using a derivative of the CC equation:

$$CCL = -norminv\left(\frac{\alpha}{2N}\right) \quad (4.1)$$

```

% -Eliminate outliers from the data using Chauvenet's Criterion
% -Only consider the fdr and the sml outliers
% -Opening the "net" too wide risks eliminating data anomalies
pb.Indeterminate = 'on';
pb.Message = 'Eliminating outliers..!';
clearvars conditions;

% -Calculate CC outliers
avg = mean(datArr(:, [4,5,6]));
sd = std(datArr(:, [4,5,6]));
CCL = -norminv(0.5/(2*size(datArr,1)));
CCo = (abs(datArr(:, [4,5,6]) - avg([1,2,3])) ./ sd([1,2,3])) > CCL; %outliers
conditions = CCo(:,1) | CCo(:,2) | CCo(:,3);

% -Eliminate CC outliers from datArr and save.
datArr(conditions,:) = [];
OArr{sLp,2} = datArr;

```

Figure 4.21. MATLAB script for first implementation of CC filter

Where CCL is the CC limit, the size of `datArr` along the first dimension ( $size(datArr,1)$ ) gives the number of samples in the data set (N) and  $\alpha$  is the chosen outlier band. The CCL indicates the threshold within which approximately 95% of the data should reside. Any SRS, RFR or SML samples beyond the threshold should be considered outliers. To apply the CCL to the SRS, RFR and the SML, each parameter is standardised using:

$$\frac{x - \bar{x}}{\sigma} \quad (4.2)$$

Where the mean ( $\bar{x}$ ) of the dataset is subtracted from each value, which is then divided by the standard deviation ( $\sigma$ ) of the dataset. Any standardised values greater than the CCL are eliminated by logical indexing. The width of the SML peak is significant and can result in shielded outliers (indicated in Figure 4.20). As such it is necessary to apply the CC filter twice to eliminate these. However, to avoid eliminating important data, the CC is targeted specifically at the SML for the second filter. The application of the second CC filter is presented in Figure 4.22.

```

% -Ask operator if X2 filter is required
if strcmp(filt2,'YES') == 1
clearvars conditions;

% -Calculate CC outliers
avg = mean(datArr(:,6));
sd = std(datArr(:,6));
CCL = -norminv(0.5/(2*size(datArr,1)));
CCo = (abs(datArr(:,6) - avg(1)) ./ sd(1)) > CCL; %outliers
conditions = CCo(:,1);

% -Eliminate CC outliers from datArr and save.
datArr(conditions,:) = [];
OArr{sLp,2} = datArr;
end

```

Figure 4.22. MATLAB script for second implementation of CC filter

The second filter is kept optional as some processes may be better implemented with only the first filter. Some processes may not have such broad outlier peaks for the SML. Equally, some processes may have very broad outlier peaks for the SML and therefore require three CC filters. It is suggested that data sets are given a cursory assessment by a competent engineer to identify which approach is suitable. It is acknowledged that statisticians argue over whether outliers, or shielded outliers should be removed at all. However, this argument is not relevant to this application of CC, as these outliers

represent non-cutting activities and therefore *need* to be removed. It is also noted that the second and third implementations of the CC filter are targeted exclusively at the SML to reduce the likelihood of removing samples relevant to the cutting process.

After the CC filter has been applied and the outliers eliminated from the data, the filtered data is saved to the overall storage array and the metaplots are created. It is noted that no data is truly deleted at this stage due to the system being a proof of concept. It is envisaged that industrial implementations would retain only the condensed information to reduce the necessary storage.

#### 4.2.2.4 Trim repeating values

The final process exclusive to the DENSE algorithm is the filtering of repeating data, herein referred to as a repetition filter. The repetitive data arises from a mismatch between the sampling frequency of the PC and the sampling frequency of the COMX and an additional mismatch between the COMX and the MT itself. To prevent data loss, it was established that the sampling frequency of the PC must be greater than either the COMX or the MT. This also allows for scalability, as when the sampling frequency of the MT or the COMX are increased, data loss should *not* increase proportionally.

The approach was developed based on the concept that the MT should not stop during the cutting process unless there is an intervention by the controller or operator. If the data suggests that the MT has stopped, that data can be ignored. A stopped MT is no longer cutting and a MT not cutting does not need to be monitored for cutting tool health. It may be argued that a machine may be stopped by the operator due to a cutting tool breakage. However, by the time the MT is stopped either the breakage has occurred or is close to occurring and the relevant data will already be captured.

Based on this premise, when the axis position reading repeats the MT is stationary and the data can be eliminated. The application of this approach is presented in Figure 4.23. It is shown that the

```

% -Trim the data to remove repeating values (use XYZ)
temp = zeros(size(OArr{sLp,3},1)+1,17,2);
temp(1:end-1, :, 1) = OArr{sLp,3};
temp(2:end, :, 2) = OArr{sLp,3};
strip = temp(temp(:,10,2) ~= temp(:,10,1) | ...
    temp(:,11,2) ~= temp(:,11,1) | temp(:,12,2) ~= temp(:,12,1), :, 2);

% -Store reduced data in OArr(5)
OArr{sLp,5} = strip;

% -Split the reduced data according to the cutting tool
clearvars tmp;
for M = 1:29
    tmp{M,1} = OArr{sLp,5}(OArr{sLp,5}(:,2) == M, :);
end
OArr{sLp,6} = tmp;

```

Figure 4.23. MATLAB script for repetition filter

approach is based on the logic that axis 1 sample N is not equal to axis 1 sample N-1 OR the same logic for axis 2 OR the same logic for axis 3. It is accepted that this repetition filter is applied quite late in the process. Applying the filter earlier on will speed up the process due to the relatively smaller data sets; however, other optimisations are likely to be necessary before the DENSE application is a

polished or finished system. Therefore, the time penalty arising from the late-stage implementation of this repetition filter is not considered to be a significant concern.

#### 4.2.2.5 Apportion data and plot

The data is now reduced significantly from the initial file size and can be separated according to the cutting tool utilised. This process is straightforward as the cutting tool index has been acquired for each entry. The data can thus be separated sequentially according to the cutting tool index. The implementation of this split was included in Figure 4.23. Following the implementation of the repetition filter and the separation of data into cutting tool groups, the data can be plotted for investigation. Two approaches are taken at this stage:

1. Create a tool path plot to show the combined efforts of the utilised cutting tools. An example MATLAB implementation is provided in Figure 4.24 for the OMI-body application. For the provided example the cutting tools are specified in the “for loop” and the cutting tool details are extracted from the data array (OArr) to populate the plot legend.
2. Populate a GUI plot tool with the imported processes, all tools, and all variables. The tool is illustrated in Appendix D.2. Creation of such a tool enables an initial investigation into the MTData results for each of the imported processes. Currently, however, the tool does not create or enable a direct comparison between the imported processes. This is primarily due to the programming required falling outside the scope of this project. The tool is currently useful for directing subsequent investigations and/or comparisons between processes.

```

% Create a plot separating each tool
figure('Name','3D-ToolPath Plot','NumberTitle','off','Color',[0.94 0.94 0.94]);
for N = [2,3,4,7,8,12,17,21,22,23,24,25,26];
    plot3(OArr{1,4}{N,1}(:,10),OArr{1,4}{N,1}(:,11),OArr{1,4}{N,1}(:,12), ...
        'DisplayName',extractBefore(TI{1,1}{N},5));
    daspect([1 1 1]);
    hold on;
end
hold off;

legend('Location','South','Orientation','Horizontal');
set(gca,'Visible','off');

```

Figure 4.24. MATLAB script for visualising process data by creating plot of cutting tool paths

#### 4.2.2.6 Additional memory improvements

The principle of the DENSE process is to reduce the data set by removing non-cutting activities and repeated data. This should result in a significant reduction in the file size. The original (reduced) file size was approximately 10MB following PAc (see Section 4.1.5). Following the implementation of DENSE, the file sizes are reduced to approximate 7.5MB. This indicates a 25% improvement. However, five additional (derivative) parameters are generated and included, increasing the output from 12 to 17 total parameters. The derivation of these parameters is discussed in Section 4.3. Including the additional parameters increases the information content by roughly 42%; however, the file size only

increases by approximately 32% to roughly 11MB. This indicates that the increase in the available information is a positive trade-off and worth keeping.

Nevertheless, it is acknowledged that the file sizes have increased relative to the PAc output and will now be 95.6% smaller than the original (sub-optimal) output. Putting this into perspective indicates that it would still be possible to monitor a continuous manufacturing process for just under 23 hours, needing the same storage capacity as the PAc output over 24 hours. This difference is considered negligible versus the value gained by including the additional five parameters. However, if this is deemed to be unacceptable, the output could be further refined by replacing original parameters with derived parameters – for context refer to Section 4.3. This would result in a file size like the PAc output but with two additional parameters (17% more information content) and no penalty to storage capacity.

### 4.3 Converting unsuitable data

Depending on the level of insight from the OEMs in enabling the capacity for DAQ from MTs, the output may not be in a state suitable for exploitation from the off. For this reason, conversion from the raw state to a more suitable state is likely to be necessary. Of the process data generated herein, it was identified that the motor load signals were acquired in an unsuitable state. In response, it was identified that many of these signals may be converted into usable states when enough information is gathered regarding the specific capabilities of each motor.

#### 4.3.1 Convert spindle motor output

One such motor found to be generating initially unsuitable process output is the spindle motor. The SML is output as an integer percentage (quantised), where the magnitude of that percentage value is relative to the specific motor characteristic employed. This percentage value is not relative to the maximum capability of the spindle and can thus exceed 100% on occasion and being out of context makes little sense during analysis. It is therefore appropriate to change the output format into one more descriptive of the process and more understandable to those assessing the data. For the studies herein, the output format is converted into units of energy (Joules).

For the spindle used herein the specific motor characteristic employed is the five-minute rating. Using the five-minute characteristic, the raw data can be reverse engineered into energy consumption using the OEM motor specification. A simple power law relationship can be applied to identify the rated power ( $P_{max}$ ) and rated torque ( $T_{max}$ ) for any individual rotational speed:

$$P_{max} = A.\omega^B \quad (4.3)$$

$$T_{max} = C.\omega^D \quad (4.4)$$

The power law relationships were derived from the spindle speed-power-torque (SPT) characteristic presented in Figure 4.25. Coefficients A, B, C and D have been derived and are presented in Table 4.2 for the different speed ranges.

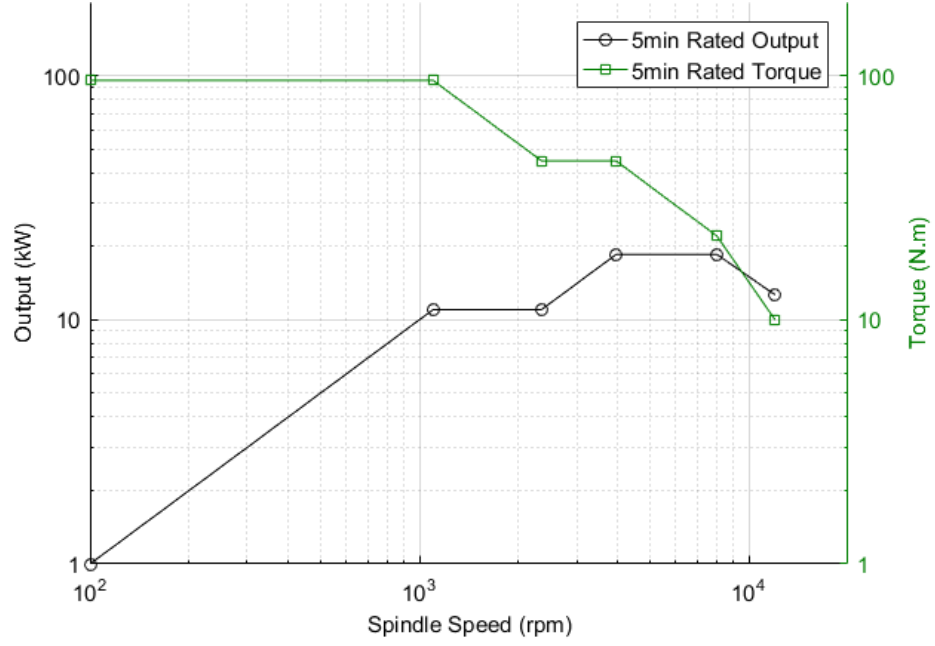


Figure 4.25. Spindle speed-power-torque characteristic, recreated from Yamazaki Mazak (2015b)

Table 4.2. Spindle speed-power-torque characteristic ranges and power law coefficients

Speed range (rpm)	Power range (kW)	Torque Range (N.m)	A	B	C	D
$100 \leq \omega < 1100$	$1.0 \leq P < 11.0$	$T = 95.5$	$1.000 \times 10^{-2}$	$1.000 \times 10^0$	$9.550 \times 10^1$	$0.000 \times 10^0$
$1100 \leq \omega < 2347$	$P = 11.0$	$95.5 \geq T > 44.7$	$1.100 \times 10^1$	$0.000 \times 10^0$	$1.063 \times 10^5$	$-1.002 \times 10^0$
$2347 \leq \omega < 3950$	$11.0 \leq P < 18.5$	$T = 44.7$	$4.736 \times 10^{-3}$	$9.987 \times 10^{-1}$	$4.470 \times 10^1$	$0.000 \times 10^0$
$3950 \leq \omega < 8000$	$P = 18.5$	$44.7 \geq T > 22.0$	$1.850 \times 10^1$	$0.000 \times 10^0$	$1.833 \times 10^5$	$-1.005 \times 10^0$
$8000 \leq \omega < 12000$	$18.5 \geq P > 12.6$	$22.0 \geq T > 10.0$	$8.438 \times 10^4$	$-9.375 \times 10^{-1}$	$8.556 \times 10^8$	$1.945 \times 10^0$

Obtaining the rated power for each instantaneous speed allows an equation for the process energy consumption (PEC) to be derived:

$$E = \frac{10P_{max}}{F_S} \cdot \int_b^a \text{SML} dt \quad (4.5)$$

Where the units for the calculated PEC are Joules, the sampling frequency ( $F_S$ ) is the rate of data acquisition (in Hz), and the limits “a” and “b” are the start and end of each machined part respectively. This is simplified further when the quantised nature of the signal is accounted for, allowing the integral to be approximated by the sum of the samples per part:

$$E = \frac{10P_{max}}{F_S} \cdot \sum \text{SML} dt \quad (4.6)$$

Equations (4.5) and (4.6) enable the generated SML to identify the energy required to machine each part when the data is apportioned appropriately, or to represent the energy per sample when applied to the individual samples. Applying Equation (4.6) to individual samples replaces the sum with a single multiplier:

$$E = \frac{10P_{max}}{F_S} \cdot \text{SML}_i \quad (4.7)$$

### 4.3.2 Convert axes motor output

The other motors investigated belong to each of the axes. Key information regarding each axis motor is provided in Table Table 4.3. Further information regarding each axis motor is provided in the Appendix. It is interesting to note that the X-axis motor is not as powerful as both the Y-axis and Z-axis motor. This difference is discussed in Chapter 6. It is noted that the axis motors do not have an indicated SPT characteristic. This implies that they have a uniform power and torque response to their speed ranges. Whilst this may not strictly be true, it may be assumed for the purposes herein. As such, the conversion from percentage to energy use for each axis motor requires the same equations as for the spindle motor, but without any power law relationships to derive the maximum power and torque. The single maximum power embodies the linear nature for these motors. This employs Equation (4.6) for parts or processes, or Equation (4.7) for individual samples, and uses the maximum rated power of each motor (provided in Table 4.3).

Table 4.3. Axis motor characteristics

Axis	Max load (kW)	Additional detail
X	1.5	—
Y	3.5	—
Z	3.5	Electromagnetic brake
TC	1.5	Tool change motor

### 4.3.3 Calculate resultant force and direction

Whilst each component of the load is useful (in this context each component being the SML, XML, YML and ZML), it is also useful to consider the combined information provided by the loads acting on the cutting tool. This may better indicate the health of the cutting tool, or the health of the process. The SML cannot feasibly be combined with the other three components as the load is acting tangentially to the cutting tool, whereas the axis loads act radially, or normal to the surface of the tool. The axis loads on the other hand may be combined to find the resultant force magnitude and the direction in which the resultant force is acting. The load on the cutting tool should be predominantly opposing the direction of travel; however, deviation from this may indicate markers of cutting tool health. The resultant load on the cutting tool (R) may be calculated using:

$$R_{XYZ} = (X^2 + Y^2 + Z^2)^{0.5} \quad (4.8)$$

Where X, Y and Z represent the loads on each respective axis. Neglecting the Z-axis from the Equation gives the planar resultant force:

$$R_{XY} = (X^2 + Y^2)^{0.5} \quad (4.9)$$

The direction ( $C_X$ ) in which the resulting loads are acting can be calculated using the inverse tangent of X and Y to find the planar resultant direction (relative to the X-axis):

$$C_X = \tan^{-1} \left( \frac{Y}{X} \right) \quad (4.10)$$

To find the angle between the X and Y resultant force and the Z-axis ( $C_Z$ ), it is possible to use the inverse cosine of  $R_{XY}$  and Z:

$$C_Z = \cos^{-1} \left( \frac{Z}{R_{XY}} \right) \quad (4.11)$$

#### 4.3.4 Implementing data conversions

The implementation of the load conversions, and the calculation of the resultant forces and directions is given in Figure 4.26. This is currently enacted within the DENSE program; however, it would be reasonable for future implementations to be enacted at the source (during DAQ). This was not implemented within this project due to the time and resource constraints.

```

% -Calculate XY kW load and direction
A = [0.01,11,0.004736,18.5,84376.62];
B = [1,0,0.998651,0,-0.93748];
C = [1100,2347,3950,8000,12000];
SL = datArr(:,6);

for i=1:5
    if i==1
        SL(datArr(:,4) < C(i),1) = ...
            ((10*A(i) * datArr(datArr(:,4) < C(i),4) .^ B(i)) / 64) .* ...
            SL(datArr(:,4) < C(i),1);
    else
        SL(datArr(:,4) >= C(i-1) & datArr(:,4) < C(i),1) = ...
            ((10*A(i) * datArr(datArr(:,4) >= C(i-1) & datArr(:,4) < C(i),4) .^ B(i)) / 64)
        .* SL(datArr(:,4) >= C(i-1) & datArr(:,4) < C(i),1);
    end
end

XL = (1.5/100) .* datArr(:,7);
YL = (3.5/100) .* datArr(:,8);
YL = (3.5/100) .* datArr(:,9);
XYMag = hypot(XL,YL);
XYDir = atand(YL./XL);

```

Figure 4.26. MATLAB script for implementing conversion of percentage load data

The SML (represented as SL in the code) requires a nested if-else within a for loop to implement the SPT characteristic. This enables the appropriate maximum power for each speed range. The Pmax coefficients are provided for the five-minute characteristic as an indexable array. Each axis motor is simply applied as a single equation as the motor characteristic is assumed to be linear for those motors. It is acknowledged that the SML could be re-calculated in the same way as each of the axis motors if a process had a single rotational speed throughout; however, it cannot be assumed that any process would be run in such a way. It is also noted that the axes may have SPT characteristics. Where these are made available, they should be implemented in the same way as the spindle motor. The X-Y force magnitude was calculated using the hypot() MATLAB function – calculating the hypotenuse using Pythagoras’ theorem. The resultant direction was calculated using the atand() MATLAB function - the inverse tangent of the YML over the XML (YL and XL in the code respectively).

## 4.4 Summary

This Chapter has discussed the novel developments required to enable the use of MTData for the assessment of both cutting tool and process health. The information enabling optimised communication with NC units was outlined and the initial steps taken towards the development of algorithms for on-line monitoring of cutting tool health were described. This can be built upon in subsequent Chapters in progress towards the engineering of a suitable monitoring system for cutting tool wear. Having established the foundation for generating appropriate process data, it follows that suitable investigation is necessary into the use of such process information. Specifically, for evaluating the past and current markers of cutting tool health and whether the information gained can improve process health awareness.

## 5 | Cylinder Wear Investigation

This Chapter considers the output from the Cylinder application. The Cylinders were developed to enact exaggerated wear on cutting tools through use of a sufficiently hard workpiece, a relatively soft set of cutting tools, and a specifically unoptimized cutting regime. This was implemented to establish the general wear curves for the cutting tools and to establish the efficacy of the acquired MTData for deriving the condition of cutting tools in lieu of geometry or surface finish information. The aim is to establish the value in each MTData signal with consideration for the inherent features and/or trends that could be employed for determining the condition or health of a cutting tool. The characteristics that show promise shall be considered in later Chapters. The Cylinders are noted to be a laboratory-specific application. That is to say that the wear enacted on the cutting tools is not representative of a practical application as it has been exaggerated to deteriorate the cutting tools in a shorter timescale. This was implemented as wearing the cutting tools normally would require a substantial volume of contact time per tool. Nevertheless, this work has not used artificially damaged or worn cutting tools. Whilst not necessarily normal, the accelerated wear enacted on the cutting tools is natural and is therefore assumed to be representative of normal cutting conditions. Three further assumptions are:

1. All process variation is attributable to the condition, deterioration, or breakage of the cutting tool and that the other notable system interactions (Chapter 2) are negligible within that respect
2. At the start of each test series the cutting tool employed is unused and all are equivalent in geometry, style, and material unless indicated otherwise
3. Each cutting tool should last for 200 cycles (and thus produce 200 parts) before being in an unusable state. For that reason it was established that each cutting tool would be used to machine no more than 200 parts.

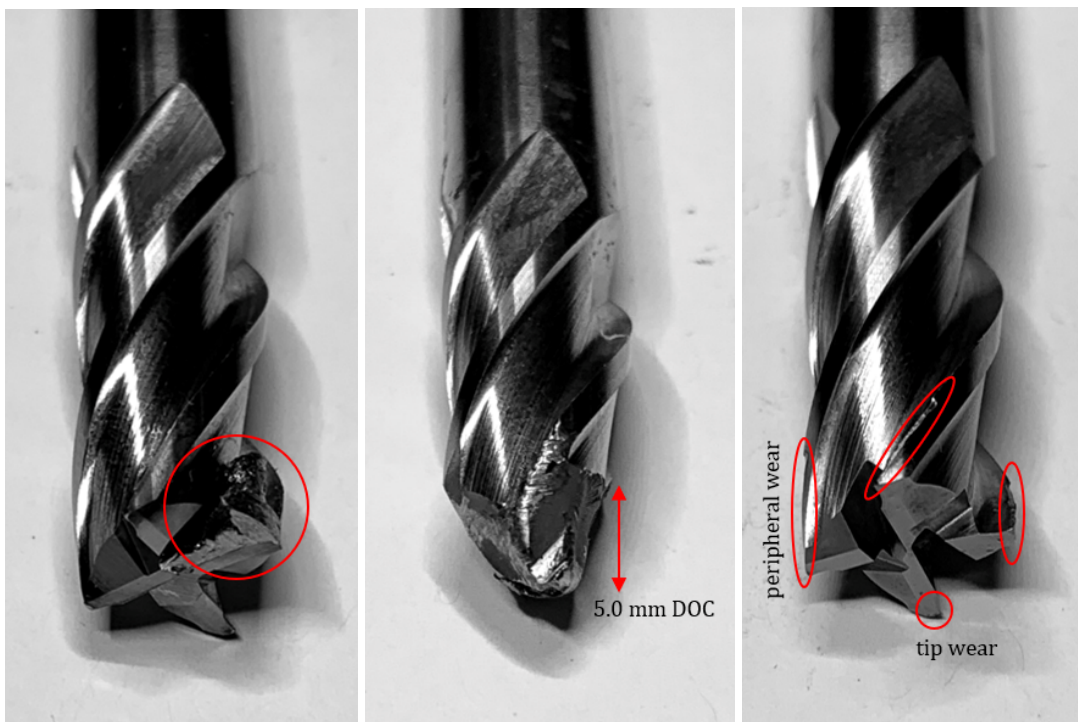
It is appreciated that these assumptions potentially raise dispute with the remarks in Chapter 2. Especially that commercial-specific applications are warranted and that not all process variation will be caused by the cutting tool. It is noted that the Cylinder application was deliberately laboratory focussed to simplify the necessary processing of the results. Immediate industrial deployment would result in more data than could be realistically managed. Therefore, the Cylinders represent a sensible first step towards eventual industrial deployment. Whilst not all the process variation will be attributable to the cutting tool, for a healthy system, the majority should be cutting tool related. Where potential conflict arises, it will be acknowledged.

Fifty Cylinder tests were attempted with 13 cutting tools under fully flooded cutting conditions. Six cutting tools failed to complete the full 200 parts before catastrophic failure. Seven cutting tools managed the full 200 parts. These tests were conducted as a single factor experiment on wear in order to evaluate the previously developed acquisition systems. Out of the 50 tests, 32 were enacted

without any process adjustments to account for the changes in part geometries. A further 14 tests were enacted with a fixed offset adjustment to account for peripheral cutting tool wear, four were enacted with a measured adjustment to account for peripheral cutting tool wear. Most of the tests utilised a 10mm diameter cutting tool, a few considered a 16mm cutting tool to consider the difference; however, it was noted that the conditions employed could not enact sufficient wear on the 16mm cutting tools. The employed cutting tools are identified in Chapter 3. It is noted that tests are grouped based on the relative batch (where a batch consisted of four tests totalling 200 parts). The naming convention employed (and used herein) is identified in Appendix D.1 for the Cylinders and for subsequent applications. The rest of this Chapter investigates the Cylinder application and the observed health of the employed cutting tools. It is noted that aspects of the investigations presented in this Chapter have been published by Hill et al. (2018) and Hill et al. (2019).

## 5.1 Qualitative condition assessment

Prior to investigating the acquired process data, it is sensible to consider qualitatively how the cutting tools are deteriorating and to consider how this deterioration is affecting the workpieces. For a qualitative assessment of the process, images were taken of the workpiece at various stages of tool wear, whilst the cutting tools were assessed when introduced and when replaced. Figure 5.1 presents three of the observed failure modes. The most common damage to the cutting tools was peripheral



a. BUE

b. Tooth shear

c. Flank wear

Figure 5.1. Observed cutting tool states following Cylinder application

(flank) wear. This was accompanied by notch wear at the level of the depth of cut. It is speculated that the notch wear was instigated by the aggressive cutting strategies employed. It is thought that

the pocket cycle encouraged a level of deflection in the cutting tool that increased the loads acting on the cutting tool from the surface of the workpiece. The peripheral wear was also exaggerated by the aggressive cutting strategies; however, this was intentional. It is noted that the degree of flank wear enacted on the cutting tools is extreme and not a condition that would be reached in typical machining processes. The notch wear and flank wear are shown in more detail in Figure 5.2.

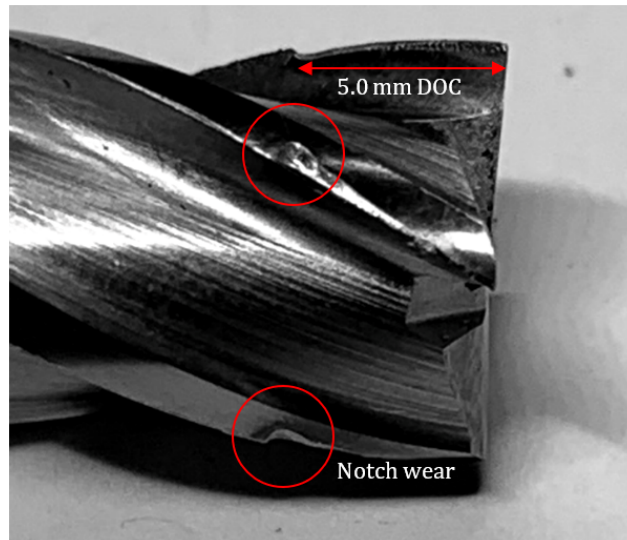


Figure 5.2. Flank and notch wear observed following Cylinder application

The most common catastrophic failure was noted to be loss of the cutting edges (teeth). It is suggested that this was primarily instigated by the notch wear weakening the cutting tool structure as the failure was always up to the notch and no further. However, it is appreciated that other failure modes may have further contributed to the catastrophic failure. Nevertheless, the cutting edge was sheared, rather than the material of the workpiece shearing. Other failure modes encountered included BUE, thermal cracking, and “disintegration” caused by a faulty collet (Figure 5.3).



Figure 5.3. Disintegrated tool (catastrophic failure)

Figure 5.3 highlights the potential hazard when cutting tools are allowed to fail catastrophically. This failure mode increases the risk of damage to the machine tool from both shrapnel, and from excessive or abnormal loads on the spindle and the tool holder. It would be useful to be able to detect each instance of the presented failures to enable a response that protects the machine tool or the operator from harm. It would be more valuable to be able to detect health markers to show the development of these failures, such that they may be predicted and therefore mitigated, or avoided entirely. The condition of the workpiece can be another victim of catastrophic failures. This brings added costs:

**Scrap cost** – arising from the wasted material and the need to replace the workpiece with new material.

**Time cost** – accumulation of hours invested in the part prior to the cutting tool failing. This is in addition to the subsequent downtime caused by the failure and the intervention by operators.

**Machine cost** – attributed to the wasted machining and the subsequent downtime.

**Labour cost** - attributable to lost time and intervention due to the failure. Where the process is mostly automated the labour cost may be lower accordingly.

Figure 5.4 presents examples of the more severe damage inflicted on the workpieces during the Cylinder application. It is also the case that the cutting tool may fail without causing irreparable damage to

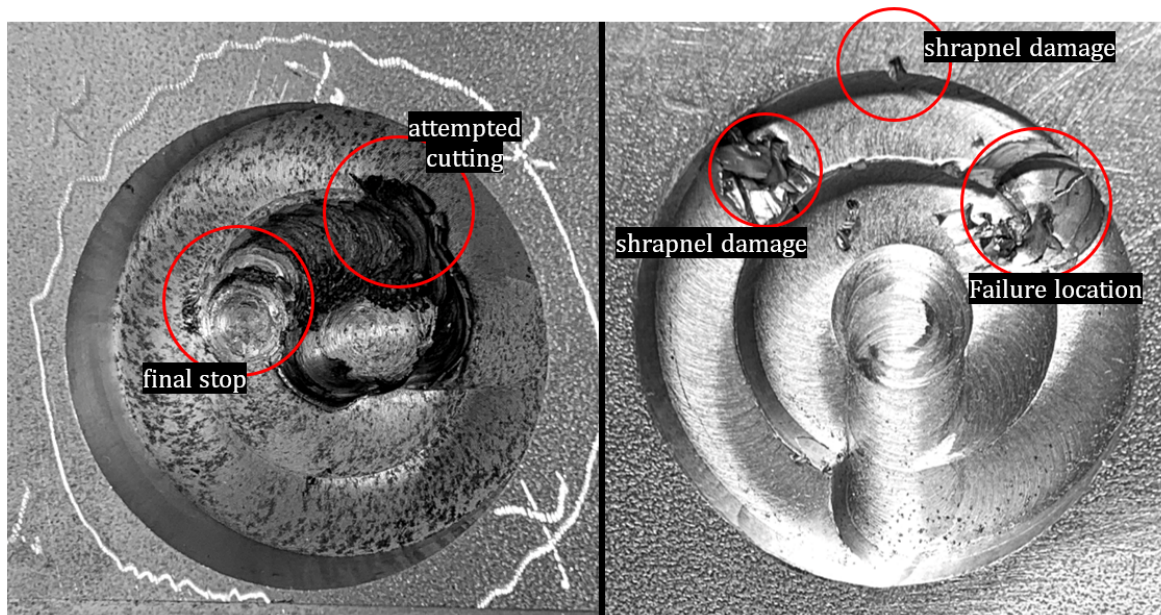


Figure 5.4. Irreparably damaged Cylinders due to catastrophic cutting tool failures

the workpiece. Figure 5.5 presents an example of this, where the cutting tool failure was identified by the operator as it happened. The intervention by the operator means that with a replacement cutting tool the process may continue. It is suggested that as the operator was able to identify the occurrence of the cutting tool failure in reasonable time, it is reasonable that an automated system should also be capable of identifying the occurrence in a reasonable time. The figure notes an increase in both scuffing and smearing in the build up to the breakage, thus these would be a good place to start.

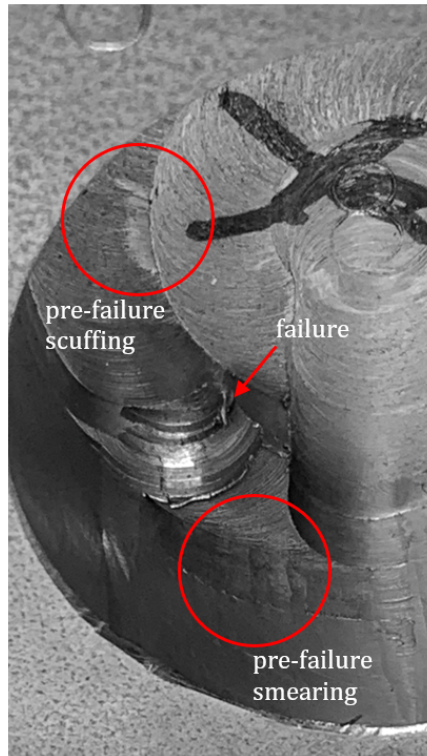


Figure 5.5. Cutting tool failure with minimal workpiece damage

Other than cutting tool failures, the condition of the workpiece should also indicate the progressive condition of the cutting tool as noted in Chapter 2. Figure 5.6 presents images of the workpieces at various stages in the cutting process. It is noted that visually the condition of the workpieces

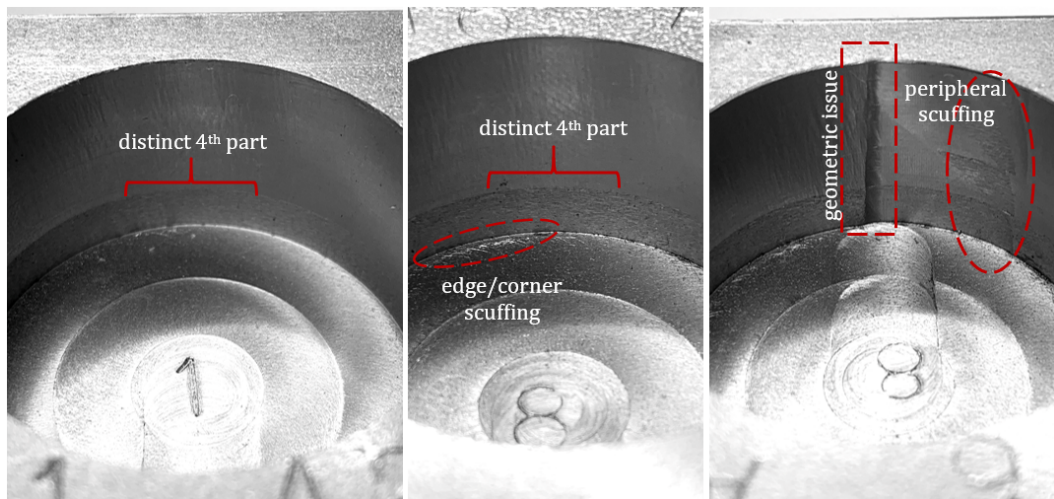


Figure 5.6. Qualitative analysis of Cylinder condition at stages in the cutting process

deteriorates significantly over the course of the process. This indicates that the surface finish is deteriorating, especially within the fourth part indicating the increased effort from that part of the cutting tool. There is also evidence of smearing, scuffing, and of geometrical inconsistencies; however, the important dimensions (diameter, depth) cannot be inferred accurately from the images. Additionally, any influence of the observed condition on the structural or mechanical properties of the final product cannot be identified without explicit testing.

Notwithstanding, the allowable condition of the workpieces, as affected by the cutting tools, depends on any subsequent processes and is subject to human opinion and preference. If a workpiece will be subject to further processing that may conceal or nullify the damage caused to the surface by the cutting tool, then such damage is inconsequential unless it causes structural or mechanical weaknesses. As the quality of manufactured parts is most often assessed by individuals, it is their judgement that determines whether the quality is acceptable or not. It is noted that this may not be the case when equipment is employed to determine the true condition, such as dimensional accuracy, or surface finish. However, even in those cases the applied thresholds are often a matter of preference unless appropriate tolerances are employed and adhered to.

## 5.2 Quantitative condition assessment

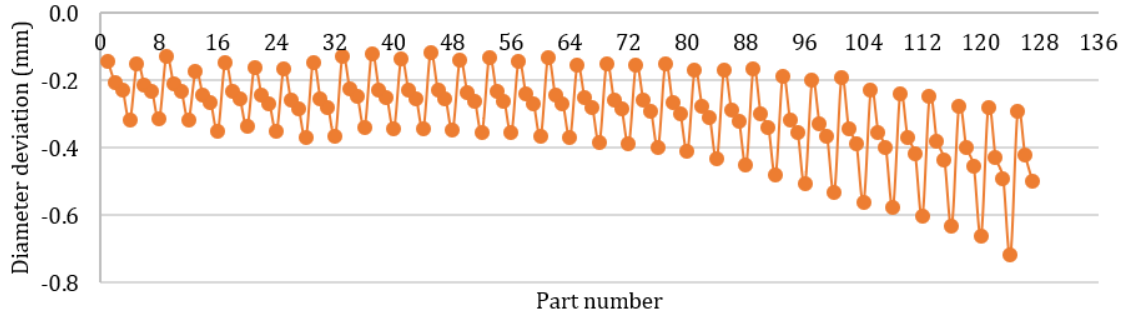
### 5.2.1 Form measurement

It is thus implied that a structured approach to determine the cutting tool condition is necessary. Whilst the aim is to achieve this using an MTData oriented approach, this must first be validated against other researched methods. The initial approach taken is to quantitatively assess the variations in the form of the manufactured parts. This was achieved through CMM measurements, enabled using MODUS software. The alignment steps to generate the part coordinate system (PCS) can be identified from the DMIS program provided in Appendix C.1. It is noted that scanning techniques were employed as the workpieces were not perfectly flat. By scanning the surfaces to align the PCS the error accountable to the variable flatness was reduced. The datum origin was aligned with the top surface (Z-origin) and the centre of the first Cylinder machined (X-origin and Y-origin). It was ensured that the manual alignment was overwritten by the programmed alignment (D(ABC)) to prevent any later conflict arising due to multiple saved datums.

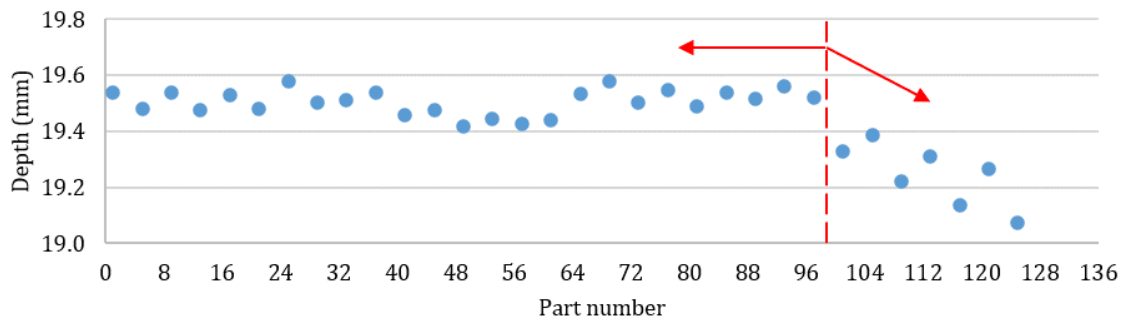
The Cylinders were scanned twice in each 5mm part to give an average diameter and circularity (per part). The floor of the Cylinders was scanned in two arcs to provide an average total depth. It is noted that measurement of the depth per part was impossible to quantify using the CMM. All measurements were taken every 0.5mm during a scan, at a fixed scanning velocity of 100mm per second, and always starting the scan at the 3o'clock position in the Cylinders.

#### 5.2.1.1 Depth, diameter and cylindricity variation

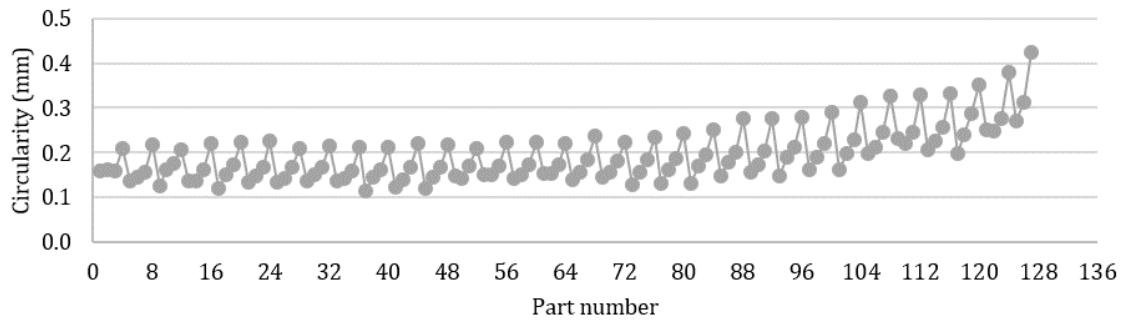
Figure 5.7 presents the formatted results for CD011014 (CD). The test employed a pre-used cutting tool and the cutting speed was increased from 36m/min near to the start of the test, to 52m/min for the rest of the test. It is noted that the cutting tool failed catastrophically following 127 parts (189 parts considering the slots). Figure 5.7 shows that the diameter measurements fluctuate every four parts (each part within a Cylinder); however, there is a clear trend away from zero. This indicates a measured reduction in the Cylinder diameters and thus an inferred increase in the cutting tool flank wear. The fluctuations are noted to be a result of DFW (acknowledged in Chapter 3) and each



a. Diameter deviation from nominal (40mm)



b. Cylinder total depth measure (nominal 20mm)



c. Cylinder circularity (tolerance 0.1mm)

Figure 5.7. Trends in form measurements for CD

part can be distinguished as a potentially different trend within the plot. A further observation is that the measurement difference between each part within each Cylinder increases over the life of the cutting tool. This is primarily affected by the first and the fourth parts. It is suggested that this is instigated by the different amount of material contact observed for each region of the cutting tool, whereby the fourth part is employed considerably more than the third (and so on). However, it is also noted that the effect of cutting tool deflection may further contribute to the discrepancy for the first part. The circularity measurements indicate a similar pattern to the diameters albeit with a greater difference between the fourth part in each Cylinder and the first three parts. As only the fourth part is affected by the hardest working 5mm of the cutting tool, that part will be isolated further. The depth measurements on the other hand are only available once per Cylinder due to the removal of each bottom surface during the machining cycles. It is noted that a redesign

of the application with deliberately staggered diameters may enable the depth for each part to be considered. It is appreciated that the depth measurements are not explicitly affected in the same way as the diameter measurements. This infers that the wear on the front edge of the cutting tool does not progress gradually and instead appears to deteriorate rapidly towards the end of life. However, firstly the depth measurements should be considered further by comparing the results from different tests. Figure 5.8 indicates the depth measurements for CD, CE015018 (CE), CF019022 (CF), and CG023026 (CG). It is noted that the cutting tool fails during CD and CF, but not during CE or CG.

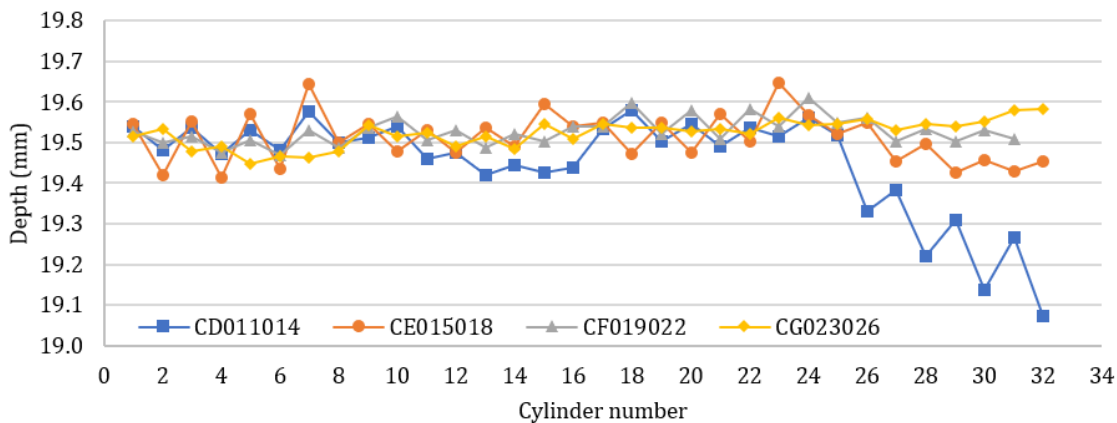
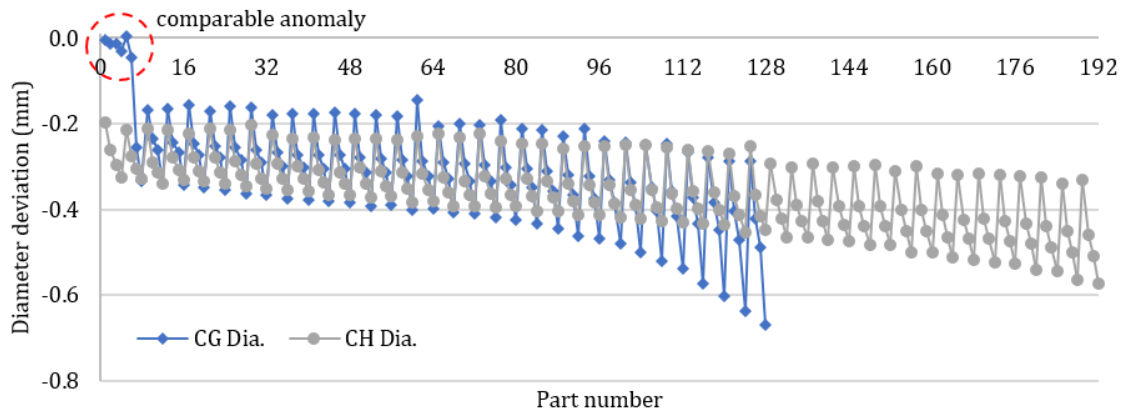


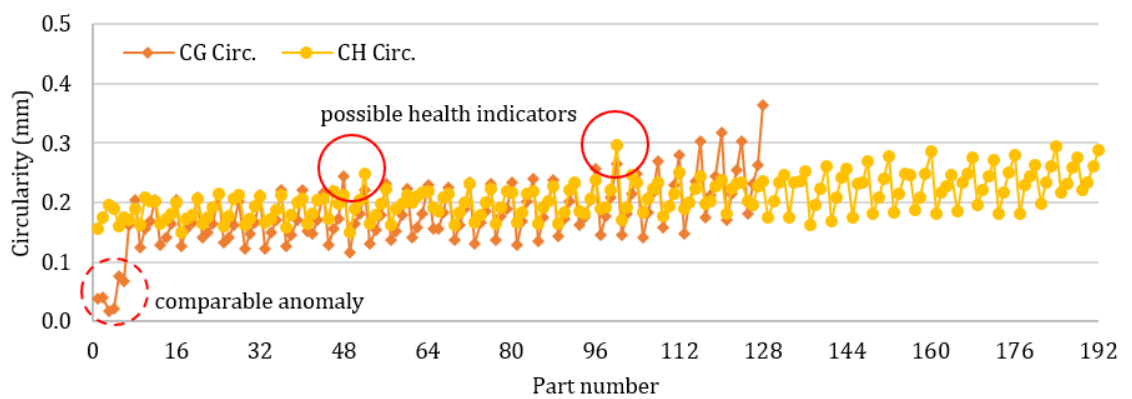
Figure 5.8. Comparison of depth measurements from four tests

Figure 5.8 indicates that only CD observes a significant decline in the measured depth in the run up to a cutting tool failure. It could be argued that the cutting tools employed for both CE and CG do not deteriorate sufficiently to observe a similar decrease in the depth; however, as the cutting tool failed during CF, this suggests that perhaps CD is the anomaly. An argument could be made that perhaps CF failed abruptly; however, the results for tests CI, CJ, CK, CL, and CM also fail to observe a decrease in the measured depth and therefore do not corroborate such an argument. As the depth measurements do not show any explicit evidence of cutting tool health, they will not be considered during the remainder of the Cylinder application. Depth results for CI, CJ, CK, CL, and CM are available in the electronic Appendix E.4.

Returning to the diameter and circularity measurements, Figure 5.9 presents the formatted results for CG and CH027032 (CH). Figure 5.9 has been included to illustrate that the diameter and circularity results are perhaps linked to a degree as noted by the comparable anomaly noted at the start of CG illustrated with a dashed circle. Although, there are still differences between the two measures, with the circularity perhaps more sensitive to the condition of the cutting tool. Possible health indications are circled. Nevertheless, the observed anomalies may be just that, anomalies. It is further appreciated that the circularity is potentially an overly abstract measure of the cutting tool condition. Without an appropriate (and relevant) tolerance for the circularity of the Cylinders, it cannot be taken forward as a primary measure of cutting tool health. It will, however, be employed in later sections for the consideration of process anomalies.



a. Diameter deviation from nominal (40mm)



b. Cylinder circularity (target 0.1mm)

Figure 5.9. Form measurements for CG and CH

It is also the case that there is no upper limit, or threshold, considered for the diameter deviation and therefore no effective indication of the cutting tool condition prior to either breakage or the end of the test. In response, to provide a point of reference, the 0.3mm flank wear limit is employed from ISO 8688-2:1989 in Figure 5.10. It is noted that the use of 0.3mm from ISO 8688-2:1989 is purely for reference as it should be appreciated that the true flank wear will not be as high as is inferred by the diameter difference (not least because the flank wear will be, at most, half the provided value). Notwithstanding, the limit provides a suitable threshold in the absence of a better one. The direct comparison of just the fourth part for CD, CE, CF, and CG not only simplifies the figure by presenting only the high-value information, but also indicates that the change in the cutting speed for CD has little effect on the process other than a notable anomaly between parts three and nine.

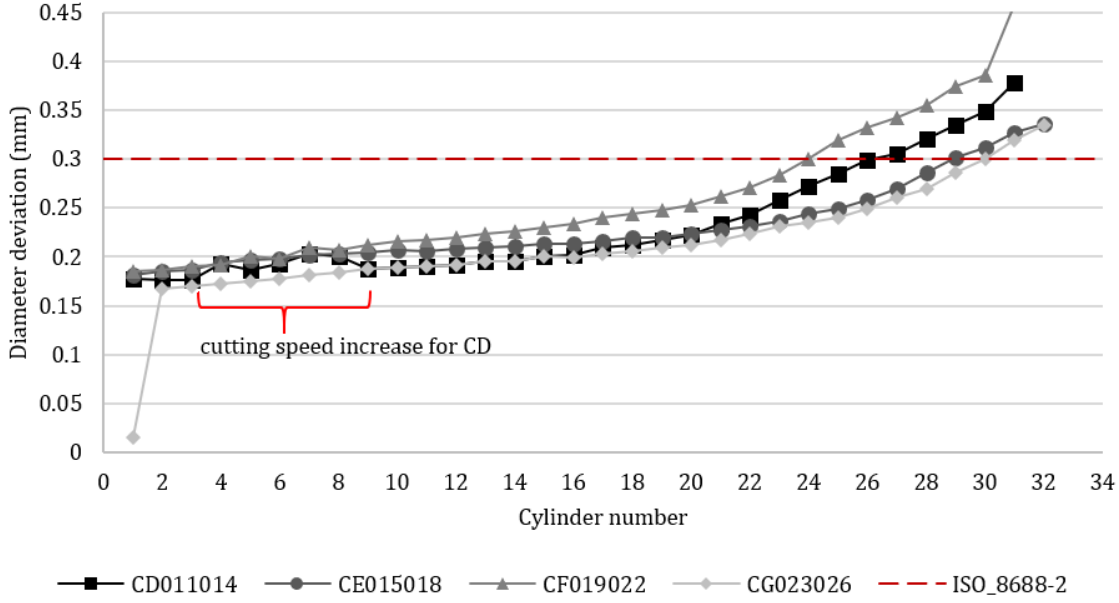


Figure 5.10. Diameter deviation for four tests considering an appropriate upper threshold

### 5.2.1.2 Developed equation for cross-section wear

It is therefore considered that the diameter measure considered is insufficient for modelling the changing conditions of the workpiece as past and current health indications have little to no bearing on the subsequent trend. This is evidenced by the change in the cutting speed for CD being evidenced in Figure 5.10, but then not contributing to the overall effective condition. The trend for CD is similar to CF, which is logical as the processes have the same cutting speed (52m/min); however, there is a greater similarity observed between CE and CG (both of which had a 36m/min cutting speed). It is noted that “health indications” is herein used to represent process changes or anomalies. It is suggested that an appropriate approach would be to develop an algorithm that enables health indications to be carried forward.

To implement this change first required a departure from the diameter deviation. This was affected as a measure of the change in the cross-sectional area of the Cylinders (CSAM). This thus indicates the cross-section of material *not* machined that *should* have been machined. It is noted that the cross-section was used rather than a measure of the volume as an accurate measure of the depth of cut per part could not be derived. Additionally, by using the cross-section, the 0.3mm ISO threshold may be converted into an equivalent threshold and may therefore continue to be applied. The conversion from diameter was implemented with Equation 5.1.

$$CSAM_i = 0.25\pi (d_0^2 - d_i^2) \quad (5.1)$$

Where  $d_0$  is the nominal part diameter and  $d_i$  is the diameter of the part being considered. Using Equation 5.1 the ISO equivalent CSAM threshold is 37.42mm<sup>2</sup>. The variation in cross-section for CD, CE, CF, and CG is provided in Figure 5.11.

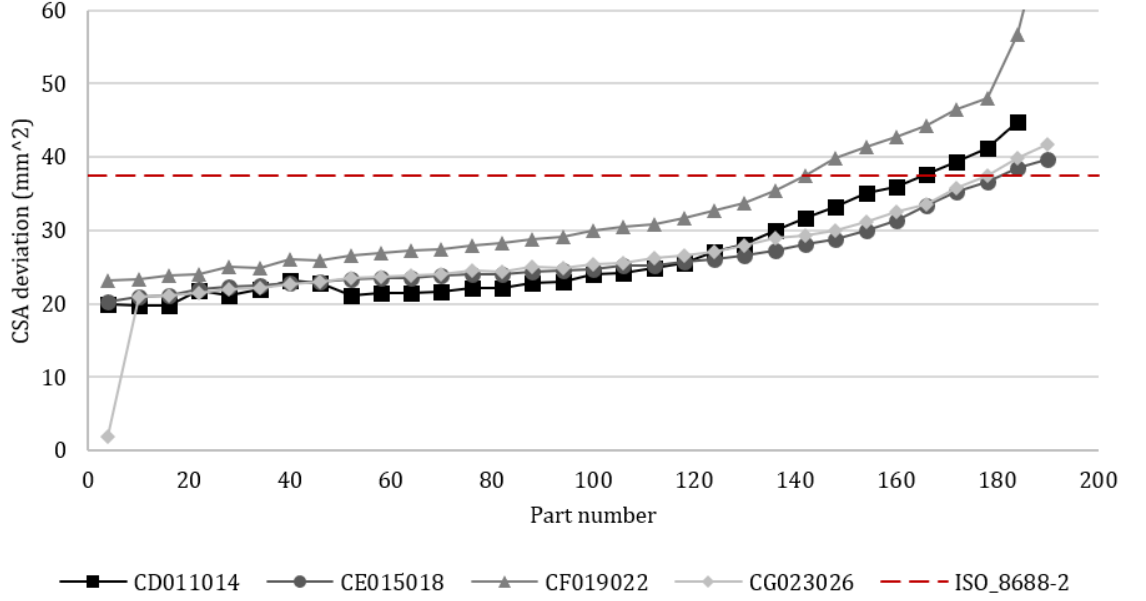


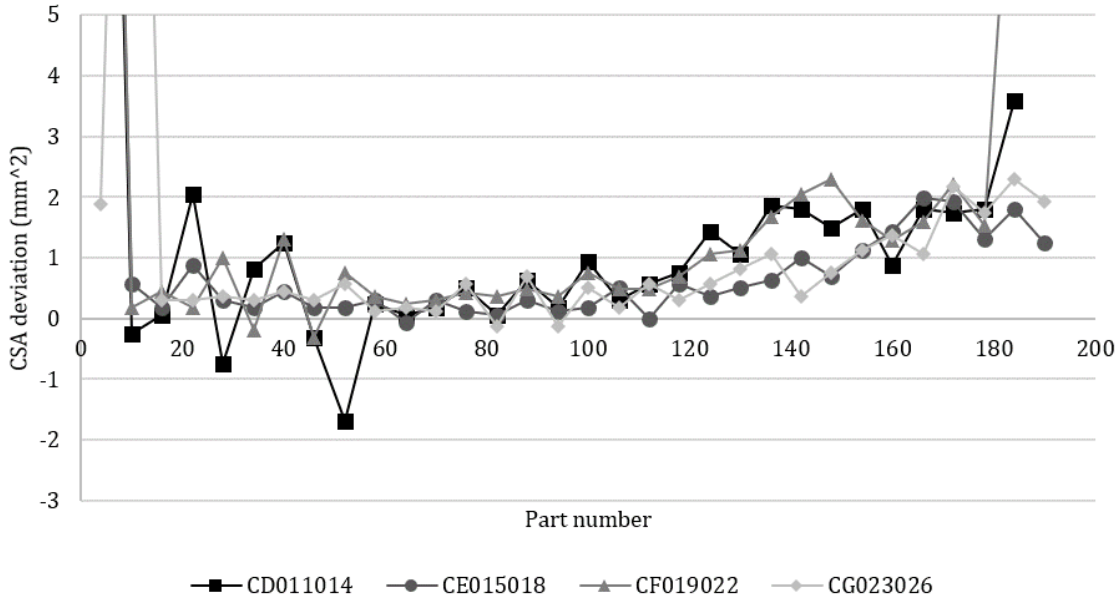
Figure 5.11. CSAM deviation for four tests

Figure 5.11 shows that converting from diameter to the cross-section moderately changes the four trendlines. It should also be noted that the part numbers have been updated to account for the machining of two slots after each Cylinder. Each slot thus contributes an additional part to the work of the cutting tool. Nevertheless, despite the changes the health indications are yet to be accounted for. Therefore, to account for the health indications the CSAM variation can be considered relative to each previous part, with the first ( $i = 1$ ) still relative to  $d_0$ . The equation for each subsequent part ( $i \geq 2$ ) is therefore:

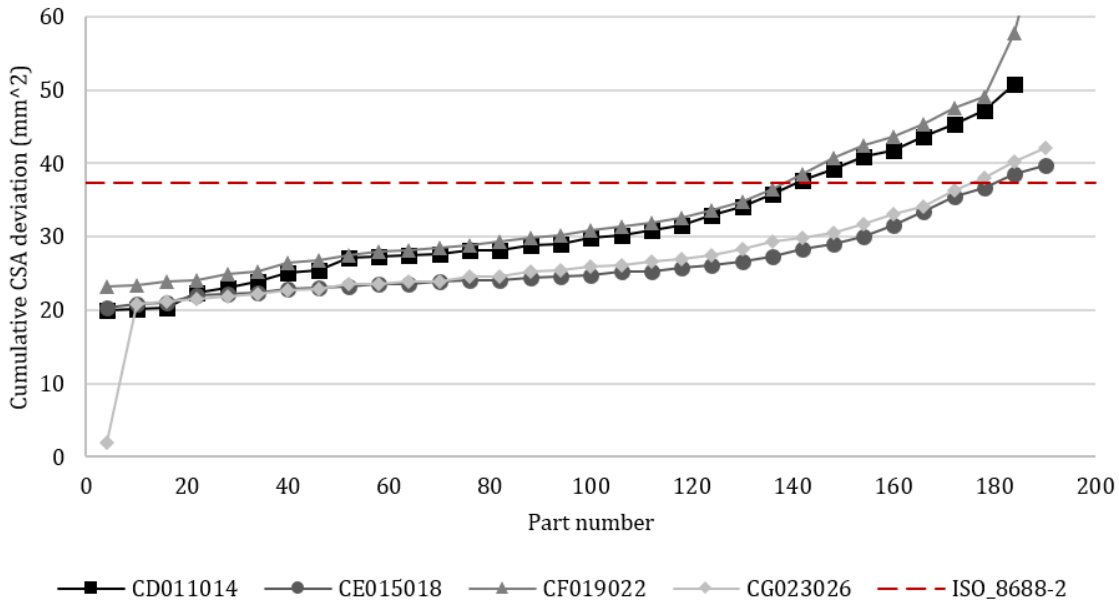
$$\text{CSAM}_i = 0.25\pi (d_i^2 - d_{i-1}^2) \quad (5.2)$$

Where  $d_{i-1}$  is the diameter of the previous part. The part-part CSAM variation is presented in Figure 5.12a. It is noted that the change in the cutting speed for CD is more noticeable; however, the overall trend has been lost. Therefore, to complete the integration of the health indications, whilst maintaining an overall trend, the part-part variation in the cross-section can be accumulated by considering the absolute value of each previous part-part variation in cross-section. The cumulative CSAM deviation is presented in Figure 5.12b. The adjusted equation is:

$$\text{CSAM}_i = |0.25\pi (d_i^2 - d_{i-1}^2)| + \text{CSAM}_{i-1} \quad (5.3)$$



a. Variation in part cross-section relative to previous part



b. Accumulative variation in part cross-section relative to previous parts

Figure 5.12. Cumulative CSAM deviation for four tests

It is observed that the developed algorithm accounts for the change in the cutting speed for CD, increasing the observed trendline proportionally. Separate research by Kundrak and Palmi (2014) indicates that such a shift should be observed when the cutting speed changes. This indicates that the developed algorithm is appropriate. The other observation is that the cutting tools fall into two distinct groups, those that failed within 200 cycles and those that did not. The cumulative CSAM deviation for tests CI, CJ, CK, and CL are considered in Figure 5.13 along with CD and the ISO-based threshold for reference.

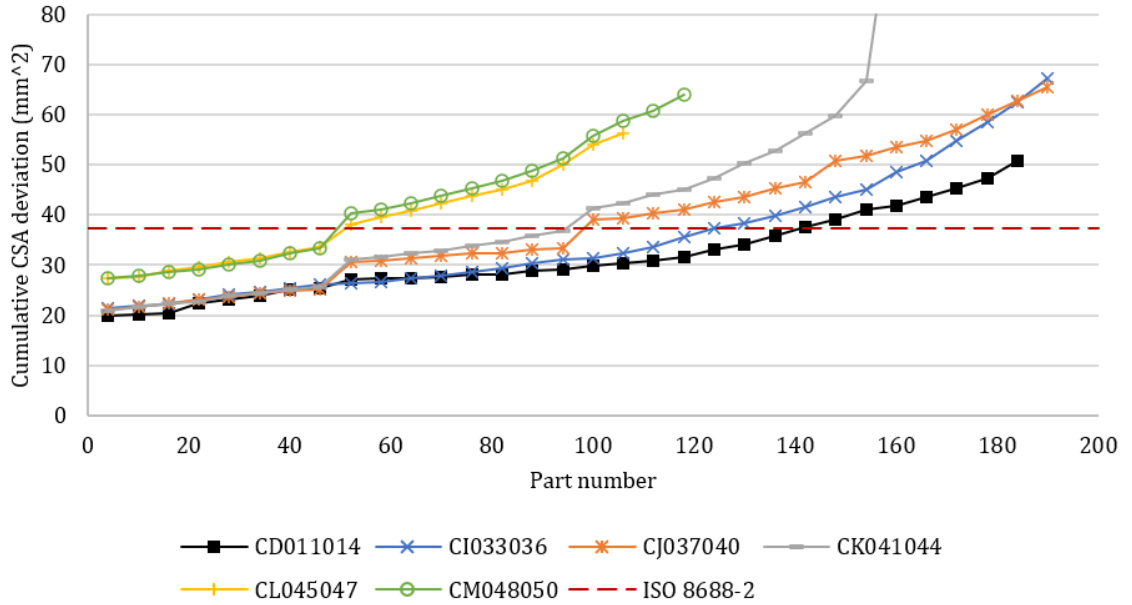


Figure 5.13. Cumulative CSAM deviation for tests CD, CI, CJ, CK, CL, and CM

It is noted that all trends are (more or less) representative of the general wear curves indicated in Chapter 2, albeit with less pronounced initial, gradual and rapid wear stages. For CJ, CK, CL, and CM the curves are noticeably staggered. This was due to introducing a fixed 0.1mm offset to the cutting tool diameter to approximate the implementation of ICG. It is noted that the rate of wear increases for the cutting tools with a regularly adjusted diameter. Notwithstanding, a 0.1mm adjustment is a worst-case scenario; with a proper implementation of ICG the increase in the rate of wear may not be as significant as has been presented. It is noted that all trendlines far exceed the ISO-based limit, although this perhaps indicates that it is not appropriate as a limit when more that the cutting speed is changed between processes. It is also noted that none of the curves hint at the instantaneous condition of the cutting tool and instead only indicate the overall, or general, trend from new to worn (or new to failed). This is a limitation of the geometry information.

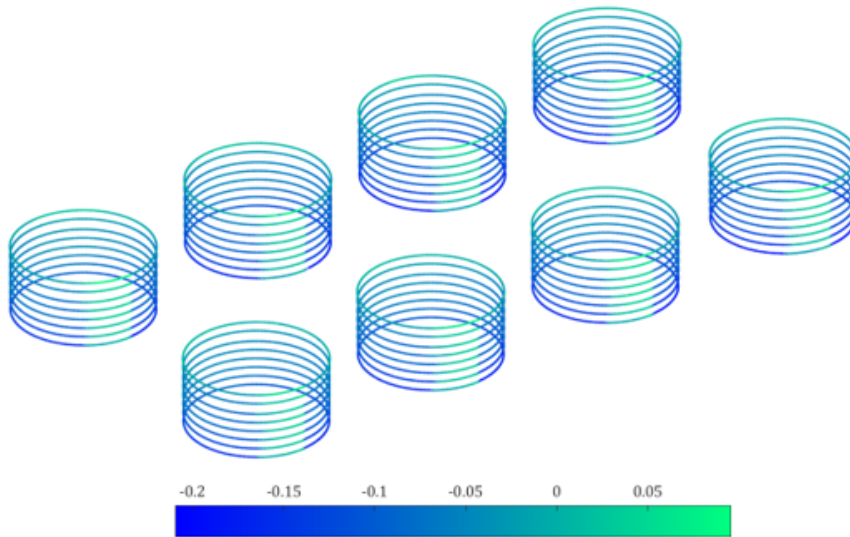
### 5.2.1.3 Form observations from scanned measurement

The cumulative CSAM deviation shows the general deterioration of the parts and therefore indirectly shows the general deterioration of the cutting tools. However, the actual instantaneous condition cannot be inferred from the line plots. Instead, the scanning data acquired from the Cylinders can be considered using 3D scatter plots. A novel program was developed by the author, in the MATLAB environment, to evaluate the scanning data using the nominal part dimensions. Access to the full MATLAB (live) script is provided in Appendix A.4 along with an inline worked example. The developed program employs the Scatter3() MATLAB function and can be summarised in five-stages:

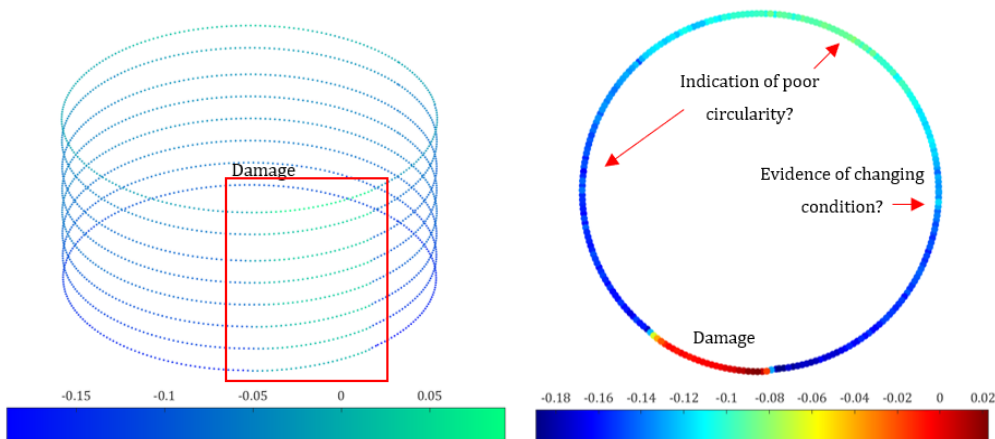
1. Filter the data to remove point touches – the scan data includes all CMM actions, including the point touches taken during the part alignments. These are removed as they do not represent the geometry of the Cylinders and will skew the later data analysis.
2. Find each scanning arc – the scanning data was all appended into a single data file. This required

each scanned arc, within each part, within each Cylinder, to be isolated and evaluated relative to the nominal dimensions.

3. Process data – the centre of each part was translated to (0,0,0). This simplified the calculation of the resultant distance from the centre of the part to each scanned point. The sorted data is then checked based on a nominal diameter of 40mm and an allowable deviation of 20% of this.
4. Compile errors – with the data sorted and filtered, the deviation of each point can be calculated as a relative error. The error is calculated from a combination of the difference from an equivalent “perfect circle” and the difference from the nominal circle. The two differences are compiled to create a colour matrix that may accompany the scan data.
5. Evaluate – the colour matrix can be superimposed on the plotted geometry to provide a visual aid for determining the condition of the Cylinder. Using colour allows subtle variation to be noted without having to exaggerate the relative variation. Figure 5.14 shows the results for an arbitrary workpiece, the first Cylinder, and two scanning arcs.



a. Example 3D scanned geometries (isometric view)



b. Single Cylinder (isometric view)

c. Arbitrary, annotated, part (top view)

Figure 5.14. Example 3D plots of geometry variation in the Cylinder applications

Figure 5.14 does not have any axes as the colour should provide the relevant information. It was determined that the axes undermined that when included. The figure is primarily monochromatic to simplify the image and to prevent distorted or false patterns emerging (see Borland and Taylor (2007) for information). Although, Figure 5.14c is provided in a Jet colourmap to emphasise the colours of each marker. It is noted that the 3D plots are a useful visual aid for determining, and comparing, the condition of the Cylinders without needing the physical part available. The plots identified the main process issues, including the potential deflection of the cutting tool evidenced in the first part of each Cylinder, the DTW evidenced as a gradual reduction in deviation magnitude, and the imperfection caused by the cutting tool retracting at the end of each Cylinder. The plots may possibly be useful for identifying the instantaneous condition of the cutting tool. However, this will be limited to occurrences during the final pass, and will only be appropriate for the fourth part in each Cylinder (as with the 2D investigation). Nevertheless, the 3D geometry plots have potential for providing process feedback during the cutting process. For systems employing ICG, such information (currently reserved for determining cutting tool offsets) may be presented in the same format, thus providing engineers with smart condition-based data during each process. This could complement other data-visualisation systems developed for Industry 4.0, the IIOT, and connected factories. It is utilised in the approaches developed further here in.

### 5.2.2 Finish measurement

The geometry provides a useful indication of the component condition; however, the nuances of the cutting tool are perhaps obscured by the imperfections in the cutting process. It is further the case that if ICG is implemented correctly, there should be negligible post-process information provided by the geometry of the workpiece. Therefore, the surface finish of the components may be considered as an added measure of cutting tool condition. The surface finish measurements were taken with a Renishaw SFP2 using the SFM-2 cranked tip. The full DMIS program written to measure the surface finish is in Appendix C.1. The scans were enacted using a custom macro M(SURFINJ):

```
M(SURFINJ)=MACRO/X1,Y1,Z1,SCNLEN,I1,J1,K1,VA,VB,VC,@FTNAM,DRAGDIR
```

Where the start coordinates X1, Y1, and Z1 were required, but the end coordinates were calculated based on the drag direction (DRAGDIR) and the scan length (SCNLEN). I, J, and K were the direction cosines and VA, VB, and VC were the vector cosines. Each surface finish measurement was calculated from three separate scans, each offset 0.5mm along the Z-axis to consider the average surface finish of the surface rather than a single path. Scans were enacted at a probe yaw of 10 degrees to prevent the SFM-2 from colliding with the workpiece (the angle was chosen arbitrarily). Measurements were evaluated every 0.5mm at a velocity of 1mm/s. The three evaluation lengths were each 6.4mm, including a total cut-off distance of 0.8mm (0.4mm each end), and seven sampling lengths of 0.8mm. The cut-off distance was employed to remove the probe acceleration and deceleration movements. It is noted that the scans were taken within the unidirectional slots (relative parts five and six) as these were easier to access than the fourth part within the Cylinders. Additionally, measurement within the Cylinders would not be perpendicular to the lay.

### 5.2.2.1 Ra versus Rz

It can be gathered from the DMIS program in the Appendix that 28 different applicable tolerances are calculated. However, herein only the roughness average (Ra) and variations of the roughness max (Rz) will be considered. Figure 5.15 indicates the Ra and two Rz values for CD. Where RzDIN is the max peak to valley distance averaged from each sampling length and RzISO is the max peak to valley distance averaged from the highest 5 peaks and the deepest five valleys from each sampling length.

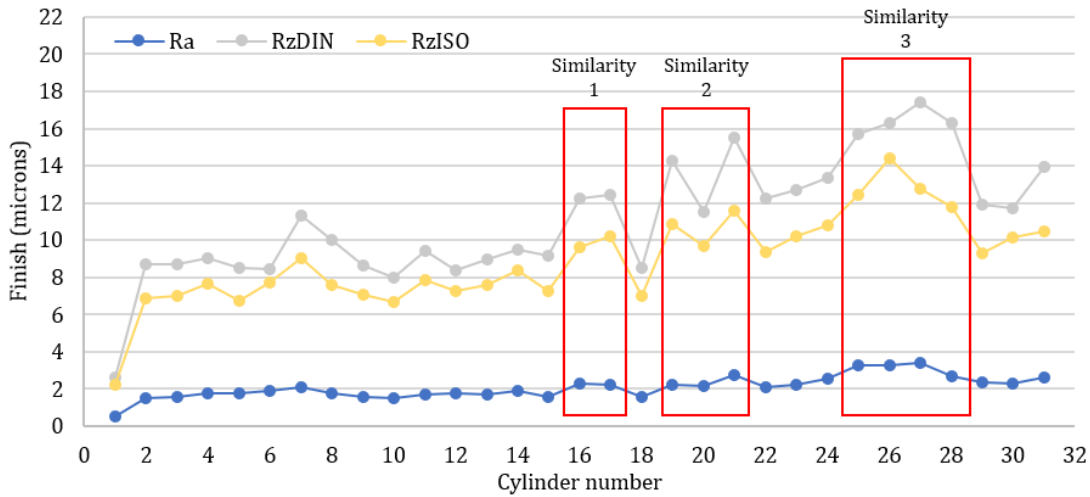


Figure 5.15. Roughness measurements for CD, comparing Ra, RzDIN, and RzISO

Figure 5.15 shows that all three measures present similar information. However, the output from Ra is significantly muted in comparison with the two Rz measures. This is understandable as the Ra is an average measurement and therefore the peak-valley impact is lessened. Mitutoyo (2016) also states that Ra is not useful; Rz is better. Notwithstanding, the usefulness of each Rz measure is also questionable. Both measures will be highly susceptible to scratches and severe damage. It is also the case that the roughness varies significantly with process variation. Figure 5.16 shows the RzISO measures for CD, where (a) is the left-hand wall and (b) is the right-hand wall of the slot.

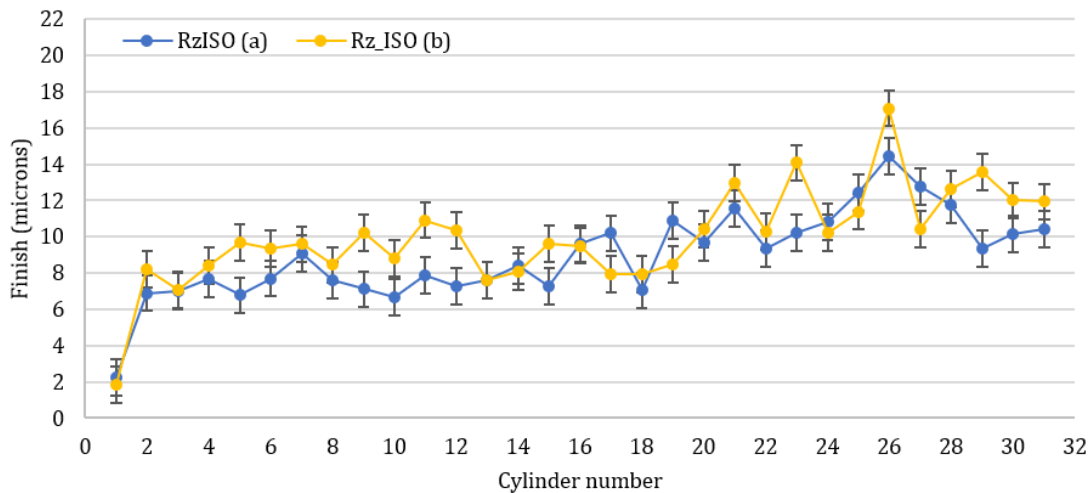


Figure 5.16. Comparing RzISO for each side of the slot wall (set CD)

Figure 5.16 includes  $1\mu\text{m}$  fixed value error-bars. Whilst both sides of the slot were machined in an equivalent way, there was a difference in the relative engagement of the cutting tool. For the left side, the cutting tool was cutting at full width (slotting), whilst for the right side the cutting tool was cutting at 60% width. The difference between the two trends for Rz implies that the surface finish is overly sensitive to process variation, hence, associating regions of the signal with the condition of the cutting tool may be challenging. Herein only the right side will be considered (side B).

### 5.2.2.2 Best-fit polynomial and cumulative sum

Whilst the surface finish may be susceptible to scratches, and sensitive to any variation in the cutting process, the general upward trend is not dissimilar to the geometry trends. This is especially the case when the signals are smoothed to remove the point-to-point variability. Figure 5.17 shows an envelope plot for CD, CE, CF, and CG, illustrating the potential curve characteristics that are reminiscent of the general wear curves, and the geometry trends. Figure 5.17 includes a 3rd order polynomial (cubic) trendline based on the combined average of the four tests. The cubic trendline illustrates the initial, steady, and rapid wear regions. It is noted that part 4 and part 10 for CG were omitted as outliers.

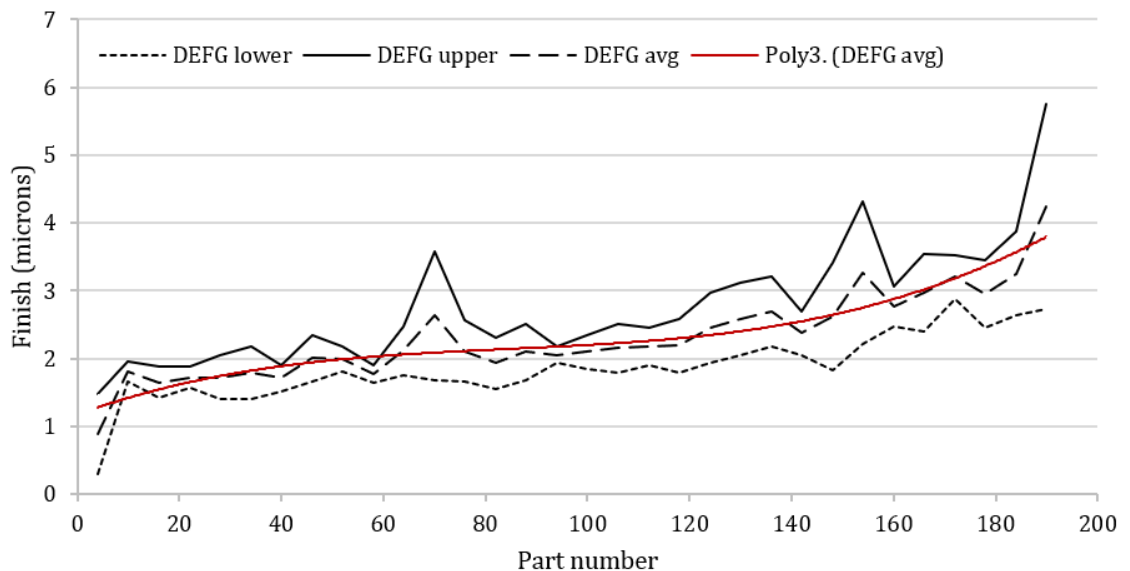


Figure 5.17. Surface finish envelope plot for CD, CE, CF and CG, showing the combined average trend

A similar plot for the geometry is provided in Figure 5.18. The most notable difference (besides the Y-axis scale) is the smoother nature of the plot (fewer peaks and valleys). To compare the actual similarity between the two trendlines provided in Figure 5.17 and Figure 5.18, one may compare the EOL between the two measures. This will be the point at which statistically the trends are deviating significantly (more than three standard deviations) from their average.

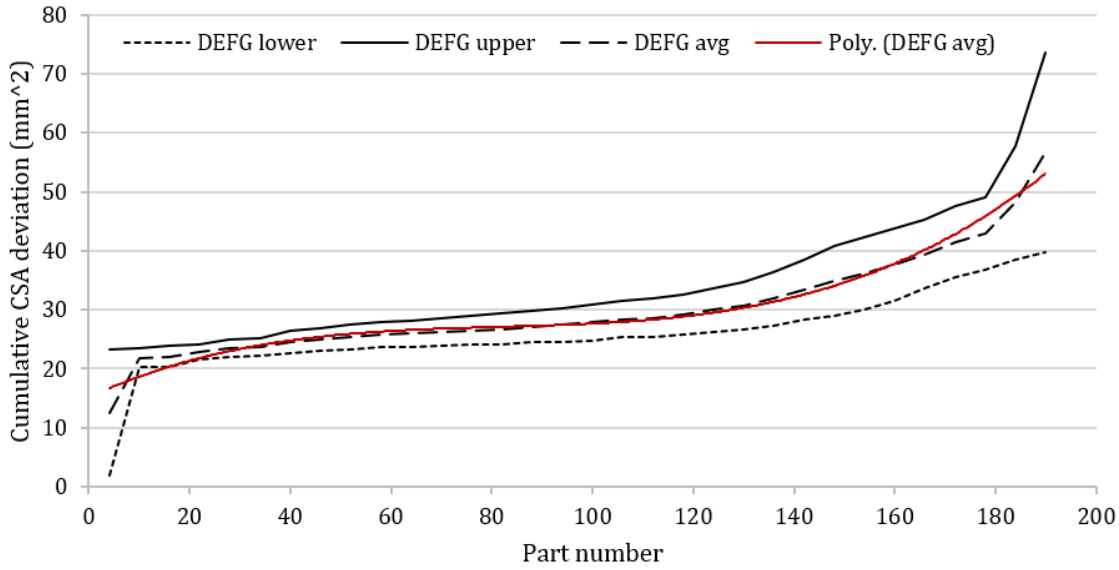
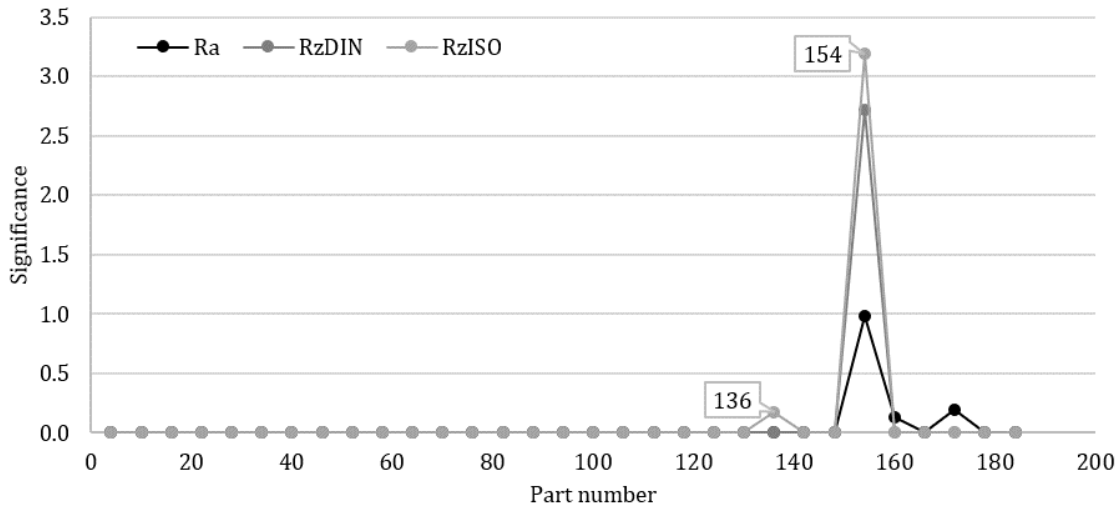


Figure 5.18. Geometry envelope plot for CD, CE, CF, and CG, showing the combined average trend

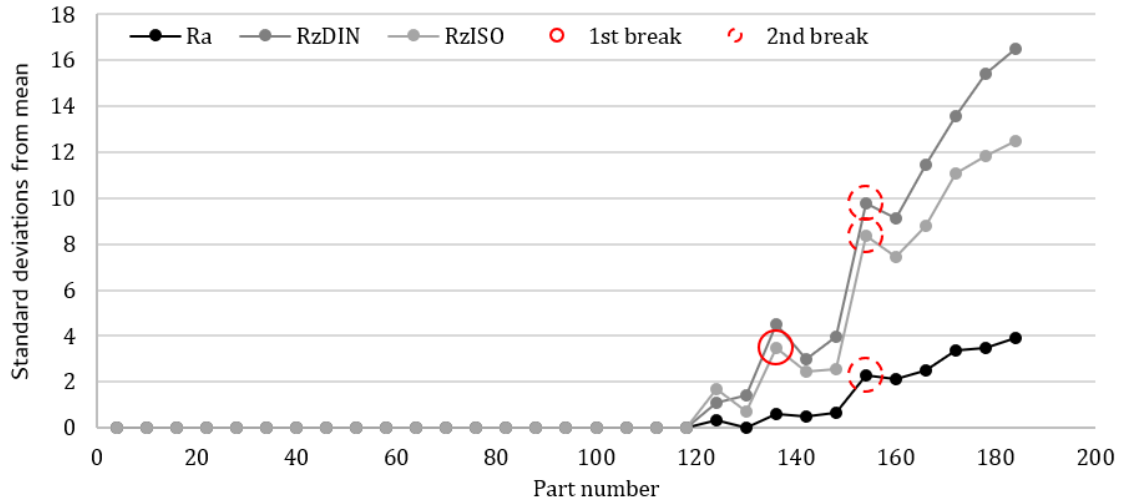
This is implemented by considering the upper cumulative sum (CUSUM, or QSUM) for each test individually. The QSUM is implemented using Equation (5.4) (Matlab 2020):

$$U_i = \begin{cases} 0 & i = 1 \\ \max(0, U_{i-1} + x_i - \bar{x} - 0.5n\sigma_x) & i > 1 \end{cases} \quad (5.4)$$

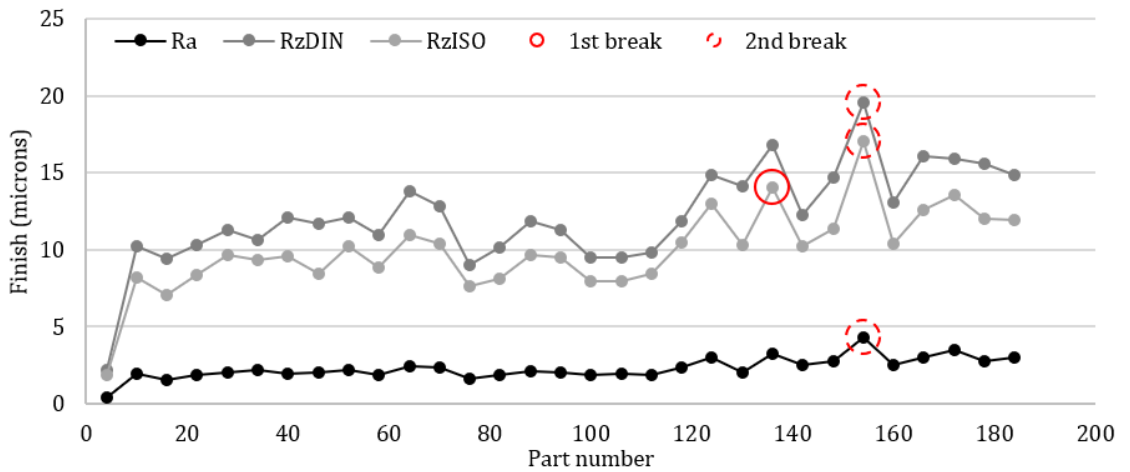
Where  $U_i$  is the upper sum,  $U_{i-1}$  is the earlier iteration,  $x_i$  is the current value,  $n$  is the significant number of standard deviations,  $\bar{x}$  is the mean of all samples and  $\sigma_x$  is the standard deviation of all the samples. All values will be zero unless more than the given number of standard deviations from the mean. For CD, the surface finish QSUM is given in Figure 5.19.



a. Upper QSUM breakpoints for CD surface finish measures with  $3\sigma$  threshold



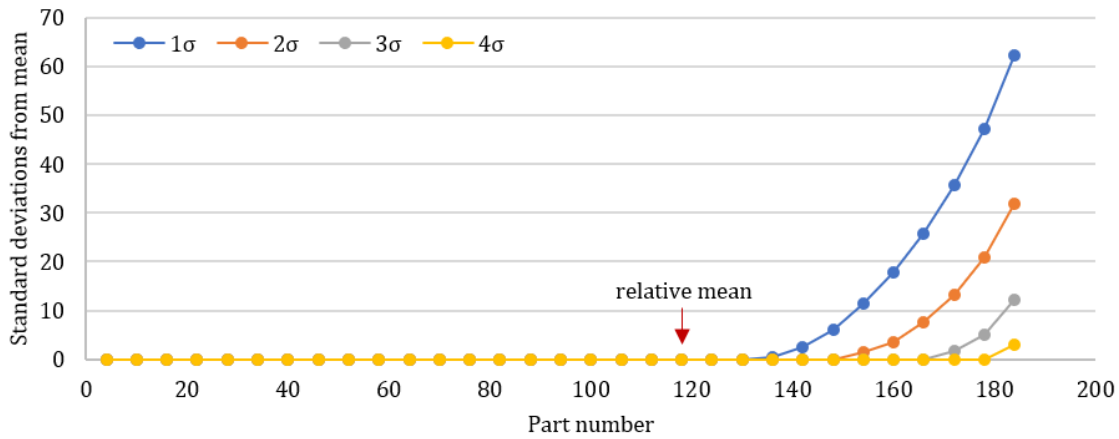
b. Upper QSUM full plot for CD surface finish measures showing breakpoints



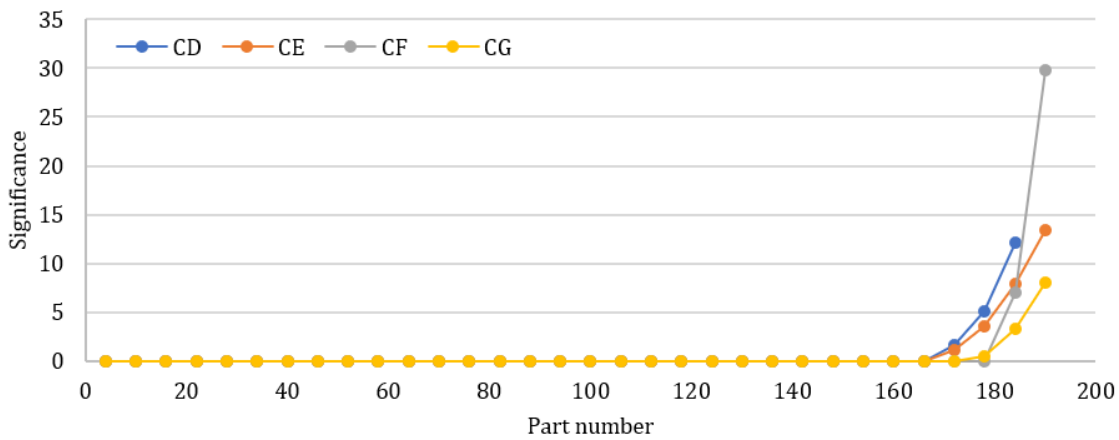
c. Roughness measurements for CD, comparing QSUM breakpoints for Ra, RzDIN, and RzISO

Figure 5.19. QSUM investigation for CD surface finish trends

Figure 5.19 shows that RzISO is the first to deviate at 136 parts. However, all measures are noted to deviate at 154 parts with a greater significance. The breakpoints are superimposed on the full QSUM plot and the original plots to illustrate when they occur. It is considered that the QSUM approach is good at finding an EOL from an otherwise ambiguous signal. The geometry QSUM is given in Figure 5.20 for comparison. Figure 5.20 shows that the geometry does not appear to deviate until much later; however, this is due to the mean of the trends being skewed towards the latter parts. It is shown that using a lower significance threshold can find the deviation earlier. However, this says that - whilst good at finding a suitable EOL within an ambiguous signal - the QSUM approach can arguably be manipulated to return an EOL that suits the desired narrative, rather than the true, or most suitable EOL. Table 5.1 gives the breakpoints for CD, CE, CF, and CG, for both the geometry and the surface finish measurements, using a  $3\sigma$  upper QSUM significance.



a. Upper QSUM trends for CD CSAM with 1, 2, and 3σ thresholds



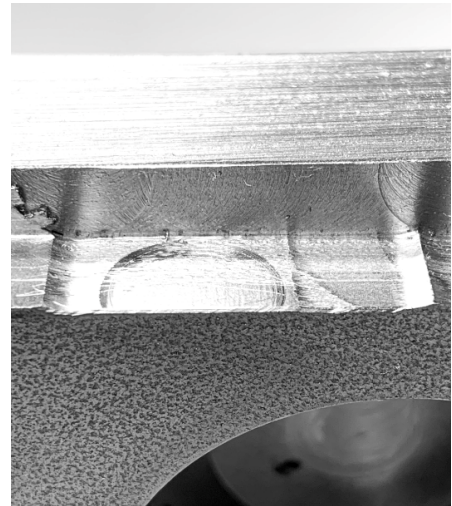
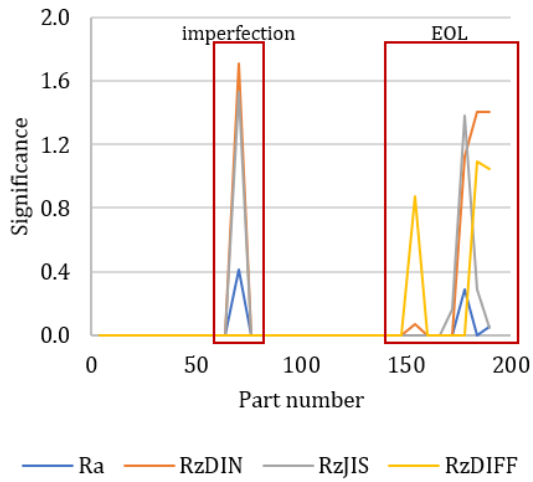
b. Upper QSUM breakpoints for CD, CE, CF, and CG CSAM trends with 3σ threshold

Figure 5.20. Upper QSUM plots for CD, CE, CF, and CG geometry data sets

In Table 5.1 the ISO column for the geometry considers the parts at which the deterioration goes beyond the ISO 8688-2:1989 threshold. All breakpoints stand for the fourth part in each Cylinder, despite (in actuality) being the sixth part. CG is noted as the first significant breakpoints correspond to an imperfection on the part surface. These were discounted when populating Table 5.1. The imperfection is illustrated in Figure 5.21. The breakpoints are compared using a radar plot in Figure 5.22.

Table 5.1. Breakpoints for CD-CG, for both geometry and surface finish measurements

Test	Geometry		Surface finish		
	ISO	CSAM	Ra	RzDIN	RzISO
CD	142	172	154	154	136
CE	184	172	166	166	166
CF	142	184	184	148	166
CG*	178	178	178	154	172



a. Upper  $3\sigma$  QSUM

b. Part photograph

Figure 5.21. CG surface imperfection

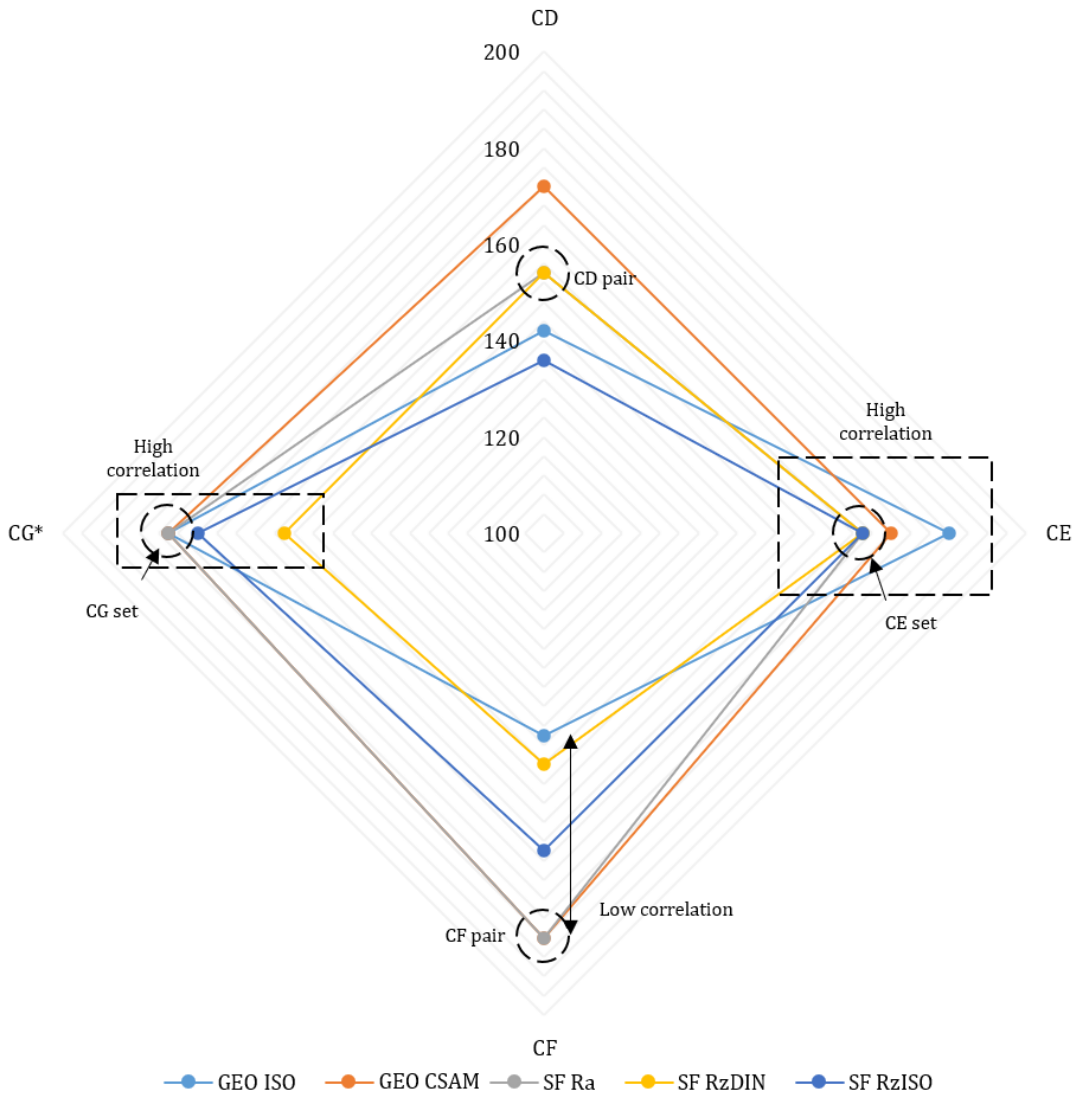


Figure 5.22. Qualitative breakpoint correlation using radar plot for CD, CE, CF, and CG

Using Figure 5.22 the correlation within each test may be considered:

- CD** – shows a match between Ra and RzDIN, but overall a low correlation between all measures. Between the geometry and the surface finish, the closest match is GEO ISO and SF RzISO with a difference of six parts. RzISO defines the EOL earliest at 136 parts.
- CE** – shows a match between all surface finish measures and overall a high correlation with a range of 18 parts for all trends. The smallest difference between the geometry and the surface finish is between GEO CSAM and all three surface finish measures, with a difference of six parts. Like CD, the surface finish was earliest to define the EOL.
- CF** – shows one match between GEO CSAM and SF Ra, and a small difference (six parts) between GEO ISO and SF RzDIN. However, the overall range is 42 parts (almost 25% of the total parts), indicating a low overall correlation.
- CG** – shows a match between GEO ISO, GEO CSAM, and SF Ra, with a difference of six parts from SF RzISO. SF RzDIN defines the EOL 18+ parts earlier than any of the other results; however, this may be because RzDIN is more affected by the surface imperfection than the other measures.

It is noted that RzDIN defines the EOL earlier (on average) than all the other measures (detecting the EOL at an average 155.5 parts). The closest geometry prediction is by GEO ISO at 161.5 average parts. A side-by-side comparison of the geometry and the surface finish results is given in Figure 5.23.

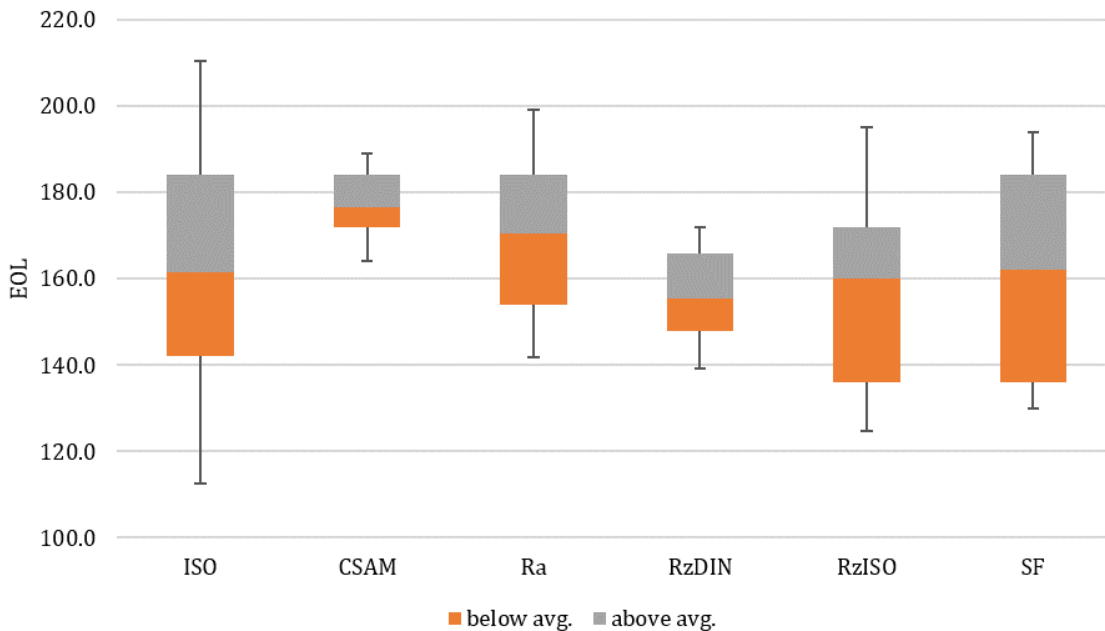


Figure 5.23. Box-plot comparison of the geometry and surface finish measures estimates for EOL

Figure 5.23 keeps the two geometry measures separate for clarity. ISO is the effective tolerance provided by the standard, while CSAM is the EOL calculated by the QSUM. The error bars show 95% significance for each observation, showing that none of the results are significantly different from

one another. The individual ranges show that CSAM and RzDIN more closely correlate the different tests, while RzISO differentiates better between them (inferred by the bigger range). It may also be inferred that the RzDIN is better for earlier definitions of the EOL, whilst the CSAM is better for later definitions. Which is better cannot be easily determined; however, based on the CSAM predictions falling later than ISO it may be inferred that earlier is better to avoid significant part deterioration. Nevertheless, it is noted that the above comparison is exclusively based on the definition of the EOL and thus a direct comparison of individual numbers. This is a challenging comparison to make; therefore, any similarity is a bonus. The qualitative comparison of the overall trend is enough to warrant that both the geometry data sets, and surface finish data sets provide useful information. This enables them to be employed for calibrating the in-process data.

### 5.3 Application of MTData: Spindle motor load

Having considered the indications of the cutting tool condition from the product quality, attention is drawn to the information derived from the machine tool itself. The first signal considered is the spindle motor load (SML). It was noted in Chapter 4 that the data needed to be converted from the raw percentage load into PEC to consider the motor rating and to change the format into one that is more descriptive of the process. Figure 5.24 shows the raw data for “cutting tool 1” (test CD).

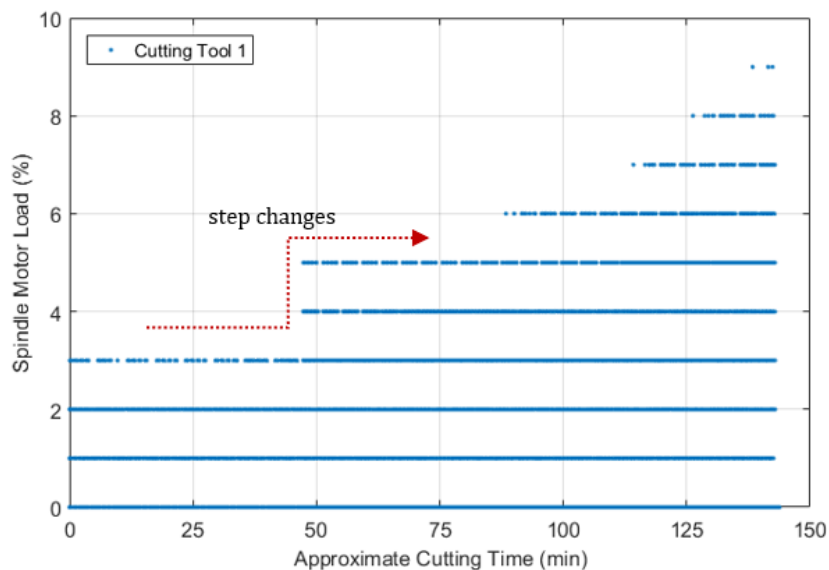


Figure 5.24. Quantised SML MTData for CD

Figure 5.24 is given as a scatter plot and shows that there is a general upward trend in the data. This indicates similar information to that provided by the geometry and the surface finish; however, it is notably staggered and discontinuous. Figure 5.25 presents the same data but processed following the steps outlined in Chapter 4; using Equation (4.6) to find the energy per part, rather than per sample. Figure 5.25 shows that the unidirectional slots in the centre of the Cylinder block present as a challenge in the resulting SML data set. This is because the PEC for the slots is much less than the PEC observed for each part of the Cylinders. As the primary concern (for this application) are the Cylinders, the slots may be filtered using a Hampel filter (Figure 5.26).

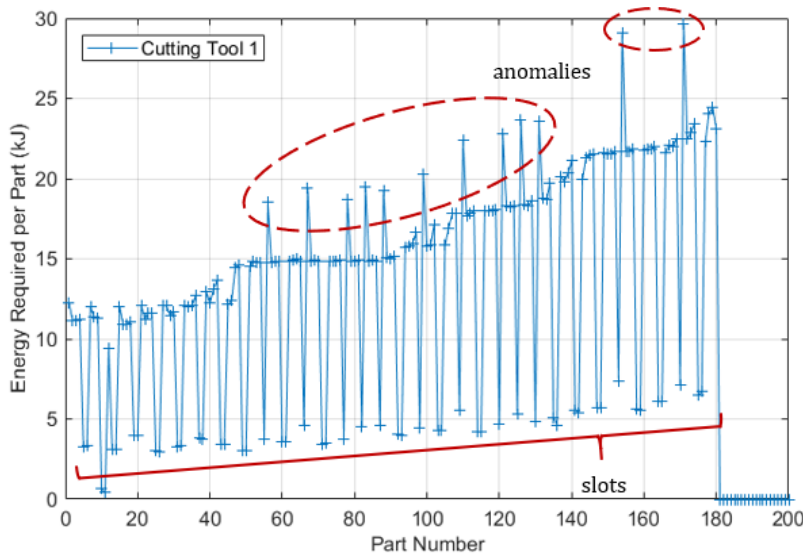


Figure 5.25. PEC for CD prior to Hampel filter

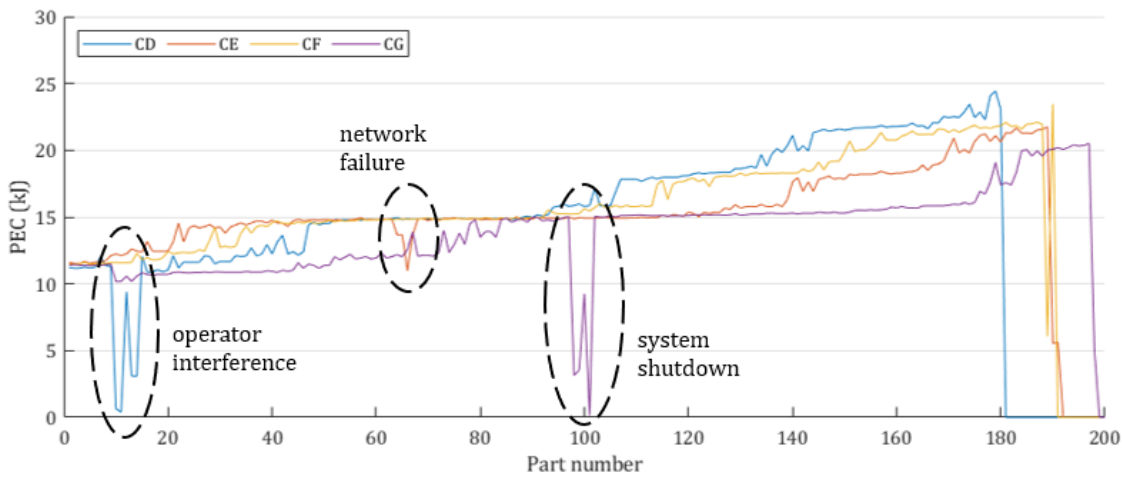


Figure 5.26. Process energy consumption plots for CD, CE, CF, and CG, after a single Hampel filter

Using the Hampel filter keeps the correct number of parts. This is better than just eliminating the slots as outliers altogether. It is noted that this method of reducing the process data into a simple trend does hide all the potential anomalies noted in Figure 5.25. This may hamper any assessment of the instantaneous cutting tool condition. Figure 5.26 shows that the quantised nature of the MTDData is still observable for all of the included cutting tools with significant “steps” in the chart data. It is acknowledged that these steps limit the precision of the system; however, this potentially benefits the system by filtering some signal noise. It is noted that improving the resolution of the MTDData will significantly reduce the observed “staircase effect”, but will also increase the data quantity and complexity. There may also be an increased need to filter the acquired data to remove noise. Figure 5.26 also illustrates the system sensitivity to process/data interruptions. All interruptions result in a significant drop in measured PEC and artificially add to the number of parts (most notably for CG). These are acknowledged in Figure 5.26 and correspond to:

**Operator interference** – process stop for cutting fluid replacement

**Network failure** – interruption to the communication between controller and PC (data loss)

## System shutdown – process stop/shutdown for an extended period

In two of the observed interruptions (interference and shutdown) the process is stopped, adding unplanned machine downtime. The resulting energy signature is repeatable, suggesting these occurrences could be monitored. However, as the information is derived from the spindle load, abrupt changes in the spindle speed will result in a similar energy signature. Identifying the exact nature of these signatures in a practical application would therefore require the consideration of additional information, including the spindle speed. The remaining of the three observed interruptions (network failure) is a fault arising in the transfer of MTData, resulting in a gap in the signal acquisition. The fault could, in theory, be confused with a process or condition change and hence may be difficult to identify in practice. However, the system recovered in reasonable time and the error code, incident time, and incident duration were recorded. If this information remains available, the fault is classifiable. It is important to state that the system accommodated all process interruptions and continued to operate normally when they were resolved. It should be noted that whilst attention has been primarily directed towards the translation of the SML into PEC, the data in the raw state will still be of use for investigating the instantaneous condition of the cutting tool. When the signal is manipulated in such an extensive way the micro changes in the progressing signal are no longer an exact representation of the cutting tool condition. This is a side-effect of prioritising the overall deterioration trend and RUL of the cutting tool. The version of the signal to consider depends on the analysis being undertaken.

### 5.3.1 Signal and condition observations

#### 5.3.1.1 Micro value

Two approaches may be taken when analysing cutting tool condition using the SML. The first is to consider the “micro value” of the raw signal. The micro value refers to the value of the instantaneous signal, or the real-time process changes. This micro format can be used to illustrate the current machining process and show actual contact time between the cutting tool and the material/part. In the first instance this can be evaluated by considering a cutting tool that failed within a single Cylinder. This is shown in Figure 5.27.

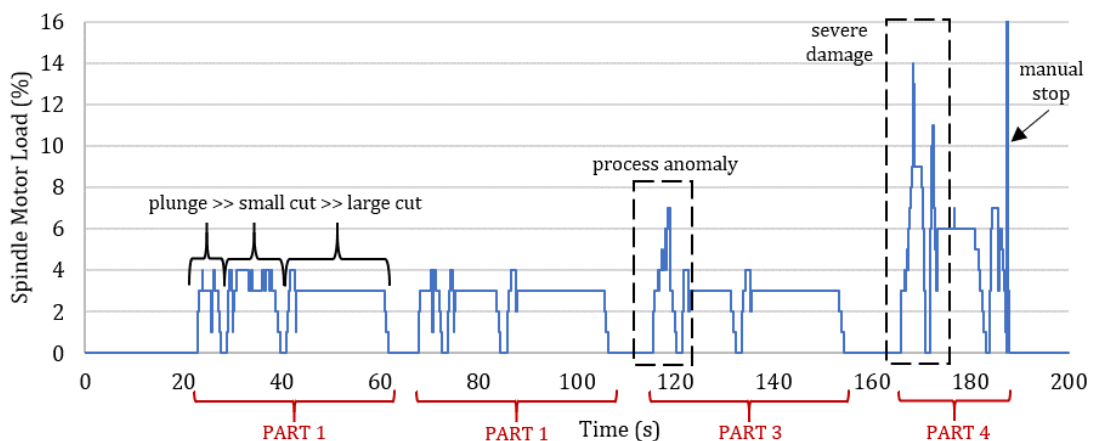


Figure 5.27. Single Cylinder spindle motor load for a 10mm cutting tool (with failure)

Figure 5.27 (like the PEC trends) notes the quantised nature of the signal. It is noted that this again raises the issue that slight, gradual or incremental changes cannot be observed, especially at this resolution. For the process considered, the cutting tool successfully removed material to a depth of 15mm, then failed whilst machining the final 5mm. The total cutting time was 128 seconds with an average SML of 3% and a peak to 14% at failure. 80% of the part was completed prior to the cutting tool failing. There is a noted separation between cutting processes with the first entry cycle (plunge) distinct from the inner (small) circular cut which is distinct from the outer (large) circular cut. Potential damage is visible at 118 seconds with a 7% peak in the SML. The peak was initially attributed to a build-up of swarf affecting the cutting tool as noted by watching the process. Failure of the cutting tool then occurred after 160 seconds with the SML peaking to 14% before settling to a (higher than average) SML of 6%. The machine tool was manually stopped at this point, this can be observed in the SML signal. A more in-depth evaluation of the process provided in Figure 5.27 is given below, using data from Table 5.2. The RAUC is the relative area under the SML signal.

Table 5.2. Data for single Cylinder machined using an arbitrary 10mm cutting tool (with failure)

Part	Process	Modal SML (%)	Peak SML (%)	Start (s)	Finish (s)	Process time (s)	Part time (s)	Process RAUC	Part RAUC
P1	Plunge	3	4	23.01	27.53	4.52	36.05	863	7201
	Inner	4	4	28.92	39.73	10.81		23.49	
	Outer	3	4	41.01	61.73	20.72		3989	
P2	Plunge	3	4	67.92	72.53	4.61	35.94	858	6846
	Inner	3	4	73.81	84.53	10.72		2033	
	Outer	3	4	85.92	106.53	20.61		3955	
P3	Plunge	3	7	115.51	120.23	4.72	36.16	1216	7267
	Inner	3	4	121.51	132.23	10.72		2053	
	Outer	3	4	133.51	154.23	20.72		3998	
P4	Plunge	9	14	165.91	170.92	5.01	19.86	2271	7731
	Inner	6	11	171.81	183.23	11.42		4258	
	Outer	7	7	183.91	187.33	3.42		1202	

**Part 1** was machined in 36.05 seconds. The plunge and the inner loop were accompanied by fluctuations in the SML indicating potential cutting tool vibrations or interactions between the cutting tool and swarf. Part 1 took 36.05 seconds to complete with the total relative area under the SML signal being 7201. The relative area is given here to enable the comparison between separate cuts and hence no units are given.

**Part 2** follows with a total cutting time of 35.94 seconds. Fewer fluctuations are observed, indicating an improvement in conditions relative to part 1. The relative area for part 2 is 6846. This quantitatively corroborates the visual improvement.

**Part 3** was the final, fully completed, part taking 36.16 seconds. Large fluctuations during the plunge took the SML to a peak of 7%. Observations during the experiment indicated trapped swarf impeded operation with implied damage to the cutting tool. It was later also noted that an issue with the g-code caused the cutting tool to enter the material in a drilling motion, rather than helical entry. This may suggest that the peak corresponds to an inefficient (bad) process causing damage to the cutting tool. The relative area for part 3 is 7267.

**Part 4** was the intended final depth. The cutting tool managed 19.86 seconds before being manually stopped. The SML curve shows a sharp rise to 14% followed by a sustained peak of 9% during the plunge indicating severe damage to the cutting tool. During the machining of the following loop the average SML rose from the prior part averages of 3% to a sustained 6%. The increased effort from the machine infers that the cutting tool was no longer capable. The relative area for part 4 was 7731, an increase over the previous parts, despite the part being only 50% completed. This is a relative increase of 126% versus part 2 (healthiest part).

Using Figure 5.27 and Table 5.2 it is possible to draw discussion towards the identifying factors in the signal that preceded the imminent failure. The cutting tool suffered severe damage during the plunge stage in the fourth part. The failure was characterised by a sharp peak in the SML output to double that of the past highest peak. The past highest peak also occurred during a plunge process. As there was a known issue during the plunge process, it is considered that these difficulties contributed to the eventual failure. Acknowledging the SML peak (anomaly) during the plunge of part 3 suggests that the failure may have been avoided if the anomaly was accounted for in-process. However, this is challenged by both inner and outer loops of part 3 completing without further indication of cutting tool deterioration. Further evidence of the micro value can be considered by using another arbitrary cutting tool that did not fail (Figure 5.28). It is noted that the Y-limit is half that of Figure 5.27.

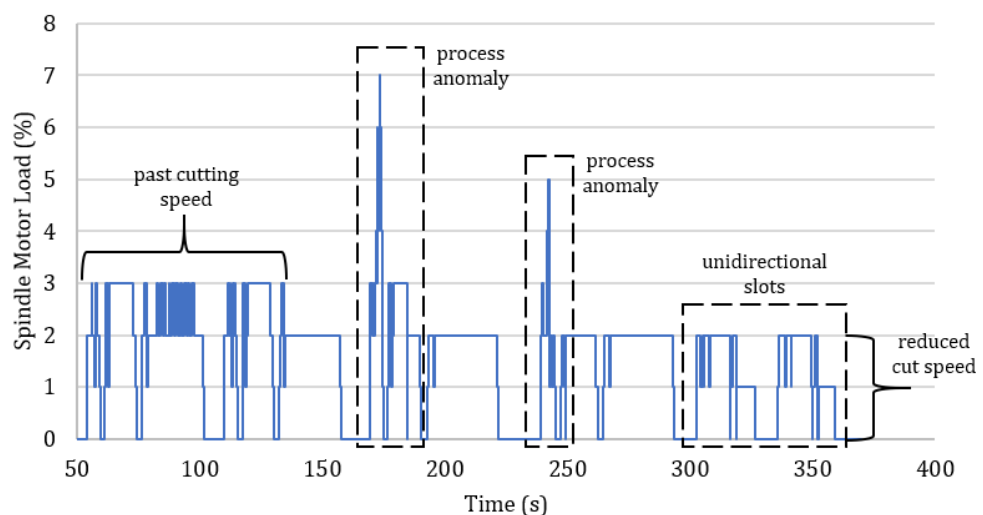


Figure 5.28. Single Cylinder spindle motor load for an arbitrary 10mm cutting tool (no failure)

Figure 5.28 illustrates that the SML signal enables the process variations to be observed. The first few cuts are taken at the same cutting speed as the previously considered cutting tool (magnitude is not

important). The cutting speed is then reduced for the rest of the Cylinder, indicated by the reduced average SML (2%). It is seen that the unidirectional slots are distinct from the other processes. This shows that the process characteristics may be used to enable a data-driven method for determining the occurring process. It is noted that the process anomalies continued to occur during the plunge process with a peak to 7% and to 5%. This reinforces that the inefficient process was causing damage to the cutting tool and shows that the issue can be reliably observed using the SML data. This would (and did) enable the issue to be raised and thus rectified.

The micro value of the SML has shown that there are potential health indicators in the form of rapid integer fluctuations and peaks in the raw SML signal. Although not useful for estimating remaining life it could be useful to prevent catastrophic damage to the machine tool and/or machined part. The SML was assessed using the absolute (raw) values plotted against the cutting time (given in seconds). It was shown that the spindle signal does successfully illustrate the machining process. This potentially enables a feedback loop to provide engineers with actual cutting times and indication of inefficient cycles, poor processes, and bad practice. The SML also demonstrated process change and cutting tool failure. It is reminded that the signal is quantised and a resolution smaller than an integer is not (herein) obtainable. It is noted that for the purposes considered it is not necessary to convert the raw data from percentage load into energy use. The only noticeable difference would be the Y-axis scale and the units used. The processing required to convert the signal would be more valuable employed elsewhere.

### 5.3.1.2 Macro value

The second approach for analysing cutting tool condition using the SML is to consider the “macro value” of the raw signal. The macro value refers to the value of the overall signal, or the general changes in the condition of the cutting process from new and healthy, to used and broken. First the general nature of the SML data must be appreciated. Figure 5.24 in Section 5.3 considered CD and noted the discontinuous, staggered data. Figure 5.29 considers the same information as a line plot.

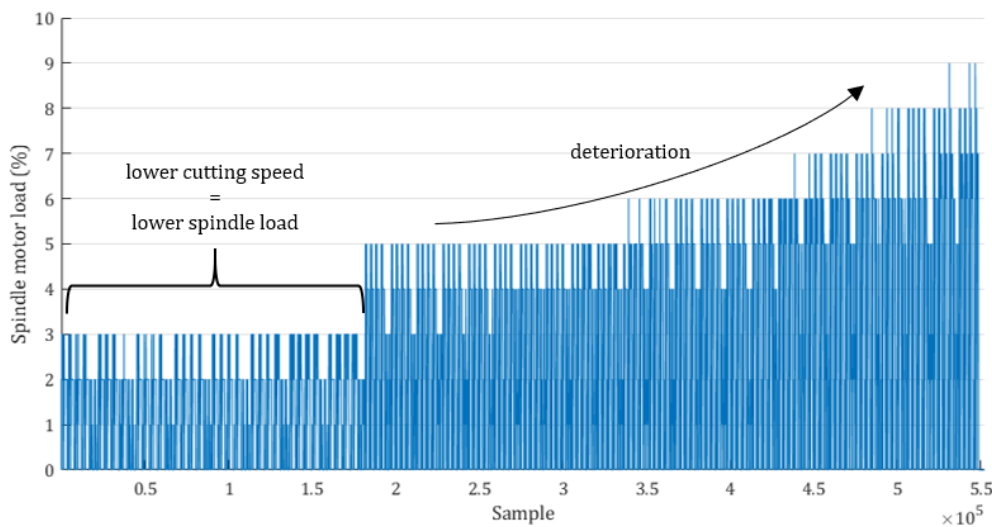
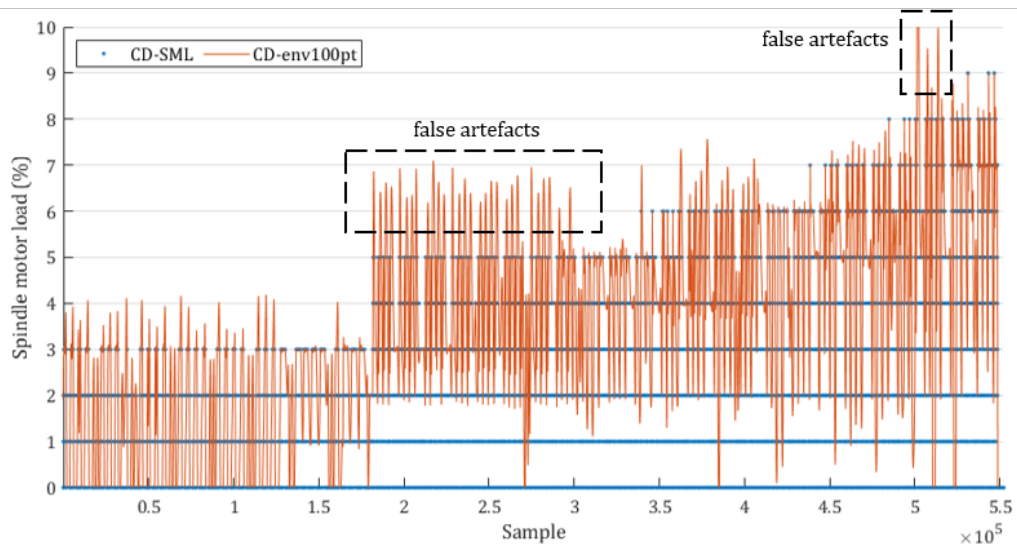


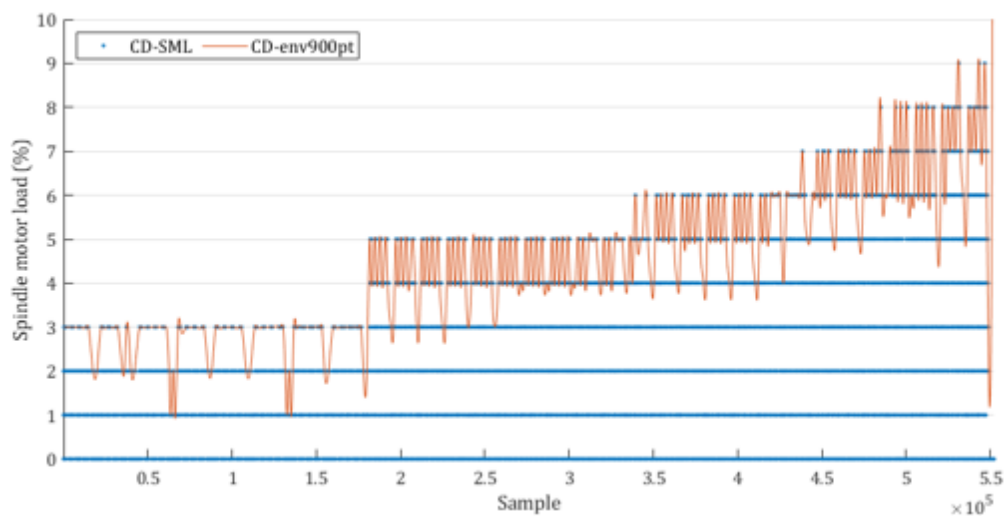
Figure 5.29. Unprocessed spindle motor load line plot for CD

The instantaneous condition can no longer be observed (easily) and it is seen that the general trend is increasing. However, there is not a clear sign of failure at the end of the process. It is also the case that the transitions between integers is significant (quantised data) yet the various stages of cutting tool wear are not so easily distinguishable. Knowing the maximum SML at which the cutting tool failed (9%) and knowing how the signal changed over the life of the cutting tool enables awareness into where the cutting tool should have been stopped; however, like the instantaneous condition (micro value), an amount of information in advance would be useful. As such, efforts have been made to evaluate the changing signal to determine whether the general trend may be defined or predicted, and whether there are indications of the changing condition that are not explicit without a little coaxing. Currently two approaches have been developed:

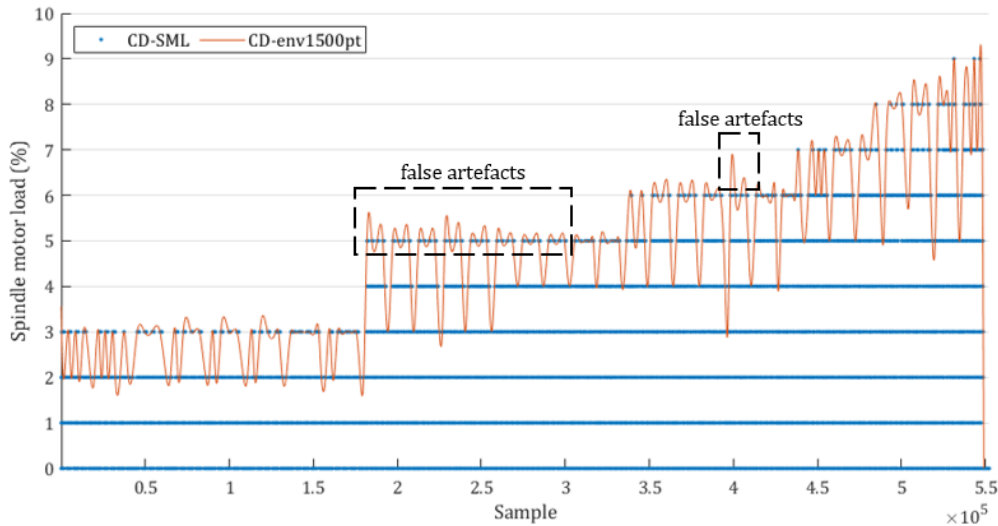
1. To calculate the upper peak envelope for the SML - calculated from the local maxima
2. PEC curves – introduced in Chapter 4, and Section 5.3 above.



a. SML upper peak envelope with 100pt separation



b. SML upper peak envelope with 900pt separation



c. SML upper peak envelope with 1500pt separation

Figure 5.30. Variations in SML upper peak envelope for CD based on peak distribution

The envelope plots presented in Figure 5.30 were calculated using the MATLAB “envelope()” function considering three peak distributions of 100pts, 900pts, and 1500pts. The peak distribution smooths the envelope whilst keeping the underlying signal information. It is seen that the 100pt distribution (and less) was unsuitable as the resultant information was still noisy and false artefacts were introduced that did not represent the original signal. Conversely, the 1500pt distribution more appropriately smoothed the signal; however, false artefacts returned in the resultant information due to over-smoothing. On the other hand, the 900pt distribution was found to appropriately smooth the data, did not introduce false artefacts, and kept a sensible amount of the underlying signal information. Figure 5.31 considers a 900pt envelope for CD and CE.

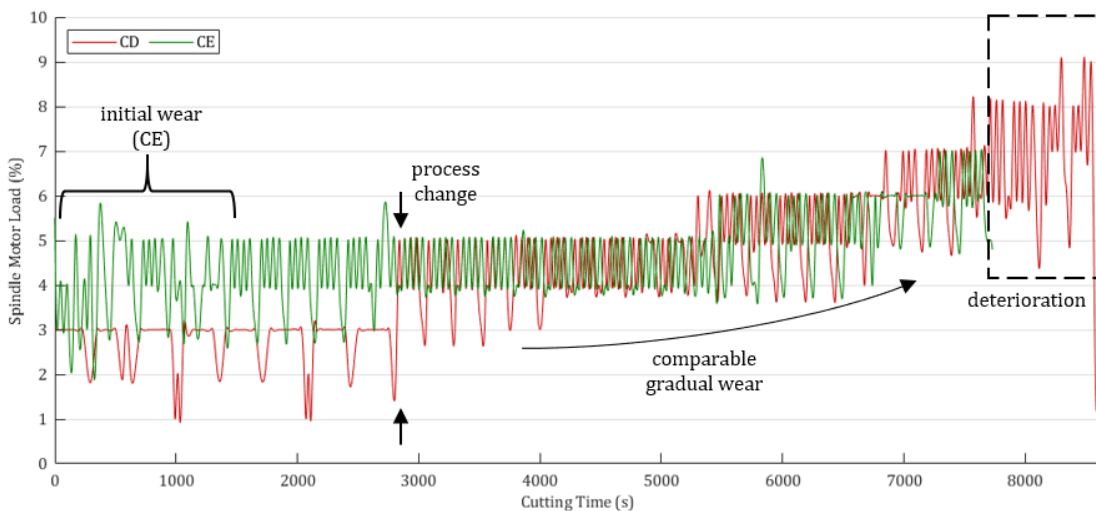


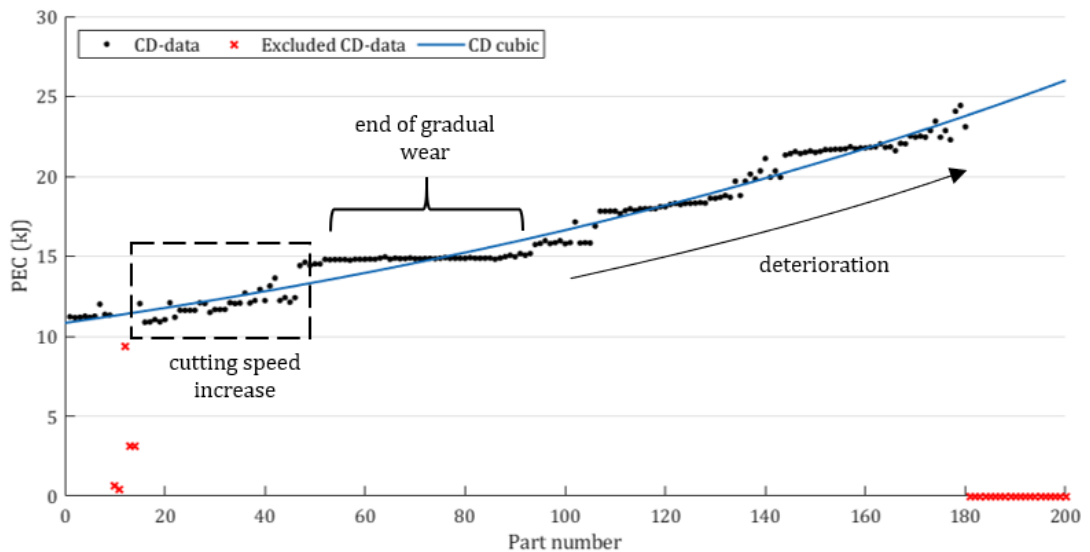
Figure 5.31. SML upper peak envelope with 900pt separation for CD and CE

Figure 5.31 shows a comparison between CD and CE because they are two similar processes yet still covering a range of process variations. CD illustrates the effect of changing the process (early increase

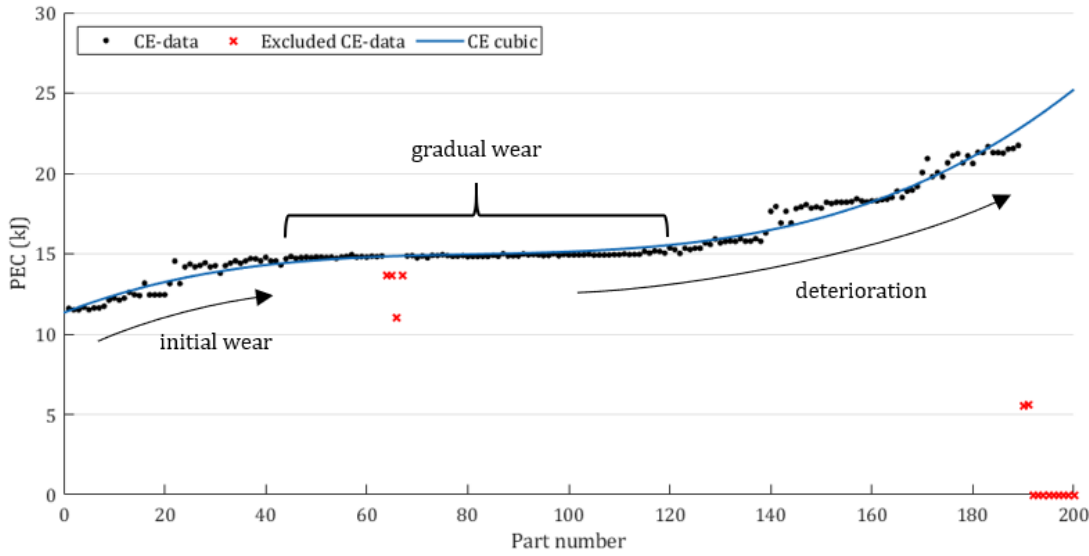
in the cutting speed), the cutting tool is pre-used and therefore lacking the initial wear stage, and the process ends in a failed cutting tool. On the other hand, CE shows a uniform process, for a brand-new cutting tool, which ends before failure can occur.

It is noted that (as expected) CE shows evidence of an initial wear phase, whilst CD does not. It is also noted that CD sees a jump in the observed SML when the cutting speed is increased. However, the change is not proportional as the cutting speed is increased by 44% (32m/min to 52m/min) whilst the SML increases by >50% (challenging to quantify due to the fluctuations). It is noted that the two trends illustrate a similar phase of gradual wear with CD noting an increase in the SML earlier than CE. The deterioration for CD is not seen as a significant peak in the data; however, the “stability” of the trend decreases substantially with sustained fluctuations noted over a range of two (or more) integer values. This is not observed at any other point in either signal; although, the initial wear phase for CE has the closest resemblance.

The envelope plots are a novel way of extracting information from the process signals, without resorting to the micro value. Their value lies in keeping signal variation, whilst still stripping back the noise. They are also a sensible method of combatting the discrete nature of the raw data, providing an estimated continuity between values. However, the limitations of the envelope plots are that they estimate the signal characteristics and are heavily influenced by the chosen peak distribution. As such, the features occurring in the envelope plots cannot be used quantitatively to determine the instantaneous condition of the cutting tool, and (ultimately) must be seen as being limited. Whilst the stages may be determined qualitatively by examining the change in the relative stability of the SML envelope plot, it may also be possible to determine the distinct changes quantitatively. This requires a different approach for understanding the macro value. The second developed approach has already been defined in this thesis. Figure 5.32 shows the PEC curves for CD and CE, noting qualitative characteristics beyond those considered in Section 5.3. The process interruptions are excluded as outliers.



a. Cubic best-fit for CD PEC excluding process outliers



b. Cubic best-fit for CE PEC excluding process outliers

Figure 5.32. PEC plots for CD and CE illustrating general trend

Figure 5.32 clearly distinguishes between the three general wear stages for CE. CD does not have such distinct stages; however, the increased rate of wear versus CE is more noticeable. The gradual wear region is not noted for CD; however, this may be due to the increase in the cutting speed marked by the corresponding shift in the PEC. This shift interrupts what otherwise would be the general wear phase. It is noted that the PEC curves are not necessarily better than the envelope plots. Instead, they provide additional value in that they avail the general wear trend without any noise and without any ambiguous data. It is considered that the PEC curves better illustrate the distinct stages in the general wear. The PEC curves will therefore be considered for the development of a RUL algorithm. The macro value of the SML has shown that the condition of the cutting tool may be determined from the whole data set by utilising envelope plots, or PEC curves. The macro format shows potential for a superficial analysis of the progressive tool condition and easily illustrates the differences between cutting tools performing similar processes, despite minimal differences in the micro format. The PEC curves seem suitable for the estimation of RUL; however, this is still from a diagnostic perspective. Effort must be directed at the developing signal characteristics and whether there is value in estimating the developing change.

### 5.3.2 Development of RUL algorithm

It has been shown that the general wear curves seek to split the condition of a cutting tool into three stages: rapid initial wear, gradual wear, and rapid wear to failure. It is considered that whilst these three stages accurately describe the recognised changes in the deterioration of the cutting process, they cannot easily be determined from process data, other than by a qualitative assessment that relies on the opinion of the investigator. Chapter 2 showed that this results in questionable statements as to the occurrence of, and the limits of, each stage.

It was decided that there must be a mathematical approach for benchmarking the curves, and therefore the deterioration of the cutting tools. The wear curves are generally based on Taylor's Equations (or derivatives of) and thus rely on process knowledge, including cutting parameters, material, and cutting tool information. However, it is desirable (in the short term) to not approach the problem in a knowledge-based fashion, but in a data-driven way. The aim is to find the key changes in the rate of cutting tool deterioration. To achieve this aim, independent of the material process conditions, requires a deviation from the accepted application of Taylor's equation for cutting tool wear. To quantify the part-process correlation and to quantitatively identify the distinct stages in the cutting tool condition, steps were taken to define the variation based on a polynomial approximation of the process signal. This can be developed based on the relatively straightforward third order polynomial (cubic). It is recognised that employing a cubic function will introduce challenges. Especially that fitting a cubic to a relatively low number of points may result in a relatively unstable method of modelling the deterioration of the cutting tool. However, it is noted that a cubic function was employed to simplify the mathematics involved and because it can be derived relatively easily using linear regression.

$$f(x) = Ax^3 + Bx^2 + Cx + D \quad (5.5)$$

Equation 5.5 does not consider error because the function is intended as a rough approximation rather than a full or exact model. A three-stage algorithm was then developed by the author based on the cubic change-points:

1. The curve was shifted to zero at the stationary point. This was found to be more stable when using partial data sets than shifting by the mean average of the data. This also accounted for the propensity for each wear curve to be tail heavy. In other words, the data mean is skewed towards the cutting tool failure
2. The data was split across zero with values normalised between zero and  $\pm 1$  according to their sign. This exaggerates the process change (and general trend) in the positive and negative gradients and separates the process data into two parts. The first part shows the "new" cutting tool and the second part shows the "worn" cutting tool
3. The magnitude change in the slope of the first differential was calculated, per part, from the general equation. The resulting maximum and minimum values were taken as the change between stages (termed the characteristic curve).

Using Excel this required the LinEst() function, which is implemented using two VBA (Visual Basic for Applications) functions. Full VBA functions are provided in Appendix A.5. Developing functions enabled a simple formula for the calculations. This allowed for shorter array formulae and reduced excel file sizes by 90%. The prerequisite information includes the total part list (e.g. 0-200 (in as many cells as appropriate)) to populate the X-axis, and the input data (either MTData or CMM data) to populate the Y-axis. The two data sets *must* have an equivalent cell-range. It is then necessary to use new equation POLY3(), input as an array formula over as many cells as the two input data sets. POLY3() will employ the separate COEFFPOLY3() function to determine the equation coefficients and will return the best-fit cubic for the provided data. An example is provided in Figure 5.33.

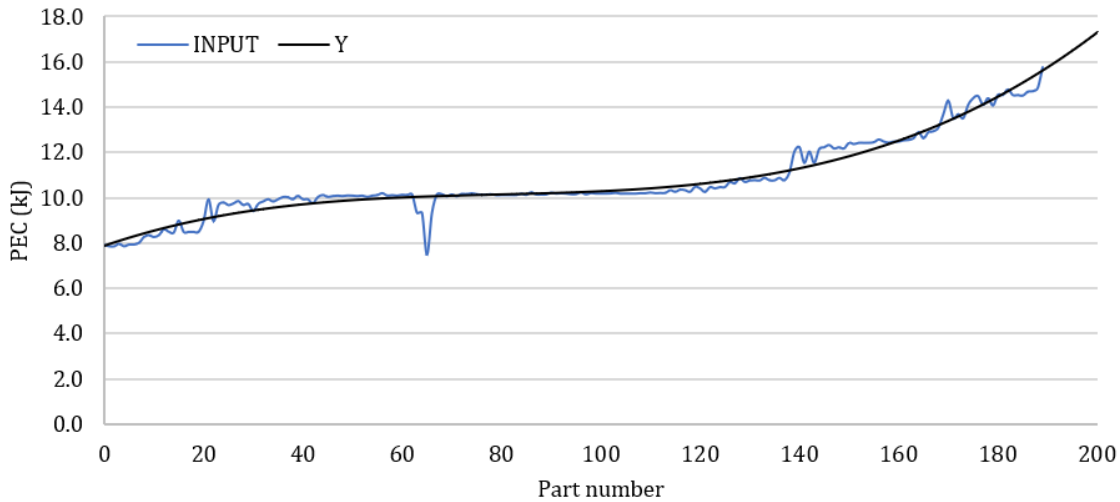


Figure 5.33. Best-fit cubic for CE PEC trend

The coefficients A, B, C and D are estimated from the given data. It is noted that the PEC data is used after eliminating the process variations that correspond to known interruptions (e.g. downtime) and removing zero values. Keeping the interruptions and zero values results in the cubic tending to zero. With the best-fit cubic now representative of the general wear trend, the process may be standardized to separate the healthy cutting tool from the unhealthy cutting tool. This considers four step changes in cutting tool condition, allowing greater flexibility over the shape of the model. These four stages are shown in Figure 5.34.

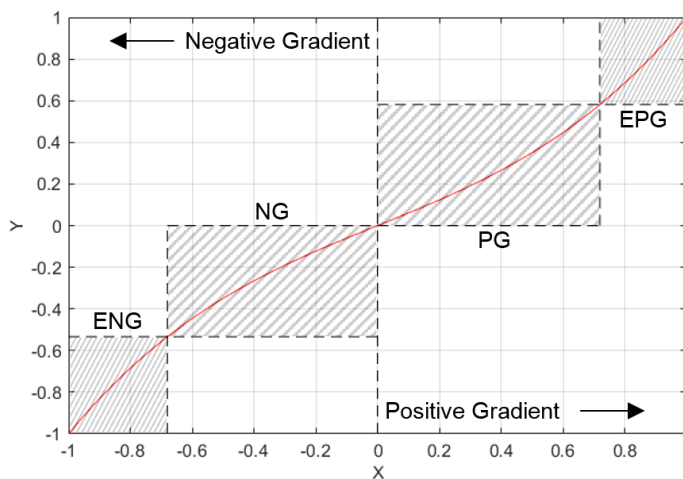


Figure 5.34. Standard cubic illustrating four condition stages based on inflection points

The four stages presented in Figure 5.34 are defined as:

1. Extreme Negative Gradient (ENG); Healthy
2. Negative Gradient (NG); Used
3. Positive Gradient (PG); Worn
4. Extreme Positive Gradient (EPG); Failing/failed

This is achieved by effectively splitting the second stage (gradual wear) in two and is based on the novel idea that a significant shift in the condition of the cutting tool may be quantitatively determined from the trend inflections. In other words:

- At the first instance the shift in gradient is greatest, the condition is changing from new to used (change from initial wear to gradual wear)
- At the stationary point, when the gradient is zero (or closest to), the condition is changing from used to worn (change from first half of gradual wear to second half of gradual wear)
- At the second instance the shift in gradient is greatest, the condition is changing from worn to failing (change from second half of gradual wear to final wear and failure).

This first required the calculation of the stationary point, as the signal mean is not always within the gradual wear region. The stationary point can be calculated by making the second derivative of Equation (5.5) zero, and rearranging for  $x$ .

$$\frac{d^2y}{dx^2} = 6Ax + 2B = 0 \quad (5.6)$$

$$x = -\frac{B}{3A} \quad (5.7)$$

Where A and B are the same as in Equation (5.5). The signal can then be translated to zero by subtracting the magnitude of the stationary point (SP) from all values. Subtracting the SP prevents the X-axis intersect from excessive variation during active monitoring - both the mean and median averages vary considerably when monitoring in-process. Additionally, whilst the mean and median averages end up weighted toward the latter stages of the process due to the relatively heavy skew towards a positive gradient data (PG), the SP remains centrally located. The resulting polynomial ( $f(x, k)$ ) is derived below, where  $k$  represents  $x$  from Equation (5.7).

$$f(x, k) = A(x^3 - k^3) + B(x^2 - k^2) + C(x - k) \quad (5.8)$$

As the signal is now at zero, values below zero represent the healthy state of the cutting tool and values above zero represent the unhealthy state of the cutting tool. Neither side is equal, as a greater proportion of the data will be more than zero due to the propensity for each wear curve to be tail heavy. To then exaggerate the gradient changes, the curve is normalised between zero and  $\pm$  one, following the rule:  $-1 \leq NG < 0 \leq PG \leq 1$ . This can be represented by  $f(x, k)_\alpha$ . The normalised curve is shown in Figure 5.35 for the CE PEC data set.

$$f(x, k)_\alpha = \begin{cases} \frac{f(x, k)}{\min f(x, k)} & f(x, k) < 0 \\ \frac{f(x, k)}{\max f(x, k)} & f(x, k) \geq 0 \end{cases} \quad (5.9)$$

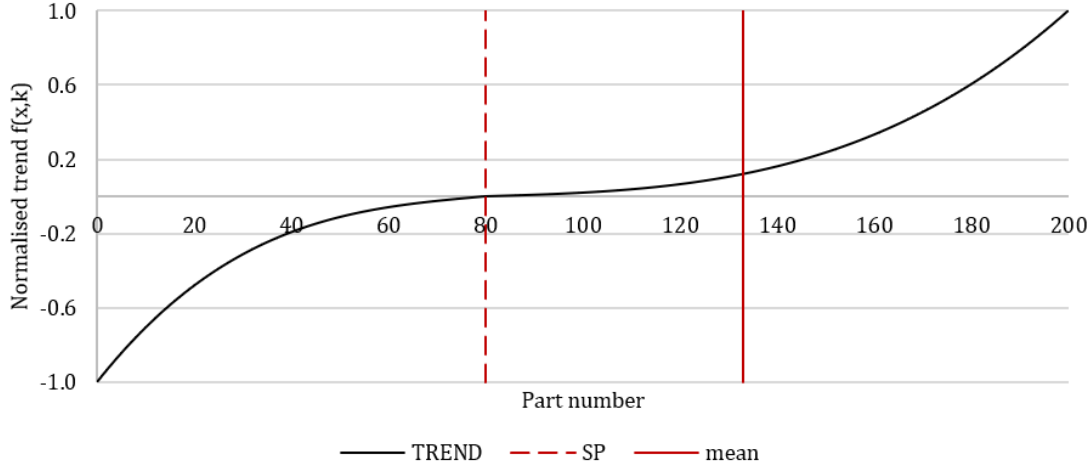


Figure 5.35. Normalised best-fit for CE PEC, showing SP and mean part numbers

Figure 5.35 shows the difference between the SP and the mean by number of parts. It is also shown that the Y-scale is now dimensionless, thus the only remaining metric is the number of parts. Returning to Equation (5.5), the first differential ( $f'(x)$ ) is needed, from which the “probable fit” curve (p-fit or  $g(x)$ ) can be calculated from the magnitude change in the slope.

$$f'(x) = 3Ax^2 + 2Bx + C \quad (5.10)$$

$$g(x) = \frac{3Ax_n^2 + 2Bx_n + C + \gamma - \min f'(x)}{3Ax_{n-1}^2 + 2Bx_{n-1} + C + \gamma - \min f'(x)} \quad (5.11)$$

p-fit should also be normalised using similar rules to  $f(x,k)$ .

$$g(x)_\alpha = \begin{cases} \frac{g(x)}{\min g(x)} & g(x) < 0 \\ \frac{g(x)}{\max g(x)} & g(x) \geq 0 \end{cases} \quad (5.12)$$

It is noted that  $\gamma$  is the adjustment factor, indicating the unit shift needed to avoid p-fit tending to infinity and adjusting the decay for each tail.

$$\gamma = ae^{\frac{b \text{FRL}}{100}} + ce^{\frac{d \text{FRL}}{100}} \quad (5.13)$$

Table 5.3. Initial coefficients for p-fit adjustment factor

Coefficient	Initial value
a	0.01
b	-50
c	0.02
d	-10

The forced remaining life (FRL) considers a fixed remaining life as an integer “percentage” of the total parts machined. This is included to enable the adjustment of the predicted EOL; however, is herein fixed at a value of 10 unless explicitly noted. The coefficients a, b, c, and d are different from A, B, C, and D (used in other equations) and may be calculated iteratively by using the initial values given

in Table 5.3 to generate a new sequence of shift values. The plotted results can be fit with Equation (5.13) using non-linear least squares to generate new coefficients. The p-fit is given in Figure 5.36 (illustrating the effect of changing  $\gamma$ ).

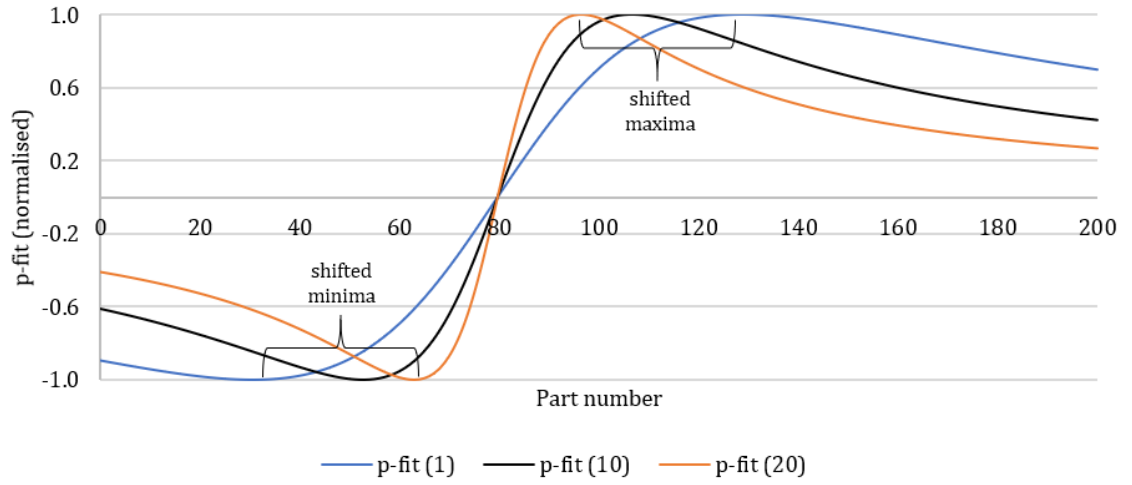


Figure 5.36. p-fit curves for CE PEC indicating FRL effect for values of 1, 10, and 20

Figure 5.36 shows that changing the FRL artificially changes the relative maxima and minima of the p-fit curve. When the FRL is zero, these maxima and minima correspond to the change points in the original cubic best-fit. If those changepoints are taken to represent the changing condition of the cutting tool, shifting them artificially allows the estimated EOL to be adjusted. This allows the algorithm to be updated based on observed cutting tool capabilities. Lastly, the two generated plots,  $f(x, k)_\alpha$  and  $p\text{-fit}(g(x)_\alpha)$ , can be subtracted from one another to generate a representative condition plot, or estimated difference plot (e-fit). This follows the logic given below, with an example PEC e-fit for CE given in Figure 5.37.

$$\text{e-fit} = |g(x) \cdot (g(x) > 0)| - |f(x, k) \cdot (f(x, k) > 0)| \quad (5.14)$$

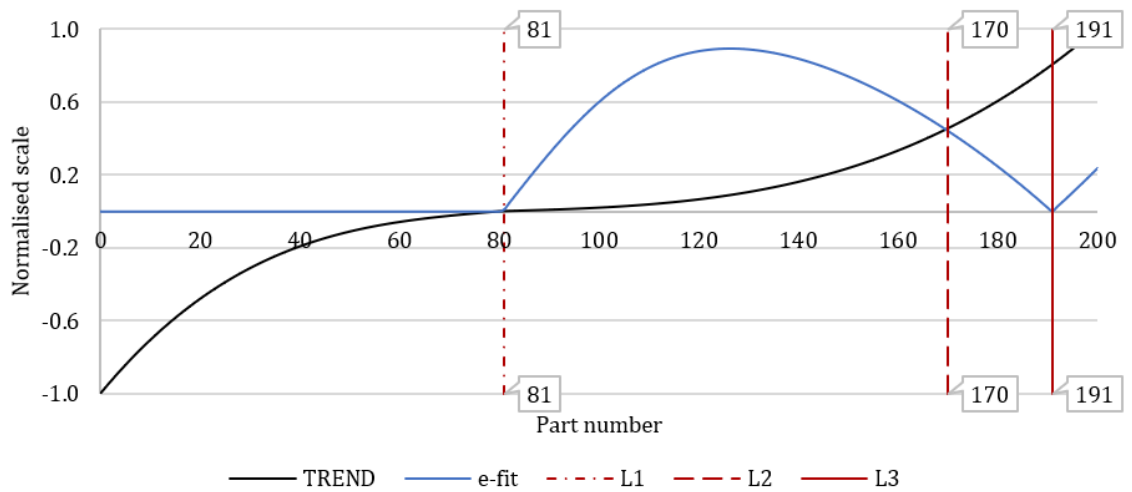


Figure 5.37. e-fit plot for CE PEC (FRL=0)

Where TREND is the normalised best-fit cubic, L1 shows the cubic inflection point, L2 shows the instance where the gradient change is greatest, and L3 indicates the estimated catastrophic failure based on the total allowed parts (here 200) and the observed gradient. This results in two plots that enable the changing condition of the cutting tool to be quantitatively estimated. Using the p-fit enables the condition to be separated into the previously defined stages:

1. ENG - From the first part to p-fit minimum
2. NG - From p-fit minimum to zero (stationary point)
3. PG - From zero to p-fit maximum
4. EPG - From p-fit to the process ends

On the other hand, using the e-fit the changing condition of the cutting tool can be quantitatively separated into a different four parts.

1. Healthy - Until e-fit deviates from zero
2. Used - Until e-fit equates to  $f(x, k)_\alpha$
3. Worn - Until e-fit equals zero
4. Failed - Until the process ends

The e-fit plot is exploited to determine the different stages using VBA functions written by the author. These novel algorithms track the relative value of e-fit versus the TREND and the X-axis to determine the values for L1, L2, and L3. The full VBA functions are included in Appendix A.5. The difference in the separation of the process is that e-fit combines ENG and NG into a single “healthy” metric. This does not distinguish the initial wear phase; however, for the calculation of the EOL or the RUL the initial wear phase is unnecessary. The e-fit then considers the cutting tool to be “used” until the first EOL, at which the cutting tool is “worn” until the second EOL. These descriptions have been chosen because the EOL is unlikely to be an exact value. Considering the e-fit for CE shown in Figure 5.37, the first EOL is 170, the second is 191. The point the cutting tool should be retired is within that range, depending on the acceptable level of cutting tool wear.

The other predominant difference between p-fit and e-fit is that e-fit enables an estimate of the EOL from the intercept between e-fit and  $f(x, k)_\alpha$ , and the point e-fit equals zero. This can be considered by simulating the CE test and introducing each machined part in sequence. Figure 5.38 illustrates the change in the e-fit curves as the simulated process continues from 48 parts completed, through to all 190 parts completed.

Figure 5.38 is given to show that the e-fit curves improve as more parts are machined. This is sensible as the process cannot be reliably forecast forward until sufficient data has been acquired. Predictions with less than 48 parts have been omitted as forecasting the process with less than 25% of the data results in highly variable responses. Figure 5.39 has been plotted to demonstrate the e-fit response over time.

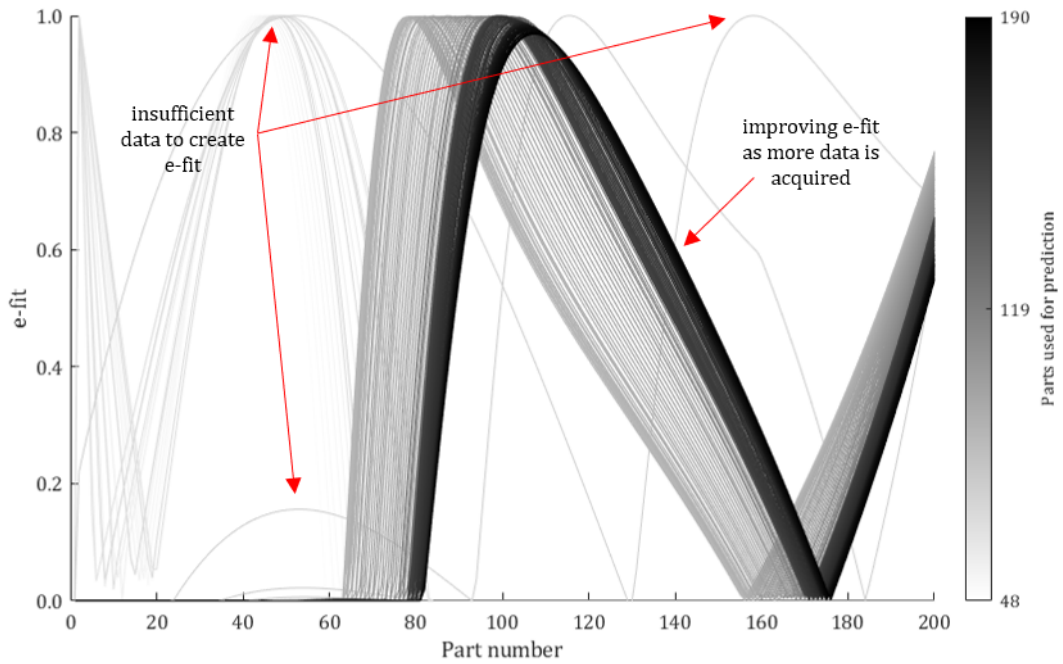


Figure 5.38. CE PEC predicted e-fit curves from 48-190 parts

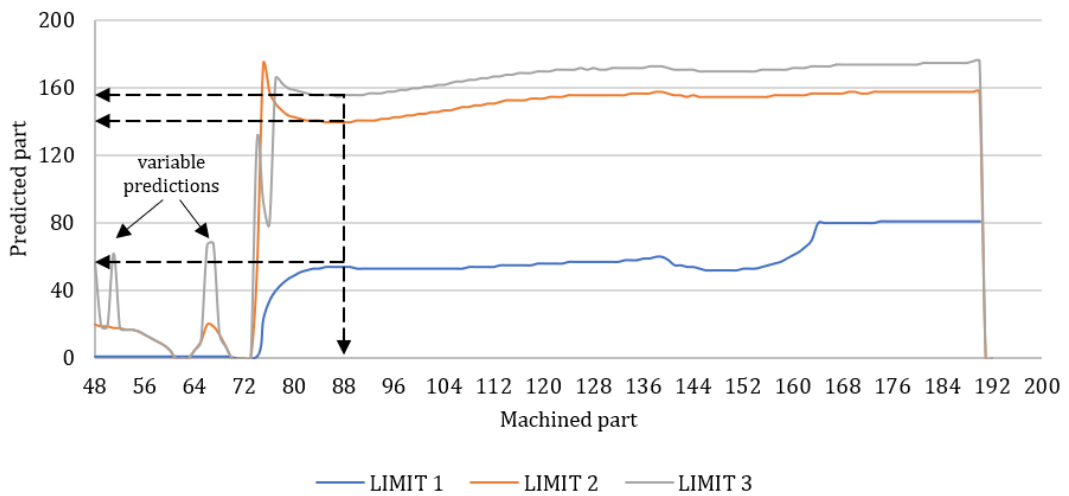


Figure 5.39. CE response plot for PEC e-fit predictions of cutting tool condition

Figure 5.39 includes LIMIT1 (L1) to show the estimated cubic inflection point, LIMIT2 (L2) showing the estimated instance where the gradient change will be greatest, and LIMIT3 (L3) to show the estimated catastrophic failure based on the total allowed parts and the observed gradient. For example, when manufacturing Cylinder 88, L1 is *calculated to have occurred* at Cylinder 54, L2 is *predicted to occur* at Cylinder 140, and L3 is *predicted to occur* at Cylinder 156. Figure 5.39 shows that the prediction response is highly variable until the actual stationary point is passed (here Cylinder 81) after which predictions become more stable. It is observed that the predicted limits constantly change over the course of the process. This is sensible as the algorithm has more data to use, making the predictions more accurate. Figure 5.40 considers the estimated RUL for CE, CD, and CF.

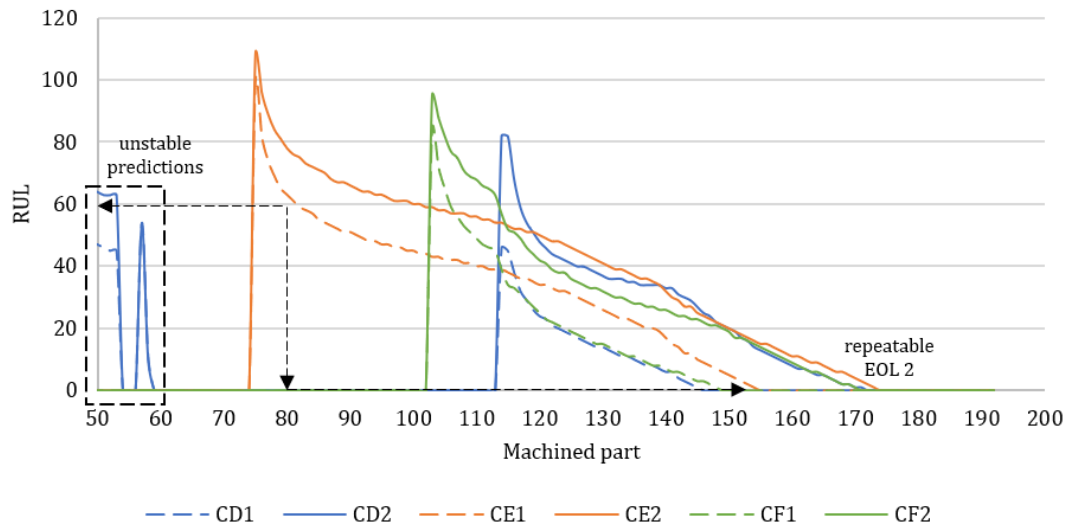


Figure 5.40. RUL predictions for CD, CE, and CF

Two values for the RUL are provided, the first indicates the remaining parts until the gradient change will be greatest (L2, or EOL1), the second indicates the remaining parts until the estimated catastrophic failure (L3, or EOL2). It is appreciated that due to the iterative nature of the RUL predictions, the remaining parts may be greater than predicted. For example, at 80 parts the predicted RUL for CE is 60 remaining parts (EOL1). The first EOL is eventually found to be 155 parts – a discrepancy of 15 parts. This should not be a problem as it is better to under predict the RUL (as a rule of thumb); however, when the continued use of a cutting tool relies on it surviving a specified number of parts, said cutting tool may be scrapped based on those 15 parts. This highlights a challenging aspect of predicting the RUL for cutting tools. Over predicting the RUL may result in using cutting tools that are not fit for purpose but under predicting may result in waste. Nevertheless, this should still be less waste than conservative approaches.

Figure 5.40 shows that applying the approach to CE produced the earliest prediction of the RUL at 75 parts (37.5% of the way through the process). This is sensible as the process was best matched with the cubic trendline and had appropriately distinct wear phases. When applied to CD the approach was the slowest to predict the RUL, requiring more than 110 parts before a prediction was possible (60% of the way through the process). It is noted that all three predicted remarkably comparable results for the second EOL, indicative of the similar cutting process. It was noted that applied to CD and CF the approach predicted a similar first EOL, whilst using CE the approach predicted the first EOL to be occurring 10 parts later. This is sensible since the cutting tool used for CE survived whilst the cutting tools used for CD and CF failed.

It is noted that when considering CG the applied approach was incapable of a stable RUL prediction due to the cubic trend-line not settling. This could be rectified by further smoothing the PEC data for CG. It is appreciated that the cubic is an unstable way of predicting the deterioration of the cutting tool. Better and perhaps more stable representations may be found using Weibull equations. It is suggested that in future these should be investigated and compared with the cubic response. It should be noted that despite the data-driven nature of the developed algorithm, the result can only

be guaranteed when implemented for trends that conform to the general wear curves in a fashion that is easy to interpret.

### 5.3.3 RUL correlation with form and finish

It is necessary to corroborate the observations made using the developed algorithm with the previously determined properties related to form and the finish. This is necessary as both the form and finish are verified against the manufactured parts. On the other hand, the PEC is more indirect and may be influenced by other conditions within the machine tool, such as the condition of the spindle, the internal processing, or the external processing (including the DENSE algorithm). It is appreciated that the general trends noted for all three parameters (form, finish, PEC) are comparable as noted in earlier Sections. This indicates that (in general) the three parameters are presenting similar process deteriorations. As the machine tool is unlikely to deteriorate within a single test, this deterioration may be attributed to the deterioration of the cutting tool. The similarities may be further reinforced when the uncertainty in the PEC is considered. Figure 5.41 considers a direct comparison of the PEC and CSAM (both standardised) for CE.

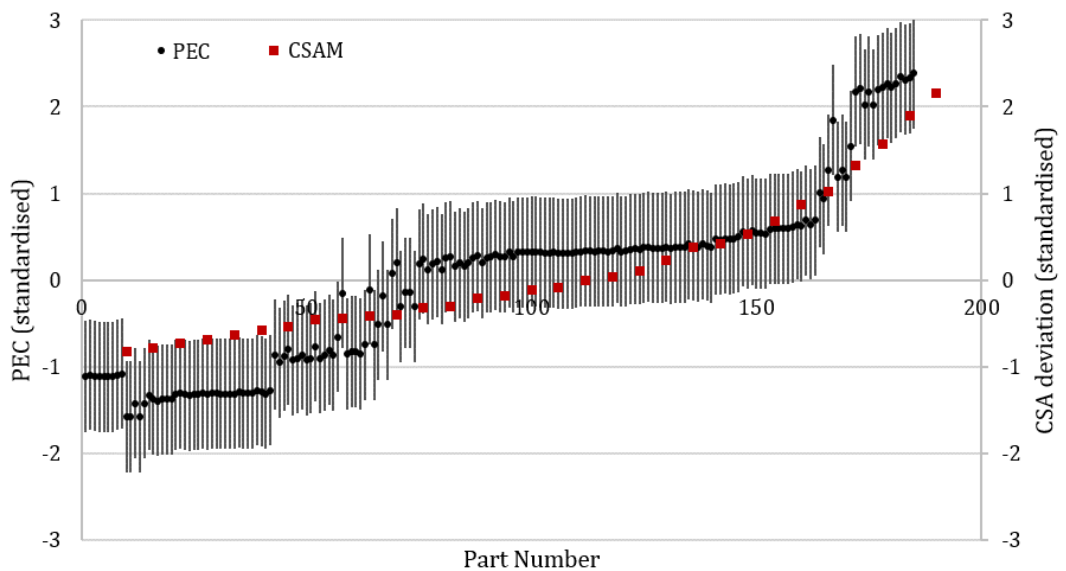


Figure 5.41. Standardised comparison of CE PEC (with uncertainty) and CSAM trends

Figure 5.41 considers the PEC measurement uncertainty, accumulated due to the discrete nature of the MTData. This assumes that the quantised nature of the original output equates to the actual value being within the range of one equivalent unit. For example, 4% has the value  $\alpha$ , where  $3.5\% \leq \alpha < 4.5\%$ . Figure 5.41 shows that the CSAM trend is within the equivalent PEC range. However, it is noted that the uncertainty margin is large (1.26 units compared with a maximum measurement range of 5.20 units). This means that the probability the CSAM trend falls within the given PEC range is high, irrespective of correlation. The PEC potential range could be reduced with the acquisition of more precise MTData, or other sources of MTData.

Figure 5.42 compares the PEC uncertainty with the surface finish measurements. It is noted that, much like with the CSAM, both follow a similar trend; however, unlike the CSAM, the surface finish

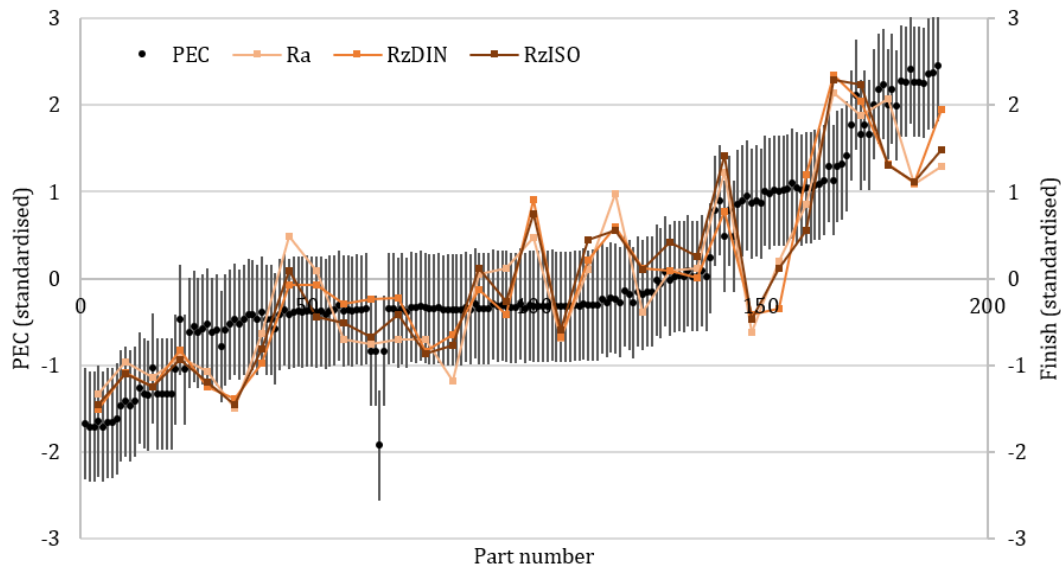


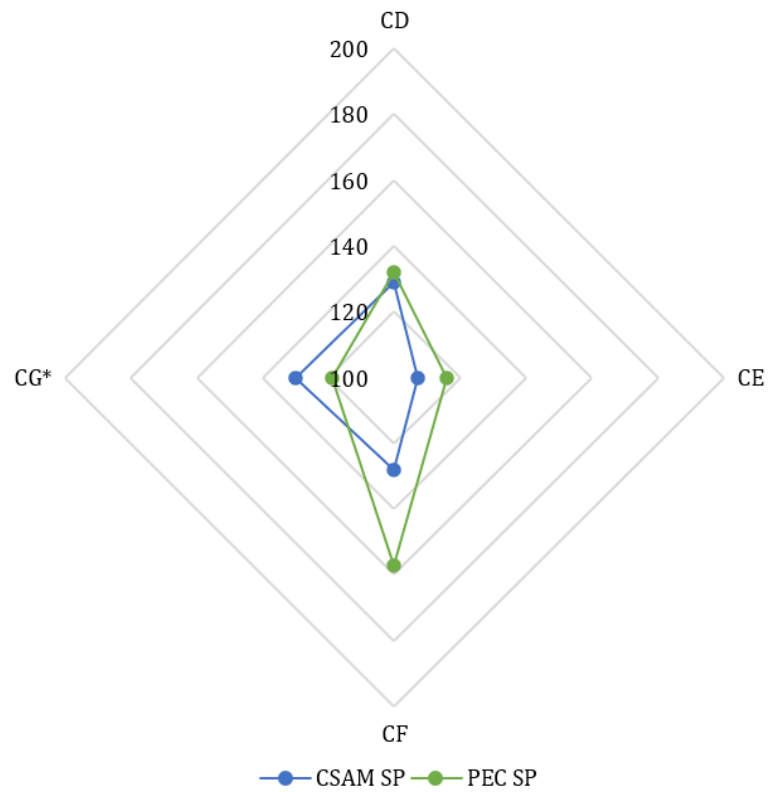
Figure 5.42. Standardised comparison of CE PEC (with uncertainty) and surface finish trends

observations do not remain within the PEC range due to significant fluctuations. This is not entirely surprising as the PEC considered the fourth part in each Cylinder, whilst the surface finish was taken in the unidirectional slots (sixth part). Variation may therefore be expected due to the difference in the part number and the difference in the cutting process (pocket milling versus slotting). It should also be appreciated that the PEC has been filtered to remove significant fluctuations. Beyond the similarities in the overall trend, the three parameters may be compared quantitatively by acquiring the relative curve inflections and the diagnosed EOL. Table 5.4 gives the e-fit characteristics derived for the CSAM plots and the PEC plots. These are presented as radar plots in Figure 5.43.

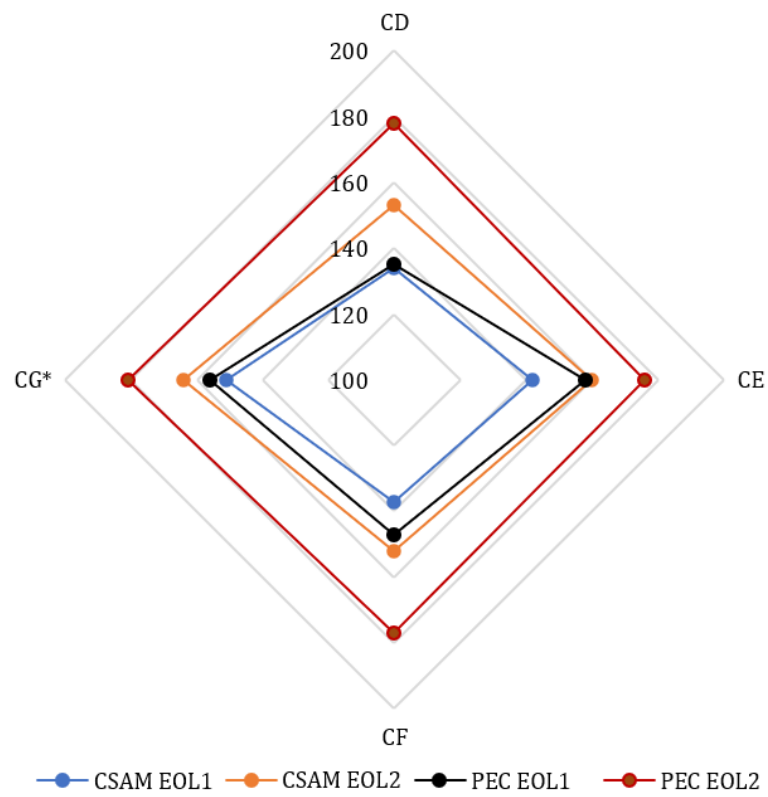
Table 5.4. CD, CE, CF, and CG e-fit characteristics, calculated for both CSAM and PEC

Test	CSAM		PEC			
	SP	EOL1	EOL2	SP	EOL1	EOL2
CD	72	134	153	43	135	178
CE	70	142	160	81	158	176
CF	71	137	152	68	147	177
CG*	93	151	164	84	156	181

Figure 5.43a shows that the SP for each test varies between the CSAM and the PEC signals. This is understandable as the characteristics of each are quite different. However, only CF noted significantly different values with the PEC SP occurring much later in the process. It is noted that despite the cutting tool failing for CF, there are no signs in the PEC signal to show this. It is noted that the breakage is not seen in the given PEC signal as it occurred during the slot (hence filtered out). This implies that either the breakage was sudden, or unexpected, or that signals in the build up to the failure were also filtered out. This would warrant investigation into micro value of the raw signal and evidences the potential value in considering all process stages. Figure 5.43b shows that both EOL



a. Comparison of stationary points for CSAM and PEC signals



b. Comparison of EOL estimates for CSAM and PEC signals

Figure 5.43. CSAM and PEC inflection comparison using radar plot for CD, CE, CF, and CG

estimates for the CSAM signal are more comparable to the first EOL estimate for the PEC signal. This is suitable, as the second EOL estimate for the PEC signal corresponds to a failed cutting tool. Figure 5.44 compares the PEC EOL estimates with the surface finish EOL estimates. It is noted that the PEC estimate for EOL1 is remarkably like the RzDIN results for all tests. This is useful as the EOL for RzDIN indicates an increase in significant surface damage. It is noted that Ra has been omitted from Figure 5.44 as the remaining signals are more relevant. RzNOV has also been introduced by the author, being the difference between RzISO and RzDIN, and shows the significance of the extreme peak to valley distances. RzNOV is particularly similar to the PEC EOL1 estimate (bar CD). On the other hand, estimates for RzISO more closely resemble the PEC EOL2 estimate.

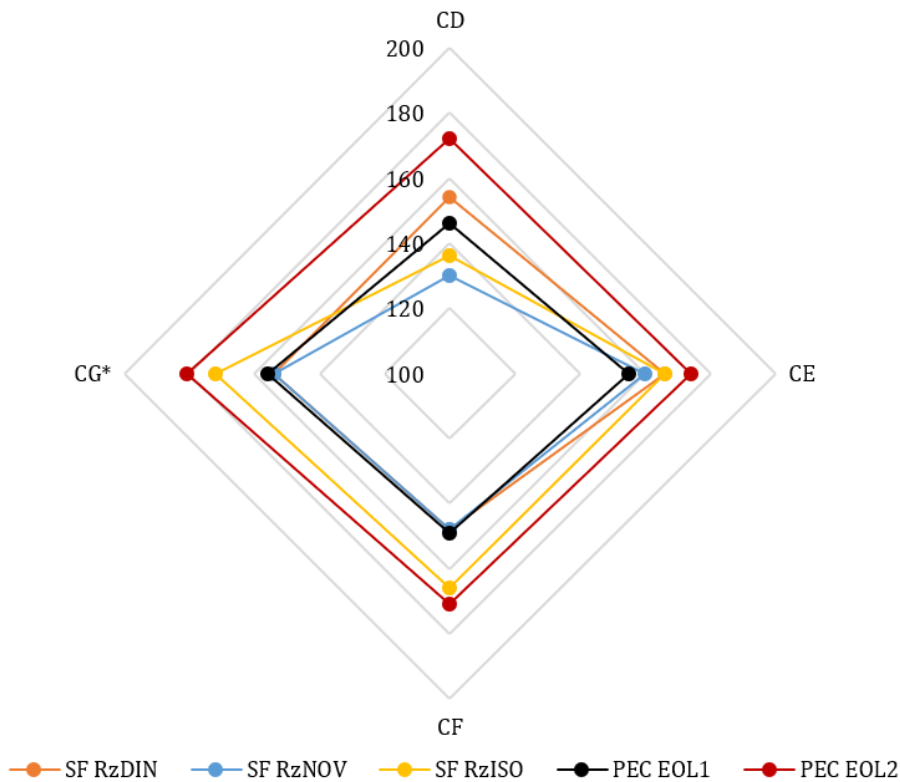


Figure 5.44. Surface finish and PEC EOL comparison using radar plot for CD, CE, CF, and CG

It has thus been shown that the form and finish observations can be used to validate the PEC and e-fit observations. This is important as both the form and finish are verified against the manufactured parts. Therefore, the similarities indicate that the PEC signal, and the e-fit algorithm are suitable for determining the condition of the cutting tool. However, whilst the SML has proven to be effective in providing in-process information relating to the condition of the cutting tool, as well as information that has value in predicting the RUL of the cutting tool, the signal has a large amount of uncertainty due to the quantised nature and the impact from in-process activities. It is noted that without sufficient additional detail from other signals, any decisions regarding cutting tool condition are lacking in evidence. Therefore, more MTData signals should be considered to determine whether they have value to add to the value of the SML signal.

## 5.4 Application of MTData: Spindle rotation

The rotational speed of the cutting spindle is a challenging signal to investigate as it is controlled by the machine tool to a greater extent than most of the other acquired signals. When changes in the process occur, including deterioration of the cutting tool, this results in a change in the resistance to cutting and therefore a change in the rotational speed of the cutting tool. However, as the rotational speed is controlled, any variation in the rotational speed will be slight, and eliminated rapidly to support a consistent cutting behaviour. Nevertheless, the machine tool cannot (yet) predict changes in the cutting process and therefore maintenance of the cutting speed will always be in response to a change. These responses may be investigated to determine whether they have value. Figure 5.45 presents the rotational speed for CE015.

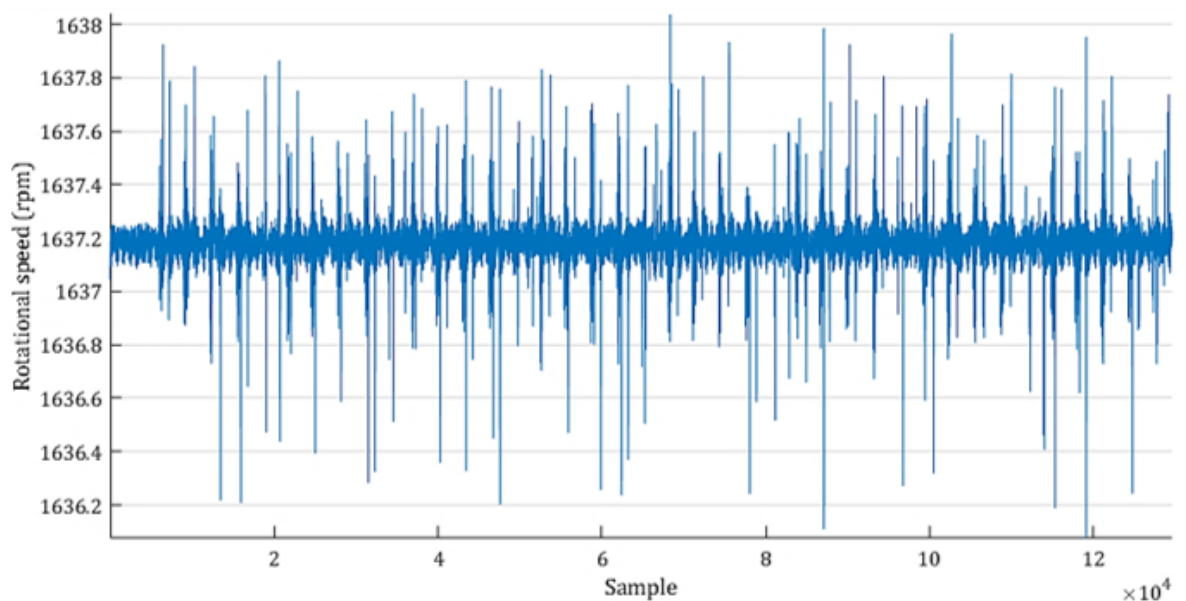


Figure 5.45. Spindle rotational speed for CE015

Figure 5.45 shows the nature of the rotational speed and illustrates the response of the controller. From the figure it can hopefully be appreciated that comparing CE015 (the first test in CE) with CE018 (the final test in CE) would be challenging, if not impossible qualitatively. In response, two structured methods of comparing CE015 with CE018 have been considered. The first is to consider the probability densities of the upper and lower peak envelopes of the signals. Figure 5.46 gives the density plots for the two SRS signals for CE.

Figure 5.46 indicates that there is negligible difference in the PDF for each lower envelope. However, there is a noted difference between the two upper envelopes. The PDF for CE015 has a tighter distribution indicating fewer outliers and a greater proportion of the signal being close to the signal average. This implies that the first test (when the cutting tool is healthy) is more able to maintain the desired rotational speed value than the last test (when the cutting tool is unhealthy) due to less resistance. Figure 5.47 introduces CE016.

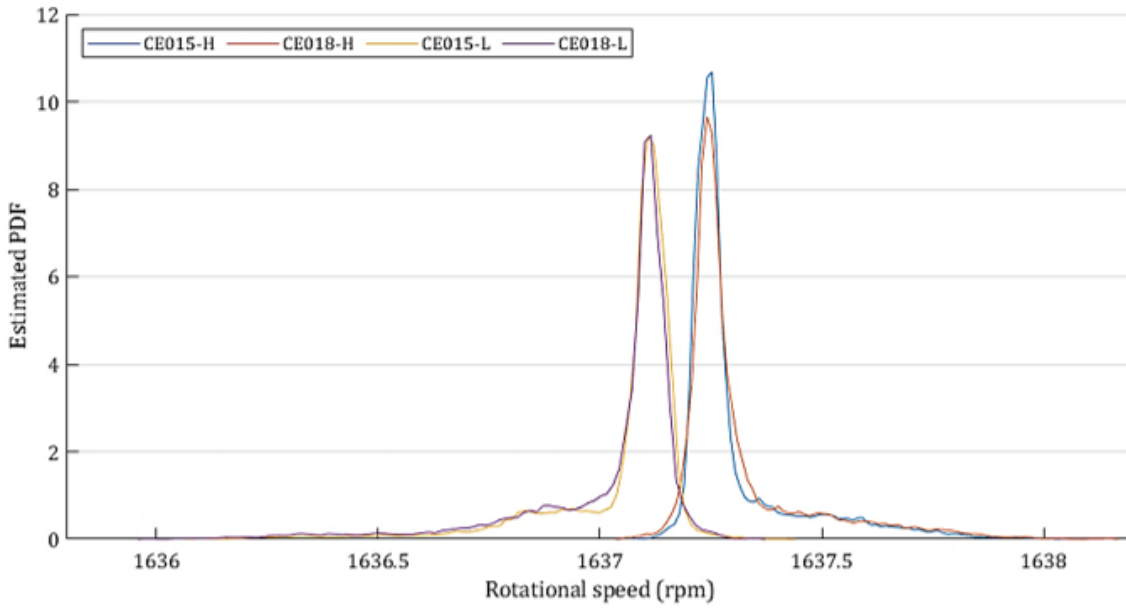


Figure 5.46. Probability density functions for two CE peak envelopes (upper and lower)

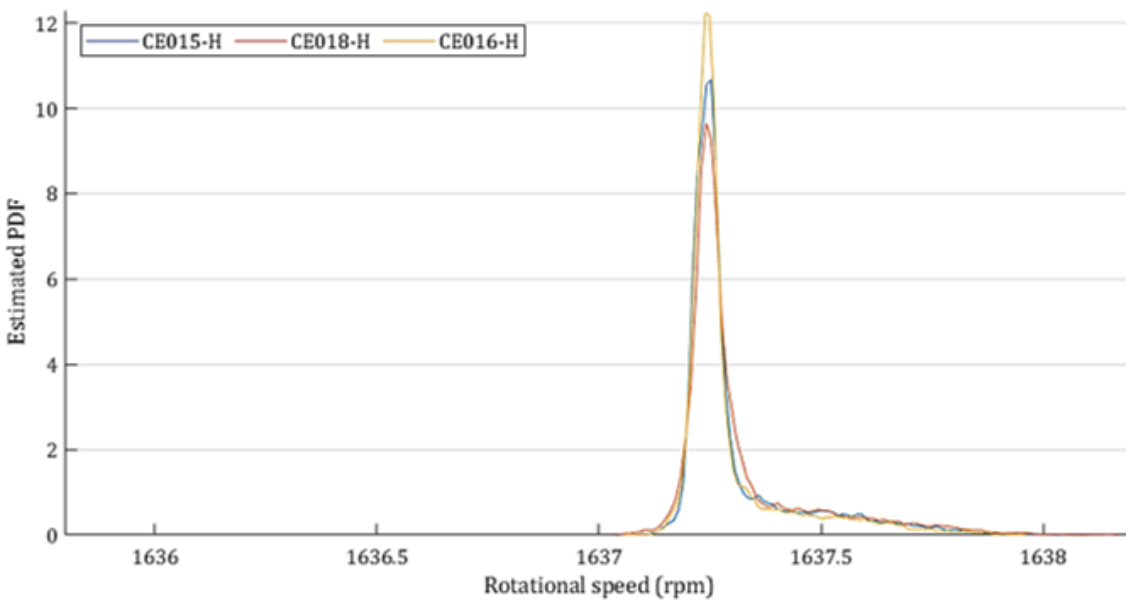


Figure 5.47. Probability density functions for three CE peak envelopes (upper)

Figure 5.47 indicates that the SRS peak envelope improves between the first and second test. This may indicate the condition of the cutting tool improving between new and slightly used. This perhaps indicates that the cutting tool is in a better (healthier) state *after* the initial wear phase, rather than before, or during. This behaviour is known in practical terms by experienced MT users. The second method to compare the change between the healthy cutting tool (CE015) and the unhealthy cutting tool (CE018) is to consider the frequency components of the SRS signals using the FFT. Figure 5.48 gives the frequency response for each test in CE.

Figure 5.48 is challenging to evaluate due to the amount of information given. There are notable similarities between the four tests (between braces); however, it is tricky to quantify what these,

and the differences, equate to in terms of the cutting tool health. Qualitative statements have been provided per test based on the PDF results. It is noted that CE015 and CE017 are the most similar (between the braces); however, decisions cannot be made reliably due to the complexity (and hence uncertainty) in the data. The plots may be improved by dividing the signal further. The health of the cutting tool will vary significantly within a single test and by evaluating a test as one signal will obscure some of that variation. Evaluating each part, or each Cylinder, separately may better show the change in the cutting tool health.

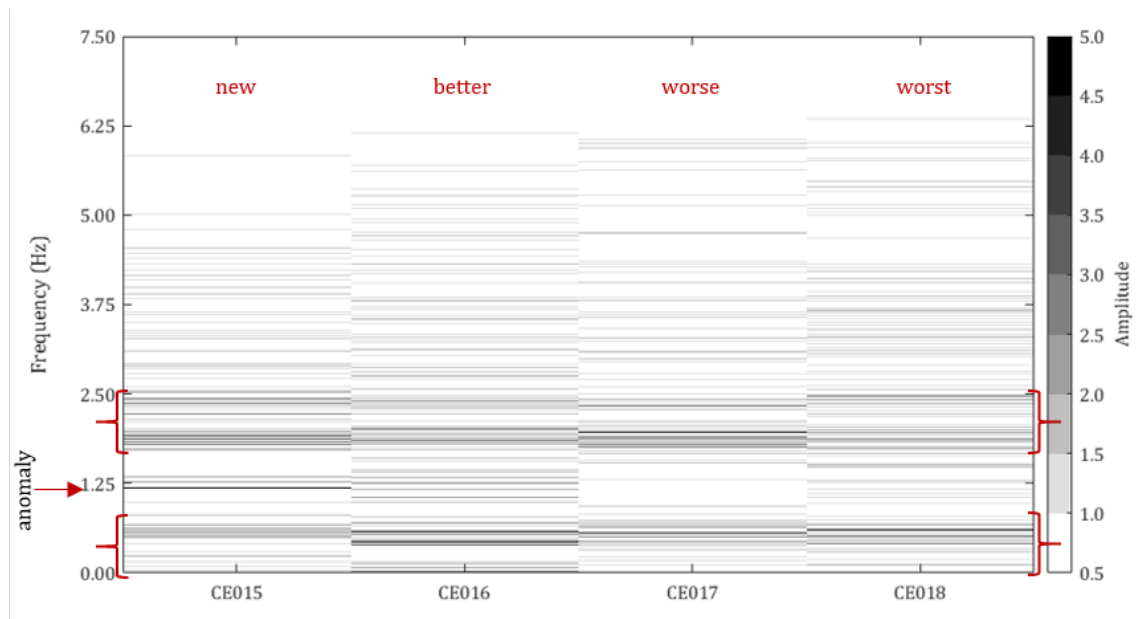
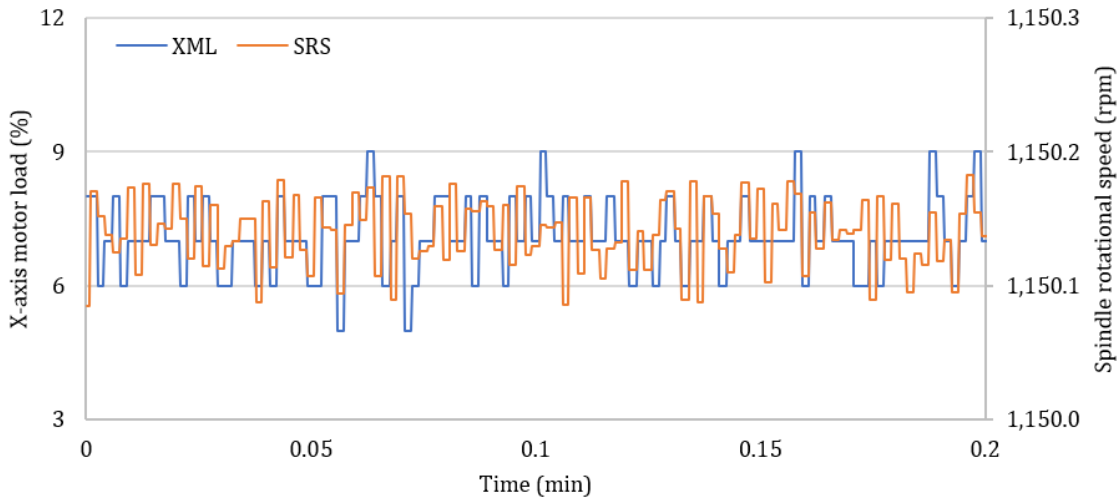


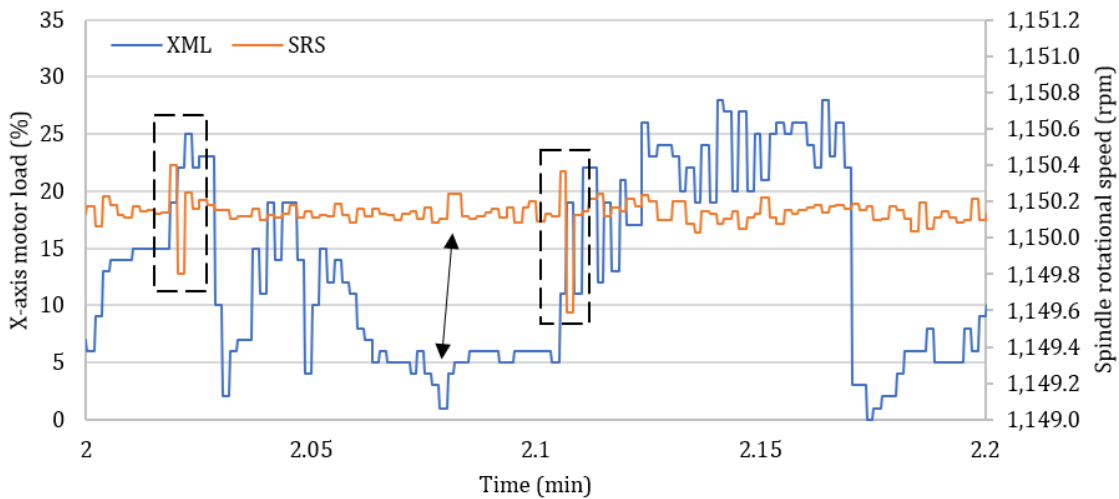
Figure 5.48. Frequency-amplitude image for CE SRS

#### 5.4.1 Applications, advantages, limitations and disadvantages

It has been shown that the SRS indicates changes in the process, noting a relative improvement when the cutting tool progresses from new to used, and a deterioration when progressing from used to worn. This is useful as it may help to corroborate other signals that show similar information. It is also interesting as it provides evidence that a new cutting tool is often improved by a wearing-in process before first use. This shows that there is value in monitoring the rotational speed of the spindle, acknowledging that changes are slight and at a micro level the responses may be inferred from other measurable changes. Figure 5.49 compares the SRS and the X-axis motor load to show that when the process is idling (the spindle is rotating but there is no cutting) there are qualitative similarities between the two signals. This illustrates an interaction between the two signals. When cutting is taking place, there is more distinction between the two signals. There are also changes in the rotational speed that could be inferred from the changes in the process – increase in SRS in anticipation of cuts. This may suggest that analysis of the SRS is unnecessary as equivalent information may be gleaned from the axis signals. However, the SRS is an important process variable, and therefore should be acquired on principle. If the necessary processing is not significant, there is no reason the SRS cannot be used to corroborate analysis or reinforce decisions drawn from other process signals.



a. SRS versus X-axis motor load with no cutting

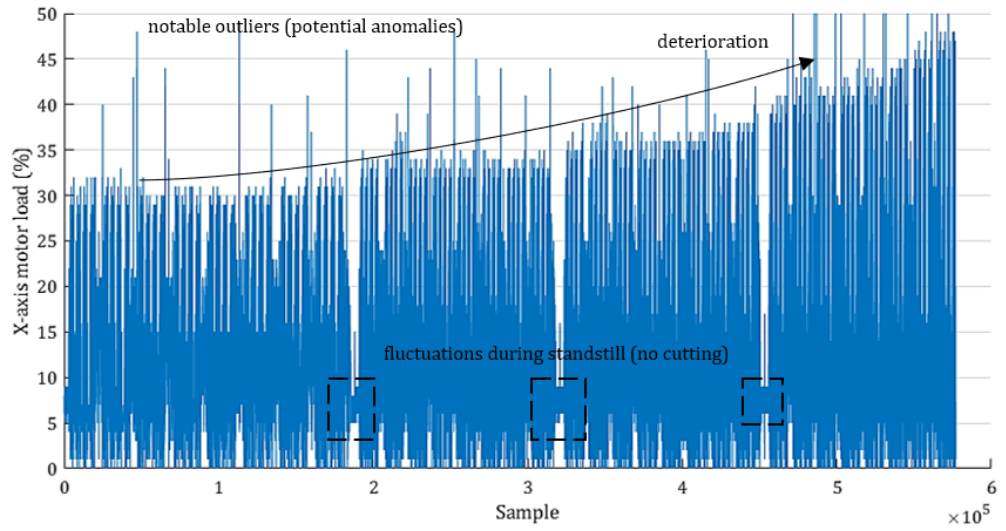


b. SRS versus X-axis motor load during cutting

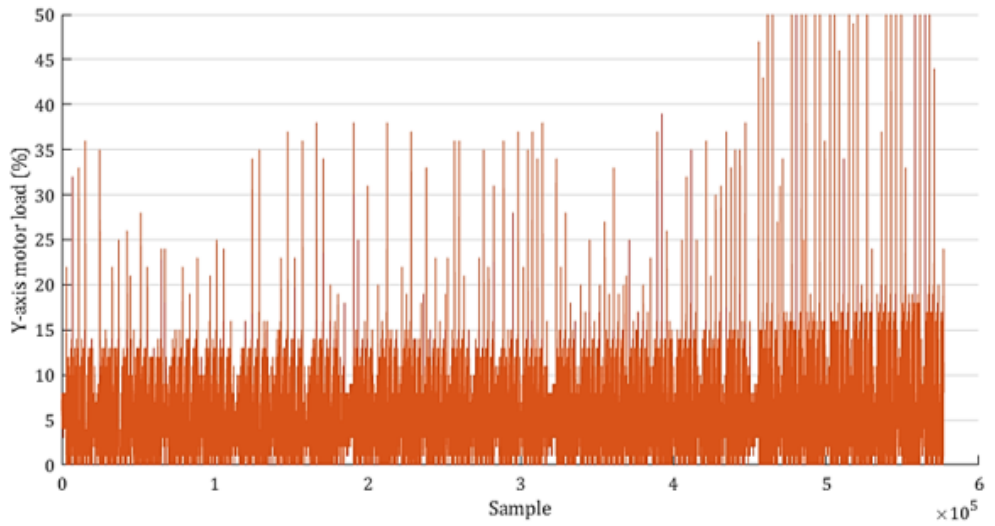
Figure 5.49. Comparison between SRS and X-axis motor load, with and without cutting

## 5.5 Application of MTData: Axis motor load

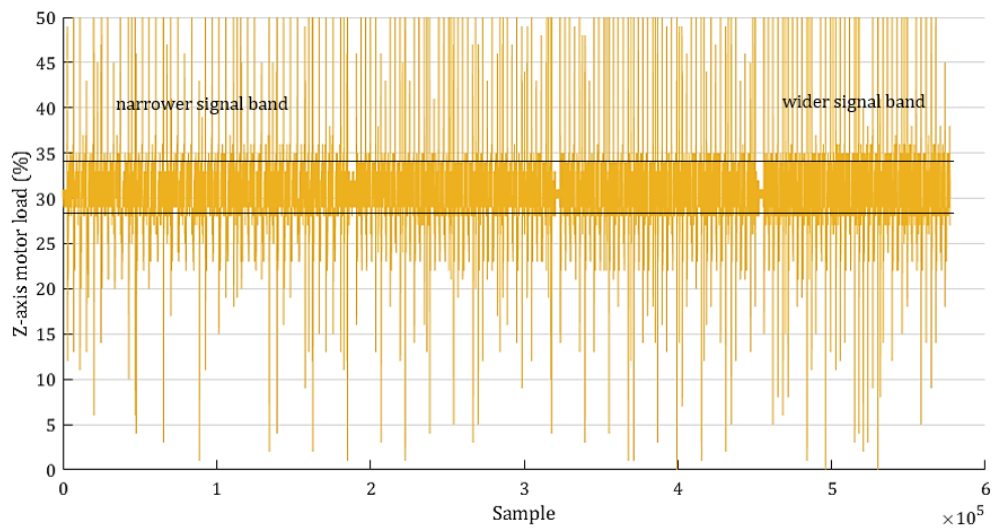
Besides the spindle, useful information may be determined by exploiting the axis loads. This was also inferred in Section 5.4.1 when considering the comparison between the X-axis motor load and the spindle rotational speed. Figure 5.50 presents the raw signals for the X, Y, and Z axis motor loads. Figure 5.50 shows that all three signals are noisy. This is partly due to each signal fluctuating even at a standstill. These fluctuations correspond to vibrations in the machine (not related to the cutting process) and to each axis (other than Z) compensating for the lack of a brake. It is noted that the overall X-axis motor load (XML) trend is reminiscent of the SML and PEC trends. The same trend is observed for the Y-axis motor load (YML) but not as significant. The difference is on account of the Y-axis motor being more than twice as powerful as the X-axis motor (3.5kW versus 1.5kW) and therefore it may be less affected by the deteriorating cutting tool.



a. X-axis motor load



b. Y-axis motor load



c. Z-axis motor load

Figure 5.50. Axis motor loads (raw signals) for CD

It is noted that the three signals are also prone to outliers because of the rapid traverse (see Chapter 4). However, there is the possibility that actual process anomalies (corresponding to the condition of the cutting tool) are masked by the rapid traverse outliers. Due to the complex (and noisy) nature of the axis signals, it is considered that a qualitative comparison of the changing signal would be challenging. Therefore, to appreciate the implicit variation in the load signals the frequency components of the axis signals will be considered. The frequency variations for CD are illustrated in Figure 5.51.

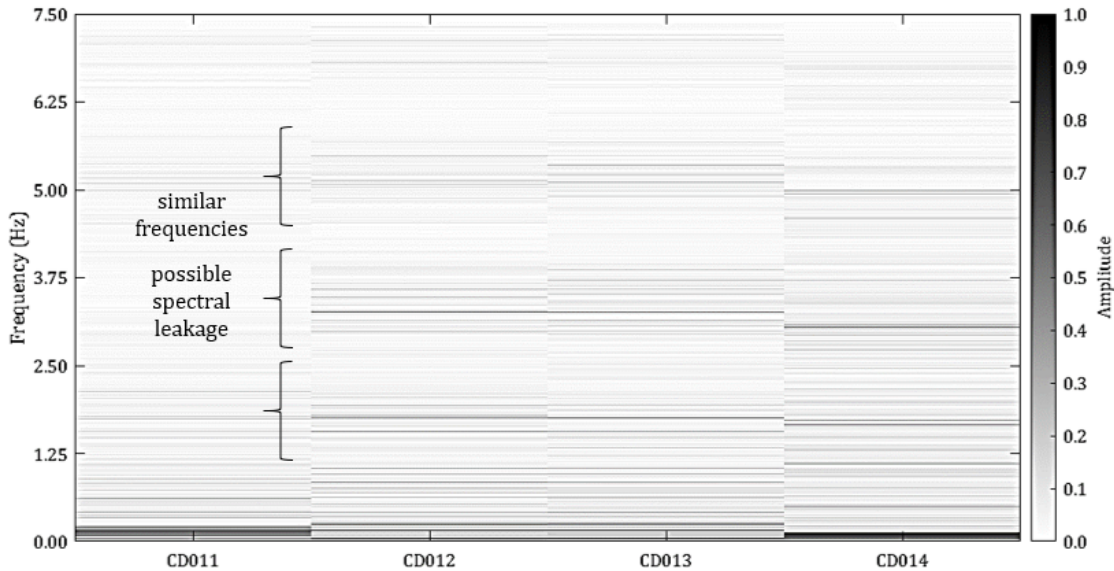


Figure 5.51. Frequency-amplitude image for CD XML

Figure 5.51 indicates very little similarity between CD011 and the subsequent tests. CD012, CD013, and CD014 indicate comparable principal frequencies. This indicates that the underlying frequencies in the signals have value for identifying the changing condition. However, like the SRS frequencies, it is tricky to quantify what these, and the differences, equate to in terms of the cutting tool health. It is possible to consider the micro value of the axis loads to understand the reasoning for this. The micro value is illustrated in Figure 5.52.

Figure 5.52 shows that the main problem with evaluating the axis loads for a pocket milling application is the constant change in the direction of the cutting process. This change makes it challenging to clearly attribute signal changes or underlying signal frequencies to the condition of the cutting tool. This means that the instantaneous condition of the cutting tool is not explicit in the given form. It also makes any information contained within the signals hard to find. It is thus considered that the process could be simplified to ascertain the instantaneous axis contributions. This is considered in Chapter 6.

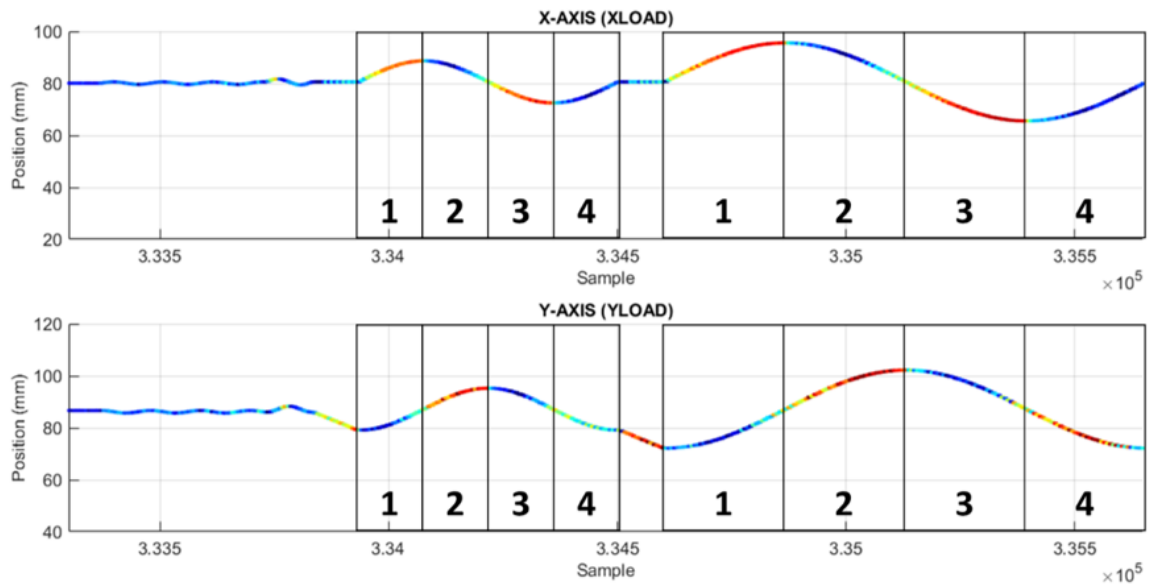


Figure 5.52. Change in axis load over a single (arbitrary) Cylinder (Jet colourmap)

## 5.6 Application of MTData: Ancillary signals

Other signals were acquired to complement those previously considered. These signals are ancillary signals (not primary signals) as their value lies in complementing the information generated by the others in categorising the process and enabling better, or simpler, comparisons between processes. On their own such signals cannot give a meaningful contribution to the determination of the cutting tool condition. Ancillary signals include:

**Feed rate** - The feed rate is beneficial due to the rapid movements employed by the machine tool. As the movements between features are much faster than movements during the cutting of features, it enabled the feed rate to be employed in the filtering of these movements. This was discussed in Chapter 4.

**Cutting tool number** – The acquisition of the cutting tool number allows the MTData to be associated with the correct cutting tool. The cutting tool number is the pocket from which the cutting tool originates. The controller requires this information to know which tool is needed for each operation as specified in the process g-code. As this information is critical for the successful operation of the machine tool, it can be relied on to remain consistent throughout a process. It is also the case that, if processes are properly organised, the cutting tool numbers will be consistent between operations and indeed known in advance of each operation. This knowledge enables the creation of a database of cutting tool parameters that allows specific information relating to each cutting tool to be correlated with the generated process information. This enables a better understanding of this information, especially when certain cutting tools behave in specific ways as this can be acknowledged before the behaviour is noted to be an anomaly.

**Axis positions** – The axis position information was gathered in response to the value gained from the scanning measurements shown in Section 5.2.1.3. It was determined that the acquisition of

the position data would enable a comparison between the post-process measured geometry and the in-process acquired geometry. Figure 5.53 presents a cropped view of a single Cylinder.

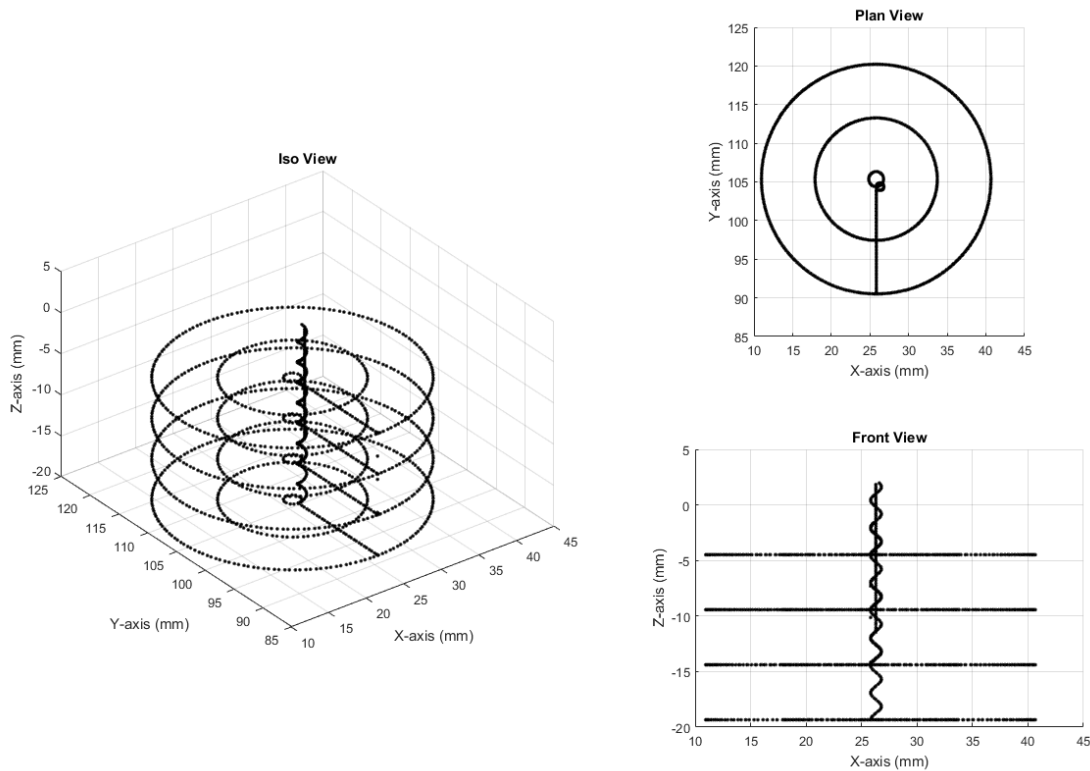


Figure 5.53. 3D process visualisation compiled using in-process axis position data

Figure 5.53 illustrates that the in-process geometry has the advantage of representing the entire process, rather than just the finished result. However, beyond facilitating visualisation of the process, it is limited in that the specific geometry of the cutting tool is not known. The values given relate to the reference points for the spindle and hence do not account for the length or diameter of the cutting tool used. This is not a concern for the Cylinder application as only one cutting tool was employed for each test; however, it should be remembered for when more cutting tools are used. Adding relevance to this will require the cutting tool number and the related cutting tool geometries.

### 5.6.1 Potential applications, advantages and complementary uses

As previously noted, the feed rate had value in complementing the DENSE algorithm and enabled a robust way of determining process movements from the actual cutting process. Likewise, the cutting tool number enables the segregation of MTData into separate categories. Where different cutting tools are employed the acquired information will not cause confusing or overlapping results. The position data on the other hand has multiple applications that could benefit the optimisation of the cutting process. Three novel uses of this data that will be demonstrated in later Chapters are further considered below in the context of the Cylinder application:

**DENSE** – The DENSE algorithm suggested that due to the difference in the amount of time spent

during cutting versus the time spent moving around within the machine tool volume, the relative density of the position data allows the part/process to be determined without prior knowledge. This was outlined in Chapter 4. It is appreciated that the right cut-off, or density threshold may require a degree of trial and error to best capture the final part information.

**Quality assessment** – A further application of the position data is to optimise the quality assessment of parts and features generated using the machine tool. Current post-process operator centred actions rely on the visual/manual inspection of every specified “nth” part machined. This will be a combination of a check for severe damage or for surface imperfections, followed by hand-gauges to assess feature suitability (e.g. go/no-go gauges). Incorporating visual information into this process enables the nth part machined to instead be the part that has not been machined to tolerance, or that, according to the data, shows signs of damage or imperfections. It also enables the attention of the engineer to be directed to the feature or issue in question, thereby increasing the speed of visual inspections and further improving the efficiency of the process. Figure 5.54 is given to illustrate this novelty. Figure 5.54 shows the potential wealth

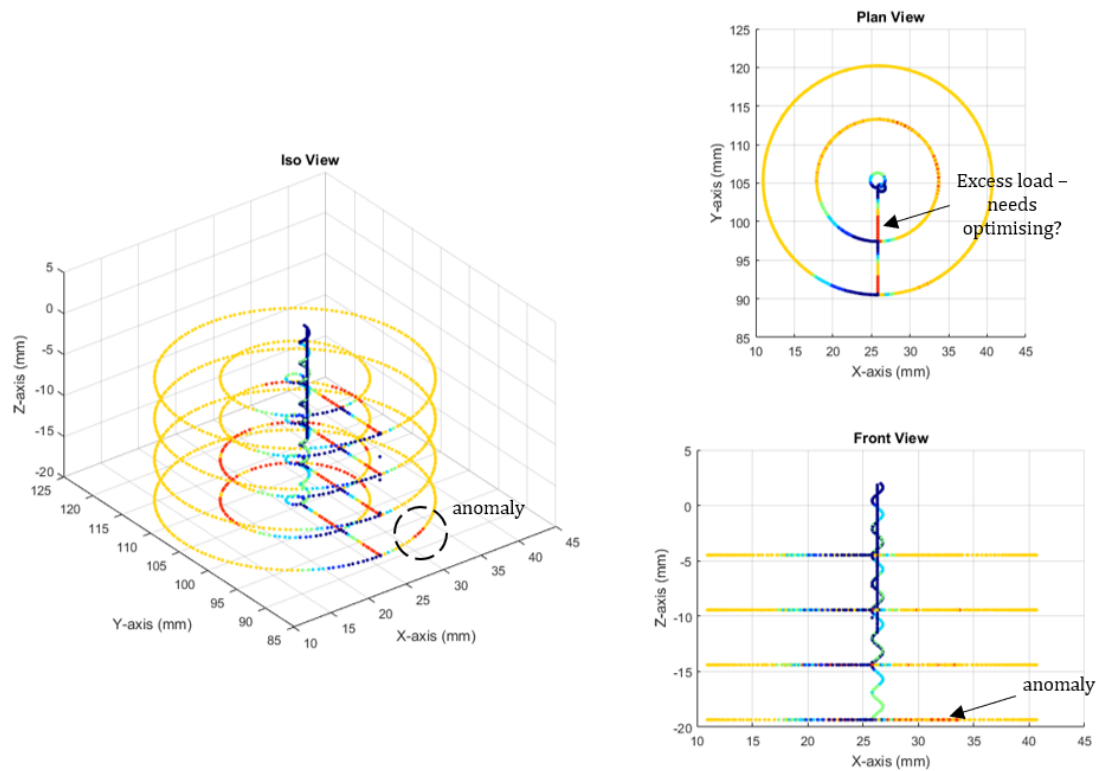


Figure 5.54. 3D process visualisation illustrating feature quality using SML overlay

of information provided by overlaying the SML on the position data for a single Cylinder. The figures are not monochromic and therefore there is a risk that distorted or false patterns may be observed; however, the Jet colourmap was given to emphasise potential anomalies and high-load signal regions. Nevertheless, it is seen that an abnormal load occurs at the start of the fourth part. This may show surface damage and should be investigated.

**Process optimisation** – In addition to post-process optimisations, the position data may also be

used to optimise the process itself. By correlating the information present in the data with the position data allows for an informed investigation into the behaviour of the cutting tool throughout the cutting process. This information should enable engineers to find cycles that could be improved to promote an increased cutting tool life. Equally, where conditions are favourable, cycles may be optimised to promote shorter process times. It may also be the case that when damage is consistently occurring during certain cycles, those may be updated to reduce the occurrences or mitigate the damage entirely. Figure 5.54 indicated that the Y-axis movements to expand the part diameter resulted in higher loads on the spindle. These may be mitigated by considering alternative strategies for expanding the part, rather than slotting.

Like the 3D geometry plots, the position data is potentially a useful resource for providing process feedback during the cutting process. For systems employing ICG, physical measurements may be combined with the position feedback, thus providing engineers with a smart combination of condition-based data during each process. This has potential as a data-visualisation system, especially considering Industry 4.0, the IIOT, and connected factories.

## 5.7 Challenges - limitations of the Cylinder application

This Chapter considered the output from the Cylinder application. A set of general wear curves were established using measurable attributes including the geometries and surface finish of the Cylinders, as well as using process generated data, such as the SML, the axis loads, and the spindle rotational speeds. The measurable attributes helped to prove the efficacy of MTData for deriving the condition of cutting tools in lieu of such attributes, such as in-process. The value of each MTData signal was considered for the inherent features and/or trends that could be employed for determining the condition or health of a cutting tool.

Notwithstanding, it is noted that the Cylinder application was (and is) limited in that the process is too simple and the disconnect between the application and commercial processes is too great. There was only one cutting tool employed for each test, and the process was developed to enact exaggerated wear on the cutting tools. The use of a single cutting tool prevented any insight into the interaction between different cutting tools and did not enable any investigation into different wear modes for cutting tools taking on different processes. It is appreciated that a single cutting tool will not be employed for both the roughing operations as well as the finishing operations. These different applications will have distinctive characteristics and perhaps distinctive features and/or trends for the cutting tools used. Similarly, the exaggerated wear enabled the wear of cutting tools within 200 parts; however, due to the aggressive attempts to wear the cutting tool, the general wear trends dominated the results. It should be appreciated that “normal” cutting processes may not be as clear-cut as those presented. Differences in the speeds, feed rates, and the specific uses of each cutting tool may present different magnitudes in the measured PEC or axis loads. These changes may not conform to the general wear curves in a fashion that is easy to interpret. As such, further investigations are required to understand the possible challenges in transitioning from a laboratory-based application towards a commercial or industry-based application.

## 6 | Slotting Investigation

This Chapter presents the developments that were introduced to simplify the processing of key MT-Data signals. This was introduced after the Cylinder application to build on the data acquisition and analysis approaches developed during the wear testing. The aim is to establish the value in each of the presented signals, and to explicitly show how each MTData signal complements the overall deterioration of the cutting tools. The Slotting application was designed to be a straightforward process that enables signal variation to be attributed directly to the cutting tool condition. It was noted in Chapter 5 that some variation was potentially attributable to the cutting process rather than the cutting tool. By reducing the complexity of the process, this can be mitigated (to a degree). Additionally, reducing the complexity will better enable the interpretation of some results. To progress from the Cylinder application considered in Chapter 5 three decisions were continued for the Slotting application

- The Slots are another laboratory-specific application. At this stage it was recognised that this was unlike any complete commercial process. They have been designed to simplify the results and the processing stages, rather than to represent a practical or entirely realistic process.
- A single cutting tool was employed throughout to reduce the complications arising from using different tools. Comparisons of different cutting tool types could be considered once the approach was proven
- The cutting regime was fixed to simplify the results and enable a comparison between monitoring methods

The second and third decisions marking the single factor strategy of the experiments conducted. The machining of the Slots was less aggressive than the Cylinders, to avoid tool breakages; however, like the Cylinders the wear enacted on the cutting tools will be entirely natural. No artificially induced damage will be considered. The cutting tools do not fail in this way; however, the deterioration is realistic (if slightly accelerated). It is also noted that two of the three assumptions given to the Cylinder application are further applied to the Slotting investigation, namely:

- All process variation is attributable to the condition, deterioration, or breakage of the cutting tool and that the other notable system interactions (outlined in Chapter 2) are negligible within that respect
- Each cutting tool employed is initially unused and all are equivalent in geometry, style, and material unless indicated otherwise.

Whilst not all the process variation will be attributable to the wear on the cutting tool, for a healthy system the majority should be cutting tool related. Where potential conflict arises, it will be acknowledged. Two Slotting tests were enacted using two cutting tools. The first test employed a 10mm diameter cutting tool, the second considered a 12mm cutting tool. The cutting parameters

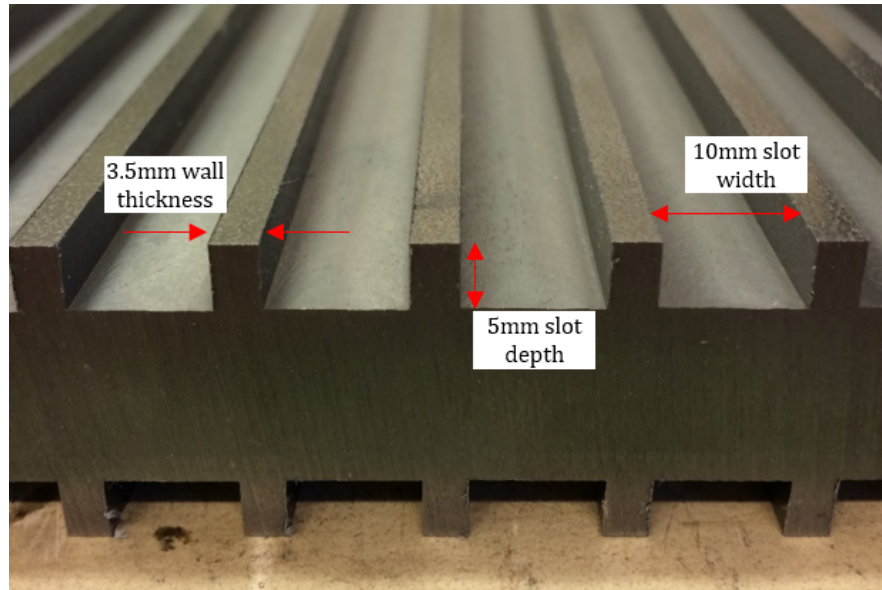
are provided in Table 6.1. It is noted that neither of the cutting tools failed. Table 6.1 shows that the acquisition of the MTData was still a work-in-progress during SA with both the rotational speed (SRS) and the feed rate (RFR) being acquired as unprocessed (individual) registers. For that reason, the results for SA will not be presented herein. It is also noted that the cutting tool used for SB003 is the same cutting tool used for SB004026. Herein references to SB will refer exclusively to SB004026, whilst SB003 will only be noted when referred to explicitly.

Table 6.1. Slotting test information and cutting parameters

Test	Cutting tool	Material removed	Acquired MTData	Settings
SA001002 (SA)	HSS (10mm $\varnothing$ )	X18 Slots (198000mm <sup>3</sup> )	SRS (raw)	SRS: 912 (rpm)
			SML (%)	CS: 29 (m/min)
			RFR (raw)	RFR: 201.6 (mm/min)
			XML (%)	RT: 22 ( $^{\circ}$ C)
			YML (%)	OT: 4 ( $^{\circ}$ C)
			ZML (%)	DOC: 5 (mm)
SB003	HSS (12mm $\varnothing$ )	X7 Slots (92400mm <sup>3</sup> )	SRS (0.001rpm)	SRS: 1375 (rpm)
			SML (%)	CS: 52 (m/min)
			RFR (0.1mm/min)	RFR: 275 (mm/min)
			XML (%)	RT: 22 ( $^{\circ}$ C)
			YML (%)	OT: 19 ( $^{\circ}$ C)
			ZML (%)	DOC: 5 (mm)
SB004026 (SB)	HSS (12mm $\varnothing$ ) (12mm $\varnothing$ )	X161 Slots (2125200mm <sup>3</sup> )	SRS (0.001rpm)	SRS: 952 (rpm)
			SML (%)	CS: 36 (m/min)
			RFR (0.1mm/min)	RFR: 190.4 (mm/min)
			XML (%)	RT: 22 ( $^{\circ}$ C)
			YML (%)	OT: 19 ( $^{\circ}$ C)
			ZML (%)	DOC: 5 (mm)

## 6.1 Qualitative condition assessment

The rate of material removal during the Slotting application was 8% less than the material removed during the Cylinder application (184800mm<sup>3</sup> versus 201062mm<sup>3</sup> per block respectively). It is also noted that the cutting tool employed was 20% larger in size for SB. For these reasons, the cutting tool was not expected to fail catastrophically within the tests conducted; although, it could still wear beyond reasonable use. This enables the cutting tool condition to be evaluated and compared with the condition of the workpiece and the implied condition from the MTData signals, without concern for damaging cutting tool failure, unexpected or otherwise. This chapter will henceforth consider the end of useful life (EOUL) of the cutting tool, in place of the EOL, indicating the point a cutting tool should be retired, even if the general condition indicates that continued use may be possible.



a. Front view (angled) of Slots



b. Top view of Slots

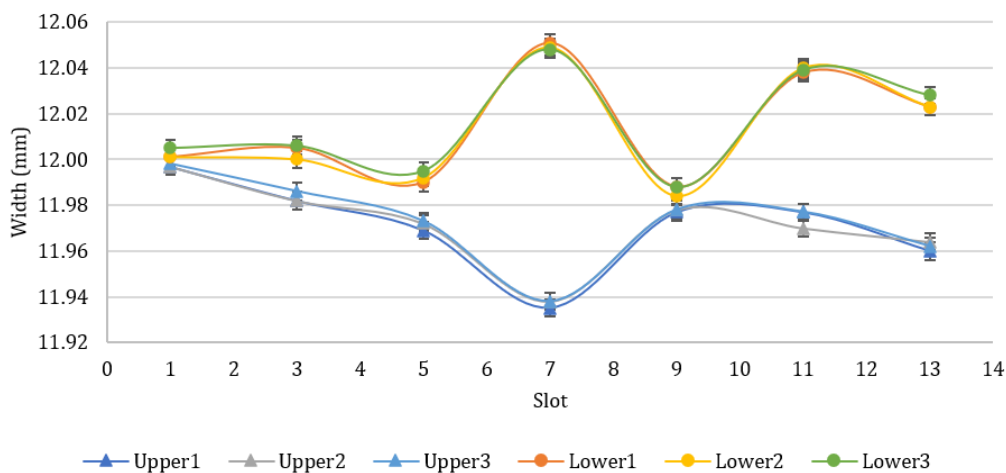
Figure 6.1. Photographs of the 10mm Slots (SA), illustrating the workpiece dimensions

Figure 6.1 shows that the Slots were machined into both sides of the workpieces. This required each block to be manually rotated and re-fixed to the bed of the machine tool. Prior to machining, each block was probed to set up the local coordinate axes and to find the centre of the workpiece. This enabled a consistent process despite the need to remove and re-fix. Each Slot was machined in a single pass, from the left side of the workpiece to the right side. The cutting tool entered the material at the cutting depth (5mm) and exited the material at the same cutting depth. The entry and exit should be notable when processing the MTDData. The consistent cutting approach limited the main mode of cutting tool wear to the peripheral edges and reduces the work of the front edges of the cutting tool. It was noted during visual part inspection that the quality varied significantly. SB003 suffered from excessive chatter due to the 52m/min cutting speed. To mitigate this, all subsequent Slots were

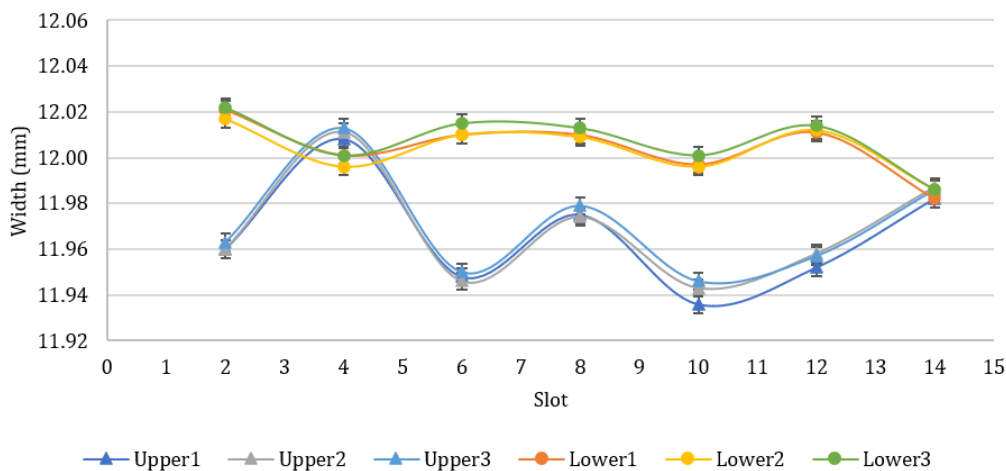
machined at a reduced speed of 36m/min. It was also observed that the surface quality was poor. This was due to aggressive cutting speeds and the lack of a finishing cut. It was further seen that the Slots accumulated a significant amount of oil, dust, and debris. The implication being that each block should be cleaned prior to tactile measurements. It is noted that all workpieces warped following removal from the machine tool. It is suggested that this was due to the machining of the Slots just 3mm apart (resulting in thin walls) and the lack of stress relief before and after the cutting process. The warp was noted for both visual part inspection and quantitative measurement of each test.

## 6.2 Quantitative condition assessment

Investigating the quantitative measure of cutting tool wear, it was found that workpiece quality had a notable impact on the acquired measurement attributes. Figure 6.2 shows the difference between the top and bottom of the Slots (as measured) and the variation between the beginning and end of each Slot.



a. Arbitrary point 1



b. Arbitrary point 2

Figure 6.2. Slot width variation (top and bottom) for arbitrary points (SB003)

Figure 6.2 shows that there is considerable variation in the measurements. It is noted that the Slot-to-Slot variation is excessive and varies depending on the discrete points used to generate the measure of Slot width. This indicates that taking discrete points is not a suitable measurement technique in this instance. However, it is also considered that the variation is on account of the workpiece warp and the surface roughness affecting the measurement repeatability. The measurement of these features was undertaken using the CMM. Attention is drawn to the large number of CMM/Modus programs included in the Appendix C.1. A small-tipped probe was used in the measurement (RSP3) due to the capability for Z-plane surface scanning. This will not benefit from the filtering effect afforded to larger tips and shows that for future applications (where possible) the RSP2 probe should be employed for the larger tip size. The measurement deviation due to the surface quality is evidenced in Figure 6.3.

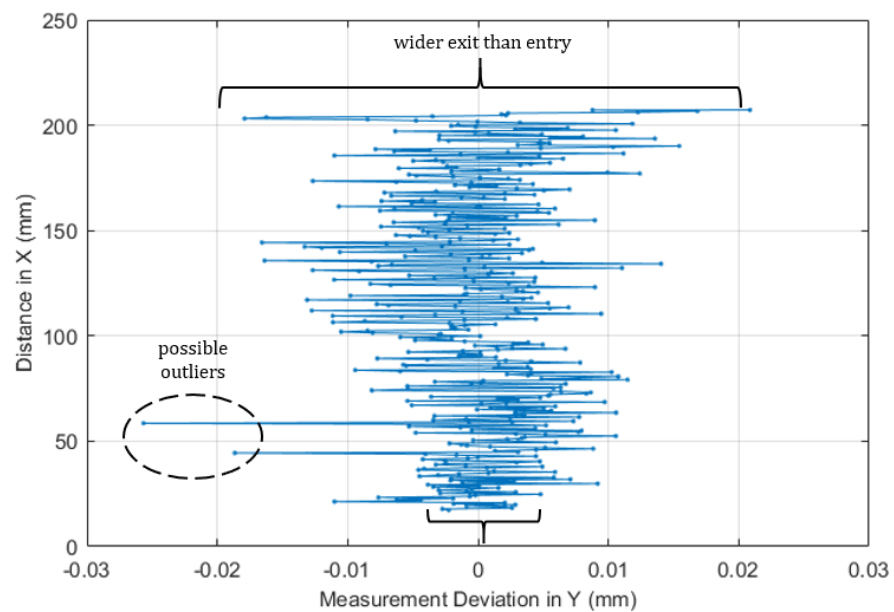
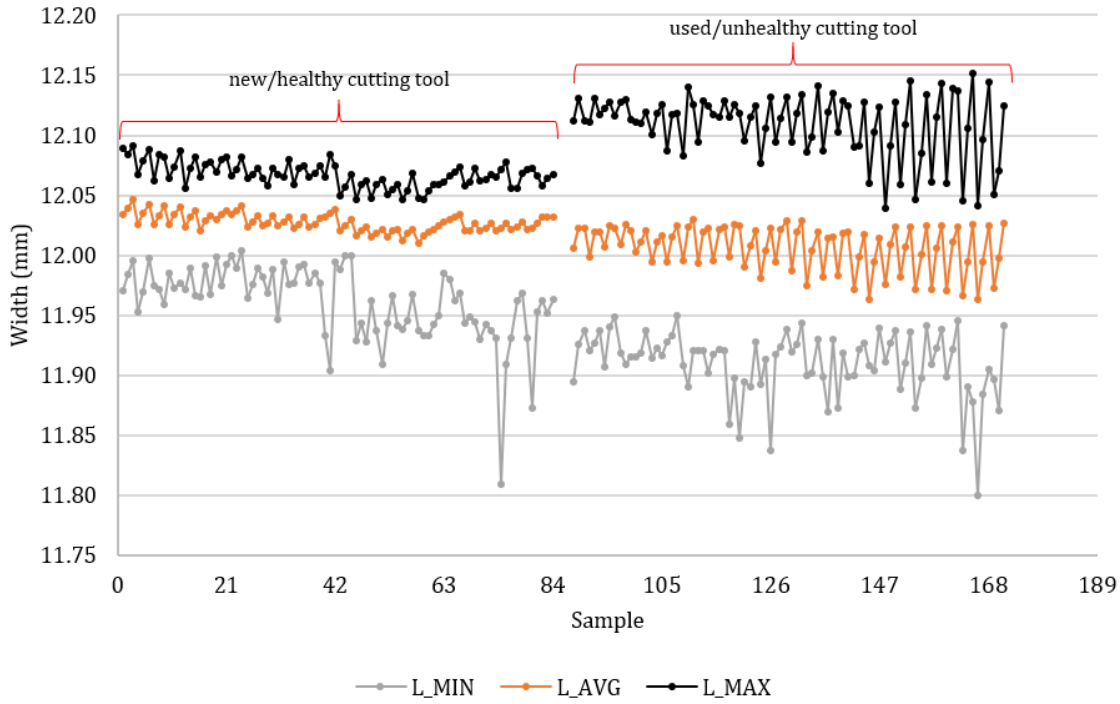


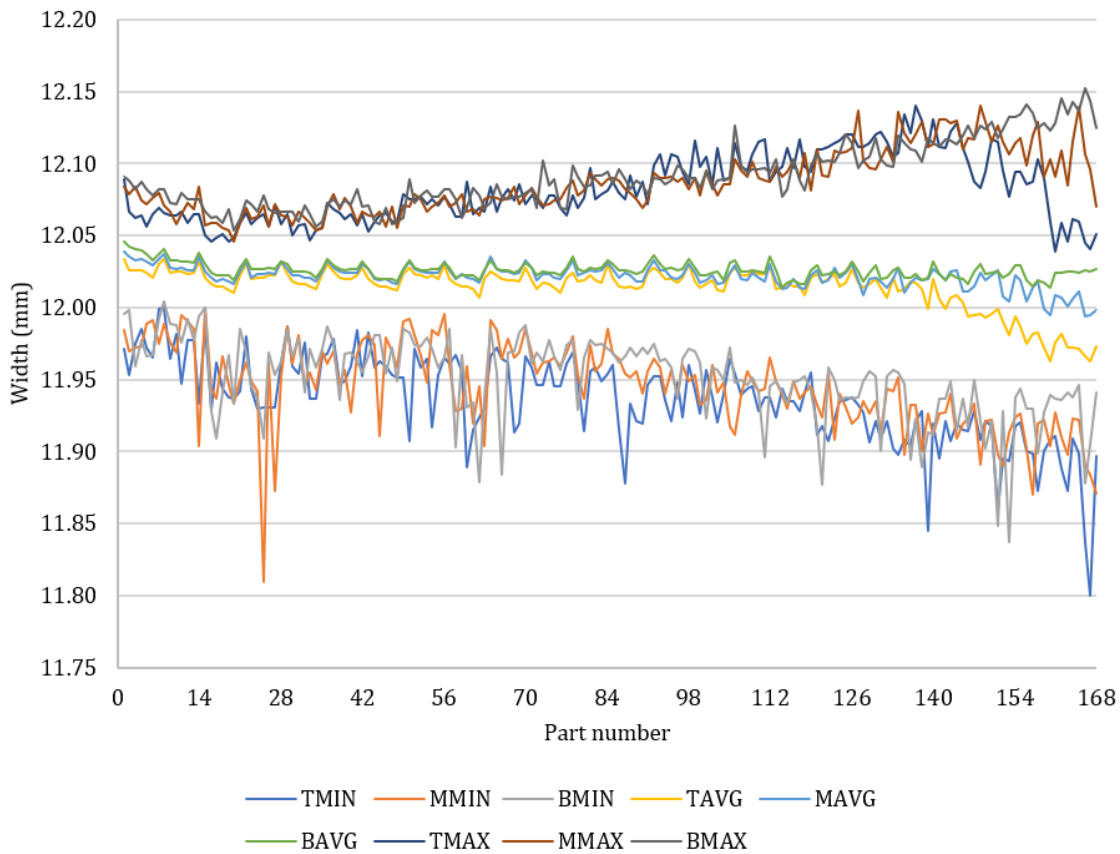
Figure 6.3. Surface waviness along Slot wall

Figure 6.3 shows that the measurement range is  $50\mu\text{m}$  on account of the surface waviness. It is considered that the best measurement approach is to scan the Slots and take an average over the full length rather than taking discrete measurements. Each Slot is scanned nine times, three scans per wall and three along the Slot floor. Opposing scans (wall pairs) are used to generate three width measurements – minimum width, average width, and maximum width. The three width measurements, for all wall pairs, are given in Figure 6.4.

Figure 6.4a shows that there is a notable difference between the minimum, average, and maximum width measurements. This is again due to the poor surface quality, which is retained to illustrate the change as the cutting tool deteriorates. It is noted that the moving range increases for all measures. It is also noted that the distances between each measure increases. The increase in the distance between each measure is on account of the surface quality deteriorating over the course of the machining process. This correlates to the deterioration of the cutting tool. Figure 6.4b further separates the measurements into their relative position within the Slots (top, middle, and bottom). This gives a better picture of the changing condition of the cutting tool. The minimum width measurements are



a. Width measurements for top, middle, and bottom scan pairs (concatenated)



b. Width measurements for top, middle, and bottom scan pairs (separated)

Figure 6.4. Min, avg, and max scanned width measurements for SB (inc. SB003)

unstable and trend towards a smaller width as the process continues. Other than the general trend (in smaller minimum widths) there are no other notable changes in the minimum width measurements as the process progresses. The maximum width measurements are much more stable (than the minimum measurements) and tend towards a greater width as the process continues; however, when the process reaches 145 parts, the maximum width changes depending on the position within the Slot:

**Bottom MAX width** – continues trend towards greater width with no discernible change in the pattern

**Middle MAX width** – slight drop in maximum width with general trend changing towards reduced values

**Top MAX width** – notable drop in the maximum width with the general trend noticeably changed towards reduced values.

These changes suggest that the wear on the cutting tool is like that observed during the Cylinder application with the development of notch wear 5mm up the cutting tool (at the 5mm cutting depth). This would explain the top of the Slot suddenly decreasing in maximum width, whilst the bottom of the Slot remains (relatively) unchanged. The average width measurements follow a similar pattern to the maximum width measurements; however, as the average have fewer fluctuations the late-stage change in the trend is clearer from a slightly earlier part (140 versus 145). The noticeable difference is that a repeating pattern can be observed in the average width measurements. This repeating pattern corresponds to the warping of the workpieces and the effect of the thin walls (primarily at the edges of the workpiece). The outer Slots on each workpiece are notably wider than those within due to the thin walls (at the edges of the workpieces) deflecting more for the first and last Slot on each side. Additionally, the side of the component machined first has wider Slots than the opposing side (machined second). This is likely to be due to the release of residual stresses and the workpiece warping when rotated to machine the second side. The most useable information is thus the average width measurements. These may be separated for further consideration, given in Figure 6.5.

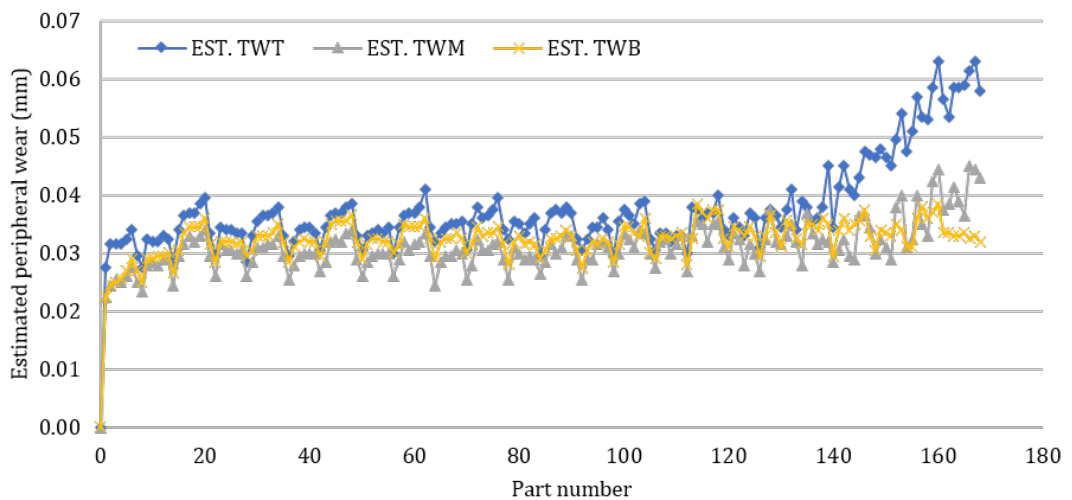


Figure 6.5. Estimated (average) peripheral edge wear based on a 12mm Slot width

Figure 6.5 considers the average width measurements adjusted against a nominal Slot width of 12mm to give a measure of the estimated peripheral wear. It is noted that the repeating pattern due to the workpiece warp is significant. It is noted that the estimated wear falls way below the ISO 8688-2:1989 recommendation of 0.3mm. This suggests that the wear is minimal and the changes perhaps indicate the relative health of the cutting tool, rather than the explicit condition of the cutting tool. It is considered unlikely (with the variation exhibited) that there is any visible occurrence of cutting tool deflection and/or vibrations. Cutting tool deflection and cutting tool vibration are therefore not considered in any particular depth herein. Figure 6.6 reduces the information further to consider the inferred cutting tool wear using just the top of each Slot.

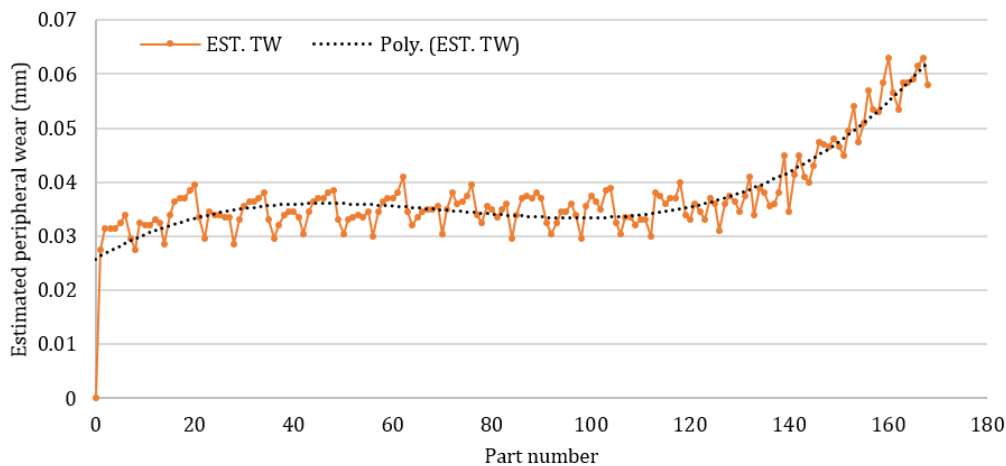


Figure 6.6. Estimated (average) peripheral edge wear based on the upper width of a 12mm Slot

Figure 6.6 includes a cubic trendline to show the general trend. It is noted that the pattern is akin to the general wear curves; however, it should be appreciated that if the measurements were taken at the middle or the bottom of the Slots, the trend would be negligible and/or non-existent. Nevertheless, as the predominant mode of cutting tool wear was notch wear, it is sensible to consider the corresponding variation as representative of the localised cutting tool health. In other words, the estimated change in the Slot width at the top may indicate development of notch wear, whilst the variation at the middle or at the bottom of the Slots will not indicate the development of notch wear. Therefore, using the middle or the bottom of the Slots will underestimate the health of the cutting tool. Figure 6.6 shows that the effect of the workpieces warping presents as a challenge for the assessment of cutting tool wear through measurement of the components. The variation attributable to the warp will be difficult to apportion appropriately when assessing the instantaneous changes. It will also obscure the subtle changes in the condition of the cutting tool. Considering the estimated EOUL for the cutting tool employed for the Slots, a QSUM may be considered, given in Figure 6.7, using the approach outlined in Chapter 5 using Equation 5.4.

Figure 6.7 shows that the estimated EOUL depends on the chosen threshold. For a significance threshold of a single standard deviation, the EOUL is 141. On the other hand, three standard deviations are not exceeded until 152 parts. Both could be considered sensible places to replace the

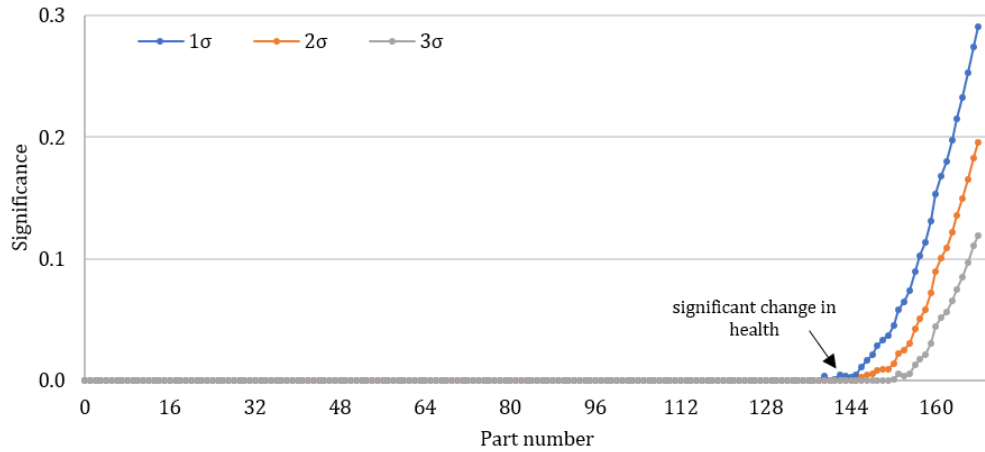


Figure 6.7. Upper QSUM trends for SB peripheral wear, with 1, 2, and 3 $\sigma$  thresholds

cutting tool as it has begun deteriorating. However, considering the data given in Figure 6.4, 141 is the better EOUL as it precedes the significant decline in condition. It may be prudent to also consider an adaption of the QSUM to consider the moving average, or the continuous (instantaneous) estimate of the QSUM. This simulates the response should the approach be implemented whilst a process is ongoing. Figure 6.8 presents the moving average QSUM. Figure 6.8 shows an in-process issue with the workpieces warping. It is acknowledged that if the 1 $\sigma$  threshold was implemented the process would give false alarms throughout the process. Even the 2 $\sigma$  threshold gives several false alarms. It is noted that avoiding the warp occurring would enable both thresholds to be used. However, accounting for the warp, 3 $\sigma$  may be employed, which gives a predicted EOUL of 139 parts. As this is two parts different from the standard QSUM it is considered reasonable.

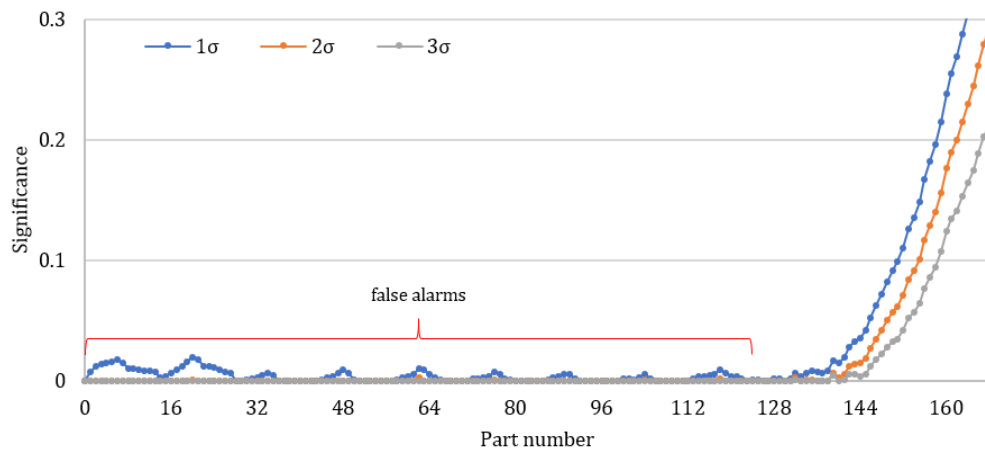


Figure 6.8. Upper QSUM moving average for SB peripheral wear, with 1, 2, and 3 $\sigma$  thresholds

### 6.3 Application of MTData: Spindle motor load

The deterioration of the workpiece shows a gradual progression in cutting tool wear. The challenge is to show this deterioration using the MTData. Like the Cylinder application, the macro value of the SML may be considered. Figure 6.9 shows the impact of the higher cutting speed used for SB003 and further evidences the need to process the data. It is noted that the general trend is towards higher

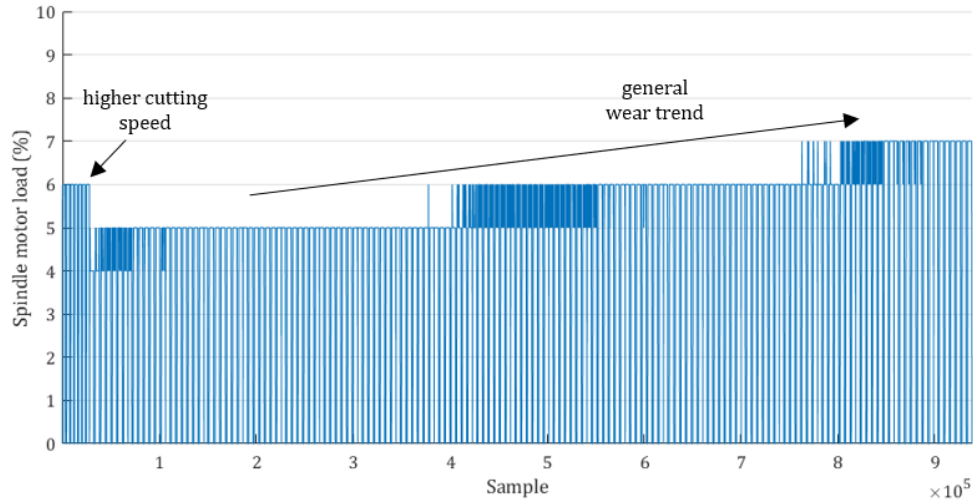


Figure 6.9. Raw SML signal for all 12mm Slots (SB003 and SB004026)

spindle loads as the cutting tool wear progresses; however, there are limited indications as to whether the wear is accelerating towards the end of the completed tests. The main indication is the increased rate of change (as inferred by the shorter transition) from 6% SML to 7% SML versus the change from 5 SML to 6% SML. Figure 6.10 presents the PEC for the Slot, accounting for the differences in the rotational speed between SB003 and SB004026.

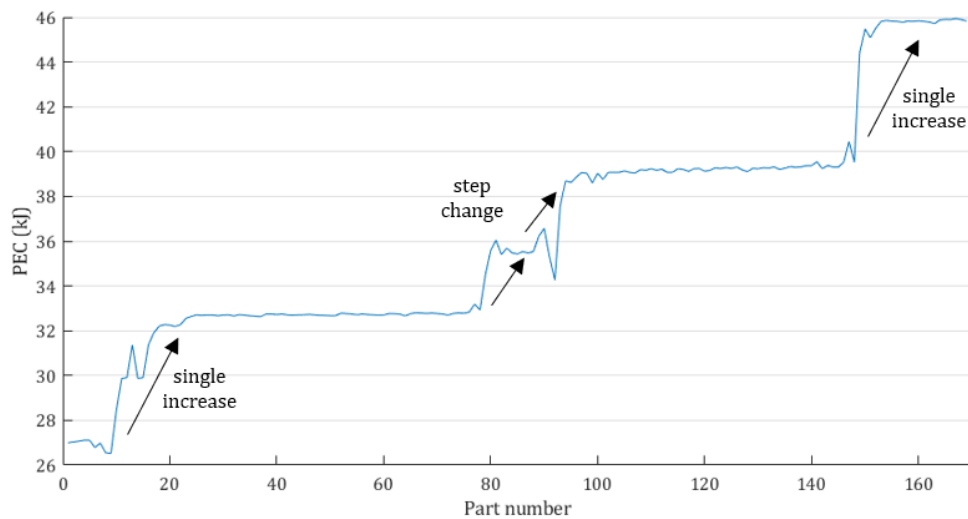


Figure 6.10. PEC trend for all completed 12mm Slots

Figure 6.10 shows that by accounting for effect of the rotational speed and the maximum spindle power, the magnitude of SB003 is broadly back in line with the expected values versus the rest of the process (in terms of the cutting tool wear). The general trend is noted to be like the unprocessed trend, although there is a more notable difference between the stages. The magnitude changes at the beginning of the signal and at the end of the signal are greater than the magnitude change between parts 80 and 100 (6kJ changes at the start and end versus 3kJ changes between parts 80 and 100). This differentiates between the initial and final rapid wear phases and the gradual wear phase between them. Despite the trend being notably staggered, it is possible to fit a cubic trendline to the data to

establish the EOUL using the cubic changepoint detection (CCPD) algorithm developed in Chapter 5. Figure 6.11 demonstrates the cubic trend. Figure 6.11 indicates that a cubic trendline in this

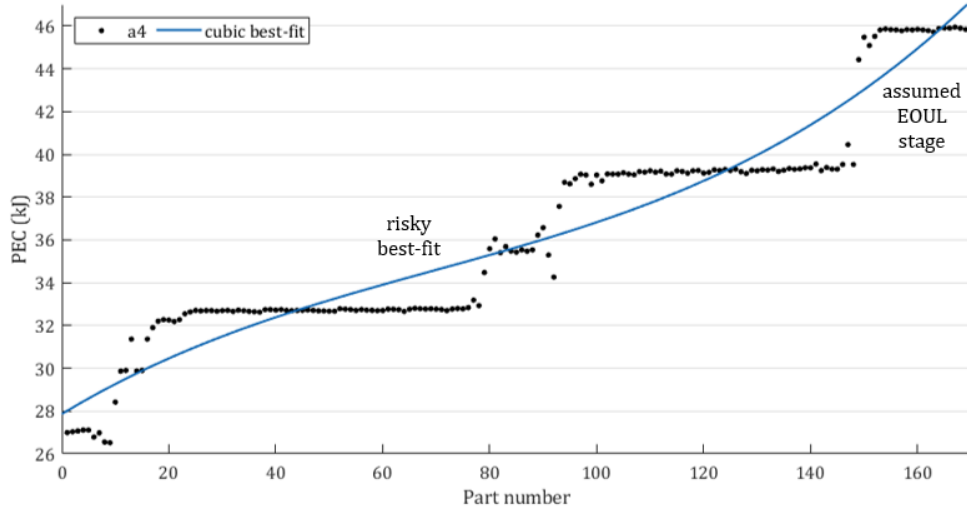


Figure 6.11. PEC trend with cubic best-fit for 12mm Slots (SB)

instance is not (perhaps) a best-fit trend. The staggered nature of the signal makes it challenging to model precisely, reinforcing the notion that getting more detail (e.g. less discrete data) would be of greater benefit. Nevertheless, working with the data that is available, the trendline changepoints may be considered to evaluate whether there are similarities to the geometry changes. The e-fit is given in Figure 6.12, produced using the methods developed in Chapter 5.

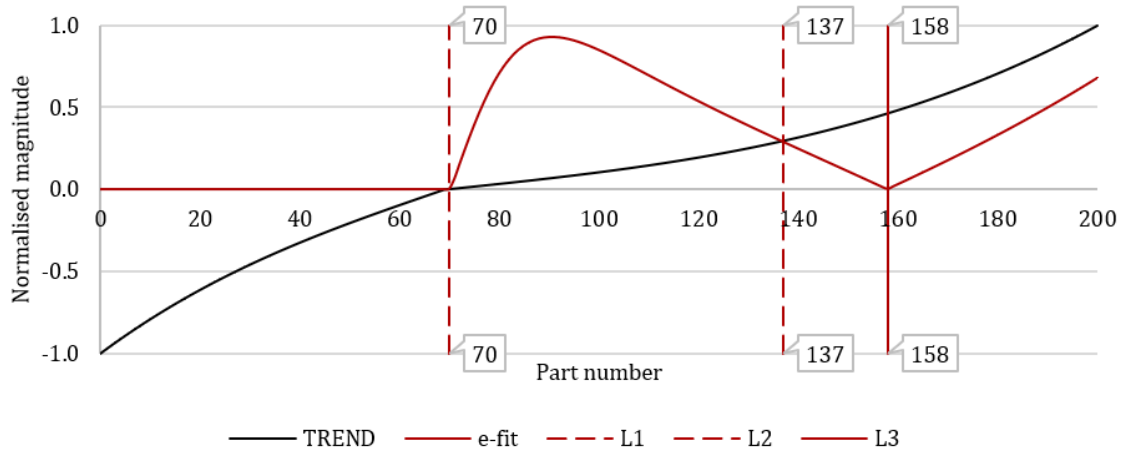


Figure 6.12. e-fit plot for SB PEC (FRL = 10)

Figure 6.12 is included to illustrate the value in using the SML for estimating the cutting tool EOUL in lieu of the geometry data and includes the SML trend inflection point (L1), the first EOUL (L2) and the second EOUL (L3). Figure 6.12 shows the calculated changes in the SML signal gradient using methods developed in Chapter 5. The predicted stationary point is at 70 parts, the first predicted EOUL is 137 and the second EOUL is at 158 parts. These are near to the geometry estimates for the EOUL at 141 parts for the full QSUM and 139 parts for the moving average QSUM. A difference of

2–4 parts is acceptable, especially considering the prediction is earlier and therefore likely to err on the side of caution. The second EOUL at 158 parts suggests that the cutting tool should be retired within 21 parts where applicable. This is again sensible as the geometry data suggests that the part quality deteriorates significantly after this (refer to Figure 6.4). The active predictions may also be considered. The in-process CCPD response is given in Figure 6.13, estimating the predicted EOUL using methods presented in Chapter 5.

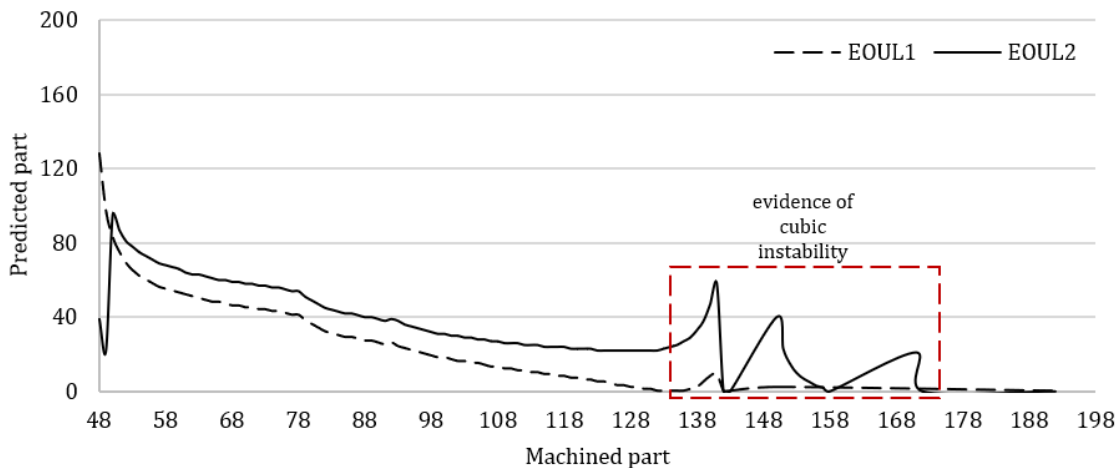


Figure 6.13. SB response plot for PEC e-fit predictions of cutting tool condition

Figure 6.13 infers that when implemented in-process the CCPD algorithm may suggest that the cutting tool is retired at (or around) 132 parts. This is an advance of five parts prior to the original EOUL prediction. It is also noted that the second EOUL response is not stable and therefore overpredicting the remaining parts. This is related to the estimated limits (change-points) becoming unstable between 139 and 150 parts and corresponds to the last step change in the PEC trend. This is further illustrated using the e-fit plots from 48 to 141 parts, given in Figure 6.14.

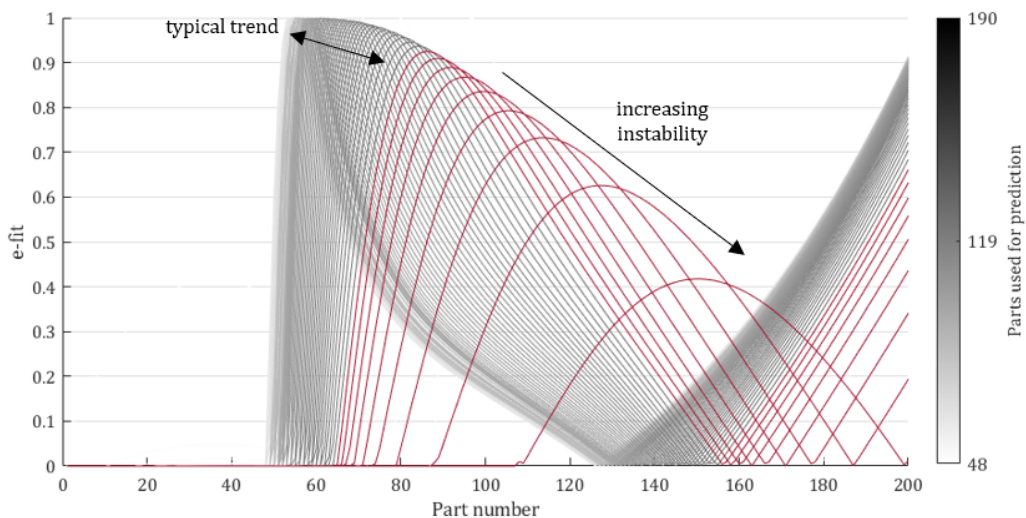


Figure 6.14. SB PEC predicted e-fit curves from 48-141 parts

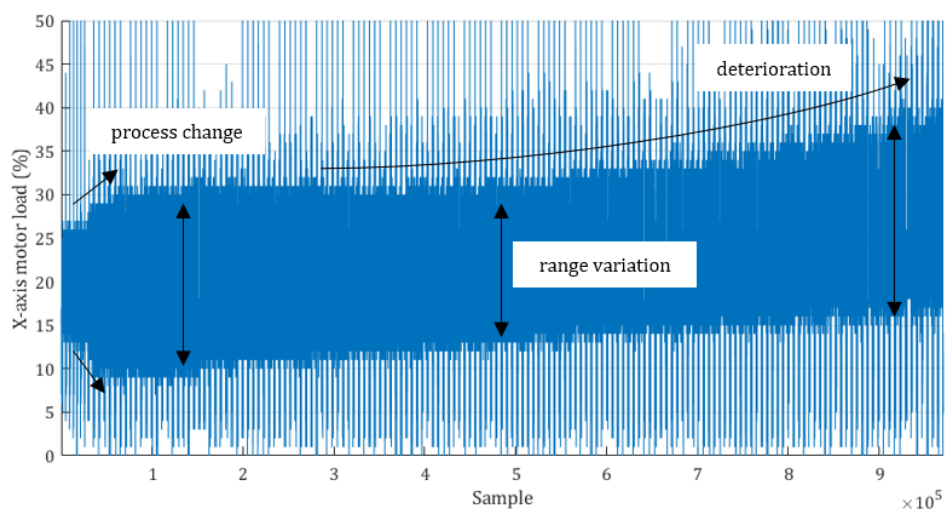
In Figure 6.14 the e-fit curves that evidence the instability of the cubic best-fit have been re-coloured

red to emphasise where they occur and how they progress. It is noted that this issue is down to the cubic best-fit tending to zero at (and after) 142 parts. This provides evidence that the CCPD algorithm may be improved by considering more stable best-fit equations. Although equally, the predictions could be weighted to account for the performances of similar cutting tools for the same (or similar) processes. The CCPD response is given to show the potential in-process value of the SML for predicting the EOUL for the cutting tool, upfront rather than retrospectively. It is shown that there is room for improvement. This could be the focus of future research.

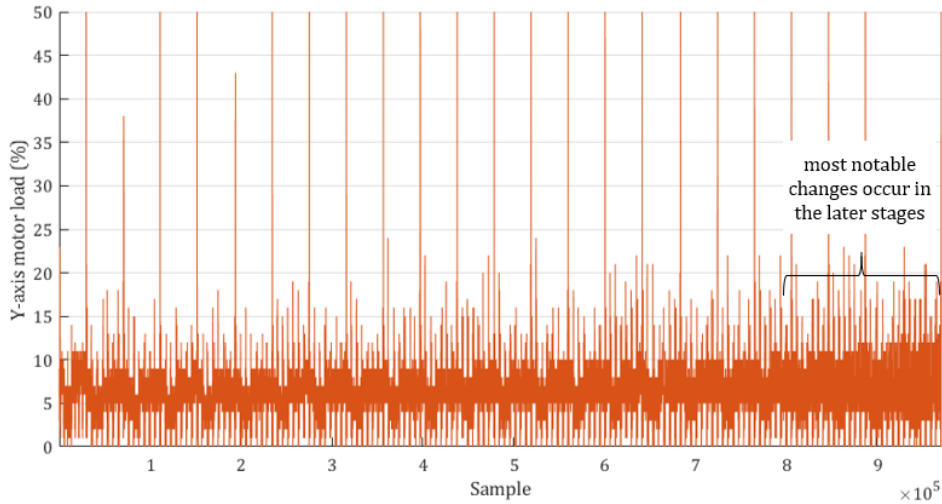
## 6.4 Application of MTData: Axis motor load

It has thus been shown that the SML for the Slotting application has value in lieu of the geometry data and that there is potential value in using the SML to estimate the EOUL for the cutting tool both retroactively (post-process) and actively (in-process). Therefore, the axis loads may be considered. The removal of material along a single axis (the X-axis) should make it easier to establish the signal changes that may correspond to the changing condition of the cutting tool. First the macro value of the axis loads may be considered to establish the overall trend for each axis. Figure 6.15 gives the percentage motor load signals for each axis.

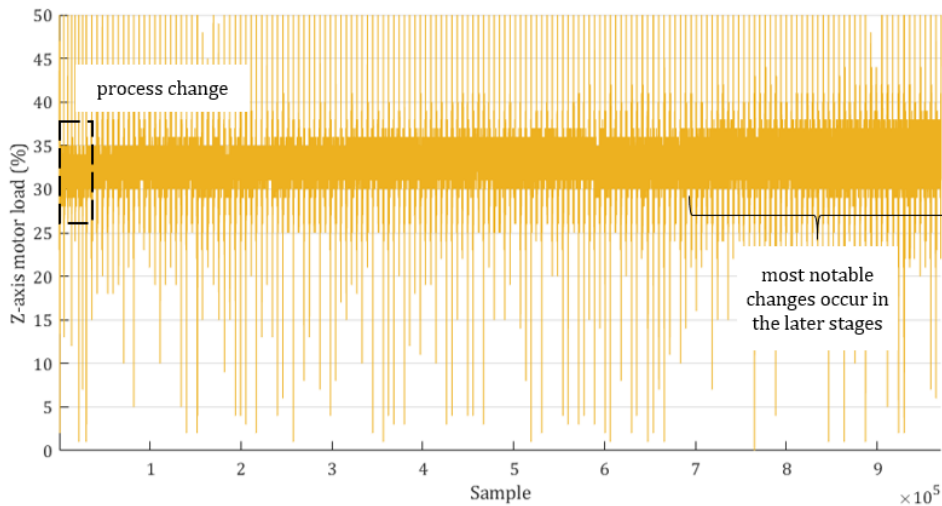
Figure 6.15 shows that, like the Cylinder application, all three signals are noisy. It is speculated that the noise may be attributable to the machine tool vibrations. It is noted that there are significant fluctuations for all three axis signals. These have been found to correspond to the rapid traverse movements; although, there is the possibility that actual process anomalies are masked by these rapid traverse outliers. Such anomalies may correspond to the condition of the cutting tool or to possible local differences in workpiece material properties. The outliers may be removed by filtering the signal with a Hampel filter; however, this may remove the actual process anomalies. The other approach is to remove the outliers using the feed rate signal as a reference. This is the approach implemented by the developed DENSE program (presented in Chapter 4), using Chauvenet's Criterion to eliminate the rapid traverse movements.



a. X-axis motor load



b. Y-axis motor load

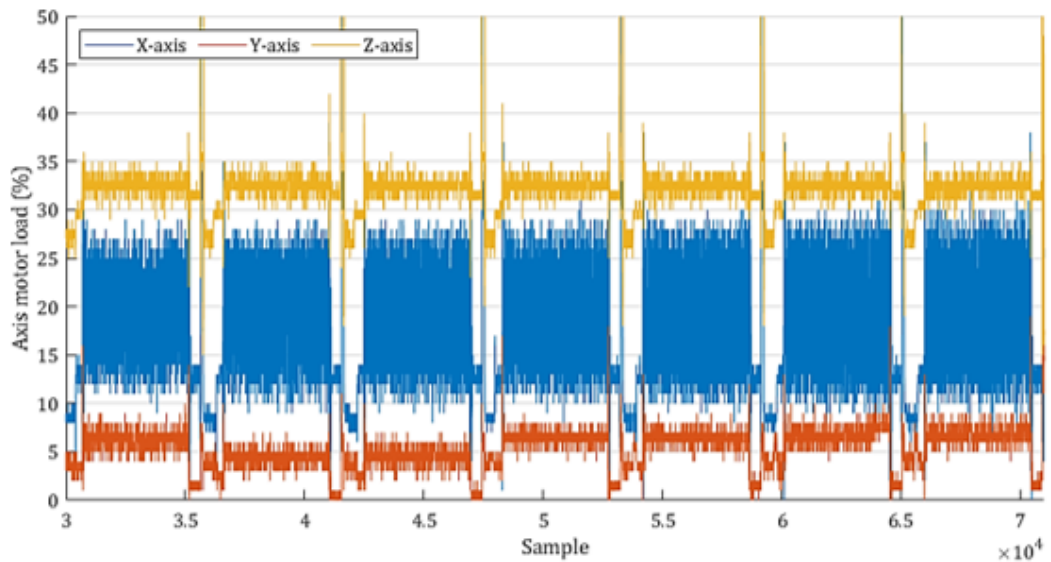


c. Z-axis motor load

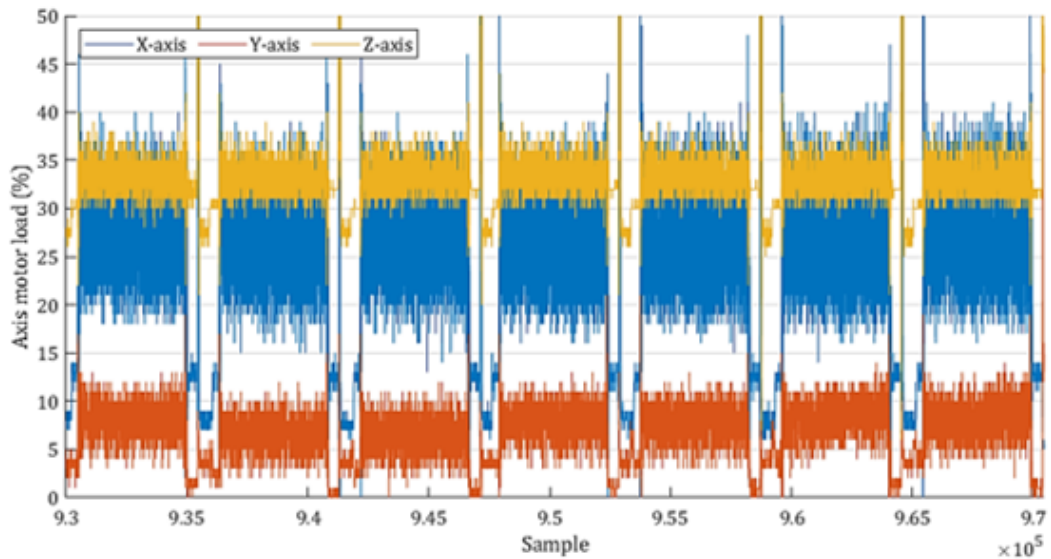
Figure 6.15. Percentage axis motor load signals for SB (including SB003)

Figure 6.15a and Figure 6.15c show a clear distinction between SB003 and the rest of the SB group. SB003 was machined 44% faster. This has resulted in a reduced load range for the X-axis and an increase in the load range for the Z-axis (versus SB004). Although the range increase for the Z-axis is limited to a reduction in the minimum values, rather than an increase in the maximum values. Beyond the differences due to the process, all three axes show the deterioration of the cutting tool through an increase in the maximum values. All three also indicate diverging trends, with the minimum values (neglecting the outliers) decreasing over the length of the process. Figure 6.15b and Figure 6.15c both indicate that the observable changes (at the given resolution) occur towards the end of the process, with negligible changes throughout the signals. This contrasts with the X-axis signal, which noticeably contracts mid-way through the process (annotated as range variation). Figure 6.15b also appears to show a signal pattern reminiscent of the variation observed for the workpiece geometry measurements (Figure 6.6); however, there is no evidence that there is a link between the two sources of variation. The predominant change over the entire process can be compared qualitatively (Figure

6.16) by reducing the plots into the first and last tests, SB004 and SB026, neglecting the test for which the process is different (SB003). Figure 6.16 emphasises the change in each of the axis signals with each covering a wider range of values. The most notable change is for the X-axis with an increase in the average magnitude from between 10% and 30% to between 20% and 40%. Nevertheless, Figure 6.16 also shows that the value within each Slot is challenging to appreciate as other than the holistic changes, the subtle differences between and within each Slot is impossible to ascertain without taking a different approach.



a. X, Y, and Z axis motor load signals for SB004



b. X, Y, and Z axis motor load signals for SB026

Figure 6.16. Percentage axis motor load signals for single test (seven Slots)

### 6.4.1 Axis separation

To show the micro value in each axis load, it is necessary to separate the acquired signals into each individual part. This is necessary to observe how each process, such as the entry/exit of the cutting

tool into the material, is impacted by the tool condition. It is also to remove all non-cutting loads to avoid them affecting the data processing. Figure 6.17 shows the signal components for a single Slot. The entry/exit loads are isolated using a Hampel filter with a window length of 300 samples.

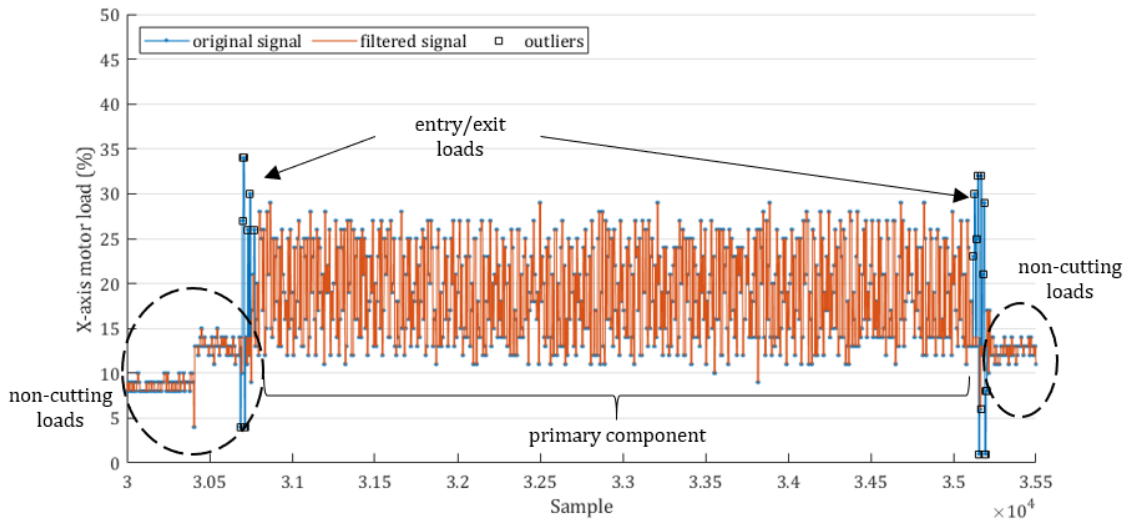


Figure 6.17. Single Slot signal components (SB004-1)

Figure 6.17 shows that the entry into the material and the exit from the material is accompanied by a significant (temporary) increase in the load range. This shows that both the entry and exit are notably different from the rest of the signal. This corroborates the increased effort required from the cutting tool and X-axis in both instances. These signals can be removed using the Hampel filter. They can also be removed by using the MATLAB function `findchangepts()` with the appropriate maximum changes and using the change in the root mean square (RMS) statistic as the threshold criteria. Using the `findchangepts()` function also enables non-cutting loads (idling loads) to be separated from the the primary component of the signal in the same step. The primary component of the signal, corresponding to the cutting process but excluding material entry and exit, is shown in Figure 6.18.

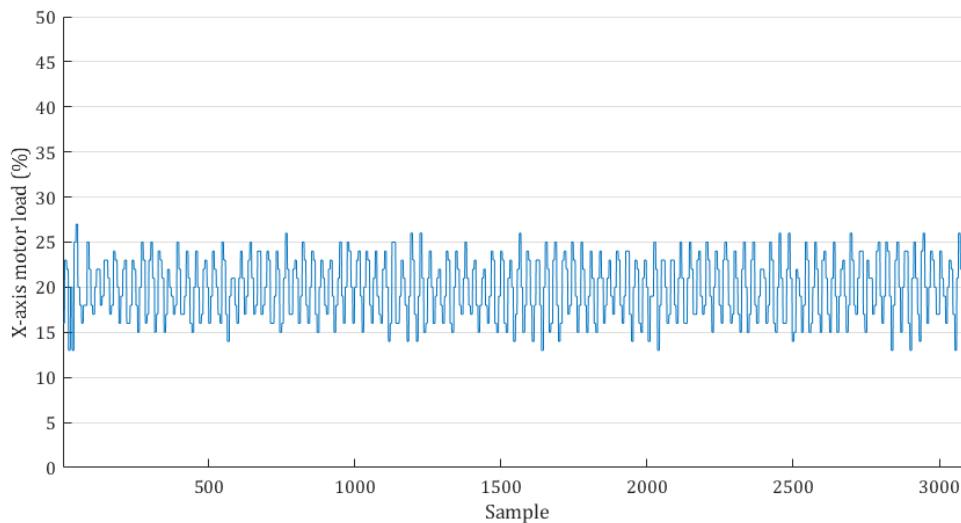


Figure 6.18. Single Slot primary signal component for SB004 (first Slot)

Figure 6.18 shows just the primary component of the first Slot XML. It is noticed that the signal is less complicated than before; however, any information regarding the cutting tool condition is still not clear. It is noted that all Slots may be processed at once, enabling the changepoints to represent start and end points of each Slot. It is also recommended that all three axes are processed using the changepoints derived from the X-axis data. Whilst the Y-axis and Z-axis signals could be processed independently, doing so may increase the uncertainty in those results.

## 6.4.2 Dispersion heat maps

Whilst investigating the Cylinder application in Chapter 5, the frequency components of the SRS and XML signals were considered using frequency-amplitude images. Such plots, employing FFT, have been utilised in other research to differentiate between processes (discussed in Chapter 2). However, it was shown in Chapter 5 that the data acquired in this study was challenging to decipher. This included identifying the differences between new and used cutting tools. This made it challenging to monitor the signal frequencies without high risk of increased false alarms. It was decided that whilst the FFT plots were useful, they did little to explicitly indicate the true changes in the behaviour or health of the cutting tool. Indeed, to properly determine the differences required significant effort. An alternative approach was deemed necessary to help determine the cutting tool health in a less complicated way and with less effort.

The alternative approach taken was to exploit the main limitation of the MTData (the quantised nature), by using the integer-based format to show the internal nature of the signals. By considering the relative recurrence of each signal integer, the approximate nature of the signal for each part may be considered and plotted as an innovative “dispersion surface” or “dispersion heat map”. These are novel plots that have been developed by the author based on the concept of the FFT image plots and the part-to-part signal density profiles considered in Chapter 5. The plots use the signal density of each part as each slice within the image. By stacking the slices the changes over time can be observed, without losing any value from the profiles of each individual part. The full dispersion heat maps and development formulae are available in Appendix E.3.

The dispersion heat maps were generated using Conditional Formatting in Excel. It is noted that the colourmaps used are arbitrary with red and green chosen for their contrast. Green denotes zero occurrences, whilst smaller values are white tending to darker red the greater the value. The Conditional Formatting is applied *per* Slot and white values are herein referred to as outliers. The explicit colour range is not important as the process is meant to illustrate the signal density. Quantifiable data can be found in Appendix E.3. Figure 6.19 shows the dispersion heat map for the XML for all 12mm Slots (SB003 (03) and SB004026 (04-26)).

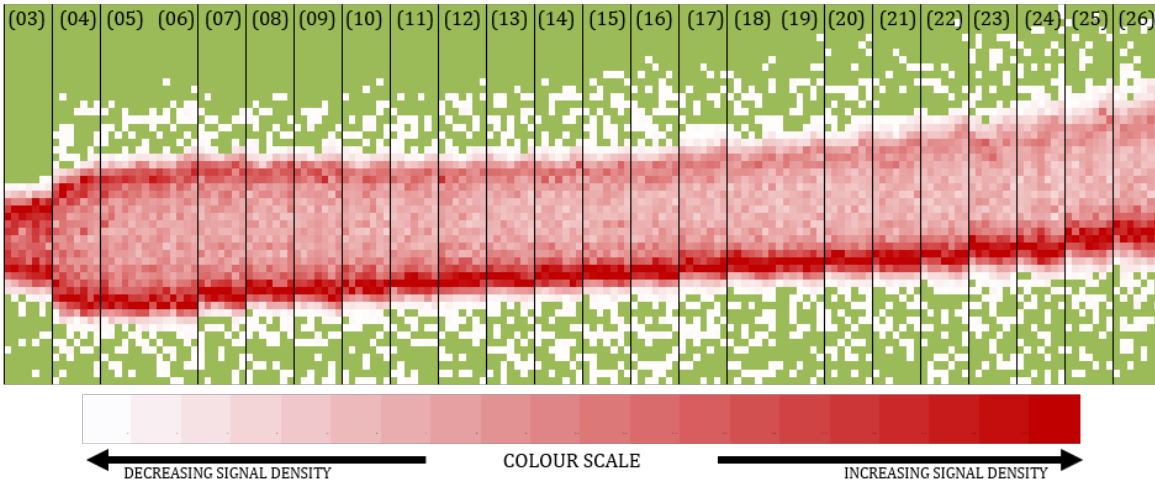
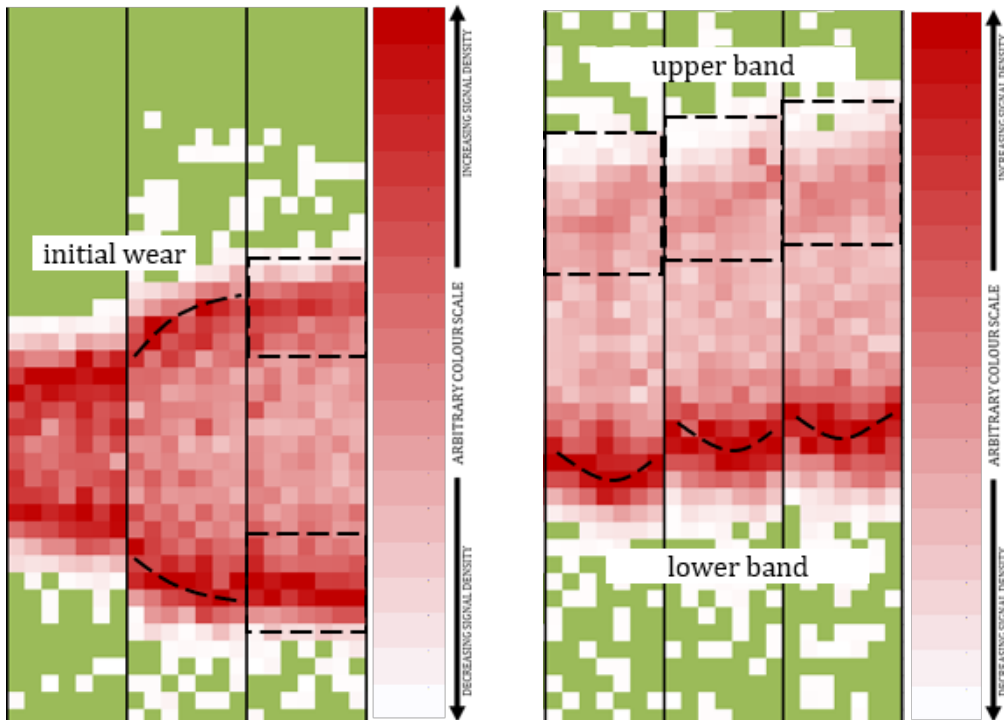


Figure 6.19. XML dispersion heat map for all 12mm Slots

Figure 6.19 considers rows 1-60, each column denotes a single Slot and every seven Slots are separated with a border to indicate each block. Figure 6.19 is valuable because it effectively illustrates the changes in the composition of the XML signal, despite it being relatively complex in the raw form. The general trend in the XML shows that initially the dispersion densities are greater at both outer extremes of the signal; however, as the cutting tool deteriorates the densities at the upper extreme of the signal (upper band) tend to reduce. Figure 6.20 directly compares SB003–SB005, and SB024–SB026 to illustrate the differences between new and worn cutting tools.



a. SB003, SB004, and SB005

b. SB024, SB025, and SB026

Figure 6.20. XML dispersion heat maps for first and last Slots

SB003 is notably different from the rest of the process, with a smaller range and a higher density. Due to this density the internal variation is challenging to determine. SB004 shows evidence of the initial wear phase with an initial rapid increase in the signal range (ignoring outliers) that is not replicated for any subsequent test. The overall magnitude shift in the signal is also more apparent by putting the start and end of the process side-by-side. The change shows that the deterioration of the cutting tool increases the required effort. Within each test there is a variation in load from Slot to Slot. The loads observed for the outer Slots are higher than for those in the middle of the workpiece. This implies that the cutting tool had to work harder at the edges of the workpiece than in the middle. Geometry measurements provided in Section 6.2 indicated that the outer Slots were not as wide as the middle Slots, most likely due to warping of the steel block. The geometrical variation may be effecting the axis loads; however this would be challenging to prove. The variation in the axis loads may also be associated with some unknown variation which occurred in-process, hence the indications in the XML signal, or possibly because the clamping force from the vice is affecting the cutting process. The Slot-to-Slot variation is primarily noticeable in the lower band and appears to be more pronounced when the cutting tool is more worn. On the other hand, the density of the upper band notably decreases as the cutting tool wears. The suggestion is that this band is expanding, rather than an equal/simultaneous expansion of the entire signal. The central band is assumed (relatively) constant, albeit with a shift towards higher loads as the cutting tool deteriorates. Figure 6.21 considers a dispersion heat map for the YML signal for all 12mm Slots (SB003 and SB004026).

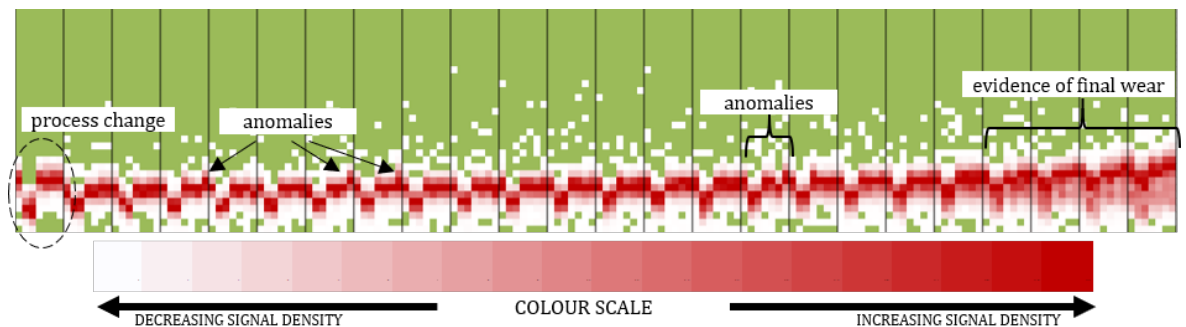


Figure 6.21. YML dispersion heat map for all 12mm Slots

Figure 6.21 shows that when the cutting tool is healthy the signal is uniform with few differences between Slots on a workpiece. However, it is noted that the second and third Slots are different from the rest demonstrating a lower mean average load. This is consistent throughout the process, irrespective of the condition of the cutting tool. When the cutting tool is worn the second and third Slots are less distinct from the others but still different. This could be due to different conditions occurring between the Slots across the test piece. Alternatively, it could be a consistent error caused during the automatic separation of the data into individual components. Although, it is noted that there appear to be no similar inconsistencies for the other axes, despite the same processing. It is noted that the YML signal does not show the first wear phase but does show the final wear phase. SB003 is distinguishable from the rest of the tests with a higher average load. However, the second and third Slots are not different to the equivalent Slots in later tests. It is noted that process anomalies

are more easily distinguishable from the signal than for the XML signal. This suggests that the YML is more valuable for determining process anomalies (showing damage) than for verifying the general deterioration of the cutting tool. Figure 6.22 gives the dispersion heat map for the ZML signal for all 12mm Slots (SB003 and SB004026).

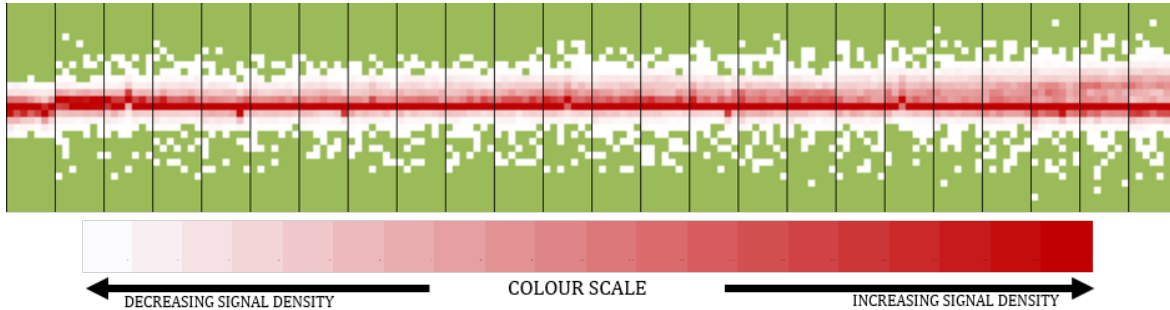


Figure 6.22. ZML dispersion heat map for all 12mm Slots

Figure 6.22 shows that there is a dominant ZML magnitude of 32% (marked by a dashed line). This is due to the lack of cutting along the Z-axis, hence the load stays consistent. It is observed that as the cutting tool becomes more worn the plot expands to encompass higher loads (above the dominant magnitude) and also expands to encompass lower loads (below the dominant magnitude). This is due to the cutting tool deteriorating but it is appreciated that the changes are slight. Additionally, there does not appear to be any notable Slot-to-Slot patterns or variation. SB003 can be distinguished by the reduced loads versus the later Slots. This contrasts with the higher loads seen in the YML signal. This may be due to the kinematics of the CNC movement, where the faster movement speed requires less effort (from the Z-axis motor) to maintain the (Z) position. The nature of the difference would require further investigation. As it is unlikely to be attributable to the wear of the cutting tool it is not investigated further. It is noted that the ZML signal may hold higher value for more involved processes that require machine movements in more than one axis.

## 6.5 Application of MTData: Spindle rotation

It was determined during the development of the Cylinder application that the rotational speed of the cutting spindle is a challenging signal to investigate as it is controlled by the machine tool. Any variation in the SRS will be slight and will be eliminated rapidly in support of consistent cutting behaviour. It was also noted in Chapter 5 that the use of FFT plots did not help with identifying changes in the SRS signal as the cutting tool deteriorated. This was predominantly because the process was (relatively) complex, but also because the influence from the machine tool controller, and the source of each frequency, was hard to determine. As the dispersion heat maps apply to all MTData sets, not just the axis loads, they may be valuable in determining the implicit value in the SRS. Figure 6.23 gives the dispersion heat map for the SRS signal for all Slots (SB003 and SB004026). Figure 6.23, like the axis dispersion heat maps, shows that SB003 is clearly different from SB004026. The magnitude is not comparable as the cutting speeds have been plotted against different axes; however, the scale is consistent and illustrates that the range is greater for SB003. This suggests

that the machine tool controller had to work harder to maintain the required SRS value at the higher speed. The general trend indicates a slight reduction in the signal range during the gradual wear

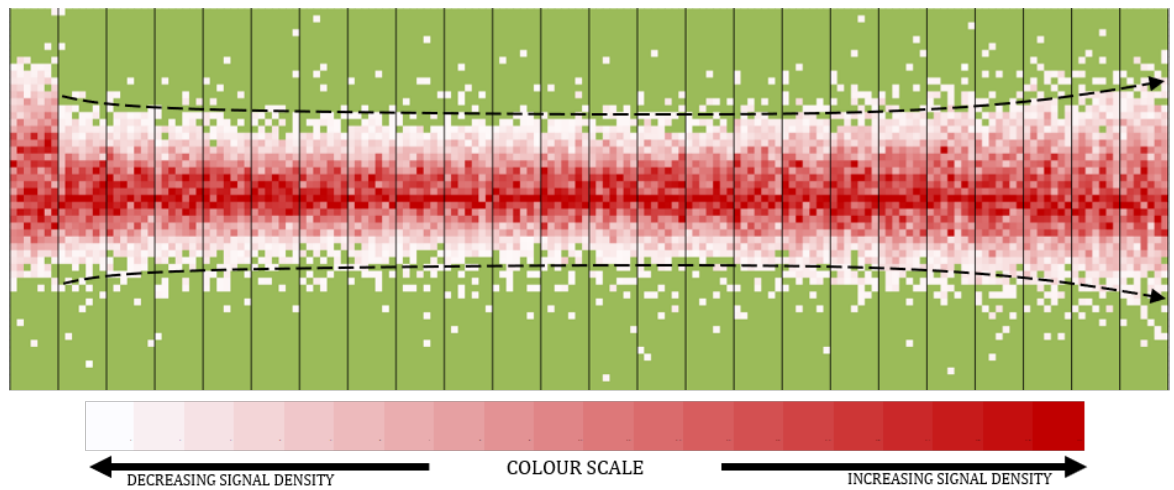
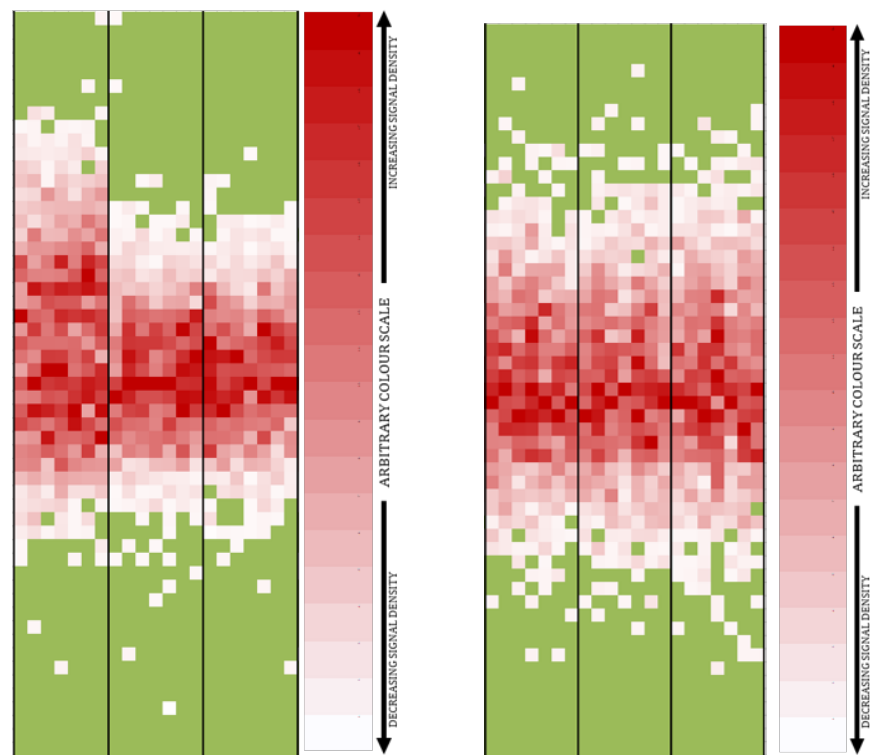


Figure 6.23. SRS dispersion heat map for all 12mm Slots

phase with a wider range for the initial wear and the final wear. The final wear phase is noticeable and therefore straightforward to determine; however, it is appreciated that the initial wear phase and the contraction indicating the general wear phase are both subtle. It is noted that the densities are higher in the central band of the signal in contrast to the observations for the XML signal. Figure 6.24 is provided to directly compare the first and last tests (SB003–SB005, and SB024–SB026).



a. SB003, SB004, and SB005

b. SB024, SB025, and SB026

Figure 6.24. SRS dispersion heat maps for first and last Slots

Figure 6.24 shows that the differences between the beginning and the end of the process are not as extensive as was noted for the XML signal. The signal average has not shifted, nor has the general distribution of the signal changed significantly. However, this is to be expected since the SRS is maintained by the machine tool controller, whereas the XML is not. Nevertheless, the signal range has increased, indicating a greater amount of fluctuation within the signal. This corresponds to an increase in the effort required to maintain the SRS magnitude and can be correlated to the deterioration of the cutting tool. It is noted that Slot-to-Slot variation is difficult to distinguish due to the MTData resolution. It is considered that the SRS has value when evaluated as a dispersion heat map; however, it is still maintained that changes are slight, and may be inferred from other signals. Nevertheless, the SRS is still valuable for supporting the decisions based on other process signals.

## 6.6 Challenges and next steps

The Slotting application enabled the axis loads to be evaluated in depth and allowed the condition of the cutting tool to be the dominating factor in the signal variation. It was noted that, like the Cylinder application, the PEC indicated the general deterioration of the cutting tool, albeit with more noticeable steps in the signal. The steps were a result of the quantised nature of the data and were more pronounced simply because there were fewer observed changes and less overall noise in the signal. The quantised nature of the data proved to be slightly unstable for the cubic trend-line used. Employing alternative trend-lines (as discussed) may solve this problem; although, a more sensible approach would be to improve the resolution of the data where possible.

The quantised nature of the signal produced the requirement for the development of the dispersion heat maps. These heat maps enabled an increased awareness of the internal composition of each axis signal and of the SRS. This enabled the general condition of the cutting process to be inferred, as well as the possible deterioration of the cutting tool and potential process anomalies. The dispersion heat maps effectively established the value in each of the axis loads and also indicated the implicit value in the SRS for indicating the cutting tool condition, despite the signal being (for the most part) determined by the machine tool controller.

It is intended that the methods created will be beneficial for the interpretation of future process signals. Whilst not all the process variation was attributable to the wear on the cutting tool, the majority was, and no conflicts arose regarding the health of the wider machine tool. However, it is appreciated that they were developed based on an uncomplicated process, with a single cutting tool, and with an aggressive cutting regime designed to exaggerate the wear on the cutting tool. Future applications should attempt to progress towards commercially viable processes to further illustrate process efficacy.

## 7 | Con-Rod Investigation

Both previous applications, the Cylinders and the Slots, were designed to aggressively deteriorate the cutting tools used. This resulted in the general wear curve being the dominant pattern in the generated process data. This enabled the deterioration of the cutting tools to be easily identified and the EOL to be predicted. However, commercial processes may not be as straightforward and the general wear trends may not be as obvious. This Chapter attempts to bridge the gap between laboratory-based studies and industrial deployment. Methods have already been developed that enable the condition of a cutting tool to be established based on health attributes. The main aim of the Con-Rod application (pictured in Figure 7.1) is to take a step towards commercial style manufacturing processes. In other words, a cutting process that is more realistic of one enacted industrially, one that uses multiple cutting tools, and one that does not intentionally wear the cutting tools in an exaggerated fashion.



Figure 7.1. Photograph of the Con-Rod application

The Con-Rods were based upon an ongoing laboratory-based exercise developed with the industrial sponsor of this research to demonstrate their metrology equipment. This presented the opportunity to utilise them as a laboratory-based case study. The author also deemed them to be a good fit to the required narrative as they were manufactured repeatedly, consistently, and used the same range of cutting tools each time. This allowed the condition of those cutting tools to be individually evaluated. The Con-Rods were machined from aluminium. This decision brought with it an anticipated reduction in cutting loads and an associated decrease in anticipated tool wear rates as compared to the Cylinders and Slots. Both were deemed to be acceptable as the main aim of this element of work was to provide evidence that the approach could be further engineered before being deployed into more aggressive and realistic environments. The Con-Rods were still a step away from true industry-style manufacturing in terms of the metal removal rates and volume of parts made. Additionally, the cutting forces are carefully controlled as the underlying intention is to avoid damaging the machine tool and to reduce wear and tear. This means that the cutting parameters are deliberately much lower than would be considered for a realistic process. Nevertheless, this still represented a significant step towards

commercial style manufacturing. This Chapter seeks to understand the current limitations of the approaches developed in previous chapters. This meant identifying what is possible in the current state, what is necessary to improve the approaches, and what is required to enable engineers to take the ideas generated herein to develop robust systems capable of improving the economy of manufacturing processes and of reducing process waste.

A sample group of 42 Con-Rods will be appraised herein. The cutting tools used are listed in Table 7.1. It is noted that the cutting tool lengths were acquired using the on-machine (contact) tool setting probe, TSR27R; however, the diameter measurements are the nominal dimensions. It is noted that the first 17 Con-Rods were machined differently to the remaining 26 Con-Rods. This was a consequence of changes in the way the cutting process was programmed. The program changes were to make the process quicker by optimising tool paths and did not relate to any changes in the design of the artefact itself. Although not a specifically intentioned step this is typical of what may happen in an industrial context. When the cutting tools were replaced after machining Con-Rod 17, the process was optimised with R021EM12 being used in place of R020EM16.

Table 7.1. Qualitative information for Con-Rod cutting tools

Name	Type	Length (mm)	Diameter (mm)
R020EM16	Square end mill	134.59	16.00
R021EM12	Square end mill	131.50	12.00
R023EM06	Square end mill	115.74	06.00
R024EM03	Square end mill	112.29	03.00
R025ENP6	Engraving tool	121.95	00.60

## 7.1 Qualitative condition assessment

The intention is still that the measure of cutting tool wear should be determined from the process data, not from the actual cutting tool or manufactured part. For that reason, this Section will only briefly discuss the changes in part quality that may infer the general condition of the cutting tool. This may then form the basis for suggestions drawn in later Sections. Figure 7.2 shows the condition within the larger bore of the Con-Rod. Figure 7.2 shows a similar indication of wear as noted for the Cylinder application. The end-section of the cutting tool is noticeably more deteriorated than the rest of the cutting tool. The cutting tool used (R021EM12) is like those employed for the Cylinder and Slotting applications. If the use of the cutter is similar, it is sensible that the deterioration will follow a similar mechanism. It is noted that the same cutting tool used for the roughing operation is reused for the finishing cut. This should rule out any deflection of the cutting tool causing the imperfection as the load on the cutting tool should be minimal during the finishing cut. It is noted that there is evidence of poor surface quality for the Con-Rod walls and floor.

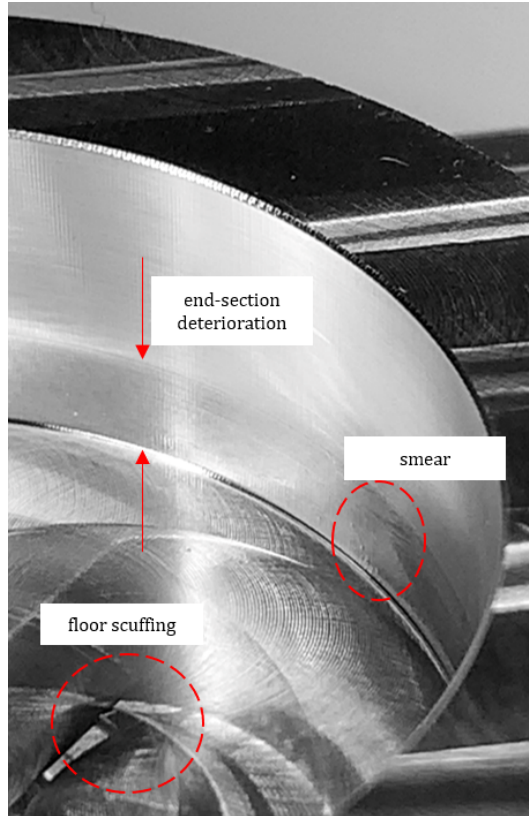


Figure 7.2. Inner-surface condition of the Con-Rod for arbitrary part (unknown cutting tool state)

Figure 7.3 shows the condition on the outer surface of the Con-Rod, showing evidence of scuffing on the exterior. This either indicates a worn peripheral edge of the cutting tool, or swarf causing damage to the surface. It is noted that the coolant is not active (dry cutting) for the exterior pass. This may be the basis for the damage and is an unintentional consequence of considering an application designed for other means. There is also evidence of tool-nose damage, shown by the poor surface quality of the chamfered surfaces. These imperfections present as an opportunity to investigate the effect on process data of suboptimal processes.

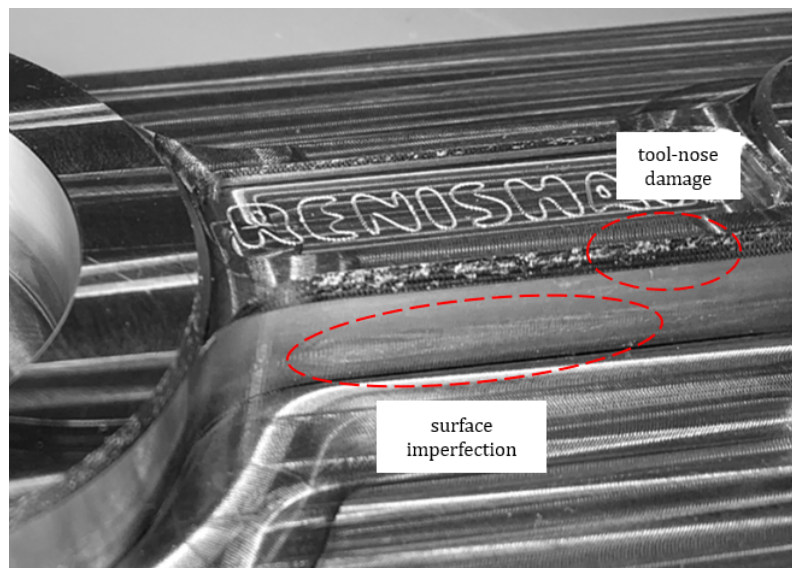


Figure 7.3. Outer-surface condition of the Con-Rod for arbitrary part (unknown cutting tool state)

## 7.2 Quantitative condition assessment

The Con-Rods may be assessed using the CMM in the same way as the Cylinders. Access to the DMIS program written by the author to enact the measurements is provided in Appendix C.1. The two bores are assessed at two different depths to include the difference noted for the end-section of the cutting tool. The diameter measurements were achieved by scanning arcs and are given as CSAM deviations (developed in Chapter 5) to consider the effect of cutting tool wear. Figure 7.4 gives the CSAM measurements for all bar the last two Con-Rods.

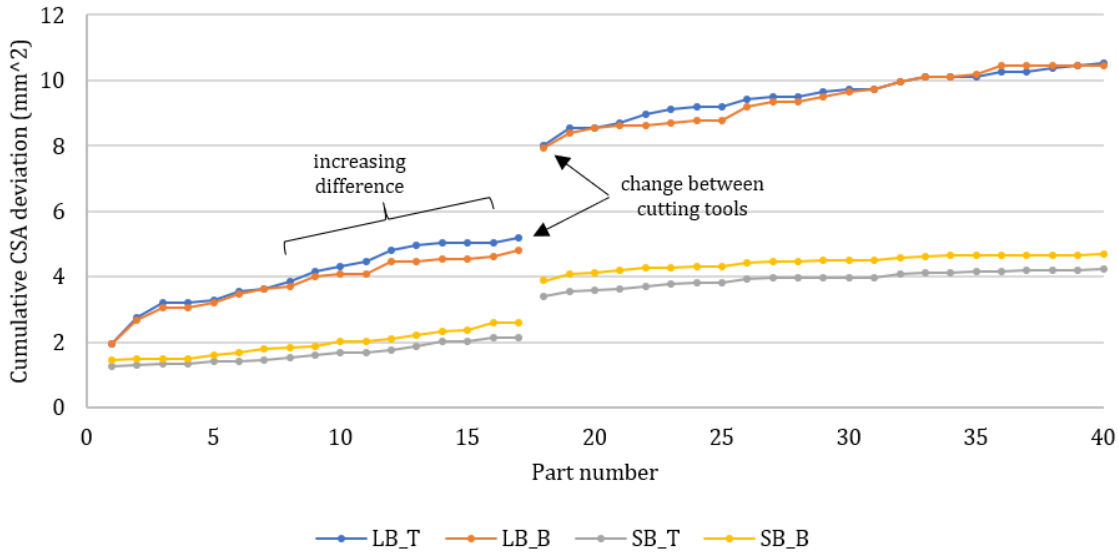


Figure 7.4. Cumulative CSAM deviation for 40 of the manufactured Con-Rods

Figure 7.4 shows the differences between the large bore (LB) and the small bore (SB). It is also shown that there is a significant shift in the values between part 17 and part 18 (where each Con-Rod is one part). This corresponds to the cutting tools being replaced and is due to the new cutting tools being undersize and therefore producing undersize features. This was deliberately not rectified using ICG and remained since the roughing and finishing cutting tools were the same. It is noted that the SB shows a consistent difference between the upper and lower scanned measurements, with the lower measurement (SB\_B) showing a reduced diameter. It is unlikely that this is due to the condition of the cutting tool as the replacements also show the same difference, despite being new.

For the new cutting tools, the LB shows no significant differences between the upper and lower scanned measurements. However, parts 1-17 (worn cutting tools) show an increasing difference, with the upper measurement (LB\_T) showing an increase in the cumulative CSAM (reduced diameter). This suggests that the failure mode is notch wear. It is noted that the LB shows an increased rate of CSAM deviation with a steeper gradient than observed for the SB. It is noted that the circularity did not show any deterioration of the cutting tools with negligible differences between parts 1-17 (worn cutting tools) and parts 18-40 (new cutting tools). The full results can be found in Appendix E.4.

The surface finish, on the other hand, did show differences between the worn cutting tools and the new cutting tools. Guided by the observations presented in Section 7.1 three surfaces were assessed:

- Within the large bore - perpendicular to the cutting direction due to difficulty accessing the surface
- On the top surface of the large bore (Z-plane)
- On the exterior wall of the Con-Rod shaft – where surface imperfections were noted in Section 7.1.

Figure 7.5 gives the three RzNOV trends (introduced in Chapter 5). It is noted that the RzNOV is presented as it was deemed the best at describing the changing condition. The results for the other surface finish attributes can be found in the electronic Appendix. Figure 7.5 indicates that each surface

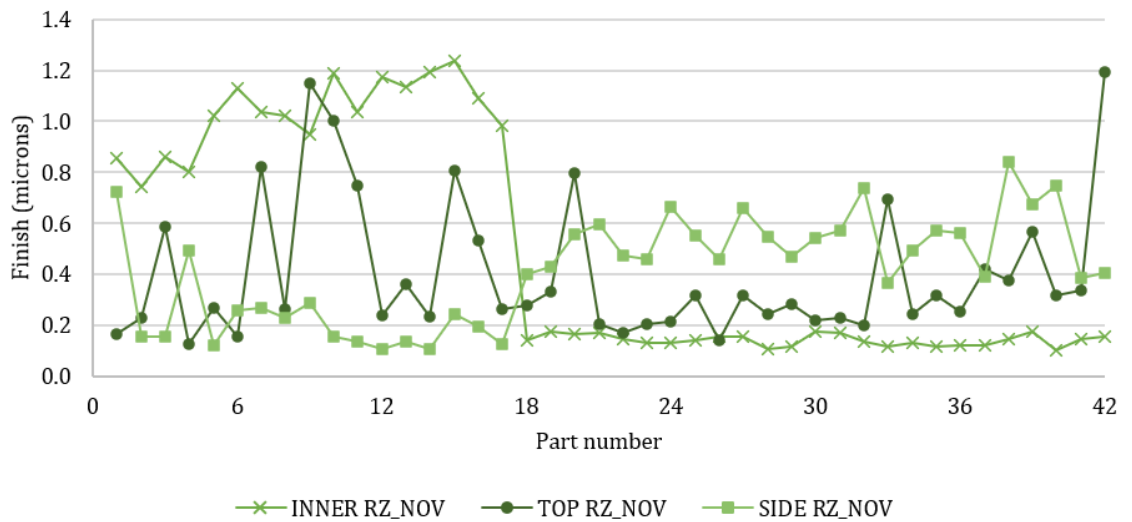


Figure 7.5. RzNOV surface finish measurements for the inner, top, and side of all 42 Con-Rods

provides different information regarding the process. The inner surface shows an increasing (overall) roughness for the worn cutting tool (1-17) followed by a step improvement in the finish for the new cutting tool (18-42). This is sensible since the worn cutting tools were replaced as they were at their EOL (according to the machine tool operator) and therefore should be rapidly deteriorating. The new cutting tools (replacements) should give a better surface finish, despite being undersize. The top surface is not as distinct in the difference shown between the worn cutting tools and the new cutting tools. The worn cutting tools have a higher mean, and a (two times) greater standard deviation than the new cutting tools. The new cutting tools also show a slight increasing trend in the surface finish. This may show the initial wear phase. The side surface shows opposing information to the inner and top surfaces. It is noted that the surface finish is good for the worn cutting tools (1-17), and worse for the new cutting tools (18-42). This is likely to be due to the process, as the coolant is switched off during the cutting for the exterior surface.

It is also possible to evaluate the full scanned information by extracting the point data from the DAT file. Figure 7.6 gives an example Con-Rod with the diameter measurements colour-coded to signify their magnitude difference from a best-fit diameter generated from the scan measurements. The author wrote a program to enact this, ensuring that alignment data is removed (Appendix A.4). Figure 7.6 is supplied to show the potential value of the scanning data. This could be used to evaluate the Con-Rod

form, although the variation in bore dimensions should be kept separate as the magnitude difference will otherwise obscure the point-to-point variation. Notwithstanding, evaluating the form in this way gives more information than is possible with just the diameter or circularity measurements. This may allow more insight into the reasons for a specific diameter and/or circularity value. It may also enable the differences in form due to different cutting tools to be established.

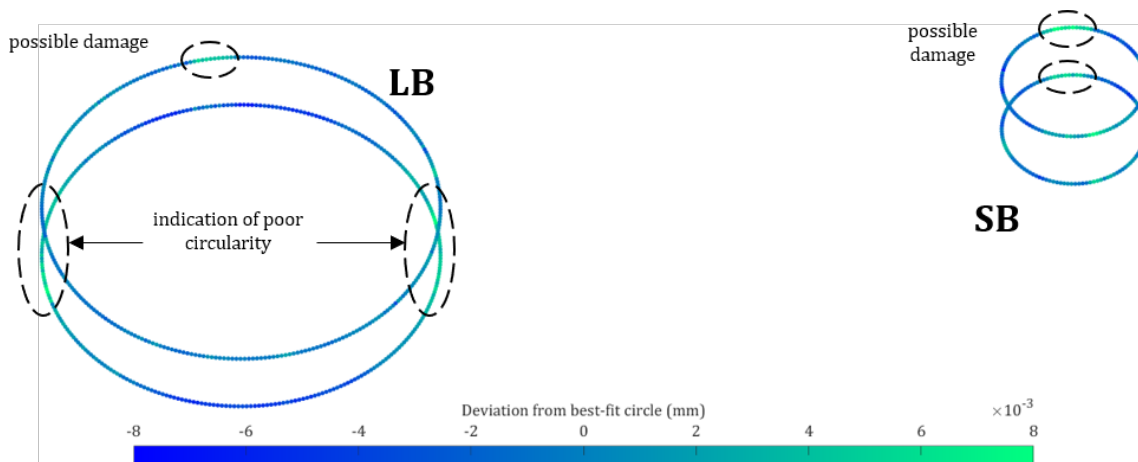
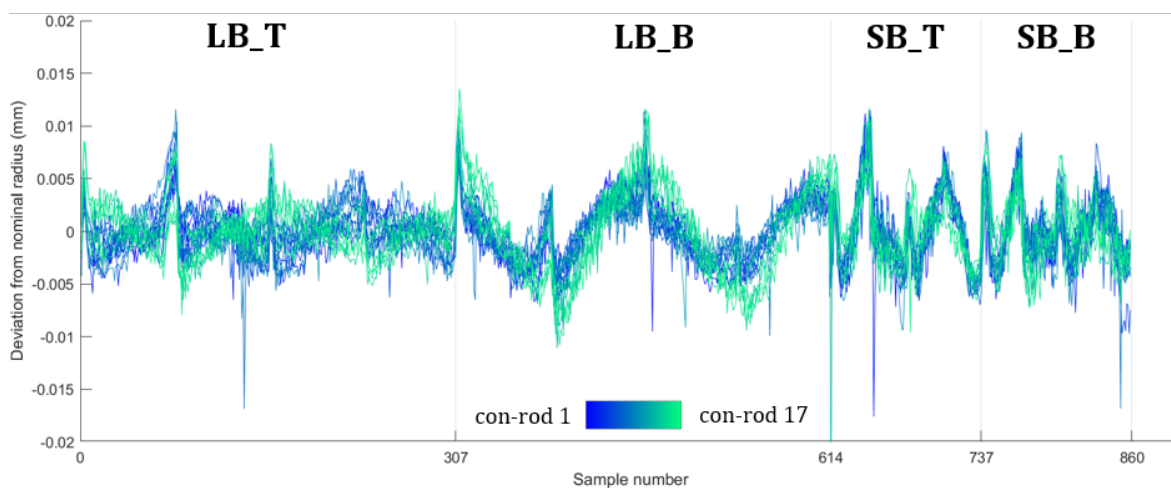
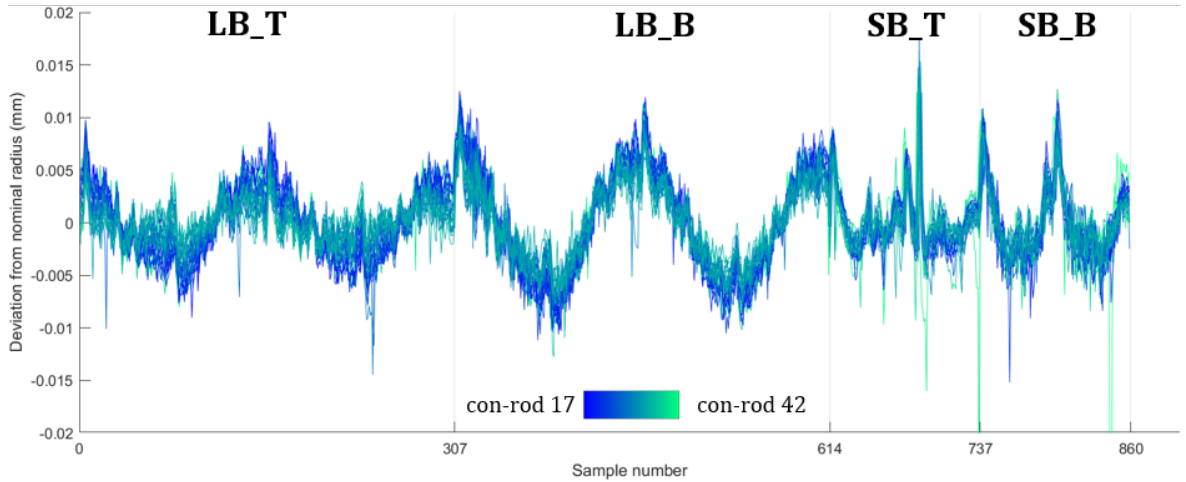


Figure 7.6. Scanned measurements for arbitrary Con-Rod indicating point-to-point variation

Figure 7.7 compares the form variation for the worn cutting tools and the new cutting tools. This is a 2D version of the information presented in Figure 7.6. It is provided as a line plot to enable an easier comparison between multiple parts, with the X-axis tick labels given to separate each scanned arc. Figure 7.7 shows that for the worn cutting tools there is higher point-to-point variation than is observed for the new cutting tools; however, there is a higher occurrence of extreme values (especially for SB.T and SB.B) for the new cutting tools. The general variation for the worn cutting tools shows less oscillation than is observed for the new cutting tools (especially for LB.T). These oscillations may be caused by dynamic effects from the machining process. The nature and exact cause of these effects is not known; however, they are observed when different programs are used to generate complex features such as circles (or bores). This is related to the algorithms the CNC employs to determine



a. Form variation for worn cutting tools



b. Form variation for new cutting tools

Figure 7.7. Point-to-point form variation measured from best-fit radius

the axis movements necessary to generate such features. The older Con-Rods used Mazatrol for the bores and were more circular, but the newer Con-Rods used PowerMill and were not so circular. The effect of the oscillations is further illustrated in Figure 7.8.

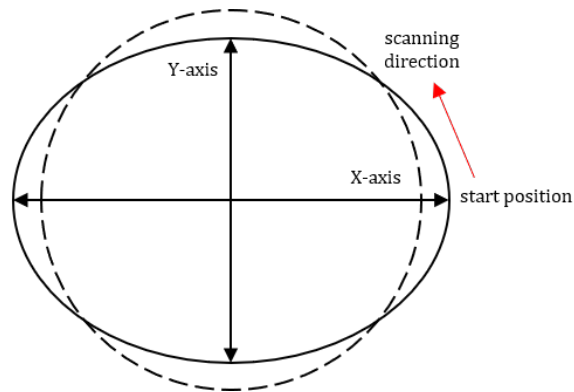


Figure 7.8. Exaggerated geometry of the Con-Rod large bore

It is noted that being able to identify minor variation is valuable; however, it must not be confused with surface damage. It is not possible to determine the form of features not scanned. This is an issue with only scanning key features, which was a deliberate approach taken to reduce the measurement time. It would not be commercially feasible to entirely scan a part using tactile measurement techniques. Therefore, whilst the scanned measurements are valuable, the possibilities are limited by the requirement for post-processing and the time required to measure enough of the part to determine the form of the entire part.

### 7.3 Application of MTData: Axis position data

It has been indicated that the scanned data for the Con-Rods is decidedly incomplete as only the dimensions of each bore are measured using the CMM. This means that to generate the entire process (visually) would require significant extrapolation from the available information. It is also the case that the specific cutting tool responsible for the measurements is not known without further knowledge

of the process. It is therefore considered that to generate a 3D model of the process, the position data generated by the machine tool may be appropriate.

A subprogram was written by the author within the DENSE program (included in Appendix A.3) to generate 3D process models by extracting the position data output from each of the axis motors and plotting these using the MATLAB plot3() function. At the time of writing such plots have never been considered before, with similar information presented using 2D plots or modelled prior to a process using the programmed tool-path information rather than process generated data. Those plots are often to prove a process is feasible, rather than to demonstrate the occurring process. It is noted that the DENSE program located the Con-Rod within the machine tool build volume thus removing the majority of the movements not related to the cutting process. The DENSE process was explained in Chapter 4. Figure 7.9 shows a 3D model generated in-process using the axis position data.

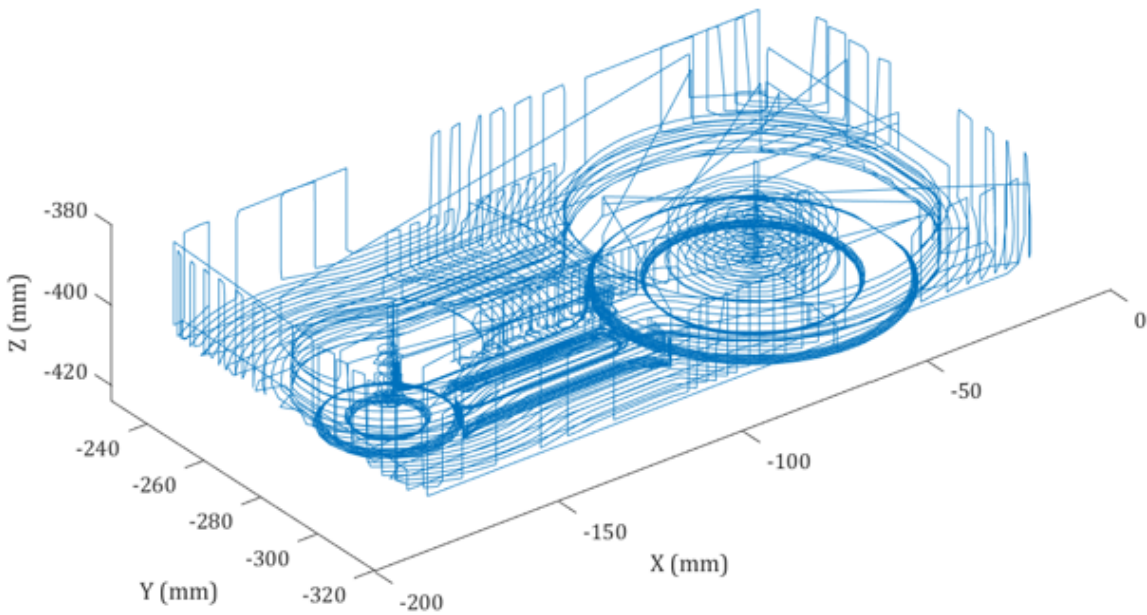


Figure 7.9. 3D process plot using axis position data (Con-Rod #2)

Figure 7.9 shows that the general Con-Rod form may be observed using the machine movements. It is illustrated that the in-process generated geometry has the advantage of showing the entire process, rather than just the measured features and thus enables complete process visualisation. However, it must be reiterated that the axis position data is limited as the values relate to the spindle and do not account for the length or diameter of the cutting tools used. This also means that the model dimensions are not relevant unless updated using information acquired using ICG techniques. The specific dimensions of each cutting tool must be provided separately. This is enabled through the definition file and applied using the DENSE program.

Figure 7.10 gives the same example Con-Rod with each cutting tool defined. Figure 7.10 shows that the Con-Rod outline is more noticeable within the plot when each cutting tool is separately considered. It is also noted that the cutting tool responsible for each feature may be isolated. This allows any damage to a particular surface to be apportioned to the cutting tool responsible. This is valuable post-process as it significantly improves the traceability of the cutting process. If this process visualisation

is also combined with ICG data, this could enable an in-process assessment of the process health.

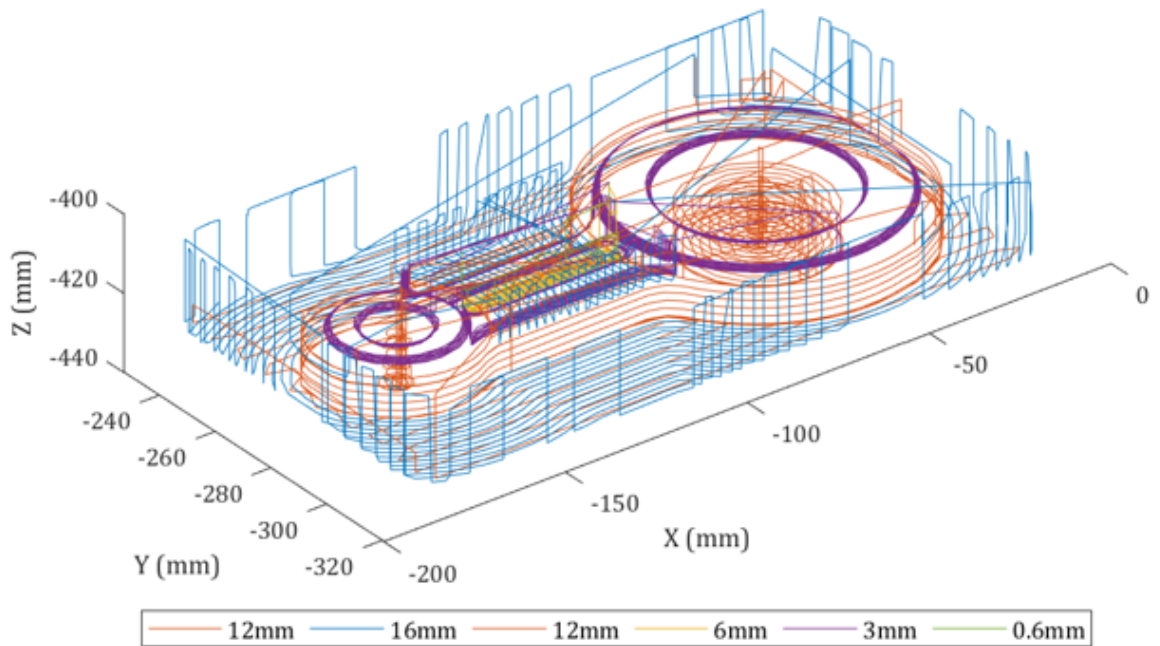
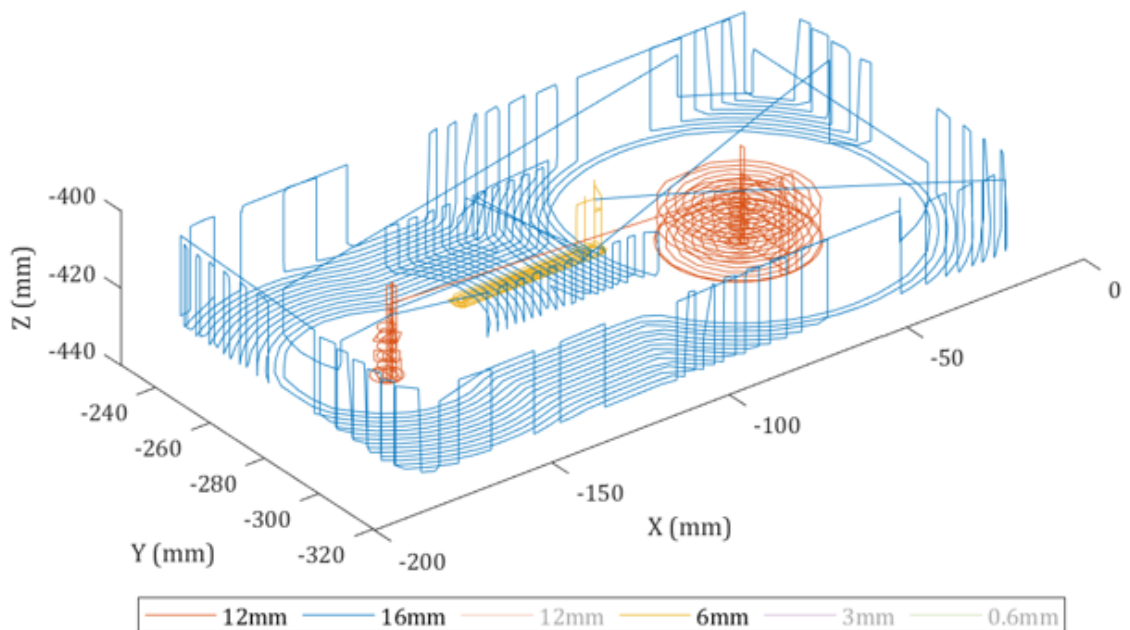
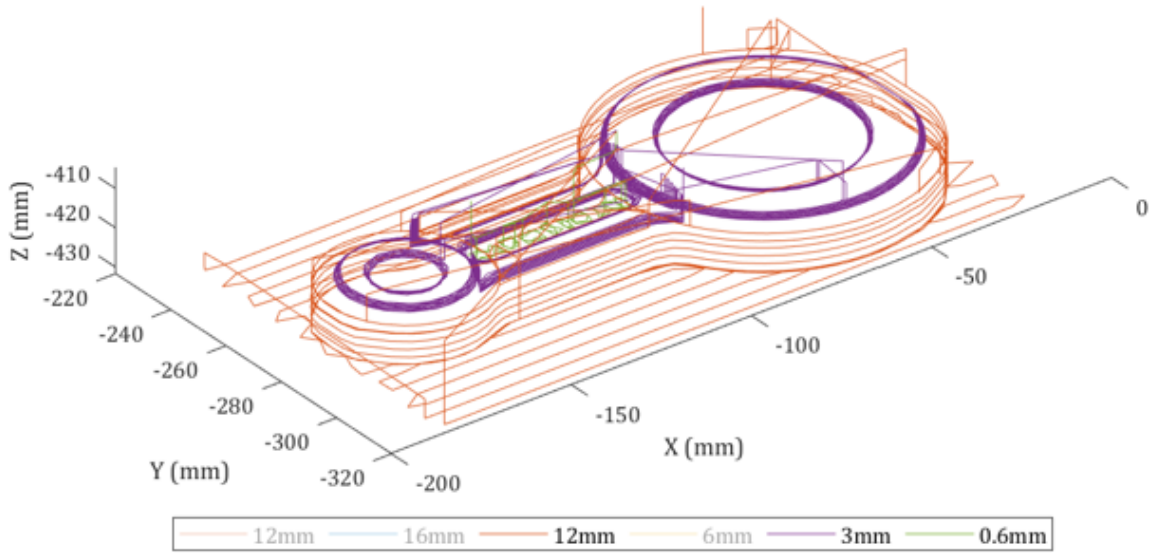


Figure 7.10. 3D process plot using axis position data – defined cutting tools (Con-Rod #2)

Separating the cutting tools also enables the separation of processes. This is critical as different actions will inevitably come with different process parameters and therefore result in different process conditions. For example, roughing cuts will have a higher average load than finishing cuts, not because the cutting tools are more worn but because they are removing a greater volume of material per cut. Separating fundamentally different processes will thus reduce any conflict between processes and prevent contrasting results. On such a basis, the Con-Rod application can be separated into roughing cuts and finishing cuts. The two processes are given in Figure 7.11.



a. Roughing cuts for example Con-Rod



b. Finishing cuts for example Con-Rod

Figure 7.11. 3D process plot separating by process - roughing and finishing (Con-Rod #2)

Figure 7.11 shows that the separation of the different processes simplifies each plot by reducing the included information. It is noted that R021EM12 (12mm) is used during both roughing and finishing processes and is therefore separated into two instances (as normally a different cutting tool would be employed for each process). Each cutting tool is identified by the nominal effective diameter. Further simplification may be achieved by further separation of the process into different cutting actions. For example, separation of slotting, pocket milling, face milling, etc. Although, if multiple cutting actions are performed per cutting tool it may be challenging to separate each without additional process knowledge. It must also be appreciated that process changes may also add to this challenge. Figure 7.12 gives an example Con-Rod for which the cutting process has been updated, making it harder to separate the Con-Rod process into manageable sub-processes without additional data processing. Figure 7.12 shows that combining stages in the machining of the Con-Rod, and using the

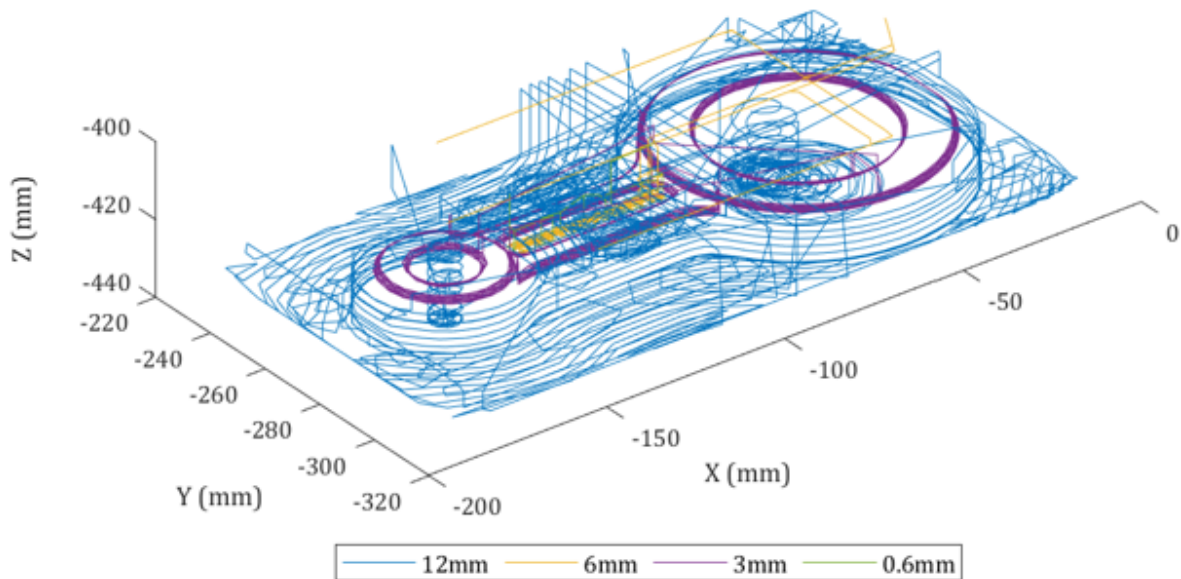
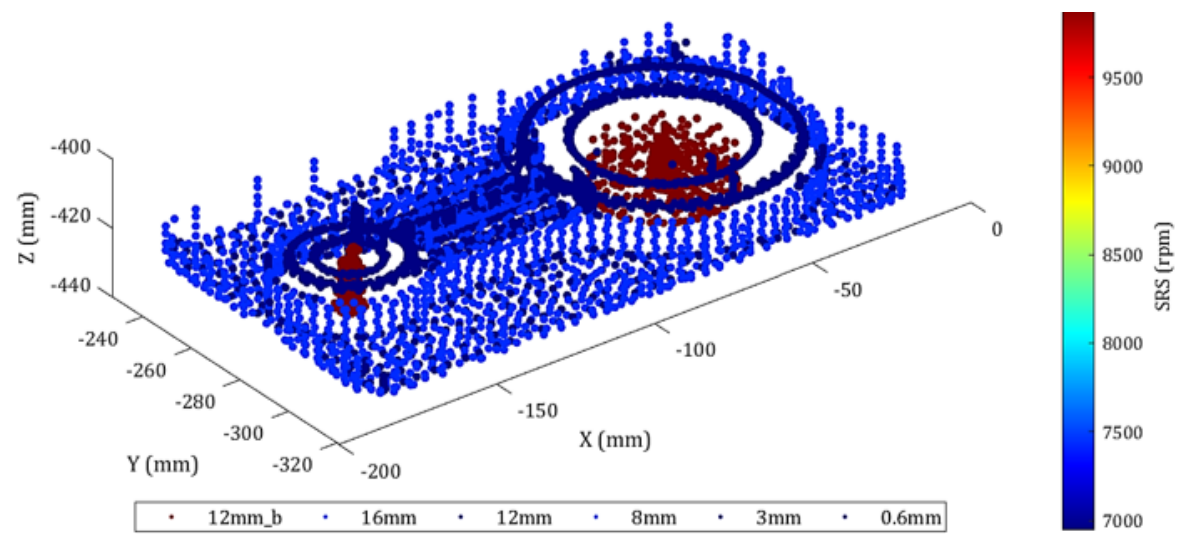
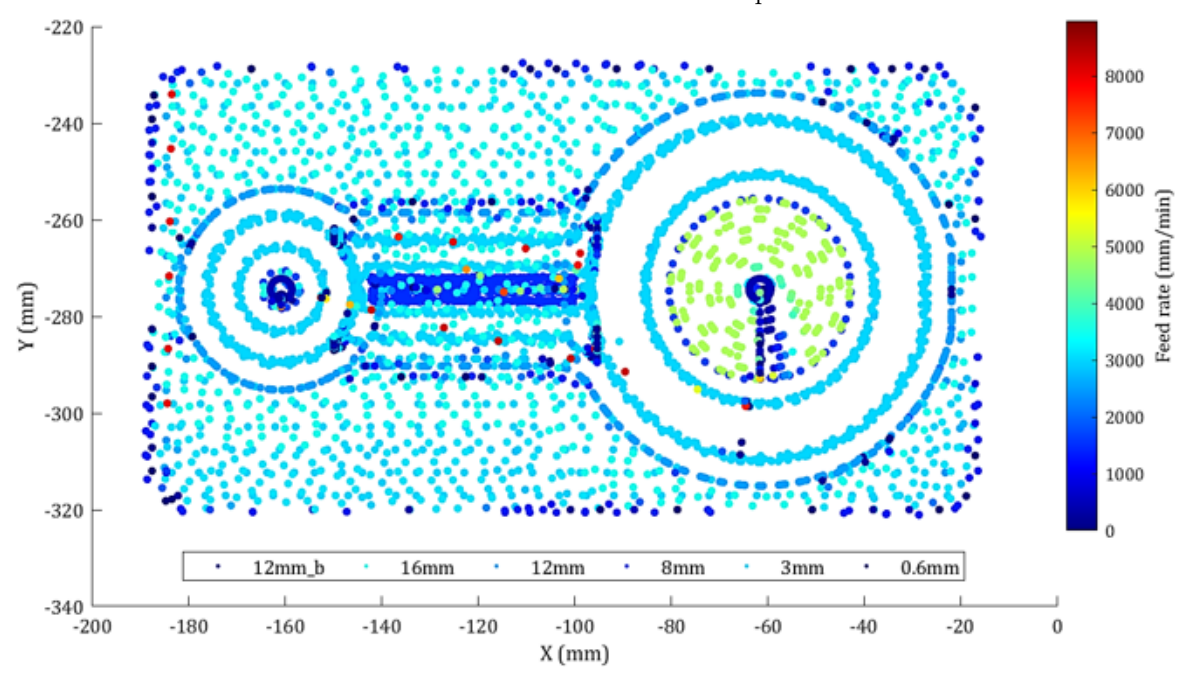


Figure 7.12. 3D process plot for optimised cutting process (Con-Rod #26)

same cutting tool for multiple processes, results in fewer components in the generated MTData. This makes it challenging to separate processes; however, this limitation just means that the results will be more complicated. Any evaluation of the condition of the cutting tools should not be affected. Further to the separation of each cutting tool and each process, the MTData may also be deployed (complementary to any ICG data) to indicate the instantaneous condition of the cutting tool. This was incorporated into the DENSE subprogram identified at the beginning of this Section and built on the value in modelling the process using generated data. The MTData signals were applied to the colour axis (CAXIS) of each plot by converting to the scatter3() MATLAB function. Whilst perhaps relatively straightforward, such an approach has not been achieved before. Figure 7.13 shows the first Con-Rod machined using worn cutting tools (part 1).



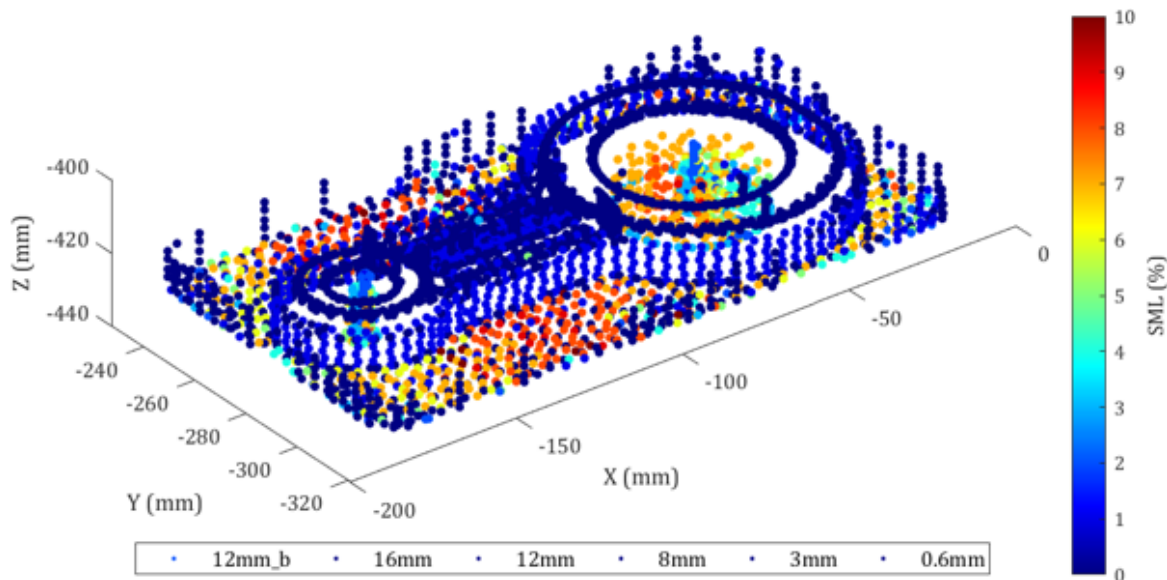
a. Isometric view of rotational speed



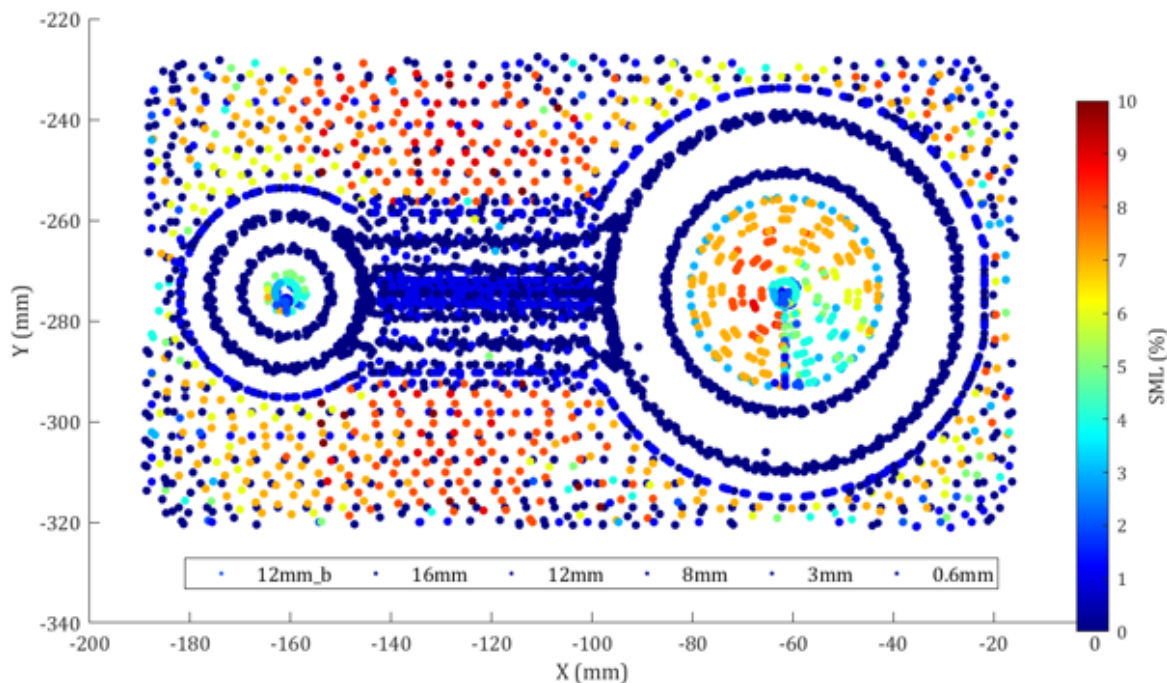
b. Top view of feed rate

Figure 7.13. 3D process plots for rotational speed and feed rate for Con-Rod #15 (all cutting tools)

The rotational speed and the feed rate shown on the CAXIS. Figure 7.13 shows that each cutting tool should be considered separately to achieve the most value from the 3D plots. The SRS does not show much detail, besides each cutting tool being utilised at different speeds. This is also the case for the feed rate; although, this plot does show a few anomalies. These anomalies correspond to rapid traverse movements that were missed by the CC filter (Chapter 4). Figure 7.14 shows the 3D plots with the instantaneous spindle load (raw %) applied to the CAXIS.



a. Isometric view for instantaneous SML

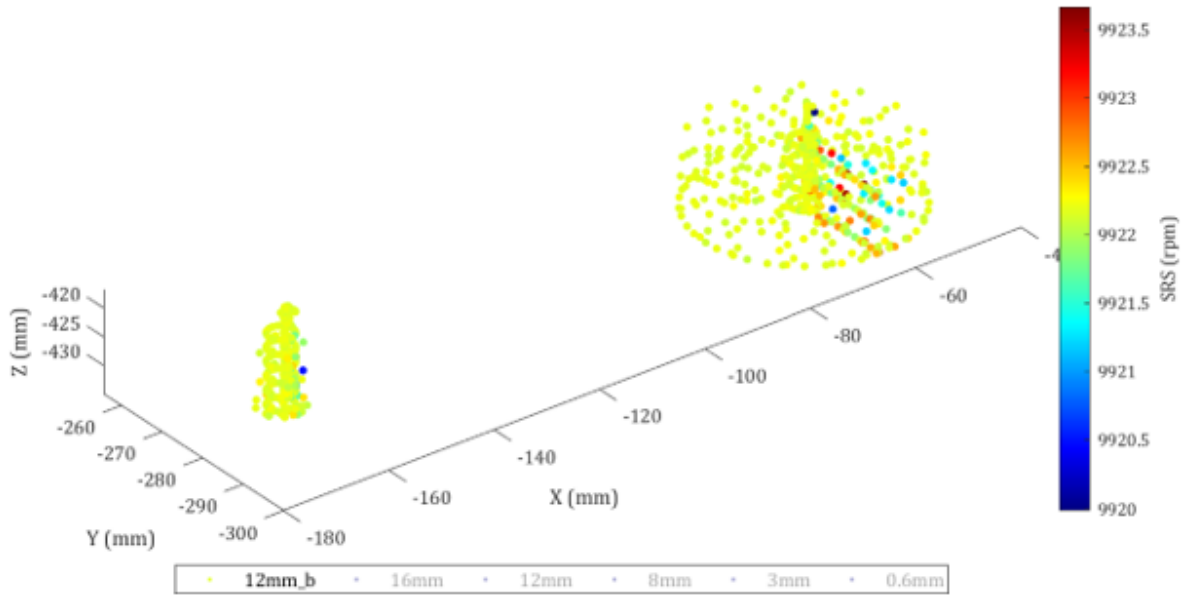


b. Top view for instantaneous SML

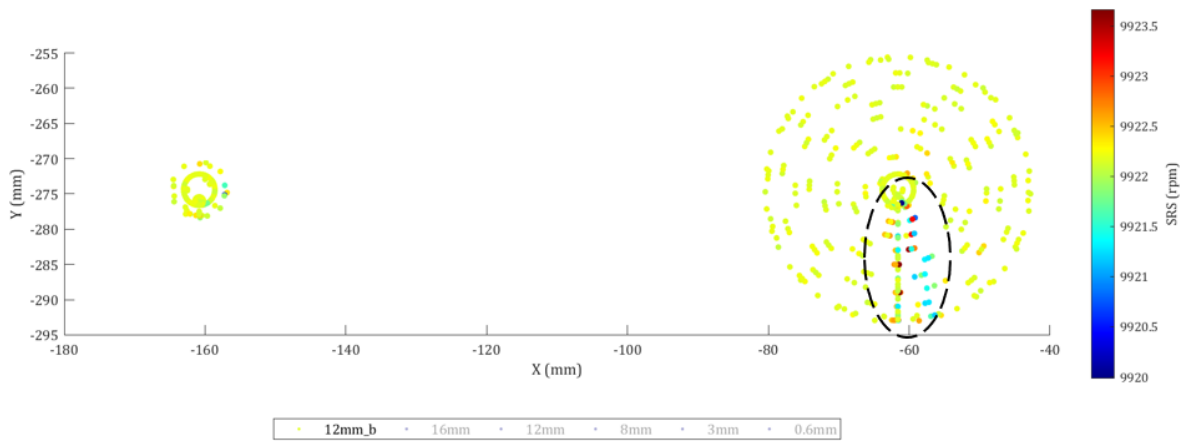
Figure 7.14. 3D process plots showing instantaneous SML for Con-Rod #15 (all cutting tools)

Figure 7.14 shows that the instantaneous SML is not as affected by considering all cutting tools at once. However, the plots would benefit from separating the roughing and finishing cuts to identify

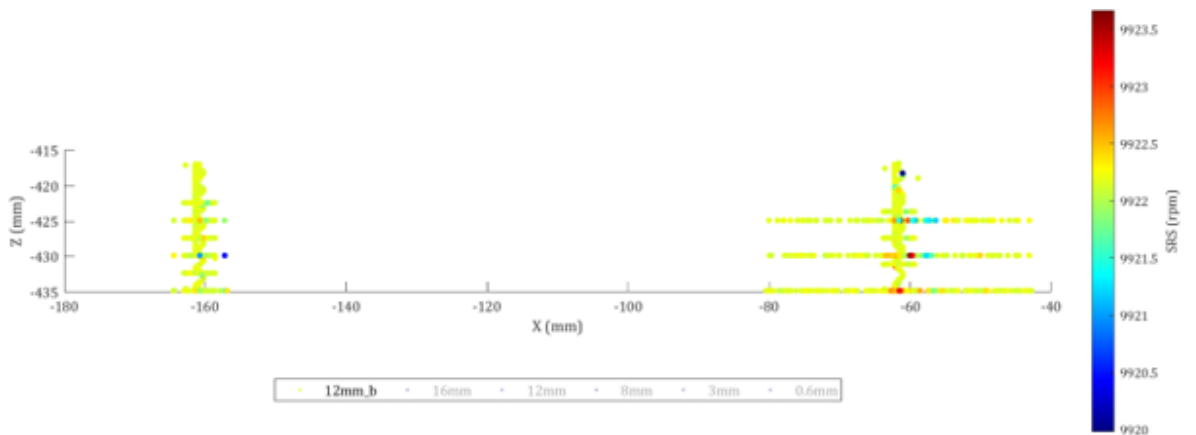
where any anomalies occur. If any occur during the finishing cuts, they could indicate damage to the part surface. Figure 7.15 and Figure 7.16 consider only R021EM12.



a. Isometric view

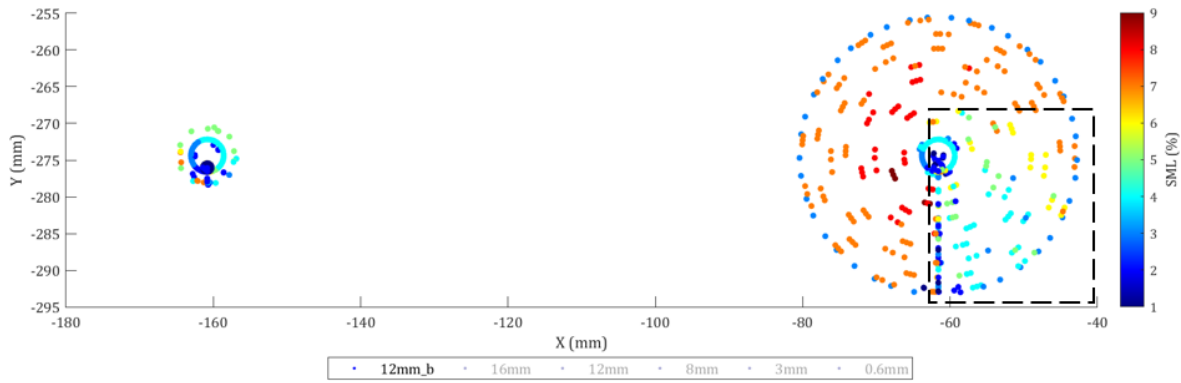


b. Top view

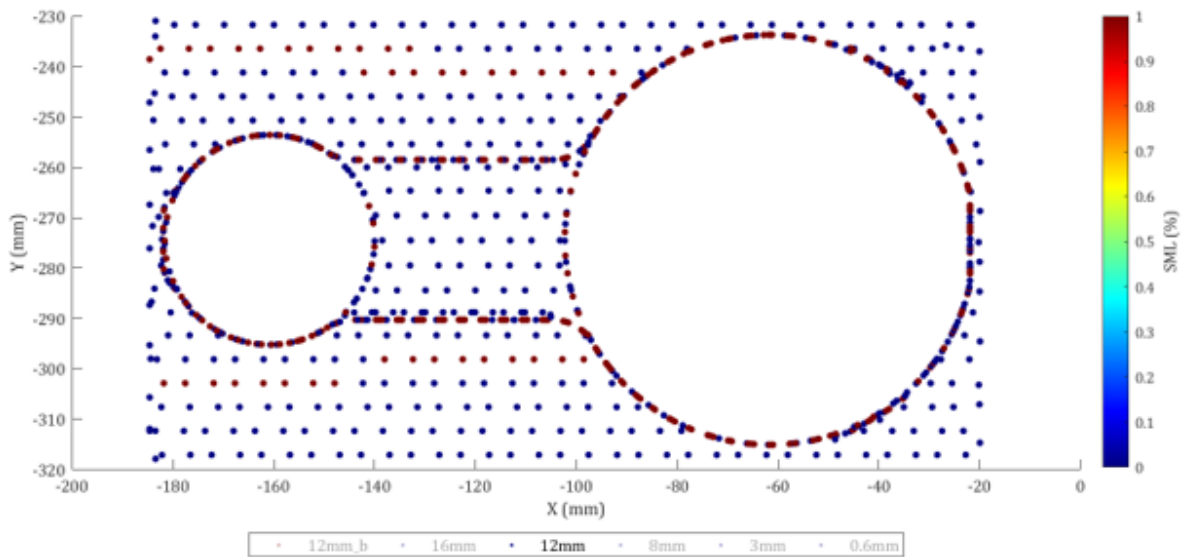


c. Side view

Figure 7.15. 3D process plots showing instantaneous SRS for R021EM12 (Con-Rod #15)



a. Top view instantaneous loads within Con-Rod bores



b. Top view instantaneous loads for Con-Rod exterior

Figure 7.16. 3D process plots showing instantaneous SML for R021EM12 (Con-Rod #15)

Figure 7.15 shows that there is minor variation in the SRS during the pocket milling process. This variation is more significant within the LB than within the SB with notable fluctuations in the SRS during the initial movement in the positive X-direction. This may correspond to the reduced feed rate in the LB observed in Figure 7.13b; however, the fluctuations in the SRS are not as consistent and do not appear to apply to the same coordinates. This discrepancy could indicate a problem with the cutting process, or with the condition of the cutting tool. Both would require investigation if raised in-process. Figure 7.16 shows that there is a similar region noted in the SML as the SRS, with low loads on the cutting tool during the initial LB cuts at each depth. Moreover, it is observed that there is a significant amount of variation in the SML throughout the LB despite the cutting process remaining consistent in terms of the rotational speed and the feed rate. This is likely caused by variation in the rate of material removed and is related to the overlap between each pass of the cutting tool (this phenomenon is investigated in-depth in Appendix B). The SML variations observed suggest that these overlaps are disproportionately affecting the conditions experienced by the cutting tool. This indicates that the employed pocket milling process could be improved. Figure 7.16b indicates that the finishing cuts mostly result in zero load on the cutting tool. This will be a consequence of the

quantised process data and suggests that a greater resolution may be necessary to best appreciate finishing cuts. Notwithstanding, the SML does peak to 1% during the last cut around the exterior of the Con-Rod. A poor surface finish was observed on the exterior of the Con-Rods (Section 7.1), therefore this peak, despite being only 1%, may be significant in showing the potential for surface damage if enacted in-process. However, if presented alongside the roughing cycles such a small peak in the data may go unobserved.

The given plots illustrate the capability of the position data, to be exploited in combination with useful MTData metrics, to show the instantaneous condition of the cutting tool. This has been shown post-process, as it is not possible to demonstrate an active version in writing. However, it is possible to apply these concepts actively using the procedure written and developed by the author to plot the data as it is acquired in real time. This would require slight alterations to the specific plot commands used, replacing individual `plot3()` and `scatter3()` commands with the `addpoints()` and `drawnow` functions as MTData is made available by the PAc program. These functions are demonstrated in the electronic Appendix. The plots are 3D, but it would also be practical to consider them in 2D and even 1D to assist in the visualisation of the process. It should be appreciated that the main issue with applying the approach in-process will be determining reliable CAXIS limits. This would require historical data to avoid a sudden change being portrayed (visually) as a possible anomaly in the process. Notwithstanding, the position data has been proven to be very useful. Like the 3D geometry plots, the position data is a valuable resource for providing process feedback during the cutting process. For systems employing ICG, physical measurements may be combined with the position feedback, thus providing engineers with a smart combination of condition-based data during each process.

## 7.4 Application of MTData: Spindle motor load

The SML has been provided in Figure 7.14 and Figure 7.16 as a data overlay for the 3D process plots. These are useful for the general presentation of information and for indicating features to investigate during quality inspections. However, in that form the SML cannot (easily) be used to determine the progressive condition of the cutting tool, nor for the estimation of the EOL or the RUL. Figure 7.17 provides the 2D plot for the SML for an arbitrary Con-Rod. Figure 7.17 shows that there is a significant difference in the signal for different cutting tools and for different processes. The roughing cycle is completed using R021EM12 and observes the highest loads and the greatest fluctuation in load on the spindle. Conversely, the finishing cycles tend to observe lower loads with fewer fluctuations. It is noted that R025ENP6 does not register a load on the spindle. This means that the SML has no discernible output for engraving tools (at the given resolution). It is also noted that R024EM03 indicates a SML of predominantly zero. This further indicates that the current resolution of 1% for the SML is inadequate for smaller cutting tools that are attempting processes that are not exaggerating the loads on the cutting tool (for example, finishing cuts).

It is noted that the cutting process was changed between Con-Rod 17 and Con-Rod 18, as well as replacing the worn cutting tools with new cutting tools. This means that a direct comparison of signals

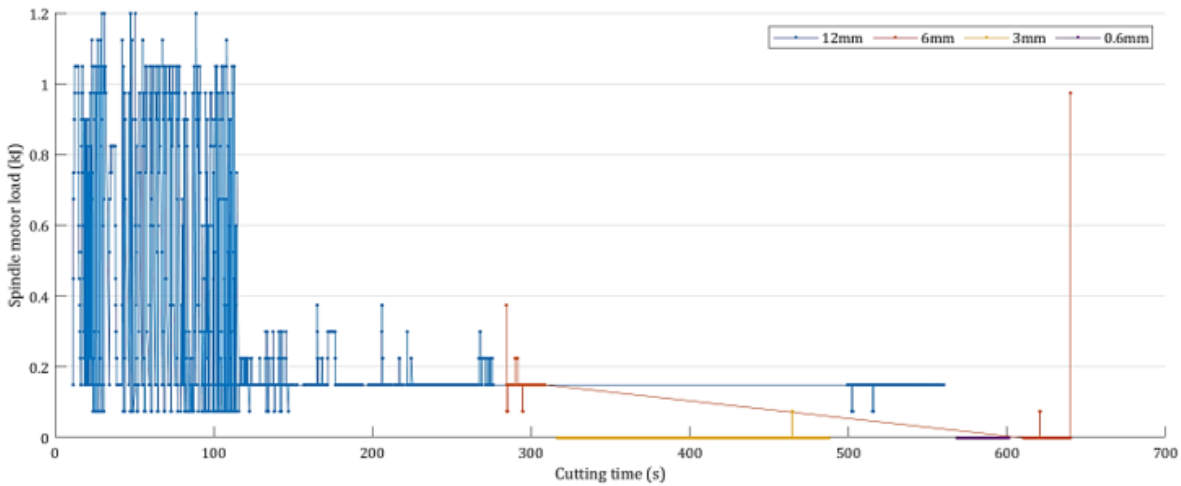


Figure 7.17. SML for arbitrary Con-Rod, separating different cutting tools

would be challenging, especially when so much of the SML signal is zero. It would be impossible to quantify changes in the condition of the cutting tool when the change in the cutting process may be responsible for differences in the signal. Nevertheless, it is possible to consider each Con-Rod as a single part, and thus evaluate the overall variation where applicable. Figure 7.18 gives the plot for spindle energy use per Con-Rod, considering only R021EM12.

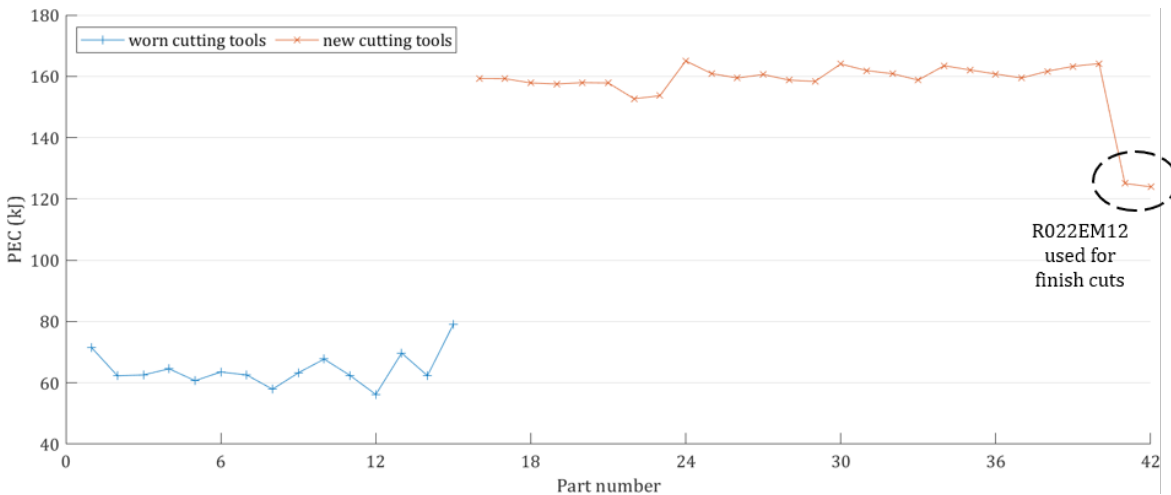


Figure 7.18. R021EM12 PEC per part for all 42 Con-Rods (one Con-Rod is one part)

Figure 7.18 shows that the process using worn cutting tools is very different from the updated process using new cutting tools. The original process included R020EM16 for much of the roughing cuts, whilst the new process (with new cutting tools) replaced R020EM16 with R021EM12. This effectively doubled the work done by R021EM12. To account for the difference, the PEC can be calculated using all cutting tools, shown in Figure 7.19. Figure 7.19 considers the energy required by all cutting tools; although, as the SML for R023EM06, R024EM03 and R025ENP6, mostly rounds to zero, their contribution to the totals is negligible. This is a consequence of the quantised process data and suggests that monitoring smaller cutting tools will need an increase in the SML resolution to enable the load on the spindle to be detected. Notwithstanding, by including all cutting tools the PEC trend for the worn cutting tools is closer to the PEC trend for the new cutting tools.

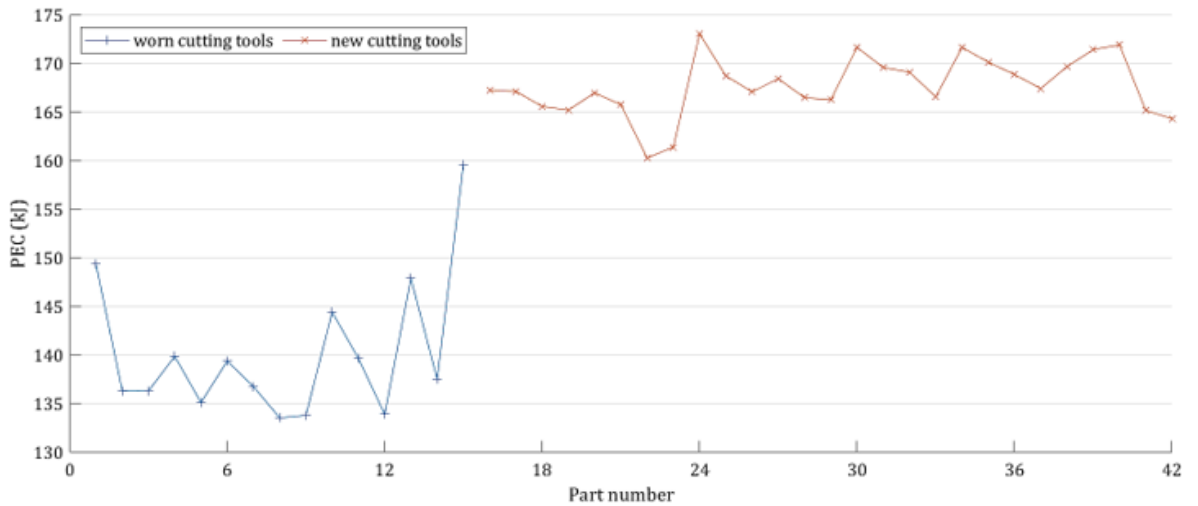


Figure 7.19. Combined PEC per part for all 42 Con-Rods (one Con-Rod is one part)

It is noted that the new cutting tools still required more energy per Con-Rod than the worn cutting tools. This may be true as it was shown in Chapter 5 that the cutting tool was in a better (healthier) state after the initial wear phase. However, it should also be noted that the cutting tool deployed to perform the roughing cuts was smaller (12 mm compared to 16 mm) and the cutting speed was increased by 30%. These changes are also likely to increase the energy required. Notwithstanding, ignoring the magnitude differences in the signals, it may be observed from Figure 7.19 that the worn cutting tools are statistically different from the new cutting tools. The PEC for the worn cutting tools has a greater standard deviation, range, and is more skewed. The values are given in Table 7.2, all rounded to integer values for clarity.

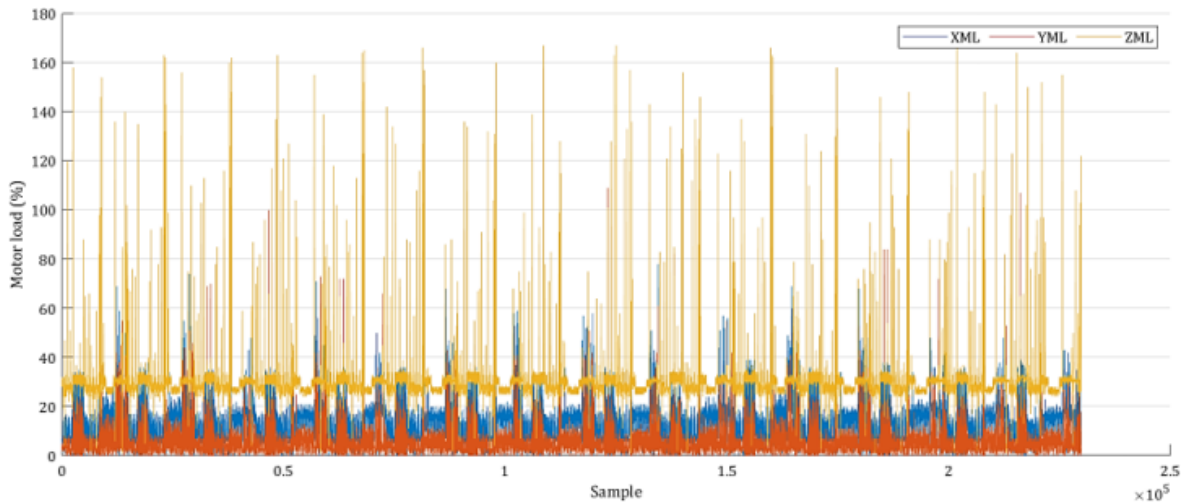
Table 7.2. Spindle PEC signal statistics for worn cutting tools and new cutting tools

Statistic	Worn cutting tools (kJ)	New cutting tools (kJ)
Average (mean)	140	168
Standard deviation	7	3
Kurtosis	2	0
Range (max-min)	26 (160-134)	13 (173-160)
Skewness	2	0

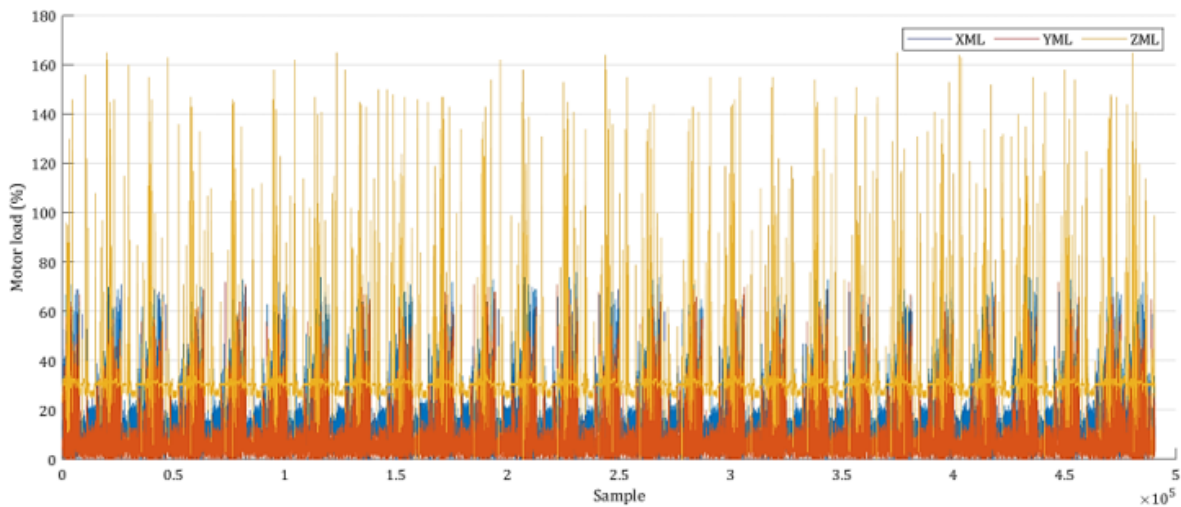
Not enough data is available to use the CCPD algorithm as more than 40% of the cutting tool life needs to be accounted for. It is also the case that the changes to the process parameters contribute significantly to the signal differences, hence any variation that may be attributable to the health of the cutting tools will be challenging to detect. It has been observed that the SML is far from self-sufficient when the cutting process gets more complicated. Whilst this could be improved by increasing the resolution of the SML signal, it may not be possible due to the limitations of the system or the communication network. As such, in the absence of an increase in the data resolution, additional signals should be considered.

## 7.5 Application of MTData: Axis motor load

The axis loads have proven to be useful for showing the general condition of the cutting tool for earlier applications (Chapter 6). Both X-axis and Y-axis signals should also have potential for determining the instantaneous condition of the cutting tool in-process using 3D process plots; however, to establish their value in determining the EOL of the cutting tool requires the 1D signal. Figure 7.20 plots the XML, YML, and ZML for R021EM12, for all 42 Con-Rods.



a. XML, YML, and ZML for worn cutting tools



b. XML, YML, and ZML for new cutting tools

Figure 7.20. Raw load signals for axis motors for Con-Rod application (R021EM12 only)

Figure 7.20 is included to show that there is no noticeable trend for either tool set (worn or new) and minor differences between the two plots. There may be micro-value within the signals, however, to establish such value would require significant investigative efforts. There is no visible macro-value. It is possible to consider an approach similar to the SML by calculating the energy required for each axis motor. Figure 7.21 gives the axis PEC plots for the X-axis motor and the Y-axis motor for the first 40 Con-Rods.

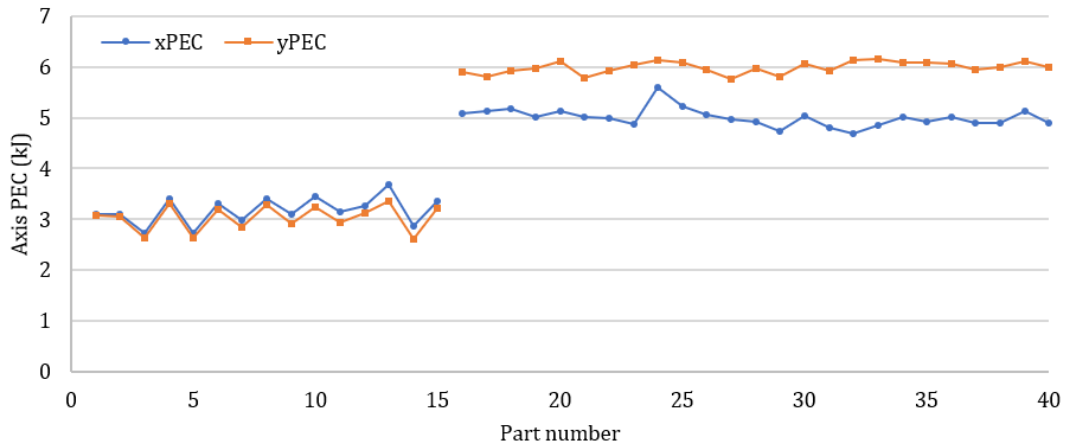


Figure 7.21. xPEC and yPEC for R021EM12 during the Con-Rod application (R021EM12 only)

Figure 7.21 does not include Con-Rod 41 or Con-Rod 42, as they employed a different cutting tool for the finishing cuts. It is noted that the difference between the worn cutting tool and the new cutting tool is predominantly due to the different amount of work undertaken by each, as stated previously. It is also shown that the yPEC is greater than the xPEC (for the new cutting tools) despite the raw signal indicating lower values. This is due to the y-axis motor having a maximum power more than twice the power of the x-axis motor (3.5kW versus 1.5kW).

It is seen that Figure 7.21 resembles Figure 7.19, showing that the efforts by each axis motor are similar to the efforts by the spindle motor. Each signal influences the others because they are all related to the same machining cycles and all motors play a role in the removal of metal. It is also likely that because the axis motors are physically connected to the bed and to the spindle, vibrations from one motor will inevitably be experienced by the others. The plot also resembles Figure 7.4. The loads do not appear to increase like the CSAM did, although the CSAM showed the accumulative trend. Nevertheless, like Figure 7.4 observed an increasing difference in the CSAM for the LB top and bottom scans, Figure 7.21 observes a similar trend in the xPEC and yPEC for the worn cutting tools. Table 7.3 lists the signal statistics for each axis, separated into worn and new.

Table 7.3. Axis PEC signal statistics for worn cutting tools and new cutting tools

Statistic	Worn xPEC (kJ)	New xPEC (kJ)	Worn yPEC (kJ)	New yPEC (kJ)
Average (mean)	3	5	3	6
Kurtosis	0	4	-1	-1
Range (max-min)	1 (3.5-2.5)	1 (5.5-4.5)	1 (3.5-2.5)	0 (6.0-6.0)
Skewness	0	1	-1	0

Table 7.3 gives integer values for clarity and does not provide the standard deviations for the signals as they round to zero. The basic statistics supplied indicate that for the xPEC the new cutting tool is more prone to outliers and is more skewed. This suggests that, in terms of the variation in cutting force the new cutting tool is similar to the worn cutting tool, although this has been shown to improve over time (Chapter 5). It is generally accepted that a cutting tool should be “worn in” as it may

initially be too sharp (the shearing action is less effectively created with a sharp edge). The yPEC statistics indicate that the worn cutting tool is worse than the new cutting tool with a greater range and more negatively skewed data. This implies that the worn cutting tools are in a worse condition than the new cutting tools. This suggests that the initial condition of a new cutting tool is not reflected by changes to the YML in the same way as the XML.

It is noted that FFT plots have shown value for previous applications; however, they have also been shown to be complicated despite being provided for relatively straightforward applications. Therefore, since the Con-Rod is a complicated process, the FFT plots will not be considered as their interpretation will be challenging. It is noted that if the Con-Rod process signals were sufficiently separated into the constituent cutting processes, the FFT plots should be valuable for comparing the changes and for determining the condition of the cutting tools used. In the absence of FFT plots, the dispersion heat maps may still be considered. Figure 7.22 gives the XML dispersion heat maps for R021EM12, for all 42 Con-Rods.

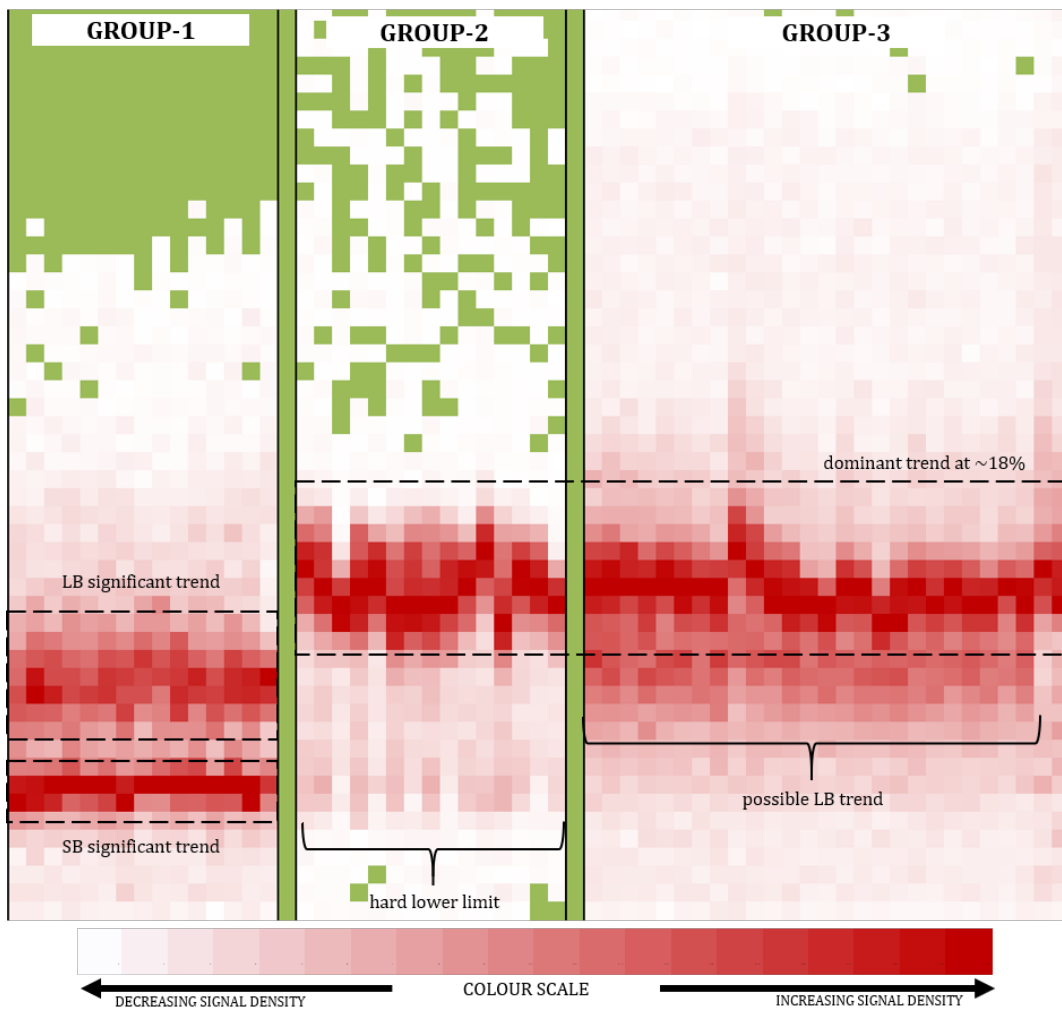


Figure 7.22. XML dispersion heat map for all 42 Con-Rods (R021EM12 only)

Figure 7.22 shows the dispersion heat maps for the Con-Rod bores machined using the worn cutting tools (Group 1), followed by the Con-Rod body machined using the worn cutting tools (Group 2),

followed by the Con-Rods machined using the new cutting tools (Group 3). These splits are necessary as the first process (with the worn cutting tools) separates the bores from the rest of the Con-Rod process. It is observed that there are two distinct load trends during Group 1. These relate to each bore, with the SB responsible for the lower load. Group 2 indicates a dominant trend fluctuating around 18%, and also evidences a lower XML threshold at 5-6%. This lower limit corresponds to the underlying machine tool vibrations and the compensation for no axis brake, raised in Chapter 5. It is noted that Group 3 is comparable to both Group 1 and Group 2 combined, indicating the dominant trend averaging 18%, and a possible LB trend; however, there is no clear indication of the SB. Nevertheless, this indicates that the dispersion heat maps do confirm the behaviour of the cutting tools within these processes are similar, despite the changes between them. There is little visual evidence to indicate the condition, or changing condition, of the cutting tool with the amount of information available. This is repeated for the YML dispersion heat map given in Figure 7.23.

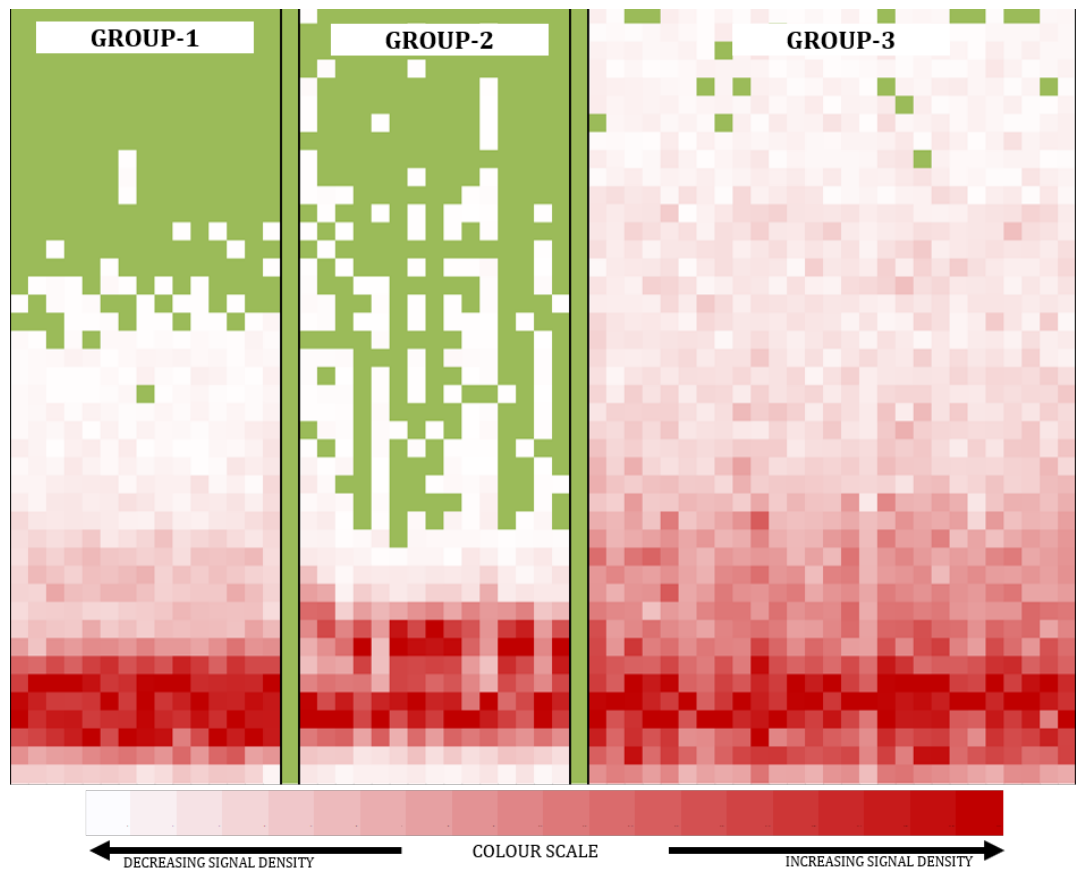
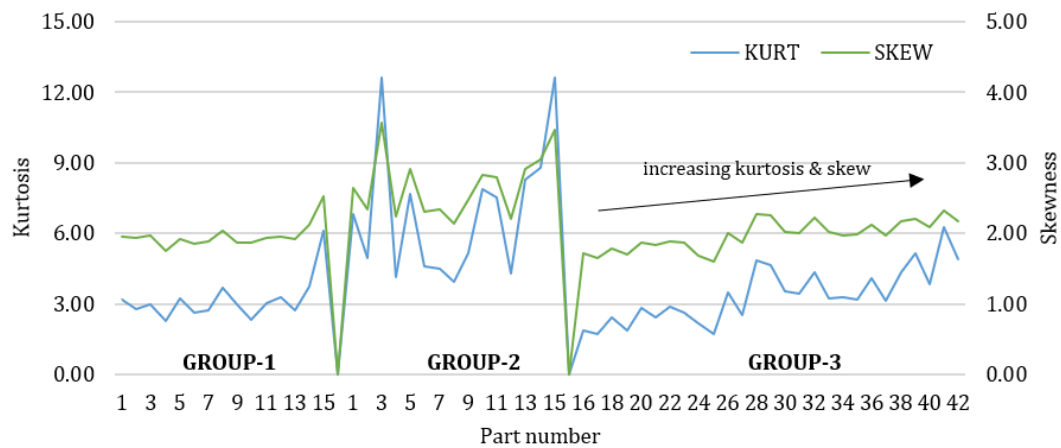


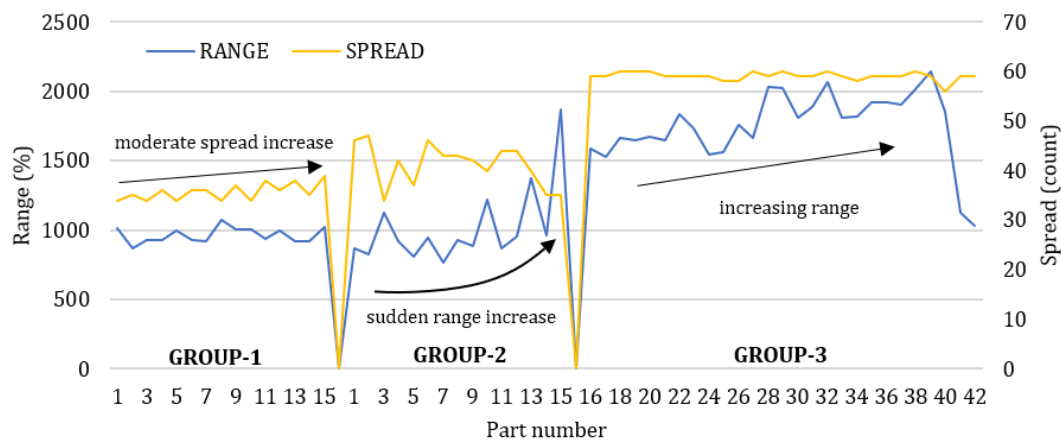
Figure 7.23. YML dispersion heat map for all 42 Con-Rods (R021EM12 only)

Figure 7.23 shows that that there is no noticeable difference between the worn cutting tools and the new cutting tools. There is a difference in the range of each plot; however, this is likely to be due to the process. Notwithstanding, the dispersion heat maps should gain value as more parts are monitored using the new cutting tools with the new cutting process. Bar any further changes to the cutting processes, the changes as the cutting tool wears should become more explicit. It is also observed that further isolating each cutting process and/or action should better indicate the changing condition of

the cutting tool. Some cutting processes will inevitably affect the cutting tool more than others. Whilst the axis loads do compare appreciably to the loads on the spindle, there is not currently enough comparable data to reliably comment on the changing condition of the cutting tool. Notwithstanding, it is noted that there are implicit trends in the dispersion heat maps. Figure 7.24 shows the trends for the XML dispersion heat maps, providing four plot statistics. The full results are given in the electronic Appendix.



a. Kurtosis and skewness trends



b. Range and spread trends

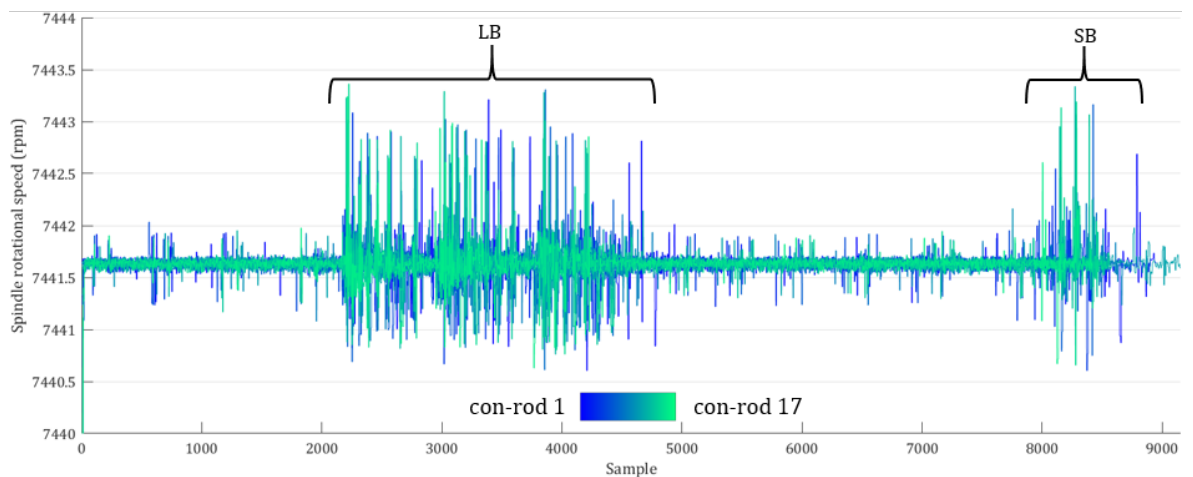
Figure 7.24. Trends in core statistics for the given XML dispersion heat maps

Figure 7.24a shows that whilst there is no discernible trends for the worn cutting tool (Group 1 and Group 2) in either kurtosis value or skewness, there is a notable upward trend for the new cutting tool (Group 3). On the other hand, Figure 7.24b shows that there are increasing trends for all dispersion heat maps when evaluating their range and their spread. It is reiterated that the range is the difference between the smallest measured XML value and the largest measured XML value, whilst the spread is the count of all integers greater than zero. It shown that there is a slight increase in the spread for Group 1, but no change in the range, this indicates mild fluctuations in the XML (fewer instantaneous changes of 2% or greater) as the cutting tool deteriorates. Group 2 observes a sudden decrease in the spread and a sudden increase in the range. This indicates a rise in sharper signal fluctuations

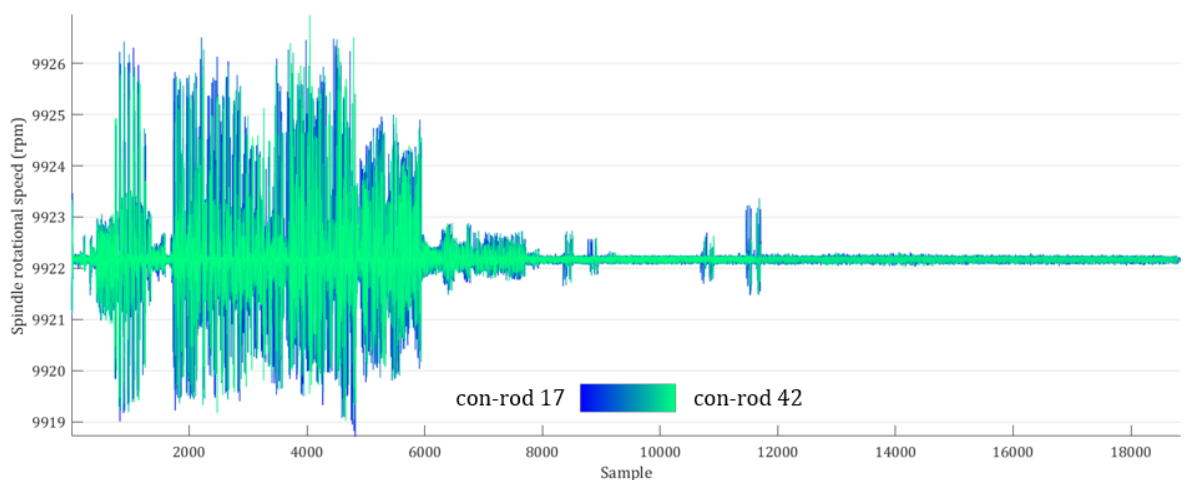
(more instantaneous changes of 2% or greater) as the cutting tool deteriorates. The contrast with Group 1 suggests different behaviour for different processes. Group 3 indicates an increasing range, with a constant spread. This is similar to Group 2, albeit with a more subtle increase in the signal fluctuations. The changes indicate that the deterioration of the cutting tool may be observed when evaluated in more depth than a visual check. It is relevant to state that these initial set of tests do indicate that the wearing-in process associated with new tools could be investigated using the deployed approach. This was not the intention of this research. Nevertheless, more data is required to establish the significance of the trends and whether the observed trends continue. It is also noted that only R021EM12 has been evaluated. Additional cutting tools should be evaluated to establish whether they all conform to the same, or similar, trends in the axis loads.

## 7.6 Application of MTData: Spindle rotation

The SRS may also (briefly) be considered in a comparable way to the axis loads. Figure 7.25 provides the SRS signals for R021EM12. Figure 7.25 shows that there is no effective comparison to be made



a. SRS for machining bores using worn cutting tools



b. SRS for machining [entire] Con-Rod using new cutting tools

Figure 7.25. SRS results for worn and new cutting tools

between the worn cutting tools and the new cutting tools due to the differences in the process. The magnitude SRS for the two are different, the cutting processes are different, and the signal fluctuations are different. This suggests that the SRS explicitly confirms the changes to the cutting process; however, it does not make it possible to compare the differences between the worn cutting tools and the new cutting tools. Instead, the worn cutting tools and the new cutting tools may be considered separately. Figure 7.26 gives a dispersion heat map of the SRS signal for the new cutting tool (R021EM12).

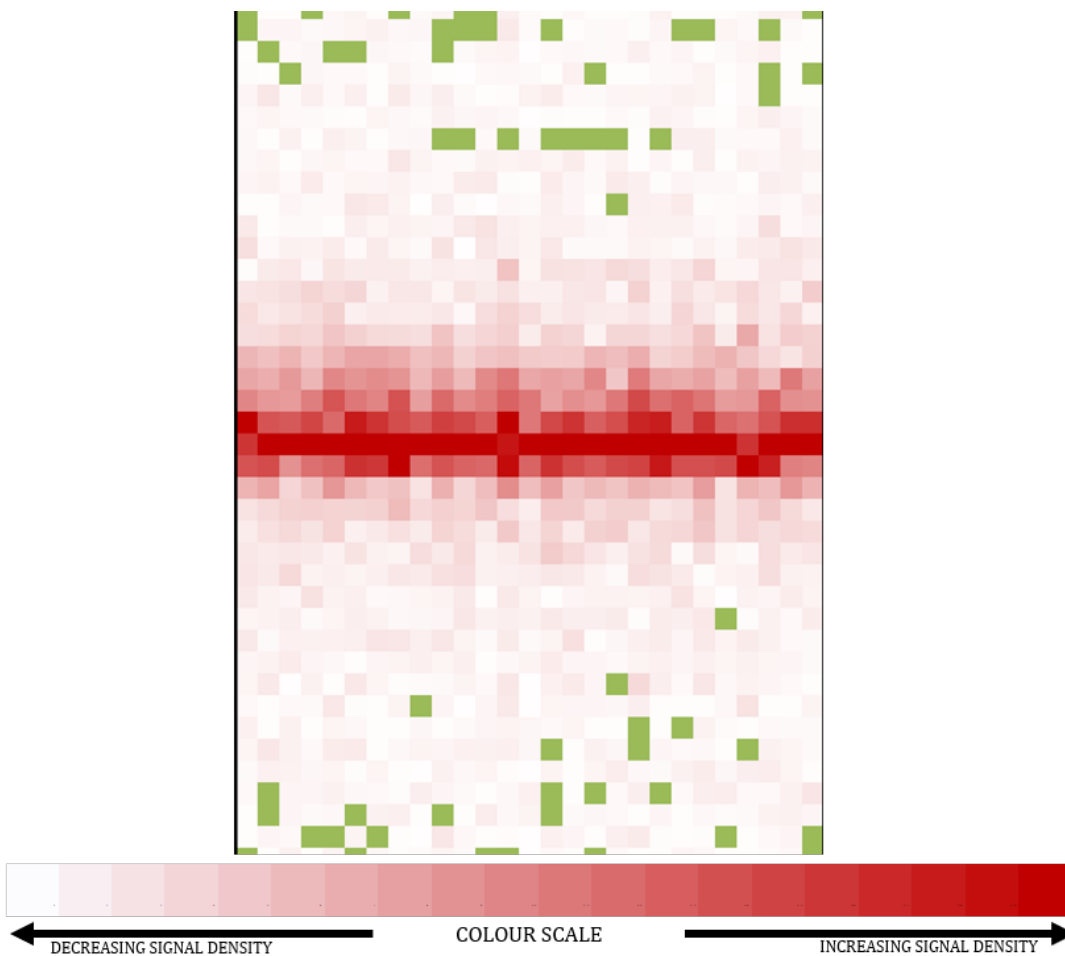


Figure 7.26. SRS dispersion heat map for R021EM12 (parts 16-42)

Figure 7.26 shows that there are no notable changes within the signal for the new cutting tools (Group 3). This is also acknowledged by the signal statistics with no variation in the results available. This suggests that the condition of the cutting tool cannot be derived from the SRS. However, it must be appreciated that the controller is acting on the SRS to maintain the desired value. This will make it harder to ascertain the condition of the cutting tool from the data as the controller will be acting to prevent the variations needed to provide the evidence. Nevertheless, the SRS signal is inherently valuable anyway, as it enables the derivation of Pmax (Chapter 4) and the calculation of the sPEC.

## 7.7 Challenges and next steps

The Con-Rod application was laboratory-based case study established to explicitly test the systems developed in previous Chapters. The step change being that the cutting process was optimised for the benefit of the process, part, and audience, rather than to explicitly deteriorate the cutting tools used. The Con-Rods also noted the addition of multiple cutting tools and the introduction of roughing cuts separate from finishing cuts. The addition of process complexity further highlighted the impact that different actions will have on the cutting process and the subsequent process signals. It was shown that separating individual cutting tools was important and that the system produced by this research was capable of separating the signals in an appropriate manner in real time. It was also shown that separating different processes was equally important, even for individual cutting tools. Only the separation of roughing and finishing cycles was attempted here, however, there would be potentially greater benefit to separating the processes as much as is possible. Indeed, it may become necessary to isolate the important signals in the MTData.

The results indicated that the SML was not sufficient by itself for the indication of the cutting tool condition; neither was it capable of predicting the RUL for the cutting tools used. However, it should be appreciated that the changes to the process parameters dominated the results and made subtle changes challenging to determine. This is a feature associated with any load-based cutting tool monitoring approach and has been a barrier to the development of previous CM systems. This work did however indicate that including the axis and rotational speed data enabled more insight into the condition of the cutting tool. Although, it was noted that the process variation still dominated with only the axis loads able to indicate the potential condition of the cutting tool through quantitative evaluation of the dispersion heat maps. The results indicated that for commercial or industrial processes the deterioration of the cutting tool cannot be dominant. Therefore, determining the condition will require additional effort and data, and enough uniformity to enable effective assessments and to determine reliable trends.

It was also consistently shown that the resolution of the MTData has become a potential issue. This was anticipated in previous Chapters; however, it is shown as only an issue for certain cutting tools and for certain processes. Increasing the resolution would be beneficial and would enable further information to be gleaned from the MTData. This may also enable any variation attributable to the changing condition of the cutting tool to be more explicit and easier to establish. However, more information may be itself challenging as this would require further data processing. It may also increase unwanted noise into an already noisy system. The need to increase the data resolution should be weighed against the potential benefit of increasing the data sampling frequency.

## 8 | OMI-body Investigation

This Chapter aims to “close the loop” by appreciating the future value for the control data when deployed in a commercial manufacturing environment. This Chapter presents the deployment of the developed system in a Manufacturing Center. The system was installed for a chosen application, the OMI-body, which was first investigated in a laboratory setting to establish any necessary adjustments to the system. Following this, the system was deployed in a comparatively high-volume manufacturing environment to study the system response, to generate information, and to establish the value in the generated information. This Chapter aims to explicitly demonstrate to machine tool manufacturers and users the potential for better utilising the information they currently generate to control and enact machining processes. The aim will be achieved by presenting the post-process value in the generated MTData and proving the potential for deployment in-process. The novel techniques developed in previous Chapters will be considered to evaluate their performance (and thus value) for real-world application. It is noted that, compared to previous applications, there are significant changes to the environment and to the process conditions. The main changes include:

- A different machine tool environment, using a lower-volume version of Renishaw’s Automated Milling, Turning and Inspection Centre (RAMTIC) system
- Deployment of ICG systems to ensure process repeatability – such would be deployed as standard
- Use of different cutting tools, using a variety of styles, sizes, and geometries and using carbide for the cutting tool material (rather than HSS)
- Remote monitoring and analysis – such that part/process condition can only be inferred from the acquired data (grey box).

It is noted that, like the Con-Rod application, the process parameters are not implemented with the intention of enacting wear on the cutting tools. This is because actual processes are not designed to intentionally wear, or break, the cutting tools used. The industrial process considered herein is the manufacture of OMI-bodies using the RAMTIC system.

### 8.1 RAMTICs

Remote manufacturing is an ideal desired by many manufacturing organisations. Being able to reduce the human involvement in a system significantly reduces cost and can also reduce lead times and process errors. These are sometimes referred to as flexible manufacturing systems (FMSs), especially when the system can adapt to changes in production (Kosky 2013) allowing economies of scope as well as economies of scale (Manthou 2001). One application would be a carousel-based implementation such as the RAMTIC system (Renishaw 2020b). RAMTIC systems, shown in Figure 8.1, consist of a conventional machine tool with modifications to allow the integration of a retrofit carousel intended to prolong and to semi-automate the machining process. The system is like a robot cell; however,



Figure 8.1. RAMTICs at Renishaw, reproduced from Renishaw2020b

parts are pulled into the machine from the side, rather than pushed in from the front. Raw material is fixed to custom “wings” that are loaded into each carousel. This effectively forms a rotary pallet changer, where each wing is a separate pallet. The carousel also holds the required cutting tools and is paired with a program that matches the tools, materials, and parts to be made. RAMTIC processes can last upwards of eight hours depending on the carousel contents but do have an upper duration as the carousels must be eventually be replenished.

The required cutting tools can be fed into the machine tool from the carousel. Cutting tools must last for an entire process to avoid costly failures. As such the cutting tools are checked prior to all processes using ICG methods. If the total lifetime remaining is less than the next cycle duration the cutting tools will be removed, replaced, and in some instances sent for re-sharpening (Section 8.1.1). However, in many cases the cutting tools will be disposed of and contribute to process waste (Meier 2019). This is a concern when the predicted life results in cutting tools being replaced when the actual life remaining is greater than the subsequent cycle duration.

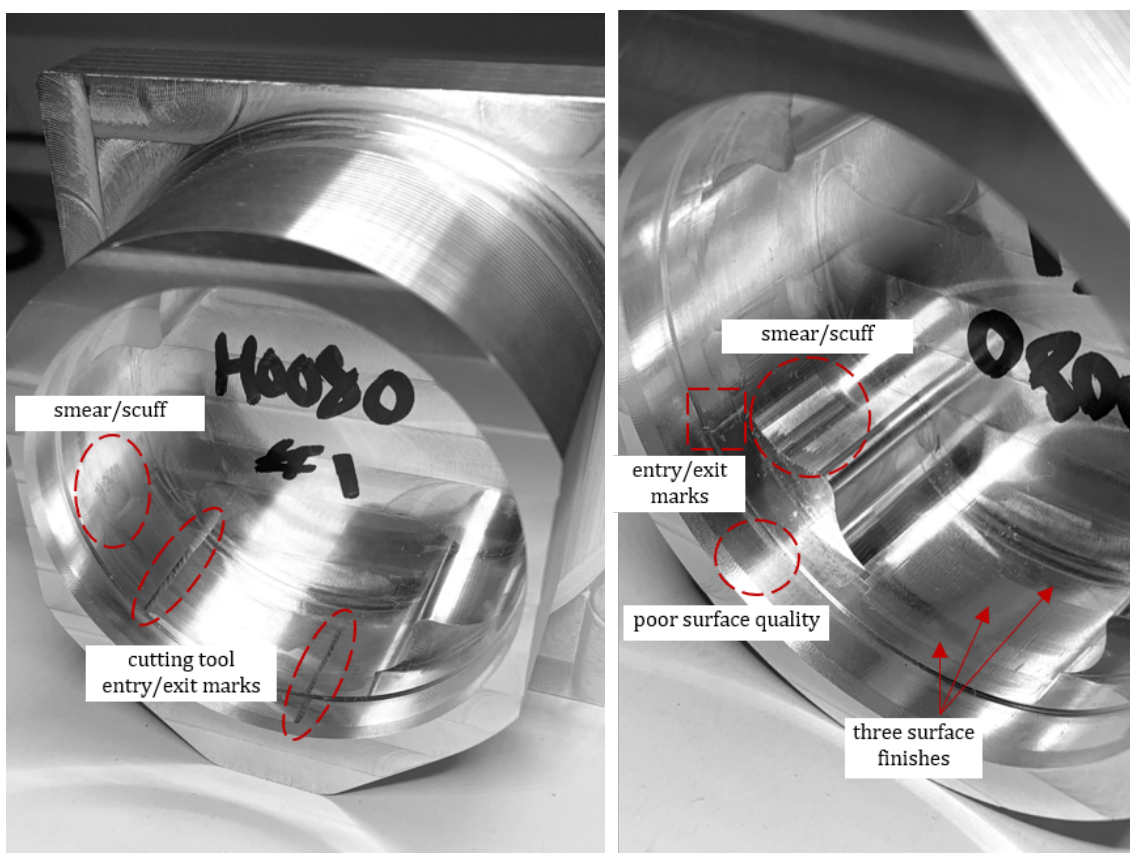
### 8.1.1 Refurbished cutting tools

Regrinding of cutting tools has become popular in recent years with services offering to take used cutting tools and return them almost as-new (MSC 2020, Ceratizit UK 2020, Mikron Tool 2020). Companies claim to offer (almost) the same cutting tool life and performance for reground cutting tools as new, as well as original geometries and surface finishes. Clearly this comes with the strong caveat that seriously damaged cutting tools cannot be serviced, nor can cutting tools that have been reground multiple times (there is a limit). It is noted that these statements perhaps stretch the truth for greater sales, however it has been commented by the industrial sponsor that regrind cutting tools *will* often be treated the same as new cutting tools. Research by Conradie et al. (2017) notes that the economic benefit of regrinding cutting tools can be significant. This alone can be a strong motivation to start regrinding cutting tools to reduce costs. However, Conradie et al. (2017) does note that the process reduces cutting tool length by up to 12% and reduces cutting tool diameter by up to 4%.

This contrasts with the claims by Ceratizit UK (2020) that geometries are unchanged; however, if employing ICG it is not unreasonable to assume that changes to the cutting tool geometry will have little effect on the final component dimensions. Nevertheless, more significantly Conradie et al. (2017) notes that reground tools do wear differently and have a shorter life than new cutting tools. They note that reground tools introduce management issues that require investigation identifying that, bar the cost savings, the introduced issues perhaps outweigh the benefits of regrinding. It is noted that due to the process of cutting tools being refurbished, such cutting tools will inevitably be included in results provided within this Chapter. The refurbished cutting tools will be acknowledged where possible to distinguish them from the new cutting tools. This will hopefully reduce any unintended impact on the analysis of cutting tool condition.

## 8.2 Laboratory implementation

To address the changes in the machine tool environment, the OMI-body was first manufactured using the same machine tool as the earlier applications. This was intended to address the differences attributable to the machine tool rather than the cutting tool and involved the testing of a series of similar cutting tools, each subject to different amounts of use. To support these tests a reduced cycle was considered due to the size difference between a typical RAMTIC machine tool and the VCS430A employed in the laboratory. The laboratory manufactured OMI-body is shown in Figure 8.2.



a. H0080#1 first view

b. H0080#1 second view

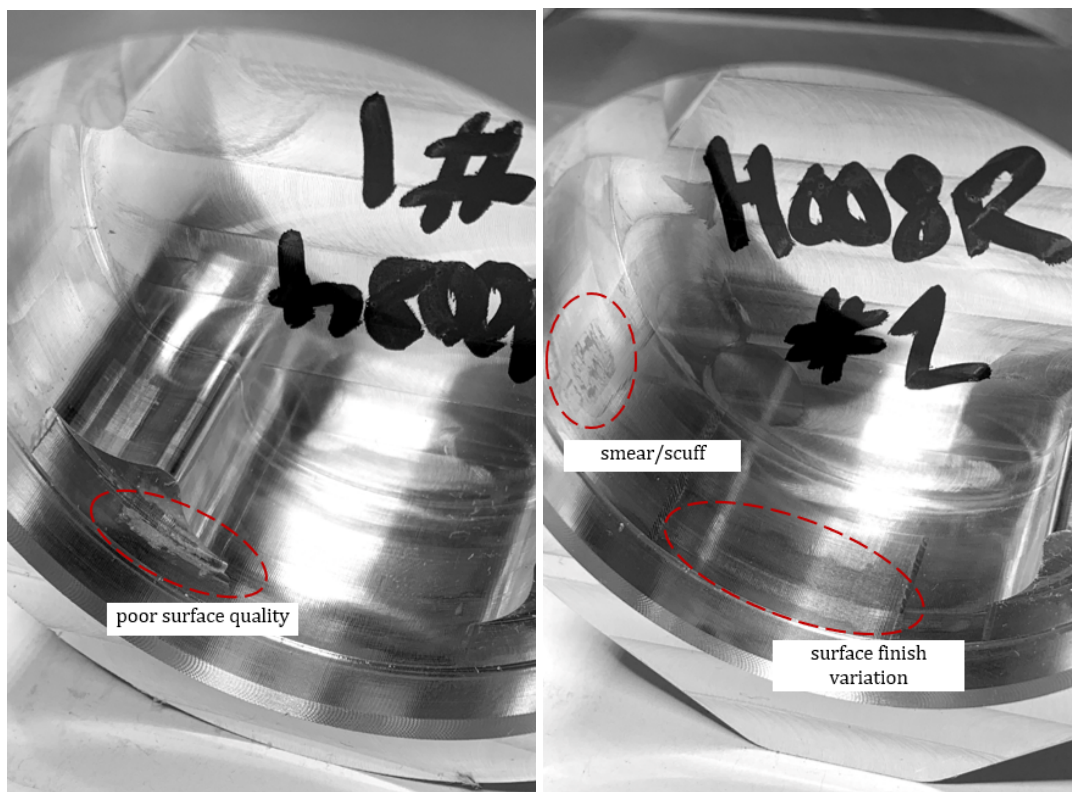
Figure 8.2. Photographs of laboratory made OMI-bodies (new cutting tools)

Figure 8.2 shows that the surface quality of the OMI-body is lacking. This is due to the process being a stripped back version of the original with only the roughing cuts completed. The visual damage to the surface of the machined parts is likely caused by the cutting process and not the condition of the cutting tools. However, there are observations of surface smear/scuffing and noticeable changes in the surface finish at different depths. The different cutting tools evaluated are given in Table 8.1. The details for the ripper cutter are provided for information but the tool is not investigated further.

Table 8.1. OMI-body cutting tool details (laboratory version)

Cutting tool	AKA	Details	Diameter (mm)	OEM life (s)	Remaining life (s)
D806N	T0	New 3-flute ripper cutter	16.0	40000	40000
H0080	T1	Pre-used 3-flute slot drill	12.0	40000	39013
H0082	T2	Pre-used 3-flute slot drill	12.0	40000	23183
H0083	T3	Pre-used 3-flute slot drill	12.0	40000	15275
H0084	T4	Pre-used 3-flute slot drill	12.0	40000	7355
H008R	TR	Reground 3-flute slot drill	12.0	40000	39035

There were minor differences observed in the workpiece finish when using the different cutting tools. The main differences were in the degree of and amount of scuffing. This is shown in Figure 8.3.



a. H0084#1 surface damage

b. H008R#2 surface damage

Figure 8.3. Photos of laboratory made OMI-bodies (worn cutting tools)

Figure 8.3 illustrates that for the more worn cutting tool (T4), there were regions indicating more

severe surface damage on the manufactured part. This fits all previous observations that a damaged cutting tool imparts damage on the workpiece. For the reground cutting tool, there were also indications of more variable surface finish. Whilst the newer cutting tools had three distinct surface finishes at different depths, the reground cutting tool used in this study resulted in more visible variation as illustrated in Figure 8.3b. Further investigation will not be pursued in this thesis. The different H008 cutting tools (12mm nominal size) may also be compared by considering their pre-process measurements, Figure 8.4. The diameters were measured twice (M1 and M2) using the TS27R. Both are given to illustrate the minor variation between measurements.

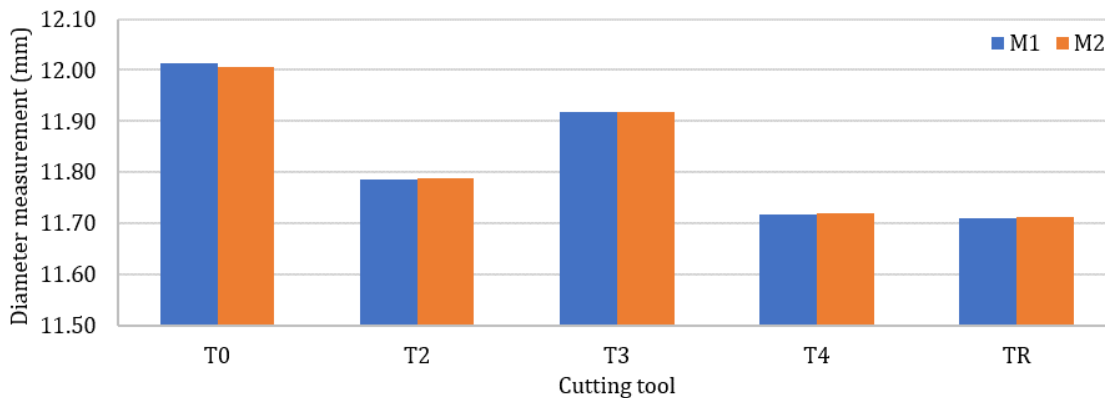


Figure 8.4. Measured (M) cutting tool (H008) diameter using TS27R

Figure 8.4 shows that T2 is visibly undersize compared to T0 and T3. This suggests that T2 may be a reground cutting tool as T3 is a used tool provided by Renishaw that has been active for 7908 additional seconds and thus should be smaller. This indicates that T4 may also be a reground cutting tool as the relative difference between T4 and T3 is proportional. However, this cannot be confirmed with the data available. The manufactured OMI-bodies were not assessed formally using a CMM as their exact dimensions and surface finish is not relevant to this experiment. In a commercial environment the manufactured parts will not likely be assessed beyond a short visual check of every “nth” part. Such checks should identify the damage imparted by the H0084 cutting tool (although with a finishing cut this damage should be negated). Without (or in lieu of) the part geometries, the MTData metrics may be considered. Figure 8.5 compares the spindle motor PEC results for each of the H008 cutting tools. It is noted that each cutting tool was used to manufacture two OMI-bodies. Figure 8.5 presents the data as a box plot to show the differences between cutting tools, and to show the variation between cutting tool uses. The plot shows similarities to Figure 8.4, with tool-to-tool variation indicating a similar pattern. However, it is highlighted that the cutting tool diameters were not accounted for. This would mean that T2, although undersize, was treated as 12mm in diameter. The relative engagement of the cutting tool would therefore be lower and the cutting tool would not have to work as hard (hence the lower PEC). This may explain the relative differences in the PEC between cutting tools being reminiscent of the relative differences between the cutting tool diameters (Figure 8.4). This also indicates that there is no significant or clear general trend in the comparative condition of the cutting tools. This is likely to be compounded by the relative lack of data.

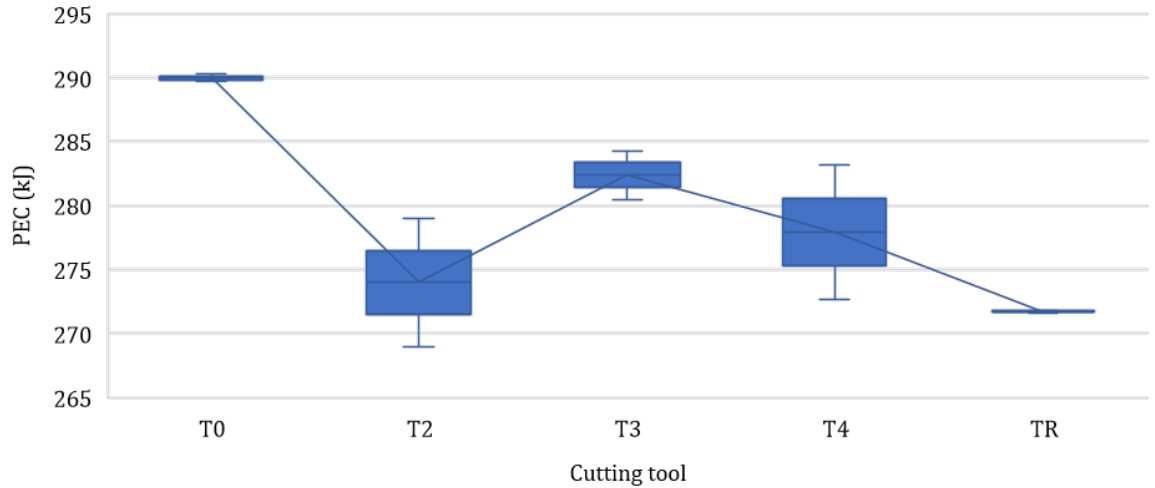


Figure 8.5. Spindle motor PEC results for the laboratory-made OMI-bodies

It is suggested that the differences between cutting tools is difficult to appropriately quantify. It should be noted that despite each cutting tool being at distinct stages of relative deterioration, they are all different cutting tools and hence comparing them is challenging. Different cutting tools will inevitably deteriorate at different rates. It is also unknown which are reground cutting tools (other than TR). Any of the included cutting tools could be since such information is not kept (all are considered as new). It is also the case that there is limited data available as the economies of scale are not present.

### 8.3 Industrial implementation

Following the brief laboratory investigation, which demonstrated the efficacy of the OMI-body monitoring set-up put in place by the author, the process was installed in the Renishaw Miskin Manufacturing Center (MMC). This was achieved by the author with cooperation from the machine tool manufacturer Mazak, and assistance from Hilscher Engineers. A COMX-CIFX link was established between a VCN530C machine tool and a standalone PC. This local communication network was established according to the same parameters as the VCS430A with the same RPI and the same (480 byte) range of output registers. The network was set up using SYCON.net, using the same processes outlined in Chapter 4 and using the supplementary documentation included in Appendix D.3 and D.4. It is noted that the only installation process requiring interruption to the operation of the machine tool was the adjustment of NC parameters to make the required MTData available through the COMX-CIFX link. This process took only a few minutes. The remainder of the installation and the subsequent acquisition of MTData had no impact on the ordinary operation of the machine tool. This evidences the value of this approach in avoiding unnecessary downtime and intrusion into the working capacity of the machine tool. A total of 92 MTData sets were acquired. Each set lasted approximately 1.03 hours ( $\pm 12$ s) of machining time. Each data set included an entire wing and therefore consisted of eight OMI-bodies. This resulted in 736 OMI-bodies manufactured, each machined in under eight minutes. Of the 92 data sets:

- 42 results included only the spindle motor load with the run time and tool numbers. These cycles were to establish the system response, to gauge the volume of information, and to identify

any issues with the data acquisition

- 31 results included the spindle motor load as well as an additional eight variables, including the axis loads, axis positions, feed rate, and rotational speed
- Four sets were interrupted cycles. One of these occurred when a cutting tool failed, the rest occurred for unknown reasons. As the manufacture of the OMI-bodies is treated as a grey box, these interrupted cycles will herein be treated as partially failed cycles (because the two parts may be combined manually if necessary)
- One result was abnormally large (but successful so also included in the 42 above). On inspection it was noted that the second process (using T25) took 17.6 times longer than normal (4919.6s versus 279.4s). As the SML values drop to zero for most of this process it is suspected that the machine tool is idling. The reason for the machine tool idling is unknown
- 15 results included incomplete and corrupt data sets. These will be treated as completely failed cycles as the processes cannot be recovered. The cause of the failures is unknown.

The acquired data indicated a success rate of 69% for the initial cycles (SML only, first batch) and a success rate of 94% for the subsequent cycles (SML+8, second batch). This indicates that improvements made to the PAc program by the author, between the two cycles, were beneficial. The cutting tools used were the complete set necessary for the manufacture of the OMI-bodies using a RAMTIC. These are listed in Table 8.2, not including the cutting tool that failed catastrophically.

Table 8.2. OMI-body cutting tool details (MMC version)

Cutting tool	AKA	Details	Diameter (mm)	OEM life (s)	Remaining life (s)
H008SD01	T2	New 3-flute slot drill	12.0	136.0	40000
H008SD02	T3	New 3-flute slot drill	12.0	136.0	40000
C900SD01	T4	New Spot drill	06.0	115.0	Unknown
H058SD03	T7	New 3-flute slot drill	08.0	110.0	Unknown
H008SD04	T8	New 3-flute slot drill	12.0	136.0	40000
C853CD01	T12	New Carbide drill	02.6	134.0	Unknown
E800CD02	T17	New Carbide drill	04.3	154.0	Unknown
F363GC01	T21	New Grooving cutter	12.0	122.0	Unknown
E616CD03	T22	New Carbide drill	02.8	139.0	Unknown
E801CD04	T23	New Carbide drill	03.3	143.0	Unknown
D635TM01	T24	New 1.0 pitch threadmill	12.0	120.0	Unknown
D806RC01	T25	New 3-flute ripper cutter	16.0	155.0	40000
E950TM01	T26	New 15-degree tapermill	12.0	130.0	Unknown

It is not known whether any of the cutting tools employed are reground cutting tools as such information is not retained. It is also noted that the OEM defined life for most of the cutting tools is unknown. The information is not needed herein as primarily only the H008 cutting tools will be evaluated but it could be obtained if necessary. The information provided in Table 8.2 can be included within the

DENSE definition file to populate the cutting tool information during the MTData processing.

### 8.3.1 Initial observations

Following the installation in the MMC and the acquisition of MTData, a few initial observations may be made regarding the acquired information. These are outlined below.

**Abnormal data sets** – One results file suggested a problem with T25 due to an abnormally prolonged process time. As the SML was zero for the majority of the process length, it is suggested that the process was stopped manually by the machine tool operator. This is also evidenced by the occurrence of a stop signature in the SML signal at 132.226 seconds (Figure 8.6). The cycle started at 15:37; therefore, the machine tool was stopped between 15:47 and 17:04 for a total of 77 minutes and 25 seconds. This observation evidences the opportunity for optimising machine tool availability using the MTData. This may be employed to improve the OEE.

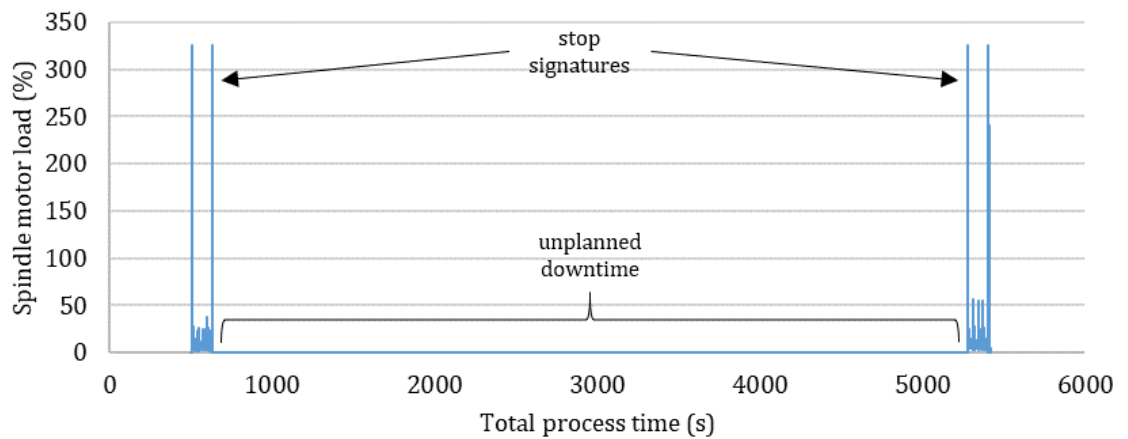


Figure 8.6. Evidence of stop signatures in the SML signal for abnormal MTData set

**Cutting tool breakage** – It was identified following the acquisition of all cycles that one of the H008 cutting tools failed catastrophically at around 450 parts. This was not initially reported; however, it was said to have occurred on 25/11/2019 at approximately 16:30. This corresponds to the second instance of an interrupted cycle and suggests that the cutting process was stopped to replace the failed cutting tool. The failed cutting tool was not located. It was suggested by the machine tool operator that it sheared completely (perhaps similar to Figure 5.3).

**MTData precision** – It is noted that there is no increase in the precision of any MTData signals. The extra precision (hundredth of a decimal) for the SML was made available within the machine tool controller. However, to make the data available to the communication network would require a significant revision to the PLC output.

**Volume of data** – There is a significantly increased volume of data versus previous applications and versus a laboratory-based process. This is simply because more parts are being manufactured within a shorter period. In a reflection of the production methods used, eight OMI bodies were manufactured in one cycle, requiring the use of an eight-part fixture. This added greatly to the

challenges associated with monitoring this process. It should be appreciated that if the MTData precision were increased, the volume of data would also increase.

**Laboratory-MMC comparison** – The VCS430A (laboratory) and the VCN530C (MMC) may be contrasted directly (using the MTData) by comparing the stop signature from each. It was observed that the MMC processes were run 20% faster than in the laboratory, and the stop signature was 120% larger with a magnitude of 326 versus a magnitude of 148. This is considered to be an excessive difference and either suggests that the 20% increase in speed has a significant impact on the stop signal, or suggests that the spindle motor in the VCN530C is not as healthy as the spindle motor in the VCS430A. This is plausible as the VCN530C will have been more active in the MMC than the VCS430A could be in the laboratory.

It is also relevant to compare the mean and median spindle load magnitudes, rounding to the nearest integer to account for the quantized nature of the data (and excluding the stop signatures). The VCS430A (for the OMI-bodies) sees a mean of 5% and a median of 2%. The VCN530C sees a mean of 28% and a median of 16%. This indicates that the impact of the quantized data has reduced relative to the process. In other words, an uncertainty of 0.5 versus a mean value of 5 indicates a 10% impact in the laboratory; however, the same uncertainty of 0.5 versus a mean of 28 has an impact of just 1.8% in the MMC.

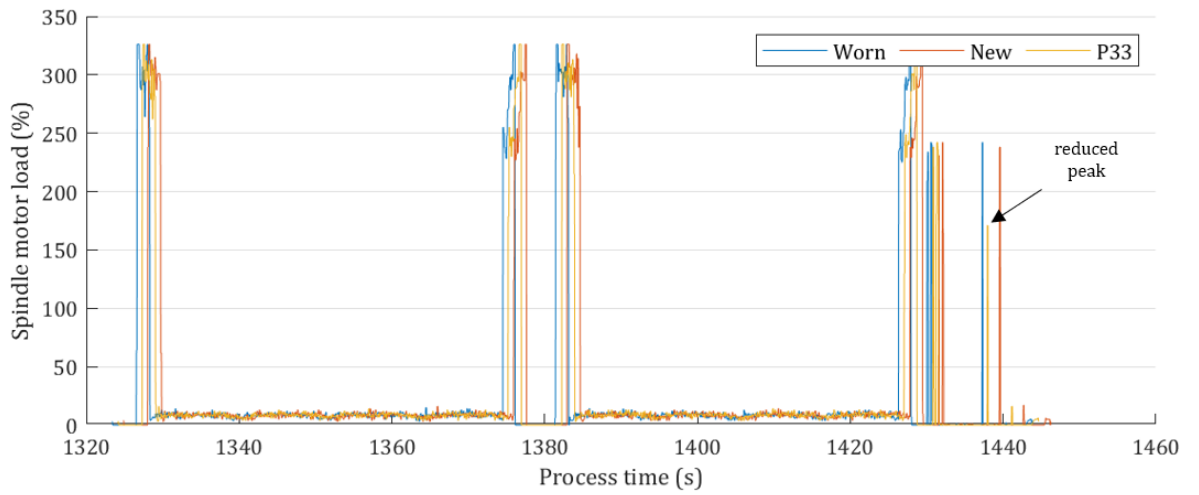
The initial observations indicate immediate value in applying the developed approach in a manufacturing setting. The installation was unobtrusive, whilst the improved monitoring capabilities enabled gains from the available MTData, even unprocessed. For example, allowing the machine tool downtime to be allocated to a specific process, at a specific time. This evidences that the developed monitoring system has immediate value in complementing existing process monitoring technologies. Nevertheless, more value may be gained from processing the results and thus reducing the volume of the MTData retained. This may also evidence how the collection of MTData may further dovetail and be complimentary to existing process monitoring technologies.

### **8.3.2 MTData investigation**

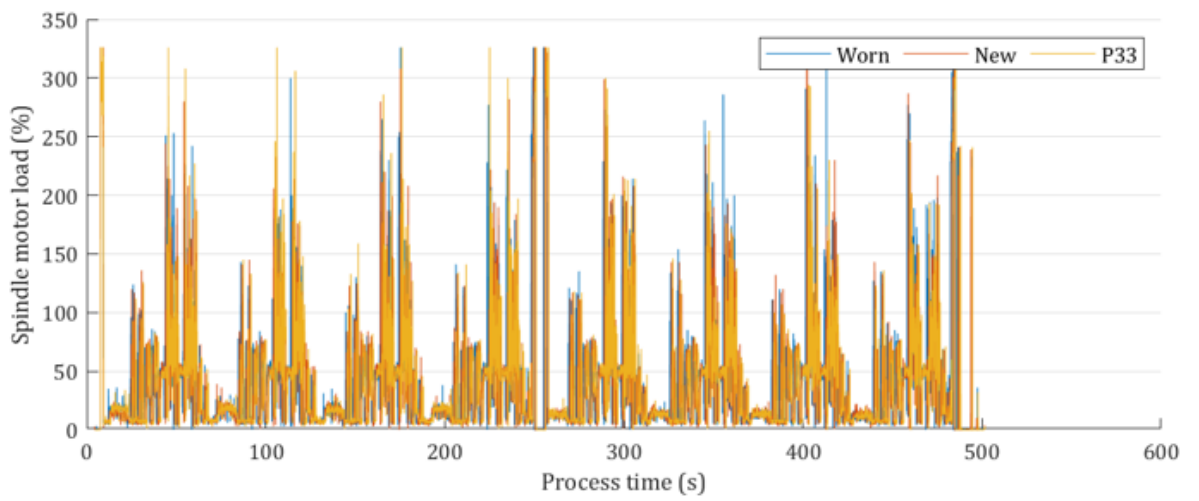
This Section presents a brief investigation into the MTData acquired for the OMI-bodies manufactured in the MMC. No direct measurements, nor observations, are available regarding the health of the cutting tools or the condition of the process. Therefore, the health of the cutting tools will be inferred from the differences between the processes completed using new and worn cutting tools where possible. This will further be deployed from the perspective of a closed system. In other words, any upper and lower thresholds will be derived from the available data, rather than taken from alternative sources.

#### **8.3.2.1 Cutting tool breakage**

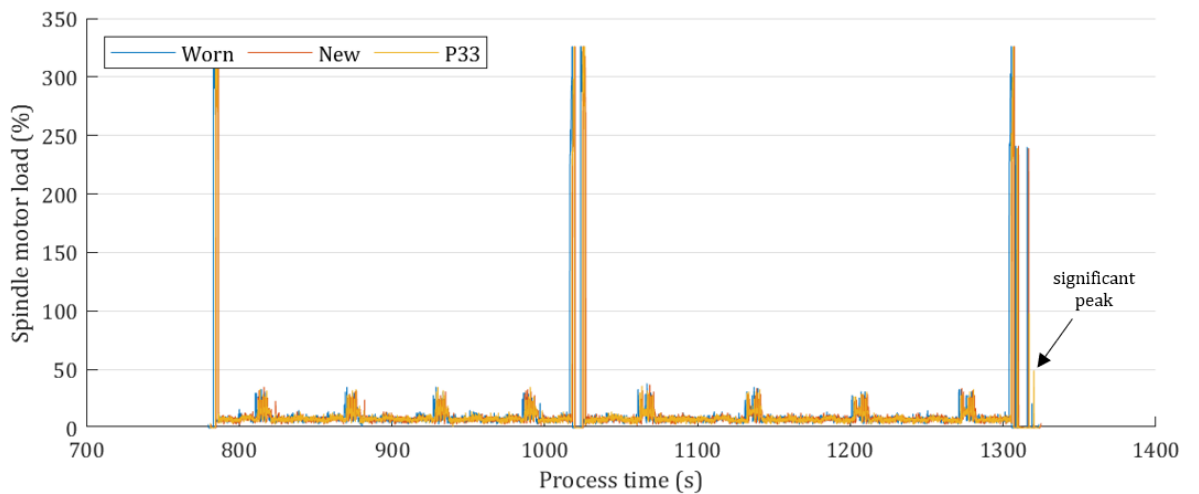
The MTData may be investigated to determine the effects (if any) of the H008 breakage on the cutting process. Figure 8.7 presents the SML signals for the three H008 cutting tools and compares a worn process, with a new process, and with the process for which a breakage occurred, process 33 (P33). Figure 8.7 indicates that the different process signals, for each cutting tool individually,



a. H008SD01 (T2)



b. H008SD02 (T3)



c. H008SD04 (T8)

Figure 8.7. SML plot to compare worn and new cutting tools with a potential breakage

are mostly comparable. T3 does not indicate any significant differences between any of the three included processes. This suggests that T3 did not fail. T2 indicates a reduced load just before 1440 seconds for P33; however, subsequent signals are equivalent to both the other included processes. This

suggests that T2 also did not fail. T8 indicates an additional SML peak to 50% at the end of the cycle for P33. This may indicate the failure of H008SD04. The signal is reproduced in Figure 8.8 for clarity. Figure 8.8 shows that the worn process also indicates a (smaller) peak at the same point in the process (offset slightly due to the time axis not being exactly in sync). This indicates a potential prior indication of the cutting tool failure (worn represents P32). The actual peak in the SML for P33 is to 50% which is significant versus the rest of the signal (except for the stop signatures). To verify this is associated with the breakage, the process G-code would have to be investigated to confirm what process is occurring. The existing on-machine breakage detection (using a TS27R) could also be utilised to confirm that T8 is the cutting tool that failed. It is noted that this challenge highlights the value in proper reporting on process events. A suitable report, or note, that the cutting tool failed would improve the traceability of the process, thus eliminating the guesswork required to identify the breakage and the potential consequences. If the data acquired does indicate the failure of one of the H008 cutting tools it shows that the signals are highly valuable and highly complementary to existing breakage detection technologies deployed in the MMC.

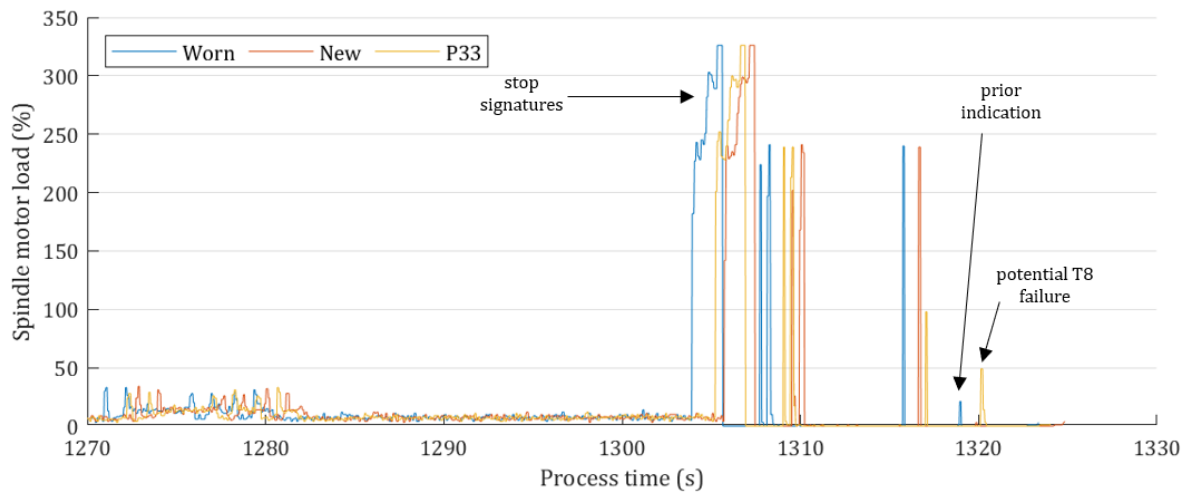


Figure 8.8. Final 60 seconds of the cutting process for T8 (possible cutting tool failure)

### 8.3.2.2 Instantaneous condition

One of the main objectives is to enable the accurate assessment of cutting tool condition in the context of current and imminent machining requirements. In response, concepts were presented in Chapter 7 showing the deployment of process position data to identify the cutting process, with additional MTData metrics included on the CAXIS to indicate the instantaneous cutting tool condition and general health. The same concepts will be included here to show the value in modelling the process for finding the instantaneous condition for a complex process. As the first 44 cycles did not acquire any position data, they will be omitted from any results presented in this Section. Figure 8.9 shows the full process, for all cutting tools, for an arbitrary OMI-body. This was generated using the DENSE program, introduced in Chapter 4 and included in Appendix A.3. The deployment of the process plots for indicating the instantaneous condition was outlined in Chapter 7. Figure 8.9 views the process in three orientations. This was enabled by the author manually by replicating the 3D process plot

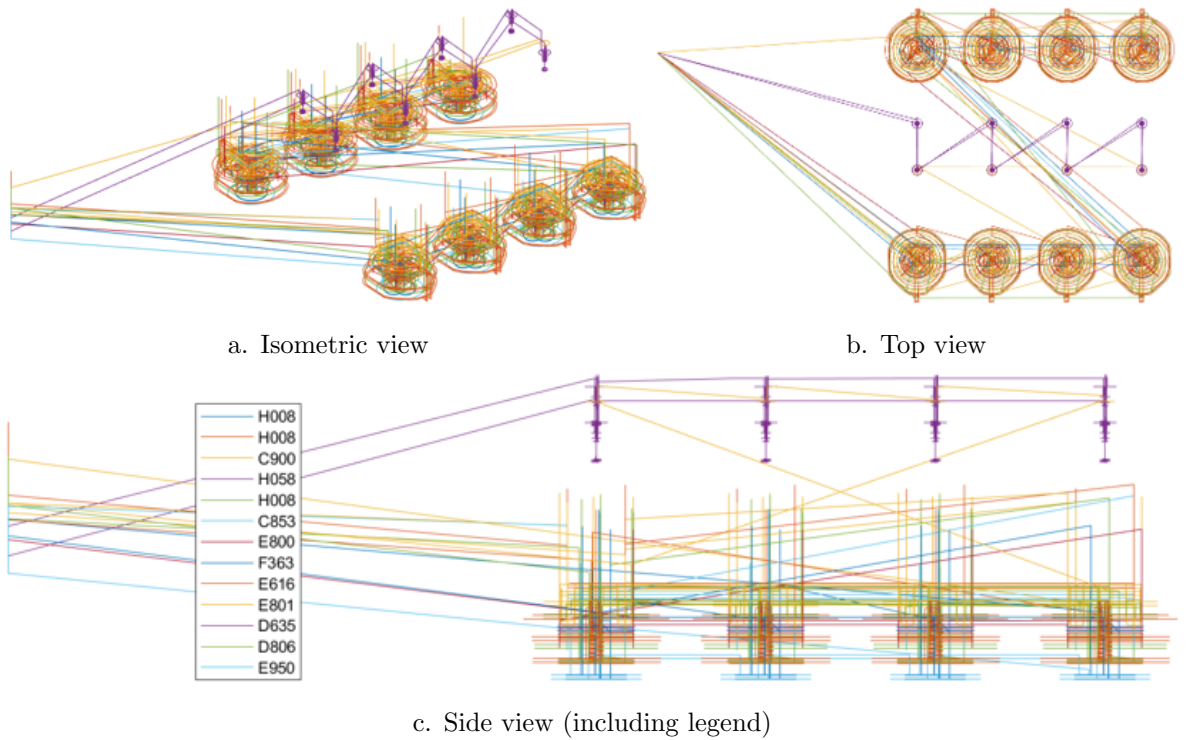


Figure 8.9. OMI-body process position data - all cutting tools (MMC)

three times and using the MATLAB `view()` function. Figure 8.9 shows that the process takes place in multiple locations. This is due to the wing fixture used, which can rotate to allow cutting access from multiple angles. This enables the cutting process to continue without needing an operator to rotate each component for machining complex features. To demonstrate how this information may be best used Figure 8.10 provides a process model for just the H008 cutting tools. This was enabled by the data being sorted and plotted according to the cutting tool deployed. The author enacted this to allow specific cutting tools to be filtered and plotted separately.

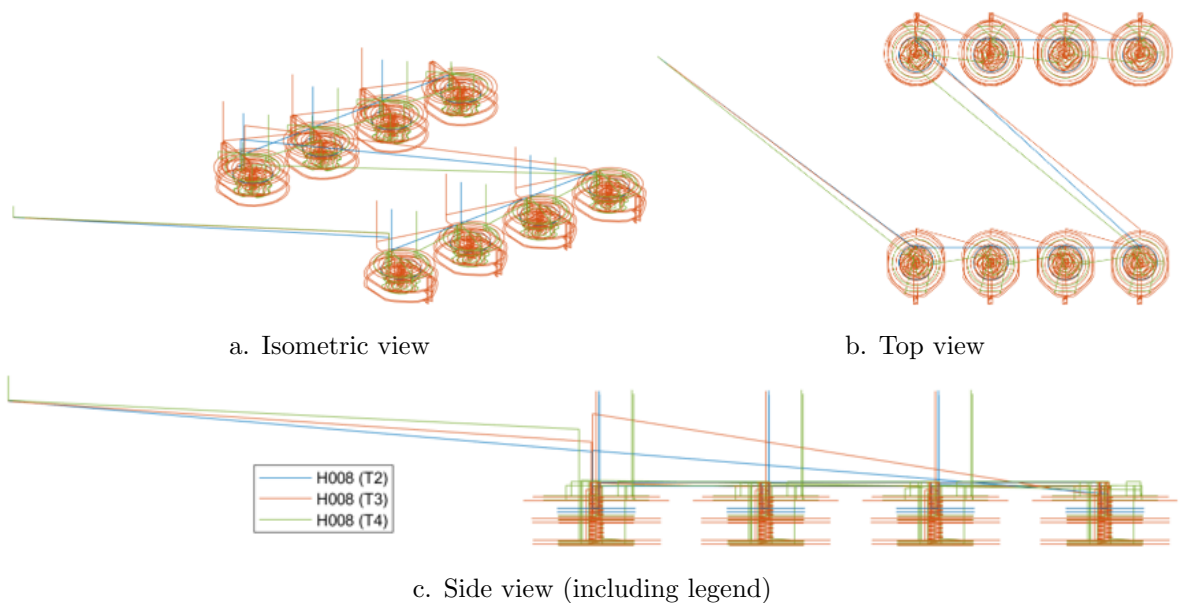


Figure 8.10. OMI-body process position data for only H008 cutting tools (MMC)

Figure 8.10 again views the process in three orientations. The figure shows that (visually) the process may be streamlined simply by considering only individual cutting tools at any one time. Figure 8.10 is noted to be remarkably similar in layout and pattern to the Cylinder application (see Chapter 5). This was not by design and has no effect (intended or otherwise) on the process data, the data acquisition, or the data processing. It should be noted that the cutting tool lengths have not been incorporated. Figure 8.9 would be affected as the cutting tools are of various lengths; however, here it is only provided for illustrative purposes. Figure 8.10 will not be affected as all three H008 cutting tools have the same nominal length. The plots may be revised, to indicate the instantaneous condition by employing various MTDData metrics on the CAXIS. An example is given in Figure 8.11. The figure is produced by deploying the process modelling developed by the author and incorporating the condition of the cutting tool as the fourth plot axis, also referred to as the CAXIS. The method developed by the author is outlined in Chapter 7.

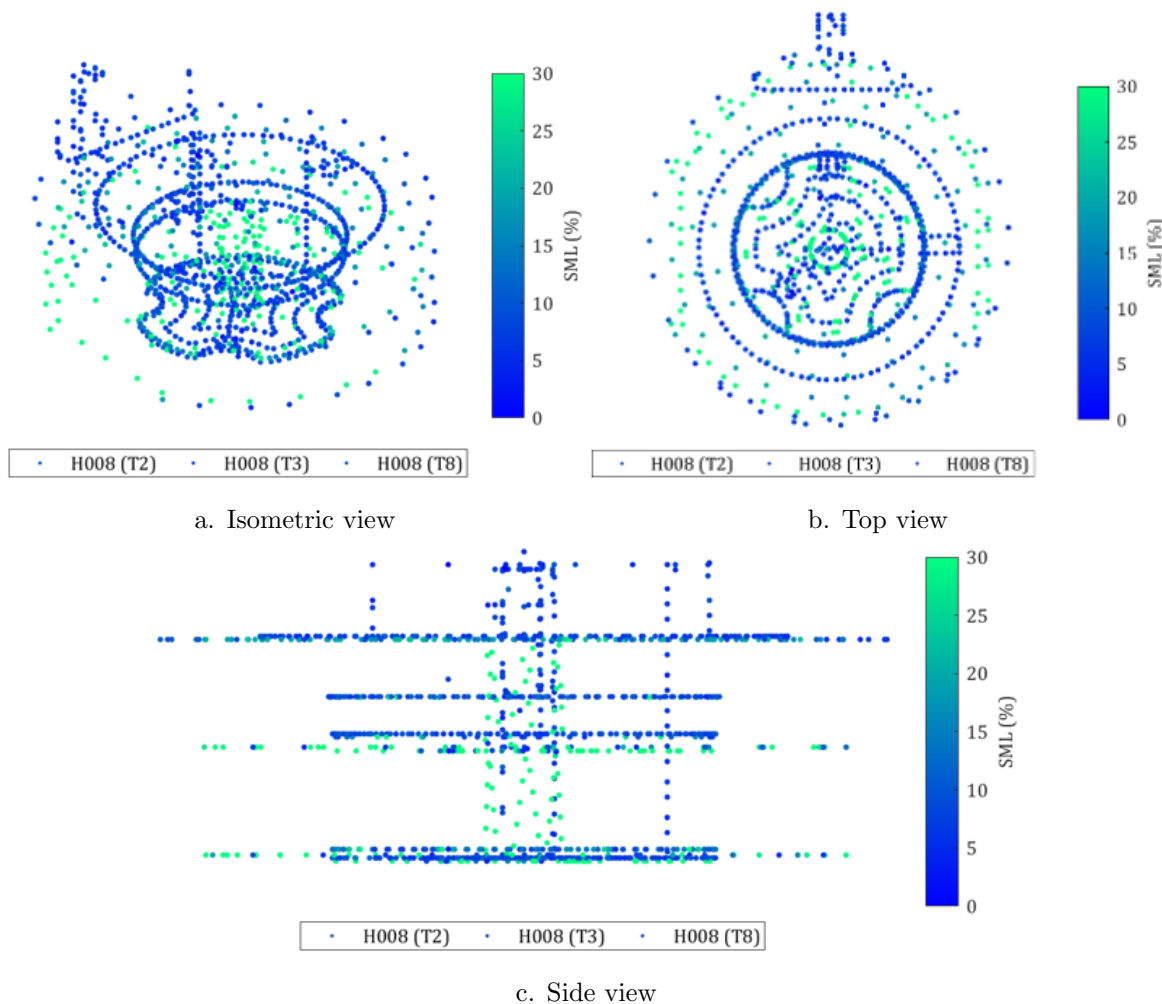


Figure 8.11. OMI-body process model for H008 indicating instantaneous SML (MMC)

Figure 8.11 shows that the finishing cuts (using T2 and T8) are notable as the slower feed rate results in less distance between points. This also highlights that the loads on T3 for the roughing process are higher than for the finishing process. This was also shown in Chapter 7 and indicates that when different cutting tools are used for roughing and finishing cuts, it may be easier to separate them and

consider the different processes separately. To infer the health of the cutting tools requires each to be evaluated in turn; however, to also infer the quality of the manufactured part (the workpiece), requires the cutting tools responsible for finishing cuts to be evaluated. The quality of the manufactured parts cannot be verified herein (being unknown). Therefore, the health of T3 (H008 responsible for roughing cuts) shall be considered as it should observe the greatest change between the first and last manufactured part (being monitored). Figure 8.12 compares the first and last OMI-bodies and shows that the differences between the first and last (monitored) OMI-bodies are subtle.

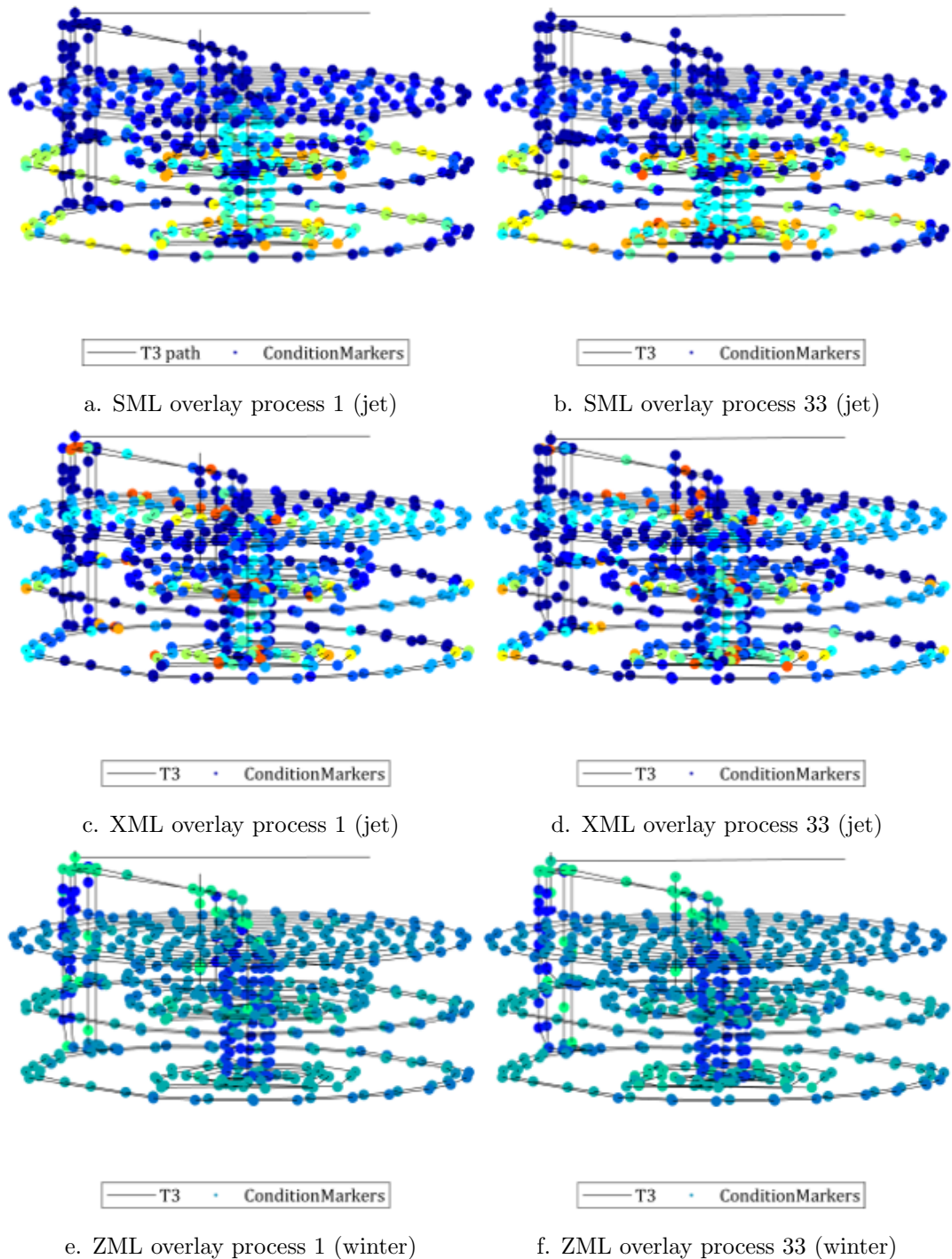


Figure 8.12. OMI-body process model for T3 comparing relative health using MTData overlays

It is noted that 256 parts have been machined between the two, observing that each cutting tool should be capable of machining approximately 530 parts (specified by Engineers from the MMC). This suggests that T3 is halfway through the life expectancy. As process 1 is not the first using T3, it is suggested that both of the OMI-bodies (process 1 and process 33) remain within the gradual wear phase of the cutting tool and thus differences should be subtle. Nevertheless, the fact that even subtle differences may be observed highlights the value of this approach in illustrating the relative condition (and thus health) of the cutting tool. The CAXIS is not explicitly provided as the plots are intended for direct comparison. The CAXIS for equivalent signals is fixed to be equal. The process generated models may also be used to show opportunities for process optimisation. Figure 8.13 shows that excessive loads occur during regions for which the volume of material removed is relatively low. The rotational speed also tends to peak in the same regions. This indicates that the process could be improved as these variations will put unnecessary stress on the spindle motor. This information may be used in conjunction with ICG data to better inform Engineers during later design stages and may enable further optimisation of machining processes. The CAXIS is again omitted as the exact magnitudes are not important; however, the CAXIS data is available in the Appendix. The regions noted in Figure 8.13 and the variation in both SML and SRS show evidence of the impact of pre-mill. This is discussed at length in Appendix B.

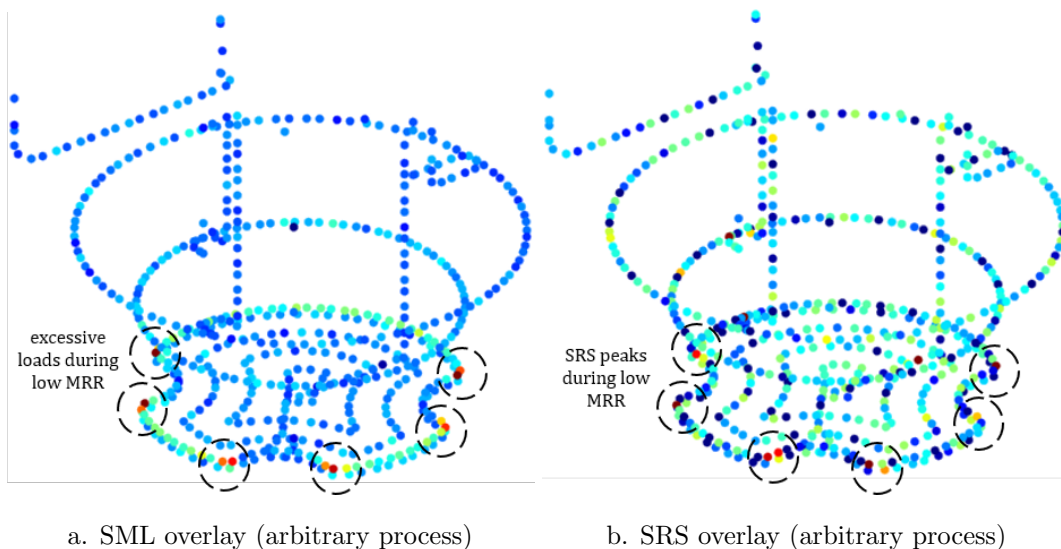
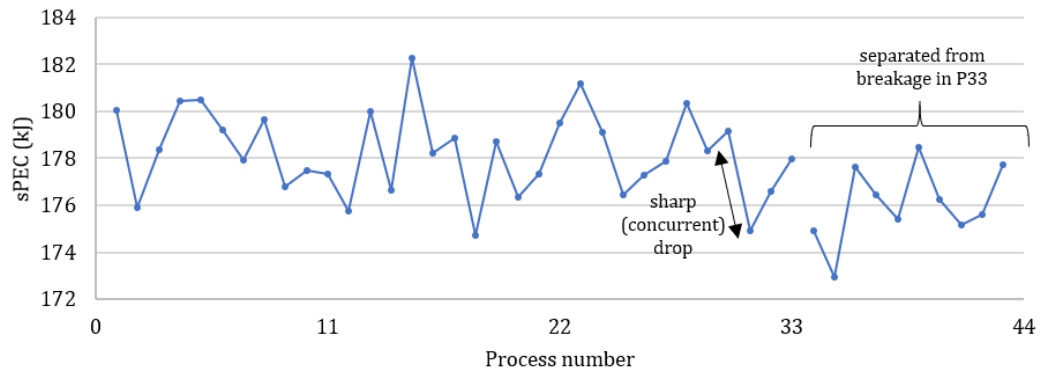


Figure 8.13. OMI-body process model for T8 showing potential process anomalies

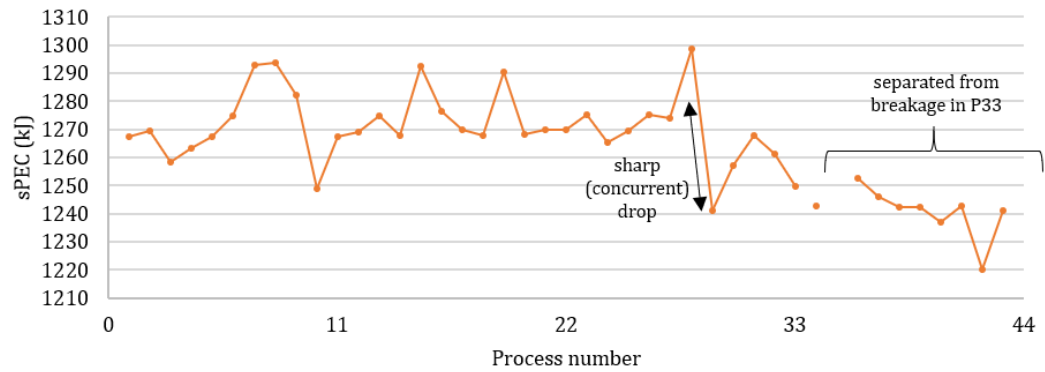
### 8.3.2.3 Spindle signals

The spindle signals may also be evaluated for their progressive value. That is, the change over time rather than the instantaneous conditions. The PEC can thus be determined for each process. The process for deriving the PEC is outlined in Chapter 4. Each process is herein representative of an entire wing (eight OMI-bodies). The separation of the data in this way was chosen entirely for simplicity. To separate each OMI-body would either require manual separation of each process, or a specialist program written to identify and sort each OMI-body. This was not considered a priority; therefore, the wings shall be considered as single entities. Both first and second batches of OMI-bodies may be

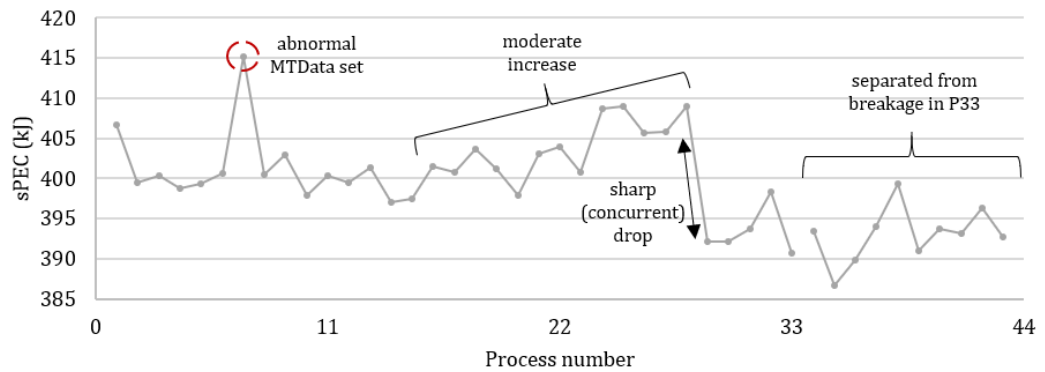
considered as the SML was acquired for both. Figure 8.14 gives the PEC trends for each H008 cutting tool (first batch) and shows that the abnormal MTDData set discussed in Section 8.3.1 is notable in the sPEC for T8. It is noted that T8 is employed immediately after T25 in the cutting process.



a. sPEC for H008 T2



b. sPEC for H008 T3

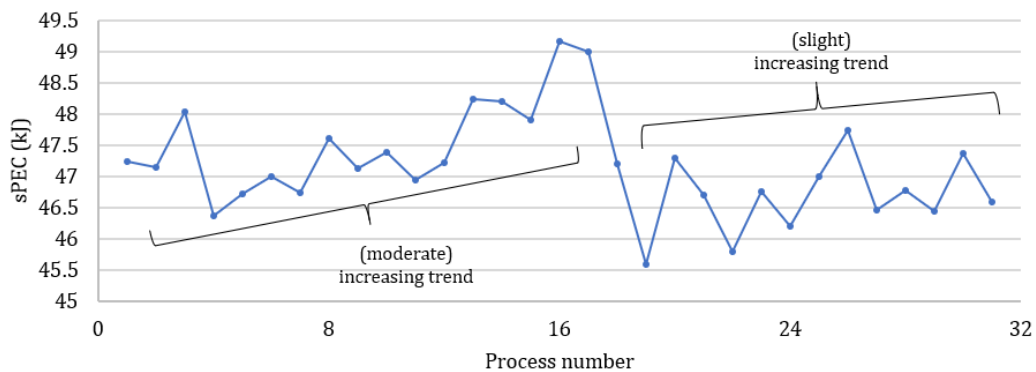


c. sPEC for H008 T8

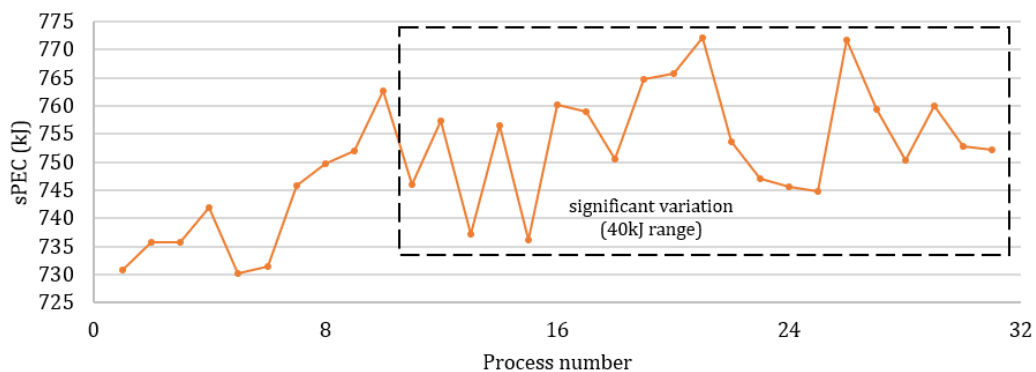
Figure 8.14. Spindle PEC trends for the MMC OMI-bodies (first batch, H008 cutting tools)

This suggests that the unknown problem during the use of T25 has impacted on the subsequent use of T8. The sPEC is 15kJ greater suggesting that T8 is working (approximately) 3.75% harder (assuming a local median sPEC of 400kJ). This raises further evidence that the abnormal process, and the excessive idling during T25, should be investigated. Also notable from Figure 8.14 is a sharp

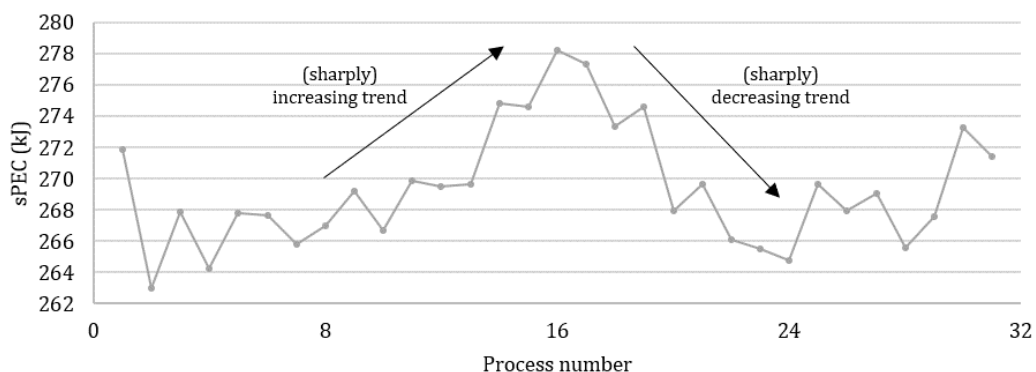
drop in the sPEC for all three H008 cutting tools. This occurs between processes 30 and 31, and suggests that either the process, or the cutting tools have changed. For T3 and T8 the subsequent sPEC magnitudes remain lower than before the drop, with T2 trending towards successively lower values. The reason for this change is unknown without additional information. The PEC trends for each H008 cutting tool (second batch) are given in Figure 8.15.



a. sPEC for H008 T2



b. sPEC for H008 T3



c. sPEC for H008 T8

Figure 8.15. Spindle PEC trends for the MMC OMI-bodies (second batch, H008 cutting tools)

Figure 8.15 shows that the three H008 cutting tools are behaving very differently. This is sensible as the three are not performing equivalent tasks. It is observed that for T2 the sPEC trends towards

greater magnitudes before dropping significantly between processes 17 and 19. The cause of this drop is unknown. The sPEC then continues to trend upwards from the lower magnitudes. The sPEC trend for T3 indicates a general upward trend, albeit more rapid earlier on and leading to significant fluctuations in the signal over a range of 40kJ during the later processes. This may suggest that the quality of the manufactured components should be investigated to confirm that this variation is not characteristic of the process quality. On the other hand, T8 indicates a sharply increasing trend in the sPEC, followed by an equally sharp decline in the sPEC (approximate change of  $\pm 4\%$ ). It should be noted that the sPEC values for the second batch of OMI-bodies are significantly lower than the sPEC values noted for the first batch of OMI-bodies. This is because the second batch was available with the full set of MTDData signals and could therefore be processed appropriately using the DENSE program. The first batch included only the SML signals with cutting time and the cutting tool number. This enabled the data to be appropriated to the specific cutting tools but did not allow the data to be suitably filtered to remove the stop signatures, rapid traverse movements, and other non-cutting signals. This evidences the value in acquiring key MTDData signals beyond just the SML. Earlier applications have shown the rotational speed to be complex in the raw form. However, the dispersion heat maps have proven to be an effective method for displaying the signal information. The SRS dispersion heat maps for the three H008 cutting tools are given in Figure 8.16 for the second batch of OMI-bodies. Annotations are included, but labels are omitted to avoid obscuring the images.

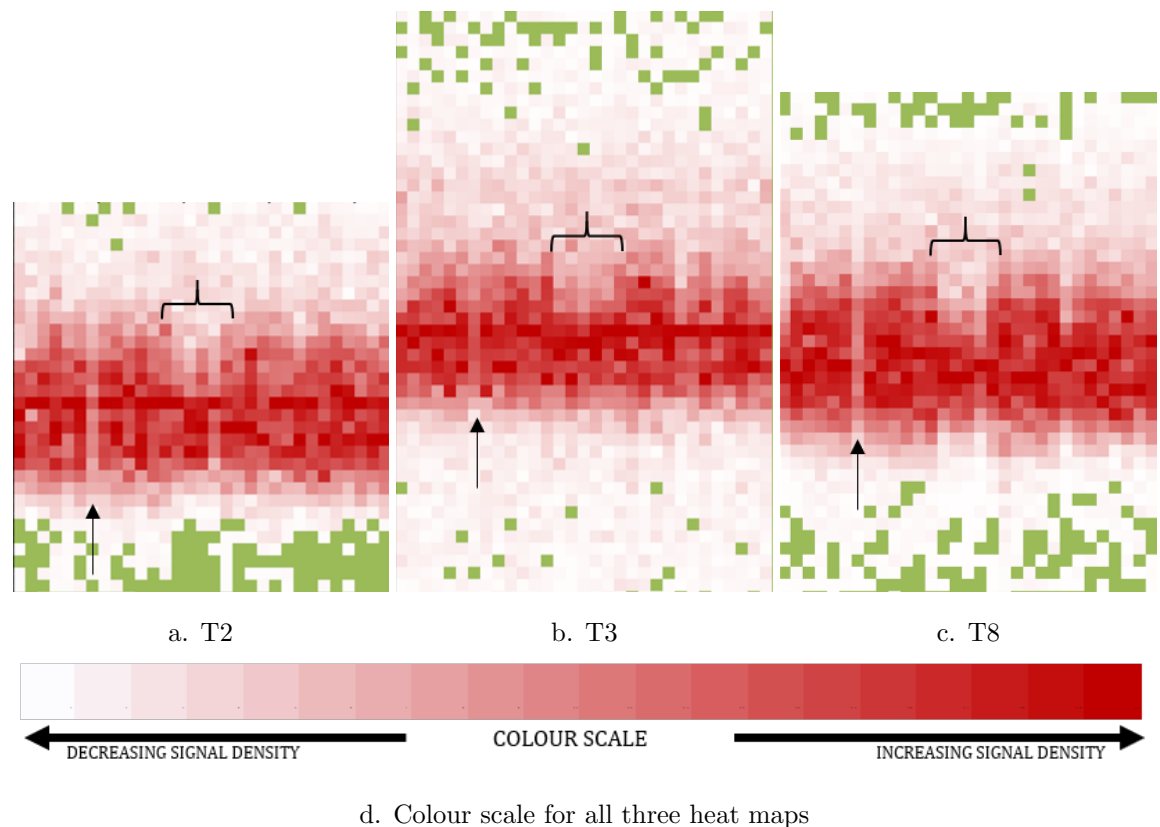
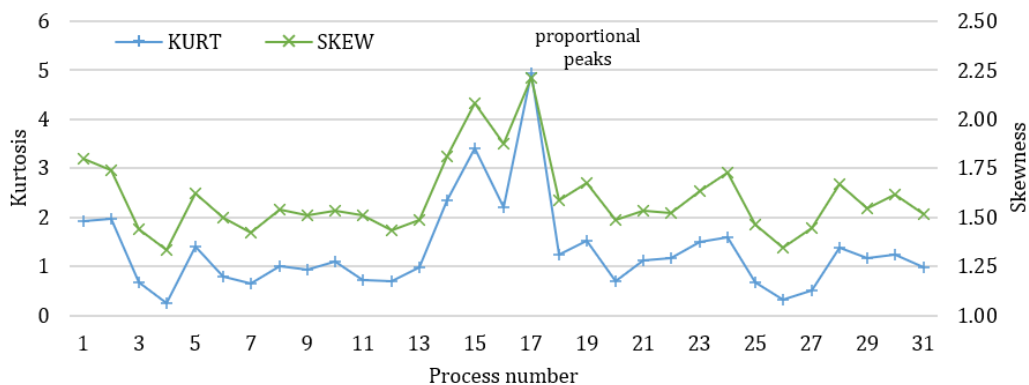
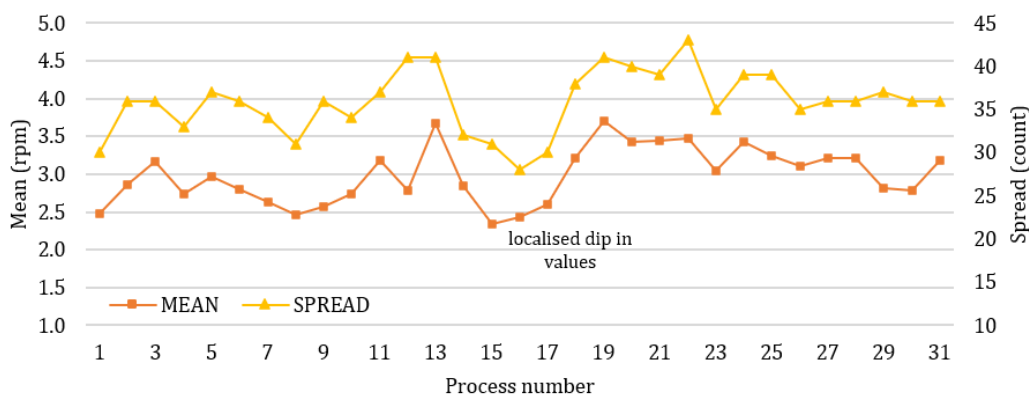


Figure 8.16. SRS dispersion heat maps for the three H008 cutting tools (second batch of OMI-bodies)

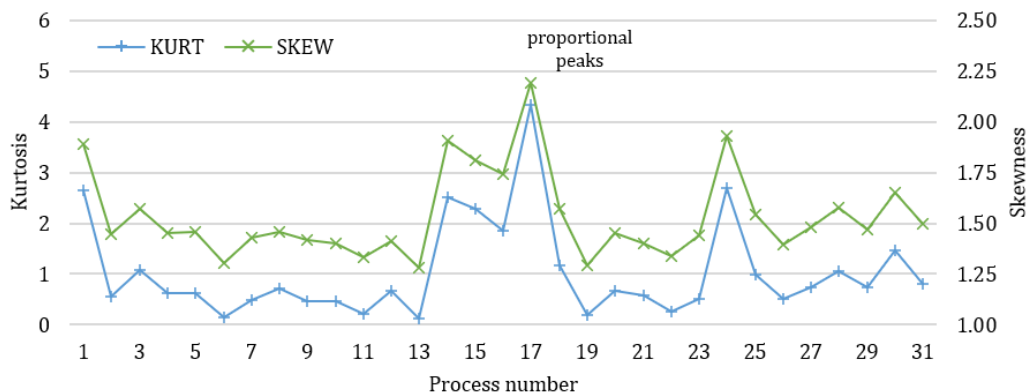
It should be noted that the resolution for all three dispersion heat maps is the same at 0.005rpm per pixel. This resolution was chosen arbitrarily to keep the figure a reasonable size. Figure 8.16 shows that the dispersion heat maps for the three H008 cutting tools show similar changes between processes. The similarities have been marked with similar annotations and show a discrepancy for the seventh process and a dip in the middle of each plot. These may be assessed by evaluating each dispersion heat map. Two sample statistics for each cutting tool are given in Figure 8.17. The statistics for all dispersion heat maps can be found in the electronic Appendix E.3.



a. Kurtosis and skewness trends for T2 SRS dispersion heat map



b. Mean and spread trends for T3 SRS dispersion heat map



c. Kurtosis and skewness trends for T8 SRS dispersion heat map

Figure 8.17. Trends in core statistics for the H008 SRS dispersion heat maps (MMC)

Figure 8.17 shows that (for the statistics provided) none of the plots indicate a discrepancy for the seventh process. This suggests that statistically it is not different. On the other hand, processes 13 to 19 (approximately) do note discrepancies. Both T2 and T8 behave in a comparable way with an observed increase in both Kurtosis and Skewness measures. As both handle finishing processes this may be sensible. T3 on the other hand does not see an increase in either Kurtosis or Skewness, but instead observes a drop in the SRS mean and spread. As T3 handles the roughing process, it may be that T3 is worn and thus removed less material. In response T2 and T8 had to remove more material. It is also noted that the SML peaks in a similar fashion suggesting that the slight drop in the rotational speed increases the relative load on the spindle. The SML dispersion heat maps (including statistics) are available in Appendix E.3. It is considered interesting that the three cutting tools have been found to behave differently, yet the visual effect on the signal consistency is similar. This again suggests that further research would be valuable to determine the nature of process variation on presented signals. It is appreciated that the sPEC plots and the dispersion heat maps include eight OMI-bodies per process. This was necessary to reduce the data processing needed. Nevertheless, this means that there is even more potential value within the data as the relative resolution of the plots may be improved if the OMI-bodies were distinguished. This has not been undertaken herein as the data processing already undertaken was considerable. However, it does present an opportunity for future research and development.

#### 8.3.2.4 Axis loads

The axis motors may also be investigated beyond their instantaneous effects as illustrated in Section 8.3.2.2. This may be approached by considering the PEC for each of the machine tool axes (X, Y, and Z); however, only the zPEC for T3 will be considered herein. The aim here is to demonstrate that the deployed approach achieves the intended monitoring aims. Further investigation into the information acquired lies outside of what was possible in this research programme. The PEC trends for all H008 cutting tools and for all axes can be found in the Appendix. Figure 8.18 provides the zPEC trend (second Y-axis) superimposed on the sPEC trend (first Y-axis).

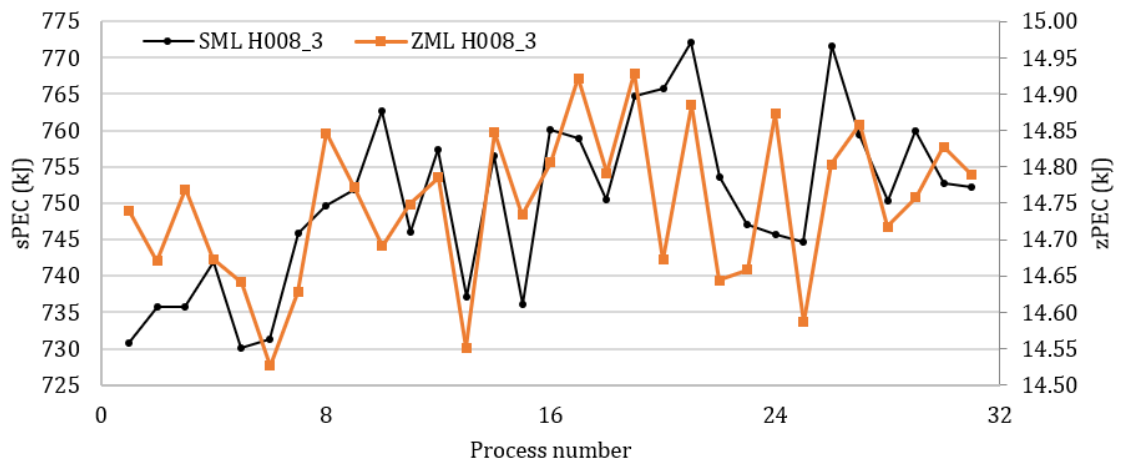


Figure 8.18. sPEC compared with zPEC for T3 (second batch) illustrative purposes.

Figure 8.18 shows that the zPEC corroborates some of the patterns noted in the sPEC signal for T3; although, it is noted that the Y-axis scales are hugely different in magnitude. The sPEC is plotted over a 50kJ range and the zPEC is plotted over a 0.5kJ range. Nevertheless, despite the obvious difference in absolute magnitude, the proportional variation is similar with similarities in the pattern and general signal trends. This suggests that the Z-axis motor signals may corroborate the spindle motor signals; however, to confirmation this theory would require significantly more investigation, including into the specifications of the axis motors (it is assumed here that they are equivalent to the VCS430A). The axis motor signals may also be considered using the developed dispersion heat maps. Figure 8.19 provides the XML dispersion heat maps for the three H008 cutting tools.

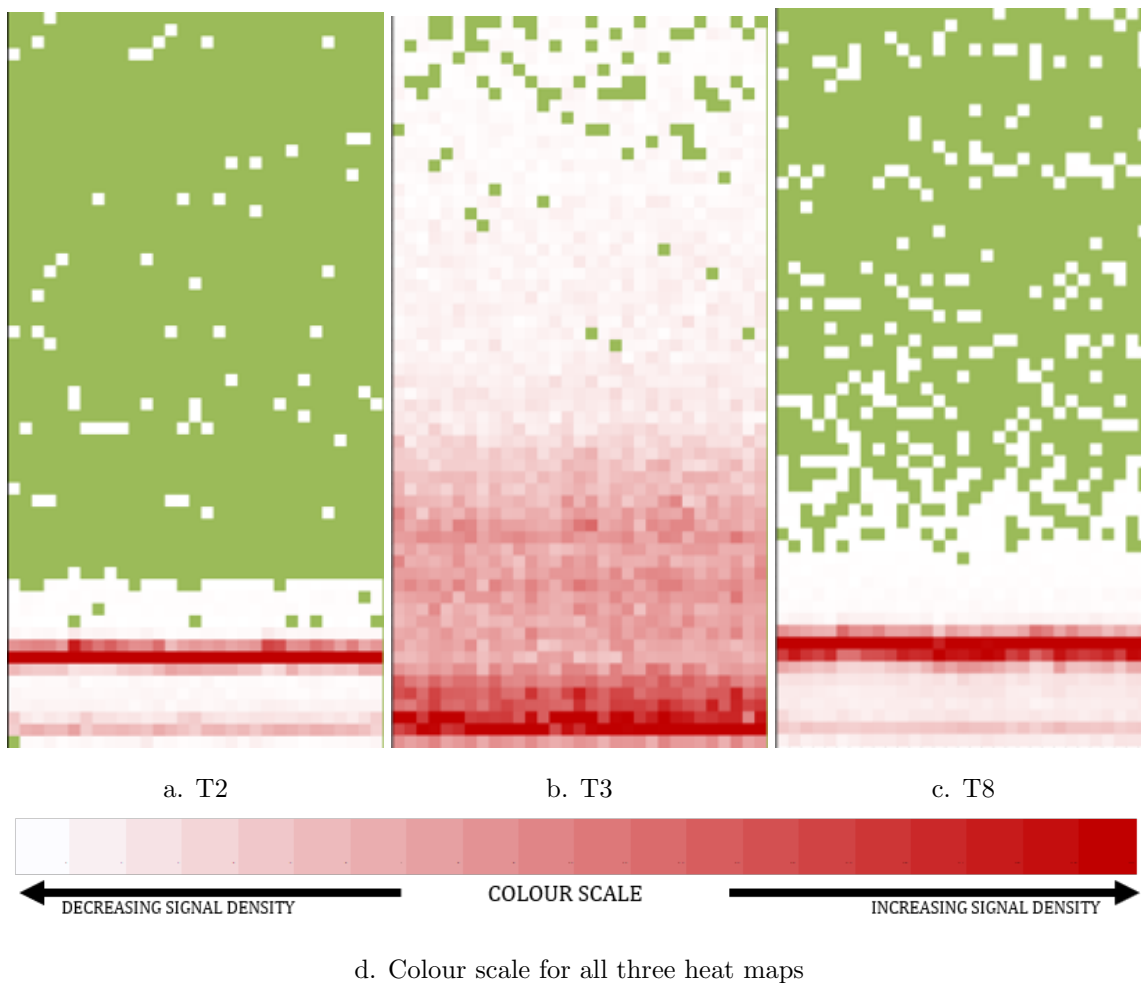


Figure 8.19. XML dispersion heat maps for the H008 cutting tools (second batch of OMI-bodies)

Figure 8.19 shows that the two H008 cutting tools (T2 and T8) responsible for the finishing processes are similar, whilst T3 - responsible for the roughing process - is quite different. However, it is noted that the statistics for T2 and T8 are not comparable, suggesting that in general the two processes are similar but implicitly they differ significantly. This would be a sensible observation as whilst they are both employed for finishing cuts, the actual processes completed by each is quite different. Figure 8.19 also shows that the lower threshold is notable, as separately noted for the VCS430A in Section 8.2. For the VCS430A this corresponded to the underlying machine tool vibrations and the compensation

for no axis brake. It is suggested that the same applies here to the VCN530C; however, again the specification of the axis motors should be confirmed.

It is reminded that the dispersion heat maps have been intentionally simplified to treat every eight OMI-bodies (one wing) as a single process to reduce the necessary processing of the data. It may be considered that there is value in separating each OMI-body to better understand the subtle changes in the condition of the cutting tools used. Further separation would also help to establish the variation within each process and the potential differences between the eight OMI-bodies on a single wing. This is an opportunity for future research and development and is not undertaken herein. It is noted that the dispersion heat maps for the remaining axes (Y and Z) along with all plot statistics can be found in the electronic Appendix E.3.

## 8.4 Challenges and next steps

This Chapter used the OMI-body application to close the loop in the research and development of management strategies for cutting tools. The OMI-body investigation provided explicit evidence of the value of the work developed throughout this research when applied in a high-volume (commercial) manufacturing environment. The developed systems were deployed in the MMC and focussed on the manufacture of a component from an important product range from within the partner company. This gave access to real life manufacturing at high levels of production.

It has been shown that the acquired data is valuable for showing the condition of the cutting tools presented. It was shown in a laboratory setting that there were differences between the presented cutting tools. However, it was demonstrated that the limited testing made it hard to draw reliable comparisons. It was later demonstrated from deployment in the MMC that all acquired MTData signals are potentially valuable. This was emphasised when several of the initial tests acquired only the SML (deliberately for testing purposes). It has been shown that it is possible to identify the instantaneous condition based on current and imminent machining using 3D process plots and overlaying key MTData attributes using the CAXIS. This built on the initial development of the approach shown for the Con-rod application. It was also shown that there was value in the overall process signals, illustrating variation between processes and illustrating those that would benefit from further investigation.

The implementation did identify a number of challenges. The health of the cutting tools could not be explicitly inferred from the generated information due to the restricted information available about the process. This highlighted that more of the basic information about a process would be necessary to reliably determine how the observed conditions relate to the health of each cutting tool. Such information could easily be made available and is information needed by the current methods for determining and monitoring dimensional performance (tool-setting, tool breakage detection, and ICG). With such information the approaches presented in this thesis will dovetail and be complimentary to these approaches.

## 9 | Discussion

It cannot be denied that Industry has progressed towards smarter manufacturing and a degree of condition-based monitoring. The current state-of-art of Industry, machine tools, cutting tools, the machining process and cutting tool condition monitoring has progressed rapidly in the last decade with significant contributions from both academics and manufacturing organisations. However, this research has shown that effective implementations of such systems and ideas are currently severely limited, with industry specific solutions for active TCM and tool/process prognostics still highly desirable. It was further evidenced that gaps remain in the current state of research, with investigations often frustrated by exaggerated wear detection, accelerated modes of cutting tool wear and laboratory-based solutions that fail to appreciate the necessary changes needed for commercial implementation.

These deficiencies mean that cutting tools are still the weakest link in the manufacturing process and heavily impact on the process economy, with high costs for SMEs estimated to be measured in terms of millions of pounds per annum. It is also the case that cutting tools continue to hinder both the automation and sustainability of the machining process. In the review of the state of art conducted for this research current industrial approaches were determined to be conservative and further improvements were considered possible and necessary. It was determined that a unique perspective was needed. The one adopted in this work enabled optimised management of cutting tools based on the efficient use of smart process data acquired from machine tool architecture. This tacit knowledge, relating to the management and control of specific cutting processes, was shown to enable smart operations and also enable access to process information without demanding significant alteration to the system or process. This is unique as most other systems require significant space for the necessary sensors and systems and often need the process to be taken offline for an unnecessary length of time for installation.

It has been proven that there is significant value in the MTDData acquired throughout this study. The data was used to show the condition of the cutting tools deployed based on current and imminent machining requirements. It was also used to estimate the RUL of specific cutting tools and to model the process to enable Engineers to improve the cutting processes and to enable the assessment of cutting tool condition and life. Numerous systems, programs and algorithms were developed through the course of this research project through the deployment of four applications. These are briefly discussed in the following paragraphs.

The Cylinder application presented exaggerated deterioration of the cutting tool through the manufacture of cylindrical pockets. The reducing diameter of the pockets and the key surface finish metrics (including RzDIN, RzISO and the novel RzNOV) were shown to indicate the general state of the cutting tool condition. These were correlated with the SML signals gained from the machine tool controller and proved that the SML was capable in lieu of the physical feature measurements for

indicating the condition of the cutting tool and of the process. It was further shown that the SML could be converted into the PEC. This was shown to be as good as (and in some instances better than) geometry and surface finish metrics at estimating the RUL of the cutting tool. The developed CCPD algorithm was shown to be effective at calculating the changes in the condition of the cutting tool by determining each meaningful change in the gradient of the process signal. These change points were mathematically calculated and shown to be able to determine the changes quantitatively and objectively. This did not rely on the opinion of the operator or any other third party. This is an improvement over qualitative, or opinion-based approaches as the changes cannot be different, or variable, when attempted by different individuals. A limitation of the CCPD algorithm was the deployment of a cubic for the process model. It was shown that the cubic was slightly unstable and that alternatives should be sought to improve the method.

The Slotting application considered a simplification of the cutting process to draw the value from each of the axis loads. The application enabled the axis loads to be evaluated in depth and allowed the condition of the cutting tool to be the dominating factor in the signal variation. It was noted that, like the Cylinder application, the PEC indicated the general deterioration of the cutting tool. However, the quantised nature of the data was more pronounced because there were fewer observed changes and less overall noise in the signal. It was shown that the axis signals had value in complementing the SML and the PEC. Novel Dispersion Heat Maps were developed by the author and illustrated that the tacit nature of a complex signal may be considered easily. The dispersion heat maps enabled an increased awareness of the internal composition of each axis signal and of the SRS. This enabled the general condition of the cutting process to be inferred, as well as the possible deterioration of the cutting tool and potential process anomalies. The dispersion heat maps effectively established the value in each of the axis loads and also indicated the implicit value in the SRS for indicating the cutting tool condition, despite the signal being manipulated by the machine tool controller.

It was acknowledged that both the Cylinder application and the Slotting application were (and are) limited by their simple processes and the disconnect between the application and commercial processes was noted. There was only one cutting tool employed for each test and the process was developed to enact exaggerated wear on the cutting tools. The use of a single cutting tool prevented any insight into the interaction between different cutting tools and did not enable any investigation into different wear modes for cutting tools taking on different processes. The methods created are beneficial for the interpretation of future process signals. However, it was also noted that they were developed based on two uncomplicated processes, using a single cutting tool and with relatively aggressive cutting regimes designed to exaggerate the wear on the cutting tool. They were designed to simplify the results and the processing stages, rather than to represent a practical, or entirely realistic process.

The Con-Rod application bridged the gap between the previous two laboratory investigations and true commercial manufacturing. The Con-Rod application was established to explicitly test the limitations of the developed systems by including multiple cutting tools and introducing roughing cuts separate from finishing cuts. It was shown that significant changes to the cutting process dominated the

observed variation in all process signals. This supported the evidence provided throughout this work that the analysis of the different processes should be kept separate, even if the differences are small. This should enable any variation attributable to the changing condition of the cutting tool to be more explicit and easier to prove.

It was also shown that the resolution of the MTData was an issue. This was more significant for certain cutting tools and for certain processes. Increasing the resolution of the motor load signals (spindle and axis loads) would be beneficial. However, acquiring more information is itself challenging as this would require further data processing and would add to the already challenging task of acquiring and storing the MTData securely and efficiently. It may also increase the noise in an otherwise noisy system. It is also appreciated that increasing the sampling frequency would be equally beneficial. It is unlikely that increasing both would be feasible without significantly affecting the operation of the machine tool. This was confirmed in discussions with the machine tool manufacturer, Mazak. Therefore, the need to increase the data resolution should be weighed against the potential benefit of increasing the data sampling frequency.

The Con-Rod application illustrated that the dispersion heat maps were valuable for corroborating similar processes, despite distinct differences in the cutting stages. The dispersion heat maps further indicated the deterioration of both the worn and the new cutting tools employed. However, it was shown that there needed to be more data and further separation of the different cutting processes is necessary. The instantaneous condition of the cutting tool was shown through innovative 4D process plots, with key health metrics shown on the CAXIS of 3D models derived from the cutting process. The process plots illustrated the capability of the position data to be exploited in combination with useful MTData metrics. This was shown post-process but could be applied actively using the procedure written and developed by the author to plot the data as it is acquired in real time. The position data was shown to be very useful. Like the 3D geometry plots, the position data is a useful resource for providing process feedback during the cutting process. For systems employing ICG, physical measurements may be combined with the position feedback, thus providing engineers with a smart combination of condition-based data during the manufacturing process.

Lastly the OMI-body investigation was presented to close the loop in the research and development of management strategies for cutting tools. The OMI-body investigation provided explicit evidence of the value of the work developed throughout this research when applied in a high-volume (commercial) manufacturing environment. The developed systems were deployed in the MMC and focussed on the manufacture of a component from an important product range from within the partner company. This gave access to real life manufacturing at high levels of production.

It has been shown that the acquired data is valuable for determining the condition of the cutting tools presented. It was shown in a laboratory setting that there were differences between the presented cutting tools. However, it was determined that the limited testing made it hard to draw reliable comparisons. It was later demonstrated from deployment in the MMC that all acquired MTData signals are potentially valuable. This was emphasised when several of the initial tests acquired only the SML

(deliberately for testing purposes). It has been shown that it is possible to identify the instantaneous condition based on current and imminent machining using 3D process plots and overlaying key MT-Data attributes using the CAXIS. This built on the initial development of the approach shown for the Con-Rod application. It was also shown that there was value in the overall process signals, illustrating variation between processes and illustrating those that would benefit from further investigation.

Nevertheless, the implementation did identify a number of challenges. The health of the cutting tools could not be explicitly inferred from the generated information due to the restricted information available about the process. It is noted that more basic information would be necessary to reliably determine how the observed conditions relate to the health of each cutting tool. Such information could easily be made available and is information needed by the current methods for determining and monitoring dimensional performance (tool-setting, tool breakage detection and ICG). With such information the approaches presented in this thesis will dovetail and be complimentary to these approaches.

There were also indications that reground cutting tools behaved differently to new cutting tools, despite them being treated as new. This could only be investigated during the laboratory-based testing as during testing at the MMC, being a grey box, the nature of, or origins of, each cutting tool was unknown (related to the previous challenge). There were also reports of a cutting tool breakage. This information was acted on to illustrate potential indications within the MTData signals; however, again the lack of effective reporting limited the investigation making it impossible to verify the observations.

It should be stressed that the lack of data is not a wider issue and instead illustrates one of the potential challenges with implementing monitoring systems within commercial manufacturing centres. Unless there are robust systems to maintain process traceability the use of any generated data is limited. It is perhaps ironic that the evaluation of such a significant volume of process-generated data is hindered by a relative lack of process data. Nevertheless, it is fully anticipated that complete and proper integration of this (or a similar) system within the MMC would not face this challenge in accessing process information.

It has been consistently stated that further work and further research would be necessary to extract the most benefit from the acquired signals. This is due to the significant volume of data acquired. Whilst the author has put a considerable number of hours into the processing and analysis of the available data, it is impossible (within the available time) to assess it all. This illustrates the value in separately proving systems and processes in a laboratory and away from the high-volume manufacturing environment. To begin at the MMC with this amount data would have been overwhelming.

## 10 | Conclusions and future opportunities

This thesis considered five distinct objectives. The first was to consider the current understanding and state-of-art of both academic and commercial innovations with respect to Industry 4.0 enabled manufacturing and cutting tool condition monitoring. This was met in Chapter 2 and was further discussed in Chapter 9. The second objective was to design and test a prototype monitoring system capable of acquiring control data from a modern machine tool. The third objective was to develop concept software capable of evaluating process data to identify the cutting process and the instantaneous cutting tool condition or general health. These objectives were covered in Chapter 3, Chapter 4 and Chapter 5. It was proven that the developed system was feasible and it was established that such approaches have intrinsic value, with the data acquired having high value. The proposed algorithms, including CSAM, DENSE and CCPD were developed with explicit consideration for the potential uncertain nature of the data employed. The tacit value in the data signals was established through the three algorithms and with the addition of dispersion heat maps in later chapters. Data that had less value for enabling cutting tool condition monitoring was intelligently filtered from the data and archived for future research and development. The fourth objective was to investigate any acquired process information to identify the likely sources, causes and ramifications of the data in terms of the cutting tool health, cutting tool or process diagnostics and cutting tool or process prognostics. This objective was covered in Chapter 6 and Chapter 7. It was shown that the developed systems could differentiate between processes and could show variations attributable to the cutting tool health. However, it was also evidenced that wider process knowledge was necessary to draw the most value from the acquired data. Further processing would be of further benefit to better establish the cause of variation in the data and top reduce the uncertainty. The final objective was to establish the efficacy of the developed systems. This was concluded in Chapter 8, showing that it was feasible to apply the developed concepts to a commercial manufacturing process. This established that the developments were robust and had been effectively managed in order to translate them from controlled laboratory-based conditions through to the relatively aggressive environment of industrial manufacturing.

It is noted that an appreciation has been shown for the necessary stages required to take a laboratory-based concept through to commercial use. This was shown through Chapter 5 through to Chapter 8. This thesis considered options for active TCM and tool/process prognostics targeted specifically towards practical or commercial applications. These were developed and tested extensively during a laboratory-based formative process and were eventually installed within a true manufacturing environment. Each development step was crucial for establishing a robust, reliable and accurate prototype system that could be commercially viable. The key advancements from each development step are summarised in the following paragraphs:

**Cylinder application** - The reducing diameter of the pockets and the key surface finish metrics (including RzDIN, RzISO and the novel RzNOV) were shown to indicate the general state of the

cutting tool condition. These were correlated with the SML signals gained from the machine tool controller and proved that the SML was capable in lieu of the physical feature measurements for indicating the condition of the cutting tool and of the process. It was shown that the SML could be converted into the PEC. It was concluded that this was as good as, and often better than, geometry and surface finish metrics at estimating the RUL of the cutting tool.

**Slotting application** - Explicitly proved the value in each of the axis loads. It was shown that each had value in complementing the SML and the PEC. Novel dispersion heat maps were developed by the author and enabled the implicit nature of complex signals to be illustrated. It was concluded that the dispersion heat maps effectively demonstrated the value in each MTData signal considered.

**Con-Rod application** - Bridged the gap between the previous two laboratory investigations and shifted focus towards commercial manufacturing. The Con-Rod application illustrated that the dispersion heat maps were valuable for corroborating similar processes, despite distinct differences in the cutting stages. The dispersion heat maps further indicated the deterioration of both the worn and the new cutting tools employed. However, it was concluded that more data and further separation of the different cutting processes is necessary. The instantaneous condition of the cutting tool was demonstrated through innovative process plots, with key health metrics shown on the CAXIS of 3D models derived from the cutting process. It was concluded that the position data was highly useful and was utilised for more in-depth investigations into the impact of small cuts, given in Appendix B.

**OMI-body application** - Proved the concept beyond “ideal” or “formative” conditions. The OMI-body investigation provided explicit evidence of the value of the work developed throughout this research when applied in a high-volume (commercial) manufacturing environment. It was shown that the novel 3D process plots were able to identify the instantaneous condition of the cutting tools. The OMI-body investigation also evidenced the value in effectively documenting the machining process, ensuring that details are available when a cutting tool fails unexpectedly, or when an operator intervenes in the cutting process. It was concluded that the MTData was capable of indicating such events; however, it was determined that greater value would be gained if this information was used to complement data from other in-process sources (such as ICG or operator reports).

The novel systems developed by the author have significant individual value for determining the current and imminent condition of the cutting tool and of the cutting process. They have even more value when considered in complement with the current methods for determining and monitoring dimensional performance (for example: tool-setting, tool breakage detection and ICG). At present these technologies are widely deployed to provide process monitoring in manufacturing organisations. Collection of MTData from the controller of the machine tool will dovetail and be complimentary to these approaches. The deployed approach will thus enable researchers to engineer machine systems that can provide more accurate, reliable and repeatable machine operations, with less waste and better managed processes.

## 10.1 Research contributions

This thesis has presented innovations that will enable the accurate assessment of cutting tool condition and life in the context of current and imminent machining requirements. Further detail on the notable contributions by the author are outlined below:

- Investigated the complexity of the enactment of a cutting process on a modern machine tool and identified the likely sources, causes and ramifications of the available information arising from such complex systems. No similar investigation has been attempted previously.
- Developed a prototype monitoring system capable of acquiring control data from a modern machine tool. The derived system proved that the concept is feasible and established that the approach has value for gaining access to control data without impacting on the manufacturing process or capabilities.
- Derived a novel set of equations for determining the geometrical condition of circular manufactured parts (CSAM). This was based on the actual versus the nominal cross-section of the features. The cumulative magnitude change in the cross-section enables the progressive deterioration to be modelled, with proper impact accredited to sudden or significant process variation.
- Developed a novel method for processing CMM scanning data to build a 3D model of the feature with visual representation of the geometrical inconsistencies. The prototype implementation was written in the MATLAB environment.
- Reverse-engineered the percentage spindle signals to gain access to the spindle energy. This enabled an indication of the relative effort required during subsequent machining operations on separate machines and thus indicated the condition of the cutting tool and the cutting process.
- Developed concept software capable of evaluating process data to identify the cutting process and the instantaneous cutting tool condition or general health. The innovative DENSE algorithm considered the relative density of the machine tool coordinates and thus stripped the process of all non-cutting movements. This significantly improved the accuracy of later modelling and processing systems.
- Provided explicit mathematical evidence of the similarities between the geometrical condition of manufactured parts, the surface finish of manufactured parts and the process energy consumed manufacturing parts.
- Derived a novel method for mathematically determining the changing state of a process when modelled using a 3rd order polynomial representative of the general wear curves. The CCPD algorithm provided p-fit and e-fit curves enabling the state of the cutting tool to be attributed to each of the established wear stages, including new, used, worn and failed.
- Developed novel “dispersion plots” by calculating the MTData density spectrum per part and overlaying this information over the original MTData signal.
- Developed novel 3D process plots using implicit control data. By modelling the process move-

ments with an overlay of the process conditions it was shown that the instantaneous condition could be observed. This approach for modelling the process has not been attempted previously. The use of high-value process data for the fourth plot axis is a further novel addition.

- Installed the developed systems within a commercial manufacturing environment. The system was installed for a high-value component and identified that the developed systems were robust, valuable and could contribute significantly to the management of cutting tools and for generic process monitoring and modelling.
- Conducted a significant investigation into the impact of small cuts on the machining process. It was established that the information acquired from a cutting process may not explicitly inform engineers of the health of a process, but rather that the process is simply occurring. This contribution enables engineers to properly appropriate health features to their source.
- Established an ongoing collaborative project between the partner company (Renishaw) and the machine tool OEM (Mazak) entirely based upon the installation and operation of the system devised by the author.

## 10.2 Future development

### Incremental

Whilst a significant amount of the work establishing the monitoring approach has been completed, it is appreciated that opportunities still remain for future research endeavours. More research is necessary to understand the complexity of modern machine tools and vertical machining centres. This would require a more in-depth investigation into the interaction between systems within the machine tool. For example, how the vibrations of individual axes may affect the signal readings at other axes and the spindle. As all components of a machine tool are effectively connected, the interactions between components will be present within the MTDData. These interactions should and could be established to improve the accuracy and reliability of any monitoring system.

In addition, certain processes may be investigated for use in optimising condition-based maintenance strategies for the machine tool. Valuable MTDData signals for this includes the idle (non-cutting) axis loads and the spindle stop signatures. Such signals were noted to be repeatable for individual machines yet differed between machines. This suggests that they could, with further work, be used to generate baseline health indications for machine tool components such as spindle or axis motors. This would increase the possible applications enabled by this and similar systems.

Regarding the systems developed herein, most represent proof of concept and therefore there is value in further developing, improving and/or combining the approaches. For example, the developed CCPD algorithm for estimating the remaining useful life of the cutting tool needs further improvement to make it applicable to more complex and variable processes. This would require a shift away from the deployment of a third order polynomial and instead consideration of more stable models, for example Weibull. In addition, the post-process systems, including the DENSE algorithm and the 3D process

plots, could be further developed to better enable their use in-process. This would require their incorporation into the PAc acquisition program. It is very encouraging to report that the machine manufacturer has been provided with the means to replicate the installed system and is thus engaged in progressing the application of this research. This will be initially within the partner company but could lead to further implementations.

## **Horizon**

It is also expected that the systems developed herein could reasonably be integrated within future smart machine tool controllers. This would be valuable to machine tool manufacturers looking to improve their product capabilities and to further enhance their Industry 4.0 offerings. This would further reduce the impact of installation and enactment of such systems on the operation and availability of machine tools and would negate the need to have one (or many) dedicated PCs on the shop-floor of manufacturing organisations. These improvements would increase the desirability of this and similar systems.

By providing machine tool data in such a way, the need to employ middle-management systems to obtain data will be eliminated. Also, current systems that already benefit the manufacturing process, such as ICG and digital twins, will further benefit from an additional source of valuable data. This can only be a complement to such systems and will enable the means to dovetail the effectiveness of and the opportunities available to the control and management of advanced manufacturing processes. This makes approaches similar to that detailed within this thesis highly valuable as a means of enabling the availability of such data and thus improving those processes. The value of smart systems and data will inevitably increase over time as factories are upgraded and Industry 4.0 is more widely adopted. It is important to note that this research has introduced the potential for the use of embedded controller information to the VMC OEM. They are thus provided with the opportunity to embrace the potential that this can provide in the context of machine and process management.

## 11 | References

- Abbass JK, Al-Habaibeh A (2015) A comparative study of using spindle motor power and eddy current for the detection of tool conditions in milling processes. In: IEEE international conference on industrial informatics
- Abdullah H, Ramli R, Wahab DA (2017) Tool path length optimisation of contour parallel milling based on modified ant colony optimisation. *Int J Adv Manuf Technol.* 92(1)
- Acuna DE, Orchard ME (2018) A theoretically rigorous approach to failure prognosis. In: Tenth annual conference of the prognostics and health management society
- Adesta EYT, Hamidon R, Riza M, Alrashidi RFFA, Alazemi AFFS (2017) Investigation of tool engagement and cutting performance in machining a pocket. *IOP Conf Ser: Mater Sci Eng* 290 (<https://doi.org/10.1088/1757-899X/290/1/012066>)
- Ahmed ZJ (2018) An integrated approach to tool life management. PhD Thesis, Cardiff University
- Ahmed ZJ, Prickett PW, Grosvenor RI (2017) Assessing uneven milling cutting tool wear using component measurement. In: Thirtieth conference on condition monitoring and diagnostic engineering management
- Albert M (2007) RAMTIC system still ticking.  
<https://www.renishaw.com/en/ramtic-system-still-ticking-8985>
- Albert M (2017) 3 perspectives on machine monitoring.  
<https://www.mmsonline.com/articles/3-perspectives-on-machine-monitoring>
- Allcock A (2018) The nuts & bolts of Industry 4.0 – Mazak.  
<https://www.machinery.co.uk/machinery-features/the-nuts-bolts-of-industry-4-0-mazak>
- Amer W, Grosvenor R, Prickett P (2007) Machine tool condition monitoring using sweeping filter techniques. *Proc Inst Mech Eng Part I: J Syst and Control Eng* 221(1):103
- Astakhov VP (2004) The assessment of cutting tool wear. *Int J Mach Tool Manuf* 44(6):637
- Astakhov VP (2007) Effects of the cutting feed, depth of cut, and workpiece (bore) diameter on the tool wear rate. *Int J Adv Manuf Technol.* 34(7-8)
- Astakhov VP, Davim JP (2008) Tools (Geometry and material) and tool wear. In: *Machining*. Springer, London, pp 29-57 ([https://doi.org/10.1007/978-1-84800-213-5\\_2](https://doi.org/10.1007/978-1-84800-213-5_2))
- Axinte D, Gindy N (2004) Assessment of the effectiveness of a spindle power signal for tool condition monitoring in machining processes. *Int J Prod Res* 42(13), pp 2679-2691 (<https://doi.org/10.1080/00207540410001671642>)

- Azmi AI (2015) Monitoring of tool wear using measured machining forces and neuro-fuzzy modelling approaches during machining of GFRP composites. *Adv Eng Softw* 82, pp 53-64  
(<https://doi.org/10.1016/j.advengsoft.2014.12.010>)
- Bain KT, Orwig DG (2000) F/A-18E/F Built-in-test (BIT) maturation process. In: Third annual systems engineering & supportability conference
- Bhushan B, Gupta BK (1991) Handbook of tribology-materials, coatings and surface treatments. McGraw-Hill, New York
- Bither B (2016) Empower your operators with machine monitoring / machinemetrics.  
<https://www.machinemetrics.com/blog/empower-your-operators-with-machinemetrics>
- Black JT, Kohser RA (2012) Degarmos materials and processes in manufacturing, John Wiley & Sons, New Jersey, p594-596
- Borland D, Taylor RM (2007) Rainbow color map (still) considered harmful. *IEEE Comput Graph Appl* 27(2), pp 14-17 (<https://doi.org/10.1109/MCG.2007.323435>)
- Cai Y, Starly B, Cohen P, Lee YS (2017) Sensor data and information fusion to construct digital-twins virtual machine tools for cyber-physical manufacturing. *Procedia Manuf* 10, pp 1031-1042 (<https://doi.org/10.1016/j.promfg.2017.07.094>)
- Camacho PYS, Ruiz GH, Ocampo JBR., Correa JCJ (2011) Tool breakage detection in CNC high-speed milling based in feed-motor current signals. *Int J Adv Manuf Technol* 53, pp 1141-1148 (<https://doi.org/10.1007/s00170-010-2907-9>)
- Cao H, Zhang X, Chen X (2017) The concept and progress of intelligent spindles: a review. *Int J Mach Tool Manuf* 112, pp 21-52 (<http://dx.doi.org/10.1016/j.ijmachtools.2016.10.005>)
- Ceratizit UK (2020) WNT restart – regrind instead of buying new.  
<https://www.wnt.com/uk/cutting-tools/regrindservice.html>
- Cerce L, Pusavec F, Kopac J (2015) A new approach to spatial tool wear analysis and monitoring. *Strojniski vestnik - J Mech Eng* 61(9), pp 489-497 (<https://doi.org/10.5545/sv-jme.2015.2512>)
- Conradie PJT, Oosthuizen GA, Dimitrov D (2017) On the effect of regrinding cutting tools for high performance milling of titanium alloys. *Int J Adv Manuf Technol* 90, pp 2283-2292  
(<https://doi.org/10.1007/s00170-016-9550-z>)
- Conroy M, Armstrong J (2005) A comparison of surface metrology techniques. *J Phys: Conf Ser* 13(106), pp 458-465 (<https://doi.org/10.1088/1742-6596/13/1/106>)
- Cosgrove J, Doyle F, Broek Bvd (2019) A case study analysis of energy savings achieved through behavioural change and social feedback on manufacturing machines. In: Ball P, Huatuco LH, Howlett RJ, Setchi R (eds) Sustainable design and manufacturing 2019. Springer, pp 323-337
- Danesh M, Khalili K (2015) Determination of tool wear in turning process using undecimated wavelet transform and textural features. In: Eighth international conference inter-eng: interdisciplinarity in engineering

- Dasarathi G (2016) CNC machining: Work hardening, its effects.  
<https://www.cadem.com/single-post/work-hardening-cnc-machining>
- Davidhazy A (2006) Introduction to shadowgraph and schlieren imaging.  
<http://scholarworks.rit.edu/article/478>
- Davim JP (2020) Additive and subtractive manufacturing: Emergent technologies. Walter de Gruyter GmbH & Co KG, 2020 (<https://doi.org/10.1515/9783110549775>)
- Dolinsek S, Sustarsic B, Kopac J (2001) Wear mechanisms of cutting tools in high-speed cutting processes. *Wear* 250(1-12), pp 349-356 ([https://doi.org/10.1016/S0043-1648\(01\)00620-2](https://doi.org/10.1016/S0043-1648(01)00620-2))
- Dornfeld D, Min S, Takeuchi Y (2006) Recent advances in mechanical micromachining. *CIRP Annals* 55(2), pp 745-768 (<https://doi.org/10.1016/j.cirp.2006.10.006>)
- Dove J (2014) Hold it right there: improve inspection results by re-evaluating fixture systems.  
<https://www.qualitymag.com/articles/92041-hold-it-right-there>
- Elattar HM, Elminir HK, Riad AM (2016) Prognostics: a literature review. *Complex Intell Syst* 2(2), pp 125-154 (<https://doi.org/10.1007/s40747-016-0019-3>)
- Engel SJ, Gilmartin BJ, Bongort K, Hess A (2000) prognostics, the real issues involved with predicting life remaining. In: *IEEE Aerospace Conference 2000*
- Flynn JM, Shokrani A, Newman ST, Dhokia V (2016) Hybrid additive and subtractive machine tools - research and industrial developments. *Int J Mach Tool Manuf* 101, pp 79-101 (<http://dx.doi.org/10.1016/j.ijmachtools.2015.11.007>)
- Frankowiak M, Grosvenor RI, Prickett PW (2005) A review of the evolution of microcontroller-based machine and process monitoring. *Int J Mach Tool Manuf* 45(4), pp 573-582 (<https://doi.org/10.1016/j.ijmachtools.2004.08.018>)
- Fu L, Ling SF, Tseng CH (2007) On-line breakage monitoring of small drills with input impedance of driving motor. *Mech Syst Signal Process* 21(1), pp 457-465 (<https://doi.org/10.1016/j.ymssp.2005.04.004>)
- Fuh KH, Wu CF (1995) A residual-stress model for the milling of aluminium alloy (2014-T6). *J Mater Process Technol* 51, pp 87-105
- Gebler OF, Hicks B, Yon J, Barker M (2018) Characterising conveyor belt system usage from drive motor power consumption and rotational speed a feasibility study. In: *Fourth European conference of the prognostics and health management society*
- Ghosh S, Naskar SK, Mandal NK (2018) Estimation of residual life of a cutting tool used in a machining process. In: *Fourth international conference on engineering, applied sciences and technology*
- Girardin F, Remond D, Rigal JF (2010) Tool wear detection in milling - An original approach with a non-dedicated sensor. *Mech Syst Signal Process* 24, pp 1907-1920 (<https://doi.org/10.1016/j.ymssp.2010.02.008>)

- Greenfield D (2016) Siemens positions itself as an industry 4.0 example.  
<https://www.automationworld.com/products/control/blog/13315384/siemens-positions-itself-as-an-industry-40-example>
- Grosvenor RI, Prickett PW (2011) A discussion of the prognostics and health management aspects of embedded condition monitoring systems. In: Third annual conference of the prognostics and health management society
- Gugulothu N, TV V, Malhotra P, Vig L, Agarwal P, Shroff G (2017) Predicting remaining useful life using time series embeddings based on recurrent neural networks. *Int J Progn Health Manag* 9(1): 004.
- Gupta P, Vardhan S (2016) Optimizing OEE, productivity and production cost for improving sales volume in an automobile industry through TPM: a case study. *Int J Prod Res* 54(10):2976 (<https://doi.org/10.1080/00207543.2016.1145817>)
- Heng A, Zhang S, Tan ACC, Mathew J (2009) Rotating machinery prognostics: state of the art, challenges and opportunities. *Mech Syst Signal Process* 23(3), pp 724-739 (<https://doi.org/10.1016/j.ymssp.2008.06.009>)
- Hill JL, Prickett PW, Grosvenor RI, Hankins G (2018) CNC Spindle signal investigation for the prediction of cutting tool health. In: Fourth European conference of the prognostics and health management society
- Hill JL, Prickett PW, Grosvenor RI, Hankins G (2019) The practical exploitation of tacit machine tool intelligence. *Int J Adv Manuf Technol* 104, pp 1693-1707 (<https://doi.org/10.1007/s00170-019-03963-0>)
- Hosseini A, Kishawy HA (2014) Cutting tool materials and tool wear. In: Davim JP (ed) *Machining of titanium alloys. Materials forming, machining and tribology*. Springer, Berlin, pp 31–56
- International Organization for Standardization (1989) ISO 8688-2: 1989(en). Tool life testing in milling - part 2: end milling. ISO, Geneva
- International Organization for Standardization (1993) ISO 2382-1: 1993. Information technology – vocabulary – part 1: fundamental terms. ISO, Geneva
- International Organization for Standardization (1998) ISO 4288: 1998. Geometric product specification (GPS) – surface texture – profile method: rules and procedures for the assessment of surface texture. ISO, Geneva
- International Organization for Standardization (2009) ISO 10360-2: 2009. Geometrical product specifications (GPS) – acceptance and reverification tests for coordinate measuring machines (CMM). ISO, Geneva
- International Organization for Standardization (2009) ISO 4287:1998+A1:2009. Geometrical product specification (GPS) – surface texture: profile method – terms, definitions and surface texture parameters. ISO, Geneva

- Jain AK, Lad BK (2016) Data driven models for prognostics of high speed milling cutters. *Int J Perform Eng* 12(1), pp 3-12
- Jones T (2020) Error-proofing the machining process.  
<https://www.competitiveproduction.com/articles/error-proofing-the-machining-process/>
- Kagermann H, Wahlster W, Helbig J (2013) Recommendations for implementing the strategic initiative industrie 4.0. *Industrie 4.0 Working Group, Frankfurt*
- Karandikar JM, Abbas A, Schmitz TL (2013) Remaining useful tool life predictions in turning using bayesian inference. *Int J Progn Health Manag* 4(2):025
- Karim Z, Azuan SAS, Yasir AMS (2013) A study on tool wear and surface finish by applying positive and negative rake angle during machining. *Aust J Basic Appl Sci* 7(10), pp 46-51
- Kariuki LW, Nyakoe GN, Ikuu BW (2014) Generation and optimization of pocket milling tool paths – a review. In: *International conference on sustainable research and innovation (2014)*
- Kim HC (2007) Tool path modification for optimized pocket milling. *Int J Prod Res* 45(24), pp 5715-5729 (<https://doi.org/10.1080/00207540600919340>)
- Koepfer C (2012) Stepping up to unattended machining.  
<https://www.productionmachining.com/articles/stepping-up-to-unattended-machining->
- Kosky P, Balmer R, Keat W, Wise G (2013) Manufacturing engineering. In: *Exploring engineering*. Academic Press, pp 205-235 (<https://doi.org/10.1016/B978-0-12-415891-7.00010-8>)
- Kundrak J, Palmay Z (2014) Application of general tool-life function under changing cutting conditions. *Acta Polytechnica Hungarica* 11(2), pp 61-76
- Kwon Y, Ertekin Y, Tseng TL (2004) Characterization of tool wear measurement with relation to the surface roughness in turning. *Mach Sci Technol* 8(1), pp 39-51  
(<https://doi.org/10.1081/MST-120034239>)
- Laloix T, Vu HC, Voisin A, Romagne E, Iung B (2018) A priori indicator identification to support predictive maintenance: application to machine tool. In: *Fourth European conference of the prognostics and health management society*
- Lauro CH, Brandao LC, Baldo D, Reis RA, Davim JP (2014) Monitoring and processing signal applied in machining processes - a review. *Measurement* 58, pp 73-86  
(<https://doi.org/10.1016/j.measurement.2014.08.035>)
- Lee K, Lee L, Teo S (1992) On-line tool-wear monitoring using a PC. *J Mater Process Technol* 29(1-3):3
- Lee KJ, Lee TM, Yang MY (2007) Tool wear monitoring system for CNC end milling using a hybrid approach to cutting force regulation. *Int J Adv Manuf Technol* 32, pp 8-17  
(<https://doi.org/10.1007/s00170-005-0350-0>)
- Lee WK, Ratnam MM, Ahmad ZA (2017) Detection of chipping in ceramic cutting inserts from workpiece profile during turning using fast fourier transform (FFT) and continuous wavelet

- transform (CWT). *Precis Eng* 47, pp 406-423  
(<https://doi.org/10.1016/j.precisioneng.2016.09.014>)
- Li B (2012) A review of tool wear estimation using theoretical analysis and numerical simulation technologies. *Int J Refract Metals Hard Mater* 35, pp 143-151  
(<https://doi.org/10.1016/j.ijrmhm.2012.05.006>)
- Li H, He G, Qin X, Wang G, Lu C, Gui L (2014) Tool wear and hole quality investigation in dry helical milling of Ti-6Al-4V alloy. *Int J Adv Manuf Technol* 71(5-8), pp 1511-1523  
(<https://doi.org/10.1007/s00170-013-5570-0>)
- Li X, Ouyang G, Liang Z (2008) Complexity measure of motor current signals for tool flute breakage detection in end milling. *Int J Mach Tool Manuf* 48(3), pp 371-379  
(<https://doi.org/10.1016/j.ijmachtools.2007.09.008>)
- Limb BJ, Work DG, Hodson H, Smith BL (2017) The inefficiency of Chauvenet's Criterion for elimination of data points. *J Fluids Eng* 139(5):054501 (<https://doi.org/10.1115/1.4035761>)
- Line JK, Clements NS (2006) Prognostics usefulness criteria. In: *IEEE Aerospace Conference 2006*
- Liu C, Vengayil H, Lu Y, Xu X (2019) A cyber-physical machine tools platform using OPC UA and MTConnect. *J Manuf Syst* 51, pp 61-74 (<https://doi.org/10.1016/j.jmsy.2019.04.006>)
- Liu C, Wang GF, Li ZM (2015) Incremental learning for online tool condition monitoring using Ellipsoid ARTMAP network model. *Appl Soft Comput* 35(1):186, pp 186-198  
(<https://doi.org/10.1016/j.asoc.2015.06.023>)
- Liu C, Xu X (2017) Cyber-physical machine tool - the era of machine tool 4.0. In: *CIRP conference on manufacturing systems*
- Liu C, Xu X, Peng Q, Zhou Z (2018) MTConnect-based cyber-physical machine tool: a case study. In: *CIRP conference on manufacturing systems*
- Liu W, Kong C, Niu Q, Jiang J, Zhou X (2020) A method of NC machine tools intelligent monitoring system in smart factories. *Robot Comput Integr Manuf* 61(1):101842  
(<https://doi.org/10.1016/j.rcim.2019.101842>)
- Liu X, Zhang C, Fang J, Guo S (2010) A new method of tool wear measurement. In: *The international conference on electrical and control engineering*
- Liu ZQ, Ai X, Zhang H, Wang ZT, Wan Y (2002) Wear patterns and mechanisms of cutting tools in high-speed face milling. *J Mater Process Technol* 129, pp 222-226  
([https://doi.org/10.1016/S0924-0136\(02\)00605-2](https://doi.org/10.1016/S0924-0136(02)00605-2))
- Lopez de Lacalle LN, Lamikiz A, Fernandez de Larrinoa J, Azkona I (2011) Machining of hard materials. In: Davim JP (ed) *Machining of hard materials*, 1st edn. Springer, London, pp 33-86
- Luo M, Luo H, Axinte D, Liu D, Mei J, Liao Z (2018) A wireless instrumented milling cutter system with embedded PVDF sensors. *Mech Syst Signal Process* 110, pp 556-568  
(<https://doi.org/10.1016/j.ymsp.2018.03.040>)

- Ma J, Jia Z, Wang F, Gao Y, Liu Z (2016) A new cutting force modeling method in high-speed milling of curved surface with difficult-to-machine material. *Int J Adv Manuf Technol* 84(9), pp 2195-2205 (<https://doi.org/10.1007/s00170-015-7856-x>)
- Ma Y, Feng P, Zhang J, Yu D (2016) Prediction of surface residual stress after end milling based on cutting force and temperature. *J Mater Process Technol* 235, pp 41-48 (<https://doi.org/10.1016/j.jmatprotec.2016.04.002>)
- MacDougall W (2014) *Industrie 4.0 smart manufacturing for the future*. Germany Trade and Invest, Berlin
- Manthou V, Vlachopoulou M (2001) Agile manufacturing strategic options. In: Gunasekaran A (ed) *Agile manufacturing: the 21st century competitive strategy*. Elsevier Science Ltd, pp 685-702 (<https://doi.org/10.1016/B978-008043567-1/50035-8>)
- Marposs (2020a) Machine monitoring. <https://artis.de/eng/application/machine-monitoring>
- Marposs (2020b) Tool and process monitoring. <https://artis.de/eng/application/monitoring-solutions-for-machining-center>
- Marposs (2020c) Go no go gauges. <https://www.marposs.com/eng/application/go-nogo-gauges>
- MathWorks (2020) cusum: more about. <https://uk.mathworks.com/help/signal/ref/cusum.html>
- Meier (2019) Methods to reduce variation in cutting tool life tests. *Int J Adv Manuf Technol* 103: pp 355-365 (<https://doi.org/10.1007/s00170-019-03558-9>)
- Mikron Tool (2020) Save resources – reduce costs. <https://www.mikrontool.com/en/Services/Regrinding>
- Mitutoyo (2016) *Quick guide to surface roughness measurement: Reference guide for laboratory and workshop*. Mitutoyo America Corporation, USA
- MSC (2020) *Regrinding service*. <https://www.mscdirect.co.uk/CGI/INPAGE?PMPAGE=/solutions/regrind.html>
- MTConnect Institute (2020) *MTConnect standardizes factory device data*. <http://www.mtconnect.org/>
- O'Regan P (2020) *Process capability management for selective laser melting*. PhD Thesis, Cardiff University
- Oddy M (2015) The infamous no-go gage: remember, your gages are your best friends. *Qual* 54(1)
- Ogwell V (2018) Digital twins: beware of naïve faith in simplicity. [https://www.engineering.com/PLMERP/ArticleID/16272/Digital-Twins-Beware-of-Naive-Faith-in-Simplicity.aspx#disqus\\_thread](https://www.engineering.com/PLMERP/ArticleID/16272/Digital-Twins-Beware-of-Naive-Faith-in-Simplicity.aspx#disqus_thread)
- Okoh C, Roy R, Mehnen J, Redding L (2014) Overview of remaining useful life prediction techniques in through-life engineering services. *Procedia CIRP* 16, pp 158-163 (<https://doi.org/10.1016/j.procir.2014.02.006>)

- Othmani R, Hbaieb M, Bouzid W (2011) Cutting parameter optimization in NC milling. *Int J Adv Manuf Technol.* 54(9-12)
- Peng ZK, Chu FL (2004) Application of the wavelet transform in machine condition monitoring and fault diagnostics: a review with bibliography. *Mech Syst Signal Process* 18(2), pp 199-221 ([https://doi.org/10.1016/S0888-3270\(03\)00075-X](https://doi.org/10.1016/S0888-3270(03)00075-X))
- Prakash M, Kanthababu M (2013) In-process tool condition monitoring using acoustic emission sensor in microendmilling. *Mach Sci Technol* 17(2), pp 209-227 (<https://doi.org/10.1080/10910344.2013.780541>)
- Prickett P, Johns C (1999) An overview of approaches to end milling tool monitoring. *Int J Mach Tool Manuf* 39(1):105
- Professional Engineering (2019) FEATURE: Skills shortages, Industry 4.0... Brexit: the state of the industry in 2019. Institution of Mechanical Engineers. <https://www.imeche.org/news/news-article/feature-skills-shortages-industry-4-brex-it-the-state-of-the-industry-in-2019>
- Qin J (2019) Advanced data analytics for additive manufacturing energy consumption modelling, prediction, and management under Industry 4.0. PhD Thesis, Cardiff University
- Qin J, Liu Y, Grosvenor RI (2017) A framework of energy consumption modelling for additive manufacturing using Internet of Things. *Procedia CIRP* 63, pp 307-312 (<https://doi.org/10.1016/j.procir.2017.02.036>)
- Qin J, Liu Y, Grosvenor RI, Lacan F, Jiang Z (2020) Deep learning-driven particle swarm optimisation for additive manufacturing energy optimisation. *J Clean Prod* 245, pp 118702 (<https://doi.org/10.1016/j.jclepro.2019.118702>)
- Rance J, Hall S, Bartolomeis Ad, Shokrani A (2019) Future direction of the sustainable turning of difficult-to-machine materials. In: Ball P, Huatuco LH, Howlett RJ, Setchi R (eds) *Sustainable design and manufacturing 2019*. Springer, pp 111-120
- Red Lion (2020) Industry application: connected factory, industry 4.0 & the industrial internet of things (IIOT). <https://www.redlion.net/industry-application-connected-factory-industry-40-industrial-internet-things-iiot>
- Renishaw plc (2011) Productive process pattern: cutter parameter update AP301. Renishaw plc, Wotton-under-Edge
- Renishaw plc (2019) REVO-2 user's guide. Renishaw plc, Wotton-under-Edge
- Renishaw plc (2020a) Equator gauging system. <https://www.renishaw.com/en/equator-gauging-system-12595>
- Renishaw plc (2020b) Renishaw Stonehouse – common sense manufacturing. <https://resources.renishaw.com/en/details/news-release-renishaw-stonehouse-common-sense-manufacturing-10151>

- Renishaw plc (2020c) Smart manufacturing technologies for process control.  
<https://www.renishaw.com/en/smart-manufacturing-technologies-for-process-control-45468>
- Renishaw plc (2020d) SFP2 surface finish probe installation and user's guide. Renishaw plc, Wotton-under-Edge
- Rexroth (2019) Predictive analytics with ODIN.  
<https://apps.boschrexroth.com/rexroth/en/connected-hydraulics/products/odin/>
- Rexroth (2020) Industry 4.0 Connected automation starts now  
<https://www.boschrexroth.com/en/xc/trends-and-topics/industry-4-0/connected-industry-1>
- Rigamonti M, Baraldi P, Zio E, Roychoudhury I, Goebel K, Poll S (2016) Echo state network for the remaining useful life prediction of a turbofan engine. In: Third European conference of the prognostics and health management society
- Rivero A, Lacalle LNL, Penalva ML (2008) Tool wear detection in dry high-speed milling based upon the analysis of machine internal signals. *Mechatronics* 18(10), pp 627-633  
(<https://doi.org/10.1016/j.mechatronics.2008.06.008>)
- Sakharov GN, Ilinykh V, Konyukhov, Yu V (1990) Improvement of fastening elements in an assembled cutting tool. *Soviet engineering research* 10(11), pp 102-103
- Sandvik Coromant (2020a) Cutting tool materials. <https://www.sandvik.coromant.com/en-gb/knowledge/materials/pages/cutting-tool-materials.aspx>
- Sandvik Coromant (2020b) Wear on cutting edges. <https://www.sandvik.coromant.com/en-gb/knowledge/materials/pages/wear-on-cutting-edges.aspx>
- Santhakumar J, Iqbal UM, Prakash M (2018) Optimization of one direction tool path orientation for pocket milling of Ti-6Al-4V using taguchi based grey relational analysis. In: Second international conference on advances in mechanical engineering (2018)
- Saxena A, Celaya J, Saha B, Saha S, Goebel K (2010) Metrics for offline evaluation of prognostic performance. *Int J Progn Health Manag* 1(1): 001
- Schwab K (2016) The fourth industrial revolution: what it means, how to respond.  
<https://www.weforum.org/agenda/2016/01/the-fourth-industrial-revolution-what-it-means-and-how-to-respond/>
- Shaw MC (1984) *Metal cutting principles*. Oxford University Press, New York, p 1984
- Shaw MC (2003) The size effect in metal cutting. *Sadhana* 28, pp 875-896  
(<https://doi.org/10.1007/BF02703319>)
- Si AS, Wang W, Hu CH, Zhou DH (2011) Remaining useful life estimation – a review on the statistical data driven approaches. *Eur J Oper Res* 213(1), pp 1-14  
(<https://doi.org/10.1016/j.ejor.2010.11.018>)
- Siddiqui RA (2008) dsPIC-based digital signal processing techniques and an IT-enabled distributed system for intelligent process monitoring and management. PhD Thesis, Cardiff University

- Siemens (2020) MindSphere – Industrial IoT as a service.  
<https://www.plm.automation.siemens.com/global/en/products/mindsphere/internet-of-things-iot.html>
- Siemens (2020b) SIPLUS CMS - Stepping up your production.  
<https://www.siemens.com/uk/en/home/products/automation/products-for-specific-requirements/siplus-cms.html>
- Singh A, Garg S, Kaur R, Batra S, Kumar N, Zomaya AY (2020) Probabilistic data structures for big data analytics: A comprehensive review. *Knowl Based Syst* 188(1)  
<https://doi.org/10.1016/j.knosys.2019.104987>
- Sobie C, Freitas C, Nicolai M (2018) Simulation-driven machine learning: bearing fault classification. *Mech Syst and Signal Process* 99(1):403
- Soshi M, Raymond N, Ishii S (2014) Spindle rotational speed effect on milling process at low cutting speed. *Procedia CIRP* 14, pp 159-163 (<https://doi.org/10.1016/j.procir.2014.03.075>)
- Staufer H (2019) OT meets IT – Siemens factory in Amberg, Germany.  
<https://ingenuity.siemens.com/2019/05/ot-meets-it-siemens-factory-in-amberg-germany/>
- Stavropoulos P, Foteinopoulos P, Papacharalampopoulos A, Bikas H (2018) Addressing the challenges for the industrial application of additive manufacturing towards a hybrid solution. *Int J Lightweight Mater Manuf* 1, pp 157-168 (<https://doi.org/10.1016/j.ijlmm.2018.07.002>)
- Sui J, Kountanya R, Changsheng G (2016) Development of a mechanistic force model for CNC drilling process simulation. *Procedia Manuf* 5, pp 878-797  
(<https://doi.org/10.1016/j.promfg.2016.08.064>)
- Sui S, Li Y, Shao W, Feng P (2016) Tool path generation and optimization method for pocket flank milling of aircraft structural parts based on the constraints of cutting force and dynamic characteristics of machine tools. *Int J Adv Manuf Technol* 85(5), pp 1553-1564  
(<https://doi.org/10.1007/s00170-015-8050-x>)
- Taylor F (1906) *On the art of cutting metals*. ASME, New York, p 1906
- Tennant M (2013) *Sustainability and manufacturing. Future of manufacturing project: Evidence paper 35*. Government Office for Science, Imperial College London
- Tseng PC, Chou A (2002) The intelligent on-line monitoring of end milling. *Int J Mach Tool Manuf* 42(1), pp 89-97 ([https://doi.org/10.1016/S0890-6955\(01\)00091-8](https://doi.org/10.1016/S0890-6955(01)00091-8))
- Tyrrell M (2017) How Mazak is utilising industry 4.0 infrastructure.  
<https://www.pesmedia.com/mazak-utilising-industry-4-0-infrastructure/>
- Vogl GW, Weiss BA, Donmez MA (2015) A sensor-based method for diagnostics of machine tool linear axes. In: *Seventh annual conference of the prognostics and health management society 2015*

- Wang P, Gao RX (2016) Stochastic tool wear prediction for sustainable manufacturing. *Procedia CIRP* 48, pp 236-241 (<https://doi.org/10.1016/j.procir.2016.03.101>)
- Warfield B (2020) Chip thinning & rubbing.  
<https://www.cnccookbook.com/chip-thinning-rubbing-lesson-3-fs-email/>
- Waydande P, Ambhore N, Chinchankar S (2016) A review on tool wear monitoring system. *J Mech Eng Autom* 6(5), pp 49-53
- Wheeler KR, Kurtoglu T, Poll SD (2010) A survey of health management user objectives in aerospace systems related to diagnostic and prognostic metrics. *Int J Progn Health Manag* 1(1): 003
- Wiklund H (1998) Bayesian and regression approaches to on-line prediction of residual tool life. *Qual and Reliab Eng Int* 14(5): 303
- Wilkinson P, Reuben RL, Jones JD, Barton JS, Hand DP, Carolan TA, Kidd SR (1997) Surface finish parameters as diagnostics of tool wear in face milling. *Wear* 205(1), pp 47-54 ([https://doi.org/10.1016/S0043-1648\(96\)07253-5](https://doi.org/10.1016/S0043-1648(96)07253-5))
- Williamson RM (2006) Using overall equipment effectiveness: the metric and the measures. Columbus, OH: Strategic Work Systems
- Witte M (2020) Today meets tomorrow: the opportunities and limitations facing AI and the digital twin (Part II). <https://blogs.sw.siemens.com/thought-leadership/2020/01/22/the-possibilities-and-limitations-of-ai-and-the-digital-twin/>
- Wong SY, Chuah JH, Yap HJ (2020) Technical data-driven tool condition monitoring challenges for CNC milling: a review. *Int J Adv Manuf Technol* 107, pp 4837-4857 (<https://doi.org/10.1007/s00170-020-05303-z>)
- Xie Z, Lu Y, Li J (2017) Development and testing of an integrated smart tool holder for four-component cutting force measurement. *Mech Syst Signal Process* 93, pp 225-240 (<https://doi.org/10.1016/j.ymssp.2017.01.038>)
- Xiong Y, Wu J, Deng C, Wang Y (2016) Machining process parameters optimization for heavy-duty CNC machine tools in sustainable manufacturing. *Int J Adv Manuf Technol* 87, pp 1237-1246 (<https://doi.org/10.1007/s00170-013-4881-5>)
- Xu X (2017) Machine Tool 4.0 for the new era of manufacturing. *Int J Adv Manuf Technol* 92(5-8):1893
- Yamazaki Mazak (2015a) Mazak SmartBox launches manufacturers into the IIOT at DISCOVER 2015. <https://www.mazakusa.com/news-events/news-releases/mazak-smartbox-launches-manufacturers-into-the-iiot-at-discover-2015/>
- Yamazaki Mazak (2015b) Operating manual vertical center smart 430A: UD32SG0010E0. Yamazaki Mazak Corp, Worcester

- Yamazaki Mazak (2019) Mazak makes major investments in UK factory.  
<https://www.mazakeu.co.uk/news-events/company-news/factory-investment/>
- Yamazaki Mazak (2020a) Industry 4.0: What is Mazak's role in industry 4.0?  
<https://www.mazakeu.co.uk/industry4/>
- Yamazaki Mazak (2020b) New functions. <https://www.mazakeu.co.uk/smooth-new-functions/>
- Yamazaki Mazak (2020c) The iSMART factory. <https://www.mazakeu.co.uk/industry4/ismart/>
- Yamazaki Mazak (2020d) Mazak SmartBox.  
<https://www.mazakusa.com/machines/technology/digital-solutions/mazak-smartbox/>
- Yang Z, Liu L, Peng K, Li S, Zhang J, Gai L (2017) Monitoring method of high-speed tool wear level based on machine vision. *Int J Signal Process Image Process Pattern Recognit* 10(6), pp 23-38  
(<https://doi.org/10.14257/ijcip.2017.10.6.03>)
- Yao Q, Wu B, Luo M, Zhang D (2018) On-line cutting force coefficients identification for ball-end milling process with vibration. *Measurement*. 125(1), pp 243-253  
(<https://doi.org/10.1016/j.measurement.2018.04.084>)
- Yusup N, Zain AM, Hashim SZM (2012) Evolutionary techniques in optimizing machining parameters: Review and recent applications (2007-2011). *Expert Syst Appl*. 39(10)
- Zhang C, Zhou L (2013) Modeling of tool wear for ball end milling cutter based on shape mapping. *Int J Interact Des Manuf* 7(3), pp 171-181 (<https://doi.org/10.1007/s12008-012-0176-6>)
- Zhou G, Lu Q, Xiao Z, Zhou C, Tian C (2019) Cutting parameter optimization for machining operations considering carbon emissions. *J Clean Prod* 208, 937–950
- Zhou Y, Xue W (2018) Review of tool condition monitoring methods in milling processes. *Int J Adv Manuf Technol* 96(5-8):2509
- Zhu KP, Wong YS, Hong GS (2009) Wavelet analysis of sensor signals for tool condition monitoring: a review and some new results. *Int J Mach Tool Manuf* 49(7), pp 537-553  
(<https://doi.org/10.1016/j.ijmachtools.2009.02.003>)

# **A | Programs**

Programs written and deployed by the Author (listed below) are available on request. The PAc flowcharts and the Excel VBA functions are included below.

## **A.1 PAc**

## **A.2 PAc flowchart**

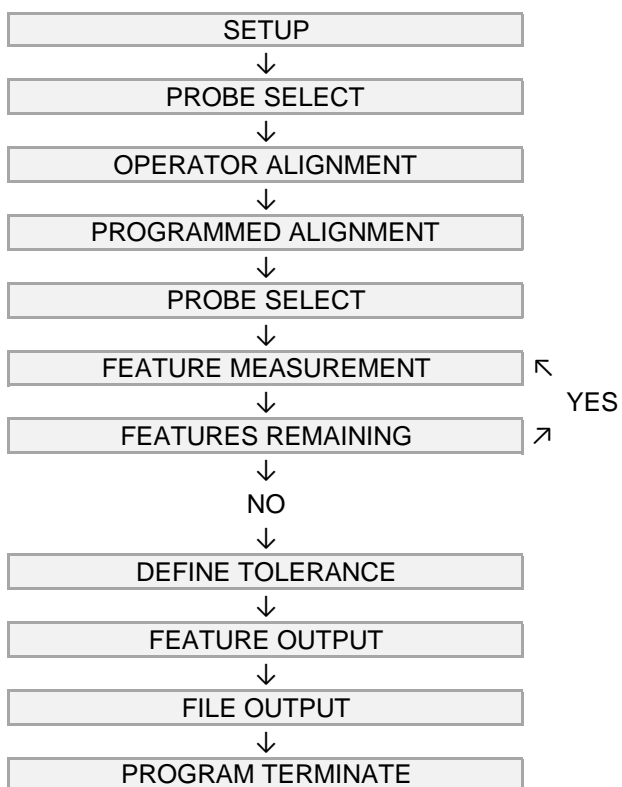
## **A.3 DENSE program**

## **A.4 CMM scan data processing**

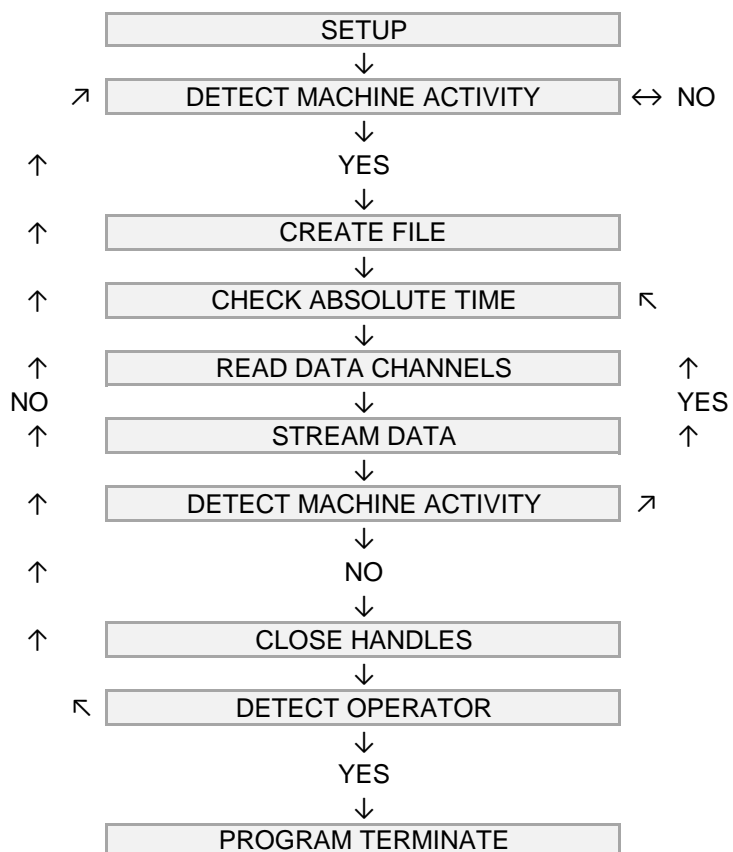
## **A.5 Excel VBA functions**

SIMPLE FLOWCHARTS

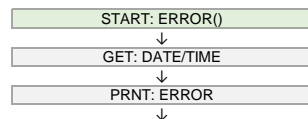
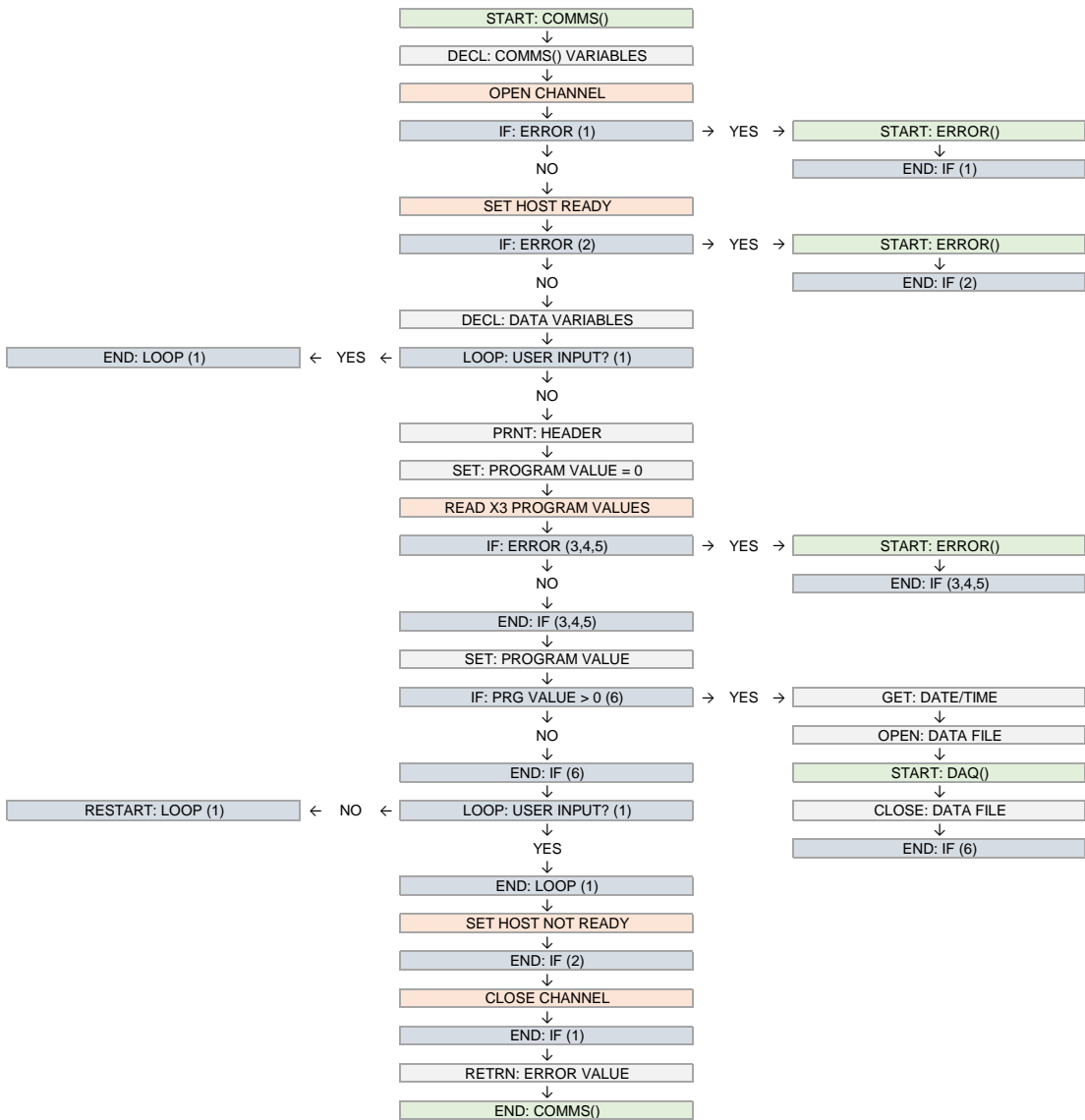
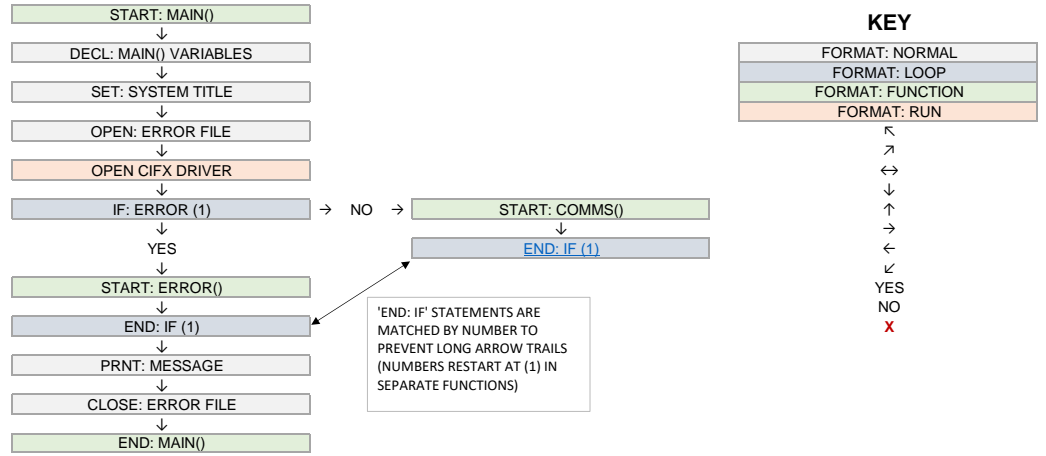
**CMM MEASUREMENT BASIC**



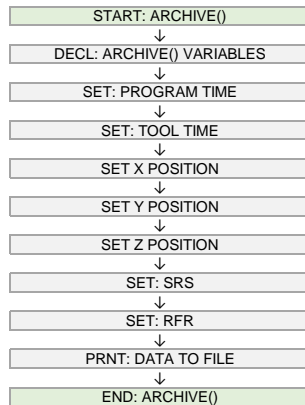
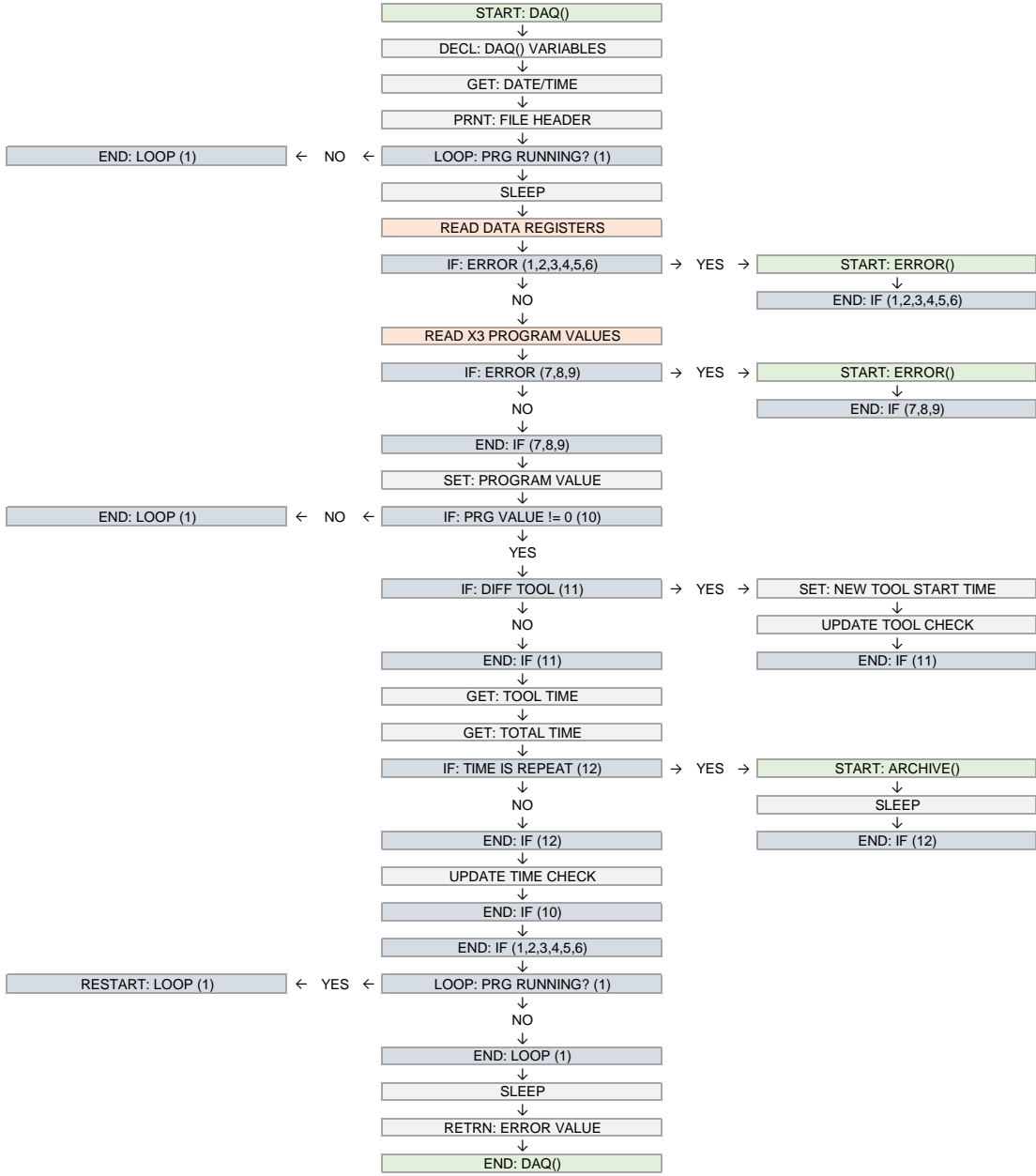
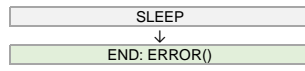
**CNC DAQ BASIC**



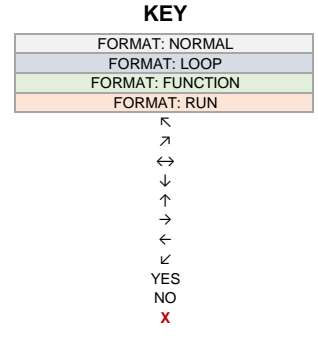
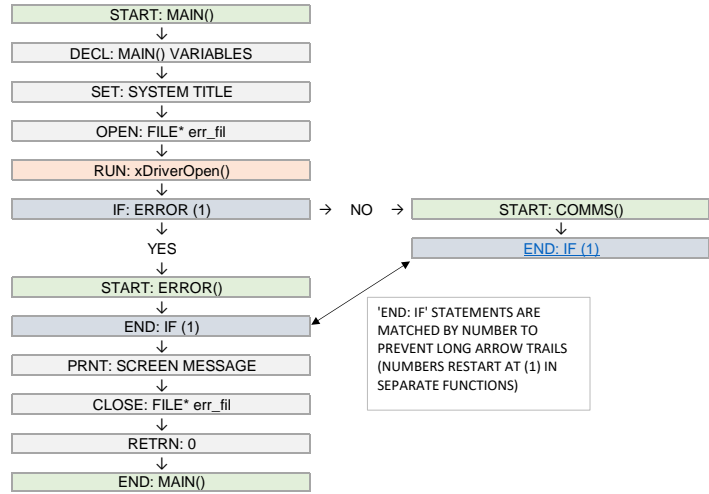
DETAILED FLOWCHARTS (DESCRIPTIVE)



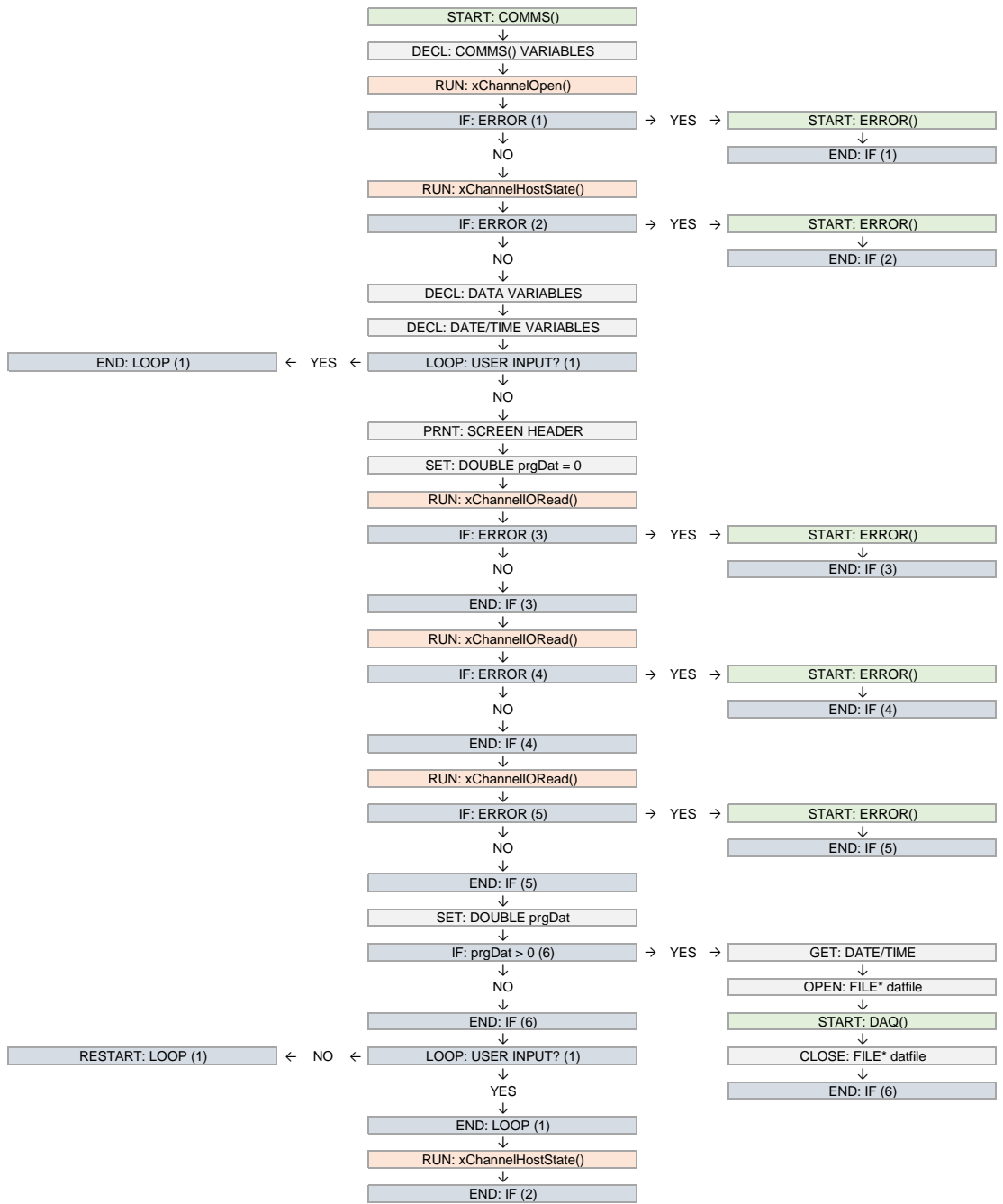
DETAILED FLOWCHARTS (DESCRIPTIVE)



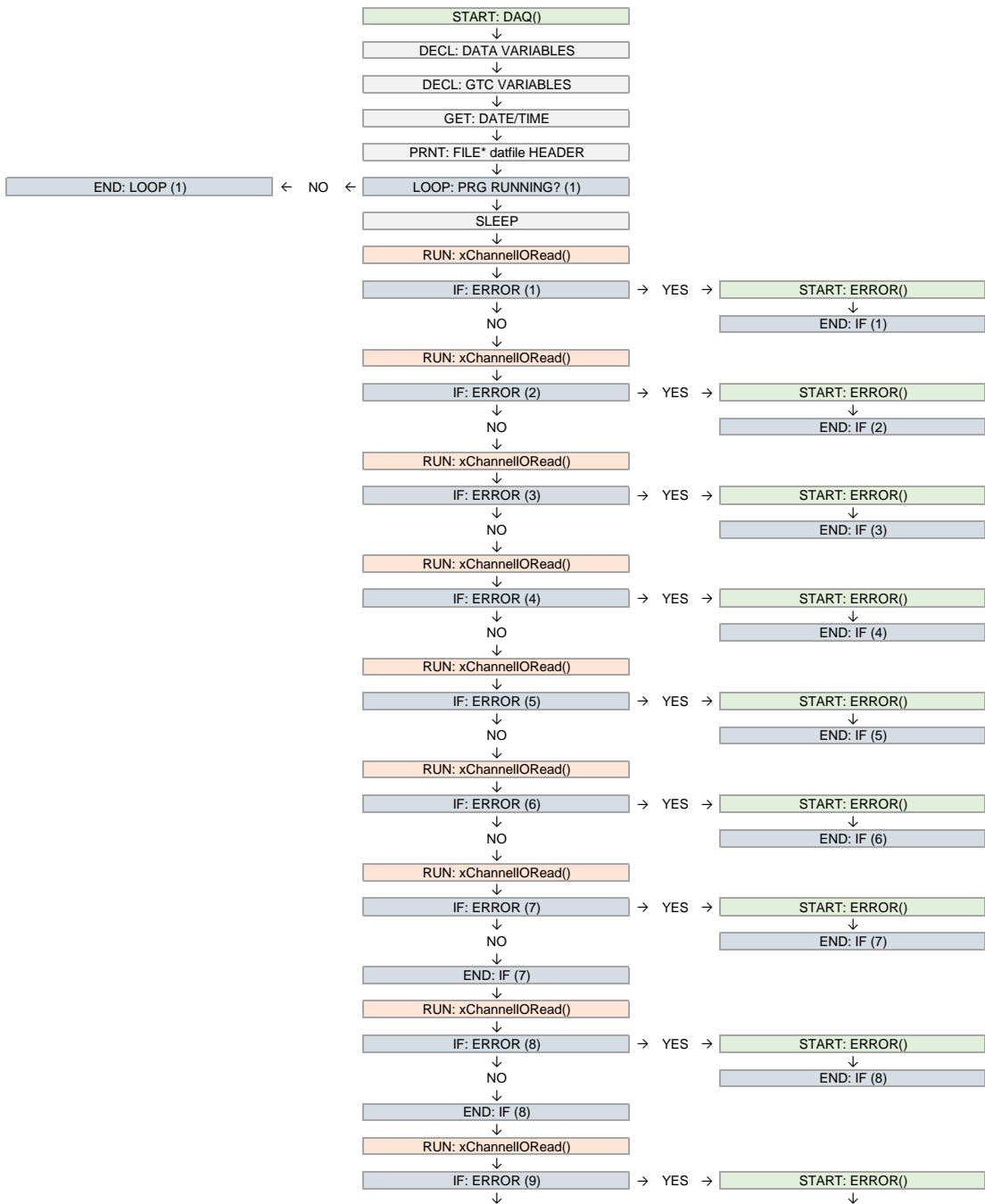
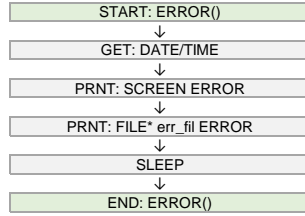
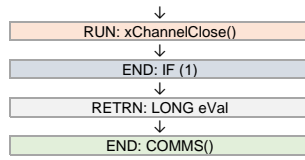
DETAILED FLOWCHARTS (CIFX API)



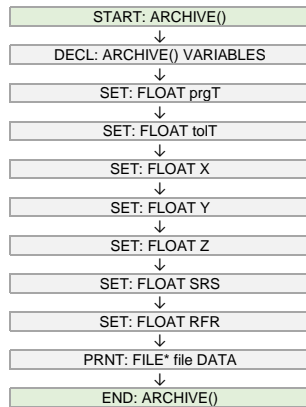
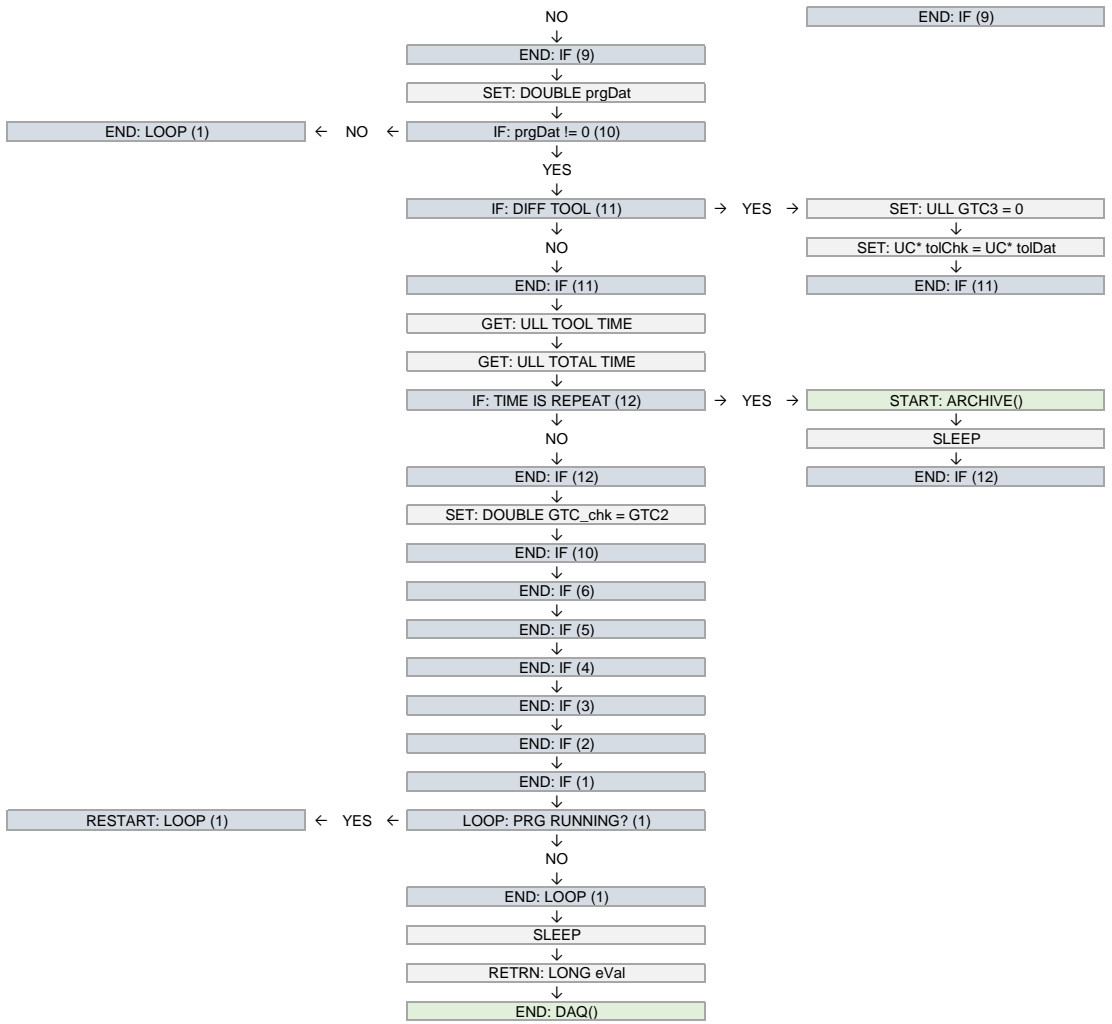
'END: IF' STATEMENTS ARE MATCHED BY NUMBER TO PREVENT LONG ARROW TRAILS (NUMBERS RESTART AT (1) IN SEPARATE FUNCTIONS)



DETAILED FLOWCHARTS (CIFX API)



DETAILED FLOWCHARTS (CIFX API)



## Excel VBA functions

Function CPOL3(X As String, Y As String, C As Integer)

- ' Calculates LS 3rd order polynomial coefficients
- ' X and Y are the string literal relative cell references for the input data
- ' C indicates the relative coefficient (A, B, C or D)
- ' XR and YR are macro specific data arrays for the actual X and Y input data
- ' XM is the macro specific matrix array for  $X$ ,  $X^2$  and  $X^3$

Dim XR As Variant, YR As Variant, XM()

XR = Range(X).Value

YR = Range(Y).Value

ReDim Preserve XM(1 To UBound(XR), 1 To 3)

For i = 1 To UBound(XR)

XM(i, 1) = XR(i, 1)

XM(i, 2) = XR(i, 1) \* XR(i, 1)

XM(i, 3) = XR(i, 1) \* XR(i, 1) \* XR(i, 1)

Next i

- ' Use inbuilt Excel functions to determine A, B, C or D

With Application.WorksheetFunction

Pass = .LinEst(YR, XM)

If C = 1 Then

CPOL3 = .Index(Pass, 1)

ElseIf C = 2 Then

CPOL3 = .Index(Pass, 1, 2)

ElseIf C = 3 Then

CPOL3 = .Index(Pass, 1, 3)

Else

CPOL3 = .Index(Pass, 1, 4)

End If

End With

End Function

---

Function POL3(x As Range, X As String, Y As String) As Variant

- ' Representative Equation:  $AX^3 + BX^2 + CX + D$
- ' x is the cell range containing the polynomial x values
- ' X and Y are the string literal relative cell references for the input data
- ' TR is the macro specific data array for the polynomial x values

Dim TR As Variant

TR = x.Value

A = CPOL3(X, Y, 1)

B = CPOL3(X, Y, 2)

C = CPOL3(X, Y, 3)

D = CPOL3(X, Y, 4)

```

If UBound(TR) = 1 Then
    TR(1, 1) =
(A * TR(1, 1) * TR(1, 1) * TR(1, 1)) + (B * TR(1, 1) * TR(1, 1)) + (C * TR(1, 1)) + D
Else
    For i = 1 To UBound(TR)
        TR(i, 1) =
(A * TR(i, 1) * TR(i, 1) * TR(i, 1)) + (B * TR(i, 1) * TR(i, 1)) + (C * TR(i, 1)) + D
    Next i
End If
POLY3 = TR
End Function

```

---

```

Function TENDR(x As Range, X As String, Y As String) As Variant

```

```

    ' Normalises POL3(x) according to the inflection point ( $f''(x) = 0$ )
    ' x is the cell range containing the polynomial x values
    ' X and Y are the string literal relative cell references for the input data
    ' TR is the macro specific data array for the POL3(x) values

```

```

Dim TR As Variant

```

```

TR = POL3(x, X, Y)

```

```

With Application.WorksheetFunction

```

```

    idxVal =

```

```

.Index(TR, .Match(.RoundUp(-2 * CPOL3(X, Y, 2)) / (6 * CPOL3(X, Y, 1)), 0), x, 0))

```

```

    For i = 1 To UBound(TR)

```

```

        TR(i, 1) = TR(i, 1) - idxVal(1)

```

```

    Next i

```

```

    SmlVal = .Min(TR)

```

```

    LrgVal = .Max(TR)

```

```

End With

```

```

For i = 1 To UBound(TR)

```

```

    If TR(i, 1) ≤ 0 Then

```

```

        TR(i, 1) = (-1 * TR(i, 1)) / SmlVal

```

```

    Else

```

```

        TR(i, 1) = TR(i, 1) / LrgVal

```

```

    End If

```

```

Next i

```

```

TENDR = TR

```

```

End Function

```

---

```

Function PFIT(x As Range, X As String, Y As String, X0EM1 As Range, XP1E As Range, SHIFT As
Range) As Variant

```

```

    ' x is the cell range containing the polynomial x values

```

```

    ' X and Y are the string literal relative cell references for the input data

```

```

    ' X0EM1 and XP1E are the string literal relative cell references for the curve fit

```

' SHIFT is the adjustment factor ( $\gamma$ )  
 ' TR is the macro specific data array for the POL3(x) values  
 ' DD is the macro specific data array for the 1st derivative

Dim TR As Variant, DD As Variant

DD = x.Value

TR = XP1E.Value

TR1 = XP1E.Value

TR2 = X0EM1.Value

'Calculate the coefficients

A = CPOL3(X, Y, 1)

B = CPOL3(X, Y, 2)

C = CPOL3(X, Y, 3)

D = CPOL3(X, Y, 4)

'Define the 1st Derivative (DD)

For i = 1 To UBound(DD)

DD(i, 1) = (3 \* A \* DD(i, 1) \* DD(i, 1)) + (2 \* B \* DD(i, 1)) + C

Next i

MnDD = Application.WorksheetFunction.Min(DD)

TR2(1, 1) = -1

'Calculate TR (primary component of PFIT)

For i = 1 To UBound(TR)

TR1(i, 1) = (((3 \* A \* (TR1(i, 1) \* TR1(i, 1))) + (2 \* B \* TR1(i, 1)) + (C)) + (SHIFT.Value - MnDD))

TR2(i, 1) = (((3 \* A \* (TR2(i, 1) \* TR2(i, 1))) + (2 \* B \* TR2(i, 1)) + (C)) + (SHIFT.Value - MnDD))

TR(i, 1) = (TR1(i, 1) / TR2(i, 1)) - 1

Next i

MnTR = Application.WorksheetFunction.Min(TR)

MxTR = Application.WorksheetFunction.Max(TR)

'IFERROR( IF( IFERROR( (TMP-1), "ERROR" ) < 0, -IFERROR() / MIN( IFERROR() ),  
 IFERROR() / MAX( IFERROR() ) ), -1 )

For i = 1 To UBound(TR)

If (TR(i, 1) < 0) Then

TR(i, 1) = (-1 \* TR(i, 1)) / MnTR

ElseIf (TR(i, 1) ≥ 0) Then

TR(i, 1) = TR(i, 1) / MxTR

Else

TR(i, 1) = -1

End If

Next i

PFIT = TR

End Function

Function EFIT(x As Range, X As String, Y As String, X0EM1 As Range, XP1E As Range, SHIFT As

Range) As Variant

```
' x is the cell range containing the polynomial x values
' X and Y are the string literal relative cell references for the input data
' X0EM1 and XP1E are the string literal relative cell references for the curve fit
' SHIFT is the adjustment factor ( $\gamma$ )
```

Dim TEND As Variant, FITR As Variant, TR As Variant

```
' Recall TENDR and PFIT macros
```

TEND = TENDR(x, X, Y)

FITR = PFIT(x, X, Y, X0EM1, XP1E, SHIFT)

TR = XP1E.Value

```
'=ABS(ABS($J$3:$J$203)*($J$3:$J$203>0)-ABS($I$3:$I$203)*($I$3:$I$203>0))
```

TR(1, 1) = 0

For i = 2 To UBound(TR)

```
TR(i, 1) = Abs(Abs(FITR((i - 1), 1)) * (FITR((i - 1), 1) > 0) - Abs(TEND(i, 1)) * (TEND(i, 1) > 0))
```

Next i

```
' Return the EFit characteristic array
```

EFIT = TR

End Function

---

Function FIT2LOOKUP2(X As Range, Fit2 As Range, ColNum As Integer, XVAR As String, YVAR As String) As Variant

```
' X is the cell range containing the polynomial x values
' Fit2 is the cell range corresponding to the best-fit trend for the current parts completed
' ColNum is the integer number of parts completed
' XVAR and YVAR are the string literal relative cell references for the input data
```

Dim TMP As Variant, TMP1 As Variant, PFIT2 As Variant, TREND As Variant, element As Variant, j As Integer

Dim RES1 As Variant, RES2 As Variant

For Each element In Fit2

```
TMP = Fit2
```

Next element

TMP1 = TRENDER(X, XVAR, YVAR)

j = 1

```
'MATCH(MAX(PFIT2),PFIT2,0)
```

With Application.WorksheetFunction

```
StatPnt = .Match(.Max(Fit2), Fit2, 0)
```

End With

ReDim TREND(1 To (UBound(TMP1) - StatPnt))

ReDim PFIT2(1 To (UBound(TMP) - StatPnt))

For i = (StatPnt + 1) To UBound(TMP)

```
TREND(j) = TMP1(i, 1)
```

```
PFIT2(j) = TMP(i, 1)
```

```

    j = j + 1
Next i
ReDim RES1(1 To UBound(PFIT2))
For i = 1 To UBound(PFIT2)
    RES1(i) = Abs(PFIT2(i) - TREND(i))
Next i
With Application.WorksheetFunction
    MIN1 = .Match(.Min(RES1), RES1, 0) + StatPnt - 1
End With
FIT2LOOKUP2 = MIN1
End Function

```

---

**Function F2L3(arg1 As Range, arg2 As Range, arg3 As Range) As Variant**

```

' arg1 is the cell range containing the x values
' arg2 is the cell range containing the pfit values
' arg3 is the cell range containing the noise cut-off value

```

**Dim X As Variant, Y As Variant, element As Variant, ANS As Variant**

**For Each element In arg1**

```

    X = arg1

```

**Next element**

**For Each element In arg2**

```

    Y = arg2

```

**Next element**

cutoff = arg3.Value

**For i = 3 To UBound(Y)**

```

'ANS = Y0 + (X2-X0)(Y1-Y0)/(X1-X0)

```

```

ANS = Y(i - 2, 1) + ((X(i, 1) - X(i - 2, 1)) * (Y(i - 1, 1) - Y(i - 2, 1))) / (X(i - 1, 1) - X(i - 2, 1))

```

```

If (ANS < 0) And (Abs(ANS) > cutoff) Then

```

```

    F2L3 = i - 1

```

```

    Exit For

```

```

End If

```

**Next i**

**End Function**

## B | Effects of variable cutter engagement

It has been identified that improper use of a cutting tool can result in a damaged product, a damaged tool and a damaged machine. All these outcomes can result in reduced economic performance. Suboptimal use can have similar consequences. Removing small cuts or overlapping with previous cuts during the milling process can result in the premature failure of the cutting tool. Such failures can be associated with abnormally high loads and/or work hardening of the part material. These factors can be exacerbated when such cuts become negligible relative to the size of the cutting tool. Innovation in this area has typically focussed on the optimisation of such cuts and the reduction in any overlap between cuts, with the aim being to optimise the economy of the cutting process. This inevitably prioritises the speed of the process, neglecting the micro-effects of such small cuts and the effect on the cutting behaviour caused by the overlap between passes. Chapter 2 discussed process optimisations and the benefits that it affords to manufacturing organisations.

Notwithstanding, whilst process optimisations may benefit one aspect of the machining cycle, the necessary changes may result in new concerns in other areas. Equally, any micro-effects neglected by the process optimisations are unlikely to disappear of their own volition. It has been observed through testing that cutting tool failures occur during cycles for which a reduced material volume is being removed. Cutting tool failures also occur during cycles when the maximum material volume is being removed by the cutting tool (Figure B.1).

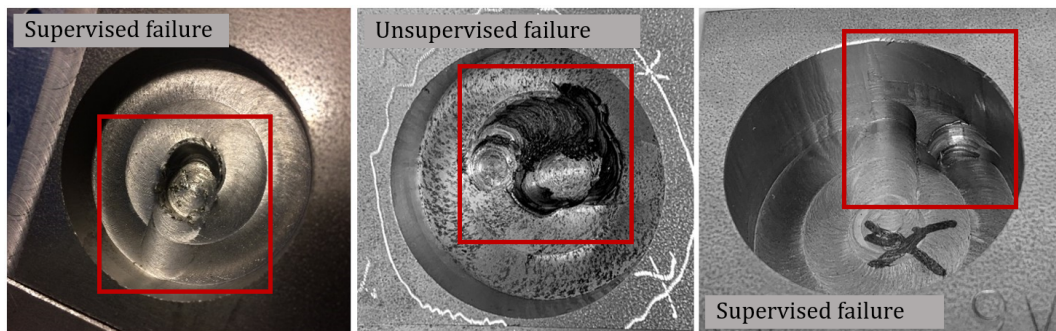
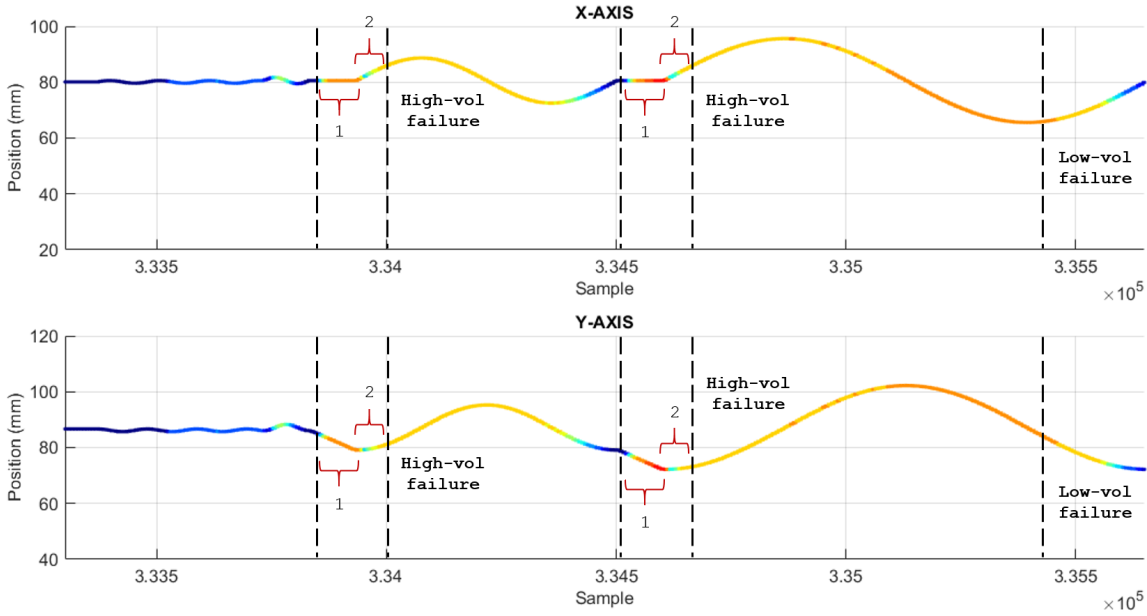


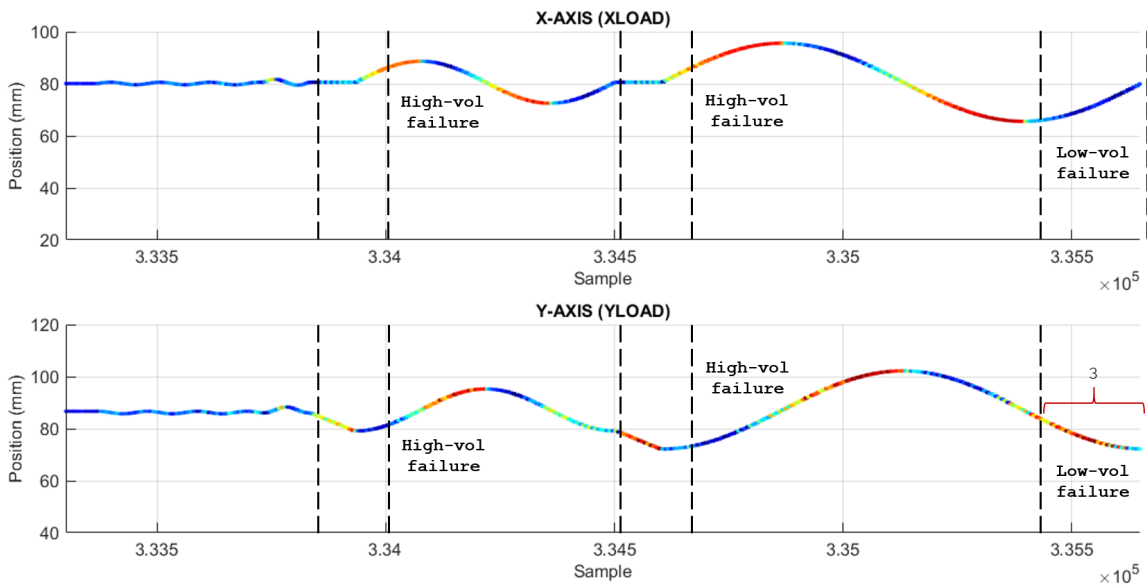
Figure B.1. Cutting tool failures for both minimum and maximum material removal

All the example failures tend to occur alongside notable variation within MTData signals (Figure B.2), including:

1. Gradual load increase during entry into material, followed by:
2. Sudden drop in the load magnitude, despite the continuous movement of the cutting tool into the material
3. Higher than expected axis loads during cycles for which a reduced material volume is being removed by the cutting tool.



a. X and Y position plots indicating spindle load



b. X and Y position plot indicating specific axis load

Figure B.2. X and Y position plots indicating relative cutting tool load

These observations may indicate the changing health of a cutting tool; however, each signal must be considered within the context of the process to prevent process variation being appropriated as process health. It is noted that the load variation identified in Figure B.2 does not explicitly raise any concerns indicating possible failures during cuts with a reduced material volume. However, the variations in available material are not accounted for. The MTData should thus be critically assessed to consider this limitation, and to consider the possible cause for failures in these regions. This prompted an investigation into whether the variations in material engagement really are significant enough to affect the conditions experienced by the cutting tool. To answer this required spatial knowledge of the process, including the position of the pocket centre, the overlap between stages and

the movements of the cutting tool. The information needed to support this was provided by the MTData, exploiting the cutting tool position data gained from the x and y axis encoder outputs.

Consequently, this chapter introduces the phenomenon of “pre-mill” and presents a novel mathematical approach for the calculation of variable engagement for a cutting tool during a circular pocket milling operation. This further develops the work presented in Chapter 4 and provides additional results to complement Chapter 5. The variation in material removal is calculated and it is discussed whether models that employ process control data, whilst accounting for such variation in material removal, exhibit different behaviour patterns/trends to models that consider process control data without such variation.

## B.1 Pre-mill theory and derivation

The removal of material *can never* be consistent for pocket milling operations due to sections where material has already been removed. This is herein referred to as previously milled (pre-mill) and refers to the overlap between tool passes and the unavoidable repeated movements through a volume. The pre-milled regions will affect the equivalent volume of material removed per rotation of the cutting tool. To evaluate the pre-mill influence on cutting conditions, a series of mathematical formulae are developed to calculate the estimated material engagement of the cutting tool. The formulae development is split into four primary actions:

1. Calculate straight line edge lengths between pre-mill vertices by considering mutual coordinates
2. Find the arc lengths that correspond to the straight line edge lengths
3. Identify an adjustment factor ( $\kappa$ ) by which to reduce the estimated material engagement
4. Calculate the effective pre-mill length (confirms the spatial boundaries)

### B.1.1 Edge lengths

The majority of significant geometries within a circular pocket can be approximated as circles, defined by the general equation;

$$(x - x_k)^2 + (y - y_k)^2 = r_k^2 \quad (\text{B.1})$$

Where  $(x_k, y_k)$  is the coordinate for the centre of the circle and  $r_k$  is the radius. This can be rearranged for  $y$ ;

$$y = y_k \pm (r_k^2 - (x - x_k)^2)^{0.5} \quad (\text{B.2})$$

When a cutting tool engages with both material and a pre-milled pocket, the position of the cutting tool relative to pre-milled volumes results in two mutual coordinates. These mutual coordinates can be found by first deriving the common chord as a function of  $x$ , using the representative circle centres and radii. Subtracting the equation for either the pre-milled pocket, or the cutting tool, from the equation for the other, and solving for  $y$  results in;

$$y = \frac{-(r_i^2 - r_j^2)}{2(y_i - y_j)} + \frac{x_i^2 - x_j^2}{2(y_i - y_j)} + \frac{(y_i^2 - y_j^2)}{2(y_i - y_j)} - \frac{x(x_i - x_j)}{y_i - y_j}$$

Which can be simplified to give the equation for the common chord;

$$y = -\alpha x(x_i - x_j) + \frac{1}{2}\alpha\beta \quad (\text{B.3})$$

Where  $\alpha$  and  $\beta$  are separated out to reduce equation complexity.  $i$  and  $j$  can interchangeably refer to either the cutting tool or the pre-milled pocket. Herein,  $j$  refers consistently to the cutting tool.

$$\alpha = (y_i - y_j)^{-1} \quad (\text{B.4})$$

$$\beta = (x_i^2 - x_j^2) + (y_i^2 - y_j^2) - (r_i^2 - r_j^2) \quad (\text{B.5})$$

The equation for the common chord (B.3) can be substituted into the general circle equation (B.1) and re-arranged to the form  $ax^2 + bx + c$  (substituting  $k$  for  $i$ ). Then a, b and c are given by;

$$a = 1 + \alpha^2(x_i - x_j)^2 \quad (\text{B.6})$$

$$b = \alpha(x_i - x_j)(2y_i - \alpha\beta) - 2x_i \quad (\text{B.7})$$

$$c = x_i^2 - r_i^2 + y_i(y_i - \alpha\beta) + 0.25(\alpha\beta)^2 \quad (\text{B.8})$$

a, b and c can be used with the standard quadratic equation to find x-values for the two mutual coordinates;

$$x_{mc} = \frac{-b \pm \sqrt{b^2 - 4ac}}{2a} \quad (\text{B.9})$$

The cutting direction dictates which one of the two mutual coordinates is relevant for the specific pocket milling process. The relevant x-value can be used with the equation for the common chord (B.3) to complete the mutual coordinate. The mutual coordinate represents the first of two pre-mill boundaries. The second boundary is unique to each of the pre-mill occurrences and is herein referred to as the "spatial boundary". The straight line edge length ( $d_{line}$ ) can be calculated using the mutual coordinate and the spatial boundary (B.10);

$$d_{line} = ((x_{mc} - x_{sb})^2 + (y_{mc} - y_{sb})^2)^{0.5} \quad (\text{B.10})$$

where  $d_{line}$  is in mm.

### B.1.2 Arc lengths

The calculation of edge lengths is a straightforward method to estimate the straight line edge length between a mutual coordinate and a spatial boundary. This is enough for small cutting tools, and when a simple estimate is appropriate. However, approximating a segment of the cutting tool circumference as a straight line results in an accuracy penalty (proportional to the size of the cutting tool and the straight line edge length). The estimate can thus be improved by accounting for the curvature of the cutting tool circumference. As the edge length subtends an angle  $\theta$  from the centre of the cutting tool footprint, the corresponding arc length can be derived using the cosine law for angles within a triangle;

$$\cos \theta_3 = \frac{l_1^2 + l_2^2 - l_3^2}{2l_1l_2} \quad (\text{B.11})$$

and the general formula for an arc;

$$S = r\theta \quad (\text{B.12})$$

Where  $\theta_3$  is the subtended angle from the centre of the cutting tool footprint. During pocket milling, the cutting tool radius is assumed constant ( $l_1 = l_2$ ). Hence, substituting  $l_2$  for  $l_1$  and replacing  $l_3$  with  $d_{ine}$ , both (B.11) and (B.12) can be combined and simplified, resulting in;

$$d_{arc} = r_{ct} \cos^{-1}\left(1 - \frac{1}{2}d_{ine}^2 r_{ct}^{-2}\right) \quad (\text{B.13})$$

where  $d_{arc}$  is the arc length (in mm) between a mutual coordinate and a spatial boundary and  $r_{ct}$  denotes the radius of the cutting tool.

### B.1.3 Adjustment factor

Due to the mechanics of the cutting process, the proportion of the cutting edge actively removing material *should* be equal to half of the cutting tool circumference ( $\pi r_{ct}$ ). However, this is often not the case due to overlaps between cutting tool passes and due to the pre-mill regions. The previously defined arc length represents a proportion of the cutting edge that is **not** actively removing material. To account for this,  $\pi r_{ct}$  can be reduced by  $\kappa$ , where;

$$\kappa = 1 - d_{arc}\pi^{-1}r_{ct}^{-1} \quad (\text{B.14})$$

Each movement of the cutting tool is assumed to be significantly smaller than the diameter of the cutting tool. Hence, the area of material removed (AMR) per cut can be approximated by a rectangular function of the diameter and the tool movement ( $d_{ct}\Delta f$ );

$$\text{AMR} = \kappa d_{ct}\Delta f$$

The AMR can also be reduced to compensate for the consistent overlap between the cutting tool and the pre-milled pockets;

$$\text{AMR} = (\kappa d_{ct} - \text{overlap})\Delta f \quad (\text{B.15})$$

where "overlap" can be any positive real number, including zero ( $\mathbb{R}_{\geq 0}$ ). For the investigated process it is noted that the consistent overlap occurs only during stages C and E.

### B.1.4 Effective pre-mill length

The length of the pre-mill region can be estimated by calculating the ratio of  $\Delta f$  against the effective pre-mill length (EPL);

$$N = 1 + (\Delta f/\text{EPL}) \quad (\text{B.16})$$

where N is the number of movements of the cutting tool. The EPL will vary depending on which of the pre-mill regions is being considered and how the cutting tool travels within that region.  $\Delta f$  represents the average travel of the cutting tool per movement. The EPL is a competent check that the correct number of MTData points have been evaluated. It is useful if the exact geometries of the process are known to ensure the calculation is accurate.

## B.2 Pre-mill examples

Using the formulae derived to calculate the material engagement of the cutting tool, the different pre-mill occurrences can be considered in detail. For these examples the calculations are based upon the 10mm Cylinder wear tests (Chapter 3) and are considered in 4 key stages:

- Identify the pre-mill occurrence and boundary vertices
- Check how many MTData points are affected by the pre-mill occurrence
- Calculate  $\kappa$  for each movement of the cutting tool within the pre-mill volume
- Apply  $\kappa$  to find the AR for all movements of the cutting tool within the pre-mill volume

The 10mm Cylinder wear tests involve a relatively simple pocket milling operation. This is re-illustrated in Figure B.3. The pre-mill regions are isolated into four occurrences (designated as Pre-mill 1 to 4) and are colour coded in Figure B.3. The constant overlap between passes - previously described as “the consistent overlap” - is not highlighted as the effect on the material engagement can be represented as a constant.

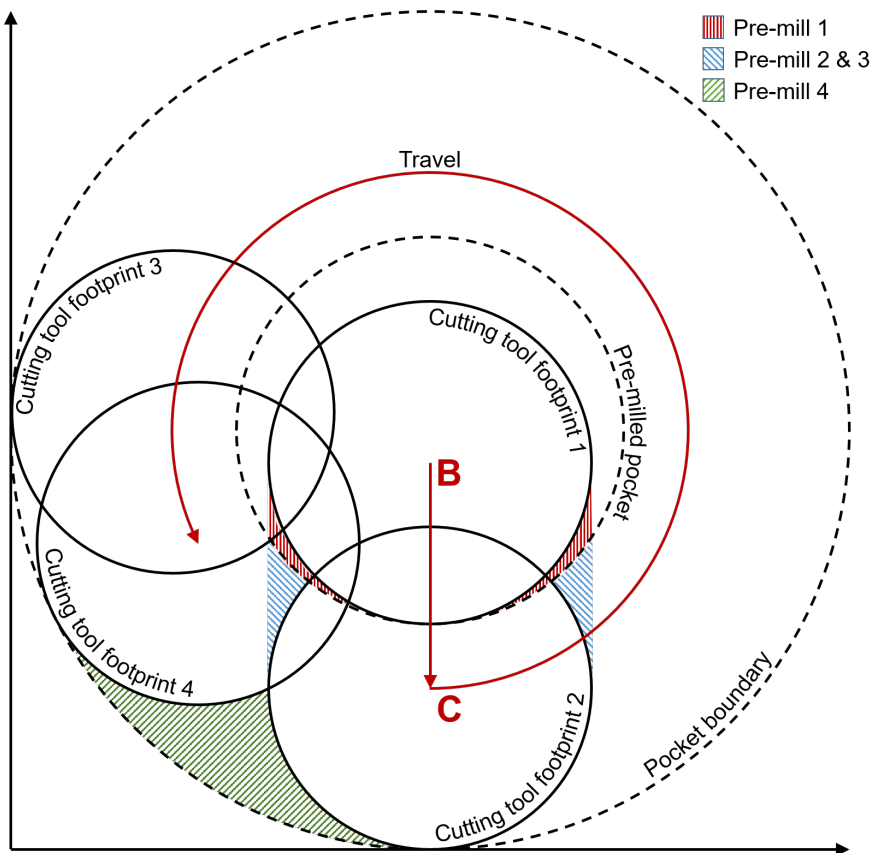


Figure B.3. Pre-mill occurrences for 10mm Cylinder wear tests (inner pocket)

**Pre-mill 1** Occurring when a cutting tool begins to break out from a pocket. This could be to increase the pocket dimensions, or simply to continue the cutting process. Pre-mill 1 occurs at the start of stage B (Figure B.3).

**Pre-mill 2** Occurring when a cutting tool changes the direction of travel. Cutting tools for milling applications will always have a circular footprint. For a change of direction, however marginal, there will be a degree of overlap between the previous path and the new path. Pre-mill 2 occurs at the start of stage C (Figure B.3).

**Pre-mill 3** Occurring towards the end of a circular partial cut around an existing pocket, if there is an overlap between the path and the pocket. If the overlap remains consistent throughout the circular partial cut, pre-mill 3 will be equal and opposite to pre-mill 2 due to process symmetry. Pre-mill 3 occurs near the end of stage C (Figure B.3).

**Pre-mill 4** During the final stage of the pocket operation the pre-milled regions account for most of the pocket volume. To account for this, the analysis is inverted for the final pass to consider the material *remaining*. The principles of the approach remain the same as for pre-mill 1-3. Pre-mill 4 occurs at the end of stage C (Figure B.3) and is herein also referred to as the final material removal (FMR).

### B.2.1 Pre-mill 1

Excluding the helical plunge into the billet, the first pre-mill occurrence (Figure B.4) is when the cutting tool travels into the material during stage B (for the inner pocket).

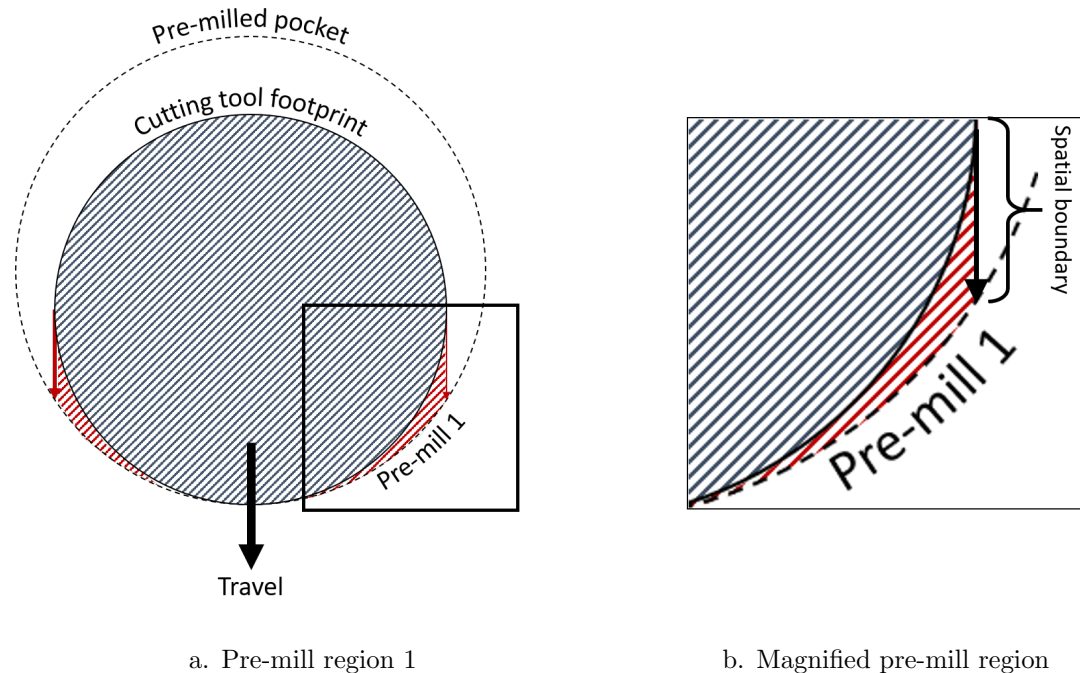


Figure B.4. Pre-mill overlap during first slotting cut

This occurs when there is a difference in size between the pre-milled pocket and the cutting tool

footprint, however, only comes into play when the cutting tool attempts to exit the pocket. As the cutting tool primarily travels along a single axis (y-axis), it can be seen that pre-mill 1 acts both sides of the leading edge of the cutting tool. Pre-mill 1 is bounded by perimeters of both the tool and the pocket, and by the cutting tool path. The cutting tool path represents the spatial boundary (occurring at  $x = x_{ct} \pm r_{ct}$  and  $y = y_{ct}$ ) and is effective until  $y_{ct} \leq y_p$  for  $x = x_{ct} \pm r_{ct}$ . Where  $x_{ct}$  and  $y_{ct}$  relate to the cutting tool and  $y_p$  relates to the pre-milled pocket.

Figure B.4b illustrates the spatial boundary. The mutual coordinates occur at each intersect between the cutting tool boundary and the pre-milled pocket boundary. Control of the MT movements dictated that pre-mill 1 will occur when the cutting tool travels solely in the negative y direction. This enables the beginning of the region to be easily identified. The end of the region will occur after enough travel in the negative Y direction. The movements of the cutting tool within the region can be estimated using Equation (B.16), where;

- The EPL is equal to the maximum y-axis travel of the spatial boundary (here 2.3mm) and can be calculated using the spatial boundary conditions for the initial position of the cutting tool with Equation (B.1)
- $\Delta f$  can be calculated using the x and y coordinates given in Table B.1 (0.416mm)

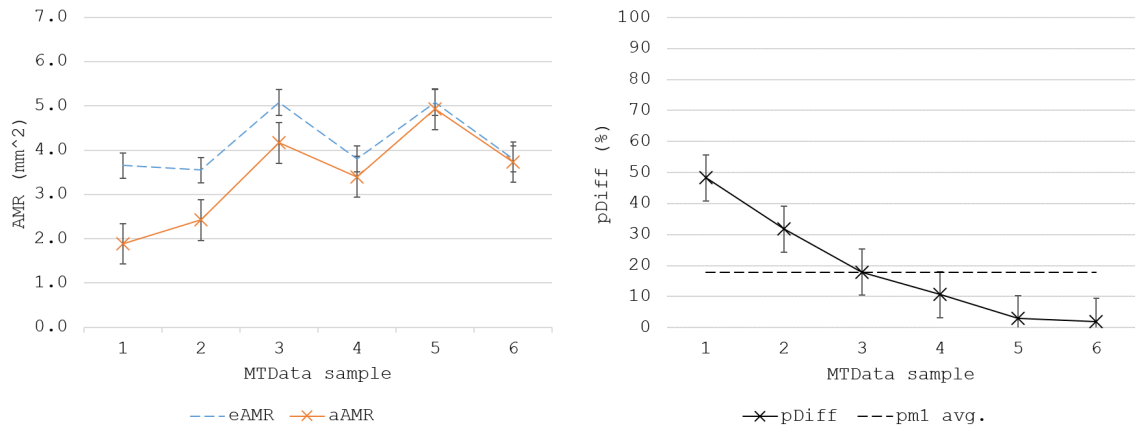
The number of the MTData entries affected by the pre-mill occurrence is estimated (using Equation (B.16)) to be  $N = 6$ . Table B.1 provides the calculated results for each MTData entry.

Table B.1. Pre-mill 1 material engagement

X (mm)	Y (mm)	$\kappa$ (%)	eAMR (mm <sup>2</sup> )	aAMR (mm <sup>2</sup> )	pDiff (%)
25.816	104.012	0.516	3.650	1.886	0.483
25.816	103.657	0.682	3.548	2.420	0.317
25.816	103.150	0.820	5.071	4.162	0.179
25.816	102.769	0.893	3.803	3.399	0.106
25.816	102.262	0.971	5.071	4.923	0.029
25.816	101.882	0.980	3.803	3.727	0.019

Where the estimated AMR (eAMR) is the simple estimate of the material removal and the actual AMR (aAMR) is the actual material removal. The eAMR is calculated using Equation B.15 when  $\kappa = 1$  and excludes pre-mill 1. The aAMR is calculated using Equation B.15 and accounts for pre-mill 1. pDiff is the proportional difference between the two. eAMR, aAMR and pDiff are illustrated in Figure B.5.

The results indicate that the active percentage of the cutting edge (proportional to the aAMR) *increases* steadily throughout the pre-mill region. This corresponds to a progressive increase in the material engagement of the cutting tool over the six consecutive MTData samples. Figure B.5b indicates this also corresponds to the aAMR tending towards the value of the eAMR. It was estimated



a. eAMR compared with aAMR

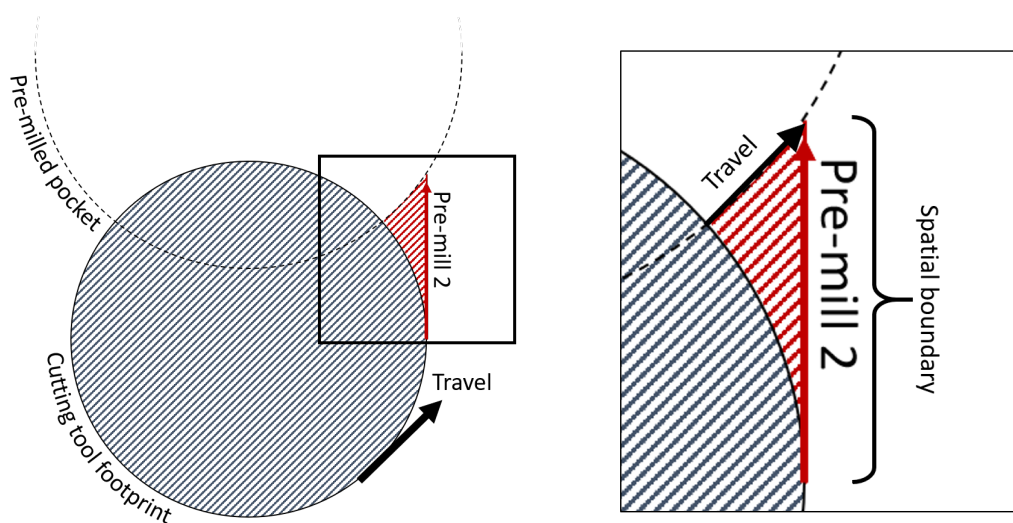
b. Proportional difference per sample

Figure B.5. Relative impact of pre-mill 1 on AMR

that the cutting tool should achieve a total AMR of  $24.9\text{mm}^2$ , yet an actual AMR of  $20.5\text{mm}^2$  is noted when pre-mill 1 is included. Hence, pre-mill 1 contributes to an overall 17.7% shift in the AMR. The standard-error bars indicate that the difference between expected AMR and actual AMR *may be negligible* for samples 4-6. However, it is noted that the standard-error bars are calculated from the six samples and are hence not necessarily representative of the true calculation error. It is observed that there is a significant "oscillating" effect in Figure B.5a. This is a consequence of a low MTData sampling frequency of 10Hz and would be improved by increasing the sampling frequency for future acquisitions.

### B.2.2 Pre-mill 2

The second pre-mill overlap (Figure B.6) occurs when the cutting tool begins the circular partial cut of stage C (for the inner pocket). Pre-mill 2 arises due to an overlap between the original path and the



a. Pre-mill region 2

b. Magnified pre-mill region

Figure B.6. Pre-mill overlap at start of circular partial cut

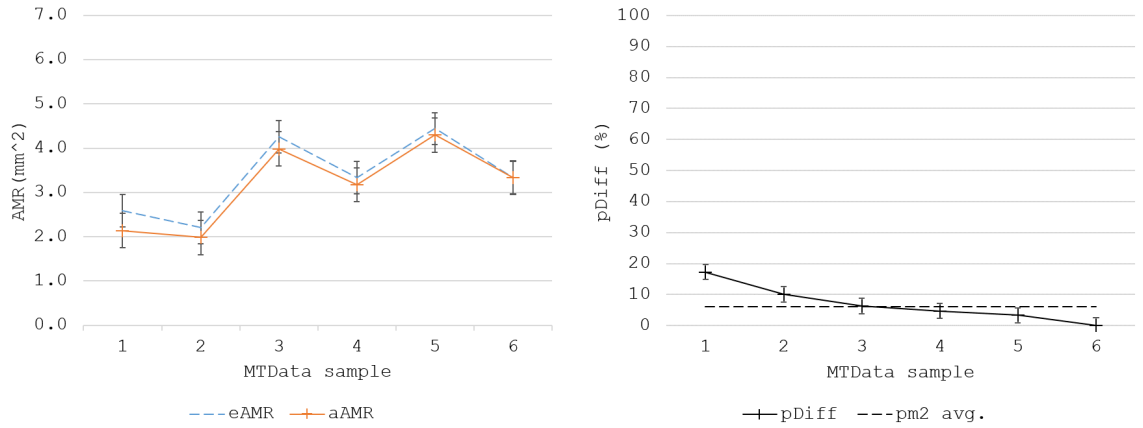
new path of a cutting tool. It is noted that for pocket milling this process is symmetrical, irrespective of up-milling or down-milling. If the path of the cutting tool travels in the opposite direction to Figure B.6 the effective pre-mill region will be equal and opposite mathematically. The behaviour of the cutting tool may change due to the differences between up/down milling. This is not investigated in this paper. Pre-mill 2 is bounded by perimeters of both the tool and the pocket (to a lesser extent than pre-mill 1) and by the boundary of the *original* cutting tool path. The limits of the original cutting tool path can be taken to represent the spatial boundary (occurring at  $x = x_p + r_{ct}$ ), where  $x_p$  relates to the pre-milled pocket. When reached by the leading mutual coordinate between the cutting tool and the pre-milled pocket, pre-mill 2 ceases to affect the AMR ( $x_{mc} \geq x_{sb}$  and  $y_{mc} \leq y_{sb}$ ). Figure B.6b illustrates the spatial boundary.

Pre-mill 2 begins when the cutting tool starts to travel in both the positive x direction and the positive y direction. The pre-mill region (in this case) ends after five subsequent MTDData entries, due to an EPL equivalent to the maximum travel around the circumference of the pre-milled pocket (2.6mm) and a  $\Delta f$  of 0.502mm. The EPL was estimated using Equation (B.13), using the radius of the pre-milled region (instead of the cutting tool) and by replacing  $d_{line}$  with the distance between the first mutual coordinate and the final coordinate of the spatial boundary. The sixth MTDData entry in Table B.2 is outside of pre-mill 2 but is included to emphasise the differences between the other corresponding eAMR and aAMR results. Table B.2 provides the calculated results for each MTDData entry. The results for eAMR, aAMR and pDiff are illustrated in Figure B.7.

Table B.2. Pre-mill 2 material engagement

X (mm)	Y (mm)	$\kappa$ (%)	eAMR (mm <sup>2</sup> )	aAMR (mm <sup>2</sup> )	pDiff (%)
25.816	97.456	0.879	2.587	2.140	0.172
26.130	97.461	0.929	2.203	1.981	0.101
26.738	97.486	0.955	4.254	3.983	0.063
27.209	97.557	0.966	3.333	3.175	0.047
27.828	97.695	0.976	4.443	4.296	0.033
28.285	97.831	0.964	3.332	3.332	0.000

The results are similar to pre-mill 1, with Figure B.7b showing the aAMR tending towards the value of the eAMR. However, the shift due to pre-mill 2 is considerably muted in comparison to the shift due to pre-mill 1. It was estimated that the cutting tool should achieve a total AMR of 20.2mm<sup>2</sup>, yet an actual AMR of 18.9mm<sup>2</sup> was noted after the addition of pre-mill 2. Pre-mill 2 thus contributes to an overall 6.2% shift in the AMR. It is noted that the standard-error bars indicate significant overlap between the eAMR and the aAMR for all samples. In practice this could indicate that pre-mill 2 is negligible and/or not observable, however, it is again noted that the standard-error bars are calculated from the given samples, thus not necessarily representative of the true calculation error. The significant "oscillating" effect can again be observed from the data, providing additional evidence that the sampling frequency should be increased.



a. eAMR compared with aAMR

b. Proportional difference per sample

Figure B.7. Relative impact of pre-mill 2 on AMR

### B.2.3 Pre-mill 3

The third pre-mill overlap (Figure B.8) occurs when the cutting tool nears the end of stage C (for the inner pocket). Pre-mill 3 arises when the end of a pocket is reached and the cutting tool overlaps with

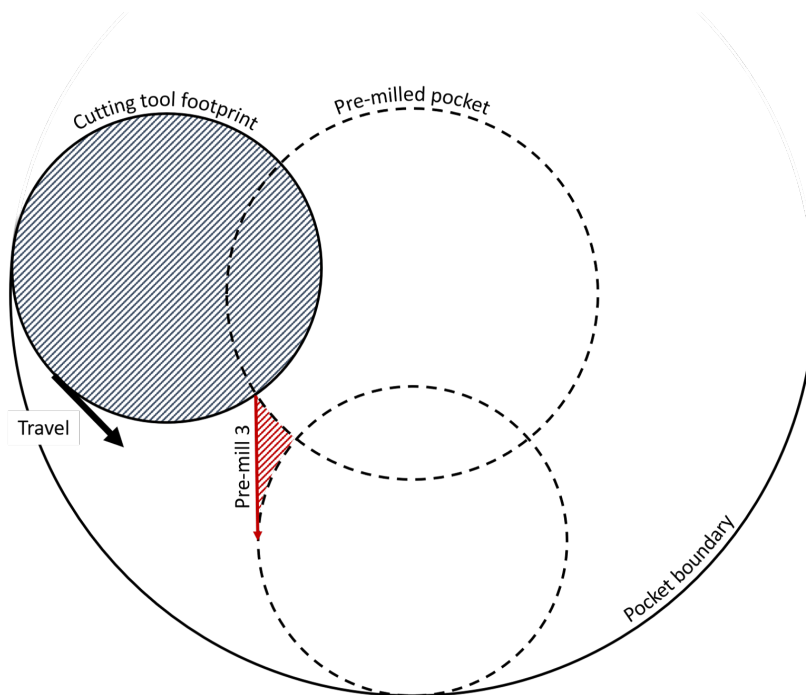


Figure B.8. Final pre-mill overlap for circular partial cut

the path created during stage B. The pre-mill region will be equal and opposite in size to pre-mill 2, however, it will affect the cutting tool differently. This will be due to the direction in which the cutting tool is travelling relative to the pre-milled region and due to the additional missing material as a result of the cutting tool movements identified during pre-mill 2. Additional differences may occur between pre-mill 2 and pre-mill 3 as a result of variations in the sampled MTData. Pre-mill 3 is bounded by the perimeter of the inner pocket, by the boundary of the *original* cutting tool path (stage B) and by the perimeter of the cutting tool at the starting position of the current pocket ( $ct_0$ )

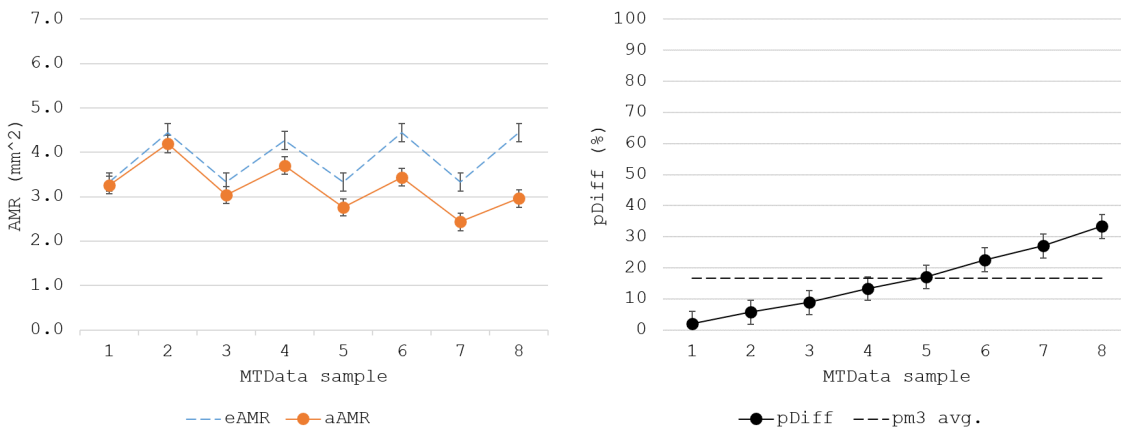
(start of stage C - indicated in Figure B.8). The spatial boundary is the perimeter of the cutting tool as it was starting stage C and is effective from the mutual coordinate between the pre-milled pocket and  $ct_0$ . Pre-mill 3 will continue to affect the cutting tool until the mutual coordinate between the cutting tool and  $ct_0$  satisfies  $x = x_{ct0} - r_{ct}$ .

Pre-mill 3 begins when the cutting tool starts to travel in the positive x direction and the negative y direction. The pre-mill region ends after eight MTData entries, due to a  $\Delta f$  of 0.541mm and an EPL equal to the distance between the first mutual coordinate of the region and the mutual coordinate satisfying  $x = x_{ct0} - r_{ct}$ . It is noted that  $\Delta f$  indicates a marginal increase in the feed rate compared to the beginning of stage C. Table B.3 provides the calculated results for each MTData entry. The

Table B.3. Pre-mill 3 material engagement

X (mm)	Y (mm)	$\kappa$ (%)	eAMR (mm <sup>2</sup> )	aAMR (mm <sup>2</sup> )	pDiff (%)
17.898	105.668	0.985	3.333	3.263	0.021
17.899	105.033	0.959	4.443	4.188	0.057
17.932	104.558	0.938	3.332	3.037	0.088
18.021	103.955	0.906	4.267	3.700	0.133
18.120	103.489	0.880	3.332	2.762	0.171
18.295	102.879	0.841	4.444	3.439	0.226
18.458	102.432	0.810	3.333	2.431	0.270
18.717	101.852	0.766	4.443	2.963	0.333

results for eAMR, aAMR and pDiff are illustrated in Figure B.9.



a. eAMR compared with aAMR

b. Proportional difference per sample

Figure B.9. Relative impact of pre-mill 3 on AMR

The results indicate that the active percentage of the cutting edge (proportional to the aAMR) *decreases* steadily throughout the pre-mill region, corresponding to a proportional decrease in the material engagement of the cutting tool. Figure B.5b indicates this also corresponds to the aAMR tending away the value of the eAMR. It was estimated that the cutting tool should achieve a total AMR of

30.9mm<sup>2</sup>, yet an actual AMR of 25.8mm<sup>2</sup> was noted after the addition of pre-mill 3. Pre-mill 3 thus contributes to an overall 16.6% shift in the AMR, increasing at an almost linear rate. It is noted that the standard-error bars indicate overlap between the eAMR and the aAMR for the first three samples, however, the points raised previously still apply. “oscillating” of the data is observed in Figure B.9a but is not replicated in the pDiff trend (Figure B.9b).

## B.2.4 Final material removal (Pre-mill 4)

The final stage of the pocket milling operation is the removal of the material region indicated in Figure B.10 as “Final MR” and previously referred to as the FMR. To calculate the impact of the FMR the

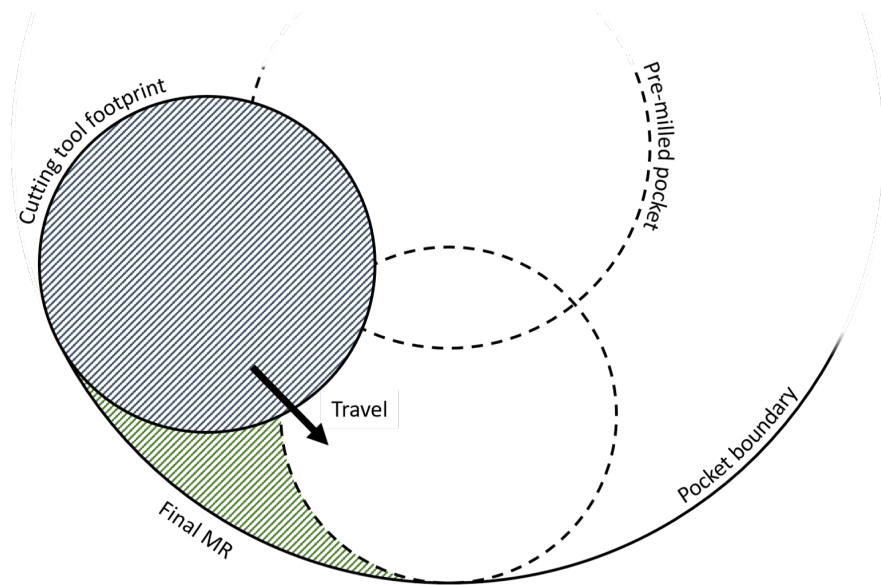


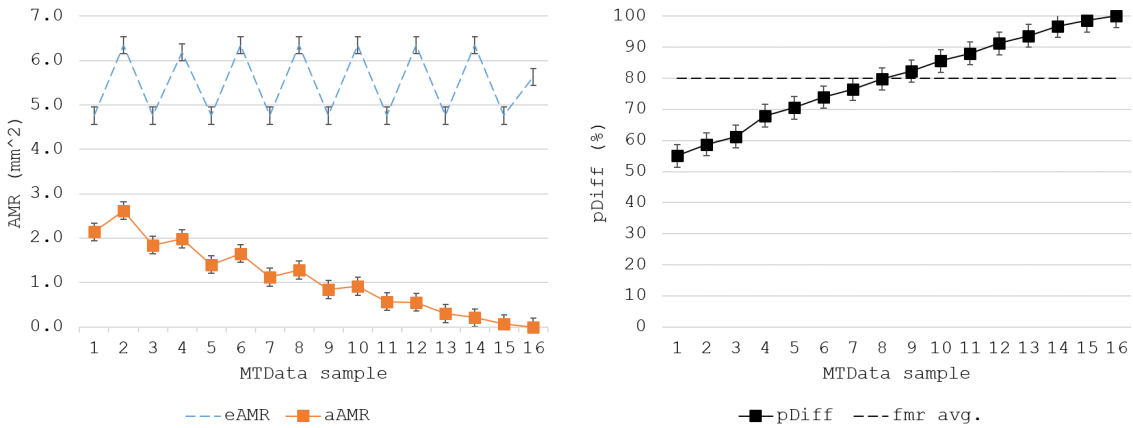
Figure B.10. Final region of metal to be removed during circular partial cut

estimation of the cutting tool engagement must be approached in a different way to pre-mill 1-3. The primary difference will be that  $\kappa$  will represent the material *to be* removed, rather than the material *being* removed.  $\kappa$  can then be employed to find the AMR for each feed increment in the region. The FMR trend should be like the AMR trend for pre-mill 3 due to the continued reduction in the material engagement of the cutter. This is opposite to pre-mill 1 and pre-mill 2, both of which observed an increase in the material engagement of the cutter. The FMR is bounded by the outer perimeter of the current pocket (pocket boundary) and by the perimeter of the cutting tool at the starting position of stage C ( $ct_0$ ). The FMR should affect the cutting tool until the end of the pocket is reached. The end of the pocket will be indicated by the start of subsequent pocket enlargement, or by rapid movements out of the pocket. The FMR begins immediately after pre-mill 3 and ends before the cutting tool travels solely in the negative y direction. Table B.4 provides the calculated results for each MTDData entry.

The results for eAMR, aAMR and pDiff are illustrated in Figure B.11. The results indicate that the active percentage of the cutting edge (proportional to the aAMR) *decreases* steadily throughout the pre-mill region. This reduction corresponds to a proportional decrease in the material engagement

Table B.4. FMR material engagement

X (mm)	Y (mm)	$\kappa$ (%)	eAMR (mm <sup>2</sup> )	aAMR (mm <sup>2</sup> )	pDiff (%)
18.941	101.432	0.449	4.761	2.140	0.550
19.278	100.894	0.412	6.348	2.619	0.587
19.558	100.509	0.387	4.761	1.842	0.613
19.941	100.023	0.320	6.187	1.984	0.679
20.273	99.681	0.294	4.760	1.402	0.705
20.745	99.257	0.260	6.349	1.653	0.739
21.120	98.964	0.235	4.760	1.119	0.764
21.647	98.610	0.201	6.348	1.281	0.798
22.060	98.373	0.177	4.762	0.843	0.822
22.631	98.095	0.144	6.346	0.915	0.855
23.073	97.918	0.119	4.762	0.570	0.880
23.677	97.723	0.087	6.347	0.554	0.912
24.139	97.608	0.063	4.762	0.301	0.936
24.765	97.499	0.032	6.348	0.208	0.967
25.238	97.450	0.014	4.761	0.067	0.985
25.801	97.455	0.000	5.630	0.000	1.000



a. eAMR compared with aAMR

b. Proportional difference per sample

Figure B.11. Relative impact of FMR on AMR

of the cutting tool. Additionally, Figure B.11 indicates this also corresponds to the aAMR tending away the value of the eAMR. It was estimated that the cutting tool should achieve a total AMR of 87.4mm<sup>2</sup>, yet an actual AMR of 17.5mm<sup>2</sup> was noted after the addition of the FMR region. The FMR thus contributes to a significant 80.0% shift in the AMR, reaching a maximum of 100.0% by the end of the pocket (corresponding to zero material remaining).

### B.3 Pre-mill effect on process data

It has been indicated that each of the pre-mill regions affect the AMR per cut by different magnitudes. Figure B.12 illustrates the difference between the eAMR per cut and the aAMR per cut for an entire pocket milling operation with labels for the pre-mill occurrences (1-4). This connects the pre-mill regions outlined in Section B.2 and includes the outer pocket stages (stage D and stage E).

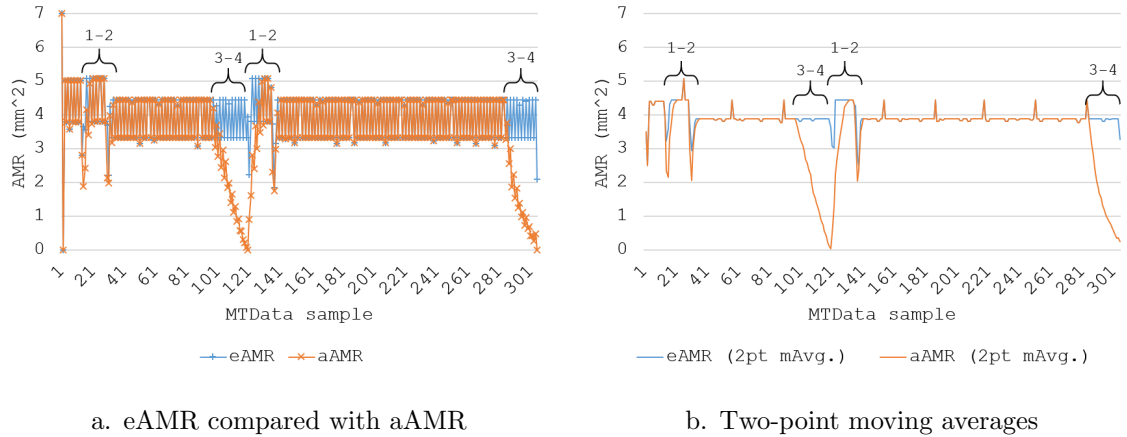


Figure B.12. Pre-mill impact on the material removal process

Figure B.12a highlights the extent of variable material engagement within the pocket milling process and shows the transition between each of the regions. The two trends in material removed are highly variable between each subsequent cut due to the 10Hz sampling frequency. This is an effect that has been repeatedly referred to as “oscillating” and can be alleviated by considering a two-point moving average for each given trend line (Figure B.12b). The two trends are visibly different as a result of the pre-mill regions, with an actual magnitude difference of approximately 10.1%. It is noted that the aAMR exhibits smoother transitions between each part of the signal, with each transition being more gradual. The key result is that the material engagement of the cutting tool is shown to be significantly changed by each of the pre-mill regions, however, it should be noted that the biggest contributor to the total difference is the FMR. Additional data sets are illustrated in Figure B.13 to indicate the efficacy of the derived pre-mill calculations.

Notwithstanding, these trends should be compared with and applied to each of the other obtained process signals and appropriate health indicators. This will indicate the true influence of the pre-mill regions on the cutting process and the behaviour of the cutting tool. The process parameters that will be considered include the spindle rotational speed (SRS), the spindle motor load (SML) and the estimated energy consumption per cut. The signals will be compared with the full aAMR for CK041-01.

#### B.3.1 Spindle rotational speed

Figure B.14 compares the SRS to a two-point moving average of the aAMR per cut.

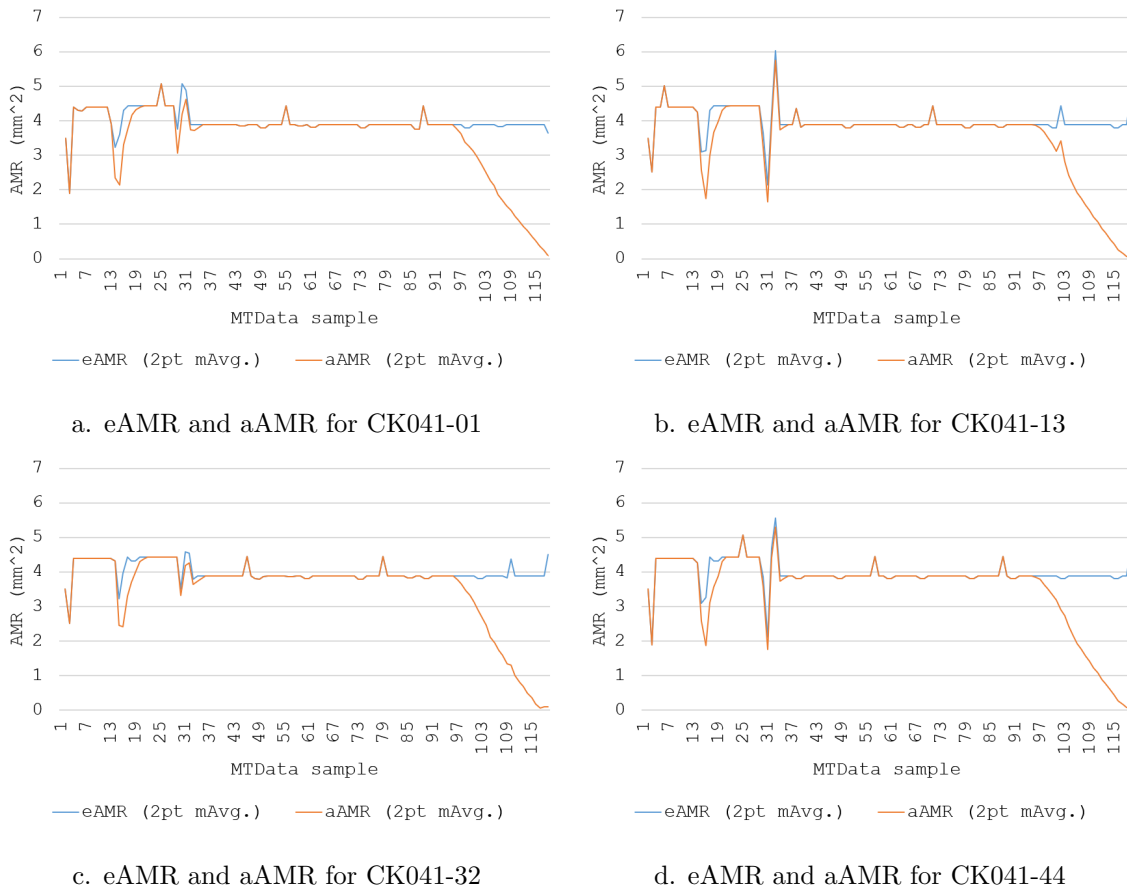


Figure B.13. Inner-pocket examples for eAMR and aAMR

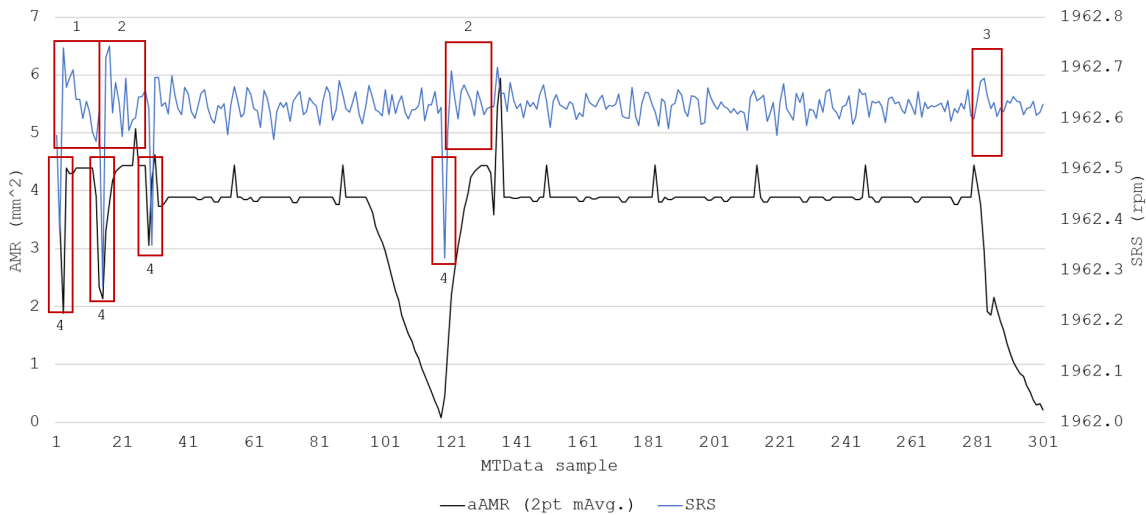


Figure B.14. Material removed per cut compared with the equivalent SRS

Several aspects of the plot are noted as follows:

1. The plunge cycle is accompanied by a local downward trend in the SRS. This may be caused by the increasing contact between the cutting tool and the material as the cutting tool plunges into the workpiece. Alternatively, the cutting tool may be affected by trapped swarf during the entry into the material, thus slowing down the tool rotation.
2. Instances in which the cutting tool exits a recently cut pocket to increase the pocket dimensions

results in a local downward trend in the SRS, like the trend noted for the plunge cycle. These patterns imply that the SRS control initially anticipates more material than is present (missing due to pre-mill 1) and hence the cutting tool enters the material at a higher rpm than expected. As the cutter engagement increases, and the control of the SRS is re-established, the SRS tends towards the desired value.

3. At the instant the cutting tool reaches the outer pocket FMR (end of stage E) a minor increase in the SRS is observed. This again implies that the SRS control anticipates a higher material engagement of the cutting tool. The sharp decrease in the engagement of the cutting tool results in a minor peak in the SRS, however this is rapidly controlled by the NC. It is not noticeable from the given signal whether a similar increase in the SRS is observed at the instant the cutting tool reaches the inner pocket FMR (end of stage C).
4. Every occurrence of negligible material in the path of the cutting tool is accompanied by a significant decline in the registered SRS. Since the decline in the SRS is slightly offset towards the subsequent material re-entry, it is implied that the drop is caused by the initial contact with, and/or engagement with, the workpiece material.

The four aspects of Figure B.14 outlined above are notable when emphasised, however, identifying them in practice *without* intervention by the machine operator, or a knowledgeable engineer, is necessary to keep the processing simple and efficient. It may also be the case that the four aspects do not indicate any significant health-related concerns with the cutting process. In these cases, the features should be identified but excessive analysis and/or investigation should be avoided. In response, Figure B.15 considers the results of an upper cumulative sum (QSUM), applied to the SRS, and presents this alongside the two-point moving average of the aAMR per cut. The plunge cycle (P) and each of the pre-mill occurrences (1-4) are indicated on Figure B.15.

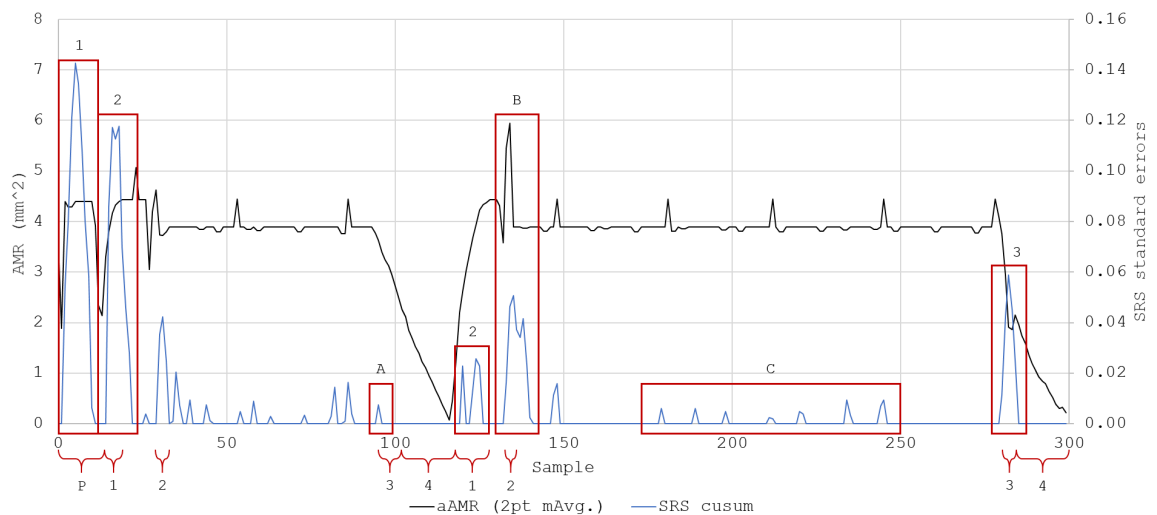


Figure B.15. Correlation of pre-mill regions with significant SRS deviations (QSUM)

The SRS QSUM identifies many of the same aspects noted in Figure B.14, with only the occurrences of aspect 4 being omitted. This is due to the lower cumulative sum not being included. It is noted

that the plunge cycle and all pre-mill regions are accompanied by peaks in the SRS standard error. The peaks that correspond to the pre-mill regions are observations that logically result from the variable material engagement of the cutting tool. These indicate that the control of the SRS was initially set too high and would correspond to there being less material than is anticipated. They do not necessarily identify the health of the cutting tool, however, they could be utilised for such a purpose if it is identified that they vary for subsequent operations. Variations would suggest changes in the health of the cutting tool, that may be causing difficulty in removing material. The peaks in the SRS QSUM indicate that the corresponding aspects are discernible from the general trend, at approximately two+ standard errors. It is noted that neither of the two FMR regions significantly affect the SRS QSUM. This is sensible since the cutting tool is removing negligible material, thus opposition to the control of the process is also negligible. A few additional observations in Figure B.15 that were absent, or not noticeable in Figure B.14 are noted as follows:

- A. There is a minor peak in the SRS standard error at the instant the cutting tool reaches the first FMR. The peak is much less than one standard error, and much less than the standard error at the instant the cutting tool reaches the second FMR. This could be challenging to identify in practice.
- B. There is an observed peak in the aAMR and an accompanying peak in the SRS QSUM. Whilst the peak in the aAMR could be assumed due to missing data (resulting in a high AMR for the subsequent cut), the corresponding peak in the SRS implies that this may not be the case. This is implied because the magnitude of the SRS should be independent of the sampling frequency. Nevertheless, the SRS peak is less than a single standard error and therefore may not be significant. Equally, the peak in the SRS may be caused by there being less material than anticipated and would infer that the peak in the aAMR is a result of pre-mill 2. This would need to be investigated for reliable conclusions to be drawn.
- C. There are numerous minor peaks in the SRS QSUM that occur during each of the circular partial cuts. These minor peaks occur outside of pre-mill regions and thus cannot be attributed to a lack of material. They may relate to key-health features of the signal, however, to confirm this would require comparison to different stages in the life of the cutting tool. Moreover, it is noted that each of the minor peaks is much less than one standard error, hence they may be negligible and/or random.

### B.3.2 Spindle motor load and relative energy

Figure B.16 considers the SML, presenting the signal alongside the eAMR per cut and the aAMR per cut. The figure illustrates the similarities between *all three* trends, however, it is noted that the aAMR more closely matches the SML than the eAMR. This is logical since loads on the spindle should correspond to the removal of material. When material is no longer present there should be negligible loading on the spindle. It is coincidental that the AMR and the SML trends are equal in magnitude as the AMR is given as an *area* of material removed. In practice the volume of material removed (VMR)

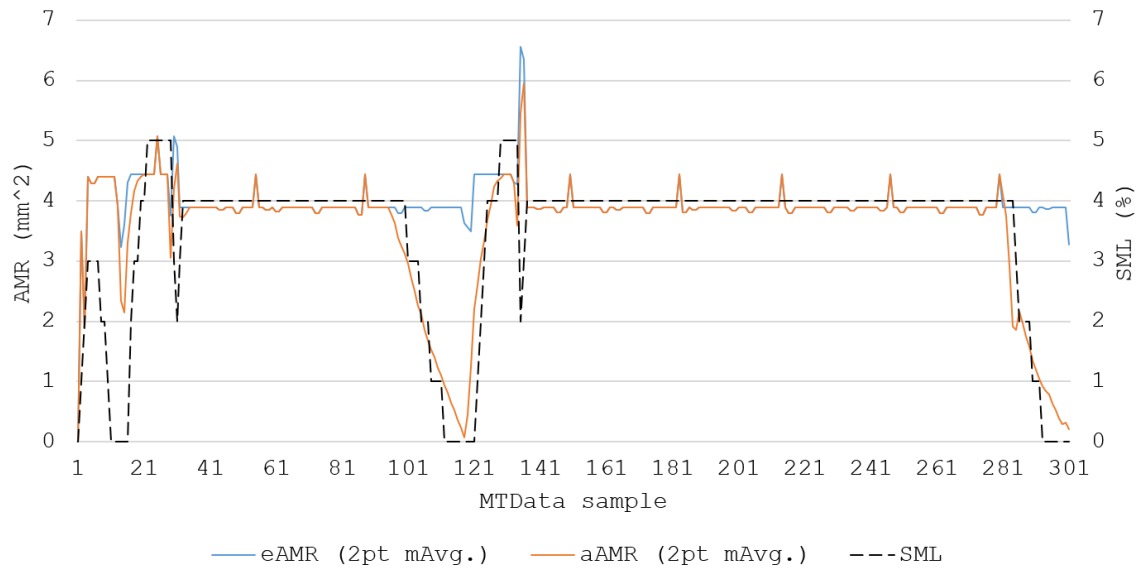
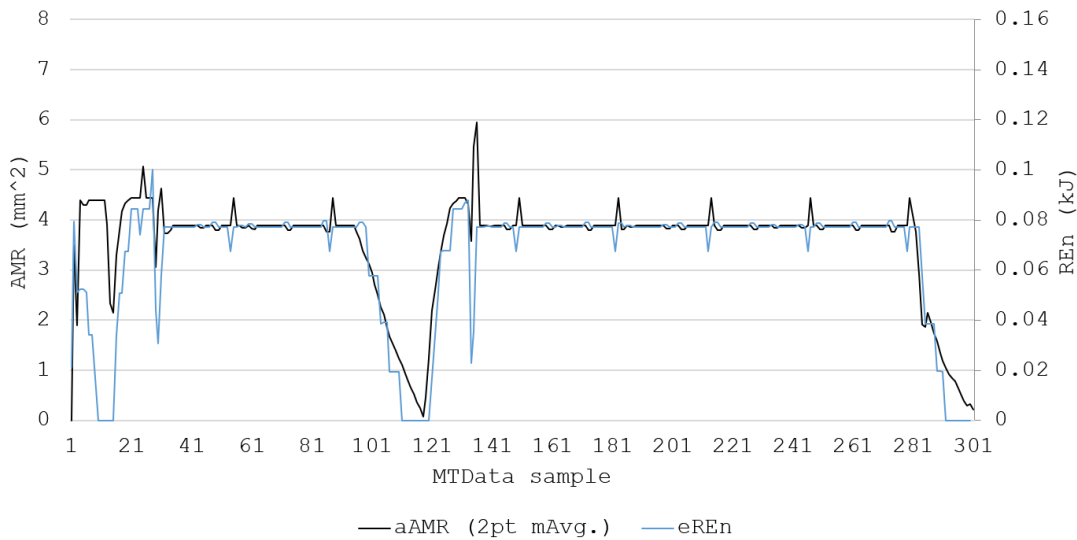


Figure B.16. Comparison of the eAMR and the aAMR with the SML

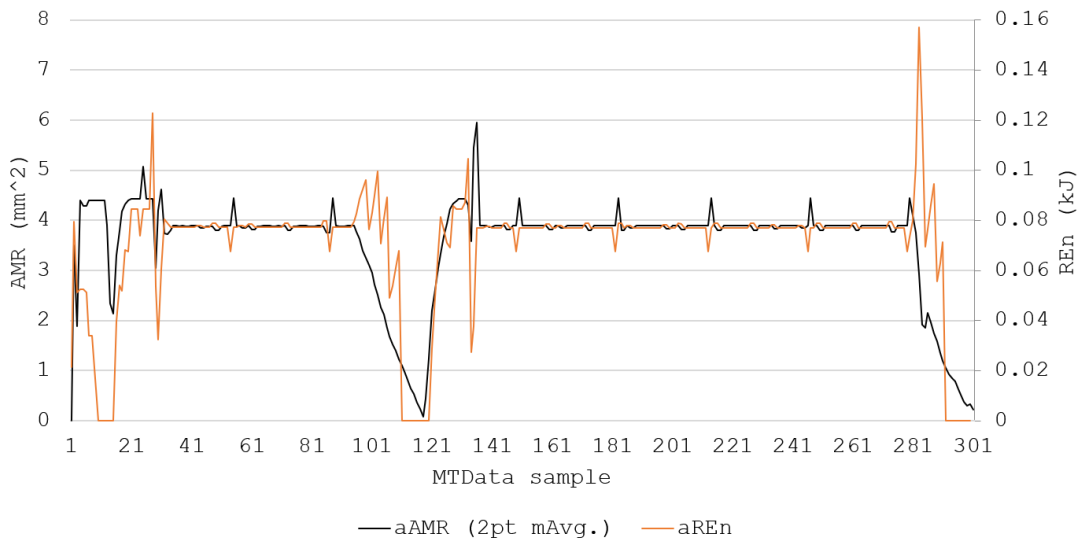
would be more usable and should be implemented. Introducing the depth of each cut to consider the VMR would not change the correlation between the material removal and the SML, however the magnitudes of each trend will be different. It should be repeated that the depth of cut is not included as the accuracy cannot be guaranteed without additional data.

Notwithstanding the similarities between the two trends, a simple comparison offers nothing of value towards the analysis of the data. To gain value, the trends in the AMR and the SML can be combined to calculate the relative energy requirements of the cutting process. Figure B.17 considers the relative energy (REn) required for the cutting tool to remove  $1\text{mm}^2$  of material. The REEn is calculated for both the eAMR per cut and the aAMR per cut. Each calculated REEn is compared with the aAMR. The y-axes are adjusted to  $0.02 \text{ REEn per AMR}$ . It is observed that the estimated REEn resembles the SML trend given in Figure B.16 and is a close match to the aAMR. These similarities are logical as the loading on the spindle tends to zero as the material engagement of the cutting tool reduces through the cut. However, it was also observed through testing that many cutting tool failures occur during, or close to, pre-mill regions. Examples were given in Figure B.1. This opposes the logic that the REEn should reduce in line with the material engagement as, if this were the case, the likelihood of cutting tool failure during the pre-mill regions should be reducing. Returning to Figure B.17, the actual REEn partially explains the higher incidence of failures occurring during pre-mill regions. The actual REEn indicates an opposing result to the expected REEn, where the energy required to remove each  $1\text{mm}^2$  of material peaks whilst the engagement of the cutting tool reduces. This is most obvious in the lead up to the end of each pocket (inner and outer). It is noted that the energy required to remove the last bit of material (per cut) is much greater than expected, considering that the material engagement is reducing AND the load on the spindle is reducing. Indeed, the actual amount of energy required is, at times, more than double the expected energy required for the material removal process.

It is observed that the peak in the REEn occurring during the inner loop FMR is not as severe as the peak during the outer loop FMR. This may be influenced by the rate at which the SML decays within



a. aAMR compared with expected REen



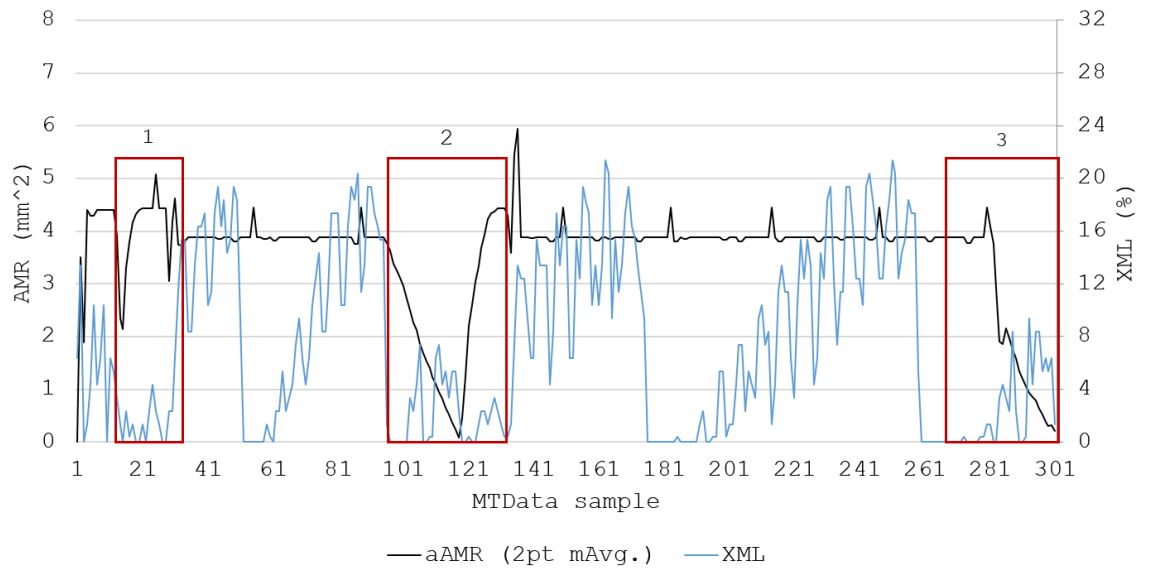
b. aAMR compared with actual REen

Figure B.17. Energy required to remove  $1\text{mm}^2$  of bright mild steel during pocket milling

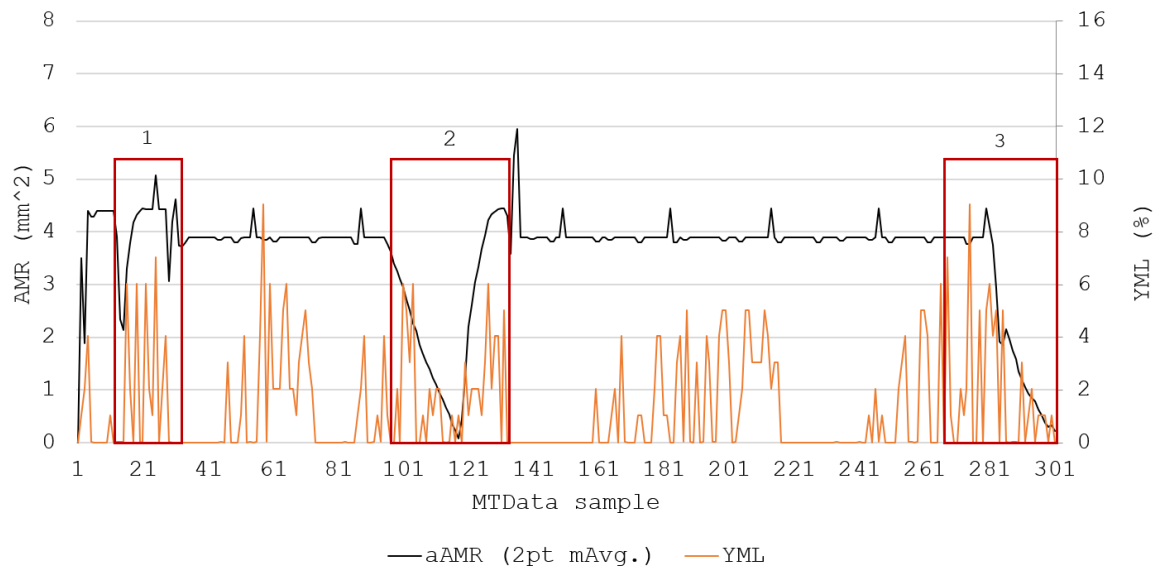
each region, as the SML decays at a slower rate following the inner loop than the outer loop. The REen may be utilised for the assessment of the health of the cutting tool in much the same way as the SRS. If the calculated REen varies between each subsequent pocket, the variations may be attributed to the health of the cutting tool. However, care should be taken to avoid appropriating the health of the process as the health of the cutting tool. Similarly, care should be taken to avoid concluding that the health of the cutting tool is changing, when the variations in the REen are simply random or negligible differences between pocket milling operations.

### B.3.3 Axis motor loads

The last of the investigated process signals are the machine axes. Figure B.18 considers the XML and the YML, presenting each (edited) signal alongside the aAMR per cut. The effects that the pre-mill



a. X-axis percentage load



b. Y-axis percentage load

Figure B.18. Axis loads versus AMR

regions may have on each of the axes are challenging to quantify due to the complexity of the signals and the inherent noise in the data (discussed in Chapters 5-8). Therefore, each trend has been edited by using the “mean resting axis load” for each axes (see Chapter 6) as a minimum threshold. By subtracting the mean resting axis load, three regions remain of interest. For the XML (Figure B.18a):

1. Region 1 should indicate negligible load as the cutter is travelling exclusively along the Y-axis. As the XML peaks above the X minimum threshold, it can be inferred that there are additional loads on the cutting tool that arise from either the health of the process, or of the cutting tool. As region 1 is concurrent to pre-mill 1, the pre-mill region may be affecting the XML.
2. Region 2 occurs at the end of the inner pocket at the point when the material engagement of the

cutting tool is dropping off rapidly. Despite the cutting direction tending towards positive X, the reducing aAMR should suppress any significant rise in the resulting XML. However, despite an initial drop in XML magnitude, the XML does peak significantly over the minimum threshold. This peak may indicate resistance to motion due to small cuts, but equally may indicate a failure of the MT to respond appropriately to a lack of material, hence “jerking” out of the material. The MT adjustment to the feed rate is not a closed loop, giving credibility to this hypothesis. Region 2 also includes the Y-axis movement indicating the start of the outer pocket. Again, the XML peaks over the X minimum threshold. The reasons for this are likely to mirror the reasons for Region 1.

3. Region 3 occurs at the end of the outer pocket and is subject to the same observations noted for Region 2. Again, the XML peaks significantly over the minimum threshold. The reason for this peak is likely to be the same, or similar, as for Region 2.

For the YML (Figure B.18b) the same three regions are noted as they encompass most of the pre-mill regions:

1. Region 1 indicates an increase in the standard deviation (from 1.9 to 3.0) over the region – compared to the samples leading up to said region – but a plateau in the moving (mean) average. As pre-mill 1 results in the aAMR increasing over the same region, it would suggest a positive trend in the YML should be expected; however, this upward trend does not materialise. It is therefore suggested that pre-mill 1 has no discernible impact on the YML according to the available data.
2. Region 2 indicates a slight peak in the YML magnitude, in line with occurrence of pre-mill 3. This peak (similarly to the XML observations) may indicate a failure of the MT to respond appropriately to a lack of material, again “jerking” forward. This indicates that pre-mill 3 does influence the process behaviour. As the aAMR tends to zero and the cutting direction tends towards positive X the YML should dissipate (fall below the Y minimum threshold). The persisting YML indicates that pre-mill 4 is also affecting the cutting tool. Region 2 also includes the Y-axis movement indicating the start of the outer pocket. However, in contrast to the inner pocket observations (Region 1) the moving (mean) average increases over the pre-mill 1 region and drops sharply upon reaching pre-mill 2. The observations are expected and indicate that in this instance pre-mill 1 and pre-mill 2 influence the process behaviour.
3. Region 3 (encompassing 42 samples) indicates another increase in the sample standard deviation (from 2.3 – 3.0) over the preceding 42 samples. There is also a marginal change in the distribution of the data (slight platykurtic shift from  $K=0$  to  $K=-0.2$ , where  $K$  is the sample kurtosis value). The load should dissipate (fall below the Y minimum threshold) as the aAMR tends to zero *and* the cutting direction tends towards positive X; however, the persisting YML indicates that pre-mill 4 is affecting the cutting tool. These affects may also be utilised to indicate cutting tool health when compared with the affects from similar regions in previous pockets.

The three investigated regions indicate that, despite the complexity of the XML and YML signals, the impact of the pre-mill regions on the process behaviour can still be identified. Additionally, the nature of such influence infers that the pre-mill regions may also affect the process health, the cutting tool health, or both. This would especially be the case for the instances of “jerky” movements. If such movements are occurring, it would suggest that the process would benefit from closing the control loop for the MT feed rate. Similarly, the process would benefit if the variation in the material engagement of the cutting tool within pocket milling cycles is accounted for. Either approach would allow the MT to protect the process and cutting tool health.

To further investigate the impact of the pre-mill regions on the XML and on the YML, a similar approach is taken as for the SRS with a QSUM calculated for the X and the Y axes. This approach explores the feasibility of simplifying the signal to better enable operators to categorise the explicit features and to potentially enable automated approaches to signal processing. Figure B.19 compares the XML QSUM with the aAMR.

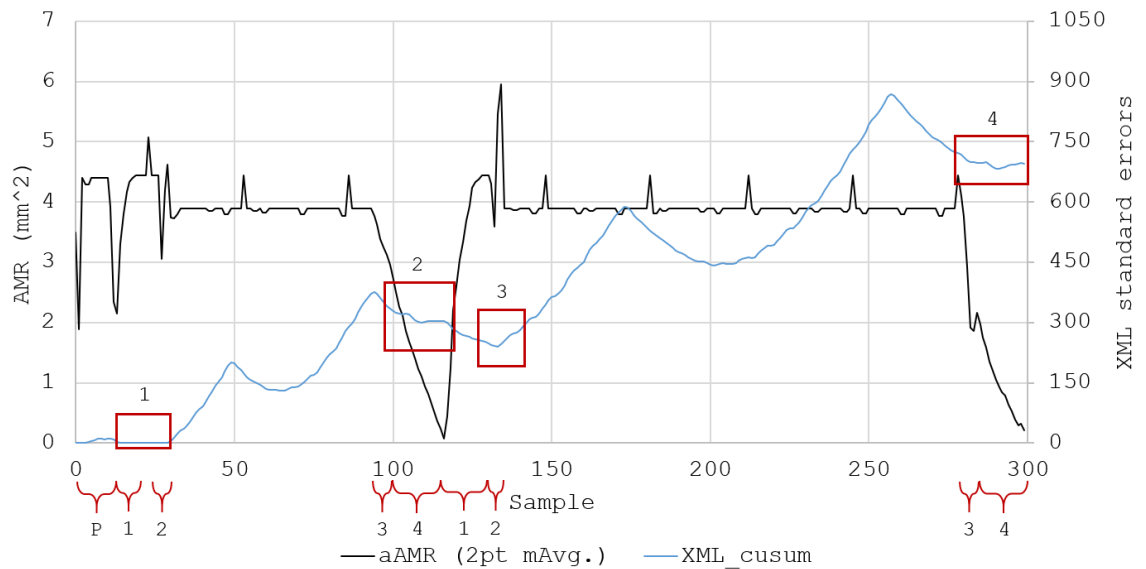


Figure B.19. Cumulative sum for X-axis percentage load compared with material removal during wear test

Firstly, it is noted that the XML peaks at close to 900 standard errors. This is due to the initial estimation of the signal mean being calculated from the first 25 samples of the signal. The implication is that the mean average of the XML is gradually increasing throughout the pocket. The cyclical nature of the XML trend results from the circular movement of the cutting tool, with each of the dips corresponding to the Y-axis travel of the cutting tool. These dips should increase in duration throughout the operation as the pocket increases in diameter. Returning to the pre-mill impact on the process behaviour; four signal regions are identified:

1. The first region has no features to indicate that pre-mill 1 has any effect on the cutting process. This infers that either the calculation of the QSUM hides any observations towards the beginning

of the sample (the mean and standard deviation are calculated from the first 25 samples – encompassing region 1), or that the observations noted from Figure B.18a are not significant enough to be observed.

2. Region two indicates that the standard error trend plateaus during pre-mill 3 and 4. It was previously noted that the XML peaks during this region. This may infer that the observations noted from Figure B.18a are not significant enough to be observed, however, it may also be the case that the XML standard error magnitude is simply too extreme to indicate the changes effectively.
3. Region 3 occurs in conjunction with the outer pocket occurrence of pre-mill 2. As there is a noticeable dip in the XML standard errors, the XML magnitude must drop suddenly. This indicates that the pre-mill region has a definite effect on the process behaviour. Care must be taken not to appropriate this feature as an indication of cutting tool health without further investigation.
4. Region 4 indicates that the standard error trend plateaus during pre-mill 3 and 4 for the outer pocket in much the same way as is observed for the inner pocket. The same inferences may be drawn as for Region 2.

Figure 3 compares the YML QSUM with the aAMR. Like Figure B.18b three signal regions are identified.

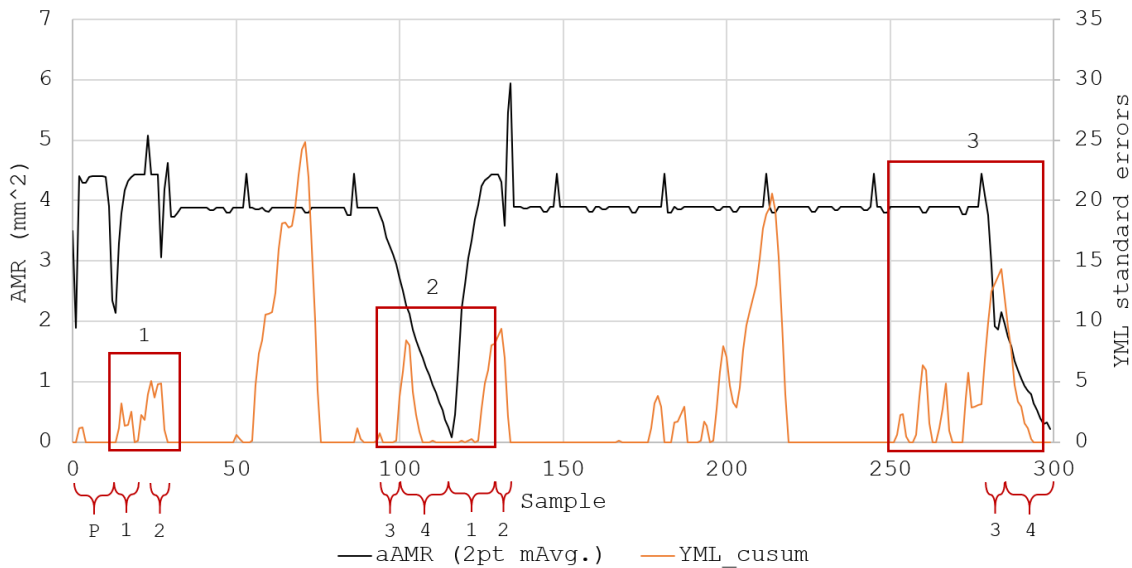


Figure B.20. Cumulative sum for Y-axis percentage load compared with material removal during wear test

1. Region 1 indicates that there is a significant YML magnitude concurrent to pre-mill 1. However, this is whilst the cutting tool is travelling along the Y-axis. This direction of cutting would imply that an increase in the YML is expected. Therefore, such a signal may be indicative of

the process, not the occurrence of pre-mill 1. Further investigation may allow the magnitude of the loads to inform the operator about the health of the cutting tool.

2. Region 2 indicates the same peak in the YML magnitude as was observed in Figure B.18b. This indicates that pre-mill 3 influences the cutting behaviour, and that this can be quantified from the YML output. This behaviour is a result of the process and therefore must not be confused with an anomaly indicative of cutting tool health. It is noted that (distinct from Figure ref) the QSUM does not indicate any influence from pre-mill 4 for the inner pocket. This implies that either the observations noted in Figure B.18b are not significant enough to be observed or that the calculation of the QSUM is masking such observations.
3. Region 3 indicates a significant rise in the YML standard errors up to, and over, pre-mill 3. This is expected due to the cyclical nature of the signal, yet the magnitude is considered extreme relative to the concurrent reduction in material engagement of the cutting tool. It is suggested that pre-mill 3 is influencing the cutting tool behaviour because of the small cuts and due to the cutting tool “jerking” out of the material. Pre-mill 4 is not considered to be having an observable effect on the cutting tool behaviour as the YML standard errors reduces as expected.

Both Figure B.19 and Figure B.20 succeeded in identifying some of the signals noted in Figure B.18. Both failed to identify some of the other observations; however, it may thus be implied that such observations are not of concern or not significant enough to warrant further investigation. It was found that the sensitivity of the QSUM was too sensitive to the stochastic nature of the data, with the XML QSUM markedly affected by both the cyclical nature of the signal, and the apparent increase in the moving (mean) average. The YML QSUM was not found to be as affected, despite the signal indicating the same cyclical nature (expected during circular pocket milling). This perhaps indicates that the differences between the two axes motors is one of the contributing factors to the dissimilarities (see Chapter 3). It is of the Authors’ opinion that the sensitivity of the QSUM approach rules it out as an approach for preparing such signals for assessment by a computer. Such an approach would be largely at the mercy of the interpretation of the data according to the QSUM algorithm rather than the true signal features and therefore prone to debilitating errors.

## B.4 Practical challenges facing implementation

In practice, determining the variations in the material engagement of the cutting tool enables a greater understanding of the relationship between the cutting process and the MTData obtained for cutting tool and/or process condition monitoring. Without this understanding the details of the MTData will at best be ignored and at worst interpreted incorrectly. A proper understanding of the MTData allows it to be leveraged for the explanation of process variation and for the indirect analysis of the health of the cutting tool and of the process.

Notwithstanding, a challenge for the calculation of process variation is the implementation in real-time. It is perhaps more realistic that the pre-mill formulae are implemented in semi-real time, thus

allowing the cutting tool to complete each cycle of the pocket milling process *before* attempts are made to identify the boundaries of any pre-mill occurrences. Indeed, the aAMR cannot be calculated if material is yet to be removed by the cutting tool. Additional considerations for implementing the pre-mill formulae include:

1. Finding the centre coordinates for the cutting tool and for the pre-milled region. The origin of the pocket will be unknown during the start of a pocket milling operation and estimated for a significant time throughout. Knowledge of the process geometry will allow the calculations to be implemented immediately.
2. The OEM tool diameters and the expected pocket diameters will affect the estimates of the AMR due to the changing dimensions of both. Including any measured/observed values will improve the accuracy of AMR estimates.
3. It is noted that the calculation of the EPL is challenging and requires a comprehensive understanding of the relative process geometries. In practice this may not be feasible or practical, especially for unique or one-off components. It is suggested that the pre-mill regions are identified using the suggested spatial boundaries and by capitalising on any known process movements.

## B.5 Summary

This work has investigated whether the equivalent volume of material removed affects the conditions experienced by a cutting tool. This only considered the removal of material during circular pocket milling, questioning the effects the overlap has on the cutting process and why these occurred. It was shown that the pre-mill phenomenon results in a significant shift in the material removed per cut during pocket milling. The difference was caused by variation in the material available following changes to the travelling direction of the cutting tool and occurrences were often linked to unexpected failures of the cutting tools, or paired with characteristic trends within the MTData signals.

The occurrence of each pre-mill were compared with acquired MTData signals representing the primary spindle outputs (SRS and SML) and two of the axes outputs (XML and YML). These comparisons identified the effects that the regions had on both the control and the behaviour of the machine and of the cutting tool. It was thus shown that the pre-mill phenomenon had a significant effect on the cutting process and provided a sound explanation for anomalies in process signals, that may otherwise be mistaken for deteriorating health of the cutting tool. Additionally, when investigated at the start of a process, these anomalies provide a potential standard for which subsequent processes may be compared. This enables the focus of post-processing to be directed towards a narrower data range, thus enabling a shorter turnaround in the data processing and reducing the quantity of data to be retained. In addition, isolating key stages of the cutting process and the variations that correlate to these key stages allows the information provided by the MTData to be categorised and to give greater prominence to any potential health features within the signal.

Further work would be necessary to identify the material removal for different pocket milling operations. However, reducing any process into simple geometries would enable this method to be applied

if the boundary conditions are implemented correctly Further development of this work would benefit from the additional consideration of the z-axis encoder output to consider the material removal in three dimensions rather than just two. This would enable the calculation of the volume of material removed, instead of the area of material removed, which in practical terms carries more significance for manufacturers.

## **C | DMIS**

### **C.1 Programs**

All DMIS programs and files, including those developed by the Author, are available on request.

### **C.2 Process assurance**

### **C.3 Calibration certificate (CMM)**

### **C.4 Calibration certificate (surface finish)**

### **C.5 I-MR charts**

## **D | Additional documents**

All additional documents are available on request.

**D.1 Naming conventions**

**D.2 DENSE additional figures**

**D.3 Sycon help file**

**D.4 Sycon project files**

**D.5 Mazak API specification**

**D.6 PC specification**

## **E | Data files**

The data identified below is available on request.

### **E.1 Experiment log**

### **E.2 Register audit**

### **E.3 Dispersion plots**

### **E.4 Application data files**